Theory of the
Interior Ballistics of Guns

Theory of the Interior Ballistics of Guns

J. CORNER, M.A., Ph.D.

NEW YORK · JOHN WILEY & SONS, INC.
LONDON · CHAPMAN & HALL, LIMITED

COPYRIGHT, 1950
BY
JOHN WILEY & SONS, INC.

All Rights Reserved

This book or any part thereof must not be reproduced in any form without the written permission of the publisher.

PRINTED IN THE UNITED STATES OF AMERICA

To the memory of
the founder of interior ballistics
BENJAMIN ROBINS, F.R.S.
1707–1751

Preface

It was in 1944 that Dr. J. W. Maccoll suggested to the writer that there was need for a modern textbook on the theory of the interior ballistics of guns. The project could not be taken up at that time, but our discussion of the plan showed that the subject was ready for an up-to-date survey.

Probably the most striking general result that has emerged from the wartime work on guns is the complexity of the physical and chemical processes involved. It is, of course, not at all obvious that this need be so. The system of gun, projectile, and charge appears at first sight to be surely one of the simplest of all heat engines. It was from this idea that interior ballistics, about a hundred years ago, began to develop towards a mathematical structure based on a few simple physical assumptions. Gradually the mathematics became more elegant, and more subtle points were discussed. As there was relatively little study of the physical assumptions, this mathematical work could not be said to be helping greatly our understanding of the behavior of real guns.

But now, a few years later, theoretical interior ballistics has completely changed its direction. This we must acknowledge to be due in the main to the use of modern instruments of research. These have revealed the complexity of the processes inside the gun and have reduced some of the basic ideas previously held to the status of mere empirical approximations. Again, the study of gun behavior under extreme conditions has led, as could have been expected, to abnormal behavior; the more important aspect is that these abnormalities can be traced in modified form right into the region of normal conditions. This explains why so many aspects of interior ballistics have eluded theoretical analysis, and have been left to "past experience" acquired over many years and reliable only in a stagnant technique.

When the physical basis of a subject becomes more complicated, the mathematics becomes simpler. When four equations are thought to sum up the whole of interior ballistics, it is natural to spend almost any length of time on their study. If, however, the subject is seen as the interrelation of a dozen different aspects, it is clearly best to keep as far as possible to simple mathematics.

In writing this book I have tried to keep the best of the classical phase while introducing also some of the methods that promise to be most valuable in the future development of the subject. It is, fortunately, not yet possible to write of ballistics as a complete and perfect structure. The new complexity implies new possibilities of rational understanding and corresponding practical advances, and we can expect research to go ahead vigorously. I have indicated the lines on which theoretical research is likely to be concentrated and have kept these in mind in choosing topics. It must be added, also, that the best classical theory, with its tendency to oversimplification of the physics and chemistry, is for that reason a valuable introduction to the subject and would earn a place in this book on that ground alone.

Permission for open publication has been kindly granted by the Chief Scientist, Ministry of Supply (England). For permission to reproduce material from my papers published in their journals I am indebted to the Royal Society (sections 2.33, 7.1–7.39, and 9.2–9.26, Figs. 7.1, 7.3, and 9.5–9.9), the Faraday Society (sections 2.41–2.44), the Franklin Institute (sections 8.1–8.16 and Fig. 8.1), the Physical Society of London (sections 3.24 and 3.32), and the *Quarterly Journal of Mechanics and Applied Mathematics* (sections 5.5–5.54). I am able to use Figs. 9.1 and 9.2 by the courtesy of Mr. F. B. Pidduck and the Royal Society. I am indebted to Mr. E. P. Hicks and Mr. C. K. Thornhill for permission to quote freely from their theory of heat transfer to gun barrels.

To my wife I am indebted not only for encouragement but also for substantial help in the preparation and editing.

J. CORNER

Contents

Chapter One: The Field of Interior Ballistics, 1

1.1 The scope of the present book 1
1.2 "Practical" and "research" ballistics 3
  1.21 The measurement of pressure in guns 7
  1.22 The measurement of muzzle velocity 9
  1.23 Other experimental research 11
1.3 The classical problem of interior ballistics 14
1.4 The future of interior ballistics 16
1.5 The history of the classical problem of interior ballistics 18

Chapter Two: Gun Propellants, 24

2.1 Propellant compositions 24
2.2 The arrangement of the propellant charge 26
  2.21 Propellant shapes and the geometrical form function 30
  2.22 The true form function 35
  2.23 The Charbonnier form of the equation of burning 41
2.3 Theories of the burning of gun propellants 42
  2.31 Surface theories 43
  2.32 Vapor-phase theories 47
  2.33 Theory of a flame zone in a gas 49
  2.34 Application to the burning of propellant 63
  2.35 The theoretical rate of burning at high pressures 66
  2.36 The influence of the initial temperature of the propellant 69
  2.37 Experimental knowledge of the rate of burning 70
2.4 "Erosion" of propellant 73
  2.41 A simple theory of the erosion of propellant at gun pressures . . 74
  2.42 Hydrodynamic considerations 76
  2.43 Effective thermal conductivity in the flame 81
  2.44 Rate of burning with turbulence 82

Chapter Three: The Thermochemistry of Propellants, 85

3.1 Sketch of closed-vessel technique 87
  3.11 Cooling corrections 85
3.2 Theory of the equilibrium state after burning without cooling or performance of work 89
  3.21 Theory without dissociation or pressure corrections 89
  3.22 Dissociation 97
  3.23 Experimental results 100
  3.24 Theory of the covolume and other pressure corrections 102

3.3 The equilibrium state after burning under constant pressure without cooling . . . 115
    3.31 Theory without pressure corrections . . . 115
    3.32 Pressure corrections . . . 117
    3.33 Specific impulse of a rocket fuel . . . 120
3.4 Thermal behavior of the propellant gases in a gun . . . 125

Chapter Four: Simple Ballistic Methods, 130

4.1 Introduction . . . 130
4.2 The "isothermal" solution . . . 132
    4.21 Notation . . . 132
    4.22 Equations of motion . . . 133
    4.23 Solution after "burnt" . . . 139
    4.24 Summary of the working formulas . . . 141
    4.25 The efficiencies of gun and charge . . . 142
4.3 Comparison with experiment . . . 145
    4.31 Some typical ballistic solutions . . . 145
        4.311 A typical AA gun . . . 146
        4.312 Cord charges in a naval gun . . . 154
    4.32 Empirical corrections . . . 156
4.4 Ballistic effects of charge and design variables . . . 159
    4.41 The web size . . . 159
    4.42 The charge weight . . . 162
    4.43 The total travel . . . 169
    4.44 Chamber capacity . . . 169
    4.45 Shot weight . . . 169
    4.46 Propellant shape . . . 170
    4.47 Nature of propellant . . . 171
4.5 The history of the isothermal model . . . 171

Chapter Five: More Advanced Ballistic Methods, 174

5.1 The energy equation of interior ballistics . . . 175
5.2 Coppock's solution . . . 177
    5.21 Assumptions . . . 177
    5.22 Equations of the problem . . . 177
    5.23 Solution of the equations . . . 178
    5.24 Summary of the working formulas . . . 182
    5.25 The nature of the effects produced by covolume and kinetic-energy terms . . . 184
    5.26 Comparison with experiment . . . 186
    5.27 The effect of heat losses . . . 189
5.3 A theory with a "shot-start pressure" . . . 189
    5.31 Assumptions . . . 191
    5.32 Goldie's solution . . . 192
    5.33 Ballistic effects of a shot-start pressure . . . 204
5.4 Rate of burning not proportional to pressure . . . 206
5.5 The ballistic effects of bore resistance . . . 213
    5.51 Disturbance of muzzle velocity by the standard bore resistance . . . 215

5.52 Accuracy of first-order theory 220
5.53 Calculation of the effect of long stretches of bore resistance . . . 222
5.54 Effect of the covolume 223
5.6 Numerical and mechanical methods 223

Chapter Six: Similarity Relations and Optimum Problems of Interior Ballistics, 226

6.1 Introduction to ballistic similarity 226
6.11 The similarity relations for a simple set of ballistic equations . . 227
6.12 The tabulation of ballistic solutions 235
6.2 Optimum ballistic solutions 240

Chapter Seven: The Interior Ballistics of Leaking Guns, 243

7.1 Introduction 243
7.2 The classical theory of nozzles 246
7.21 Covolume corrections 250
7.22 Thrust on a nozzle 251
7.3 The equations of interior ballistics of a leaking gun 253
7.31 Assumptions of the theory 253
7.32 Notation 255
7.33 Pressure and density distributions in the gun 255
7.34 Nozzle flow and energy relations 258
7.35 Summary of the equations 260
7.36 The equivalent nonleaking ballistic problem 261
7.37 Numerical integration 266
7.38 Solution with linear rate of burning 267
7.39 Solution after "burnt" 274
7.4 Gas leakage in a smooth-bore mortar 276
7.5 The ballistics of a worn gun 279
7.51 Equations of interior ballistics of a worn gun 281
7.511 Basic assumptions 281
7.512 Notation 282
7.513 Equations of the problem 282
7.514 Solution after "all burnt" 284
7.515 Approximate solution near the start 285
7.52 Analysis of the experimental data on new and worn guns 287
7.521 Ballistics of the new gun 288
7.522 Ballistics of the worn gun 289
7.53 Changes in ballistics during the life of the gun 293
7.54 Rapid estimation of the effect of leakage 294
7.6 Ballistic properties of recoilless guns 295
7.61 "Recoillessness" 296
7.611 The calculation of recoil momentum 297
7.62 The influence of design variables and loading conditions on the interior ballistics of a typical recoilless gun 299
7.621 Effect of nozzle-start and shot-start pressures 300
7.622 Effect of rate of burning or web size 304

        7.623 Effect of charge weight on nozzle throat area for zero recoil 305
        7.624 Effect of shot weight on nozzle area for zero recoil . . . 306
        7.625 Effect of changes of chamber capacity 306
        7.626 Changes in total shot travel 307
        7.627 Effect of nature of propellant 307
        7.628 Influence of nozzle design 308
    7.63 The optimum pressure for opening of the nozzle 308
    7.64 The value of a muzzle brake on a recoilless gun 309

Chapter Eight: Some Special Types of Gun, 312

8.1 The high-low-pressure gun 312
    8.11 Notation 313
    8.12 Assumptions 314
    8.13 Equations of interior ballistics up to "burnt" 316
    8.14 Interior ballistics after "burnt" 323
    8.15 Summary of the working formulas 324
    8.16 The maximum possible piezometric efficiency 326
8.2 Small arms 327
8.3 Composite charges 328
    8.31 Reduction of a composite charge to a single effective web size . . 329
8.4 Tapered-bore guns 334
    8.41 The equations of interior ballistics for a tapered-bore gun 336

Chapter Nine: The Hydrodynamic Problems of Interior Ballistics, 339

9.1 Introduction to Lagrange's ballistic problem 339
    9.11 The conventional solution 342
    9.12 The results of Love and Pidduck 347
    9.13 Pidduck's limiting solution 351
    9.14 Experimental results and future theoretical research 357
    9.15 The shock-wave equations 359
    9.16 The maximum possible muzzle velocity 361
9.2 The interior ballistics of a gun after shot ejection 364
    9.21 The initial state of the gas in the barrel 365
    9.22 Earlier work 368
    9.23 Discussion of the problem 370
    9.24 Solution before the arrival of the wave from the muzzle 371
    9.25 Comparison with an experimental breech pressure record 374
    9.26 The rarefaction zone 377
9.3 Muzzle brakes 383
    9.31 The calculation of muzzle-brake thrusts 385
    9.32 The "efficiency" of a muzzle brake 387
9.4 Conditions ahead of the shot 392
    9.41 Steady motion 393
    9.42 Riemann's method for the solution of the hydrodynamic equations 395
    9.43 Accelerated motion 397
9.5 The motion of propellant in a gun 400
    9.51 Ballistic consequences 407

Chapter Ten: Heat Transfer to Gun Barrels, 409

10.1 Introduction 409
10.2 The heat-transmission coefficient 410
10.3 The conduction of heat in the barrel 418
10.4 Results of the heat transfer in guns 422
    10.41 Semiempirical formulas for heat loss 425

Appendix A: The Numerical Solution of the Equations of Interior Ballistics, 427

A.1 Method of solution on a calculating machine 427
A.2 Solution without a computing machine 430

Appendix B: Some Constants Used in Ballistics, 432

Appendix C: Interpolation Coefficients, 433

Name Index, 435

Subject Index, 439

CHAPTER ONE The Field of Interior Ballistics

1.1 The scope of the present book

The purpose of this book is not to give results so much as to illustrate methods. The field of interior ballistics is now too wide to be covered completely in one book of moderate size, and new problems are constantly arising. The methods of attack from the theoretical side are much more settled, and they show certain themes, which occur repeatedly in different problems. We hope to illustrate these techniques in the present book.

The experimental side of ballistics is discussed here only where it affects the theory, as, for example, by fixing the accuracy which the theory need not exceed. This omission is not meant to imply that experiment is unimportant, but rather to keep this book to a reasonable size. In any case, the author cannot speak with any authority on the experimental side. He is well aware that in ballistics most of the theoretical work is directly inspired by experimental results, either as an attempt to explain the newly observed, or else as the refinement of existing theory to cope with an extra order of magnitude in the accuracy of measurement. At the same time, experiment is often held back until a theoretical examination has been made; this respect for theory is due in part, it must be admitted, to the high cost of experiments in this subject.

Our field, then, is the theory of the phenomena that occur inside a gun or that are closely associated with it. The interior ballistics of rockets we do not touch.

The aim of illustrating methods allows one a good deal of choice in the subjects discussed. The author has tried to mention most of the problems in this field and to discuss in detail all the more important; for the rest, the emphasis has fallen on those subjects that have had special interest for him. Much has been taken from the author's wartime work, for example the burning and "erosion" of propellant, the theory of the of his *Lehrbuch der Ballistik*. This is particularly valuable on the historical side, for it gives details of a number of methods which are obsolete today.

The French school is represented, in its two classical attacks on the central problem of interior ballistics, by Gossot and Liouville, *Balistique intérieure* (Paris, 1922),[1] and Sugot, *Cours de balistique*, volumes I, III, and IV (Paris, 1918). At this point we may refer to two memoirs of special value: a very clear and elegant survey of the classical problems of interior ballistics, summarizing the work of the French school, by Sugot, *Mémorial de l'artillerie française*, volume 5 (1926), page 1131; and a summary of methods up to 1922, which in some respects is clearer than Cranz's review, published by Desmazières in *Mémorial de l'artillerie française*, volume 3 (1924), page 1009.

Other books on interior ballistics either are obsolete or are covered by the treatment in Cranz. For progress since 1926 it has been necessary to go to the original papers.

Finally, one must refer to Charbonnier, *Balistique intérieure* (Paris, 1908). This book is of great historical interest, having had a strong influence on the development of ballistic theory. Though naturally obsolete in details, it is still one of the clearest expressions of the aims of interior ballistics.[2]

1.2 "Practical" and "research" ballistics

There is considerable application of ballistics to routine work, such as the testing of guns and propellants and the estimation of new charges. This may be called "practical" ballistics, as opposed to the "research" aspect. From the experimental side the distinction is that "practical" ballistics needs only relatively simple measurements, which are easily carried out in mass; "research" is that class of experiments for which a considerable preparation is necessary and which involve some analysis before the final result is obtained. The distinction may seem to be not very sharp, but it is quite clearly marked in practice. Thus a measurement of the peak pressure attained in a gun can be obtained in a minute or two from a crusher gage, and this measurement is done by the hundred in a day's work at a proving range. To obtain a pressure-time curve on a sheet of graph paper is more of a research matter: the setting up of the piezo gage and its circuit takes longer, the film on which the record is made has to be developed and fixed, and the reading of the film and its reproduction as a graph take yet more time. Furthermore, there are more possibilities of failure in work with the piezo gage. It follows that, although the piezo gage is used a good deal, yet it tends to be reserved for the more important and delicate problems, where a knowledge of the variation with time is essential.

---

[1] Also *Traité des effets des explosifs* (1919).

[2] Charbonnier restricts "internal ballistics" to the study of mechanical effects, that is, to what we call the "classical central problem" (including the closed vessel); all other matters that are considered here Charbonnier would have relegated to "the science of explosives."

The same distinction appears on the theoretical side and arises partly from this division of the experimental data. Where measurements involve a considerable amount of work, it pays to have as accurate a theory as possible. A special case arises when some quantity cannot be measured at all by current technique—it is then essential to go into the theory as carefully as possible. This is the function of the research aspect of interior ballistics.

For analysis of routine firings the ballistic theory need be only of the simplest type. All reasonable errors in the theoretical results can be removed by examining the errors recorded for previous calculations on as nearly as possible the same problem. A further reason for not pushing routine analysis too far is the variability of guns and charges. Nominally the same guns by different makers show differences of the order of 10 ft/sec, and the variation of propellant properties causes an even bigger spread, which, however, is more easily corrected by altering the charge weight in the filled round. The subject of the accuracy needed in theory is closely linked with the reproducibility of ballistics, to which we now turn.

The ballistic properties of gun propellants are sensitive to the small variations that occur during manufacture. At any one factory the ballistic properties of the individual sticks of propellant show variations, which may be quite considerable, about a mean which varies slowly with time. The mean properties of nominally the same propellant from two factories often show differences that are too large to be neglected but are not easily corrected at the factory stage; these differences are presumably due to trivial variations in the process of manufacture, though a correlation is not easy.

These variations are more easily taken into account after a smoothing process. The product of one factory is divided into successive "lots," whose size may be anything from 1 to 20 tons, depending on the output, and within each lot a blending is carried out. The efficiency of this can be checked by statistical means, and, if satisfactory, the result is a batch of propellant of fairly homogeneous character; that is, an examination of individual sticks shows, of course, the same spread of properties as before blending, but now a division into bundles of *adjacent* sticks gives the distribution of mean properties to be expected from a random sample. Without blending, the bundles of adjacent sticks would show an extra variability, because each bundle would have a common day of manufacture or be made in the same subsection of the factory.

Propellant is indexed by its lot number. Each lot is fired in a gun or a closed vessel under controlled conditions, and the effective rate of burning is determined. Both the mean and the distribution about the mean are found; although it is common to use the mean deviation or the rms deviation as the parameter measuring the variability of this or any other ballistic quantity, there are establishments that prefer a statistically less significant quantity, namely, the total spread in, say, five experiments. This was a common practice in German ballistics.

From the mean properties and the variance, the lot is either accepted or rejected; for example, the rate of burning may be so subnormal that a charge to give the specified muzzle velocity would be too bulky to be loaded into the chamber. Assuming that the lot satisfies the specification, its effective ballistic speed is taken into account by stating the charge weights of this lot to be used in service rounds.

The division of propellant into "lots" of known ballistics makes it possible to "prove" guns by using standard charges. "Gun proof" is concerned mainly with the strength of the gun, and pressures up to 20 per cent above the normal peak pressure are applied. In most countries this is done by using charges of greater weight, which is simple but not always possible (for example, even the normal charge may fill the available space). The German practice of using a heated charge, with therefore a higher rate of burning, is more logical but needs a heating chamber. A heavier shot is a possible alternative, though the supply of several weights of proof shot for each type of gun would not be liked. Proof shot, it may be mentioned, have a flat head, intended to give reproducible breaking of Boulengé screens (§ 1.22). Proof shot are normally solid, though some hollow proof shot are in use.

The proof of guns with charges of one lot reveals gun-to-gun differences of muzzle velocity and peak pressure. As the gun wears, its performance tends to approach more closely that of its fellows, taken at the same stage of wear: that is, not necessarily at the same number of rounds fired. During the initial period, when gun-to-gun differences are at their largest, it is possible to trace a common tendency among all guns from a single factory. One maker will produce guns whose velocities at proof average rather higher than those from another maker.

Another known variation occurs from day to day in the mean performance of a single gun firing charges of the same lot at a given temperature.

Until now we have tacitly assumed that equal charges of a single lot, fired one after another in the same gun, will give a set of velocities (or peak pressures) that are distributed in some permanent fashion about a fixed mean. If, for example, we calculate the mean and the variance of the first n rounds, the mean has been assumed to tend toward a fixed value, the mean of the population, as n increases; likewise, the variance has been assumed to tend to a fixed value characteristic of the frequency distribution. This assumption is a natural one, and the test, though simple, is almost always omitted. It is true that first rounds from a cold gun are invariably disregarded, being sometimes peculiar. In most firings the assumption of a true mean and a real frequency distribution are well obeyed. An exception noted recently occurred at the smallest charge in a certain class of howitzers, where the velocity was found to rise slowly by as much as 50 ft/sec in 50 rounds ("upward creep"). This shows that a mean and a mean deviation do not necessarily exist in the kind of variability encountered in ballistics.

We shall recapitulate with some typical numerical values. Individual sticks of nominally the same propellant from a single factory have rates of burning with a standard error of the order of 10 per cent of the mean. Blended into lots and subdivided into gun charges, the mean deviation, when rounds of one lot are fired in one gun on the same day, is roughly 5 to 10 ft/sec; this is a property of the gun as well as of the propellant. Equal charge weights of different lots fired in the same gun on the same day give mean velocities that can differ by as much as 30 ft/sec. This mean difference is taken up by adjustment of the filled charge weight of each lot. Charges from one lot, fired at the same time in guns of the same type, give mean velocities that can easily differ by 10 ft/sec in new guns. The mean velocity in each gun varies from day to day, by amounts of about 5 ft/sec.

The mean deviation of charges of one lot, as determined at the proving ground, is less than the spread of service rounds using charges from this lot. For the dispersion due to the charges to show up more clearly at the proving ground, the shot and charge weights are kept constant within about 1 part in 1000. In service rounds these rigorous conditions cannot be maintained. In particular, charge weights have a broader tolerance whose magnitude is naturally settled by considering the residual and unavoidable dispersion shown in the propellant proof, together with production matters.

Returning to the subject of routine calculations of interior ballistics, it will now be accepted that there is no point in computing theoretical muzzle velocities to better than 5 ft/sec. An exception must be made when differential effects (for example, the effect of a small change in shot weight) are computed by the difference between two nearly similar calculations; here the accuracy of the final result will be very low unless the two basic calculations have a high nominal accuracy. Differential effects are better calculated from an explicit formula, if such is available.

In research work on interior ballistics it is more often necessary to work to a nominal accuracy of 1 ft/sec. This can arise when individual rounds have been given a great deal of experimental attention and the theoretical worker has to make the most of each round. Information from such a detailed analysis is usually applicable only to that particular round. Where we are dealing with mean performances over a number of rounds the theoretical worker often carries his computations to 1 ft/sec, but only because he will later need to interpolate between these basic solutions. In effect, he is computing differential properties of his theoretical solutions.

To take computations beyond this accuracy is hardly ever necessary. This has arisen only once in the writer's experience: in computing differential effects to compare with an approximate explicit formula it was necessary to compute basic solutions to a nominal accuracy of 0.1 ft/sec (§ 5.52).

1.21 The measurement of pressure in guns [3]

For routine proof of guns it is desirable to be able to measure the maximum pressure quickly and simply, and the details of the pressure-time curve are not of much interest. For this the crusher gage (Fig. 1.1) serves very well. A cylinder, usually of copper, is compressed by a piston exposed to the gases, and from the measured permanent compression can be read at once the peak pressure attained in the gun. The body of the gage is heavily coated with copper to prevent damage to the gun. One or two gages are loaded with the charge at the breech end to prevent their motion. A table giving the relation between the pressure and the reduction in length is obtained by calibration in a deadweight press. Since the accuracy depends on the reproducibility of the plastic properties of the copper, it is only by strict specification and rigid inspection that the method becomes reliable.

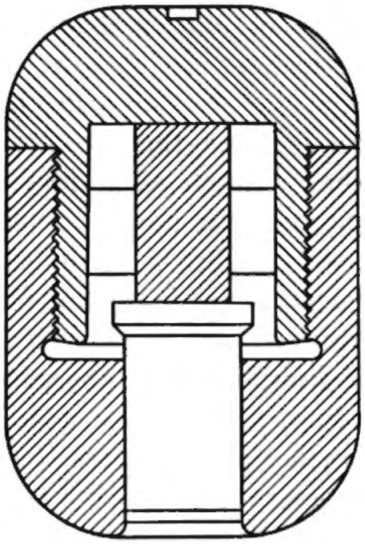

FIG. 1.1 Section through a typical crusher gage showing the copper cylinder surrounded by a centering ring and compressed by a piston exposed to the propellant gases.

---

[3] For a much more full account, though not now up to date, see Cranz, *Ballistik*, vol. 3 (Berlin, 1927).

The copper crusher gage was invented by Noble (1860), and there is still no sign of any competitor in routine pressure measurement. The copper is usually precompressed to a few tons per square inch below the expected peak pressure. It is very rare for a crusher gage to fail: apart from forgetting to load the gages at all, almost the only thing that can go wrong is the use of a copper already compressed to more than the pressure attained in the gun, and even this can be avoided by using two gages with different precompressions.

The reading of the gage depends on the temperature of the copper at the time of firing. For ordinary British gages the pressure calculated from the tables has to be reduced by 1 per cent for each 10°F that the copper temperature is above the standard. At pressures below 5 tons/sq in. the differences in length produced in the standard gage become small, and lead crushers have been used in this zone.

For routine work it is often sufficient to have an indication of the pressure, rather than an accurate value. It is not important if the "pressure" deduced is, say, 20 per cent lower than the true pressure, provided that all gages behave in the same way and that no attempt is made to use their results as true pressures. For gun design and tests of theory, such an uncertainty is not allowable. Comparison with the piezoelectric gage (discussed later) has shown that, in fact, the copper pressure should be multiplied by 1.2 to give true peak pressures. The factor depends on the dimensions of the gage, to some extent, and the value 1.2 refers only to the standard British gage. For this reason, it is desirable to use the same size of gage in all calibers except the smallest, where a miniature gage, of lower accuracy, must be used. Since a crusher gage reduces the free space inside the chamber, a correction to pressure and velocity must be made. This is easily computed from the simple ballistic theory of chapter 4. It should be added that the factor of 1.2 falls slightly below 10 tons/sq in., reaching 1.15 at about 5 tons/sq in.

The lower deformation of the copper under dynamic conditions is attributed to (1) the time lag in the plastic flow, and (2) possibly also some friction resisting the motion of the piston when the gage is subjected to a hydrostatic pressure of many tons per square inch. On the other hand, the inertia of the moving piston must tend to compensate these effects. Because of the possibility of friction, when two gages have been used the higher of the two pressures is often preferred to the mean.

In small guns, of less than 6-cm caliber, there is little room for a crusher in the cartridge case. If a crusher is used at all, it is usually screwed into the wall of the chamber opposite a hole in the cartridge case. This is the "radial crusher gage." Such gages have been used at positions down the bore, to obtain pressure-travel curves. When used in this way the gages are given a shock loading as the base of the shot passes, and it is likely that they read too high. The correction to be applied is a matter of controversy. Crusher gages down the bore are in fact useful for discovery rather than proof of ballistic phenomena.

An accurate pressure-time curve is necessary for research on guns, and for this feature it is necessary to sacrifice some convenience and speed in obtaining the answer and to accept an occasional failure to record a round. The gage must recoil with the barrel, which rules out any mechanical type. The piezoelectric gage has been found very satisfactory. A tourmaline crystal disk, diameter about ½ in., is cut perpendicular to the electric axis and secured by conducting cement to two electrodes. The crystal and electrodes are mounted in a gage screwed in the gun wall, and the interior of the gage is filled with mineral jelly as a protection against the hot gases. The crystal is thus subjected to hydrostatic pressure, and a charge, proportional to the pressure, is developed at the electrodes. This charge is led via a cable to a small condenser, whose voltage is amplified to control a cathode-ray oscillograph, which is photographed on a revolving drum.

The charges developed are small; at 20 tons/sq in. a normal charge is only 0.1 microcoulomb. Thus, in practice, much attention must be given to insulation. To calibrate the gage a dead-weight pressure is used, giving a charge-pressure relation. To convert the film record to pressure we need also the known input capacitance and the voltage-deflection characteristic of the amplifier, oscillograph, and optical system. This characteristic is recorded before each shot by switching in known voltages. The exit of the shot can also be recorded on the film by a muzzle contact.

Few other methods of measuring pressure have been applied to guns. In small arms the weapon can be mounted rigidly and a mechanical gage, such as the Thring gage, can be used. Another electrical method for finding the pressure-time curve in a gun is to measure the out-of-balance current in a bridge of which one arm is a coil of Manganin wire exposed to the gun pressure. This method has been used successfully by Rheinmetall-Borsig.

1.22 The measurement of muzzle velocity [4]

The Boulengé chronograph was invented at about the same time as the crusher gage and has for many years been the standard way of measuring muzzle velocity. Previously the only method was a ballistic pendulum, which, of course, cut short the trajectory in the act of measurement. What is actually measured by the Boulengé is the time taken to traverse the accurately known space between two "screens," of which the nearer is usually a couple of hundred calibers from the muzzle. From the observed mean velocity and an estimated retardation coefficient of the projectile, the muzzle velocity can be calculated; strictly speaking, the velocity so derived is slightly higher than the true velocity at the muzzle, because of the acceleration of the projectile in its first ten calibers or so of flight, before it gets away from the muzzle gases. It is easy to convince oneself, by an approximate calculation, that this discrepancy is never more than a few feet per second, and therefore negligible.

---

[4] For more details, see Cranz, *Ballistik*, vol. 3 (Berlin, 1927).

Each "screen" has a continuous fine wire, wound backwards and forwards to fill the gap in a rectangular frame set perpendicular to the trajectory. A current flows through the wire, which is so closely wound that the projectile in its passage must break the circuit. The spacing of the wire has to be sufficiently fine to ensure that the possible positions at which the projectile may hit the screen will cause breaking of the circuit at times equal within experimental error. Certain sensitive fuses cannot be fired through screens.

The chronograph invented by le Boulengé measures time by the free fall of an iron rod, covered with a soft metal such as copper, zinc, or cadmium. The two screens are each in series with an electromagnet. Initially the rod is held underneath the first magnet. When the projectile breaks the first current, the rod falls freely. At the breaking of the second circuit, another suspended rod falls, releasing a spring-loaded knife which marks the falling rod. The zero of the fall has been previously marked on the rod by holding it suspended by the first magnet and opening the second circuit. Thus, the height of fall is known, and, likewise, the time of fall. This must now be corrected by another constant of the instrument, namely, the time taken for the marking process. This can be found by opening both circuits together.

The Boulengé chronograph is simple, and fairly reliable if the wiring and instruments are properly maintained, and if the instrument is insulated against the vibrations common to test ranges. Disadvantages of this chronograph are the time required to rewire the screens and the restriction to firing at low angles of elevation.

A method that can be used at all angles of elevation is to fire a magnetized projectile through two coils in series at some distance apart along the trajectory. For high elevations a high gantry is needed. The passage through each coil induces an emf in the circuit, which contains an oscillograph recording on sensitized paper on a rotating drum. This "solenoid" system does not require any rewiring of circuits, unless an unlucky shot hits one of the coils, and it is less temperamental than the

Boulengé. To offset these advantages, the shot must be magnetized, the result is not known until the film has been developed and fixed, and the accuracy is poor if the projectile is yawing badly or is off the axis of the coils.

With a typical base line traversed by the shot in about $\frac{1}{10}$ sec, the error in the Boulengé method can be as small as 1 part in 1000. This is for large flat-headed shot. With small pointed shot fired at high velocities the error can rise to 20 ft/sec. The most important factor affecting accuracy in the chronograph, as distinct from the screens, is the nature of the solenoid steel. Careless electrical treatment can reduce the accuracy of a good Boulengé by a factor of 2 without outward signs of damage.

Other methods of measuring velocities have been developed, some in the direction of greater speed and convenience, others toward use on ship or in the field. Until now little has been published about these more modern methods.

1.23 Other experimental research

In this section we shall list a number of experimental techniques that are employed to test theories or to suggest problems. Some of them have been developed to such a stage that they can be applied immediately whenever the need arises. One example is the strain gage. A thin wire cemented to the surface of a gun barrel converts strains into changes of resistance, and if connected in a bridge circuit the short-lived strains during the firing of the gun can be permanently recorded by cathode-ray oscillograph and camera. Longitudinal or hoop strains can be measured, according to the direction of the wire. Full use of this technique requires a multichannel oscillograph, which makes a great difference in the convenience of the process. Much valuable and unexpected information was obtained in this way during World War II.

One measurement that is completely standardized is the determination of the firing interval. This is effectively the time from the (external) act of ignition to the emergence of the shot from the muzzle. This time interval is greater than the time required to ignite the charge by the time of travel of the shot down the bore. This latter time is roughly (travel)/(half the muzzle velocity) and is almost constant from round to round. The much larger variations in the firing interval are therefore a measure of the irregularities of ignition. In this way has been accumulated a mass of empirical results about ignition, with at present almost no theory to tie them together.

The measurement of the position of the projectile in the bore at any instant is far from being a routine matter. One way is to bore the gun walls at certain points, inserting insulated probes, which are short-circuited to the barrel by the passing projectile. This is a laborious method, and it gives only the times at which certain discrete points are passed. Moreover the recording of a number of positions on a single round requires either a multichannel oscillograph or an automatic high-speed switching device. Partial results from a number of rounds can be collected on simpler apparatus, but in many cases this would raise the problem of the reproducibility of the ballistics.

In small arms it is possible to take a flash radiograph of the barrel at a known time from ignition. This method gives less information per round than the former. Its principal advantage is the absence of any modification of the gun.

A question the importance of which will become obvious in later chapters is the resistance to motion of the shot down the bore. Experiments to determine this "bore resistance" have been conducted many times, usually on small arms. In some cases this choice may have been necessary for reasons of economy, though the effect is indeed believed to be most prominent in small arms. Unfortunately the time scale of the phenomena is shortest in such weapons, and it was not until recent years that the natural frequency of the recording systems became sufficiently high to give useful results. A full review of the work done in this field would be out of place here, being much too long; a review of the prewar literature can be found in a paper by Bodlien.[5]

All the methods are really the measurement of the acceleration of a body acted on by the bore resistance, together with measurements of all other forces acting on that body. It is easiest to take the gun barrel itself as the moving body. The forces acting on it are (1) the thrust of the recoil system, which if appreciable at the start of recoil can be measured by a pressure gage; (2) the pressure on the breech face, obtained from a piezo gage; (3) the pressure where the chamber narrows to form the seating for the shot—this pressure can be estimated by approximate theories of the pressure distribution in the gun (chapter 9) but is better eliminated by using a chamber of little more than bore diameter, if one is allowed to design a special apparatus; (4) the bore resistance. The acceleration of the gun can be determined from a piezoelectric accelerometer. The bore resistance then follows as the difference of two large and nearly equal forces. For this reason it is not sufficient to find the acceleration by double differentiation of a recoil-time record. Numerical differentiation is at best a relatively inaccurate process, and two stages make the calculated acceleration extremely sensitive to the values read from the recoil curve. Another method, which is not so objectionable, is to measure the recoil velocity directly and differentiate this. Nevertheless the use of the accelerometer is today the best method.

---

[5] Bodlien, *Z. ges. Schiess- u. Sprengstoffw.*, **34** (1939), 33, 65, 97.

The development of piezo gages sufficiently robust to be put in the projectile has made possible the use of the shot itself as the reference body. The forces acting are (1) the bore resistance and (2) the pressure at the base of the shot. A piezo accelerometer and a piezo gage exposed to the base pressure are carried in the projectile. The circuit is made via barrel and shot and is completed by insulated leads running from the muzzle down the axis of the gun. When the shot moves, the shattered pieces of wire are caught in a cup in the projectile. This method has been used in the United States and Germany[6] and gives not only the bore resistance but also equally valuable information about the relation between the pressure at the shot and that at the breech. It should be mentioned that it is possible to mount a single piezo gage in the projectile to give a direct reading of the bore resistance. The main difficulty in these experiments is the ionization of the propellant gases escaping past the shot and the spurious signals produced thereby.

Conditions at the muzzle of the gun can be studied by interferometry or by schlieren or silhouette photography. The light source has in the past been usually a spark. Recently there has been much improvement in light sources for this purpose, as can be seen from the performance of the flash sources developed for ballistic work and now available commercially.

Gun smoke has in the past been assessed by the verdict of "experienced observers." These instruments are not easily prepared, and their assessments are not in good agreement. Consequently, this situation has led to the construction of smoke meters, often based on the obscuration of a standard pattern, as seen by a cinecamera. These methods have reduced the observational uncertainty but have also demonstrated the real sensitivity of the phenomenon to such factors as direction and strength of wind and relative humidity. It must be concluded that assessment of smoke is possible only in relation to standard control rounds fired on the same occasion.

The recoil velocity of a gun is at most of the order of 30 ft/sec, and a space-time record can be obtained by simple apparatus. The Sébert velocimeter (1881) has a smoked steel tape, moving with the barrel, and marked by a tuning fork of known frequency, mounted on a non-recoiling part. This instrument was for many years the only means of obtaining a pressure-time record for a gun. The pressure, obtained by double differentiation of the space-time curve, was naturally of low accuracy, by any standards. This led to a virtual disregard of its results by about 1910, though for guns no substitute appeared until twenty years later. Where recoil is absent (closed vessels and small arms), the recording crusher gage and the mechanical spring gage were of course used. In spite of this limitation the Sébert velocimeter has great historical importance, and the theoretical work[7] based on its results had considerable influence on the development of interior ballistics.

---

[6] Rossmann, *Jahrb. deut. Akad. LFF*, **1940/41.**

Except that recording is nowadays by electric contacts spaced along an insulating rod recoiling with the barrel, the measurement of recoil distance has not changed. Direct readings of recoil velocity have recently been made by turning this into an angular velocity and thence into an induced voltage. This is more accurate than the differentiation of a space-time curve.

The ballistic pendulum is another instrument of historical importance, which is still used somewhat, though not for its original purpose. Its earliest applications were to the measurement of muzzle velocity, in interior ballistics, and to the estimation of air resistance, in exterior ballistics. Recently the ballistic pendulum has been used to determine the influence of a muzzle brake on recoil momentum; the gun on a cradle, slung by wire ropes several feet long, is itself the mass whose swing measures the momentum. When "recoilless" guns (chapter 7) have their recoil adjusted to zero, this is best done by firing in a ballistic pendulum. The largest gun tested in this way seems to have been a German 28-cm gun.

1.3 The classical problem of interior ballistics

For many years the field of theoretical interior ballistics was almost confined to a single problem: given the characteristics of shot, charge, and gun, to calculate the muzzle velocity and peak pressure. The problem was first taken in this form when both velocity and peak pressure could at last be measured, that is, from about 1860 onward. Before that time, pressure could be measured only in crude and dubious ways, and the measurement of muzzle velocity itself goes back only one century more (Robins, 1740).[8] Thus it happens that what we now regard as the central problem of interior ballistics has a history that goes back no further than the middle of the last century, though, if only muzzle velocities are in question, the history of the problem begins with Robins.

Making the shot infinitely heavy, we arrive at the problem of the "closed vessel." This apparatus first became important when Noble used his crusher gage in it to measure peak pressures; it became still more useful after Vieille's invention, about 1880, of the recording crusher gage. Since that time, it has been important in both theory and practice. For many years the "characteristics of the charge" used in the theory were derived by analysis of firings in other guns, including as a particular case the firings in closed vessels. These were for almost fifty years distinguished by the fact that pressure-time curves could be obtained in closed vessels but not in any other weapon (except small arms, whose ballistics are not in all respects representative of larger calibers). The difficulty was the disturbance of the recording by the recoil of the gun. Thus until 1930 the central problem of interior ballistics was in effect: given the characteristics of shot and gun and a knowledge of the behavior of the charge in a closed vessel, predict muzzle velocity and peak pressure.

---

[7] Sébert and Hugoniot, *Étude des effets de la poudre* (Paris, 1882).

[8] For the history of the measurement of pressure and velocity, see Cranz, *Ballistik*, vol. 3 (Berlin, 1927).

From about 1930 onward the problem was rapidly transformed. The cause was the perfection of the piezoelectric pressure gage. First suggested by Sir J. J. Thomson during the war of 1914–18, the development cannot be said to have been completed until roughly 1935. Piezo gages of fair performance had been produced before this date, but they showed defects in reliability, calibration, and especially in spurious effects on the record. Published results up to 1935 were certainly mediocre, but the knowledge that accurate pressure-time curves would soon be obtained in guns had already had its effect on the theoretical outlook.

In the first place, the pre-eminence of the closed vessel vanished. Pressure-time records could be obtained even from recoiling gun barrels. The closed vessel becoming just another gun, it was natural to wish to "explain" gun behavior from some deeper source than closed-vessel data. This had already been attempted in some directions; for instance, the rate of burning used to be taken from the closed vessel, but during the 1920's attempts began to be made toward a calculation of the rate from chemical kinetics. This tendency to connect interior ballistics with modern physics and physical chemistry is the main trend in ballistics today. In the author's opinion, the change is bound to refresh the subject. Nowadays the behavior of a gun is to be calculated, in the last analysis, from such data as Planck's constant and the mass of the electron.

Second, the advent of pressure-time records meant that theory had to concern itself more with the whole course of the phenomena in time, instead of concentrating on a few salient features. It is true that the pressure-time curve had often been discussed in theory, but this was speculation without a check, except to the extent that the special features such as peak pressure had to be correct. Nowadays we ask for all the details of the pressure-time relation. This means more work for each complete solution. However, it is pleasing to feel that one is approaching reality, and the more routine work can still be done by methods that are quicker because they lean more on past experience.

This transformation of interior ballistics may be compared with the revolution in exterior ballistics after 1914. Before that time only one point on a trajectory had any interest: the point of fall on the horizontal plane. The need for anti-aircraft fire arose in 1914. This meant that a shell might be required to burst at any time along a calculated trajectory, which therefore had to be correct at every point and not just at the point of fall. This led, as is well known, to a great development of ballistic theory on the one hand and to much more wearisome computations on the other.

Interior ballistics, likewise, is passing through a period in which its scope is being widened. The central problem is still the same, but more detail is asked for, and the matter is taken deeper into its foundations in pure science. Many accepted features of ballistics are being re-examined (for example, the "covolume," as in chapter 3), and new quantities are being measured (for example, gas temperatures are now within experimental reach).

1.4 The future of interior ballistics

The solution of the classical problem is today largely completed. The problem in which there is a substantial resistance to motion of the shot is the only division in which considerable advances are still to be expected.

The classical central problem has also been discussed for the newer and still unorthodox types of gun, such as the recoilless gun (chapter 7) and the "high-low pressure" gun (chapter 8). Other novelties will no doubt arise. Most of these types can be seen as generalizations of the orthodox gun. A striking feature of recent developments is the appearance of rocket launchers, which are all but guns, and of guns which can be discussed approximately by the concepts of rocket theory. It seems likely that a union of gun and rocket theory will occur, covering in one style of treatment the many new weapons. The present theories of gun and rocket do not have much in common, and so the generalization would not be simple, nor, for that matter, would it necessarily help our understanding of these extreme cases. It is the development of the half-and-half weapons that makes the attempt worth while.

If we turn away from the central problem, which was for so long the only one to attract attention, we find many interesting and little-touched fields. A whole set of hydrodynamic problems remain. For the orthodox gun, only two variables are involved: time, and distance down the gun. When the barrel is tapered internally (see § 8.4) one more variable is introduced into the equations. The new phenomena that this can introduce were experienced in development work during World War II. Time was then lacking to study the theory, which appears to have links with several other fields. The basic connection is that the shot velocity can be greater than the local velocity of sound in the gas, and the hydrodynamics can be those of subsonic or mixed subsonic-supersonic fields. In this way we can relate ballistic phenomena to transient phenomena in certain nozzles and diffusers. It is certain that the hydrodynamics of interior ballistics is capable of much development.

The theory of the optimum ballistic parameters of a gun and charge is well understood (see chapter 6), and relatively little remains to be done in this field. More fruitful is likely to be the physical chemistry of gun propellants. This is touched on in chapter 2, which illustrates the kind of problem that arises. The thermodynamic properties of propellants have been predicted from statistical mechanics (chapter 3), and very little remains to be done on the thermodynamic side of ballistics.

The plastic properties of present-day conventional gun propellants are understood fairly well from the empirical knowledge of many years, but the development of newer types will be slow unless the latest methods of high-polymer theory are applied. Propellants are not extremely complicated systems, and it is possible that much of the fundamental research on high polymers could be carried out on propellants themselves, where the empirical background is more extensive than for most high-polymer systems. Indeed, much of the work on swelling and gelatinization of solids has been carried out with nitrocellulose.

One of the most important of the chemical problems is the study of ignition. This has been tackled in the past by empirical methods, with only the beginnings of a theory to help. This approach has developed certain standard layouts of ignition system which have been thought to be generally satisfactory. Confidence in these methods has been shaken lately; experience has shown that they are satisfactory only for a more restricted class of charges than had been thought, while the need to consider temperatures lower than in previous experience has revealed unsuspected troubles. The more general use of the piezo gage has also shown that certain sporadic troubles can be correlated with irregular pressure-time curves on *every* round of the charge concerned. This has raised a problem of hydrodynamics as well as of chemistry. This particular difficulty has been solved by experimental methods, but it serves to show that there is much to be discovered about ignition.

Unorthodox guns are also setting new problems, often in a most violent and expensive way. The whole subject is ripe for theoretical development.

To sum up what we see as the future of interior ballistics: the classical central problem is not likely to be developed much further, except for (1) new types of projector, and (2) substantial resistance to motion of the shot; some generalization of the problem is, however, likely to be attained. The thermochemistry of ballistics is all but completed. Chemical problems set by the burning and ignition of solid and liquid propellants are capable of much development; so too is the study of plasticized polymers, both from a macro- and a microscopic viewpoint. The hydrodynamics of the gun is a field in which the problems are interesting and not insoluble.

1.5 The history of the classical problem of interior ballistics

As we have indicated in § 1.3, the classical central problem is the calculation of muzzle velocity and peak pressure for a gun with a given charge. We have indicated that this is no longer one of the more active problems of interior ballistics. Nevertheless, it is still of the greatest practical importance and covers four chapters of this book. We are now going to outline the history of this problem as an introduction to our later discussion of modern methods.

In the earliest days ballistics was not divided into exterior and interior ballistics, for the muzzle velocity was not known. All that could be said was that a certain weight of powder and a given shot in a certain gun at a given angle of elevation produced a certain range. Theories of the trajectory could be used to estimate the muzzle velocity, but the values obtained had little certainty, and there was no serious attempt to relate them to the details of the charge.

The first method of measuring velocity that was at all reliable in the crude state of early technique was the ballistic pendulum, suggested by Cassini (1707) and first used by Robins (1740) for small shot.[9] In Robins' work we see the first division into interior and exterior ballistics and astonishing progress in all aspects of gunnery. Toward the end of the eighteenth century larger pendulums were built, capable of measuring the velocities of cannon balls. Considerable improvements were made by the French (Commission of Metz) in the first part of the next century, and reliable empirical knowledge about muzzle velocities began to accumulate.

The first attack on the classical problem was purely empirical. Formulas were sought, relating velocity to weights of shot and charge and

[9] Robins, *New Principles of Gunnery*, 2d ed. (1742).

gun dimensions. This treatment was repeated again and again by various ballisticians,[10] using more reliable and more extensive data, but without essential modification.

The first reliable measurements of peak pressure in guns were obtained from Noble's crusher gage (1860). Henceforward the classical problem was clearly defined. The effect on the empirical treatments was to stimulate interest in the pressure-space relation. Forms for the pressure-time or pressure-space relation were assumed, and the parameters were determined from the observed muzzle velocity and peak pressure. This gave, it was hoped, the pressure-space relation in a gun that had been fired. When the gun existed only on paper, the only difference was that the velocity and peak pressure were obtained from empirical rules. Treatments of this nature can be traced as far back as Poisson (1826), when they were merely uncontrolled speculation, but they are especially associated with the names of Vallier,[11] Heydenreich,[12] and Leduc. The only "theory" involved is a little integration of Newton's equation of motion.

Such methods could be tested, at that time, only by double differentiation of the recoil-time record. This was very inaccurate. Nowadays one can use a piezo gage to record directly and accurately the pressure as a function of time. This has shown the wide variety of shapes taken by the pressure-time curves under different conditions. One is led to expect that such methods as those of Heydenreich and Leduc can work only over a limited range of conditions, as a way of interpolating between nearly identical guns and charges. As it happens, the only present-day applications known to the writer occur in two gun-design establishments,[13] each of which is noted for the ballistic similarity of most of its guns and its liking for one particular density of loading of charge.

Another approach to the classical problem attempts to write down all the underlying equations. This line was opened in the 1860's, notably by Résal's enunciation [14] of the energy equation for the shot and the propellant gases, followed by Sarrau's introduction of the equation of combustion.[15] Thereafter came a continuous development, especially by Sébert and Hugoniot,[16] and Liouville.[17] Without entering into details,[18] the general trend may be explained. First, the burning of gunpowder gave rise to a wide variety of assumptions, which were difficult to test because of (1) the low accuracy of the only method available for finding the pressure-time curves in guns, namely, the recoil velocimeter, and (2) the wide variation between individual grains of powder. With the introduction of colloidal propellant of more easily controlled shape and size, and the invention of the recording crusher gage for finding pressure-time curves in closed vessels, much of the difficulty disappeared and the formulation of the burning equations became more standardized, though the details still showed a wide variety.

---

[10] Such as Hélie, *Balistique expérimentale* (Paris, 1865).

[11] Vallier, *Comp. rend.*, **128** (1899), 1305; **129** (1899), 258; *Mém. poudres*, **11** (1902), 129.

[12] Heydenreich, *Kriegstech. Z.*, **3** (1900), 287, 334; **4** (1901), 292; *Lehre vom Schusz*, vol. II (Berlin, 1908).

[13] The Heydenreich method was used by Rheinmetall until 1945. Leduc's method was in use by the U. S. Navy as late as 1942.

[14] Résal, *Recherches sur le mouvement des projectiles dans les armes à feu* (Paris, 1864).

[15] Sarrau, *Les effets de la poudre dans les armes* (Paris, 1876).

As time went on, more phenomena were included in the equations, and a better understanding was obtained of the points that can be neglected in producing approximate equations at various levels of accuracy. Since by this time, toward the end of the nineteenth century, projectiles were spun in the present fashion by a driving band which was engraved by the rifling of the gun, the point that gave rise to most variety was the resistance to motion of the shot. This is still true today.

The earliest solutions of the ballistic equations were analytical solutions,[19] so complicated that they were rarely used in practice, or else exact solutions of approximations to the true equations. This latter class may be said to begin with the work of Moisson [20] (1887), and by refinement of the approximations this class has led to the ballistic methods that are most used in practice. A typical method of this sort is given in chapter 4.

The analytical solution of the (nearly) exact equations in a convenient fashion was first achieved by Charbonnier.[21] His work has been followed, in spirit though not in details, by later analytical solutions. Compared with earlier analytical solutions, the essential differences of Charbonnier's work are: (1) by breaking away from the tradition that the burning law was a geometrical property of the individual sticks of propellant, he was at liberty to make full use of closed-vessel data; (2) he showed that an analytical solution of practical value could be obtained by making certain convenient assumptions, solving exactly the resulting equations, and calculating the effect of his approximations as small perturbations; (3) in particular, he was the first to incorporate the "shot-start pressure," idealizing the initial resistance, in an analytical solution. His work is probably the clearest expression of the division of the problem into primary and secondary ballistic problems.

---

[16] Sébert and Hugoniot, *Étude des effets de la poudre* (Paris, 1882).

[17] Liouville, *Mém. poudres*, **8** (1895), 25.

[18] See Cranz, *Ballistik*, vol. 2 (Berlin, 1926).

[19] Such as those of Sébert and Hugoniot, and Liouville (*loc. cit. ante*).

[20] Moisson, *Pyrodynamique* (Paris, 1887).

[21] Charbonnier, *Balistique intérieure* (Paris, 1908).

In the earliest days, Sarrau[22] had noticed that certain parameters occurred only in association in his approximate analytical solution. This point was developed by Gossot and Liouville[23] in the following way. Writing down the ballistic equations on certain assumptions which they thought plausible, they combined the parameters in these equations to obtain a set of equations in reduced variables. To illustrate, one might replace the shot travel in the ballistic equations by the travel divided by the caliber, or by the ratio of the volume swept out by the shot to the volume of the chamber. Thus, Gossot and Liouville arrived at a set of equations between dimensionless variables, in which the properties of gun, projectile, and charge appeared only in combination in the parameters of the equations. Instead of trying to solve these equations mathematically, they used the data provided by firing trials. The muzzle velocity, for example, is a function of the "reduced" shot travel and the parameters in the "reduced" ballistic equations. Each firing gives one point of the functional relation. Gossot and Liouville fitted mathematical formulas to these empirical results, arriving at a set of formulas that are suitable for interpolation between existing guns but are of doubtful value for extrapolation to entirely different types.

It can be seen that the Gossot-Liouville method treats the empirical data in a much more sophisticated way than the earlier, purely empirical formulas. The Gossot-Liouville solution obtains a much wider generality from a given quantity of data. On the other hand, certain assumptions have to be made, such as the relation between the rate of burning and pressure, and if these are wrong the predictions of the method will be somewhat wrong; if we have several firings with nearly the same reduced parameters, the effect of an error in the basic assumptions is a discordance in the empirical results. In this way the method is adjusted for best fit. The labor of fitting may be considerable. The final formulas are, however, easy to use. As with all empirical methods, the Gossot-Liouville method and its successors (for example, the Dupuis tables) are only a synopsis of past experience and may be unreliable when applied to novel guns.

The similarity used by Gossot and Liouville was extended by Emery (1912),[24] who studied in a more detailed way the correspondence that can exist among pressure, velocity, space, and time relations in different guns. This similarity arises from the structure of the ballistic equations and, it must be pointed out, not merely from dimensional analysis. Thus, the nature of the correspondence depends on the physical assumptions and the mathematical approximations made. A fuller discussion is given in chapter 6.

---

[22] Sarrau, *Recherches théoriques sur le chargement des bouches à feu* (Paris, 1882).

[23] Gossot and Liouville, *Mém. poudres*, **13** (1905), 1; **17** (1913), 1; *Balistique intérieure* (Paris, 1922) or *Traité des effets des explosifs* (1919).

[24] See Emery, *Mém. artillerie franç.*, **2** (1923), 21.

A new kind of similarity was discovered by Röggla [25] in 1914. Previously the correspondence had referred only to charges with the same shape of propellant. Röggla was able to show that a certain relation existed between pressure-space curves even for different shapes of propellant, though the similitude held for only part of the curve.

Although in general an analytical solution of a mathematical problem is far more useful than a numerical solution, in ballistics it is difficult to obtain an exact solution except by disregarding certain factors. This is usually justified by the remark that, since so much is doubtful about the phenomena in a gun, some conscious simplification is permissible. Sometimes writers have thought that they knew so much about the phenomena that it would be a pity to throw away some of their knowledge for the sake of an analytical solution. They have therefore made numerical solutions of the equations. Usually the results have been presented in reduced variables to cut down their bulk. Such "grids" of solutions have been prepared by Charbonnier and Sugot (for the strip propellant used in France) and by Bennett for American charges of multitubular chopped grains. Furthermore, numerical solutions have sometimes been given as graphs in reduced variables, as by Röggla.[26] The production of numerical tables is likely to be the form adopted for most future work on the central problem of interior ballistics. The reason is not that we are so sure we now know all about ballistics, but, rather, that the time and expense needed to construct a grid of numerical solutions is much less than when the Charbonnier-Sugot and Bennett tables were made. Desk calculating machines are now universal; also the differential analyzer and various high-speed computing machines can mass-produce solutions at a reasonable cost, though the initial outlay is large. In England, National accounting machines have been used for such integration, as well as for their normal role of differencing the final tables; although the model of the National used has only 6 registers and multiplication has to be done on a separate desk calculator, the machine is reasonably fast in most ballistic applications.

[25] Röggla, *Mitt. Gegenstände d. Artill. u. Genie-wesens,* **45** (1914), 1, 149.

[26] Röggla, *Neue Diagramme für die angewandte innere Ballistik* (Pilsen, 1931).

Of the various lines of attack on the central ballistic problem, only the purely empirical is not illustrated in this book. For the semi-empirical approach via the theory of ballistic similarity, we may refer to chapter 6. Exact analytical solutions of nearly exact equations are given in the first part of chapter 5. An example of an exact analytical solution of heavily simplified equations is discussed in chapter 4. A table of numerical solutions is given in chapter 8.

CHAPTER TWO Gun Propellants

2.1 Propellant compositions

From the earliest days of firearms down to the 1880's, the energy was supplied by black powder. This was a mixture of potassium nitrate, charcoal, and sulphur, whose composition became stabilized at about 75:15:10 parts by weight. By the seventeenth century the fine powder had been replaced by small grains. The rate of burning depended on the degree of compactness and on the average particle size. By "burning" we mean, as usual in interior ballistics, an exothermic decomposition in the absence of air. Just before its eclipse, the ballistic properties of gunpowder were greatly improved by the invention of more strongly compressed grains of definite shape and size; these could be produced in sizes matched to particular guns.

Nitrocellulose[1] was discovered in 1845 by Schönbein. Prepared by nitration of cellulose, the product retained the porous nature of the latter. Burning could be set up, but it passed over into detonation (10^5 times as fast a decomposition), in an uncontrollable fashion. Not until the 1880's was it found that the physical macrostructure of nitrocellulose could be changed by swelling it in a solvent such as alcohol and ether, squeezing the putty-like mass through a die to give long strips, cords, or tubes, and then removing the solvent by hot air. The product was smooth and rather brittle. It could be ignited in a gun by a small quantity of black powder, and burning proceeded smoothly from the outer to the inner layers without evidence of detonation under normal conditions. The new form of nitrocellulose had many advantages over gunpowder. The charge weight needed for a given muzzle energy was divided by 2 to 3, there was far less smoke, and the pressing operation allowed the shape and size of the propellant to be chosen to suit a particular gun. Once the proper solvents had been mastered, the extent of the nitration could be varied (between about 11½ and 13½% N) to give propellants with different properties in respect to erosiveness, specific energy, and smoke. Finally, small amounts of stabilizer could be incorporated, giving a storage life of many years in temperate climates, and the nitrocellulose "powder" was less sensitive to moisture than gunpowder had been, and far less sensitive to shock and friction.

---

[1] Usually abbreviated to NC.

It was soon discovered that not all the swelling need be done by an extractable solvent. It was found that nitroglycerine[2] and nitrocellulose could be taken up by their common solvent, acetone, and only the acetone extracted after pressing. This gave greater control over the properties of the product and, if desired, greater specific energy, a quality prized in the early days. For example, the first British standard smokeless propellant was Mk I, a 40/60 nitrocellulose-nitroglycerine composition of high specific energy, very hot products, and an erosive power first appreciated in the South African war. Extruded as long cords, cut to the length of the gun chamber, it was called "cordite"; the name survived for many years and was used for all gelatinized propellants, no matter what their shape. This was no more misleading than calling them *Pulver* or "cannon powder"; however, the word "propellant" is now favored.

The unit of propellant is usually called a "grain," where it is not desired to imply any special shape such as a cord or a ribbon.

The conversion of nitrocellulose into a gun propellant had been in men's minds for forty years before it was achieved, and there had been several close approaches to the solution. It is not surprising that there has been some controversy about priority. The discovery is usually credited to Vieille (1886), but many German writers claim priority for Duttenhofer. The period was marked in England by a famous lawsuit over patents.

The time and expense involved in putting solvent into propellant and then taking it out again was made obvious in the First World War. In 1912 the Germans had in fact made an important advance,[3] which was disclosed at the end of the war. Within a few years most nations were producing "solventless" cordites[4] as part of their normal output. A typical composition is 40:50:10 parts by weight of nitroglycerine, nitrocellulose (12% N), and carbamite (ethyl centralite). Easy gelatinization with this solvent is helped by the relatively low nitration of the cellulose. The solvent here is nitroglycerine-carbamite, which is a better one than either of the separate components. The carbamite also acts as a stabilizer, by removing the products of decomposition of the propellant, which otherwise have an autocatalytic effect. This is, of course, the function of the stabilizer in solvent as well as solventless cordites, and a wide range of organic compounds can be used for this purpose. The carbamite here also serves to reduce the temperature of the propellant gases.

---

[2] Usually abbreviated to NG.

[3] Muraour, *Mém. artillerie franç.*, **2** (1923), 503.

[4] German: POL = *Pulver ohne Lösungsmittel;* French: SD = *sans dissolvant;* British: SC = solventless cordite.

Solventless cordites are almost essential for rockets, where the web is usually measured in inches; the time to dry out solvent from the interior of such a grain would be far too long to be acceptable.

Just before the Second World War the Germans introduced diethylene glycol dinitrate (DEGN) in place of nitroglycerine in much of their propellant production. The new *G-Pulver* was derived from indigenous sources, none of which were foodstuffs. This was the main aim,[5] but it is not to be assumed that this was the sole advantage. It is possible, for example, to reach lower gas temperatures in this way. Another constituent favored lately has been nitroguanidine, used, for example, by the Germans in "Gudol," a solventless cordite of nitrocellulose, nitroguanidine, DEGN, and stabilizer, the main constituents being in the ratio of roughly 40:30:30.

The question of the best constituents for a propellant has been investigated more thoroughly in the last few years. There are two possible approaches. One is to try various substances in propellants, learning how to handle and incorporate them in the gel and finally evaluating the product by closed-vessel tests. The other method has been taken up more recently, especially by Dr. Laidler in Canada. In this the thermochemical behavior is worked out theoretically for any assumed composition and the best compositions chosen; for example, the best of a series of coolants can be picked out. The best constituents being known, an attempt is made to turn these into a propellant. This is always a difficult and not always a possible task, and so it is encouraging to know that the effort is being centered on a composition which, if it can be made to burn regularly, will have very good ballistic properties. Experience has shown that the step from thermochemical calculations to approval as a standard-production propellant is difficult and long.

2.2 The arrangement of the propellant charge

It is desirable to know a little about the form of a propellant charge and its arrangement in the gun. There is a great deal of scope for ingenuity in the arrangement, particularly for howitzer charges. Here the different charges must have acceptable regularity and be easily changed without possibility of accidental overcharging, and the layout must be sufficiently rigid not to be disturbed by rough usage. The technical tricks which help to solve these problems have not, so far as the author knows, been published, nor are they essential here. Only a sketch of the general arrangement need be given.

---

[5] An interesting account of the development has been given by Gallwitz, the man chiefly responsible, in *Die Geschützladung* (Berlin, 1944). *G-Pulver* was named after Gallwitz.

Guns are classified by the method of sealing the propellant gases. In a BL gun this obturation is performed by some device in the breech mechanism, such as a pad or ring; in a QF gun the obturation is provided by the cartridge case. The names BL and QF were originally abbreviations of "bag loading" and "quick firing," but these terms no longer cover all the classes denoted by BL and QF. It is to be noted that, when a cartridge case is used, the shot can be either held in the mouth of the case (fixed ammunition) or loaded into the gun before the cartridge (separate-loading ammunition). Furthermore, the fact that a cartridge case is used is no guarantee that the gun is a QF type. There is at least one class of gun that uses a cartridge case but provides the gas sealing by a device built into the breech. This must be classified as a BL type.

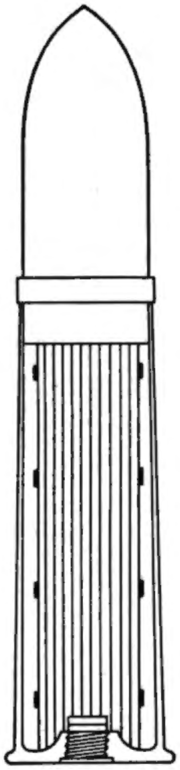

FIG. 2.1 Typical round of fixed ammunition for a QF gun, with stick propellant held in a rigid bundle by silk ties, the sticks extending the full length of the cartridge case from primer to shot base.

Figure 2.1 shows a typical arrangement of charge in a QF gun firing fixed ammunition. The propellant is cut to fit the whole length available, from shot base to primer. The propellant is therefore "made to measure." Fixed ammunition almost invariably implies that we are making full use of the capabilities of the gun, and that the charge is therefore sufficiently bulky to fill the chamber. Indeed, the difficulty is often to load into the case all the charge desired. This has led to the use of granular propellant in which the length of the pieces is of the same order as their other dimensions. American multitubular propellant is an example. Such granular propellant is easily loaded by pouring and makes full use of the available space, even in strongly necked cartridge cases. A graphite glaze is often used to reduce the risks from static electricity during the filling; the cynical insist that the graphite is really to improve the appearance of the propellant. Granular propellants are harder to ignite, probably because the gases and hot particles from the primer can reach only part of the charge surface.

QF separate-loading ammunition is used in certain large guns merely because the fixed round is inconveniently heavy and bulky. In such examples the arrangement is the same as in Fig. 2.1, except that the mouth of the case is closed by a cardboard or metal lid, which is consumed on firing. Separate loading is also used in howitzers, where, to get high accuracy at the target, the velocity is adjusted to keep the gun elevation near 45°. The number of separate charges used may be as many as ten. They are obtained by suitable choice from a number of component charges, each wrapped in a silk or cloth bag, and all carried in the cartridge case. The design of such charges needs a great deal of skill. A typical layout is shown in Fig. 2.2.

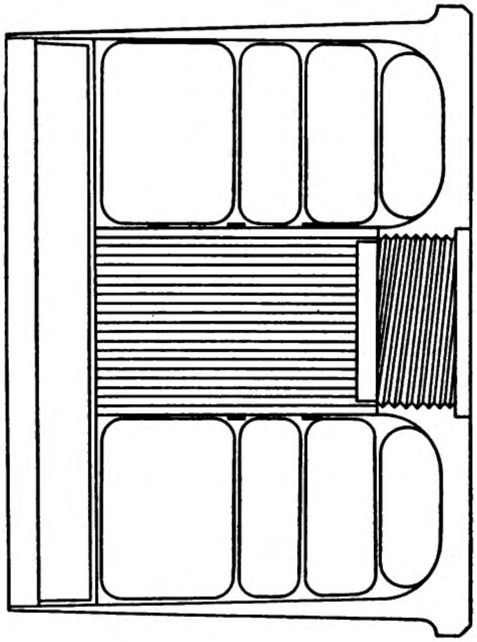

FIG. 2.2 Typical separate-loading cartridge for a QF gun. This is a relatively simple example, with four "doughnut" bags of propellant surrounding a rigid core of short sticks, sitting on the primer. The lid is of thin board or consumable metal.

In guns with long chambers it is often necessary to use supplementary igniters part way along the charge. In a really big gun a charge the full length of the chamber would be too long to handle, and so the charge is loaded in several bags, which together fill the length of the chamber. Auxiliary igniters are sewn on one or both ends of the bag. When we come to such details, the possible variety of designs becomes large, and nearly all of them could be illustrated by one or more examples from actual charges. This shows the difficulty of laying down any general rules about ignition. It can be said, however, that, when the ignition satisfies the proving ground, the matter can be omitted from any theoretical work.

In BL guns the gas and hot particles from the gunpowder igniter enter the chamber through a vent. This has the advantage that, in the event of a misfire, the main initiator can be replaced without opening the breech.

Granular propellant is not a happy choice for BL guns, since the charge lacks rigidity. Variations in the shape of the bag lying in the chamber have striking effects on the peak pressure, especially at densities of loading over 0.6 g/cc. Hence the use of "stacked" charges of multitubular propellant in bag-loaded guns. It would appear to be simpler to use long grains, of tubular or ribbon shape.

There has been little theoretical research on ignition of propellants. The early part of the pressure rise in guns is not known accurately, but it is not of much importance—the outstanding difficulty in this region is the nature of the initial motion of the shot. One obvious way to include the process of ignition is to introduce the fraction of surface burning at any instant. It is known from experiment that this is not a suitable technique and that the most promising approach would be on the lines of the theory of chain reactions. The field has been little explored, and a mass of disconnected empirical knowledge awaits a theoretical co-ordination.

With regard to the classical field, the main problem of interior ballistics, it is quite proper to neglect the process of ignition. For an igniting charge of gunpowder or fast-burning porous nitrocellulose (German: Nz Man P = *Nitrozellulose Manöver Pulver*), weighing rarely much more than 1 per cent of the main charge, is sufficient to give regular ignition, and its direct contributions to peak pressure and muzzle velocity are certainly less than 1 per cent. They may be neglected in present-day theory. For a range of weights of igniter, varying by a factor of the order of 2, the regularity of ballistics is substantially constant. It is in this range that one can, with some confidence, assume that all the propellant surface is ignited before the shot starts. This is the common assumption in theories of the central problem of ballistics.

For increasingly large igniters the peak pressure rises and the velocity tends to fall, while smoke increases. With very weak igniters the "firing interval" (between striker blow on the gun and emergence of the shot from the muzzle) increases and becomes irregular. The former indicates too small a reserve of igniting power. The irregularity of the firing interval is even more annoying in naval guns, whose firing is controlled from a roll indicator on the assumption of constant firing interval.

Gunpowder contains potassium nitrate, which helps to reduce "flash"; 1 or 2 per cent potassium nitrate or sulphate is often added to propellants to make them flashless. Big igniters are often sufficient to cure a not too violently flashing charge. The corollary is extra smoke, partly because of the hygroscopic potassium salts, and also because the explosion which gives the flash serves to dissipate smoke. Porous nitrocellulose, which was used as a main component in German ignition systems, has neither the hygroscopicity, the mechanical weakness, the smokiness, nor, on the other hand, the flash-reducing properties of black powder. A combination invented recently by the Germans is NSP, a blend of 75.8 per cent gunpowder, 24 per cent nitroglycerine and 0.2

per cent diphenylamine, which forms hard grains more resistant to rough usage than gunpowder grains, is only weakly hygroscopic, and is said to be a better igniter than gunpowder. A point that may become important is the reduction of the amount of sulphur in the charge. Sulphur reacts with the gun bore to give products that are thought to be easily eroded, and so the reduction of sulphur may be accounted a substantial virtue of nitrocellulose in ignition systems.

2.21 Propellant shapes and the geometrical form function

Consider a long cord of propellant, of initial diameter D, burning under a pressure P. Let the rate of recession of the propellant be uniform over the surface of the cord, and written as $\frac{1}{2}B(P)$. Let $C\phi(t)$ be the amount of gas generated up to time t, where C is the initial weight of the cord; ϕ therefore runs from 0 to 1. Let fD be the diameter of the cord remaining at time t.

Neglecting the small contribution from the burning of the ends of the cord, we have the *geometrical* relation,

$$\phi = 1 - f^2 \tag{1}$$

and the expression of our definition of the rate of burning:

$$D\frac{df}{dt} = -B(P) \tag{2}$$

f is found to be a convenient variable in the solution of the equations of interior ballistics, but, as it appears only in these two equations and not in the other fundamental equations, we may eliminate f, giving

$$\frac{d\phi}{dt} = \frac{2B}{D}(1 - \phi)^{\frac{1}{2}} \tag{3}$$

These equations are clearly true for any number of long cords.

The importance of the web size D in ballistics is analogous to the part played by the dimensions of the unit of fuel in a coal or wood fire. The influence of this on the rate of consumption of fuel, and especially on the rate of building up to a steady state, is familiar to everyone.

Analogous relations may be written down for other shapes. Consider, for example, long tubes of initial external and internal diameters d_1 and d_2, with

$$D = \tfrac{1}{2}(d_1 - d_2)$$

and fD as the annulus remaining at time t. Then the geometrical relation is

$$\phi = 1 - f \tag{4}$$

and the burning rate is still the same as in equation 2, leading to

$$\frac{d\phi}{dt} = \frac{B}{D} \tag{5}$$

This assumes that the rate of burning is the same on all surfaces of the propellant and that the inner and outer surfaces are coaxial.

Both shapes may be brought into the same scheme by choosing the dimension of the grain along a direction normal to the surface at two points of intersection where the direction is in one instance passing into and at the other passing out of the propellant; the smallest such dimension, *if one exists*, is called the web size D. Thus for cord, D is the diameter; for tube the diameter is the direction normal to the surface at two intersections (in fact, at four), and the smallest such dimension is the annulus, defined by

$$D = \tfrac{1}{2}(d_1 - d_2)$$

Next we define fD as the remaining web when a fraction ϕ of the propellant has been turned into gas. From the definition of the rate of burning,

$$D\frac{df}{dt} = -B(P) \tag{2}$$

For certain shapes, $\phi = 1$ when $f = 0$. For a still more restricted class of shapes, ϕ and f are related geometrically by

$$\phi = (1 - f)(1 + \theta f) \tag{6}$$

where θ is a constant for a given shape. For example, $\theta = 0$ for tubular sticks and $\theta = 1$ for long cords.

We shall use equations 2 and 6 again and again in this book, and so we must discuss the subject of how many of the shapes used in practice do obey our very special assumptions. It may be seen that we have defined D by reference to a direction which will not exist for a shape chosen at random. For shapes of fairly high symmetry D will have a meaning. The definition of f and equation 2 then follow without exception. There is, however, no guarantee that, when this dimension has been eaten away, all the solid propellant will have turned into gas; only for simple shapes does this occur. Finally, equation 6 is a very special form. We shall discuss the most common shapes, to illustrate the different possibilities.

With long cords and tubes there is no difficulty. The web is easily found, and equation 6 holds with $\theta = 1$ and 0, respectively. Equation 6 may be referred to as the "form function," with θ as the "form factor."

θ is a measure of the change in the area of the burning surface as burning proceeds: the burning surface of a long tube remains constant ($\theta = 0$); the area of a cord decreases to zero as the burning proceeds. The ratio of initial and final surfaces is $(1 + \theta)/(1 - \theta)$. Thus the larger θ, the faster the surface decreases, and the faster the drop in the rate of evolution of gas at constant pressure. Shapes of positive θ are said to be "degressive," those of negative θ to be "progressive." Shapes, such as tube, with $\theta = 0$, are sometimes said to be "neutral."

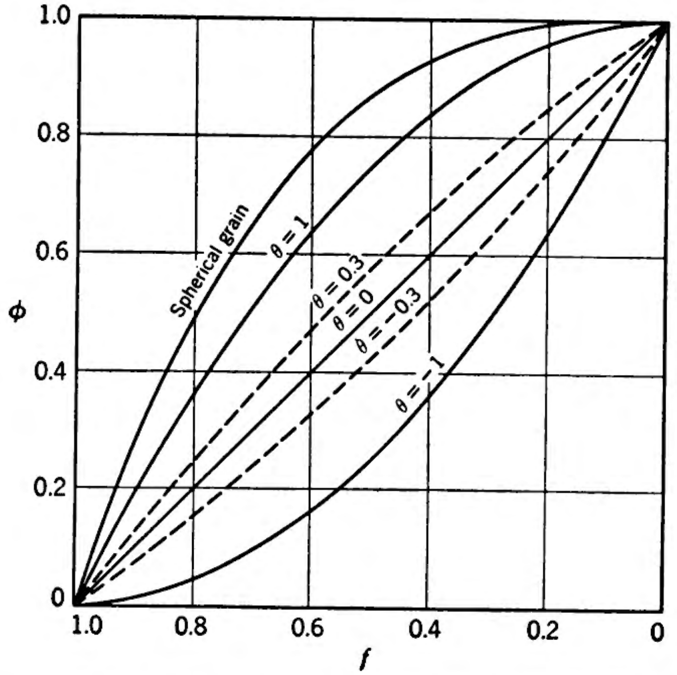

FIG. 2.3 Form functions with θ from -1 to 1, and the form function for spherical or cubical grains.

The possible range of θ is restricted. θ cannot be less than -1, for otherwise ϕ is negative for f near unity. Nor can θ be greater than unity for then ϕ would be greater than unity for some accessible range of f. This does not mean that cord, with its $\theta = 1$, is the most degressive shape possible. The sphere has a surface which decreases even more rapidly (see Fig. 2.3). In this case D comes out, by our prescription, as the diameter, and $\phi = 1$ when the remaining diameter is zero. It is not true, however, that equation 6 holds with any value of θ. The true geometrical form function is

$$\phi = 1 - f^3 \tag{7}$$

That equation 6 is not true for spheres or cubes is not a serious disadvantage. Such highly degressive shapes are but little used, except in shotguns. Cord chopped into short lengths is a near approach. This propellant is used sometimes in small arms and infantry mortars, weapons not usually given a serious theoretical study. Almost all shapes, including cubes, could be covered by writing ϕ as a cubic in f, but analytical solution of the ballistic equations is more difficult with a cubic than with a quadratic.

Between $\theta = 0$ (tube) and $\theta = 1$ (cord) lie a group of simple shapes, which have arisen as practical approximations to tubular propellant. Tube has the property that the internal perforations bring air into the the cartridge case rather than propellant. To load a desired large charge in a given chamber, one must sometimes reduce the perforation to a point at which the behavior of the whole charge becomes unsatisfactory. Occasional abnormally high pressures appear, often associated with an unusually low or even negative temperature coefficient of the peak pressure. These are believed to be due to the increased "erosion" of the wall of the perforation by the outflowing gas, with extra pressure building up inside the stick and a general tendency toward instability. The Germans, who used tubular propellant (RP = *Röhrenpulver*) for all but their howitzers, had a rule that the internal diameter should not normally be less than four thirds of the annulus. If absolutely necessary to reach a desired density of loading, the perforation was reduced further, with great caution.

Higher densities of loading can be attained by employing long thin strips, a form popular in France and used a little in Germany (Str P = *Streifenpulver*) and in England ("ribbon"). Strip has the further advantage that it needs no extrusion press. The strips are normally sufficiently long for the burning of this dimension to be negligible; the width of the ribbon is usually about ten times its thickness, which makes θ about 0.1. By reducing the length of the strip θ is increased; when the grain has become a thin square plate of side nD (British: "flake"; German: Bl P = *Blättchenpulver*) θ is $2/n$; n is usually about 5, and θ is then 0.4. As a special case, Continental secondary charges for mortar bombs are made from packets of horseshoe-shaped thin plates (*Ringpulver*), which are easily slipped on the tail shaft of the bomb. Flake propellant is often used in place of tube where the wall thickness of the latter would be so small that the grain would be fragile. Short tubes can be used in the same circumstances.

There is one popular shape for which a web size D exists, according to our definition, yet the charge is not all burnt for $f = 0$. Consider a long circular cylinder (Fig. 2.4) of radius R, pierced by two holes of radius a; their axes are parallel to the axis of the cylinder and lie a distance $(R + a)/3$ away from it, and all three axes lie in the same plane.

Then the web size is, by our definition, $(2R - 4a)/3$. As burning proceeds, the surface at first increases, so that the shape is progressive in this stage. When the shortest distance $(2R - 4a)/3$ has been burned through, f is zero by definition; yet it is obvious that two slivers of propellant remain. These burn with decreasing surface.

It is clear that

$$\phi = (1 - f)(1 + \theta f)$$

cannot be even a rough representation of the burning of this shape unless we modify the web size. Taking D as $\mu(2R - 4a)/3$, we may choose μ and θ to secure best over-all agreement with the accurate form function, which is easily calculated. μ will be rather greater than unity. Until the breakup of the shape, θ ought to be negative, and afterwards θ ought to be near unity. On balance, the best θ is slightly negative.

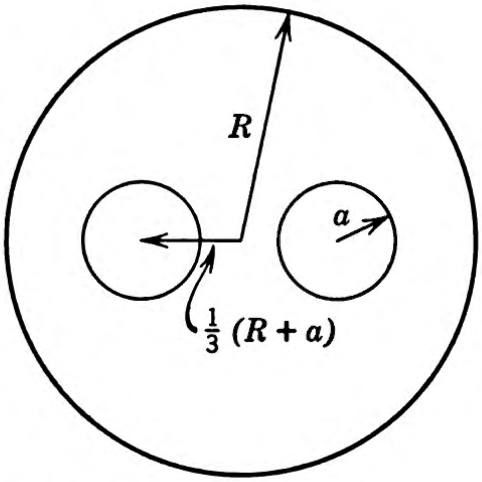

FIG. 2.4 Cross section of a twin-perforated cylindrical grain.

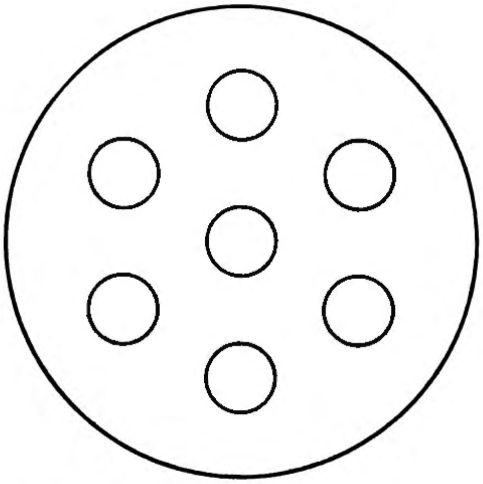

FIG. 2.5 Cross section of a seven-perforated grain.

Long twin-perforated tube has not been used, except as an experimental form in Britain in the first decade of this century, but it serves to explain how to deal with multitubular propellant. This has seven perforations, symmetrically arranged as in Fig. 2.5, and the grain is chopped short to help ignition and loading; a common shape has a length about 2½ times the diameter, or 25 times the diameter of the perforation. The effective web size is roughly 20 per cent greater than the least thickness, and, up to sliver point ($\phi = 0.85$), θ is about -0.2. Although the progressive effect of the seven perforations is rather counterbalanced by the degressive burning of the 12 slivers, still an average θ for the whole burning is slightly negative, of the order of -0.1.

Multitube is popular and, in fact, almost standard in the United States for cannon powder. Its use has spread to Russia, and it has been used to some extent in England. Although multitube has not been used much in Europe, in the recent war the Germans produced some experimental lots of 19-hole and 55-hole propellant for an 8-mm machine gun. In their search for a progressive charge they even made some blocks with 361 holes, whose performance seems to have been a disappointment. "Rosette" powder, which is multitube with scalloped exterior, was at one time used in the United States, in the hope that the elimination of the 6 outer slivers would make the propellant more progressive. It was tried again during World War II, and dropped when firings failed to show any advantage.

Inhibition of burning by coating certain surfaces of the propellant is an established technique in the design of rockets. Although it has not, to the writer's knowledge, been applied to gun propellants, except on the experimental scale, inhibition would make possible a negative θ. For example, a single-perforated tube with the external surface prevented from burning would have $\theta = -\frac{1}{3}$ if the internal diameter were half the external diameter. For a vanishingly thin perforation, $\theta = -1$.

2.22 The true form function

The form function was derived in the previous section from geometrical arguments. Whether propellants actually obey

$$D \frac{df}{dt} = -B(P) \tag{2}$$

$$\phi = (1 - f)(1 + \theta f) \tag{6}$$

is, however, a question of physics, not of geometry. The answer is found to be that equations 2 and 6 are nearly always a sufficiently good approximation, though f has no simple geometric meaning, and θ may have to be rather different from its "geometric value." Finally, the behavior in the gun is not the same as that in the closed vessel.

(*a*) *Burning in the closed vessel.* To begin, let us take those effects that are common to the gun and the closed vessel. We have assumed that the rate of burning is the same on all surfaces. Where perforations occur in the propellant grain, the gas passing out increases the rate of burning in the channel, an effect known as "erosion of the cordite." For a discussion of the mechanism, see § 2.41. The effect is most marked for cool propellants. The effect at any time depends on both the size of the perforation at that time and on the density; hence, the form function is not just a function of the grain shape but depends also on the density-time relation: that is, on the gun or closed vessel used. In practice, the result is to alter θ by an amount that can be as much as

0.2 in a pronounced case, depending on the grain shape, nature of the propellant, and peak pressure.

We have assumed that a propellant charge is composed of a number of grains, identical in shape, size, and rate of burning. A little examination with a micrometer shows that there are, in fact, considerable variations in size from stick to stick. When it is considered, also, that propellant compositions are merely nominal, in spite of being tabulated to 0.1 per cent, it can be expected that the rate of burning will also be variable from one grain to another. Records of the variation of size within a sample are made for each lot of propellant, but it is difficult to find any nondestructive test that will do the same for rates of burning. Dupuis and Chalvet[6] have graded part of one "lot" of solvent strip powder according to the web thickness, which before grading had a standard deviation of 3 per cent; this they say is about half that usually found for French solvent propellants. Samples with a close range of webs were then fired in a closed vessel. By analyzing the pressure-time curves, using the Dupuis theory[7] of the statistical distribution of the initial and final times of burning, it was deduced that these time intervals had a standard error of the order of 10 per cent. One can verify this by examining the variation of the mean rate of the samples fired and, hence, calculating an approximate standard deviation ($\sim$ 10 per cent) of the rates for single sticks.

Consider a charge of tubular propellant, with $\theta = 0$. If part of this charge has its rate of burning increased, the mean rate of burning of the charge is increased. The rate of evolution of gas, at constant pressure, drops when the faster tubes have been burnt but does not drop to zero until the slower part of the charge has been consumed. The charge has become degressive, and, if the behavior is represented by our standard form function,

$$\phi = (1 - f)(1 + \theta f)$$

the value of θ is positive. If part of the charge is made slower burning, rather than faster, the mean rate of burning falls, rather than rises, but θ increases in *both cases.* Any heterogeneity increases θ.

This is equally true if the heterogeneity is within the individual grain, instead of being a grain-to-grain variation. Dupuis and Chalvet (*loc. cit.*) have shown that the thickness of a ribbon of propellant varies from edge to center. This causes a spread of burning times between different parts of the surface of one and the same strip. Another common fault has been discussed by Kleider.[8] In dealing with tubular propellants, we have assumed that the inner and outer surfaces are coaxial, as, indeed, the manufacturer hopes they will be. Inspection of real tubes shows frequent deviations from coaxiality, amounting to a variation of web size around the tube. Kleider has calculated the geometric form function for a rather extreme case, in which the diameters are 1 and 0.6 and the axes are 0.1 unit apart. The rate of burning can be absorbed into the unit of time, and, since the rate is taken to be constant, the time is proportional to $1 - f$. In Fig. 2.6 are plotted his $\phi(t)$ curve, together with that computed from

---

[6] Dupuis and Chalvet, *Mém. artillerie franç.*, **18** (1939), 37.

[7] Dupuis, *ibid.*, **17** (1938), 799.

[8] Kleider, *Z. ges. Schiess- u. Sprengstoffw.*, **38** (1943), 131.

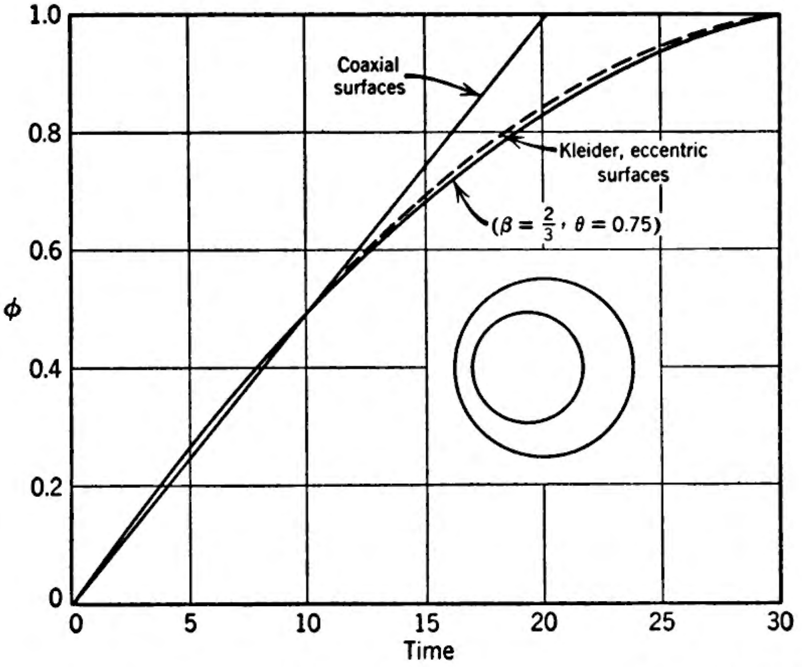

FIG. 2.6 ϕ as a function of time for tubular propellant burning at a constant rate. Kleider's result for eccentric surfaces refers to the cross section shown. An excellent approximation is obtained by the standard form function with two-thirds the normal rate of burning and $\theta = 0.75$.

$$\phi = (1 - f)(1 + \theta f)$$

$$D \frac{df}{dt} = -B$$

where D is the mean web, B is two thirds of the rate assumed by Kleider, and θ is 0.75. The curves agree to within 0.02 in ϕ at all times. This example has as large a deviation from coaxiality as could be expected. Even so, the increase of θ by 0.75 is striking. It is not unlikely that the form factor of real tubular propellant is raised by, say, 0.2 on this account.

θ is increased if there is delay in igniting any part of the surface. This is not likely to be important, except perhaps for chopped propellants at high densities of loading. A statistical analysis of the matter has been published by Dupuis.[9]

The quantity f was originally defined as the fraction remaining of the initial web size. It may now be seen to be the fraction remaining at one particular kind of place, namely, at points where D/B has the largest value attained sufficiently often to be of importance in the rate of evolution of gas. "Erosion" alters B differently at different points of the surface; the effect varies with time. Obscured by these refinements, f becomes just a convenient quantity, which splits up the burning law,

$$D\frac{d\phi}{dt} = B(P)[(1+\theta)^2 - 4\theta\phi]^{1/2} \tag{8}$$

into the mathematically more tractable set,

$$\left.\begin{aligned} \phi &= (1-f)(1+\theta f) \\ D\frac{df}{dt} &= -B(P) \end{aligned}\right\} \tag{9}$$

To sum up, the propellant burns in the closed vessel as if it has a θ, which may be 0.2 or 0.3 away from its geometrical value. The latter is almost always too low.

A word on the history of form functions may be inserted here. Piobert's law (1839), that the rate of burning is the same on all surfaces of a grain, was enunciated for gunpowder, for which it is probably untrue. After the discovery of gelatinized propellants in the 1880's, Piobert's law and the emphasis on the single propellant grain rather than on the assembly of grains led to an acceptance of the geometric form function. This was criticized by Gossot and Liouville[10] and in a still more iconoclastic manner by Charbonnier.[11] Throwing aside any geometric form, he relied on the closed vessel for the form function of a *complete* charge. Since the geometric approach gives

for cubes $$\frac{d\phi}{dt} = B(P)(1-\phi)^{2/3}$$

for cords $$\frac{d\phi}{dt} = B(P)(1-\phi)^{1/2}$$

---

[9] Dupuis, *Mém. artillerie franç.*, **17** (1938), 799.

[10] Gossot and Liouville, *Mém. artillerie marine* (1905), 122.

[11] Charbonnier, *ibid.* (1905), 591.

and for tubular propellant

$$\frac{d\phi}{dt} = B(P)(1 - \phi)^0$$

therefore Charbonnier took

$$\frac{d\phi}{dt} = B(P)(1 - \phi)^\beta$$

for nominally degressive or neutral shapes, and determined β and $B(P)$ from the closed-vessel record.

The two opposing points of view having been established, there had been little further development of ideas on the form function at the time Cranz [12] summarized the history to 1926. Since then the statistical theory of slightly heterogeneous charges has been advanced by Dupuis,[13] while "erosion" of propellant has been lately the subject of quantitative study, not yet published.

(*b*) *Burning in the gun.* The conditions of burning in a gun chamber are in one respect quite different from those in a closed vessel. In the latter, the gas streams out along the normals to the propellant surface, and, if the charge is not concentrated near one end of the vessel, the gas velocities parallel to the burning surface are nowhere large. On the other hand, it is shown in § 9.5 that in a gun the propellant moves with only a small fraction of the velocity of the shot at the same instant. The distribution of gas velocity along the bore at a given time is not known accurately for the period before the propellant has been completely burnt; it is usually assumed that the gas velocity is proportional to the distance from the breech. However, it can be said that the propellant burns in a gas stream moving parallel to its surface, with relative velocities of some hundreds of feet per second. This increases the rate of burning, an effect called "propellant erosion." This has been mentioned already, as operating in perforations of the propellant, in closed vessel and gun alike, but the application considered here is to all surfaces of the propellant; cord, for example, which has only external surface, is "eroded" in this way in the gun, and not in the closed vessel. In the gun, then, the propellant at first behaves as in a closed vessel, later showing a rate of burning greater than that found in the closed vessel at the same pressure. Near the end of burning, the effect may decrease again, since the gas velocity at the propellant increases but slowly *at this time,* while the propellant velocity rises rapidly—the relative velocity can therefore fall. Further, the very last stages of burning are marked by a decreasing burning surface.

---

[12] Cranz, *Ballistik,* vol. II (1926), p. 120.

[13] Dupuis, *Mém. artillerie franç.,* **17** (1938), 799.

The resultant of these effects is obviously complex, and changes in $B(P)$ and θ can serve only as an approximate representation. The ballistic importance depends chiefly on the relative positions of "maximum pressure" and "all burnt." The separation of these is normally greatest for cord charges, and for these the effect is chiefly a more progressive burning, that is, a decrease in θ, of the order of 0.2; there is a corresponding increase in the rate $B(P)$ to preserve the initial rate of burning, which is proportional to $(1 + \theta)B(P)$. For shapes with nominally constant burning surface, "maximum pressure" occurs nearer "all burnt," and the final effects carry more weight. There is still, on the whole, a decrease in θ and an increase in the rate $B(P)$; $(1 + \theta)B(P)$ is roughly conserved.

There is one last difference between gun and closed vessel that it is as well to note here, though it concerns not so much the way the propellant burns as the way in which we represent it. In closed-vessel analysis there is no reason for choosing any special function for the rate of burning. In dealing with the more complicated equations for a gun it is, on the other hand, convenient to write the rate as proportional to the pressure. This is almost essential if an analytical solution is wanted. Unfortunately, present-day propellants prefer to burn according to a rather different law. Forms used have included

$$B(P) = \beta P^{\alpha}$$

and

$$B(P) = \beta(P + P_1)$$

The constants depend on the composition; P_1 is usually quoted as of the order of 1 ton/sq in., and is, at any rate, positive. The "pressure index" α is commonly near 0.9, and is almost always less than unity.[14]

Both forms agree in asserting that the propellant burns more slowly at high pressures than would be expected from

$$B(P) = \beta P$$

Hence, if we analyze the behavior of a gun on the latter assumption, the burning area will appear to decrease at high pressures. For shapes with θ near zero, peak pressure tends to occur only a little before "burnt," and the decrease of apparent burning area extends over the later stages of burning. The effect can be simulated by an increase of the form factor θ by an amount of the order of 0.1.

---

[14] Among production propellants, the highest α recorded has been 1.02. Values near 2 have occurred with experimental compositions and have been attributed to disintegration of imperfectly gelatinized material; this is supported by their irregular behavior. The Boys-Corner theory of the rate of burning at gun pressures does not exclude α from rising a little above unity (§ 2.35).

For cord the matter is not so simple, for the region of high pressure is normally confined to the middle of burning. The effect reveals itself as a variation of β with peak pressure, which cannot be eliminated by altering θ.

The "cooler" the propellant, the further α lies below unity, and the bigger the effect just mentioned, but at the same time the greater the erosion. The sum of the two effects is not likely to vary greatly from one composition to another.

2.23 The Charbonnier form of the equation of burning

In the mathematical theory of interior ballistics it is convenient to use

$$\left.\begin{aligned} D\frac{df}{dt} &= -B(P) \\ \phi &= (1-f)(1+\theta f) \end{aligned}\right\}. \tag{9}$$

rather than the single equivalent equation,

$$D\frac{d\phi}{dt} = B(P)[(1+\theta)^2 - 4\theta\phi]^{\frac{1}{2}} \tag{8}$$

The preference for equation 9 is justified by the variable f being convenient for the analytical solution of the main equations of interior ballistics. On the Continent the form 8 is now preferred, or rather, equations which, like equation 8, are all included in the Charbonnier form:

$$D\frac{d\phi}{dt} = B(P)g(\phi) \tag{10}$$

D is a length characteristic of the size of a grain of the propellant; for instance, for a charge of cord D could be the mean diameter, or equally well the radius. Such ambiguities have to be corrected by proper choice of the form function $g(\phi)$. $B(P)$ is the rate of burning at pressure P, a function depending only on the composition of the propellant.

The form function $g(\phi)$ is a property of the whole charge, being affected not only by the mean shape of the grains but also by the heterogeneity of the charge. Furthermore, the form function varies somewhat with the conditions of use of the charge; for example, the extent of erosion of the propellant depends on the peak pressure and the muzzle velocity, and this has an effect on $g(\phi)$.

The form function is proportional to the integral of the rate of burning per unit area, taken over the whole surface of the charge at pressure P and fraction-burnt ϕ. When the rate of burning is the same at all points of the surface at a given time, $g(\phi)$ is simply the relative area of the propellant.

This form of the burning equation is convenient for theoretical discussion of the effects of heterogeneity and erosion—in fact, for study of all these instances where the variable f has not a simple geometrical interpretation. By the introduction of this form function, Charbonnier at last broke away from the geometrical arguments that were associated with equation 9. However, the latter form is still useful if we remember that θ is to be found from the gun, not from geometry.

2.3 Theories of the burning of gun propellants

There have been very few such theories, and they can be summarized quickly. Before doing this, it is worth considering whether there is any need for a theory. One result of a fully developed theory will be a formula showing how the rate of burning depends on composition, initial temperature, and pressure. There will be perhaps one or two constants to be determined by fitting to a few observed rates of burning. The possibility of predicting rates of burning is not, however, a justification for a theory of burning; the rate of a propellant can be guessed from its composition [15] sufficiently closely for the purpose of predicting compositions with required characteristics. This assumes a knowledge of the rates of a number of propellants of similar physical nature: colloidal propellants with an emulsion as stabilizer (for example, mineral jelly) are noticeably faster than colloidal propellants of the same explosion temperature but with stabilizer distributed homogeneously (for example, carbamite); likewise, nitroguanidine propellants contain this substance as crystals enmeshed in the gel, and so it is perhaps not surprising that the rate depends on the size of the crystals. Many data have been accumulated about all these types of propellant, so that it is not necessary to appeal to theory for the dependence of rate on composition. The variations with pressure and initial temperature are also obtainable from closed-vessel experiments. In short, the rate of burning can serve as a check on a theory or as a way of evaluating its constants but cannot be a reason for setting up the theory.

---

[15] One way is to plot the rates of burning (at a given pressure) against the uncooled temperature of explosion or against the calorimetric value (see chapter 3). The points lie near a smooth curve. These properties can be calculated from the composition, as explained in the next chapter. Hence, the rate of burning can be estimated from composition.

Muraour, *Comp. rend.*, **187** (1928), 289, found that the logarithm of the rate of burning was a linear function of the uncooled explosion temperature for a series of colloidal propellants (NC-NG-carbamite). This form of relation gives quite a good fit to British data for propellants of this type, though the fit is not so close as found by Muraour.

The real value of a theory of burning lies in its physical and chemical picture of the process. If this picture is reasonably close to the truth, it helps us to understand various phenomena associated with burning (for example, "erosion" of propellant and ignition). A successful theory would provide a general understanding of these phenomena and would indicate the possibilities of control; it might also extend to quantitative predictions, but this is perhaps too much to expect. Even a qualitative theory would be a valuable guide in the choice of significant experiments. Therefore, a theory of the burning of a propellant may give small discrepancies from experiment, showing that it is not the complete story, and yet it may provide an understanding of the process sufficient for many needs.

All theories put forward can be divided into two types: the first may be called the "surface theories," in which the burning is controlled by the rate at which energy, in the right form, is transmitted from the hot gaseous products to the surface of the solid propellant; the second class of theories fix attention on the reactions in the gas phase, which are thought to control the over-all rate. The latter may be called "vapor-phase" theories.

2.31 Surface theories

These have been suggested by Létang,[16] Schweikert,[17] Muraour,[18] Yamaga,[19] and Crow and Grimshaw.[20] Muraour's work has also been reviewed by Schmidt.[21]

These theories consider the rate at which energy is transferred from the hot gas to the solid. The molecule of the propellant may be supposed to react if it receives a sufficiently large amount of energy by being struck by a fast-moving gas molecule. This is the essential part of the theories of Muraour, Yamaga, and Létang. An important point is, therefore, the energy distribution of the molecules striking the surface. These molecules had their last collision at various distances from the surface; however, nearly all come from a thin layer close to the surface. What energy distribution is to be assumed for the molecules (that is, the "average temperature of their origin") is a point at which the theories differ.

---

[16] Létang, *Mém. artillerie franç.*, **1** (1922), 955.

[17] Schweikert, *Innere Ballistik* (1923).

[18] Muraour, *Bull. soc. chim. France*, **41** (1927), 1451; **47** (1930), 261; *Comp. rend.*, **192** (1931), 227. Muraour and Schumacher, *Mém. poudres*, **27** (1937), 87.

[19] Yamaga, *Z. ges. Schiess- u. Sprengstoffw.*, **25** (1930), 60.

[20] Crow and Grimshaw, *Phil. Trans. Roy. Soc. (London)*, **230A** (1931), 387.

[21] Schmidt, *Z. ges. Schiess- u. Sprengstoffw.*, **27** (1932), 1, 45, 82.

These theories give a rate of burning proportional to the number of sufficiently energetic collisions per unit area per second; and, if the energy distribution of the impinging molecules does not depend on the pressure, the rate of burning is proportional to pressure. Muraour has discussed the energy distribution in a qualitative way. The average temperature of the gas layer is supposed to be somewhat less than the final temperature of the products, the temperature of "uncooled explosion";[22] and at low pressures the surface layer of gas is more mixed with the final products and is therefore hotter than at high pressures. Hence the rate of burning, M grams per square centimeter per second, is greater at low pressures than would be expected from a linear law. Muraour has therefore used the relation,

$$M = a + bP$$

where P is the pressure. The calculation of a and b has not been attempted. Part of the a term is attributed to transmission of large energy quanta by radiation, which is supposed to be independent of pressure. From experiment the ratio a/b is known to depend on whether the stabilizer is distributed homogeneously or as an emulsion.[23]

At high pressures the number of impacts per unit area per unit time is not exactly proportional to the pressure, being altered by the finite size of the molecules.[24, 25]

Muraour has also discussed qualitatively the dependence of the rate on the uncooled temperature of explosion. This affects the speed of the reactions in the gas phase, and therefore the extent to which the "temperature of the surface layer" of gas falls short of the final temperature of the products. Muraour concluded that with change of composition the rate of burning would increase somewhat faster than the explosion temperature.

---

[22] This is the temperature attained by the products when formed without loss of heat or performance of external work. Another name is the "adiabatic flame temperature." It is shown in the next chapter that this temperature is almost independent of the density of the products. When the products are formed against a pressure P, their temperature is the "explosion temperature at constant pressure" or "isobaric flame temperature." This has a fairly strong dependence on P.

[23] Muraour and Aunis, *Comp. rend.*, **192** (1931), 418.

[24] Muraour, *Bull. soc. chim. France*, **41** (1927), 1451.

[25] Anticipating the definitions of the next chapter, we shall refer to the results of the finite size of the molecules as "covolume effects."

Muraour's picture involves a decomposition of the solid, which may be only incomplete and followed by reactions in the gas phase, ending in the usual equilibrium products. This is much the same as the process assumed by Boys and Corner (§ 2.34), but the controlling rate is very different in the two theories. For Muraour the rate of the whole process is fixed by the rate at which decomposition occurs at the surface of the propellant.

Muraour has illustrated his theory by experiments on many features of the burning of propellants. The theory has certainly been of value in guiding experiment, but it has not received a quantitative development.

Yamaga's theory[26] assumes that decomposition occurs when an "activated" surface molecule is struck by a fast molecule from the gas. The surface molecules are assumed to be at the temperature T' of the original propellant, and their "activation energy" is E', so that at any instant only a fraction $e^{-E'/RT'}$ of the surface molecules are capable of reaction. The bombarding gas molecules are taken to have the energy distribution appropriate to a temperature T; the number of impacts (per unit time) by molecules whose translational kinetic energy is greater than the activation energy E, is proportional to $T^{-\frac{1}{2}}e^{-E/RT}$ as a function of T. The rate of burning M is therefore proportional to

$$T^{-\frac{1}{2}}e^{-E/RT-E'/RT'}$$

in its dependence on T and T'. Yamaga took T to be the temperature of uncooled explosion; he determined E from the experimental rates for different propellants at the same initial temperature, and E' from the rates of the same propellant at different initial temperatures.

The identification of T with the temperature of uncooled explosion is a weakness of this theory. The assumption permits a quantitative treatment, as opposed to Muraour's rough and qualitative discussion, but the more quantitative theory is based on less acceptable physical ideas. The values found for E and E', 19.1 kcal/mole and 274 cal/mole, respectively, are probably somewhat in error.[27] Lesauskis[28] has applied the same theory to the slow low-temperature decomposition of propellants. In this application there is no difficulty about the appropriate value of T, which is just the same as T', the temperature of the propellant and the whole system. The impinging gas molecules are of different nature in the two cases, which would be expected to affect the results; nevertheless, Lesauskis obtained a satisfactory temperature dependence of the reaction rate by using Yamaga's values of E and E'.

---

[26] Yamaga, *Z. ges. Schiess- u. Sprengstoffw.*, **25** (1930), 60.

[27] In finding the theoretical change of rate with T', the corresponding change of T was neglected, although the latter contributes about 30 per cent of the whole effect. The experimental change of rate with T' was given as about 1.7 per cent per 10°C, which is about half that found by Crow and Grimshaw, *Phil. Trans. Roy. Soc. (London)*, **230A** (1931), 387.

T was found by calculation and ran up to 4100°K for the hottest powder (Mk I). This is certainly too high and suggests that T was overestimated.

[28] Lesauskis, *Mém. artillerie franç.*, **14** (1935), 487

Létang's theory [29] was the earliest of this type. It differs from that of Yamaga in that there is no activation of the solid by its own thermal energy. Létang assumed that every sufficiently violent impact of a gas molecule with the propellant would generate another gas molecule and that the energy distribution of the bombarding molecules was that appropriate to the temperature of explosion. He found the velocity necessary for a successful impact by working back from known rates of burning and explosion temperatures.[30] The theory gave a rate of burning proportional to pressure, as with all these "surface theories." Létang applied this theory to the slow low-temperature decomposition of propellant and to ignition.

The theory of Crow and Grimshaw [31] assumed that a molecule of the propellant requires extra internal vibrational energy before it will decompose. This energy was supposed to be supplied by the internal vibrational energy of the impinging gas molecules coming from the layer outside the solid. The temperature of the gas molecules was taken to be the temperature of uncooled explosion. The vibrational energy obtained by the propellant is manifested by an increase of temperature, and the amount necessary for decomposition is measured by the ignition temperature or "touch-off temperature." The rate of transfer of vibrational energy from impinging molecule to solid is governed by an accommodation coefficient. The two arbitrary parameters for each propellant were chosen to reproduce the rate of burning and its dependence on the initial temperature of the propellant. The touch-off temperature varied considerably over the four types of propellant studied, and its prediction from composition would appear to be difficult.

---

[29] Létang, *Mém. artillerie franç.*, **1** (1922), 955.

[30] He found that the kinetic energy of the molecule had to be greater than 35 kcal/mole, roughly. This is considerably more than Yamaga's 19 kcal/mole. The discrepancy is explained by the difference in their methods of finding the activation energy, and it indicates that their formula for the rate of burning cannot account for both (1) the rate of a certain propellant, and (2) the variation of the rate with the temperature of explosion. Létang used (1); Yamaga used (2). Létang's table of results (p. 962) confirms this explanation; for there are effectively three distinct explosion temperatures listed, and the activation energy increases with the explosion temperature; that is, the property (2) of the propellants studed by Létang demands an activation energy much *below* 35 kcal/mole.

[31] Crow and Grimshaw, *Phil. Trans. Roy. Soc.* (*London*), **230A** (1931), 387.

All these theories lead to the result that the rate of burning depends on the gas temperature near the solid. From experiment[32] it is known that the rate of burning is not affected by proximity to a different propellant. This shows that the effective gas layer round any piece of propellant contains only gas emitted from this propellant; mixture of the products of the various pieces takes place further from their surfaces. For the same reason the temperature of uncooled explosion should be replaced, where it occurs in these theories, by the temperature of combustion at constant pressure. This lies below the temperature of uncooled explosion, the difference being of the order of 500°C (see § 3.31).

Another result common to these theories is that the rate of burning is proportional to pressure, except at high pressures where the effect of the finite size of the gas molecules becomes significant. Crow and Grimshaw concluded that the rate of burning was proportional to density and not to pressure; this has been challenged from the experimental side,[33] and its deduction from the assumptions of their theory might also be questioned.

2.32 Vapor-phase theories

A possible criticism of all the previous theories is that they pay insufficient attention to the reactions in the layer of gas just outside the solid. The bombarding molecules come from a layer that is at most a few mean free paths thick. Their effective temperature is supposed to be the temperature of explosion, or very near it. The reactions of the gas leaving the surface are therefore assumed to evolve no heat outside this thin layer. Moreover, no appreciable reaction can occur in the few collisions suffered in traversing this layer. This means that these theories assume the surface decomposition of the propellant to give the final products in one stage, or, if not the final products, then gases which transform into the final products without evolution of heat.

Such a conception is hardly in accord with modern views on chemical reactions. These lead us to expect a primary decomposition of the solid into gases, which probably undergo many reactions before the final products are reached. Reaction must be going on in the gas for a distance of some hundreds of free paths from the solid. Boys and Corner have therefore proposed a theory that considers the gradual progress of reaction in this zone. The reactions were idealized to a single reaction leading from the "intermediate products" of the primary decomposition of the solid, up to the final equilibrium products. It was assumed that most of the heat of explosion was given out in this gas reaction. This sweeping idealization of the actual reactions was made necessary by difficulties of handling any more complicated case, and also by the lack of information (at that time) of the probable intermediate products. A theory of flames in gases[34] was used to find the mass consumption of the flame zone, and so the rate of burning of the solid.

---

[32] Muraour, *Z. physik. Chem.*, **139A** (1928), 163.

[33] Hunt and Hinds, *Proc. Roy. Soc.* (London), **138A** (1932), 696.

The order of the reaction decides how the rate of burning M depends on pressure P; for example, a first-order reaction leads to $M \propto P^{1/2}$ and a second-order reaction to $M \propto P$.

These results suggest that it may be possible to represent the observed variation of the rate of burning with pressure. Let it be assumed that there are *parallel* routes from "intermediate" to final products, whose over-all rates are first and second order; then at sufficiently low pressures the first-order set of reactions will predominate and $M \propto P^{1/2}$; at high pressures the second-order reaction will be the more important, and $M \propto P$ in this pressure region. This does indeed represent the general behavior of propellants. At high pressures there enter other effects. It may be mentioned here that calculation has shown at 20 tons/sq in. the ratio M/P can fall to about 80 per cent of its value at low pressure (say 5 tons/sq in.). The points to be noted are: (1) the change being the sum of at least four effects of different signs, there is no reason to expect all propellants to show closely similar high-pressure behavior; (2) the results can be expressed in terms of either the pressure or the density but not necessarily as a simple form in either case.

The earliest form of the Boys-Corner theory was not entirely satisfactory quantitatively. The strong gradient of concentration in the reaction zone causes a significant diffusion of products into reactants. Not until diffusion had been included in the theory was it possible to get agreement with experiment with reasonable assumptions about molecular weights and heats of reaction. The theory of the flame zone, allowing for diffusion, has been published by Corner.[35] In this book we shall present only the simpler theory omitting diffusion, since the latter effect does not alter the physical picture, nor does it affect the form of the dependence on pressure, whereas the equations are simpler without diffusion terms.

The theory of Boys and Corner has a close connection with the work of Belajev,[36] though it was developed in ignorance of the latter.

---

[34] Boys and Corner, *Proc. Roy. Soc. (London)*, **197A** (1949), 90.

[35] Corner, *Proc. Roy. Soc. (London)*, **198A** (1949), 388.

[36] Belajev, *Acta Physicochim.*, **8** (1938), 763; **14** (1941), 523; *Comp. rend. (URSS)*, **24** (1939), 254.

Belajev's theory refers to the burning of volatile explosives, which he distinguishes sharply from propellants. His idea is that the surface of the explosive is emitting it as vapor and that its decomposition takes place in the gas phase just outside the liquid surface. The surface temperature is the boiling point of the liquid at the given pressure. This is clearly not applicable to propellants, and is replaced in Boys' theory by the assumption that the substances being emitted from the surface into the gas reaction zone are products of the low-temperature decomposition of the propellant. Apart from these differences the two theories are much the same. Belajev used the theoretical work of Zeldowitch and Frank-Kamenetsky on flames in gases, which is in many ways similar to the treatment of Boys and Corner.

We shall now give the simplest form of the theory of a flame zone and then the application to the "vapor-phase" theory of the burning of a homogeneous propellant; we shall mention the effects that enter at very high pressures, and finally the influence of the initial temperature of the propellant.

Before passing on to these matters, it must be said that the theory to follow is applicable only at gun pressures. The phenomena at rocket pressures, of the order of a few hundred pounds per square inch, are more complicated. This field has been much studied in the United States, particularly by Professor B. L. Crawford and Professor O. K. Rice, and it appears to be necessary to consider several successive reactions to explain the observations. Reactions inside the solid are important, and it is no longer possible to speak of a purely "vapor-phase" theory. The extent of the difference between the two fields can be illustrated thus: the rate of burning of a rocket propellant has been found to depend on the mean molecular weight of the nitrocellulose, which is a long-chain polymer with a wide range of possible chain lengths; on the other hand, the mean molecular weight of the nitrocellulose has never been proved to affect the rate of burning at gun pressures.

2.33 Theory of a flame zone in a gas

A reaction zone moves through a medium by the transfer of some activating influence from the portion already reacted to an unreacted part. This in its turn reacts and again activates more unreacted material. In an exothermic reaction there are several ways in which the activating influence may be transferred. These are the flow of heat, diffusion of active particles or catalytic intermediate products, or radiation. In the case of propellants there are products at extremely high temperature, and there is a considerable flow of heat from these to the unreacted portion. We shall ignore the other possibilities of activation and merely consider the flow of heat, a picture that can conveniently be described as the simple thermal model. We shall examine the rate at which the activating heat is transferred, by calculating the thermal conduction from the distribution of temperature through the zone.

We shall examine the steady propagation of a plane reaction zone through a homogeneous medium with the following properties:

1. The medium is capable of a single exothermic reaction whose rate at any point in the medium is determined solely by the temperature, pressure, and the stage to which the reaction has proceeded, all taken at the point in question.

2. The velocity of the reaction zone is so slow that the pressure is effectively constant through this zone. Diffusion will be neglected.

We shall examine the general reaction zone and then a special case assuming constant specific heats and thermal conductivities, together with activation-energy formulas for a second-order reaction rate. The general case can always be integrated numerically, and in the special case an explicit formula for the rate of burning can be obtained.

We consider a plane reaction zone, which is in steady motion, and we wish to predict the speed for which such a steady motion is possible. We shall exclude the phenomenon of detonation, whose speed is very different from that of any flame. A complete theory would cover detonation and such nonsteady phenomena as ignition and the transition to detonation. Throughout this work we shall consider only the steady motion of flames.

This restriction leaves two points uncertain: in the first place, we do not show how such a steady motion could be generated; second, we do not prove that such a flame is stable. These are difficult questions, which do not appear to have simple general answers. However, in the application to solid propellants we can appeal to experiment as a proof that such regimes are both possible and stable.

Take an x axis of reference perpendicular to the plane, with an origin moving with the reaction zone, so that relative to our axes the unreacted medium moves from the direction of negative x, and, after passing through the flame, the products pass toward $x = \infty$. All properties of the system are functions of x alone. When U is the velocity of the medium at any point, the rate at which any property y of a given small portion of the medium varies with time is given by

$$\frac{\mathfrak{D}y}{\mathfrak{D}t} = \frac{\partial y}{\partial t} + U\frac{\partial y}{\partial x} = U\frac{dy}{dx} \tag{11}$$

U is itself a function of x.

The quantities whose variation through the reaction zone are required are U the velocity, V the volume per unit mass, T the temperature, and ϵ the fraction the reaction has progressed toward completion at the plane x, so that, of the gas passing this plane, a fraction ϵ (by mass) consists of the products of reaction. We can immediately obtain a relation between U and V. If we consider the material moving along a cylinder with walls parallel to the x axis and of unit cross section, it is apparent that the same mass is moving across any cross section of this per unit time. Representing this by M, we have

$$U = MV \tag{12}$$

Since the pressure is constant, V must be a function of ϵ and T only and is known from the equation of state for the medium with a given ϵ.

The energy crossing any normal section of the cylinder must be a constant, or energy would accumulate or disappear between two sections. The energy flow is composed of:

1. The intrinsic energy E per unit mass, transported by the mass flow.
2. The work done by the material on one side of the section by its pressure on the material on the other side of the section.
3. The flow of heat due to thermal conduction, which is described by a thermal conductivity λ.

The latter flow will be zero at large distances on both sides of the reaction zone. Denote the conditions at a large distance before the flame by T_0, V_0, etc., and at large distances past as T_m, V_m, etc. Then we have

$$M(E + PV) - \lambda \frac{dT}{dx} = M(E_m + PV_m) = M(E_0 + PV_0) \tag{13}$$

which gives

$$\frac{\lambda}{M}\frac{dT}{dx} = E - E_m + P(V - V_m) = H - H_m \quad \text{or} \quad H - H_0 \tag{14}$$

where H is the total heat content per unit mass.

We need a further relation, which is supplied by considerations of reaction velocity. The homogeneous reaction rate, expressed as $\mathfrak{D}\epsilon/\mathfrak{D}t$, will be a function of ϵ, V, and T, by our initial assumptions.[37]

---

[37] This implies that the reaction rate at any point is determined by the local temperature, just as if the gas at that point were in a large enclosure at constant temperature. This is true only if the thickness of the reaction zone is large compared with the mean free path of molecules in it. It can be shown that this condition is satisfied in flame zones outside propellants.

Hence, we have

$$U\frac{d\epsilon}{dx} = \frac{\mathfrak{D}\epsilon}{\mathfrak{D}t} = f(\epsilon, V, T) \tag{15}$$

Equations 14 and 15 can be written in terms of ϵ and T alone, since H will be a known function of ϵ, T, and V, and the latter can be eliminated by using the equation of state. In this way we can obtain two differential equations, from which x can be eliminated by dividing one by the other, giving

$$\frac{d\epsilon}{dT} = \frac{\lambda f(\epsilon, T)}{M^2V(H - H_m)} \tag{16}$$

This is possible only because x does not appear except as dx. In more general cases than we are considering here, x may appear explicitly; this happens when the phenomena in the flame zone depend on the distance from the solid boundary. In such cases there is no point in forming equation 16. In our case, however, this step is useful because the problem of the flame speed can be solved from equation 16 alone. If distances in the flame zone are of interest, the results can be substituted in equation 14, giving the relation between x and T or ϵ.

We require the integral of equation 16, which is such that $T = T_0$ when $\epsilon = 0$, and $T = T_m$ when $\epsilon = 1$. T_0 is the temperature at a large distance inside the unreacted medium, the initial temperature, which is known in any particular set of experiments. T_m follows from this by the relation,

$$H_m = H_0$$

where H_m is the total heat content for $\epsilon = 1$, and H_0 refers to $\epsilon = 0$. T_m is the temperature of the product gases when formed against a constant pressure. In the application to propellant, T_m must be distinguished from the temperature of uncooled explosion at constant volume, which is about 20 per cent higher.

Equation 16 is a first-order equation, and its solution is determined by the parameters of the equation, together with one pair of corresponding values of ϵ and T. The solution determined by the conditions at T_0 will, in general, not fulfil the condition at the upper limit T_m. There will be one value of M for which both conditions are satisfied; this determines the only velocity possible for a steadily moving reaction zone in the given medium. This value of M is a function of the other parameters in the equation.

The form of the equations ensures that ϵ and T remain constant beyond the point where $\epsilon = 1$ and $T = T_m$. This has the result that in finding M we can restrict our attention to the equation between ϵ

and T. No matter whether the point ($\epsilon = 1$, $T = T_m$) is at a finite or an infinite distance, we can be sure that everywhere beyond this point the outgoing gases will be at the temperature T_m and will be completely reacted, which is necessary for a physically satisfactory reaction zone. For distances that are large compared with the effective thickness of the flame, the gas may be subjected to cooling and consequent changes of composition, or it may be compressed against a barrier, but these cannot affect the rate of burning. The only influences that can have any effect on the rate are those that act in the region where the reaction rate is appreciable.

The velocity of the reaction relative to the unburnt medium is MV_0, which in the application to propellant is the rate of recession of the surface of the propellant. The corresponding relation between ϵ and T is the solution of equation 16 with the proper value of M; finally, the (x, T) relation can be found by substituting in equation 14. This provides a scale of distances for the variation of ϵ and T through the reaction zone.

We now examine a simple case, which can be integrated explicitly by a method of successive approximations. This case corresponds to a simple form of the reaction rate, which appears to be applicable to propellant. The method of successive approximation is not restricted to this instance.[38]

We limit our examination to a zone in perfect gases with constant specific heats per unit mass. Positions in the flame zone at which the reaction does not proceed at an appreciable rate do not affect the rate of burning; we are assuming constancy of the specific heat only at those high temperatures in the flame at which most of the reaction takes place. The assumption is therefore a good approximation for hot flames.

If Q_m is the heat of reaction at constant pressure at the temperature T_m of the final products, we have

$$H - H_m = (1 - \epsilon)Q_m + (T - T_m)[C_p'(1 - \epsilon) + \epsilon C_p] \qquad (17)$$

where C_p' is the specific heat of the reactant and C_p that of the products, both at constant pressure. It would be possible to integrate this case if the problem required this refinement, but, since a simpler case is adequate for our purposes, we shall put $C_p' = C_p = C$. We can also write Q instead of Q_m, since now the heat of reaction is independent of the temperature. Thus, finally,

---

[38] Mr. Booth has applied a similar technique to reaction zones in pyrotechnic mixtures.

$$H - H_m = (1 - \epsilon)Q + (T - T_m)C \tag{18}$$

so that

$$\frac{\lambda}{M}\frac{dT}{dx} = (1 - \epsilon)Q + (T - T_m)C \tag{19}$$

and substituting into equation 16 gives

$$\frac{d\epsilon}{dT} = \frac{\lambda f(\epsilon, T)}{M^2 V[(1 - \epsilon)Q + (T - T_m)C]} \tag{20}$$

In a simple reaction in which molecules of molecular weight W give molecules of molecular weight w, the equation of state is

$$\frac{PV}{RT} = \frac{1 - \epsilon}{W} + \frac{\epsilon}{w} = \frac{1 + n\epsilon}{W} \tag{21}$$

where $n = (W/w) - 1$, and R is the gas constant per mole (8.205×10^{-2} atm·liter·mole^{-1}·deg^{-1}). If the reactant consists of more than one type of molecule with different molecular weights, this equation will have the same form but a different value of n.

For a second-order rate from a bimolecular reaction, the value of $\mathfrak{D}\epsilon/\mathfrak{D}t$ as a function of ϵ, V, and T is

$$f(\epsilon, T, V) = \frac{\mathfrak{D}\epsilon}{\mathfrak{D}t} = \frac{B}{V}(1 - \epsilon)^2 e^{-A/RT} \tag{22}$$

The values of the constants will be discussed in § 2.34. Substituting in equation 20, we have

$$\frac{d\epsilon}{dT} = \frac{\lambda B(1 - \epsilon)^2 e^{-A/RT}}{M^2 V^2[Q(1 - \epsilon) + C(T - T_m)]} \tag{23}$$

Using equation 21 yields

$$\frac{d\epsilon}{dT} = \frac{\lambda B(PW)^2(1 - \epsilon)^2 e^{-A/RT}}{M^2(1 + n\epsilon)^2(RT)^2[Q(1 - \epsilon) + C(T - T_m)]} \tag{24}$$

Near the hot boundary of the reaction zone, $T - T_m$ and $1 - \epsilon$ are small, and these terms determine the behavior of the solution. All other functions of T and ϵ in this equation can be given the values corresponding to $T = T_m$ and $\epsilon = 1$. The equation thus simplified has a solution that at large distances, where $T - T_m$ and $1 - \epsilon$ are sufficiently small, approaches that solution of the original equation satisfying the boundary condition that $T - T_m$ when $\epsilon = 1$. This (ϵ, T) relation can then be used in the awkward coupling term $Q(1 - \epsilon) + C(T - T_m)$ but no-

$$H - H_m = (1 - \epsilon)Q + (T - T_m)C \tag{18}$$

so that

$$\frac{\lambda}{M}\frac{dT}{dx} = (1 - \epsilon)Q + (T - T_m)C \tag{19}$$

and substituting into equation 16 gives

$$\frac{d\epsilon}{dT} = \frac{\lambda f(\epsilon, T)}{M^2 V[(1 - \epsilon)Q + (T - T_m)C]} \tag{20}$$

In a simple reaction in which molecules of molecular weight W give molecules of molecular weight w, the equation of state is

$$\frac{PV}{RT} = \frac{1 - \epsilon}{W} + \frac{\epsilon}{w} = \frac{1 + n\epsilon}{W} \tag{21}$$

where $n = (W/w) - 1$, and R is the gas constant per mole (8.205×10^{-2} atm·liter·mole^{-1}·deg^{-1}). If the reactant consists of more than one type of molecule with different molecular weights, this equation will have the same form but a different value of n.

For a second-order rate from a bimolecular reaction, the value of $\mathfrak{D}\epsilon/\mathfrak{D}t$ as a function of ϵ, V, and T is

$$f(\epsilon, T, V) = \frac{\mathfrak{D}\epsilon}{\mathfrak{D}t} = \frac{B}{V}(1 - \epsilon)^2 e^{-A/RT} \tag{22}$$

The values of the constants will be discussed in § 2.34. Substituting in equation 20, we have

$$\frac{d\epsilon}{dT} = \frac{\lambda B(1 - \epsilon)^2 e^{-A/RT}}{M^2 V^2[Q(1 - \epsilon) + C(T - T_m)]} \tag{23}$$

Using equation 21 yields

$$\frac{d\epsilon}{dT} = \frac{\lambda B(PW)^2(1 - \epsilon)^2 e^{-A/RT}}{M^2(1 + n\epsilon)^2(RT)^2[Q(1 - \epsilon) + C(T - T_m)]} \tag{24}$$

Near the hot boundary of the reaction zone, $T - T_m$ and $1 - \epsilon$ are small, and these terms determine the behavior of the solution. All other functions of T and ϵ in this equation can be given the values corresponding to $T = T_m$ and $\epsilon = 1$. The equation thus simplified has a solution that at large distances, where $T - T_m$ and $1 - \epsilon$ are sufficiently small, approaches that solution of the original equation satisfying the boundary condition that $T - T_m$ when $\epsilon = 1$. This (ϵ, T) relation can then be used in the awkward coupling term $Q(1 - \epsilon) + C(T - T_m)$ but nowhere else in equation 24. The resulting equation can be integrated exactly. This provides a second approximation to the exact solution of equation 24. We do not go beyond this order of approximation, because comparison with numerical integration has shown that the accuracy of the second approximation is ample for our purposes; moreover, the differential equation in the next approximation is as difficult to solve analytically as the original equation. It is not possible to stop at the extremely simple first approximation, because the error in the rate of burning is a factor of about three. The error in the second approximation depends chiefly on A/RT_m and has not been more than 15 per cent in the examples studied until now, in which A/RT_m has been as low as 4. For A/RT_m near 8, the rate is too low by about 5 per cent.

Write $1 - \epsilon = \xi$ and $T_m - T = \eta$. The first approximation is the solution of the equation,

$$\frac{d\xi}{d\eta} = \frac{D\xi^2}{Q\xi - C\eta} \tag{25}$$

where

$$D = \frac{\lambda B(PW)^2 e^{-A/RT_m}}{(MRT_m)^2(1+n)^2} \tag{26}$$

The equation can be written as

$$\frac{d\eta}{d\xi} + \frac{C\eta}{D\xi^2} = \frac{Q}{D\xi}$$

of which we want the solution with $\xi = 0$ at $\eta = 0$. This is

$$\eta = \frac{Q}{D} e^{C/D\xi} \int_0^{\xi} e^{-C/D\tau} \frac{d\tau}{\tau} \tag{27}$$

The "exponential integral" is defined[39] as

$$Ei(-x) = \int_{\infty}^{x} e^{-t} \frac{dt}{t}$$

a well-known tabulated function. Let $\psi = C/D$. Transforming the variable of integration in equation 27 to ψ/ξ, we see that the solution can be written as

$$T_m - T = -\frac{Q}{D} e^{\psi/\xi} Ei\left(-\frac{\psi}{\xi}\right)$$

---

[39] For example, Jahnke and Emde, *Function Tables*, 1933 ed., p. 78; 1938 ed., p. 1.

Substituting in the $T - T_m$ term of equation 24, we have

$$\frac{d\epsilon}{dT} = \frac{\lambda B(PW)^2\xi^2 e^{-A/RT}}{(MR)^2(1 + n\epsilon)^2QT^2\left[\xi + \psi e^{\psi/\xi}Ei\left(-\frac{\psi}{\xi}\right)\right]}$$

which integrates to

$$\int_0^{1-\epsilon}\left[\xi + \psi e^{\psi/\xi}Ei\left(-\frac{\psi}{\xi}\right)\right]\left(\frac{1+n}{\xi} - n\right)^2 d\xi = \frac{\lambda B(PW)^2}{(MR)^2Q}\left(\frac{R}{A}\right)\left(e^{-A/RT_m} - e^{-A/RT}\right) \quad (28)$$

This solution has been made to satisfy the boundary condition at the hot end of the flame but does not necessarily do so at the beginning of the reaction zone. Imposing the condition that $\epsilon = 0$ when $T = T_0$ gives, as the equation to determine M,

$$\int_0^{1}\left[\xi + \psi e^{\psi/\xi}Ei\left(-\frac{\psi}{\xi}\right)\right]\left(\frac{1+n}{\xi} - n\right)^2 d\xi = \frac{\lambda B(PW)^2}{(MR)^2Q}\left(\frac{R}{A}\right)e^{-A/RT_m} \quad (29)$$

since e^{-A/RT_0} is negligible compared with e^{-A/RT_m}.

To simplify the equation we write $\theta = \psi/\xi$. The result is

$$g_1(\psi) - \frac{2n}{1+n}g_2(\psi) + \left(\frac{n}{1+n}\right)^2 g_3(\psi) = \frac{CT_m}{Q}\cdot\frac{RT_m}{A} \quad (30)$$

where

$$g_1(\psi) = \psi\int_\psi^\infty\left[\frac{1}{\theta} + e^\theta Ei(-\theta)\right]d\theta$$

$$g_2(\psi) = \psi^2\int_\psi^\infty\left[\frac{1}{\theta} + e^\theta Ei(-\theta)\right]\frac{d\theta}{\theta}$$

and

$$g_3(\psi) = \psi^3\int_\psi^\infty\left[\frac{1}{\theta} + e^\theta Ei(-\theta)\right]\frac{d\theta}{\theta^2}$$

These functions are presented in Table 2.1 for the whole range of ψ likely to be encountered in work on flames outside propellants.

Table 2.1 Functions for the Solution of the Flame Equation

ψ	$g_1(\psi)$	$g_2(\psi)$	$g_3(\psi)$
4.5	0.840	0.397	0.258
3.9	0.822	0.386	0.250
3.3	0.800	0.372	0.240
2.7	0.771	0.355	0.228
2.1	0.731	0.332	0.211
1.5	0.672	0.298	0.188
1.4	0.660	0.291	0.183
1.3	0.646	0.283	0.178
1.2	0.631	0.274	0.172
1.1	0.615	0.265	0.165
1.0	0.596	0.255	0.159
0.95	0.586	0.249	0.155
0.9	0.576	0.244	0.151
0.85	0.565	0.238	0.147
0.8	0.553	0.231	0.143
0.75	0.541	0.224	0.138
0.7	0.527	0.217	0.133
0.65	0.512	0.210	0.128
0.6	0.497	0.202	0.123
0.55	0.480	0.193	0.117
0.5	0.461	0.183	0.111
0.45	0.442	0.173	0.104
0.4	0.419	0.162	0.097
0.38	0.410	0.158	0.094
0.36	0.400	0.153	0.091
0.34	0.389	0.148	0.088
0.32	0.378	0.142	0.085
0.30	0.367	0.137	0.081
0.28	0.355	0.131	0.077
0.26	0.342	0.125	0.074
0.24	0.328	0.119	0.070
0.22	0.314	0.112	0.066
0.20	0.299	0.106	0.061
0.18	0.282	0.098	0.057
0.16	0.265	0.091	0.052
0.14	0.245	0.082	0.047
0.12	0.224	0.074	0.042
0.10	0.201	0.064	0.036
0.08	0.176	0.054	0.030
0.06	0.146	0.043	0.024

To find the rate of burning M corresponding to given values of n, T_m, C, Q, A, B, P, and W, we calculate the right side of equation 30 and then solve for ψ by trial and error. Since $\psi = C/D$, we have finally

$$M^2 = \frac{\lambda B(PW)^2\psi e^{-A/RT_m}}{C(RT_m)^2(1+n)^2} \tag{31}$$

Since equation 30 does not contain the pressure P, for a given reaction, ψ is independent of P, and the rate of burning is therefore proportional to the pressure.

In using these equations one point should be noted. The gas constant R appears from two sources: as it enters from equation 21, the equation of state of the gas, it has to be in the units

$$\frac{\text{Unit of pressure} \times \text{unit of volume of a mole of gas}}{\text{Unit of temperature}}$$

In other words, R is in the appropriate mechanical units. The activation energy A is conventionally given in heat units, as calories per mole, and so the R associated with the A is in heat units, namely, calories per mole per degree. To prevent possible confusion, we have written all the formulas in terms of R and A/R, so that R is in mechanical units where it stands alone; in A/R, which has the dimensions of temperature, A and R can be in any consistent units; normally heat units would be used.

The relation between ϵ and T in the second approximation is

$$(1-\epsilon)g_1\left(\frac{\psi}{1-\epsilon}\right) - \frac{2n(1-\epsilon)^2}{1+n}g_2\left(\frac{\psi}{1-\epsilon}\right) +$$
$$\left(\frac{n}{1+n}\right)^2(1-\epsilon)^3 g_3\left(\frac{\psi}{1-\epsilon}\right) = \frac{CT_m}{Q}\cdot\frac{RT_m}{A}\left(1-e^{A/RT_m - A/RT}\right) \tag{32}$$

For any set of values of A, T_m, Q, C, and n, equation 30 gives ψ, which can be used in equation 32 to find the T corresponding to any given ϵ. The error in the (ϵ, T) curve is small: a typical comparison with a numerical integration carried out with the accurate M showed that ϵ was too large by 3 per cent at $\epsilon = 0.5$, and the error was everywhere of the same amount except at low temperatures. Here T tends to zero as the ϵ of the approximate solution tends to zero, whereas the numerical integration had been started with $\epsilon = 0$ at a "surface temperature" greater than zero.

This (ϵ, T) relation can be used to find a value of M that is several per cent better than the second approximation itself. To do this we choose ϵ_1 and ϵ_2 in the neighborhood of 0.4 and 0.6, respectively, and such that $\psi/(1-\epsilon_1)$ and $\psi/(1-\epsilon_2)$ occur in Table 2.1. Equation 32 gives the corresponding temperatures T_1 and T_2 and, hence, allows one to estimate $d\epsilon/dT$ at $T = \frac{1}{2}(T_1 + T_2)$. Substitution into equation 23 gives M.

When the (ϵ, T) relation has been found, this can be used in the equation of heat conduction 19 to give the (x, T) relation. This supplies the scale of distances for the variation of ϵ and T. Let the origin of x be taken at a temperature T_s. Then,

$$x = \int_{T_s}^{T} \frac{\lambda\, dT}{M[Q(1 - \epsilon) + C(T - T_m)]} \tag{33}$$

where ϵ is expressed as a function of T. In the special case considered previously and in most possible cases, x will tend to infinity as T tends to T_m and to minus infinity as T tends to T_0. Theoretically, therefore, the reaction zone is of infinite thickness, though most of the reaction occurs in a small distance. To obtain a measure of the thickness it is convenient to take the distance between the points where $\epsilon = 0.1$ and 0.8.

A first approximation to the (ϵ, x) relation can be found from the first approximation to the (ϵ, T) law. From equations 19 and 25,

$$\frac{d\xi}{dx} = -\frac{MD}{\lambda}\xi^2 \tag{34}$$

with the solution,

$$\frac{1}{1 - \epsilon} = \xi^{-1} = \frac{MD}{\lambda}x + \text{constant}$$

and therefore an infinite flame thickness.

To get a second approximation it is easiest to tabulate ϵ as a function of T, given by the second approximation, and then to carry out a numerical integration of equation 33.

In the first approximation the "thickness of the flame" is proportional to

$$\frac{\lambda}{MD} = \frac{RT_m(1 + n)}{PW}\left(\frac{\lambda\psi}{CB}\right)^{\frac{1}{2}} e^{A/2RT_m} \tag{35}$$

As an example of the kind of result obtained, we show in Fig. 2.7 the values of ϵ and T as functions of distance through a reaction zone at 10 tons/sq in. pressure. The activation energy is 25 kcal/mole; this and other data are typical of those used in the application to propellant. In this case the (ϵ, T) relation was found by numerical integration of equation 24, and x was then calculated from equation 33. As boundary condition at the cool side of the flame, it was assumed that $\epsilon = 0$ at 750°K, though the diagram makes it clear that $d\epsilon/dT$ is so small in this region that the exact temperature assumed is of no importance. Actually a change of 200° in the temperature at which $\epsilon = 0$ produced in a typical example a decrease of only 1 per cent in the rate M.

Figure 2.7 can be used at other pressures. For it can be shown that for a second-order reaction rate the distance between two assigned values of ϵ or temperature is inversely proportional to the pressure. Hence the diagram can be regarded as valid for any pressure P tons/sq in., giving ϵ and T as functions of $xP/10$.

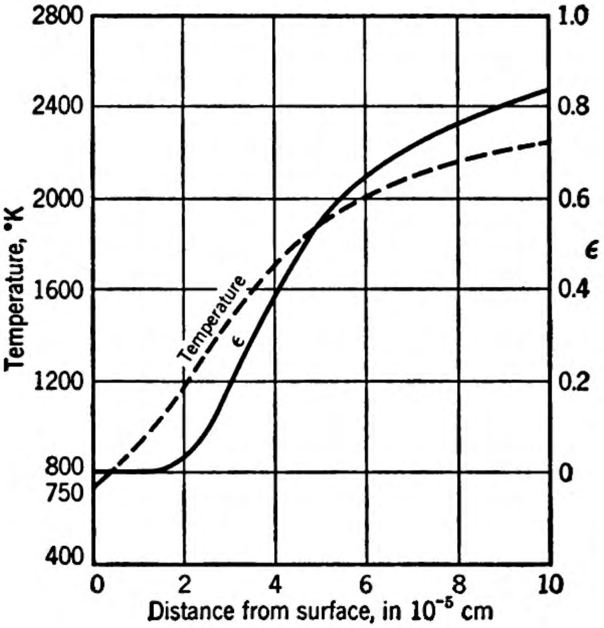

FIG. 2.7 The variation of temperature and degree of reaction in the reaction zone of a typical propellant burning at 10 tons/sq in., from the theory neglecting diffusion. British Crown copyright reserved.

We shall now explain how, by combining parameters in the general equations, one may obtain the exact dependence of the rate on certain parameters without finding an exact solution. The process is applicable to other forms of the reaction rate, though, of course, the results may be somewhat different.

We have to solve

$$\frac{M^2}{\lambda B(PW)^2}\frac{d\epsilon}{dT} = \frac{(1-\epsilon)^2 e^{-A/RT}}{(RT)^2(1+n\epsilon)^2[Q(1-\epsilon)+C(T-T_m)]} \qquad (36)$$

and the solution must fit the boundary conditions that $\epsilon = 0$ when $T = T_0$ and $\epsilon = 1$ when $T = T_m$. These conditions determine the value of the parameter $M^2/\lambda B(PW)^2$, which we may regard, therefore, as a function of the other parameters A, Q, n, C, and T_m. To get the (ϵ, T)

relation the value of the parameter $M^2/\lambda B(PW)^2$ must be inserted in equation 36, and this must be integrated; hence the (ϵ, T) relation depends on M, λ, P, W, and B only through the combination $M^2/\lambda B(PW)^2$, which is itself determined by A, Q, n, C, and T_m. Using this relation in

$$\frac{\lambda}{M}\frac{dT}{dx} = Q(1 - \epsilon) + C(T - T_m)$$

we get the result that $M(x_1 - x_2)/\lambda$ (where x_1 and x_2 are the positions with given temperatures T_1 and T_2) must depend only on A, Q, n, C, T, and T_1 and T_2. Hence, we have

$$M = K_1 PW(\lambda B)^{1/2}$$

and

$$x_1 - x_2 = \frac{\lambda K_2}{M} = \frac{\lambda K_3}{PWB^{1/2}}$$

where K_1, K_2, and K_3 depend only on A, Q, n, C, and T_m (and T_1 and T_2 in the case of K_2 and K_3). These quantities remain fixed in the case of a given reaction when only the pressure is varied, and in this instance the linear dimensions of the reaction zone vary inversely as the pressure.

For a reaction zone typical of those encountered in the application to propellant, the distance between the planes where the reaction is 10 and 80 per cent completed is about $8 \times 10^{-4}/P$ cm (where P is the pressure in tons per square inch). This distance is least for reactions with high final temperatures, though the variation is only moderate; for two propellants with final temperatures of 2000 and 3000°K the widths of the flame were found to be in the ratio of 1:0.7.

Although in this reaction the flame equations can be integrated by the approximate process already given, this is not possible with all the forms of reaction rate that one may wish to study. To take only one instance, the effect of the variation of thermal conductivity with temperature has to be investigated to help one to choose a suitable mean λ for the simpler example. The basic equation is here

$$\frac{d\epsilon}{dT} = \frac{\lambda B(PW)^2(1 - \epsilon)^2 e^{-A/RT}}{(MRT)^2(1 + n\epsilon)^2[Q(1 - \epsilon) + C(T - T_m)]} \tag{37}$$

or possibly some more complicated set. This can be integrated by a step-by-step process, for any assumed value of M. Starting from one of the boundary conditions, the solution can be carried sufficiently near to the other extreme of the reaction zone, to see whether the solution satisfies the other boundary condition. For example, suppose that the integration has been started at the cool side of the flame, in fact, at the surface of the propellant, where ϵ is practically zero and $T = T_s$. If M is less than a certain critical value, dT/dx becomes negative after a certain value of T has been reached in the integration. $d\epsilon/dx$ is still positive, so that, beyond the point where $dT/dx = 0$, ϵ continues to increase, but T decreases and never attains T_m. This is not a physically satisfactory form for the reaction zone, for it does not have the essential feature of the actual zone, that the temperature rises to the value corresponding to complete reaction. For large M the solution has the property that $d\epsilon/dT$ is so small that, when the solution has reached $T = T_m$, ϵ has not attained unity. This solution too is not physically satisfactory. There is one value of M for which the solution ϵ tends to unity as T tends to T_m. This solution is the reaction zone that would be set up in steady burning (if our equations were complete descriptions of the phenomena).

When T_m is of the order of 2000°K, steps of 100°K are convenient for the integration of the differential equation. For flames without diffusion it has been found better to start the integration of the equations at the cold side of the flame. In more complicated cases, such as have been studied recently by Professor Hirschfelder and his collaborators, it appears to be essential to start at the hot side, where unfortunately there is a singularity. For details of the methods used to get away from the singularity, we must refer to the series of papers from this group.[40]

The formulas needed for the numerical integration of differential equations are given in Appendix A. The only special point about the flame equations is that it is essential to work the computation with T as the independent variable; if ϵ were used as the independent variable, slight errors in predicting T for the next step would lead to large errors in $dT/d\epsilon$, because of the presence of $e^{-A/RT}$, and the step would have to be reworked an unusually large number of times.

Tests with thermal conductivities obeying Sutherland's law have shown that the rate of burning is the same as that given by a constant λ whose value is appropriate to a temperature somewhat above the middle of the temperature range in the flame. The conductivity at any point depends on the composition of the gas at that point: that is, on ϵ. The reactants have higher molecular weight than the products, and the conductivity is least at the cool side of the zone. Numerical solutions have shown that, for rates from this simple theory to be correct to a few per cent, it is sufficient to take an average of the initial and final conductivities as the constant of λ. Of course, the (ϵ, T, x) relations are not accurately reproduced by any constant conductivity, but this is not usually of any great importance, and the error is not large.

---

[40] Hirschfelder and Curtiss, *Third Symposium on Combustion, Flame, and Explosion Phenomena* (1948), p. 121; Henkel, Spaulding, and Hirschfelder, *ibid.*, p. 127; Henkel, Hummel, and Spaulding, *ibid.*, p. 135; Hirschfelder and Curtiss, *J. Chem. Phys.*, **17** (1949), 1076.

2.34 Application to the burning of propellant

It is assumed that the controlling rate in the burning of a colloidal propellant is the rate of a gas reaction going on between the products of the initial decomposition of the propellant. Passing through the system normal to the propellant surface, we start with unreacted propellant at the initial temperature; there is a steep rise of temperature as we near the surface and, consequently, a decomposition into intermediate products. These are assumed to be of fairly low molecular weight and therefore form a vapor phase, in which the slow controlling reaction takes place. Since the rate of burning of propellant is roughly proportional to the pressure, we must suppose that we are dealing with a second-order reaction.

If the main reaction is not proceeding appreciably at the temperature of the surface (compared with its rate in the hotter parts of the flame), then the rate of burning will be independent of the surface temperature. The initial temperature of the propellant affects the rate of burning through its effect on T_m, not because it is the point where $\epsilon = 0$. These remarks can be seen to follow from the analysis of the preceding section; the lower boundary condition that $\epsilon = 0$ when $T = T_0$ is actually used in the form: $\epsilon = 0$ when e^{-A/RT_0} is negligible, and we should get exactly the same results if we took $\epsilon = 0$ at any other temperature such that $e^{-A/RT}$ is negligible. The rate of burning is not affected by the temperature variation before the controlling reaction has commenced appreciably, provided the same over-all energy conditions hold. Hence, since we are assuming the slow reactions to take place entirely in the gaseous layer, it is the velocity of propagation of this flame that determines the rate of burning of the propellant. The surface temperature will adjust itself to supply the necessary gases at this rate, provided that this is possible at some temperature below the range in which the main reaction velocity becomes appreciable.

The variation of temperature in the solid before substantial decomposition occurs is governed by

$$\frac{\lambda_s}{M}\frac{dT}{dx} = C_s(T - T_0) \tag{38}$$

where C_s is the specific heat of the solid at constant pressure and λ_s is its thermal conductivity. If the primary decomposition in the solid evolves or absorbs only a small heat, equation 38 will still be an approximation. Using it as such, and taking a surface temperature T_s and a mean C_s, we have

$$\frac{T - T_0}{T_s - T_0} = \exp \frac{MC_s x}{\lambda} \tag{39}$$

where x is measured from the surface into the solid. For propellant λ_s is of order 8×10^{-4} cal/sq cm/(deg/cm). Taking T_s as 750°K and T_0 as 300°K, we find that for a typical propellant at P tons/sq in. the temperature has fallen to 315°K at a distance of no more than $4 \times 10^{-3}/P$ cm from the surface. Thus, the "hot zone" in the propellant is rather larger than the effective breadth of the reaction zone outside, and their ratio is independent of pressure.

By writing down the equation for $d\epsilon/dx$ from the unimolecular primary decomposition of nitroglycerine or nitrocellulose, the equation between ϵ and T can be set up just as in the preceding section. It can be shown in this way that the primary decomposition is almost complete at 750°K. The argument is only rough, since the experimental knowledge of the decomposition refers to low temperatures and small values of ϵ. However, it can be concluded that the propellant decomposes long before it can reach a temperature at which unreacted propellant would sublime or vaporize.

In the previous section we have assumed that the pressure is constant throughout the flame. This is certainly true for the reaction outside the propellant. The velocity with which the products leave the surface is

$$U_m = \frac{\text{rate of burning} \times \text{density of solid}}{\text{density of products}}$$

which is almost independent of pressure and is of order 1 meter/sec. The pressure drop across the flame is equal to the increase of momentum per unit time in the material passing through the unit cross section of the zone and so is roughly $U_m \times$ rate of burning $\times$ density of the propellant. The fractional pressure drop is almost independent of pressure and never more than about 10^{-5}.

As disposable constants in the theory we have (1) the molecular weight of the intermediate products, which is probably of the order of 75; (2) the fraction of the total heat of reaction liberated in the gas phase; (3) the activation energy A. The heat of the controlling reaction is not known but must be a substantial part of the whole heat of reaction. The activation energy A has a strong effect on the magnitude of the rate of burning, and there is little chemical evidence concerning its value.

The other quantities appearing in the equations of the flame zone can be calculated from the propellant composition. For example, the effective specific heat and thermal conductivity can be obtained from the known final products and assumed intermediate products; the latter choice is not of great importance for the calculation. Finally, an upper limit for the kinetic reaction constant B can be found from the kinetic theory of gas reactions. This upper limit must be reduced by a factor α, which allows for the fact that the intermediate products are a mixture of some complexity. Only part of the collisions will take place between a molecular pair that can take part in the controlling reaction. The result is

$$B = \frac{4N\sigma^2}{W\alpha}\left(\frac{\pi RT'}{W}\right)^{1/2}$$

where σ is the collision diameter of the reactants, N is Avogadro's number, and T' is a mean temperature in the reaction zone.

It was found that the closed-vessel rates of burning of a number of propellants could be represented by taking $\alpha = 100$, an implausibly large value, which was necessary to keep the apparent activation energy approximately the same for all the propellants. A later theory included diffusion, which reduces the rate of burning of a given gas mixture without altering the dependence on pressure. With this theory a value of $\alpha = 10$ gave satisfactory results. This amounts to taking one tenth of the collisions as suitable for the controlling reaction; part of this may of course be a steric hindrance factor. The mean activation energy for seven propellants not containing mineral jelly was 26.4 kcal/mole, which is reasonable for reactions between unsaturated organic molecules. The activation energies had a total spread of 1.8 kcal/mole, and it was shown that this range was not much larger than that introduced by unavoidable inconsistencies in the other constants used. Table 2.2 gives a comparison of observed and theoretical rates, the latter being calculated from a single set of constants for all the examples.

TABLE 2.2 COMPARISON OF OBSERVED AND THEORETICAL RATES OF BURNING

All rates are in inches per second for a single surface, at 10 tons/sq in.; initial temperature 300°K. $A = 26.4$ kcal/mole; $\alpha = 10$.

Propellant	T_m, °K	Theory with Diffusion	Observed
1	3050	8.0	7.9
2	3050	8.0	7.6
3	2700	6.8	5.9
4	2500	5.7	5.0
5	2250	4.1	3.9
6	2230	3.6	4.2
7	1900	2.6	3.2

Details of the estimation of specific heats, thermal conductivities, and diffusion coefficients in the flame zone need not be given here, though it should be mentioned that the molecular weight of the intermediate products was taken to be three times that of the final products. These were calculated from the thermochemical tables given in the next chapter. It was assumed also that all the heat of the process was liberated in the controlling reaction. The relative rates for different propellants are not sensitive to this assumption.

The single-reaction theory is inadequate at pressures below 2 tons/sq in., where reactions in the solid have important effects.

Transfer of energy through the flame by radiation has been neglected in this theory. Experiment has shown the effect to be of some importance under rocket conditions, but at gun pressures the effect on the rate is believed to be only a few per cent.

2.35 The theoretical rate of burning at high pressures

The calculations in this and the next two sections refer to the set of constants that represent SC. This was chosen because more physical data were available for this than for the other propellants and also because its temperature lies in the middle of the range for modern propellants. The experimental results are much the same for all colloidal propellants, and there seems to be no theoretical reason why the results should vary considerably from one propellant to another.

1. *Increase of density of propellant.* The theory gives M, the rate of burning in grams per second per square centimeter of true area. The rate used in interior ballistics is an apparent rate, based on the area at atmospheric pressure. In other words, the practical rate overlooks the reduction of area when burning under high pressures. This practical rate is, of course, the more convenient one for interior ballistics, and we must correct the theoretical rate before comparison. This has been pointed out by Dr. H. H. M. Pike.

Let β be the average compressibility of the propellant, up to pressure P. Provided there is isotropic compression under hydrostatic pressure, the surface of the propellant will be reduced by the factor $1 - 2\beta P/3$. The compressibility of this propellant up to 10 tons/sq in. is $\beta = 7.7 \times 10^{-11}$ cgs, which is comparable with that of a normal organic liquid. The compressibility decreases rapidly with pressure. It is estimated that at 20 tons/sq in. the apparent rate of burning will be about 12 to 15 per cent below the theoretical rate. It is likely, in fact, that the orientation of the fibers in extruded propellant will make the stick less compressible along its axis than perpendicular to it. In the extreme case when there is no reduction of length but only a decrease of the diameter of the cord, the decrease of area is 8 to 10 per cent. This anisotropy is probably greater than that actually present and shows that in any case the apparent rate of burning will be of the order of 10 per cent less than the theoretical rate, at 20 tons/sq in.

2. *Covolume effects.* The theory assumes that the gases in the reaction zone obey the perfect-gas laws. At high pressures this is a bad approximation. For example, at 15 tons/sq in. the gas density just outside the solid is predicted by the perfect-gas law to be greater than the density of the solid propellant itself. This is a region of the flame in which wide deviations from reality are fortunately unimportant in their effect on the rate of burning. Nevertheless, the deviations from the perfect-gas law in the important region of the flame can cause considerable changes in the rate of burning at pressures of this order. Computations have been carried out with the abbreviated form of Van der Waals' law

$$P(V - b) = RT\frac{1 + n\epsilon}{W} \tag{40}$$

which is conventional in interior ballistics. This more complicated equation of state prevents application of the usual method of successive approximations. Numerical integration has been carried out for a bimolecular reaction, neglecting diffusion. It was found that at 20 tons/sq in. the rate fell about 30 per cent below that calculated from the "rate $\propto$ pressure" law. The order of magnitude of the effect will not be altered by diffusion.

That the effect of a covolume is to reduce the rate of burning can be seen from the result that at very high pressures the rate would tend to a finite limit, if the equation of state given previously were accurate at such pressures.

3. *Thermal conductivity.* In the theoretical work it was assumed that the thermal conductivity of the gas in the reaction zone was independent of pressure. This is true at pressures of the order of some atmospheres. The thermal conductivity of a gas must approach that of a liquid as the pressure is raised; that is, it must increase. There appear to be few experimental data bearing on this point. Enskog has predicted a dependence on pressure, roughly parallel to the viscosity. The theory has never been tested for conductivity, but it works well for the viscosity, at pressures up to some thousands of atmospheres at room temperatures. We shall therefore use it to estimate the order of magnitude of the effect on the thermal conductivity. The formulas are taken from chapter 16 of Chapman and Cowling.[41]

---

[41] Chapman and Cowling, *The Mathematical Theory of Non-uniform Gases* (Cambridge, 1939).

Let λ_0 be the thermal conductivity at low pressures. Then Enskog has shown that the conductivity at any other pressure and the same temperature is

$$\lambda = \lambda_0 \left[\frac{1}{\chi} + \frac{6}{5} bp + 0.757(bp)^2 \chi \right] \tag{41}$$

where bp is the ratio of the covolume of the gas to the total volume, and χ is a factor that represents the increase of the probability of a collision at high densities and that can be expanded as

$$\chi = 1 + \tfrac{5}{8} bp + 0.29(bp)^2$$

for small values of bp. Inserting this expansion in equation 41, we get

$$\frac{\lambda}{\lambda_0} = 1 + 0.575bp + 0.86(bp)^2$$

The products of burning have a covolume close to 1 cc/g. Their molecular weight is about 25, and in the important region of the flame their temperature is about 2000°K and their pressure P tons/sq in. This makes the density $2.32 \times 10^{-2}P$ g/cc, and $bp = 2.32 \times 10^{-2}P$, and so the percentage increase of the thermal conductivity is

$$1.31P + 0.042P^2$$

which is 43 per cent at 20 tons/sq in. This increases the rate of burning by 20 per cent.

4. *Pressure-effect on specific heat.* The specific heat of the gases increases with pressure. This alters two quantities in the equations: it increases the average specific heat, and it reduces the maximum temperature T_m. The rate of burning is reduced. The magnitudes of these effects have been calculated for SC, from the tables of pressure corrections given in the next chapter. It has been found that this correction reduces the rate of burning at 20 tons/sq in. by 20 to 30 per cent.

5. *Change of reaction rate.* The formulas we have used for theoretical reaction velocities refer to molecular collisions in a dilute gas. At high pressures the environment of any molecule tends to become less impermanent, and the motion of any one turns from random motion with infrequent collisions to an oscillation in a "cell" with occasional escapes to another. This would be expected to alter the number of intermolecular collisions effective in producing reaction. However, theoretical investigations have led to the conclusion (Fowler and Guggenheim) [42] ". . . that the rate of bimolecular reaction in dilute solution may be

---

[42] Fowler and Guggenheim, *Statistical Mechanics* (Cambridge, 1939).

expected in general to be about the same as that for the same molecules at the same concentration in a gas." This is applicable to our case and shows that the reaction rate will not alter by a *large* factor at high pressures. Changes of, say, 50 per cent are not excluded by this general statement. Such a change would be expected to be usually an increase; that is, it would probably increase the rate of burning.

6. *Diffusion.* At normal pressures the diffusion coefficient D is known, from both theory and experiment, to be inversely proportional to the pressure P. This is assumed in the theory with diffusion, in proving that the rate of burning is proportional to the pressure. At high pressures the diffusion coefficient must depart from this assumed law, but there appears to be no experimental evidence of this. A decrease of DP seems most likely, from a theoretical discussion of Fowler and Slater.[43] A 10 per cent decrease of DP would increase the rate of burning by 10 to 15 per cent.

To summarize these effects, we may say that on balance they tend to reduce the ratio of (rate/pressure) at high pressures, by an amount which can be of the order of 20 per cent at 20 tons/sq in. The observed effect is the sum of a number of effects with both signs, and there is no reason why all propellants should show the same behavior at high pressures. A rate of burning increasing faster than the pressure is not excluded.

2.36 The influence of the initial temperature of the propellant

A rise of the initial temperature of the propellant has two effects: it increases the surface area of a given stick of propellant, and it raises T_m, the final temperature of the products.

1. *Surface area effect.* This must be added to the theoretical result before comparison with the practical result, for just the same reason as in part 1 of the previous section. The rate of change of density with temperature is known for SC, and, if we assume that the coefficient of linear expansion is the same in all directions, the area of a stick increases at the rate of 0.4 per cent per 10°C. In a highly anisotropic case in which there were no expansion along the axis of the stick, the area would still increase by 0.3 per cent per 10°C. The actual behavior, which is strongly anisotropic, lies between these two extremes.

2. *Change of T_m.* The rise of T_m can be obtained from the specific heats (at constant pressure) of products and solid propellant. It has been found that for the propellant under consideration the theoretical rate of burning increases by 2.2 per cent per 10°C.

---

[43] Fowler and Slater, *Trans. Faraday Soc.*, **34** (1937), 81.

The total rate of increase with initial temperature is therefore about 2.6 per cent per 10°C. The experimental results give 3 to 4 per cent for this propellant in cord form.

2.37 Experimental knowledge of the rate of burning

This comes from two sources: pressure-time curves in closed bombs and in chambers with nozzles venting to the open air. These are usually called closed vessels and vented vessels, respectively. Pressure-time curves in guns are not by themselves of great value, since the phenomena in the gun are more complicated than those in a fixed space. For the latter the analysis is simpler, but it has to be admitted that the flow of gas over the propellant burning in a gun chamber is not reproduced in the closed vessel. Thus closed-vessel rates are valuable for comparing different batches of nominally the same propellant, while they give but an indifferent fit to gun ballistics. The leeway is taken up by adjusting factors of one form or another. This point will be seen in chapters 4 and 5.

The vented vessel can be arranged to subject the propellant to "gas erosion" as well as to a nearly constant pressure. Almost all the work on rocket propellant has been done in vented vessels, but these have not yet been used very much at gun pressures. However, the loss of energy through the nozzle of a vented vessel can be duplicated in the closed vessel by increasing the heat loss well above the normal value. Developing this idea, Dr. Pike has invented a technique that needs only an orthodox closed vessel, is applicable from 200 lb/sq in. up to any pressure the vessel will stand, and is more accurate, particularly at low pressures, than the normal method. Details have not yet been published.

The analysis of a pressure-time curve in a closed vessel is so obvious that it need not be written out here. Correcting the peak pressure for heat loss (see § 3.11), one proceeds to correct the pressure at earlier times, a highly arbitrary process which is often omitted and which is always responsible for most of the error in the rate of burning at low pressures. Then, using also the equation of state of the products, one obtains the relation between the fraction of charge burnt ϕ and the time t.

Let this relation be

$$D \frac{d\phi}{dt} = f(\phi, P) \tag{42}$$

where D is a mean size representing the effective dimension of the propellant grain; for example, for a cord charge D would be the radius or diameter. We have to split equation 42 into factors representing the shape of the propellant and its rate of burning as a function of pressure. If

$$D\frac{d\phi}{dt} = B(P)g(\phi) \tag{43}$$

then

$$D\int\frac{d\phi}{g(\phi)} = \int B(P)\,dt + \text{constant} \tag{44}$$

Thus, if we take charges of the same shape and composition and plot $D\int d\phi/g(\phi)$ against $\int B(P)\,dt$, all such curves should be part of a single curve. This is the Schmitz process,[44] long classical in this field.

For simple shapes this process is very useful. When we deal with shapes that have perforations, we find perturbations, which indicate that the factorization in passing from equations 42 to 43 is not permissible. In this event it seems to be reasonable to use $B(P)$ derived from other shapes and to throw the remaining pressure variation into $g(\phi)$. We have mentioned in § 2.22 how these effects change $g(\phi)$.

It has long been conventional to use

$$B(P) = \beta P^{\alpha} \tag{45}$$

with parameters α and β depending only on the composition of the propellant. In the early days the value of α varied between ½ and 1. For deriving analytical solutions, $\alpha = 1$ is by far the most convenient. The values accepted now for normal propellants are, at gun pressures, between 0.9 and unity.[45] With a suitable value of α in this range it is possible to fit, to within a few per cent, the rate from 5 to 25 tons/sq in.

At lower pressures the behavior deviates from the high-pressure equation 45, and there is more variety between different propellants. For example, a plot of log B against log P for one propellant may show a point of inflection, whereas for another there may not be any inflection within an attainable range. This is consistent with the increasing sensitivity to the physical state of the propellant and to the scale of any inhomogeneities. The explanation is almost certainly the rising importance, as we go to lower pressures, of reactions which under gun pressures are not rate-determining. The combination of several reactions in series can give rise to a wider variety of behavior than a single

[44] Schmitz, *Artill. Monatshefte*, **84** (1913), 482; **86** (1914), 85.

[45] One α of 1.02 is so little above unity that the difference is not significant. Values of α between 0.8 and 0.9 were obtained in early lots of certain propellants. With increased experience in their production, α rose to 0.9. This is taken to show partial segregation of one component in the early production.

reaction, and this explains the individual peculiarities found below 2 tons/sq in.

If a formula of type 45 is to be used at rocket pressures, α must be less than at gun pressures. For example, a propellant with $\alpha = 0.96$ at 10 tons/sq in. gave, below 3 tons/sq in., a steadily decreasing α, which had fallen to roughly 0.5 at 1800 lb/sq in.[46]

This fall of α at low pressures is essential to the use of solid propellant in rockets. For the rate of flow through the nozzle of a rocket is proportional to the pressure in the chamber, and, if α were unity, the rate of generation of gas would also be proportional to pressure. Thus any steady pressure attained in the rocket would be equally a solution if multiplied by any factor. The equilibrium would be sensitive to disturbances, and the behavior would vary greatly from one round to another. If α is less than unity, the equilibrium is stable, and, the further α is from unity, the better the propellant for rocket work. A pressure exponent of 0.9 would be unacceptable in most though not in all rockets. An α of 0.7 would be much better.

The formula,

$$B(P) = \beta(P + P_1) \tag{46}$$

where β and P_1 are constants depending on the composition, has found support from French ballisticians; Muraour[47] has attempted a theoretical proof, and Dupuis and Chalvet[48] use such a formula to represent their closed-vessel results. P_1 is positive and of the order of 1 ton/sq in. The very accurate experiments on a British propellant, mentioned previously, can be fitted to within a few per cent between 0.8 and 3.5 tons/sq in., by equation 46 with $P_1 = \frac{1}{3}$ tons/sq in. For most propellants equation 46 is nearer the truth than an index law,[49] with P_1 between 0.2 and 3 tons/sq in. Unfortunately, equation 46 is inconvenient in the interior ballistic equations.

Some colloidal propellants can be made to detonate under strong confinement and a violent initiating impulse. This has sometimes led to fears that propellant might detonate at high pressures in a gun. This would be most likely in small arms, where the rate of rise of pressure is greatest. The possibility must be taken as unlikely, and there is no certain evidence that the process has ever occurred in a gun. The burning of propellant has been explored up to about 35 tons/sq in. There is no theoretical reason to expect any striking change in the burning law at higher pressures. Nevertheless, an experimental check would be interesting, and one might have been obtained if the recent war had lasted longer: in connection with the German development[50] of a gun to work at 100 tons/sq in., a study of burning at such pressures was to have been carried out in a closed vessel during 1945. It is interesting to note also that high explosives *burn* at speeds that are comparable to those of propellants.

---

[46] This latter value of α is what one would obtain from theory if the rate were determined by a single first-order reaction.

[47] Muraour, *Comp. rend.*, **192** (1931), 227.

[48] Dupuis and Chalvet, *Mém. artillerie franç.*, **18** (1939), 37.

[49] I am indebted to Dr. H. H. M. Pike for information on this point. Mansell, *Phil. Trans. Roy. Soc. (London)*, **207A** (1907), 243, used such a law to represent his early experiments.

The dependence of the rate of burning on the initial temperature is usually fairly linear over the range, 0 to 120°F, most important in practice. The rate increases by about 3 to 4 per cent for a rise of 10°C. The temperature coefficient does not vary greatly from one propellant to another, though there is some tendency to be biggest for "hot" propellants. The coefficient is substantially less in shapes that have narrow perforations, such as multitubular grains. This is believed to be due to the "erosion" process in the perforations having a different temperature coefficient from the normal burning mechanism.

2.4 "Erosion" of propellant

The excess pressure inside tubes of burning propellants and the more rapid burning at the center of the tube were noticed early, for example, by Mansell.[51] The more rapid burning just inside the ends of the tube was not mentioned by Mansell, probably because he used a "hot" propellant; as will appear later, the effect is least in such cases. The effect has been remarked several times, chiefly in its bearing on the true form function (see Winter[52]), but it was not until the matter became important in the design of high-performance rockets that the effect was studied seriously. It has been shown experimentally that the rate of burning of a propellant surface is increased by gas flow parallel to the surface. In a given geometrical setup, for instance in a rocket chamber with given dimensions, the effect can be represented as a function of velocity. This function applies only to the given setup and propellant. The same propellant burning in a different chamber gives an "erosion law" with a fairly small though significant difference. It is thought that the increase in the rate of burning is really a function of the turbulence at the point considered. For a simple layout this is related to the velocity at the point; the relation does, however, depend on the geometry.

---

[50] Although the project was directed by the German Army High Command, the essential high-pressure technique was contributed by a Frenchman, J. Bassett. When the Germans retreated from Paris in 1944 Bassett fled to Switzerland, while the plans and the gun were taken to Germany. Work on the gun continued, apparently even after the great "project purge" of late 1944.

[51] Mansell, *Phil. Trans. Roy. Soc.* (*London*), **207A** (1907), 243.

[52] Winter, *Mém. artillerie franç.*, **18** (1939), 775, esp. p. 834.

A typical propellant shows little "erosion" until the transverse flow reaches 200 to 300 ft/sec. There is a rapid increase at higher velocities. A propellant with an explosion temperature (no work done by products) of 3000°K can have its rate increased by 15 per cent at 500 ft/sec. Cooler propellants show even more striking effects.

The rate of burning may be written as the product of the rate at zero velocity (a function of pressure) and an "erosion factor" depending only on the velocity (in a given setup). The erosion factor so defined is a slowly varying function of pressure, for colloidal propellants.

"Erosion" occurs no matter what the nature of the gas that is flowing parallel to the propellant surface. The burning propellant is bathed in its own products, and these are set into transverse motion by the main stream. The hydrodynamical character of the transverse stream settles the flow in the products near the propellant surface but cannot alter the gas composition at the important distances from the surface. In practice, of course, the most common examples have only propellant products in the gas flow.

Very little is known about the variation of the erosion factor with the initial temperature of the propellant. It is very likely that the erosion factor decreases as the temperature increases.

2.41 A simple theory [53] of the erosion of propellant at gun pressures

We shall now consider propellant erosion, using the theory of ordinary burning sketched in § 2.33. Although no theory based on a single reaction appears to be adequate at rocket pressures, the results will probably be applicable to propellants in guns. However, the theory of § 2.33 neglected diffusion in the flame zone. This is permissible as an introduction to the subject of normal burning, the equations being simpler and qualitative results being largely unaltered. It can be shown, however, that diffusion makes a substantial difference in the theory of erosion. It seems best in this book to sketch the effects that are thought to cause erosion and, neglecting diffusion, to arrive as quickly as possible at such qualitative conclusions as have been confirmed by experiment.

In § 2.34 we slurred over the question of the nature of the propellant at the stage when, hot and partly decomposed, it is pouring out vapor into the flame. This omission was due in part to the evidence being mainly chemical, and well off the central line of interior ballistics. In any case, the question does not affect the theoretical rate of burning at gun pressures and zero transverse velocity.

---

[53] Corner, *Trans. Faraday Soc.*, **43** (1947), 635.

On the other hand, one can expect the erosion to depend on whether the surface layers of the decomposing propellant are solid or liquid. Most evidence points to the surface being a mush of intermediate products in a plastic if not a liquid state, and this will be swept along by high stream velocities. The whipping up of spray through the reaction zone would increase the rate of burning. We shall neglect this effect, which we expect to be small, but which emphasizes that the discussion here cannot give more than qualitative results.

To fix ideas, let us consider a large block of propellant, pierced by a long cylindrical cavity of circular section. The burning at the surface of this cavity will be studied. We shall calculate how turbulence increases the heat conductivity near the surface, and the resulting increase in the consumption of the flame. This we shall regard as the main contribution to the erosion of the propellant.

The first matter to be considered is the probable value of the Reynolds number. For flow in a cylindrical tube, Reynolds number is usually taken to be

$$R = \frac{\text{velocity} \times \text{radius}}{\text{kinematic viscosity}} \tag{47}$$

The kinematic viscosity ν is equal to μ/ρ, where μ is the ordinary coefficient of viscosity and ρ the density. Let us assume that the temperature and pressure of the gases are about 2500°K and 10 tons/sq in. If the kinematic viscosity is taken to be much the same as that of air at this temperature and pressure, its value may be found as follows: the viscosity of many gases varies with temperature according to a law closely represented by Sutherland's formula,

$$\mu \propto \frac{T^{3/2}}{T + C}$$

where C is a constant of the order of 100°K for light gases such as nitrogen. Viscosity is nearly independent of the pressure P, for small P, and in our rough theory we neglect the actual dependence. Hence, the kinematic viscosity can be taken to be proportional to

$$\frac{T^{5/2}P}{T + C}$$

Its value for air at 0°C is 0.132 cm^2/sec. Hence, the value at 2500°K and 10 tons/sq in. is about 3×10^{-3} cm^2/sec. As a typical radius we may take 0.04 in., and as a typical velocity 250 m/sec, about one quarter of the velocity of sound in propellant gases in a gun. The Reynolds number is then of the order of 10^6.

Such a high Reynolds number is sufficient to set up turbulence not only in the main flow but also in the layer near the boundary. We must consider, however, the distance down the conduit in which the turbulence is developing. For flow in a cylindrical channel with smooth entry, a laminar flow with a large Reynolds number R has a transition to turbulence within a distance

$$\frac{10^5}{R} \times \text{radius of channel}$$

This is of the same order as the radius in our example. After this transition to turbulent flow has taken place, a further distance is needed before the velocity distribution across the channel cross section takes up its final form. The distance has been calculated theoretically, assuming fully developed turbulence at the start, and has been measured experimentally. The experimental results are larger than the theoretical by a factor of about two. At $R = 10^6$, even the theoretical distance is 30 diameters. It must be concluded that the flow at any point in the conduit is not likely to be described accurately by the final velocity distribution in a long channel in which the flow has the constant Reynolds number appropriate to this point of the cavity. We use this approximation in this book; however, the reader may find it interesting to rewrite the theory to take into account the "inlet length" nature of the flow, by using experimental results for flow over a thin plate parallel to the stream (see chapter 10).

Most experiments on turbulence have been carried out in channels with smooth impermeable walls. In the kind of experiment we are considering there is an emission of gas from the walls. The velocity normal to the surface is fortunately small, of the order of 1 m/sec and almost independent of pressure. Over the greater part of the length of the channel, this velocity is certainly less than one tenth of the stream velocity at the important distance from the wall. It seems reasonable, therefore, to use the results of experiments on smooth impermeable walls.

2.42 Hydrodynamic considerations

There are three current theories of turbulence: Prandtl's momentum transfer theory; Taylor's vorticity transfer theory in its two forms (*a*) with symmetrical turbulence, (*b*) with isotropic turbulence; von Kármán's similarity theory.[54] The Prandtl momentum transfer theory is the most convenient to apply to the flow near a solid surface. The vorticity transfer theory does not give satisfactory results for the velocity distribution near a wall, which is just the region where the momentum transfer theory seems to work best.[55] We therefore use the latter theory, a description of which can be found in *Fluid Dynamics* (chapter V, especially § 81).[56]

The flow near the wall of a tube depends on the Reynolds number, and for a value of about 10^6 it has the following nature. There is a "laminar sublayer" next to the wall, in which the turbulent velocities perpendicular to the wall are small. It is obvious that the root-mean-square component of velocity perpendicular to the wall must tend to zero as the wall is approached.[57] In the "laminar sublayer" the Reynolds' stresses, which represent the transport of momentum across a surface due to the velocity fluctuations, are much less than the stresses caused by viscosity.

Outside this layer there is a transition region where the Reynolds' stresses are of the same order as the viscous stresses, both regions together forming the "viscous layer." Farther out lies the greater part of the stream, in violent eddying motion with negligible viscous stresses.

Information about the region near the wall can be obtained from the heat transfer from pipes to fluids. This work is summarized in *Fluid Dynamics,* page 654. The simplest model (Prandtl and Taylor) omits the transition zone and can be made to fit the experimental data by a suitable choice of the thickness of the laminar layer, provided the "Prandtl number" of the fluid is near unity.

This number is

$$\sigma = \frac{\text{kinematic viscosity}}{\text{thermometric conductivity}} = \frac{\mu C_p}{\lambda}$$

where λ is the thermal conductivity and C_p is the specific heat per unit mass. For air at 1 atm, σ decreases from 0.77 to 0.72 as the temperature rises from 0 to 300°C.[58] The Prandtl number σ is independent of pressure. In our problem σ is probably not very different from unity.

---

[54] These are fully discussed in vol. II of *Fluid Dynamics* (ed. Goldstein, Oxford, 1938), or Dryden, div. T, vol. VI of *Aerodynamic Theory* (ed. Durand, Berlin, 1936), p. 246, where the relation between the Prandtl and the Taylor mixing lengths is discussed. These will be referred to as *Fluid Dynamics* and Dryden.

[55] For the temperature distribution between rotating cylinders, see *Fluid Dynamics,* p. 663.

[56] See also Prandtl, div. G, vol. III of *Aerodynamic Theory,* subsequently referred to as Prandtl.

[57] Experiments on this point have been carried out by Fage and Townend, *Proc. Roy. Soc. (London),* **135A** (1932), 657.

We shall show later that the thickness of the laminar region in this model is much less than the distance from the surface to the middle of the flame.

A more detailed model has been used by von Kármán,[59] and the results are in better agreement with experiment when the Prandtl number is not near unity. In this model the laminar and turbulent regions are separated by a transition region with a modified velocity distribution. It will appear later that the flame zone lies mostly in the transition, partly in the laminar region.

Consider flow down a cylindrical channel of circular cross section, of radius r. Take the origin at the point in the surface where the rate of burning is required, with the x axis normal to the surface, and the y axis parallel to the axis of the channel. We are considering only the normal cross section Oxz. At any point in this plane the velocity of the stream down the conduit is U. This is a mean over a time long compared with the time scale of the turbulence but smaller than the time of a significant change in the flow. U is a function only of the distance from the axis of the channel. Let $\bar{U}$ be the average of U over the cross section, and let ρ be the density and C_p the specific heat at any point.

In discussing the flow in the flame zone, we may treat the wall as plane, since its radius of curvature is of the order of 1000 times the effective breadth of the flame.

In flow past an infinitely long plane wall with no pressure gradient, the shearing stress in the fluid is constant and equal to the shearing stress at the wall, the intensity of the wall friction, usually denoted by τ_0. It is convenient to introduce a velocity V_* defined by[60]

$$\tau_0 = \rho V_*^2 \tag{48}$$

(Prandtl, page 128). Let $\eta = xV_*/\nu$, which is a "dimensionless distance" from the wall, analogous to the use of Reynolds number as a "dimensionless speed."

Let the "mixing length" of the turbulence be l; this is the average length of path described by a small mass of the fluid before it mixes again with other masses. It is usually assumed in this theory that the "mixing length" is the same for the transport of both vector and scalar quantities, momentum and temperature. This does not always hold in practice, but experimental evidence shows that near a wall the two lengths are the same.[61]

---

[58] Dryden, p. 228.

[59] Von Kármán, *Proc. 4th Congr. Applied Mech.* (1934), 77.

[60] V_* is the same as the U_τ of *Fluid Dynamics*, ch. VIII, section III, where the flow through a channel is discussed on the momentum transfer theory.

Prandtl's theory assumes

$$V_* = l\left|\frac{dU}{dx}\right| \tag{49}$$

near the origin of our co-ordinates. For flow past a plane wall it is clear that l must be proportional to x, except in the laminar sublayer. Analysis of experimental velocity distributions indicates that, over the greater part of the cross section,

$$l = 0.4x \tag{50}$$

(Prandtl, page 140). This result and the constancy of V_* over the cross section can be taken as first approximations to the flow with a pressure gradient in a channel.

The relation between $\bar{U}$ and V is[62]

$$\bar{U} = V_*\left(2.5 \ln \frac{rV_*}{\nu} + 1.75\right) \tag{51}$$

To obtain V_* as a function of $\bar{U}$, this equation can be written as

$$\frac{r\bar{U}}{\nu} = \frac{rV_*}{\nu}\left(2.5 \ln \frac{rV_*}{\nu} + 1.75\right)$$

so that

$$V_* = \frac{\nu}{r} f\left(\frac{r\bar{U}}{\nu}\right) \tag{52}$$

where the function $f(R)$ satisfies the equation:

$$R = f(R)[2.5 \ln f(R) + 1.75] \tag{53}$$

We want an explicit form for $f(R)$ when R is near 10^6. Typical solutions of equation 53 are as follows:

f	R/f	R
10^4	24.8	2.5×10^5
10^5	30	3.0×10^6
10^6	36.3	3.6×10^7

These show that $f(R) \simeq R/30$ for a wide range of R near 10^6. Substituting in equation 52 gives

---

[61] Dryden, p. 249.

[62] Equation 22.21 of Prandtl, p. 143.

$$V_* = \frac{\bar{U}}{30} \tag{54}$$

It is convenient that the dependence on tube radius r and kinematic viscosity ν has vanished in this region of high Reynolds number.

We can now use equation 54 to obtain the dimensionless distances in our problem in terms of the mean velocity:

$$\eta = \frac{V_* x}{\nu} = \frac{\bar{U}x}{30\nu} \tag{55}$$

Theoretical calculations (§§ 2.33 and 2.34) on the structure of flames have shown that, for a typical case of decomposition at 10 tons/sq in., the value of x at the most important region in the flame is about 5×10^{-5} cm; if we take $\bar{U} = 250$ m/sec and $\nu \simeq 3 \times 10^{-3}$ cm^2/sec, we find that the important part of the flame is in the neighborhood of $\eta = 15$. The "flame thickness" and ν are both inversely proportional to P, so that this value for η is independent of the pressure.

The point $\eta = 15$ lies in a region where the heat transfer by conductivity and by turbulent mixing are of the same order of magnitude. The most detailed model used so far is that of von Kármán (*loc. cit.*), who distinguished three regions: (1) a laminar layer at the wall, with negligible turbulence; (2) a transition region with heat transfer by turbulence of the same order as that by conductivity; (3) a fully turbulent region extending over most of the channel. This division is only an approximation, but it gives good agreement with experimental results on heat transfer if the boundaries of the zones are taken at $\eta = 5$ and 30.[63] This shows that part of the flame lies in a region where turbulence can be neglected and that nowhere in the flame is heat transfer by turbulent mixing of paramount importance.

Up to this point we have found a relation between x the distance from the wall and η the hydrodynamical variable. To calculate the heat transfer by turbulent mixing we need also a formula for the mixing length near the wall. The result (equation 50), which is of the right form, is valid at high Reynolds numbers but only for large η, greater than 2500;[64] below this the ratio l/x becomes a function of the Reynolds number. However, equation 50 is certainly correct in order of magnitude. Von Kármán's treatment,[65] leads to a velocity distribution that can be shown to lead to

---

[63] A simpler two-zone model has been investigated by Takahasi, *Proc. Phys. Math. Soc. Japan*, **21** (1939), 672, who concluded that the transition ought to be taken at $\eta = 8$.

[64] Prandtl, p. 141.

[65] *Fluid Dynamics*, p. 657.

$$l = 0.2x \tag{56}$$

in the transition region of his three-zone model. We may write, therefore,

$$l = xg(\eta) \tag{57}$$

where g is a steadily increasing function of η, with $g(\infty) = 0.4$; $g \simeq 0.2$ for η of order 10, and g probably very small for η near unity. So far as we know, there is at present no other hydrodynamical information about the function g. The simplest formula that satisfies these requirements appears to be

$$g = \frac{0.4\eta}{10 + \eta} \tag{58}$$

These results give some support for our approximation of taking the velocity and mixing-length distributions to be those appropriate to the Reynolds number at the cross section in question and not to the Reynolds number at some section further upstream. For at these high Reynolds numbers l/x depends only on η, which, at a given x, does not depend strongly on the section chosen. Also $V_*/\overline{U}$ is independent of R.

We have now found all the hydrodynamic quantities needed in the calculation of the extra heat conductivity in the flame, due to the turbulence of the flow.

2.43 Effective thermal conductivity in the flame

The flame speed depends on the thermal conductivity of the gases in the flame zone. Turbulence enhances this conductivity and, hence, increases the flame speed. It is usual to assume that the effective heat conductivity is the sum of the ordinary thermal conductivity together with an "eddy conductivity," calculated as follows.

Let C_p be the specific heat of the fluid at constant pressure, per unit mass. In unit time the heat transferred across unit area normal to the x axis, in the direction of x increasing, is[66]

$$-\rho C_p l^2 \left| \frac{dU}{dx} \right| \frac{\partial T}{\partial x}$$

and the extra conductivity is therefore $\rho C_p l^2 |dU/dx|$, which from equation 49 is equal to

$$\rho C_p l V_* = \rho C_p \frac{\overline{U}x}{30} g(\eta) \tag{59}$$

---

[66] Prandtl, p. 163.

from equations 54 and 57. Let λ_0 be the ordinary thermal conductivity of the gas in the flame. Strictly, this varies through the flame, but only slowly, and an average value can be taken without much error. Near the surface the effective conductivity is therefore

$$\lambda = \lambda_0 + \rho C_p \frac{\overline{U}x}{30} g(\eta) \tag{60}$$

2.44 Rate of burning with turbulence

In the previous section we have derived formula 60 for the conductivity near the decomposing surface. One way of finding the rate of burning associated with such a conductivity would be to integrate numerically the equations of the flame zone. It is also possible to use an approximate method, which gives an explicit formula for the rate of burning and which is more in keeping with the order of approximation adopted up to this point. In this method we replace the constant conductivity λ_0, appropriate to burning with $\overline{U} = 0$, by a different constant value derived from equation 60 by giving the quantities, which vary through the flame, their values for the most important region. This will be in the part where the reaction is half completed. This treatment can be expected to give the right dependence on the pressure, mean velocity, and properties of the reactant and can lead to the right order of magnitude for the various coefficients. The method has been tested by comparison with the results of numerical integration of a number of typical flames, and the agreement is reasonably satisfactory.

Using suffix 0 to denote values in the most important region of the flame, we have

$$\lambda = \lambda_0 + \rho_0 C_{p_0} \frac{\overline{U}x_0}{30} g\left(\frac{\overline{U}x_0}{30\nu_0}\right) \tag{61}$$

We have shown in § 2.33 that, for a second-order reaction, $x_0 \propto \lambda^{1/2}P^{-1}$, and the rate of burning is proportional to $\lambda^{1/2}P$. We write $\zeta = (\lambda/\lambda_0)^{1/2}$, so that, with regard to pressure and turbulence, the dependence of x_0 is $x_0 \propto \zeta P^{-1}$ and the consumption by the flame is proportional to ζP. Since ρ_0 and $\nu_0{}^{-1}$ are proportional to the pressure, we have from equation 61,

$$\zeta^2 = 1 + [\gamma \overline{U} \zeta g(\overline{U} \zeta \delta)] \tag{62}$$

where γ and δ depend only on the nature of the propellant. Since in this case equation 62 for ζ does not contain the pressure, the rate of burning can be written as proportional to pressure multiplied by a function of $\overline{U}$.

For a typical propellant, yielding gases at a final temperature of 2500°K, it can be shown that C_p of the products $\simeq 0.4$ cal/g, $\rho_0 \simeq 10^{-4}P$ g/cc, $\nu_0 \simeq 5/P$ cm^2/sec, $\lambda_0 \simeq 2 \times 10^{-4}$ cal/cm^2 sec (°C/cm), and $x_0 \simeq 8 \times 10^{-2}/P$ cm at $\bar{U} = 0$. These lead to the orders of magnitude,

$$\gamma \sim \delta \sim 5 \times 10^{-4}$$

when $\bar{U}$ is measured in centimeters per second.

Table 2.3 shows our estimates of γ and δ for three propellants, giving very different final temperatures. The quantity δ appears to vary as γ^2, roughly. The effect of gas flow over the surface is predicted to be greater, the cooler the final products. This certainly agrees with observations made since this theory was first put forward. A similar effect has been noted in experiments with gas mixtures:[67] a fast-burning mixture is less affected by whirling of the gas than is a slow-burning mixture. The physical explanation is presumably analogous to that of our result. In the case of propellants the striking increase in "erosion" on going to "cooler" propellants is caused by quite small changes in the flame thickness; the magnification comes from the rapid variation of turbulence in going out from the surface. A moderate decrease of flame thickness is sufficient to suppress erosion almost entirely.

TABLE 2.3 VARIATION OF γ AND δ WITH THE FINAL TEMPERATURE

Propellant	Temperature of Products at Constant Pressure, °K	Relative Values of γ	Relative Values of δ
A37/2	3000	0.77	0.60
449	2500	1	1
S27S	1800	1.33	1.70

EXAMPLES

1. Calculate the geometrical form function up to "sliver point" for a short 7-perforated grain in terms of the fraction remaining of the geometric web size. Fit this relation by

$$\phi = (1 - f)(1 + \theta f)$$

where f refers to a new effective web size D', and θ and D' are chosen for best fit. Evaluate numerically for the typical dimensions: grain length = 2.5 × grain diameter = 25 × perforation diameter.

2. Show that, if the gases in a reaction zone obey equation 40 of § 2.35 at all pressures, the rate of burning tends to a finite limit at very high pressures.

---

[67] Kratz and Rosecrans, *Univ. Illinois Eng. Expt. Sta. Bull.* **133** (1922).

3. Show that for any reaction rate of the form $f(\epsilon, T)$ the rate of burning and the flame thickness are proportional to $\lambda^{1/2}$.

4. A first-order reaction has

$$f(\epsilon, T) = B(1 - \epsilon)e^{-A/RT}$$

Obtain a formula for the flame speed by the process used in § 2.33.

5. Write down the equations of a flame zone with diffusion coefficient D for the diffusion of products into reactants.

6. Show that, since DP is independent of P at moderate pressures, the dependence of the flame consumption on P is not altered by including diffusion, except at very high pressures.

CHAPTER THREE The Thermochemistry of Propellants

3.1 Sketch of closed-vessel technique

The closed vessel was first used extensively in ballistic research by Noble, from about 1860, and especially by Vieille, who was the first to obtain pressure-time curves. Vessels of the Vieille type had a volume of order 150 cc, and their maximum load was consequently only an ounce or two. After publication of the research carried out for Krupps by Schmitz,[1] there was a swing toward bigger vessels, which by taking bigger charges reduce round-to-round variations. Schmitz used a closed vessel of 3½ liters capacity. Such large vessels have a small surface-volume ratio, and the cooling correction, being much smaller, can be estimated with greater accuracy. Indeed, cooling corrections are often omitted when using such large closed vessels, on the ground that the cooling is of the same order as in a gun.

Closed vessels have been fired at pressures up to 35 tons/sq in., though a more normal figure is 20 tons/sq in. This is attained at a density of loading of about 0.2 g/cc. With a cylindrical vessel, built in the same manner as a gun chamber, there is no difficulty in meeting these pressures with a reasonable safety factor. Expansion of the capacity by high pressure is allowed for in the most accurate work.

It has been explained in chapter 1 that pressures are measured in guns by piezoelectric gage or by copper crusher, the latter measuring only maximum pressure. Crusher gages are now used in closed vessels only in the form of the recording crusher gage, which gives a pressure-time record. This gage is of great historical importance, because by its invention Vieille first put a time scale into closed-vessel technique. The recording crusher gage is still used in France but has been abandoned elsewhere.

The piezoelectric gage is used in the closed vessel in the same way as in a gun. Since the pressure remains on the gage for a few seconds, until the release valve is opened, the gage is more roughly handled than in a gun. The accuracy attained is better than 1 per cent.

---

[1] Schmitz, *Artill. Monatshefte*, **84** (1913), 482; **86** (1914), 85.

The most accurate method of measuring pressure in a closed vessel is by a mechanical gage. In England, for example, the gage used is a descendant of the Petavel gage. A piston, protected from the hot gases by luting, deflects a spring of high natural frequency, in the form of a tube surrounding the piston. The motion is registered by an optical lever using a mirror tilted by the piston, being finally recorded on a rotating drum. The accuracy obtained is well within 1 per cent of full deflection. The natural frequency is of the order of 5000 cycles/sec, so that the spring gage cannot be used for the most rapid phenomena, where the pressure may rise from zero to maximum in a few milliseconds. Here the piezo gage is used instead.

Piezo and spring gages are calibrated by a dead-weight press. In the former the calibration, expressed as a charge per unit pressure, changes very slowly with time. The deflection on the record depends also on the amplification of the electric circuits, which is varied to give full deflection at the expected peak pressure; the amplification is measured before each round by switching known voltages into the input, so that the deflections on the film can be interpreted as pressures.

Obturation against the hot gases is important, and in some types of gage even apparently trivial changes in the method of obturation may cause systematic changes of several per cent in the pressure. These small but important points of technique we cannot discuss in this book. Another such matter is the problem of the release valve, which has to withstand the repeated high-velocity flow of hot dense gas.

Simultaneous ignition on all surfaces of the charge can be achieved by filling the vessel with an inflammable gas mixture and passing an electric spark. This method of ignition differs substantially from that used in guns, so that a more favored (and more convenient) method is to use an electric wire, igniting a small charge of gunpowder or porous nitrocellulose. A method still nearer gun practice is to put the propellant in a cartridge case with an ordinary primer, exactly as in a gun, and to fire by a striker blow on the primer. The cartridge case also provides the obturation for the breech of the closed vessel. The approach to gun conditions is limited only by the density of loading being about half that in a gun working at the same peak pressure.

The interior shape of a closed vessel is usually a short cylinder, about 2 diameters long. Longer cylinders are apt to give pressure waves, especially with end ignition of a small charge,[2] and the pressures recorded in the waves are often substantially greater than the normal maximum pressure for this weight of charge. The first observation of such waves was made by Vieille. They are not confined to closed vessels, having been found also in guns firing charges that fill only a small part of the chamber. That the peak pressure was unusually high in such cases was known to Robins (1742), by bursting guns. In modern howitzers the lowest charge cannot be bulky if the highest charge is to be loaded easily, and so the lowest charge is fired as a small charge in a large chamber; to reduce the possibility of pressure waves, the charge must be spread along the chamber, and the bottom charge is therefore usually made up as a long bundle surrounding the primer. Another interesting application is the release of jammed shot. It sometimes happens that a shot sticks in the bore well toward the muzzle. This can happen only with small charges. To clear the bore it is not advisable to use a normal charge, for the expected low maximum pressure in the large available volume will be considerably exceeded by the peak pressure in the waves, which will usually be set up. Since one cannot hope to get any reasonable charge well distributed between breech and shot, it is best to use a very small charge.

---

[2] For recent work, see Liebessart, *Mém. artillerie franç.*, **18** (1939), 345.

To return to the construction of the closed vessel, it is usual to provide a liquid jacket to enable firings to be carried out over a wide temperature range. The limits for routine work are +60 and −20°C.

3.11 Cooling corrections

From the pressure-time curve and the equation of state of the uncooled products of the burning, one can derive the charge burnt as a function of time and, finally, the rate of burning at any stage. Before this is carried through, two corrections should be applied to the observed pressure-time curve. The first is to subtract the pressure generated by the igniter; this correction is easy to make to sufficient accuracy, since it rarely exceeds 1 per cent.

The second correction is more important. The pressure at each instant has to be corrected for the cooling loss up to that time. The effect is biggest in small vessels and may rise to 10 per cent. When large vessels are used, with a capacity of about 2 liters, cooling corrections are often neglected in closed-vessel and then in gun calculations on the ground that the effects will cancel. To make this more plausible, the closed vessel is designed to emphasize the resemblance to a gun chamber. Even so, the gas velocity along the walls, which is often considerable at the moment of maximum pressure in the gun, cannot be reproduced in the orthodox closed vessel, and the accuracy of ballistic prediction suffers thereby. If we trace the error further, it is found that the variation is absorbed, sooner or later, in some empirical factor, from which no theory of the central problem of interior ballistics is free. The variability of this empirical factor is somewhat greater than if cooling corrections were included in the closed-vessel analysis, but, if, from some other approximation, this variation is already large, the additional variation may be unimportant. If the closed-vessel results are to be used in a rough ballistic theory, it may not be worth while to apply cooling corrections.

Assuming, however, that we wish to make as good a job as possible of our closed-vessel work, we must apply cooling corrections. Closed vessels with a range of values of (surface/volume) are used, and the pressure-time curves from the different vessels, each a mean of several rounds, are extrapolated to zero surface. Two vessels, a large and a small, may be used, or the area of a low-loss vessel may be increased when needed by a removable grid. In any case the work is more than doubled, though by tabulation of corrections for various propellants the extra labor does eventually become small.

This method was first used by Petavel,[3] followed by Muraour [4] and Burlot,[5] with later work by Muraour.[6] Their results may be summed as: for a given density of loading and propellant,

$$\Delta P \propto \frac{S}{U} \cdot t^n$$

where S is the cooling area, U the volume of the vessel, and t the time to burn the propellant. n is about $\frac{1}{4}$. At constant S/U and t, $\Delta P/P$ is independent of the nature of the propellant, and, at constant S/U and web size, $\Delta P/P$ is almost independent of the density of loading.

Crow and Grimshaw [7] considered the loss of heat by conduction from the gas, at the explosion temperature, straight into the metal walls, and determined the thermal conductivity of the metal by fitting to results at two values of S/U. Since the conductivity turns out to be far less than that for steel at normal temperatures, it seems that the resistance to heat transmission must occur at some other stage. This also vitiates the recent work of Schweikert.[8] Kent and Vinti have studied the matter, assuming that the resistance to heat flow occurs mainly in a layer of gas close to the surface. They found a heat loss proportional to $(\text{web})^{1/3}$, using the data of Crow and Grimshaw. The theory of cooling corrections is not yet in its final form.

---

[3] Petavel, *Phil. Trans. Roy. Soc. (London)*, **205A** (1906), 357.

[4] Muraour, *Mém. artillerie franç.*, **3** (1924), 339.

[5] Burlot, *Mém. poudres*, **21** (1924), 411.

[6] Muraour, *Mém. artillerie franç.*, **4** (1925), 460. Muraour and Issoire, *ibid.*, **18** (1939), 13.

[7] Crow and Grimshaw, *Phil Trans. Roy. Soc. (London)*, **230A** (1931), 39.

[8] Schweikert, *Tech. Hochschule Berlin Rept.* **44/17**.

3.2 Theory of the equilibrium state after burning without cooling or performance of work

We consider the burning of a propellant in absence of air, and under conditions in which the products do no work against external forces, nor are they cooled. It is our aim to calculate the equilibrium state of the products: namely, the temperature and composition of the gases. To fix ideas we may think of the final state in a closed vessel. Here the air initially in the vessel is negligible in mass compared with the charge; the work done by expanding the walls is small and easily computed; cooling corrections can be applied, as described in the previous section. The only point to be noted is that equilibrium is attained only after a short but finite time, and, if the gases were of zero thermal conductivity and no convection currents were set up, there never would be any single equilibrium state in the vessel. For the earliest-formed gas is compressed by the later, and the former is heated by the compression, and the latter is cooled by doing work; thus the gas temperature is highest near the walls, until conduction and convection have equalized the distribution.

We begin with the simplest theory, without dissociation or pressure corrections. Then dissociation is introduced, and after a discussion of experimental results the pressure corrections, shown to be needed, are given a theoretical backing.

3.21 Theory without dissociation or pressure corrections

We consider 1 g of propellant, which for conventional types will be composed of carbon, hydrogen, nitrogen, and oxygen atoms. Small quantities of potassium salts are often added to reduce flash, and chalk is usually present in amounts up to 1 part in 1000 by weight. These constituents will be neglected here.

Let the propellant contain $\{C\}$ g-atoms of carbon, $\{H\}$ of hydrogen, $\{N\}$ of nitrogen, and $\{O\}$ of oxygen. The products consist of CO_2, CO, H_2O, H_2, and N_2 in comparable quantities, together with much smaller amounts of their dissociation products: OH, H, NO and, at temperatures around 3500°K, some O_2, O, and N. We neglect dissociation products in this section. With very cool propellants it is possible for soot to form, although, so far as we know, it has never been formed at the explosion temperature, but only after considerable cooling. Soot formation is considered in § 3.4. Methane and ammonia are formed in small quantities on cooling, but not in important quantities at the equilibrium explosion temperature.

Let $[CO_2]$ be the number of moles of CO_2 in the products, with a similar notation for other products. Let n be the total number of moles in the products of 1 g, so that

$$n = [CO_2] + [CO] + [H_2O] + [H_2] + [N_2] \tag{1}$$

Let the temperature of the propellant before burning be 300°K. It is easy to correct to other temperatures later.

Consider a state in which the temperature is T°K and the volume occupied by the gases is V cc, and let P be the pressure. If the products are in chemical equilibrium, P is determined uniquely by V and T. In this section the products are assumed to be perfect gases. Hence,

$$P = \frac{nRT}{V} \tag{2}$$

where R, the gas constant per mole, is 82.06 [9] if the pressure is in atmospheres and 0.5384 if the pressure is in tons per square inch.

We start with any values of V and T and calculate $[CO_2]$, etc., and n. These in fact depend only on the temperature, in the present approximation. Knowing the products at any temperature T°K, we can calculate the energy needed to heat such gases from 300°K to T°K and also the energy released by breaking down propellant at 300°K to these gases at 300°K. Equating these two energies gives the temperature, T_0°K, of the equilibrium products of burning without cooling or performance of external work. This may be called the "uncooled explosion temperature" or the "adiabatic flame temperature."

To calculate the composition at any temperature, we can use the conservation of atomic types:

$$[CO_2] + [CO] = \{C\} \tag{3}$$

$$[CO] + [H_2O] + 2[CO_2] = \{O\} \tag{4}$$

$$2[H_2O] + 2[H_2] = \{H\} \tag{5}$$

$$2[N_2] = \{N\} \tag{6}$$

One more equation is needed to determine the five unknowns $[CO_2]$, $\cdots$ $[N_2]$. This is supplied by the equilibrium constant for the water-gas reaction:

$$\frac{[CO][H_2O]}{[CO_2][H_2]} = K_0(T) \tag{7}$$

where $K_0(T)$ is tabulated in Table 3.1. Since V does not enter equations 3 to 7, the composition is independent of the density of the products.

---

[9] Birge, *Rev. Modern Phys.*, **13** (1941), 233.

TABLE 3.1 EQUILIBRIUM CONSTANTS AT ZERO DENSITY *

Notation explained in text. For interpolation, log K is nearly linear in $1/T$ in most parts of the table.

T, °K	K_0	K_1	K_2	K_3	K_4	K_5	K_6	K_7	K_8	K_9
800	0.2478							31.25	2.91×10^{-3}	1.35×10^{-4}
1000	0.7286							3.72×10^{-2}	5.64×10^{-4}	2.33×10^{-2}
1200	1.435							3.99×10^{-4}	1.85×10^{-4}	0.698
1400	2.270							1.55×10^{-5}	8.2×10^{-5}	7.65
1500	2.704							4.2×10^{-6}	5.9×10^{-5}	19.9
1600	3.132	6×10^{-5}						1.35×10^{-6}	4.5×10^{-5}	45.4
1700	3.555	2×10^{-4}						4.9×10^{-7}	3.5×10^{-5}	91.2
1800	3.975	4×10^{-4}	2×10^{-5}					2.0×10^{-7}	2.8×10^{-5}	170
1900	4.385	9×10^{-4}	6×10^{-5}					9.2×10^{-8}	2.3×10^{-5}	304
2000	4.782	0.0016	2×10^{-4}					4.5×10^{-8}	1.9×10^{-5}	513
2100	5.161	0.0031	4×10^{-4}	2×10^{-5}				2.4×10^{-8}	1.6×10^{-5}	802
2200	5.520	0.0057	8×10^{-4}	5×10^{-5}				1.3×10^{-8}	1.4×10^{-5}	1.20×10^{3}
2300	5.852	0.0097	0.0016	10^{-4}	10^{-5}	10^{-5}			1.2×10^{-5}	1.71×10^{3}
2400	6.155	0.0159	0.0029	2×10^{-4}	3×10^{-5}	3×10^{-5}	10^{-5}		1.1×10^{-5}	2.38×10^{3}
2500	6.433	0.0251	0.0052	4×10^{-4}	7×10^{-5}	9×10^{-5}	3×10^{-5}		1.0×10^{-5}	3.31×10^{3}
2600	6.694	0.0383	0.0090	7×10^{-4}	2×10^{-4}	2×10^{-4}	10^{-4}		0.9×10^{-5}	4.22×10^{3}
2700	6.939	0.0566	0.0146	0.0012	3×10^{-4}	5×10^{-4}	2×10^{-4}		0.8×10^{-5}	5.48×10^{3}
2800	7.167	0.0814	0.0231	0.0020	5×10^{-4}	0.0012	5×10^{-4}		0.8×10^{-5}	6.98×10^{3}
2900	7.379	0.1143	0.0355	0.0034	8×10^{-4}	0.0026	0.0010		0.7×10^{-5}	8.71×10^{3}
3000	7.574	0.1574	0.0529	0.0055	0.0014	0.0053	0.0020		0.6×10^{-5}	1.07×10^{4}
3100	7.753	0.2125	0.0768	0.0086	0.0022	0.0103	0.0038			
3200	7.917	0.2813	0.1089	0.0129	0.0035	0.0190	0.0071			
3300	8.068	0.3658	0.1513	0.0188	0.0053	0.0339	0.0126			
3400	8.205	0.4682	0.2064	0.0271	0.0078	0.0586	0.0216			
3500	8.330	0.5910	0.2760	0.0387	0.0113	0.0978	0.0358			
3600	8.443	0.7367	0.3626	0.0539	0.0161	0.1591	0.0580			
3700	8.544	0.9079	0.4693	0.0734	0.0225	0.2516	0.0917			
3800	8.633	1.1070	0.6001	0.0982	0.0309	0.3886	0.1412			
3900	8.710	1.3360	0.7589	0.1300	0.0417	0.5878	0.2132			
4000	8.775	1.5970	0.9495	0.1693	0.0554	0.8711	0.3157			

* *References.* All equilibrium constants taken from a compilation by Professor J. L. Hirschfelder, except for K_4, from tables of Dr. Pike, and K_9, from Kassel, *J. Am. Chem. Soc.* **56** (1934), 1838.

For tables 3.1 to 3.4 and 3.18 I am indebted to Professor J. O. Hirschfelder and Dr. H. H. M. Pike, whose compilations of data have found many ballistic applications.

This is, of course, due to the number of molecules remaining constant during the water-gas reaction

$$CO_2 + H_2 \rightleftharpoons CO + H_2O$$

$[CO_2]$ is the solution x of

$$(K_0 - 1)x^2 + x[\{O\} + K_0(\tfrac{1}{2}\{H\} + \{C\} - \{O\})] + \{C\}(\{C\} - \{O\}) = 0 \quad (8)$$

and

$$[CO] = \{C\} - x \quad (9)$$

$$[H_2O] = \{O\} - \{C\} - x \quad (10)$$

$$[H_2] = \tfrac{1}{2}\{H\} - \{O\} + \{C\} + x \quad (11)$$

$$[N_2] = \tfrac{1}{2}\{N\} \quad (12)$$

with finally

$$n = \tfrac{1}{2}\{H\} + \tfrac{1}{2}\{N\} + \{C\} \quad (13)$$

Thus the pressure can be calculated, in this approximation, without knowledge of the water-gas equilibrium constant.

We now find the energy required to heat these gases at constant volume from 300°K to T°K. This can be done for each gas by a summation over the energy levels of the isolated molecule (for we are assuming perfect gases), and these levels are known from spectroscopy. Table 3.2 gives the internal energy so computed, relative to 300°K, in the form of the mean specific heat from 300°K to T°K. The specific heat is used only because it is a more slowly varying function than the internal energy. The specific heats of Table 3.2 are for 1 mole of each substance.[10] Multiplying by the numbers $[CO_2]$, etc., and summing over the 5 constituents, we find the internal energy of the products at temperature T°K, relative to the same gases at 300°K. We write the energy as

$$E = \Sigma[CO_2]E_{CO_2,0} \quad (14)$$

where the suffix 0 indicates that this is strictly the energy at zero density. In § 3.24 we shall add terms proportional to the first and second powers of the density.

The energies of formation of the propellant from graphite, hydrogen gas, nitrogen gas, and oxygen gas, all at zero density, 300°K, and without performance of work on the external pressure, can be calculated from Table 3.3. There the energies of formation of the common constituents are listed. In passing from the separate constituents to the gelatinized propellant there is an energy change that is known to be

---

[10] The calorie used in these tables is 4.1833 international joules.

TABLE 3.2 MEAN SPECIFIC HEATS $\bar{C}_V$, AT ZERO DENSITY

The values tabulated are the mean specific heats from 300°K to T°K, in calories per mole per degree. These are specific heats at constant volume; to obtain specific heats at constant pressure add 1.987. For monatomic gases $\bar{C}_V = 2.980$. For interpolation over short intervals, use may be made of the fact that $\bar{C}_V$ is nearly linear in $1/T$.

T, °K	CO_2	H_2O	CO	H_2	N_2	OH	NO	O_2	CH_4	NH_3
800	8.896	6.599	5.244	5.019	5.179	5.092	5.432	5.570	9.870	8.322
1000	9.409	6.883	5.403	5.059	5.326	5.136	5.597	5.759	11.129	9.021
1200	9.824	7.176	5.553	5.117	5.468	5.197	5.744	5.915	12.243	9.672
1400	10.165	7.467	5.684	5.191	5.598	5.288	5.871	6.044	13.235	10.270
1500	10.313	7.612	5.743	5.232	5.658	5.337	5.927	6.100	13.683	10.548
1600	10.449	7.752	5.799	5.275	5.714	5.385	5.979	6.152	14.098	10.811
1700	10.574	7.887	5.851	5.318	5.767	5.432	6.026	6.202	14.486	11.061
1800	10.690	8.017	5.899	5.362	5.816	5.477	6.069	6.248	14.849	11.298
1900	10.797	8.142	5.944	5.407	5.862	5.520	6.109	6.292	15.188	11.523
2000	10.896	8.263	5.986	5.451	5.906	5.563	6.147	6.335	15.506	11.735
2100	10.989	8.380	6.026	5.495	5.946	5.606	6.183	6.375	15.798	11.936
2200	11.075	8.492	6.063	5.538	5.984	5.648	6.217	6.413	16.083	12.126
2300	11.156	8.599	6.098	5.580	6.020	5.691	6.250	6.450	16.347	12.307
2400	11.233	8.702	6.131	5.621	6.054	5.734	6.281	6.486	16.595	12.478
2500	11.305	8.801	6.162	5.662	6.086	5.774	6.309	6.522	16.828	12.640
2600	11.373	8.896	6.191	5.702	6.117	5.812	6.335	6.557		
2700	11.437	8.988	6.218	5.740	6.146	5.849	6.360	6.591		
2800	11.498	9.076	6.244	5.778	6.174	5.885	6.384	6.625		
2900	11.556	9.160	6.269	5.815	6.200	5.922	6.406	6.658		
3000	11.611	9.241	6.293	5.851	6.225	5.957	6.427	6.690		
3100	11.664	9.319	6.315	5.886	6.249	5.990	6.448	6.721		
3200	11.714	9.395	6.336	5.920	6.271	6.023	6.468	6.752		
3300	11.762	9.468	6.356	5.953	6.293	6.054	6.487	6.782		
3400	11.808	9.538	6.376	5.985	6.314	6.085	6.505	6.812		
3500	11.852	9.605	6.394	6.017	6.333	6.114	6.522	6.841		
3600	11.895	9.670	6.412	6.047	6.352	6.143	6.539	6.869		
3700	11.936	9.733	6.429	6.077	6.370	6.170	6.555	6.896		
3800	11.975	9.794	6.446	6.106	6.385	6.197	6.570	6.923		
3900	12.013	9.852	6.462	6.135	6.404	6.223	6.585	6.949		
4000	12.050	9.908	6.477	6.163	6.420	6.248	6.599	6.974		
Source:	*a*	*b*	*c*	*d*	*c, e*	*f*	*g*	*h*	*i*	*i*

[a] Kassel, *J. Am. Chem. Soc.*, **56** (1934), 1838.

[b] Gordon, *J. Chem. Phys.*, **2** (1934), 549; Stephenson and McMahon, *ibid.*, **7** (1939), 614; E. B. Wilson, *Chem. Rev.*, **27** (1940), 17.

[c] Johnston and Davis, *J. Am. Chem. Soc.*, **56** (1934), 271.

[d] Davis and Johnston, *ibid.*, 1045; Giauque, *ibid.*, **52** (1930), 4816.

[e] Giauque and Clayton, *ibid.*, **55** (1933), 4875.

[f] Johnston and Dawson, *ibid.*, **55** (1933), 2744, above 3000°K; otherwise, from Lewis and von Elbe, *Combustion, Flames, and Explosions of Gases* (1938).

[g] Johnston and Chapman, *J. Am. Chem. Soc.*, **55** (1933), 155, above 2000°K; otherwise, from Lewis and von Elbe, *loc. cit.*

[h] Johnston and Walker, *J. Am. Chem. Soc.*, **57** (1935), 682, corrected for $^1\Delta$ state by Hirschfelder.

[i] Hirschfelder.

small and is always neglected. It is thought to be a few calories per gram.

Table 3.4 lists the energies of formation of the product gases, when formed from graphite, hydrogen gas, nitrogen gas, and oxygen gas, all at 300°K and zero density and without performance of external work.

Table 3.3 Energies of Formation and Atomic Composition of Propellant Constituents *

For Formation from Graphite, Hydrogen Gas, Oxygen Gas, and Nitrogen Gas at 300°K and Zero Density; Constant Volume Conditions; Compositions in Units of 10^{-5} mole/g

	Mol.	Atomic Composition				*EF*,	
Substance	Wt.	C	H	N	O	cal/g	Ref.
Nitrocellulose, 11.5% N		2335	3070	821	3587	694	*a*
12.0		2275	2935	857	3609	657	
12.2		2251	2881	871	3618	643	
12.4		2228	2828	885	3626	629	
12.6		2204	2774	899	3635	614	
12.8		2180	2720	914	3644	600	
13.0		2156	2666	928	3653	586	
13.2		2132	2612	942	3662	571	
13.5		2097	2531	962	3675	550	
Nitroglycerine, $C_3H_5N_3O_9$	227.1	1321	2202	1321	3964	349	*b*
Ethyl centralite (carbamite), $C_{17}H_{20}N_2O$	268.2	6339	7458	746	373	55	*c*
Mineral jelly, $C_{20}H_{42}$	282.3	7084	14876	0	0	422	*d*
Acetone, C_3H_6O	58.1	5168	10336	0	1723	996	*d*
Diphenylamine, $C_{12}H_{11}N$	169.1	7096	6505	591	0	−204	*e*
Nitroguanidine (picrite), $CH_4N_4O_2$	104.1	961	3844	3844	1922	207	*f*
Camphor, $C_{10}H_{16}O$	152.2	6569	10510	0	657	445	*d*
Dinitrotoluene, $C_7H_6N_2O_4$	182.1	3843	3294	1098	2196	14	*g*
Dibutylphthalate, $C_{16}H_{22}O_4$	278.3	5748	7904	0	1437	679	*h*
Diamylphthalate, $C_{18}H_{26}O_4$	306.4	5875	8486	0	1306	678	*h*
Ethyl alcohol, C_2H_5OH	46.1	4343	13030	0	2172	1393	*i*
Diethylene glycol dinitrate, $C_4H_8N_2O_7$	196.1	2040	4079	1020	3569	517	*j*

* For the data in this table I am indebted to a compilation by Dr. Pike.

[a] Interpolated from mean data of Prettre, *Mém. poudres* **24** (1930), 223, and Schmidt and Becker, *Z. ges. Schiess- u. Sprengstoffw.*, **28** (1933), 280.

[b] Mean value from Schmidt and Becker (*loc. cit.*) and Rinkenbach, *Ind. Eng. Chem.*, **18** (1926), 1195.

[c] Schmidt and Becker, *loc. cit.*

[d] Kharasch, *Bur. Standards J. Research*, **2** (1929), 359.

[e] Mean of three values, two by Kharasch (*loc. cit.*) and one by Schmidt and Becker (*loc. cit.*).

[f] Determined in Armament Research Department, Ministry of Supply, England.

[g] Schmidt, *Z. ges. Schiess- u. Sprengstoffw.*, **29** (1934), 262.

[h] Ambler, *J. Soc. Chem. Ind.* (*London*), *Transactions*, **40** (1936), 291.

[i] Bichowsky and Rossini, *Thermochemistry* (1936).

[j] Rinkenbach, *Ind. Eng. Chem.*, **19** (1927), 925.

Thus we find

$$\Delta(EF) = \text{energy of formation of products} - \text{energy of formation of propellant}$$

and, finally, $\zeta = E - \Delta(EF)$. The temperature of uncooled explosion T_0 is that which makes $\zeta = 0$. Since the nature of the products depends on T, not only E but also the term $\Delta(EF)$ is a function of T.

A numerical example will help. Propellant X has $\{C\} = 2238$, $\{H\} = 3014$, $\{N\} = 1044$, $\{O\} = 3468$, all in 10^{-5} mole/g, and the energy of formation of the propellant is 470 cal/g. The atomic ratios

TABLE 3.4 ENERGIES OF FORMATION OF PRODUCTS

From Graphite, Hydrogen Gas, Nitrogen Gas, and Oxygen Gas at 300°K and Zero Pressure; Constant Volume Conditions; Energies in Kilocalories per Mole

Substance	Molecular Weight	Energy of Formation	Reference
CO	28.01	26.69	*a*
CO_2	44.01	94.03	*a*
H_2O liquid	18.02	67.43	*a*
H_2O gas		57.50	*a*
CH_4	16.03	17.27	*a*
NH_3	17.03	10.38	*b*
NO	30.01	−21.53	*c*
OH	17.01	−9.31	*c, d*
N	14.01	−85.25	*e*
O	16.0	−58.75	*e*
H	1.008	−51.79	*e*

[a] Rossini, *J. Research Natl. Bur. Standards*, **22** (1939), 407; also Fiocke, *ibid.*, **5** (1931), 479.

[b] Bichowsky and Rossini, *Thermochemistry* (1936).

[c] Lewis and von Elbe, *Combustion, Flames, and Explosions of Gases* (1938).

[d] Dwyer, *Phys. Rev.* **59** (1941), 928.

[e] Herzberg, *Molecular Spectra* (1939).

have been calculated from the nominal composition by the data given in Table 3.3.

The product composition at various temperatures, computed from equations 8 to 13 with Table 3.1, are given in Table 3.5. Tables such as 3.3 are sufficiently smooth to permit computation of such quantities as $[CO_2]$ to the nearest $\frac{1}{2} \times 10^{-5}$ mole/g, with the assurance that the results will be smooth if the computation has been correct. $\Delta(EF)$, E, and ζ are also given in Table 3.5. By linear interpolation between 300 and 3100°K, ζ is found to vanish at $T_0 = 3090$°K. The error in using

TABLE 3.5 MAJOR PRODUCTS AT VARIOUS TEMPERATURES, FROM PROPELLANT *X*

Compositions in 10^{-5} mole/g; Energies in cal/g

T,°K	$[CO_2]$	$[CO]$	$[H_2O]$	$[H_2]$	$[N_2]$	$\Delta(EF)$	E	ζ
1000	797	1441	433	1074	522	913.0	185.4	−727.6
2000	429	1809	801	706	522	876.8	493.9	−382.9
2500	377	1861	853	654	522	871.7	662.6	−209.1
3000	350	1888	880	627	522	869.0	836.9	−32.1
3100	346	1892	884	623	522	868.6	872.2	3.6
3090	346	1892	884	623	522	868.6	868.6	0.0

linear interpolation is about ½°K, which is smaller than the nominal uncertainty in our tables and a good deal smaller than the real error in the simple theory used here.

Some points about Table 3.5 deserve mention. To begin with, it can be seen that $\Delta(EF)$ is not constant, though it varies much more slowly than E, the internal energy of the products. Furthermore, at all temperatures there are 4267×10^{-5} moles of gas formed from a gram of the propellant, and the mean molecular weight is therefore 23.4. The values for conventional propellants cover the range from 20 to 25, the "hot" propellants giving the higher mean molecular weights.

The ratio γ of the effective specific heats at constant pressure and volume can be calculated from Table 3.5. A mean value for gun calculations would correspond, for this propellant, to the range 2000–3000°K. Between these temperatures the internal energy of the products changes by 342.97 cal/g, and the change in heat content is larger by $1000nR =$ 84.79 cal/g. The effective γ is therefore $1 + (84.79/342.97) = 1.247$. Since the equilibrium constant K_0 is a function of temperature, the value of γ at any temperature is not a mean of the values of γ for the separate gases. Thus the mean values of γ (at constant composition) over the range 2000–3000°K are 1.244 for the 2000°K composition and 1.245 for the 3000°K composition.

In a gun emptying after the shot has left, the temperature falls by the adiabatic expansion. At a time when the temperature of the products of this propellant has fallen to 1000°K the composition would not be that listed in Table 3.5. For the latter gives the equilibrium composition, which is attained only in a relatively long time at such low temperatures. The equilibrium constant of gases in a gun follows the temperature down until K_0 is about 2, after which the equilibrium "freezes." This must be remembered when calculating the properties of gases flowing out of a gun. In a bomb calorimeter, used to measure the "calorimetric value" (see § 3.4), the cooling gases "freeze" at about the same equilibrium constant. Fortunately, the heat evolved is almost independent of the exact point at which the equilibrium freezes.

The proportion of hydrogen in the products changes substantially over the temperature range of Table 3.5. This causes a pronounced change in certain properties, notably the thermal conductivity.

The explosion pressure, corrected for cooling, is, by equation 2,

$$P = \frac{nRT_0}{V} \tag{15}$$

The quantity nRT_0 is the "force constant" or "force" of the propellant. The dimensions are energy per unit mass, and for gun calculations it is convenient to use as the unit (ton/sq in.) × (cc/g). For propellant X the force is 70.99 in these units; hence, when it is fired at 0.2 g/cc the pressure expected is 14.2 tons/sq in. In many problems $(nRT_0)^{1/2}$ enters as a characteristic velocity and is obtained in the unit (ft/sec) by multiplication by 407.7. For example, for propellant X, $(nRT_0)^{1/2}$ is 3435 ft/sec.

It is conventional to absorb the n into R, giving the latter symbol to the gas constant per gram. This is possible since the gas constant per mole does not appear in classical interior ballistics. In this chapter we use R for the molar quantity; elsewhere we follow the ballistic convention, so that, for instance, the "force" is written as RT_0. This abbreviation is possible because n is all but constant during the variations of pressure and temperature in the gun. The water-gas equilibrium does not alter the total number of molecules in the gas, while minor products will be shown, in the next section, to cause only small variations in the mean molecular weight.

The velocity of sound in the uncooled products is $(\gamma nRT_0)^{1/2}$, where γ is taken at the temperature T_0. For propellant X the velocity of sound is 3824 ft/sec.

3.22 Dissociation

At high temperatures and low pressures small quantities of dissociation products such as OH, H, and NO are formed, while the very hottest products contain traces of O_2, O, N_2O, and N. The dissociation products have only a small effect on the number of molecules present, but the energy absorbed in the dissociation makes a considerable difference to the energy balance which decides the equilibrium temperature. At higher pressures the effect is less, and it may be seen from the equations immediately following that at a given temperature the total amount of dissociation products is roughly proportional to $P^{-1/2}$.

The equilibrium constants governing the dissociation are simple and are listed in their normal order of importance:

$$[\mathrm{H}] = ([\mathrm{H_2}])^{1/2}\left(\frac{V}{82.06T}\right)^{1/2} K_1(T) \tag{16}$$

$$[\mathrm{OH}] = [\mathrm{H_2O}]([\mathrm{H_2}])^{-1/2}\left(\frac{V}{82.06T}\right)^{1/2} K_2(T) \tag{17}$$

$$[\mathrm{NO}] = [\mathrm{H_2O}]([\mathrm{N_2}])^{1/2}[\mathrm{H_2}]^{-1}\left(\frac{V}{82.06T}\right)^{1/2} K_3(T) \tag{18}$$

$$[\mathrm{N}] = ([\mathrm{N}_2])^{1/2}\left(\frac{V}{82.06T}\right)^{1/2} K_4(T) \tag{19}$$

$$[\mathrm{O}] = [\mathrm{H}_2\mathrm{O}]([\mathrm{H}_2])^{-1}\left(\frac{V}{82.06T}\right) K_5(T) \tag{20}$$

$$[\mathrm{O}_2] = \left(\frac{[\mathrm{H}_2\mathrm{O}]}{[\mathrm{H}_2]}\right)^2\left(\frac{V}{82.06T}\right) K_6(T) \tag{21}$$

where $K_1, \cdots K_6$ are functions of T alone and are given in Table 3.1. The dissociation products can be calculated, once we know the major products, and the number of gram-atoms of carbon, etc. available for the major products is diminished by those going into the minor products. The process of computation, therefore, goes as follows.

The minor products are guessed. It is simple and usually means little extra work if one starts with zero values. Then the number of gram-atoms of hydrogen, nitrogen, and oxygen available for the major products are computed as, say, $\{H\}'$, $\{N\}'$, and $\{O\}'$. The major products are calculated from equations 8 through 12, where now $\{H\}'$ replaces $\{H\}$, and so on. The minor constituents follow by using equations 16 through 21 and are compared with the original estimates. If they do not agree, the cycle is repeated until the results are consistent to $\frac{1}{2} \times 10^{-5}$ mole/g. The process converges rapidly for all propellants at gun pressures. At the lower pressures used in rockets, the dissociation is more intense, and, in the worst cases, the convergence becomes very slow; this indicates that our division into major and minor products is inappropriate, and the solution can be speeded up by rearranging the solution in an obvious way.

The minor products increase rapidly with temperature, roughly doubling for a rise of 200°K. Below 2500°K there are only negligible traces at pressures above 1 ton/sq in., and for many "cool" propellants it is not necessary to consider dissociation products. Table 3.6 shows the products at 0.2 g/cc for the propellant X previously used as an ex-

TABLE 3.6 DISSOCIATION PRODUCTS FROM PROPELLANT X, AT 0.2 G/CC

All Compositions in 10^{-5} mole/g

T, °K	[OH]	[H]	[NO]	[O_2]	[O]	[N]	Pressure, tons/sq in.
2500	0.3	1	0.02	10^{-4}	3×10^{-4}	2×10^{-3}	11.5
3000	3	6	0.3	8×10^{-3}	0.02	0.05	13.8
3500	13	19	2	0.1	0.2	0.3	16.1
4000	41	48	7	1	2	2	18.6

ample. The conditions at 3500 and 4000°K are, of course, attainable only by compressing the products and are included only to show how rapidly the dissociation increases with the temperature.

The temperatures at which these reactions are important are so high that it is safe to assume that the dissociation does not "freeze" at the rates of cooling found in guns.

Below about 2000°K there appear a set of minor products, which, to distinguish from the high-temperature dissociation products, we shall call the "combination products." They are formed in gases cooling in an explosion calorimeter or in the gases from an emptying gun and are therefore not usually of much importance, nor do the circumstances suggest that chemical equilibrium is attained. However, the matter is sometimes raised in connection with ultracool fuels, and so we add the formulas for the only two such products of any real importance:

$$[\mathrm{CH_4}] = \frac{[\mathrm{CO}]^2[\mathrm{H_2}]^2}{[\mathrm{CO_2}]}\left(\frac{82.06T}{V}\right)^2 K_7(T) \tag{22}$$

$$[\mathrm{NH_3}] = ([\mathrm{N_2}])^{1/2}([\mathrm{H_2}])^{3/2}\,\frac{82.06T}{V}\,K_8(T) \tag{23}$$

where the functions K_7 and K_8 are listed in Table 3.1. These products are formed from the major products by reactions in which the number of molecules decreases, and, consequently, the combination products are most pronounced at high pressures and, of course, low temperatures.

The effect of the dissociation products on the explosion temperature and pressure is now to be considered. The energy of the products is calculated from Table 3.2, which covers all the gases likely to be encountered. The energy of formation of all the products comes from Table 3.4; the energy of formation of the propellant is still the same as in the treatment without dissociation. The large negative energies of formation of the free radicals magnify their small mole ratios into substantial effects on the explosion temperature. For example, the splitting of hydrogen molecules into atoms requires 104 kcal/mole.

In Table 3.7 we show the energy balance for the products of propellant X, at 0.2 g/cc, allowing for dissociation. The uncooled explosion temperature is now 3072°K, instead of the 3090°K calculated without dissociation. The more accurate calculation makes the force 70.67 instead of 70.99 (tons/sq in.) × (cc/g). T_0 and the force now depend on the density of the products, the deviation from the result without dissociation being roughly proportional to $V^{1/2}$.

TABLE 3.7 ENERGY BALANCE FOR THE PRODUCTS OF PROPELLANT X, AT 0.2 G/CC

Minor Products Included, but No Pressure Corrections. Energies in cal/g

T, °K	E	$\Delta(EF)$	ζ
2500	662.6	871.0	−208.4
3000	836.8	864.1	−27.3
3100	872.2	861.8	10.4
3072	862.4	862.4	0.0

3.23 Experimental results

If only the major products are included,

$$PV = nRT \tag{24}$$

where n is independent of V and T. In particular, at the uncooled explosion temperature T_0,

$$PV = nRT_0 \tag{25}$$

where the right-hand side depends only on the nature of the propellant.

When dissociation is included, n and T_0 are altered by terms that are very roughly proportional to $V^{1/2}$. For the maximum uncooled pressure set up in an explosion at a density of loading of V^{-1} g/cc, we have

$$PV = \alpha - \beta V^{1/2} + O(V)$$

which can be written as

$$PV = \alpha - \beta\alpha^{1/2}P^{-1/2} + O(P^{-1}) \tag{26}$$

where α and β depend only on the composition of the propellant, and both are positive.

If we plot PV against P, the simpler theory gives a horizontal straight line, while the effect of dissociation is to lower PV below this line by an amount roughly proportional to $P^{-1/2}$.

Experimental data show quite a different behavior. The graph of PV against P is nearly straight, but not horizontal. The curve can be represented very closely by

$$PV = \alpha + P\eta \tag{27}$$

where η is positive and varies slowly with V. Since η is in effect defined by

$$\eta = V - \frac{\alpha}{P} \tag{28}$$

the value of α is chosen to make η as constant as possible. Equation 27 with constant η is the Noble-Abel equation of state, and η, whose dimensions are those of volume per unit mass, is called the "covolume" of the propellant.

The effect of dissociation can be seen sometimes with "hot" propellants at pressures under 10 tons/sq in. The effect is not really large and can easily be obscured by the difficulty of estimating consistent cooling corrections over a wide range of pressures.

The discrepancy between the present theory and the experimental results is most marked at high pressures, which indicates that the effect is due to our assumption of the perfect-gas laws. The deviations of real gases from these laws alter the equilibrium constants and the internal energies of the products. These effects are taken into account in the next section.

The observed covolume is about 1 cc/g and shows relatively little variation from one propellant to another. Those with hot products have small covolumes, though the whole range for present-day propellants is only 0.9–1.1 cc/g.

There have been few serious attempts to find a better equation of state than the Noble-Abel equation. This with a constant covolume represents the observed behavior of the product gases more accurately than most assumptions made in the theory of gun ballistics, and the form of the equation is not mathematically inconvenient. It should be remembered, however, that the closed vessel can prove that

$$P(V - \eta) = \text{constant}$$

only at the explosion temperature, whereas, in the application to guns, it is assumed that

$$P(V - \eta) = \text{constant} \times T \tag{29}$$

where T is any temperature less than T_0; it is assumed that η is independent of temperature, without any supporting evidence. It can be shown by the theory of the next section that, in fact, the covolume alters by less than 1 per cent over the range 2000–3000°K, for a typical propellant with $T_0 = 3000°\text{K}$. It is found also that

$$PV = nRT\left(1 + \frac{\beta}{V}\right) \tag{30}$$

is, at each temperature, a better representation of the theoretical equation of state than

$$P(V - \eta) = nRT \tag{31}$$

If best values of β and η are used the errors in PV for a typical propellant are of order 0.7 and 2 per cent, respectively.

3.24 Theory of the covolume and other pressure corrections

The specific heats and equilibrium constants tabulated in previous sections refer to zero pressure, and the explosion temperatures, pressures, and product compositions calculated from these tables are therefore incorrect. Of these quantities only the pressure can be measured experimentally. The theoretical temperatures and compositions are in error by unknown amounts.

The tables in the present section are intended to give real pressures of explosion, and this is confirmed by comparison with experimental results. To put it another way, we may say that these tables enable covolumes to be predicted. The tables also give true temperatures and compositions, both of which are difficult to test by experiment. At the same time this fact makes theoretical results all the more important in physical and chemical problems of interior ballistics, such as questions of erosion by heat transfer and chemical action. When this work was begun, there was a belief that the temperature of adiabatic explosion might decrease by 150°C under a pressure of 20 tons/sq in. It has now been found that the explosion temperature is in fact almost independent of pressure and within a few degrees of that calculated without pressure corrections. The temperature of burning under constant pressure is another important property of a propellant, with applications in the theory of rates of burning (chapter 2) and the interior ballistics of rockets. This temperature turns out to be strongly pressure-dependent (§ 3.32).

The composition of the explosion products is rather different from that calculated by the simpler tables without pressure corrections. This has important effects on the heat conductivity and viscosity of the product gases, since these quantities are sensitive to the amount of hydrogen in the products.

Work of a very similar nature has been carried out by Hirschfelder and his collaborators (published only as classified documents); the details are rather different, but the viewpoint is the same as our own.

We begin by explaining the general idea. We have to find the internal energy and heat content of the gases that occur in guns and closed vessels, at pressures up to 40 tons/sq in. and at temperatures in the range 1500 to 4000°K. The values at zero density are given in earlier sections. The pressure corrections can be derived from the equations of state of the products, by thermodynamic formulas. This use of the equation of state to obtain theoretical specific heats is now common in chemical engineering, but we have been able to find only one application at the temperature encountered in interior ballistics. Burlot[11] calculated the specific heats of CO_2 and N_2 from an empirical equation of state, claimed to hold up to 100°C and 300 atm. This is too slender a basis for even qualitative results under ballistic conditions. The only other early work that bears on this subject is that of Crow and Grimshaw,[12] who attempted to derive molecular radii from dielectric constants. When suitably corrected, the results fitted the observed covolumes of nonflashless propellants. This has no more than an empirical significance, for, in fact, the "covolume" may arise not only from the volume occupied by the molecules but also from the resulting change in the specific heat, which cannot be calculated from the rough equation of state used by Crow and Grimshaw. It is true that this change of the explosion temperature can be shown from the tables of the present section to be negligible; this result, however, could not have been deduced from any approximate equation of state.

---

[11] Burlot, *Mém. poudres*, **25** (1932), 314.

The calculation of heat and energy contents requires an accurate equation of state. Experimental results do not go beyond 700°K, and so there is a wide range to be covered by extrapolation before we reach the region, 1500–4000°K, of interest in ballistics. The extrapolation is, in fact, sufficiently wide to be unbridgeable in a purely empirical way. Fortunately, there is now a considerable body of theory to help. It is perhaps as well to emphasize that this theory has been verified by the equations of state of gases at normal temperatures, so that, in effect, the theory is being used as an extrapolation formula, which has the blessing of statistical mechanics. The work is straightforward, and the only doubtful point is whether our equations of state and specific heats are really sufficiently accurate to give a reasonably correct result at ballistic temperatures. Tests will be described later. Meanwhile, we may say that the basic data (the equations of state of the pure gases up to 600–700°K) and the theory are well established, and future modifications are likely to be small; also, there seems to be little hope of working back from experiments at ballistic temperatures. Accordingly, these tables are not likely to be much improved by new experimental data at low temperatures and not likely to be superseded by a more direct method.

In a purely empirical extrapolation to ballistic temperatures, the only reason for confidence in the results would be the accuracy of fit to experiments at normal temperatures and possibly the successful prediction of covolumes. The essential new feature of a theoretical extrapolation is the reasonable nature of the intermolecular forces assumed. For example, we treat N_2, CO, and H_2 as having fields of spherical symmetry, for this assumption is not only sufficient to account for their low-temperature equations of state but also reasonably consistent with what we know of their molecular structure. The same applies to H_2O, except that here we have used a dipole field with a short-range repulsion of spherical symmetry; the equation of state of a gas of such molecules has been given by Stockmayer.[13] The other main product of propellant combustion is CO_2, which presents the only real difficulty in our program. This molecule has the shape of a cigar, roughly, and it is not plausible to use a field of spherical symmetry, even though this gives a good fit to experiments at normal temperatures. We have therefore devised a molecular field of cigar or cylindrical shape, roughly speaking, and we have found the equation of state of a gas of such molecules. This equation we have fitted to observations on CO_2 up to 300°C, to find the parameters of the potential for this molecule. From this point the calculation of heat and energy contents at high temperatures has followed the same course as for the simpler molecules.

---

[12] Crow and Grimshaw, *Phil. Trans. Roy. Soc. (London)*, **230A** (1931), 39.

The pressure of a mixture of real gases can be written as

$$\frac{PV}{nRT} = 1 + \frac{B}{V} + \frac{nC}{V^2} + \cdots \tag{32}$$

In this series B, C, and the higher coefficients are functions of temperature and composition. It can be shown that the pressure of a pure gas can be represented by a convergent series of this form, up to the density at which the gas becomes a saturated vapor. At ballistic densities, which run up to about $V^{-1} = 0.35$, only the coefficients B and C need be retained. This is fortunate, since B and C are the only coefficients whose theoretical expressions have been evaluated numerically.

B has the dimensions of volume per unit mass, and, to be consistent with the definition of V, the units of B must be cubic centimeters per gram. B is obtained from the linear sum:

$$B = [CO_2]B_{CO_2} + [CO]B_{CO} + \cdots + [N_2]B_{N_2} \tag{33}$$

The coefficients B for the pure gases are given in Table 3.8. They are the "second virial coefficients" and are given in the units of cubic centimeters per mole, customary in physical chemistry. How best to derive B for a mixture from the values of the second virial coefficients of its constituents is still not conclusively settled. In our case only the simplest method (equation 33) can be considered, because the alternative methods lead to excessively complicated formulas for the internal energy and heat content of the mixture. In a typical case the two other well-known combination rules, the "square-root" and Lorentz methods,[14] gave values of B that were, respectively, 8.5 and 5.5 per cent smaller

---

[13] Stockmayer, *J. Chem. Phys.*, **9** (1941), 398.

[14] See Beattie and Stockmayer, *Rept. Progress Phys.* (1940), 195.

TABLE 3.8 CORRECTIONS TO PRESSURES

Temperature, °K	Table of B, cc/mole				Table of C, (cc/mole)^2			
	H_2	N_2, CO	CO_2	H_2O	H_2	N_2, CO	CO_2	H_2O
1600	16.4	32.1	45.7	−4.2	20	210	1385	220
1700	16.3	32.3	47.3	−2.5	20	200	1305	210
1800	16.2	32.4	48.7	−1.1	20	190	1235	195
1900	16.1	32.6	49.9	+0.2	20	180	1170	185
2000	16.0	32.6	50.9	1.2	15	170	1110	175
2100	15.9	32.7	51.8	2.2	15	160	1055	170
2200	15.8	32.7	52.6	3.0	15	155	1010	160
2300	15.7	32.8	53.2	3.7	15	150	965	155
2400	15.6	32.8	53.8	4.4	15	140	925	145
2500	15.6	32.8	54.4	5.0	15	135	885	140
2600	15.5	32.7	54.8	5.5	15	130	855	135
2700	15.4	32.7	55.3	6.0	15	125	825	130
2800	15.3	32.7	55.6	6.4	10	120	795	125
2900	15.3	32.6	56.0	6.8	10	120	765	120
3000	15.2	32.6	56.2	7.1	10	115	740	120
3100	15.1	32.6	56.5	7.5	10	110	720	115
3200	15.0	32.5	56.7	7.7	10	105	695	110
3300	15.0	32.4	56.9	8.0	10	105	675	105
3400	14.9	32.4	57.1	8.3	10	100	650	105
3500	14.8	32.3	57.3	8.5	10	95	635	100
3600	14.8	32.3	57.4	8.7	10	95	615	100
3700	14.7	32.2	57.5	8.9	10	90	600	95
3800	14.7	32.2	57.6	9.1	10	90	585	95
3900	14.6	32.1	57.7	9.3	10	85	570	90
4000	14.5	32.0	57.8	9.4	10	85	555	90

Hydrogen. Intermolecular forces from de Boer and Michels, *Physica*, **5** (1938), 945.

Nitrogen. Force constants from Corner, *Trans. Faraday Soc.*, **36** (1940), 780.

Steam. Parameters from Hirschfelder, McClure and Weeks, *J. Chem. Phys.*, **10** (1942), 201.

Carbon dioxide. Intermolecular potential by Corner, *Proc. Roy. Soc. (London)*, **192A** (1948), 275.

than the results of equation 33. These rules are usually more accurate than equation 33. A 5.5 per cent change in B corresponds to a 2 per cent change in the pressure, at 30 tons/sq in. The covolume from our tables, along with assumption (equation 33), turns out to be slightly too small, which suggests that an attempt to improve equation 33 may not improve the agreement with experiment. It is doubtful, too, whether the real accuracy of our individual values of B for the pure gases at high temperatures is great enough to justify a superstructure of complicated combination rules.

It may be noticed that in the linear sum (equation 33) we have omitted the minor products. The values of B for these gases are difficult to obtain (except in the case of hydrogen atoms). Their orders of magnitude can be guessed, however, and the error due to their omission can be estimated. The error is appreciable only for the hottest propellants at the lowest densities of loading. Calculation has shown that, for a propellant with a temperature of uncooled explosion over 3600°K, the inclusion of minor products increases the theoretical covolume by 2 per cent at a loading density of 0.1 g/cc, and by less than 1 per cent at 0.2 g/cc; these densities correspond to pressures of about 8 and 18 tons/sq in. Both pressures would be altered by 0.2 per cent by these covolume changes. The contribution of the minor products to the covolume is therefore negligible at gun pressures, even for the very hottest propellants. The direct effect on the pressure by increasing n is, of course, taken into account.

The values of B in Table 3.8 have been computed from the intermolecular forces, which were themselves derived from low-temperature experimental values of B.[15] The number of places retained in the table of B, and indeed in all the tables of the present section, is greater than the real accuracy of the quantities tabulated. The number of places was decided by the need for smoothness in the intermediate steps of computations to be made with the tables. These are adequate to give quantities such as $[CO_2]$ to $\frac{1}{2} \times 10^{-5}$ mole/g and explosion temperatures to 1°K. Ragged differences in calculations of this accuracy indicate an error of computation.

The coefficient C is obtained by a summation:

$$C = [CO_2]C_{CO_2} + [CO]C_{CO} + \cdots + [N_2]C_{N_2} \qquad (34)$$

The individual third virial coefficients C are listed in Table 3.8. They were calculated from the intermolecular forces derived from low-temperature values of B. Theoretical results for C as a function of these intermolecular forces have been given by de Boer and Michels[16] and Mayer and Montroll.[17] We have extrapolated to ballistic temperatures by power series, using the numerical results of Mayer and Montroll. C is of minor importance until pressures rise above 40 tons/sq in., and so the probably low real accuracy attained in its calculation is sufficient.

It may be worth pointing out that the three-term power series in equation 32,

---

[15] For details of the work, see Corner, *Proc. Phys. Soc.* (*London*), **58** (1946), 737.

[16] de Boer and Michels, *Physica*, **6** (1939), 97.

[17] Mayer and Montroll, *J. Chem. Phys.*, **9** (1941), 626.

$$\frac{PV}{nRT} = 1 + \frac{B}{V} + \frac{nC}{V^2} \tag{35}$$

is considerably more accurate than the series,

$$\frac{PV}{nRT} = 1 + B'P + C'P^2 \tag{36}$$

which is often used in chemical engineering. The latter equation has the form $V = f(P, T)$, which is a virtue in that field. In ballistics the more convenient form is $P = f(V, T)$, which is fortunately a property of the more accurate equation 35.

Throughout our tables we have taken N_2 and CO to have the same equation of state. This is known to be true to a few per cent in the second virial coefficient, as in most properties of these molecules.[18]

The virial coefficients B and C are functions of temperature. Inspection of the tables shows that the values of B for H_2, N_2, and CO are nearly constant over the range 1600–4000°K. C is not so constant, but, in view of its limited importance, it would be possible to take a mean value for the C of each molecular species. Our tables show that B_{H_2O} changes sign in passing from 1800 to 3600°K. The variation in B_{CO_2} is also appreciable. We have retained the temperature dependence of B and C on the grounds that it does not increase the labor involved in using the tables, and it may have an effect on the trend of covolumes from "hot" to "cool" propellants.

The ratio of the major products in the gases at any given density and temperature is determined by the equation,

$$\frac{[CO][H_2O]}{[CO_2][H_2]} = K \tag{37}$$

where K is the effective equilibrium constant for the water-gas reaction. If the gases were perfect, K would be $K_0(T)$, the function of temperature listed in Table 3.1. Since, however, the equation of state is really equation 32, it can be proved that

$$K = K_0(T) \exp\left(-\frac{n\Delta B}{V} - \frac{n^2\Delta C}{2V^2}\right) \tag{38}$$

where

$$\Delta B = B_{CO} + B_{H_2O} - B_{CO_2} - B_{H_2} \tag{39}$$

and

$$\Delta C = C_{CO} + C_{H_2O} - C_{CO_2} - C_{H_2} \tag{40}$$

---

[18] Grimm and Wolf, *Handbuch der Physik*, 2d ed., **24,** pt. 1 (1933), 977.

ΔB and $\frac{1}{2}\Delta C$ are given in Table 3.9. They are not zero; indeed, they have the same magnitude as the B and C of N_2. The effective equilibrium constant is increased by this effect, by as much as 50 per cent at pressures of order 30 tons/sq in. The composition of the products of explosion is therefore considerably different from that obtained from the simpler tables. Examples are discussed later.

TABLE 3.9 CORRECTIONS TO EQUILIBRIUM CONSTANTS

Temperature, °K	$-\Delta B$, cc/mole	$-\frac{1}{2}\Delta C$, (cc/mole)^2
1600	34.2	490
1700	33.8	460
1800	33.5	435
1900	33.2	410
2000	33.0	390
2100	32.8	370
2200	32.6	355
2300	32.5	340
2400	32.4	325
2500	32.2	310
2600	32.1	300
2700	32.0	290
2800	31.9	280
2900	31.8	270
3000	31.7	260
3100	31.6	255
3200	31.5	245
3300	31.4	235
3400	31.4	230
3500	31.3	225
3600	31.2	215
3700	31.1	210
3800	31.1	205
3900	31.0	200
4000	30.9	195

The amounts of minor products are determined by equilibrium constants, which can be corrected for gas imperfection in the same way. The guessing of B for molecules such as OH introduces some uncertainty, which is not important in view of the small amounts of these products. In fact, the correction could be omitted without introducing an error greater than 10^{-5} mole/g in the minor products, except at temperatures over 3000°K and pressures less than 10 tons/sq in. Taking rough values of the virial coefficients, chosen to be of the right order and to give convenient numerical quantities, we find that the only equilibrium constants that need correction are those for OH and NO:

$$[OH] = \frac{[H_2O]}{([H_2])^{1/2}}\left(\frac{V}{82.06T}\right)^{1/2} K_2(T)\exp\left(-\frac{20n}{V}\right) \tag{41}$$

$$[NO] = \frac{[H_2O]([N_2])^{1/2}}{[H_2]}\left(\frac{V}{82.06T}\right)^{1/2} K_3(T)\exp\left(-\frac{20n}{V}\right) \tag{42}$$

which replace equations 17 and 18.

We must now correct the internal energy and heat content. From the thermodynamic relations,

$$\left(\frac{\partial E}{\partial V}\right)_T = T\left(\frac{\partial P}{\partial T}\right)_V - P$$

and

$$\left(\frac{\partial H}{\partial P}\right)_T = V - T\left(\frac{\partial V}{\partial T}\right)_P$$

it can be shown that the internal energy E and heat content H of the products of 1 g of propellant are

$$E = \Sigma[CO_2]E_{CO_2}(T, \text{perfect gas})$$
$$-\frac{nRT}{V}\Sigma[CO_2]T\frac{d}{dT}B_{CO_2} - \frac{n^2RT}{2V^2}\Sigma[CO_2]T\frac{d}{dT}C_{CO_2} + O(V^{-3})$$

and

$$H = \Sigma[CO_2]H_{CO_2}(T, \text{perfect gas}) + \frac{nRT}{V}\Sigma[CO_2]\left(B_{CO_2} - T\frac{d}{dT}B_{CO_2}\right)$$
$$+\frac{n^2RT}{V^2}\Sigma[CO_2]\left(C_{CO_2} - \frac{1}{2}T\frac{d}{dT}C_{CO_2}\right) + O(V^{-3})$$

where the summations are over all the types of product, with CO_2 as the typical one. We may write these results in the form,

$$E = \Sigma[CO_2]E_{CO_2,0} + \frac{n}{V}\Sigma[CO_2]E_{CO_2,1} + \left(\frac{n}{V}\right)^2\Sigma[CO_2]E_{CO_2,2} \tag{43}$$

$$H = \Sigma[CO_2]H_{CO_2,0} + \frac{n}{V}\Sigma[CO_2]H_{CO_2,1} + \left(\frac{n}{V}\right)^2\Sigma[CO_2]H_{CO_2,2} \tag{44}$$

where $E_{CO_2,0}$ and $H_{CO_2,0}$ denote the internal energy and heat content at zero density, computed in the usual way from tables of mean specific heats. The quantities E_1 for the various gases are given in Table 3.10. As we shall not need heat contents until § 3.32, we do not give H_1 at this point. E_2 and H_2 vary by only a few per cent over our range of temperatures and have been given mean values.

TABLE 3.10 CORRECTIONS TO INTERNAL ENERGIES

Temperature, °K	$E_1/100$, cal-cc/mole			
	H_2	N_2, CO	CO_2	H_2O
1600	45	−110	−870	−935
1700	50	−95	−840	−895
1800	55	−80	−810	−855
1900	65	−70	−785	−825
2000	70	−55	−755	−795
2100	75	−40	−730	−770
2200	80	−25	−700	−745
2300	90	−15	−675	−725
2400	95	0	−645	−705
2500	100	15	−620	−685
2600	105	25	−595	−665
2700	110	40	−565	−650
2800	120	55	−540	−635
2900	125	65	−515	−620
3000	130	80	−490	−605
3100	135	95	−465	−590
3200	140	105	−440	−580
3300	145	120	−415	−565
3400	150	130	−390	−555
3500	160	145	−365	−540
3600	165	155	−340	−530
3700	170	170	−315	−520
3800	175	185	−290	−510
3900	180	195	−265	−500
4000	185	210	−240	−490

At all temperatures in this range, use:

	H_2	N_2, CO	CO_2	H_2O
$10^{-4}E_2$	3	34	220	35 cal-(cc/mole)^2

The energy zero for closed-vessel calculations is the initial temperature of the propellant, which we are supposing to be 300°K, and zero density; that is, equations 43 and 44 give the energy and heat contents of the products at (V, T) relative to *the same* gases at 300°K and zero density.

Reference to the tables of E_1 will show that the values for the different gases include both signs, and, accordingly, the summation over all constituents tends to be small. E itself lies in the range 600–1000 cal/g, and of this about −3 cal/g comes from the E_1 terms and about

1 cal/g from the E_2 terms (both these figures refer to pressures of 20 tons/sq in.). In the calculations of interior ballistics H is of the order of 600–1000 cal/g, while H_1 terms contribute about 40 cal/g, and the H_2 terms 4 cal/g at 20 tons/sq in. This demonstrates how small are the pressure corrections to the internal energy, compared with those to the heat content. As a corollary, the tables without pressure corrections give temperatures of uncooled explosion at constant volume correct to within a few degrees; on the other hand, the temperature of burning at constant pressure is really lower than that computed from the simple tables, to the extent of 150°C at 20 tons/sq in.

Computation with these tables is a little longer than if pressure corrections are omitted, but the principles are the same. The explosion temperature T_0 at any given specific volume is the temperature which makes

$$\zeta \equiv E - \Delta(EF) = 0 \tag{45}$$

The corresponding composition gives n, the number of moles of product per gram of propellant. To find the pressure and the covolume, the correction factor to the ideal-gas laws, namely,

$$1 + \frac{B}{V} + \frac{nC}{V^2}$$

is calculated for the two temperatures bracketing the explosion temperature, and its value at the latter is deduced by linear interpolation. The explosion pressure is

$$P = 0.5384 \frac{nT_0}{V}\left(1 + \frac{B}{V} + \frac{nC}{V^2}\right) \text{ tons/sq in.} \tag{46}$$

The pressure, by the conventions of interior ballistics, is written as

$$P = \frac{\lambda_0}{V - \eta} \tag{47}$$

where λ_0 is the "force constant." The "observed covolume" reported from experiments is calculated from the observed pressure and a force constant computed without pressure corrections at about 0.2 g/cc. The theoretical covolumes listed later (Table 3.11) are for the sake of consistency calculated with the same force constant.

We should say something about the real accuracy of these tables and the nominal accuracy to be achieved in computations. The real accuracy refers to the difference between theoretical and experimental results for a sample of *known* composition. The fact that this will not usually be the same as the "nominal composition" of this variety of propellant is important in practice but has no connection with the real accuracy of the thermochemical tables. This is decided by (*a*) errors in the theory used, and (*b*) errors in the data. Under *a* we must include: (1) neglect of virial coefficients above the third; errors of the order of 0.2 cal/g in ζ, the energy balance, and 0.5 cal/g in μ, at 20 tons/sq in.; μ is the quantity analogous to ζ in explosions at constant pressure; (2) neglect of energy changes in gelatinization; error usually about 2 cal/g; (3) neglect of gas imperfection at 300°K and 1 atm; errors of a fraction of a calorie per gram in the calculation of explosions under constant pressure; (4) treatment of the minor products as perfect gases; even for the hottest propellants the maximum error is rarely more than 0.2 cal/g in ζ and 1 cal/g in μ.

For comparison with these errors we may quote the pressure corrections in the tables of this section and § 3.32. These amount to changes in ζ of 2 cal/g, in μ of the order of 50 cal/g (at 20 tons/sq in.). It requires changes of about 40 cal/g in ζ or μ to move the appropriate explosion temperatures by 100°K.

Errors of type *b* occur in both the tables without pressure corrections and in the present supplement. It is believed that the errors in the main tables may introduce errors of the order of 10 cal/g in ζ and μ. It is difficult to estimate the uncertainties in our tables of pressure corrections, since these errors arise from many points: the accuracy of the low-temperature observations, which are the basis of the tables; errors in the form of the intermolecular potentials; and errors in the curve fitting, which yields the parameters of the potential. We estimate the uncertainty to be 5 to 10 cal/g in ζ and μ. This is consistent with the differences between observed covolumes and those calculated from our tables.

To sum up this discussion of the real accuracy, we may say that these tables of pressure corrections have reduced the real errors to the same order as those in the *thermochemical data* of the earlier tables.

We shall now show the kind of result obtained by using the tables of pressure corrections. We take the same propellant X discussed in earlier sections. Table 3.11 shows the theoretical temperature, products, pressure, and covolume at various product densities. Similar calculations without pressure corrections lead to considerable differences in the main products, which can be inferred also from the rapid variation of the main products, although the explosion temperature changes only slowly. The minor products are little affected, and the total number of moles of product is almost unaltered. So is T_0, which is moved only a few degrees by the pressure corrections. Consequently the "covolume" comes almost entirely from the factor

$$1 + \frac{B}{V} + \frac{nC}{V^2}$$

in equation 46. This simple interpretation is true only because the pressure alters the energy of the products substantially but in both directions, so that the effect on T_0 is small.

The most interesting result in Table 3.11 is the "theoretical covolume" η, computed from equation 47 with $\lambda_0 = 70.67$. At pressures over 5 tons/sq in., η decreases with increase of density. The accepted figure for this propellant is 0.95 cc/g, determined by closed-vessel firings at 27 tons/sq in. Our value at this pressure is 4 per cent too low.

TABLE 3.11 UNCOOLED EXPLOSION OF *X* AT CONSTANT VOLUME

Product Density, g/cc	0.01	0.05	0.1	0.2	0.35
T_0, °K	3024	3058	3068	3073	3073
$[CO_2]$, in 10^{-5} mole/g	346	336	325	302	267
$[CO]$	1892	1902	1913	1936	1971
$[H_2O]$	870	888	900	925	961
$[H_2]$	617	610	600	577	542
$[N_2]$	521	522	522	522	522
$[OH]$	13	6	5	3	2
$[H]$	27	13	9	7	5
$[NO]$	1	½	½	½	½
$10^5 n$	4287	4277	4274	4272	4271
P, tons/sq in.	0.7061	3.723	7.878	17.471	35.161
$\Delta(EF)$, cal/g	845	856	858	858	857
Covolume, cc/g	−0.1	1.02	1.03	0.96	0.85

As the maximum pressure is reduced below 5 tons/sq in., the covolume begins to decrease again, until it becomes negative at pressures of the order of 1 ton/sq in. This behavior is due to the increasing dissociation causing low temperatures of explosion. This suggests also that a "hot" propellant will show the same effect at a higher density of loading, and computation has confirmed this expectation.

TABLE 3.12 DEPENDENCE OF THEORETICAL COVOLUME ON λ_0, FOR PROPELLANT *X*

	Covolume (cc/g) at a Loading Density of				
λ_0 (tons/sq in.) × (cc/g)	0.01	0.05	0.1	0.2	0.35 g/cc
70	0.9	1.20	1.11	0.99	0.87
70.67	−0.1	1.02	1.03	0.96	0.85

The covolume is not very sensitive to the λ_0 used (Table 3.12) except at small densities of loading, where the covolume exerts a trivial influence on the pressure. For ballistic purposes the best single covolume (for any assigned λ_0) is that for the highest densities of the products, say, at 0.3 g/cc. The error at lower pressures is small and varies slowly with λ_0; it seems best, therefore, to retain the conventional λ_0 calculated without pressure corrections and to take the corresponding covolume at 0.3 g/cc.

Table 3.13 shows calculated and observed covolumes for a series of propellants, listed in order of their values of T_0. Most of the experimental results refer to the neighborhood of 0.2 g/cc. From the results for propellant X, it appears that our theoretical covolume at 0.2 g/cc is likely to be 1 or 2 per cent higher than the accepted single value of the covolume, and this is confirmed, in the main, by Table 3.13. Both theoretical and observed covolumes show a decrease in passing to "hotter" propellants. The experimental values do not show the same smooth progression as the theoretical results, which indicates the uncertainty in these observed values to be about 0.02 cc/g.

TABLE 3.13 SOME THEORETICAL COVOLUMES USING STANDARD VALUES OF λ_0

		Covolume, cc/g, at			Observed
T_0, at 0.3 g/cc	λ_0	0.1	0.2	0.3 g/cc	Covolume
2430	61.7	1.14	1.02	0.93	0.99
2780	66.9	1.10	0.98	0.90	0.96
2800	65.6	1.04	0.96	0.89	1.01
3070	70.7	1.03	0.96	0.88	0.94
3300	72.6	0.98	0.93	0.87	0.91
3620	75.8	0.91	0.91	0.86	0.94

It is useful to have a simple means of estimating the covolume, which can be done from the formula:

$$\eta\ (\text{cc/g}) = 1.18 + 6.9\ \{\text{C}\} - 11.5\ \{\text{O}\} \qquad (48)$$

This was obtained by noting that the covolume appears to be a function of the calorimetric value of the propellant and, hence, of the heat of formation (at constant volume and 300°K) of the products at low temperatures (water liquid). This heat is, by Table 3.4, nearly independent of the equilibrium constant at which the reaction freezes, and is roughly

$$\epsilon = 67.4\ \{\text{O}\} - 40.7\ \{\text{C}\}\ \text{kcal/g}$$

The theoretical covolumes at a density of loading of 0.2 g/cc are represented by $\eta = 1.20 - 0.017\epsilon$ with rms deviation 0.01 cc/g. Reducing all these covolumes by 0.02 cc/g to improve agreement with experimental values, we arrive at equation 48 as a formula for the covolume in the neighborhood of 20 tons/sq in.

3.3 The equilibrium state after burning under constant pressure without cooling

Until now we have considered only processes at constant volume. They can be realized in practice in the closed vessel. If we now think of reactions in a vessel with a valve to hold the pressure steady, we are led to study the thermodynamics of reaction at constant pressure. The most important application is to rockets, where the valve is a nozzle; here the pressure is effectively constant during the reaction of any sufficiently small part of the charge. Another application is to the thin reaction zone at the surface of burning propellant, for here also each element of reaction passes through the zone under an effectively constant pressure exerted by preceding elements.

We discuss processes at constant pressure although their only application to the interior ballistics of guns is in connection with the theory of burning. The tables and the methods are so closely related to the process at constant volume that only a brief discussion is needed.

3.31 Theory without pressure corrections

For any assumed temperature of the product gases, their composition can be calculated, given (1) the equilibrium constants of Table 3.1, and (2) the atomic composition of the propellant. This has been explained in §§ 3.21 and 3.22.

The heat of formation of the propellant at constant pressure, 300°K, and 1 atmosphere is greater than the energy of formation at constant volume (Table 3.3) by the work done by the external pressure during the disappearance of $\frac{1}{2}[\{\mathrm{H}\} + \{\mathrm{O}\} + \{\mathrm{N}\}]$ moles of nearly perfect gas. This work is $300R$ per mole, with $R = 1.987$ cal/deg. Hence the heat of formation at constant pressure is

$$\text{Energy of formation at constant volume} + 298[\{\mathrm{H}\} + \{\mathrm{N}\} + \{\mathrm{O}\}] \text{ cal/g}$$

The heat of formation of the products can be calculated from Table 3.4 by a similar process. To eliminate frequent recalculation, the relatively few values needed are given in Table 3.14.

We can thus obtain $\Delta(HF)$, the difference in the heats of formation of propellant and products. For equilibrium this must be equal to the heat content of the products at the explosion temperature T_m. Since, for a perfect gas,

$$C_p - C_v = R$$

we obtain H, the heat content, at temperature T, as (*a*) the internal energy E, computed from Table 3.2, and (*b*) with $1.987(T - 300)n$ cal/g in addition. Writing

$$\mu = H - \Delta(HF) \tag{49}$$

we have to find the temperature at which μ vanishes.

We run over the calculation in brief. We wish to find the equilibrium state at pressure P tons/sq in. We guess the temperature T_m, which is roughly $0.8T_0$, and n, which is roughly $\frac{1}{2}\{N\} + \frac{1}{2}\{H\} + \{C\}$. The products at the assumed T_m are calculated as in § 3.22, it being noted that, in equations such as 16,

$$\frac{V}{82.06T} = \frac{n}{152.42P}$$

The products lead to a better n, and the process is repeated until it is self-consistent. The heat content of the products is computed with the help of Table 3.2 and $\Delta(HF)$ from Tables 3.3 and 3.14. We thus find μ.

We repeat with other values of the temperature until T_m is bracketed. If the bracket is an interval of 100°K, linear interpolation is sufficient, the maximum error being about ½°K.

Table 3.15 compares the equilibrium states for propellant X under constant-volume and constant-pressure conditions. The temperature under the latter conditions lies about 600°K lower than when the gases

TABLE 3.14 HEATS OF FORMATION AT CONSTANT PRESSURE

At 300°K, 1 atm, from Graphite, Hydrogen Gas, Nitrogen Gas, and Oxygen Gas

Substance	Heat of Formation, kcal/mole
CO	26.39
CO_2	94.04
H_2O liquid	68.33
H_2O gas	57.80
CH_4	17.87
NH_3	10.97
NO	−21.53
OH	−9.31
N	−85.55
O	−59.05
H	−52.09

TABLE 3.15 EQUILIBRIUM STATE FOR PROPELLANT *X*, STARTING AT 300°K

Conditions	Temperature, °K	Molar Composition, 10^{-5} mole/g				
		CO_2	CO	H_2O	H_2	N_2
Constant volume, 0.2 g/cc	3072	347	1891	879	622	522
Constant pressure, 20 tons/sq in.	2493	377	1861	853	654	522

do no work. This difference can be obtained, in order of magnitude, by a simple argument. Let γ be the mean ratio of specific heats at temperatures between T_0 and T_m. Then,

$$\begin{aligned} H(T_m) &= E(T_m) + nR(T - 300) \\ &= E(T_0) + \frac{nR}{\gamma - 1}(T_m - T_0) + nR(T_m - 300) \\ &= \Delta(EF) + \frac{nR}{\gamma - 1}(T_m - T_0) + nR(T_m - 300) \end{aligned}$$

Neglecting the difference between $\Delta(HF)$ and $\Delta(EF)$, we have

$$H(T_m) = \Delta(EF)$$

and so,

$$T_0 - T_m = \frac{(\gamma - 1)(T_0 - 300)}{\gamma} \qquad (50)$$

Since for propellant X, γ is about 1.25, $T_0 - T_m$ is about one fifth of $T_0 - 300$.

3.32 Pressure corrections

From the thermodynamic relation,

$$\left(\frac{\partial H}{\partial P}\right)_T = V - T\left(\frac{\partial V}{\partial T}\right)_P \qquad (51)$$

it can be shown that the heat content H of the products of one gram of propellant is

$$H = \Sigma[CO_2]H_{CO_2}(T, \text{perfect gas}) + \frac{nRT}{V}\Sigma[CO_2]\left(B_{CO_2} - T\frac{d}{dT}B_{CO_2}\right) + \frac{n^2RT}{V^2}\Sigma[CO_2]\left(C_{CO_2} - \frac{1}{2}T\frac{d}{dT}C_{CO_2}\right) + O(V^{-3}) \qquad (52)$$

where the summations are over all the types of product. We write this as

$$H = \Sigma[CO_2]H_{CO_2,0} + \frac{n}{V}\Sigma[CO_2]H_{CO_2,1} + \left(\frac{n}{V}\right)^2\Sigma[CO_2]H_{CO_2,2} \qquad (53)$$

and list H_1 and H_2 for the various gases in Table 3.16.

There is little cancelation in the summation of H_1 values, and the effect of pressure corrections is correspondingly large, compared with the effect in a closed vessel. The temperature falls with pressure, at the rate of about 7½°K per ton/sq in., with very little difference between various propellants.

TABLE 3.16 PRESSURE CORRECTIONS TO HEAT CONTENTS

Temperature, °K	$H_1/100$, cal-cc/mole			
	H_2	N_2, CO	CO_2	H_2O
1600	565	910	585	−1065
1700	600	995	760	−975
1800	635	1080	930	−895
1900	670	1160	1100	−820
2000	705	1240	1265	−745
2100	740	1325	1430	−680
2200	775	1405	1595	−615
2300	805	1485	1760	−555
2400	840	1560	1920	−495
2500	875	1640	2080	−440
2600	905	1720	2240	−385
2700	940	1795	2400	−330
2800	970	1870	2555	−280
2900	1005	1950	2710	−230
3000	1035	2025	2865	−180
3100	1065	2100	3015	−135
3200	1100	2170	3170	−85
3300	1130	2245	3320	−40
3400	1160	2320	3470	+5
3500	1190	2395	3620	50
3600	1220	2465	3770	90
3700	1250	2540	3920	135
3800	1280	2610	4065	175
3900	1310	2680	4210	220
4000	1340	2750	4355	260

At all temperatures in this range, use:

	H_2	N_2, CO	CO_2	H_2O
$10^{-4}H_2$	10	101	661	106 cal-(cc/mole)^2

Computation of the equilibrium state is not greatly lengthened by the inclusion of pressure corrections. Let the pressure be P tons/sq in. The first step is to estimate T_m from equation 50. The specific volume, V cc/g, of the products at P tons/sq in., is estimated, and a neighboring simple value of V^{-1} is chosen. Calculations of the products are made at two temperatures 100°K apart, bracketing T_m. The heat content H

of the products, relative to 300°K and zero density, is computed from equation 53. $\Delta(HF)$ comes from Tables 3.3 and 3.14, and then we calculate

$$\mu = H - \Delta(HF)$$

for two different temperatures for each V; by linear interpolation we find the temperature at which $\mu = 0$. This gives T_m for the assumed product density V^{-1} g/cc. The corresponding pressure P is found from equation 32. We have now found T_m at one pressure P, and the calculations must now be repeated at other values of V until the specified P can be reached by interpolation. Linear interpolation with respect to P gives compositions with errors of about 10^{-5} mole/g. To find T_m by linear interpolation, it is most accurate to interpolate T_m^{-1}. This gives T_m to about 1°. Of course, these interpolations are not necessary if our object is to find T as a function of P; they are necessary only if we are interested in one special value of P.

In the previous calculations we have omitted the heat content of the products due to gas imperfections at 300°K and 1 atmosphere. The error is a fraction of a calorie per gram and is smaller than the uncertainties in the heats of formation of the propellant constituents and products, and also smaller than the neglected change in the energy when the ingredients gelatinize to form the colloidal propellant.

The results for our typical propellant X are shown in Table 3.17 and Fig. 3.1. The temperature of the products has a maximum just below 1 ton/sq in., decreasing at smaller pressures because of the increasing dissociation and at higher pressures because of the increasing heat content of the imperfect gases. At 25 tons/sq in. the T_m is about 180°K lower than that calculated without pressure corrections. Above 1 ton/sq in., the main products and $1/T_m$ are nearly linear functions of pressure.

TABLE 3.17 EXPLOSION OF X UNDER CONSTANT PRESSURE

Pressure, tons/sq in.	0.577	3.00	6.255	13.56	26.46
Product density, g/cc	0.01	0.05	0.1	0.2	0.35
T_m, °K	2482	2468	2440	2389	2309
$[CO_2]$ in 10^{-5} mole/g	376	368	358	336	302
$[CO]$	1862	1870	1880	1902	1936
$[H_2O]$	853	862	872	894	928
$[H_2]$	652	644	634	612	579
$[N_2]$	522	522	522	522	522
$[OH]$	1	½	½	0	0
$[H]$	4	2	1	½	½
$10^5 n$	4270	4268	4268	4267	4267
$\Delta(HF)$, cal/g	843	844	844	842	839

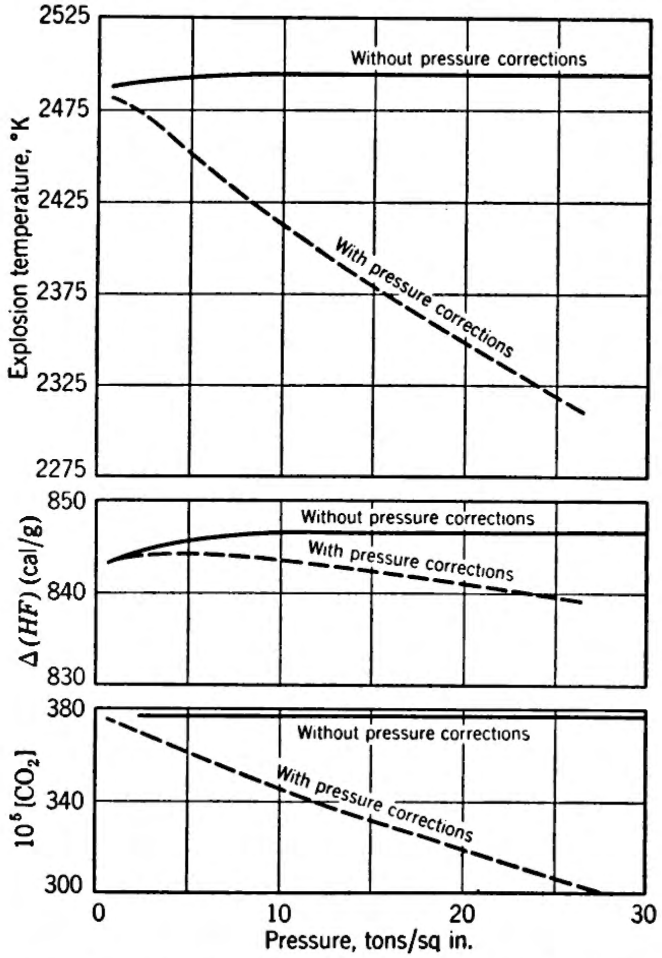

FIG. 3.1 Theoretical results for the explosion of propellant X under constant pressure conditions at 300°K, showing the effects caused by pressure corrections to the simple thermochemical tables.

3.33 Specific impulse of a rocket fuel

From the equilibrium state after reaction at constant pressure it is easy to calculate the energy released by an adiabatic expansion of a stream of gas. In particular, this gives the thrust on a nozzle, neglecting heat loss to the walls.

The formulas are easily written down. Rocket-chamber pressures are rarely more than 1 ton/sq in., and it is permissible to neglect pressure corrections. Dissociation is reduced, compared with gun calculations on the same propellant, by the lower temperatures in the rocket, whereas the lower pressures have the opposite effect. On the whole, dissociation is of the same order as in gun calculations.

Dissociation complicates the theory and introduces some uncertainty into the results. If it is assumed that the dissociation is at each stage at equilibrium with the temperature, the accurate calculation of the entropy change in the expansion becomes extremely laborious, though it can be and has been done for sufficiently important fuels. In this section we give a short method, which is a good approximation even for the highest temperatures.

Whether the reactions can preserve equilibrium conditions in a rapidly moving element of gas is difficult to say, the temperatures being rather far from laboratory conditions. This makes the physical basis of the preceding method a little uncertain. Computation from alternative extreme assumptions have been made by Dr. Pike, who has concluded that the uncertainty in the final results is nevertheless quite small. The matter has been studied in some detail by Penner and Altman.[19]

When dissociation is small and the expansion ratio of the nozzle is not too great, the formulas can be given an explicit form, in terms of T_m and a mean γ.

We begin with the most general case, in which gas at pressure P_m and temperature T_m is expanded adiabatically to final pressure P_f and temperature T_f. The final pressure P_f is specified, and we have to find the thrust obtained from the fuel. This appears, as may be seen later, in the form of a momentum per unit mass of the fuel, the "specific impulse" of this fuel between pressures P_m and P_f. The details of the nozzle influence the specific impulse only insofar as they alter the hydrodynamic and heat losses, which occur in real nozzles but are neglected in the theory. The specific impulses of propellants between 100 and 1 atm are of the order 200 lb wt × sec/lb mass, that is, about 6000 ft/sec.

We assume that the final pressure P_f is equal to the external atmospheric pressure. If not, there is an extra contribution to the thrust, consisting of the product of the exit area of the nozzle and the excess of the gas pressure over the external pressure. We shall also omit pressure corrections, since the pressure rarely exceeds 1 ton/sq in.

Let us suppose that we can calculate the final temperature T_f. Then the final velocity v of the gas is such that the kinetic energy gained in the expansion is equal to the change in the heat content of the gases:

$$\tfrac{1}{2}v^2 = H(T_m) - H(T_f) \tag{54}$$

where $H(T)$ is the heat content of the gas at temperature T, per gram. The heat content is obtained by calculating the composition at temperature T (§§ 3.21, 3.22) and then using Table 3.2 with

---

[19] Penner and Altman, *J. Franklin Inst.*, **245** (1948), 421. Altman and Penner, *J. Chem. Phys.*, **17** (1949), 56. Penner, *J. Applied Phys.*, **20** (1949), 445. Penner, *J. Am. Chem. Soc.*, **71** (1949), 788.

$$C_p - C_v = R \tag{55}$$

The specific impulse is v. Hence, the problem reduces to finding the final temperature T_f.

If heat losses to the walls of the combustion chamber and nozzle are neglected, the expansion is adiabatic. The heat content of the gases at temperature T and mole numbers [CO_2], etc., is

$$\Sigma[\mathrm{CO_2}]\left[\int_{300}^{T} C_p\,dT + HF(\mathrm{CO_2})\right]$$

where the summation is over all constituents and $HF(CO_2)$ is the heat of formation of a mole of CO_2 at 300°K and 1 atm from the standard substances. The heat absorbed in a change dT is

$$\Sigma d[\mathrm{CO_2}]\left[\int_{300}^{T} C_p\,dT + HF(\mathrm{CO_2})\right] + \Sigma[\mathrm{CO_2}]C_p\,dT$$

and the change in entropy is this expression divided by T:

$$dS = \sum \frac{d[\mathrm{CO_2}]}{T}\left[\int_{300}^{T} C_p\,dT + HF(\mathrm{CO_2})\right] + \Sigma[\mathrm{CO_2}]C_p\frac{dT}{T}$$

so that the change in entropy from the chamber temperature T_m to the temperature T_f at the exit of the nozzle is

$$\Delta S = \sum \int_{T_m}^{T_f}\left[\int_{300}^{T} C_p\,dT + HF(\mathrm{CO_2})\right]\frac{d[\mathrm{CO_2}]}{T} + \Sigma[\mathrm{CO_2}]_f\int_{300}^{T_f} C_p\frac{dT}{T}$$
$$- \Sigma[\mathrm{CO_2}]_m\int_{300}^{T_m} C_p\frac{dT}{T} - \sum\int_{T_m}^{T_f} d[\mathrm{CO_2}]\int_{300}^{T} C_p\frac{dT}{T} \tag{56}$$

This is exact. The total entropy change in the expansion from (T_m, P_m) to (T_f, P_f) is given by ΔS, together with the further term due to the expansion:

$$\int_{P_f}^{P_m} R\Sigma[\mathrm{CO_2}]\frac{dP}{P}$$

where $R = 1.987$ cal/mole·deg is the gas constant.

Hence, the final temperature T_f is determined by

$$\Delta S + \int_{P_f}^{P_m} R\Sigma[\mathrm{CO_2}]\frac{dP}{P} = 0 \tag{57}$$

and this depends on how closely the composition of the products follows the equilibrium function of temperature. Equation 57 can be used in its exact form but is wearisome to compute, nor is there usually any need to do so. In a process suggested by Dr. Devonshire, we approximate to ΔS by

$$\Delta S = \sum \frac{([CO_2]_f - [CO_2]_m)}{T_1}\left(HF(CO_2) + \int_{300}^{T_1} C_p\, dT - T_1 \int_{300}^{T_1} C_p \frac{dT}{T}\right) + \Sigma[CO_2]_f \int_{300}^{T_f} \frac{C_p\, dT}{T} - \Sigma[CO_2]_m \int_{300}^{T_m} C_p \frac{dT}{T} \quad (58)$$

where T_1 is a mean temperature at which most of the change in $[CO_2]$ takes place; T_1 may have to be different for the various molecular species.

Let us now consider the computation of equation 58. The function $\int_{300}^{T} C_p\, dT/T$ is tabulated for each of the main constituents in Table 3.18. Terms such as $[CO_2]_m$ are known for the main constituents from the gas composition at the initial temperature, and $[CO_2]_f$ can be calculated on the basis of no dissociation and a water-gas equilibrium constant K_0 of 2. HF for the main products is given in Table 3.14 and $\int_{300}^{T} C_p\, dT$ can be computed from equation 55 and Table 3.2. For the T_1 corresponding to the main products we take a temperature some few hundred degrees below T_m. A glance at Table 3.1 will suggest a suitable value. Hence we can compute all those terms in equation 58 belonging to the major products CO_2, CO, H_2, H_2O, and N_2.

For a minor product such as OH, $[OH]_f = 0$, and the terms in equation 58 reduce to

$$-\frac{[OH]_m}{T_1}\left[HF(OH) + \int_{300}^{T_1} C_p\, dT\right]$$

which can be computed from Tables 3.2 and 3.14. The dissociation falls rapidly as the temperature goes down, and so T_1 should be taken at, say, 100°K below T_m. The exact value is not important. Hence we can calculate all the terms appearing in ΔS.

We have now to compute

$$R \int_{P_f}^{P_m} \Sigma[CO_2] \frac{dP}{P}$$

which is simplified by $\Sigma[CO_2]$ being constant ($= n$) except at the very highest temperatures, where dissociation occurs; we can write, with very good accuracy,

$$R \int_{P_f}^{P_m} \Sigma[CO_2] \frac{dP}{P} = nR \ln \frac{P_m}{P_f} \quad (59)$$

TABLE 3.18 $\int_{300}^{T} C_p\,(T')\,dT'/T'$ FOR THE PRODUCT GASES

At Zero Density. Unit Is cal/mole·deg

T, °K	CO_2	H_2O	CO	H_2	N_2	OH	NO	O_2	NH_3	CH_4
800	10.403	8.321	7.039	6.846	6.987	6.953	7.209	7.333	9.786	11.05
1000	13.230	10.455	8.776	8.452	8.699	8.566	8.992	9.165	12.627	14.66
1200	15.647	12.312	10.245	9.784	10.148	9.915	10.494	10.697	15.166	17.95
1400	17.757	13.970	11.518	10.939	11.406	11.101	11.789	12.027	17.467	20.96
1500	18.719	14.742	12.097	11.470	11.979	11.644	12.377	12.631	18.544	22.38
1600	19.628	15.48	12.642	11.974	12.519	12.157	12.931	13.196	19.574	23.74
1700	20.487	16.18	13.158	12.454	13.031	12.644	13.455	13.731	20.561	25.04
1800	21.302	16.86	13.648	12.910	13.517	13.107	13.951	14.240	21.509	26.29
1900	22.079	17.51	14.114	13.343	13.980	13.547	14.421	14.724	22.420	27.49
2000	22.821	18.13	14.558	13.758	14.421	13.970	14.868	15.185	23.298	28.64
2100	23.531	18.74	14.981	14.158	14.841	14.377	15.295	15.625	24.144	29.75
2200	24.213	19.33	15.386	14.544	15.243	14.770	15.704	16.047	24.959	30.82
2300	24.867	19.89	15.775	14.916	15.629	15.147	16.097	16.453	25.746	31.85
2400	25.495	20.43	16.149	15.275	15.999	15.511	16.476	16.845	26.509	32.84
2500	26.100	20.96	16.508	15.622	16.356	15.862	16.841	17.224	27.248	33.80
2600	26.684	21.47	16.854	15.958	16.700	16.200	17.191	17.590		
2700	27.248	21.96	17.188	16.283	17.032	16.527	17.527	17.944		
2800	27.792	22.44	17.510	16.598	17.353	16.845	17.851	18.287		
2900	28.321	22.90	17.822	16.905	17.663	17.154	18.165	18.619		
3000	28.834	23.35	18.123	17.202	17.963	17.455	18.470	18.942		
3100	29.331	23.79	18.414	17.491	18.254	17.747	18.766	19.256		
3200	29.813	24.22	18.697	17.772	18.536	18.030	19.054	19.562		
3300	30.281	24.64	18.972	18.046	18.810	18.306	19.333	19.860		
3400	30.737	25.04	19.239	18.313	19.076	18.574	19.603	20.150		
3500	31.181	25.44	19.499	18.573	19.335	18.834	19.865	20.431		
3600	31.614	25.83	19.751	18.827	19.587	19.088	20.120	20.704		
3700	32.036	26.21	19.997	19.074	19.832	19.336	20.368	20.969		
3800	32.448	26.58	20.237	19.316	20.071	19.579	20.610	21.232		
3900	32.850	26.93	20.471	19.553	20.304	19.816	20.845	21.488		
4000	33.242	27.28	20.699	19.785	20.532	20.048	21.074	21.738		
Source	*a*	*b*	*c*	*d*	*c*	*e, f*	*f, g*	*h*	*i*	*j*

[a] Kassel, *J. Am. Chem. Soc.* **56** (1934), 1838, with slight modifications by J. O. Hirschfelder.
[b] Gordon, *J. Chem. Phys.*, **2** (1934), 68, 549; E. B. Wilson, *J. Chem. Phys.*, **4** (1936), 526; Stephenson and McMahon, *ibid.*, **7** (1939), 614.
[c] Johnston and Davis, *J. Am. Chem. Soc.*, **56** (1934), 271.
[d] Davis and Johnston, *ibid.*, 1045.
[e] Johnston and Dawson, *J. Am. Chem. Soc.*, **55** (1933), 2744.
[f] Lewis and von Elbe, *Combustion, Flames, and Explosions of Gases* (1938).
[g] Johnston and Chapman, *J. Am. Chem. Soc.*, **55** (1933), 153.
[h] Johnston and Walker, *ibid.*, 172; **57** (1935), 682.
[i] J. O. Hirschfelder.
[j] Wagman, Kilpatrick, Taylor, Pitzer, and Rossini, *J. Research Natl. Bur. Standards*, **34** (1945), 143.

This gives the last of the data needed for the calculation of T_f, which proceeds by computation of

$$\Delta S + nR \ln \frac{P_m}{P_f}$$

for trial values of T_f, until a bracket 100°K wide is obtained. The value of T_f is then found by linear interpolation and the specific impulse calculated from equation 54.

Combination products such as methane should be omitted from thrust computations even when they would be formed in the equilibrium state at the final temperature T_f; the expansion in a nozzle is too fast for equilibrium to be reached in such reactions.

If the initial temperature T_m is not much above 2000°K, it is possible to neglect dissociation, and the water-gas equilibrium changes so little that we can neglect all changes in composition during the expansion. Thus the final temperature T_f is decided by

$$\Sigma[\mathrm{CO_2}]\int_{T_f}^{T_m} C_p \frac{dT}{T} = nR \ln \frac{P_m}{P_f} \tag{60}$$

Let the mean value of C_p over the range T_m to T_f be $\gamma R/(\gamma - 1)$; then equation 60 becomes

$$\frac{\gamma}{\gamma - 1} \ln \frac{T_m}{T_f} = \ln \frac{P_m}{P_f}$$

the ordinary adiabatic for a nonreacting gas. The specific impulse is

$$\left[\frac{2n\gamma RT_m}{\gamma - 1}\left(1 - \frac{T_f}{T_m}\right)\right]^{1/2} = \left[\frac{2n\gamma RT_m}{\gamma - 1}\left\{1 - \left(\frac{P_f}{P_m}\right)^{(\gamma-1)/\gamma}\right\}\right]^{1/2} \tag{61}$$

This shows that to get a high specific impulse at a given upper temperature T_m, the molecular weight $(1/n)$ of the products should be low. There is also an optimum γ for each pressure ratio P_m/P_f; for example, if the pressure drops in the nozzle by a factor of 30, the optimum γ is in the neighborhood of 1.1.

So far we have assumed that a nozzle can be designed to give expansion from pressure P_m to pressure P_f. The dimensions of the nozzle are not needed for the calculation of the thrust. The pressure as a function of cross section in a nozzle is discussed in § 7.2, on the assumption of a slowly varying specific heat.

3.4 Thermal behavior of the propellant gases in a gun

The gases in a gun have a temperature that starts at T_0, since the shot is at first not abstracting energy from the gas. With increase of shot velocity the temperature soon begins to fall steadily and is down to

$0.6T_0$–$0.7T_0$ at the moment the projectile emerges. This means a high rate of cooling; for example, in a gun of 3 in. caliber and a muzzle velocity of 3000 ft/sec, the rate of cooling is about 150°K/msec, and in small arms the rate may be six times as great. Nevertheless, the temperatures are so high that, for all but the coolest propellants, and possibly in certain small arms, the composition of the gases shows a negligible lag behind the equilibrium state. Thermal properties can therefore be calculated as in the preceding sections.

An important point is the value of γ in the gun. The quantity that appears in the conventional equations of a gun is actually $nR/(\gamma - 1)$, which is equal to C_v, the specific heat (at constant volume) per gram of gas, only when the gases are perfect. For real gases C_v is not equal to $nR/(\gamma - 1)$ with $\gamma = C_p/C_v$. Now it is C_v that ought to be used in ballistics, whereas $nR/(\gamma - 1)$ is always used in its place. This practice can be tolerated if γ is *defined* by

$$\frac{nR}{\gamma - 1} = C_v \tag{62}$$

With this definition, γ is not equal to C_p/C_v, except in the case of perfect gases. Since C_p does not occur in the equations of interior ballistics, this point is in practice not a source of confusion.

To find this "gun γ," then, we compute a mean C_v over the range T_0 to $0.7T_0$ and use equation 62. We have

$$\overline{C_v} = \frac{E(T_0) - E(0.7T_0)}{0.3T_0}$$

where $E(T)$ is the internal energy, at temperature T, of the products existing at temperature T. These products and the corresponding energies are easily calculated by the methods explained in §§ 3.2 to 3.24. Pressure corrections for the 5 main products tend to cancel, summing to a small net amount, which is, in this connection, hardly worth the extra computation. In general, therefore, it is sufficient to calculate C_v by omitting all pressure corrections. This has already been done in § 3.22 for propellant X.

For propellants of high energy content γ is around 1.22, changing to 1.28 for very "cool" flashless propellants. Where a mean has to be taken over all types, $\gamma = 1.25$ is a convenient value.

Ballistically the propellant has only six characteristics: nRT_0, the "force constant"; $nR/(\gamma - 1)$, the specific heat per gram at constant volume at temperatures near T_0; η, the covolume, and δ, the density of the solid propellant; two more parameters suffice to describe the burning law of the propellant. The force constant and the covolume decide the pressure obtained in a closed vessel and its variation with loading density; the specific heat settles the rate at which the temperature falls in the gun; the density of the solid is important chiefly because it decides how much propellant can be loaded into a gun.

The specific heat may be replaced by the more easily visualized quantity that is obtained by multiplication by T_0, and this "potential," $nRT_0/(\gamma - 1)$, has the physical significance that it is roughly proportional to the useful energy obtained from unit mass of the propellant in a given gun.

For routine inspection during propellant manufacture it is desirable to use some characteristic that is more easily measured. For this purpose the "calorimetric value" is suitable. It is obtained by measuring the heat evolved when propellant is burned in a bomb calorimeter in an inert atmosphere. The temperatures are near 300°K. Corrections are applied for the imperfection of the product gases in their final state, for water present as vapor, and for the formation of methane during the cooling. The first correction arises chiefly from the carbon dioxide, whose state is not far removed from the critical point. The water-gas equilibrium "freezes" at an equilibrium constant around 2. We shall now show that the variations observed in this final equilibrium make very little difference to the calorimetric value.

Let the number of moles of CO_2 per gram of propellant be $[CO_2]$. The other products are

$$\begin{aligned}
[CO] &= \{C\} - [CO_2] \\
[H_2O] &= \{O\} - \{C\} - [CO_2] \\
[H_2] &= \tfrac{1}{2}\{H\} - \{O\} + \{C\} + [CO_2] \\
[N_2] &= \tfrac{1}{2}\{N\}
\end{aligned}$$

The energies of formation of these gases at constant volume have been given in Table 3.4. The total is

$$67.4\,\{O\} - 40.7\,\{C\} - 0.1[CO_2]\text{ kcals} \quad \text{(water liquid)}$$

which depends very little on the actual value of $[CO_2]$. The heat measured by the calorimeter is the difference between this energy of formation and the energy of formation of the propellant and is therefore itself nearly independent of the point at which the water-gas equilibrium freezes.

This calorimetric value is for water present as liquid in the products, and is usually distinguished by the addition (WL). With water present as steam the calorimetric value (WV) is about 10 per cent less. This particular calorimetric value is rather more dependent on the final value of $[CO_2]$, since the heats of formation do not so nearly cancel. The calorimetric value (WL) is therefore some 10 per cent less than $E(T_0)$, which itself may be written as $nR(T_0 - 300)/(\gamma_1 - 1)$, where γ_1 is a mean over the range 300°K to T_0. The relation of the potential to the calorimetric value (WL) is finally

$$\frac{\text{Potential}}{\text{Calorimetric value (WL)}} \simeq \frac{0.9T_0}{T_0 - 300}\left(\frac{\gamma_1 - 1}{\gamma - 1}\right)$$

which varies between about 1.05 for "hot" to 1.15 for "cool" propellants. This is a useful rough relation. High calorimetric values are correlated with high values of the potential, though propellants of very different composition and small differences of potential may show a reversal of this order when considered with respect to calorimetric value.

Certain cool propellants with calorimetric value less than 700 cal/g do not obey this relation between potential and calorimetric value. The latter is up to 20 per cent bigger than that expected from the calculated potential, which itself is confirmed by trials in guns. The explanation is the deposition of soot from the gases when cooled in the bomb calorimeter. This does not occur in the gun, though it may help to explain the dense smoke from such propellants. Under the relatively slow cooling down to room temperature in the calorimeter, there is time for carbon to be deposited in amounts comparable with the equilibrium value. This can be calculated easily.

The equilibrium condition is that graphite is deposited if

$$\frac{[CO]^2}{[CO_2]} > \frac{V}{T} K_9 \tag{63}$$

where K_9 is a function of temperature alone, given in Table 3.1. The energy of formation of the products increases by 3.4 kcal/g of carbon deposited, and this is enough to raise the calorimetric value by as much as 100 cal/g in some compositions. A numerical example is given at the end of this chapter.

The deposition of soot in a bomb calorimeter can be avoided by mixing the cool propellant with a larger amount of some normal propellant. The calorimetric value of the cool propellant can then be found by proportion, and compared with the potential deduced from gun firings. The familiar relation is confirmed.

Another way to verify this explanation of the anomalous calorimetric value is to fire mixtures of the cool propellant with a hot propellant and plot the heat evolved (per gram) against the mixture ratio. The relation is linear, for small amounts of the cool propellant, and deviates toward higher values as soon as soot begins to appear.

EXAMPLES

1. Calculate the temperature of uncooled explosion without performance of work, for a propellant consisting of 99 per cent nitrocellulose (13% N) and 1 per cent diphenylamine, at a loading density of 0.2 g/cc, without pressure corrections.

2. Repeat with pressure corrections.

3. Calculate the temperature of burning at constant pressure for the same propellant, at a pressure of the order of 20 tons/sq in.

4. At what temperature would soot begin to be formed from the products of a propellant with composition 62 per cent nitrocellulose (12% N), 28 per cent diethylene glycol dinitrate, and 10 per cent carbamite, at a loading density of 0.1 g/cc? If the equilibrium amount were formed at 300°K, what would be the effect on the calorimetric value?

5. The second virial coefficient of methane has been estimated to be about 30 cc/mole at temperatures of the order of 1500°K. Find an approximate correction to the methane equilibrium (equation 22), for pressure effects.

6. Calculate (third virial coefficient)/(second virial coefficient)^2 for the Noble-Abel equation, and compare with the values for the separate gases, found from Table 3.8. Hence, show that equation 30 can be expected to be a better representation of the theoretical equation of state at ballistic temperatures than equation 31.

7. The fuel ratio of the V2 rocket was roughly 1 part by weight of liquid oxygen: 0.6 part ethyl alcohol: 0.2 part water. Calculate the temperature attained in reaction under a pressure of 20 atm and the specific impulse in an expansion to 1 atm. The heats of formation of liquid oxygen and ethyl alcohol may be taken as 2.9 and 66.3 kcal/mole, respectively.

CHAPTER FOUR Simple Ballistic Methods

4.1 Introduction

There are numerous ways of treating the interior ballistics of orthodox guns [see Cranz, vol. 2 (1926)], and these ways may be divided into two extreme types with many intermediate gradations. As one extreme we have the type that attempts to be "exact" and is usually called a "theory." The other extreme has the virtue of utility rather than physical plausibility, and few of this type are ever referred to as "theories." Both types are valuable in their own fields. In this book the two classes are represented by the methods of this chapter and the next. The basis of the simple methods is the use of all the known firings to build up a semiempirical system. The methods used are rapid, and, when assisted by various empirical rules, they give useful results for charge estimations and prediction of performance of weapons of familiar types.

The more exact theories attempt to include all the main phenomena, up to a certain order of magnitude, and to use fewer parameters determined from firing data. This leads to more complicated methods of working, and as a rule these theories are not suitable for routine ballistic calculations. Their most useful applications are to weapons of unusual form, for which firing data are not available, and to the study of various design parameters, which are not easily measured by experiment. These are fields in which the differential analyzer has been found useful.

The method we describe in this chapter belongs to the more elementary of the two classes just sketched. The two main difficulties of interior-ballistics theory are, first, the representation of the resistance to motion, especially that arising during the engraving, and, second, the Résal term, corresponding to the kinetic energy of the projectile, in the equation of energy. The method to be described avoids the first difficulty by using an "effective" rate of burning. The second point is taken into account by using a constant gas temperature somewhat smaller than the temperature attained when the gases are generated without the performance of external work.

There are other approximations in this method. Their importance is, however, secondary to those previously listed. In considering the main approximations, it is possible to take a purely empirical viewpoint; it can be said that experience has shown how the ratio of effective to measured web depends on the charge conditions in various guns, so that the practiced ballistician can predict maximum pressures to within a few per cent. Furthermore, the errors in calculated and observed muzzle velocity have been found to be independent of some of the ballistic variables and to be predictable from past experience. Thus a ballistic "scheme" can be evolved, with the backing of an approximate ballistic solution and anchored to experience by the analysis of a mass of past firings. Such a scheme ("RD 38") is, in fact, the basis of charge estimation in British practice, and it has proved to be both rapid and reliable for normal guns. In the present book we cannot give the rules that have been evolved for the various correction factors that are responsible for the agreement with experiment.[1] We can give only the bare bones, in the form of the approximate mathematical solution. Although this in itself is not sufficient to account for the detailed ballistics of guns, it does make clear certain important parameters, which appear in the more refined but more elaborate ballistic theories.

In short, this simple ballistic theory gives a clear introduction to the properties of ballistic solutions, provided attention is drawn to those features that demand corrections. Taking such residual factors from the mass of practical experience at the disposal of a ballistic computing section, we arrive at a scheme that gives accurate results for pressure and muzzle velocity.

Before leaving this use of a ballistic scheme as a device for interpolating between the results of past firings, there are certain points that ought to be mentioned. In the first place, it is essential that the basic calculation should be short, for the time involved plays a part not only in the prediction of a new solution but also in the analysis of the allied data from which, eventually, any prediction must start. Speed is one of the outstanding virtues of the method described here.

Other rapid solutions on other lines have been developed, and some of these are mentioned in chapter 5. There is no reason to think that graphical solutions offer any substantial saving of time over the "RD 38" scheme. Indeed, the multiplicity of grain shapes found in most services would demand a correspondingly large number of graphs, whereas they are all covered by single, simple formulas in the analytical method favored here.

---

[1] A comment made to the writer was "Britain can fake it."

One point that has caused some discussion is how to adapt this method to use rates of burning from closed-vessel tests. The "RD 38" scheme uses a rate of burning (of a given propellant) chosen to fit observations in a number of guns. The closed vessel need not be used; in fact, the rate of burning derived from closed-vessel experiments gives but indifferent results when applied to the gun. This is less of an inconvenience to the working ballistician than might be thought, provided, of course, that he has good facilities for obtaining special gun firings. The closed vessel is then redundant (for this particular purpose), though if its results could be adapted to the simple ballistic method they would provide a valuable check. Their chief use would be in deciding whether abnormal firing results were arising from the propellant or from the gun and projectile. We shall show in chapter 9, however, that the effective rate of burning in the gun is liable to be greater than that in the closed vessel, by an amount of the order of 10 per cent. This shows that the failure of CV rates in this simple ballistic scheme is no condemnation of the latter. As proof of this explanation of the failure of CV rates, we may mention that, the cooler the propellant gases, the worse the CV rates. This is just what would be expected from the theory of chapter 9.

4.2 The "isothermal" solution

4.21 Notation

Let the volume of the gun, between the breech and the base of the shot in its starting position, be U. In this space is the charge, of weight C; the ratio C/U is the "density of loading." We write the shot weight as W, the bore area as A, and the caliber as d. Let the travel, velocity, and breech pressure at time t be x, V, and P, respectively.

Let the fraction of the charge burnt up to this time be ϕ. The initial web size being D, the remaining web is written as fD. The connection between ϕ and f has been discussed in chapter 2 and is expressed here by a quadratic form function:

$$\phi = (1 - f)(1 + \theta f) \tag{1}$$

where θ, the form factor, is unity for cord propellants and close to zero for tubular, ribbon, and chopped multitubular shapes. Taking the diametral rate of burning to be βP, we have

$$D \frac{df}{dt} = -\beta P \tag{2}$$

The rate of recession (along the normal) of a single propellant surface is therefore $\frac{1}{2}\beta P$.

The way in which β, D, and θ are chosen in practice is explained in § 4.32. The simple theory given here takes a rather unsophisticated view of the process of burning, and D and θ have to be chosen, therefore, to allow for the erosion by the gas streaming along perforations and by the general flow out of the chamber. Furthermore, the present theory neglects resistance to motion of the shot. Initial resistance has an important effect on peak pressure, which has to be counterfeited in practice by a suitable variation of β with the ballistic details. Actually β has been found empirically to be expressible as

Function of propellant composition × function of maximum pressure

for given gun and driving band. The variation of β with propellant shape and composition and with the details of the interior ballistics is therefore much more special and certainly more convenient than might have been expected. This is the basis of the use of this treatment as a practical ballistic method. About these points more will be said in § 4.32; here we shall work in terms of f, β, D, and θ, as if they really had the simple definitions that we have used.

Other properties of the propellant, which have been introduced in earlier chapters, are the force constant RT_0, the density δ, and the covolume η.

4.22 Equations of motion

We have already assumed that the propellant stays in the chamber, burning under the breech pressure P. We assume that the temperature of the gases *during burning* can be replaced by a mean value, corresponding to an effective mean force constant λ. This is a fair approximation, since the continuing conversion of thermal energy of the gas to kinetic energy of the shot is largely compensated by the generation of energy by the reaction of more propellant.

The space available to the gas behind the shot at time t is

$$U + Ax - C\frac{1-\phi}{\delta}$$

and the equation of state is therefore

$$P_1\left(U + Ax - C\frac{1-\phi}{\delta} - C\phi\eta\right) = \lambda C\phi \tag{3}$$

where P_1 is the mean pressure through the volume behind the shot. There is a pressure gradient from breech to shot base, this drop of pressure supplying the force needed to accelerate the gas in the gun. This subject of "Lagrange corrections" [2] is discussed in chapter 9. Here we shall simply quote the conventional results, which, though not accurate, are generally accepted and are at least as good as our other approximations. The space-mean pressure P_1 at the instant considered is

$$P_1 = \frac{P\left(1 + \frac{C}{3W_1}\right)}{1 + \frac{C}{2W_1}} \tag{4}$$

where P is the pressure at the breech, and the pressure on the base of the shot is $P/[1 + (C/2W_1)]$, where W_1 is an effective mass of the shot, discussed later.

We simplify equation 3 by taking $\eta = 1/\delta$. Since η is about 1 cc/g, whereas $1/\delta$ is about 0.6 cc/g, the error in this approximation may be considerable at high densities of loading. The effect of η being greater than $1/\delta$ is that the peak pressure is higher than would be expected; this can be simulated by an increase of β or of λ. It is shown in the next chapter that the effect can be represented by adding to λ a term proportional to the peak pressure P_m. A change in λ from one firing to another is inconvenient; therefore λ is increased by a constant amount, and the variation with P_m then appears as part of the variation of β with peak pressure. It follows that, having once neglected initial resistance and thereby forced β to vary with the ballistics, it causes little further inconvenience to assume that $\eta = 1/\delta$. This assumption is frequently made in the simpler ballistic theories and is usually referred to as "neglect of covolume." Some ballisticians take a mean of η and $1/\delta$, say 0.9 cc/g (Gossot and Liouville) or 0.78 cc/g (Charbonnier and Sugot); this tends to reduce the difference between "observed" and closed-vessel rates of burning, without removing the trend of β with the maximum pressure. The same remark applies to the use of the closed vessel η as the appropriate value of $\eta = 1/\delta$; this has been done by Langweiler.[3]

The idea of using a mean of η and $1/\delta$ is actually most valuable when their difference is to be taken into account. For, if we expand the solution in powers of $\eta - \eta'$, where η' is some mean of η and $1/\delta$, the series is much more rapidly convergent than if the solution were expanded in powers of $\eta - (1/\delta)$. A series solution in $\eta - \eta'$ is in fact the way in which Sugot [4] takes $\eta - (1/\delta)$ into account, and is one of the chief reasons for using η' in the tabulated solutions of Charbonnier-Sugot.

---

[2] First studied by Lagrange, *J. école polytech. (Paris)*, **21** (1832), 13.

[3] Langweiler, *Z. ges. Schiess- u. Sprengstoffw.*, **33** (1938), 273, 305, 338.

[4] Sugot, *Mém. artillerie franç.*, **5** (1926), 1131.

Equation 3 now simplifies to

$$P\left(U + Ax - \frac{C}{\delta}\right) = \frac{\lambda C\phi\left(1 + \frac{C}{2W_1}\right)}{\left(1 + \frac{C}{3W_1}\right)} \tag{5}$$

We write

$$U - \frac{C}{\delta} = E = Al \tag{6}$$

E is the initial free space behind the shot. The length l is a more convenient measure. Hence, equation 5 becomes

$$P(x + l) = \frac{\lambda C\phi}{A} \frac{\left(1 + \frac{C}{2W_1}\right)}{\left(1 + \frac{C}{3W_1}\right)} \tag{7}$$

The equation of motion of the shot is

$$W\frac{dV}{dt} = \frac{AP}{1 + \frac{C}{2W_1}} \tag{8}$$

neglecting resistances to motion, the recoil of the gun, and the rotational inertia of the shot. To include these we replace equation 8 by

$$W_1\frac{dV}{dt} = \frac{AP}{1 + \frac{C}{2W_1}} \tag{9}$$

where W_1 is the effective shot weight. If the twist of the rifling is 1 turn in n calibers and the radius of gyration of the shot, about the longitudinal axis, is k, then the kinetic energy of the shot at velocity V is

$$\frac{1}{2}WV^2\left[1 + \left(\frac{2\pi k}{nd}\right)^2\right]$$

The thrust of the driving edges of the lands rotates the projectile, and the component along the axis of the bore reduces the force available for acceleration of the shot. The shot weight has to be increased in the ratio,

$$m = 1 + \left(\frac{2\pi k}{nd}\right)^2 \tag{10}$$

giving

$$W_1 = mW \tag{11}$$

if equation 9 is to be used. For proof shot or solid steel armor-piercing shot, $k/d \simeq 1/3$, and for HE shell $k/d \simeq 3/8$. In guns the twist n is usually of the order of 30, making $m \cong 1.005$. This is hardly worth bothering about. Long shell need a more rapid spin for stability just outside the muzzle, and howitzers also have steeper twists than $n = 30$. The dependence of m on n^2 makes the effect increase rapidly as n decreases. For $n = 15$, for example, m is about 1.02 for proof shot. The lowest values of n used in practice are around 10.

The driving band exerts a normal pressure on the bore as well as the pressure on the lands, which rotates the shot. Both these forces give rise to frictional resistances, which oppose the motion of the shot along the bore. The resistance associated with the normal pressure is much the bigger, and it is pedantic to pay any attention to the friction corresponding to the rotational thrust. In the present treatment we make no mention of bore friction, though, if desired, a resistance proportional to the gas pressure can be included by simply increasing the effective mass of the projectile. Such a form for the resistance gives a rough allowance for the energy lost against friction but fails to represent the relatively high resistance in the very earliest stages and is probably never a good approximation to the true resistance.

Let M_0 be the mass of the recoiling parts. While the shot is in the gun, the recoil is effectively free. It is easy to show that to allow for the motion of the gun one should (1) reduce the effective shot weight to

$$W_1 = mW\left(1 - \frac{W}{M_0}\right) \tag{12}$$

and (2) take the velocity of the shot, relative to the ground, to be $(1 - W/M_0) \times$ the calculated velocity relative to the gun.

These results are correct only to terms of the order of W/M_0. This is rarely more than 2 per cent, so that higher-order terms are in fact not needed. When empirical corrections of the order of 2 per cent have to be made to the calculated velocities because of imperfections in the theory, it is possible to omit this correction for recoil of the gun.

The effective shot weight W_1 is therefore a quantity whose calculation depends greatly on the nature of the problem: for example, whether one is considering only one gun or comparing several types at once.

The fundamental equations are thus

$$\phi = (1 - f)(1 + \theta f) \tag{1}$$

$$D\frac{df}{dt} = -\beta P \tag{2}$$

$$P(x + l) = \frac{\lambda C\phi}{A}\frac{\left(1 + \dfrac{C}{2W_1}\right)}{\left(1 + \dfrac{C}{3W_1}\right)} \tag{7}$$

$$\left(W_1 + \frac{1}{2}C\right)\frac{dV}{dt} = AP \tag{9}$$

with the initial conditions $x = V = 0$ at $f = 1$.

Eliminating P from equations 2 and 9 and integrating, we get

$$V = \frac{AD}{\beta(W_1 + \frac{1}{2}C)}(1 - f) \tag{13}$$

If we use equation 13 in equation 9 and eliminate P by using equation 7,

$$\frac{dx}{df} = -M\frac{x + l}{1 + \theta f} \tag{14}$$

where

$$M = \frac{A^2D^2\left(1 + \dfrac{C}{3W_1}\right)}{\beta^2W_1C\lambda\left(1 + \dfrac{C}{2W_1}\right)^2} \tag{15}$$

λ is an energy per unit mass, the square of a velocity; $AD/\beta W_1$ is a velocity; M is therefore dimensionless, as it should be to be consistent with equation 14. M is the "central ballistic parameter" of this method. M, or an equivalent, can be identified in nearly all the ballistic theories that lead to explicit solutions.[5] M can be thought of as a dimensionless parameter showing the importance of the shot motion in reducing the pressure from the value that would be attained in a closed vessel.

---

[5] For example, in Langweiler's method (§ 4.5) there appears a fundamental parameter D, which is proportional to the inverse of our M.

Integrating equation 14, with $\theta \neq 0$,

$$x + l = l\left(\frac{1+\theta}{1+\theta f}\right)^{M/\theta} \tag{16}$$

whereas, if $\theta = 0$,

$$x + l = le^{M(1-f)} \tag{16A}$$

The pressure P can now be obtained from equations 7 and 16, as

$$\theta \neq 0: \qquad P = \frac{\lambda C\left(1+\dfrac{C}{2W_1}\right)(1-f)(1+\theta f)}{E\left(1+\dfrac{C}{3W_1}\right)}\left(\frac{1+\theta f}{1+\theta}\right)^{M/\theta} \tag{17}$$

$$\theta = 0: \qquad P = \frac{\lambda C\left(1+\dfrac{C}{2W_1}\right)}{E\left(1+\dfrac{C}{3W_1}\right)}(1-f)e^{-M(1-f)} \tag{17A}$$

This completes the determination of x, V, and P as functions of the parameter f.

Values at "all burnt." Suffix B will be used to denote quantities at the instant at which the propellant is just burnt, $f = 0$.

$$V_B = \frac{AD}{\beta(W_1 + \frac{1}{2}C)} \tag{18}$$

$$x_B + l = l(1+\theta)^{M/\theta} \qquad (\theta \neq 0) \tag{19}$$

$$= le^{M} \qquad (\theta = 0) \tag{19A}$$

$$P_B = \frac{\lambda C\left(1+\dfrac{C}{2W_1}\right)}{E\left(1+\dfrac{C}{3W_1}\right)(1+\theta)^{M/\theta}} \qquad (\theta \neq 0) \tag{20}$$

$$= \frac{\lambda C\left(1+\dfrac{C}{2W_1}\right)}{E\left(1+\dfrac{C}{3W_1}\right)}e^{-M} \qquad (\theta = 0) \tag{20A}$$

Values at "maximum pressure." Quantities here will be denoted by suffix m. Differentiating equation 17 or 17A gives

$$f_m = \frac{M + \theta - 1}{M + 2\theta} \tag{21}$$

for all θ. Also

$$\phi_m = \frac{(1+\theta)^2(M+\theta)}{(M+2\theta)^2} \tag{22}$$

$$x_m + l = l\left(\frac{M+2\theta}{M+\theta}\right)^{M/\theta} \qquad (\theta \neq 0) \tag{23}$$

$$= le \qquad (\theta = 0) \tag{23A}$$

and

$$P_m = \frac{\lambda C\left(1 + \dfrac{C}{2W_1}\right)(1+\theta)^2(M+\theta)^{1+(M/\theta)}}{E\left(1 + \dfrac{C}{3W_1}\right)(M+2\theta)^{2+(M/\theta)}} \qquad (\theta \neq 0) \tag{24}$$

$$= \frac{\lambda C\left(1 + \dfrac{C}{2W_1}\right)}{E\left(1 + \dfrac{C}{3W_1}\right)eM} \qquad (\theta = 0) \tag{24A}$$

It is impossible to reach in the gun the mathematical solution with f negative. These results have, therefore, a physical significance only if f_m is positive, that is, if

$$M \geq 1 - \theta \tag{25}$$

Otherwise, the maximum pressure attained is that at "burnt," and the pressure-time curve has a sharp peak instead of a flat summit.

Equation 24 for the maximum pressure can be simplified while preserving the standard of accuracy of this model. To three-figure accuracy,

$$P_m = \frac{\lambda C\left(1 + \dfrac{C}{2W_1}\right)(1+\theta)^2}{E\left(1 + \dfrac{C}{3W_1}\right)(eM + 4\theta)} \tag{26}$$

This is exact for $\theta = 0$.

4.23 Solution after "burnt"

Let

$$r = \frac{x + l}{x_B + l} \tag{27}$$

At any travel x greater than x_B, the pressure is

$$P = P_B r^{-\gamma} \tag{28}$$

In later methods we shall abandon the assumption that $\eta = 1/\delta$. The only difference from the formulas of this section will be that l is replaced by $l' = (U - \eta C)/A$. This more accurate version could be used in this section too but is rarely worth the bother. The velocity is given by

$$V^2 - V_B{}^2 = \frac{2A}{W_1 + \frac{1}{2}C} \int_{x_B}^{x} P\,dx = \frac{2AP_B(x_B + l)}{(W_1 + \frac{1}{2}C)(\gamma - 1)} (1 - r^{1-\gamma}) \tag{29}$$

$$= \frac{\lambda C \Phi}{W_1 + \frac{1}{3}C} \tag{30}$$

where

$$\Phi = \frac{2}{\gamma - 1} (1 - r^{1-\gamma}) \tag{31}$$

For an infinitely long gun, $\Phi = 2/(\gamma - 1)$, which is of the order of eight. Since $\gamma - 1$ is only a small fraction, in practical guns Φ is considerably less than $2/(\gamma - 1)$. Also

$$V_B{}^2 = \left(\frac{AD}{\beta(W_1 + \frac{1}{2}C)}\right)^2 = \frac{\lambda C M}{W_1 + \frac{1}{3}C}$$

Thus the velocity at any travel after "burnt" is given by

$$V^2 = \frac{\lambda C(M + \Phi)}{W_1 + \frac{1}{3}C} \tag{32}$$

The calculation of γ from the thermochemical properties of the propellant gases has been explained in chapter 3. It is now customary to increase γ above the thermochemical value, to allow for the heat loss to the walls of the bore. This practice is of long standing in gas-engine theory, and Cranz[6] and others have suggested its use in ballistics. R. H. Kent and Dr. J. P. Vinti have shown that the modification is simple if it is assumed that the heat loss up to any epoch is proportional to the kinetic energy of the shot at that instant. Recent theoretical calculations of the heat transfer (chapter 10) have shown that this assumption is sufficiently accurate to justify its use in ballistic calculations, especially since it leads to simple formulas. If the heat loss is $\frac{1}{2} \chi W_1 V^2$, then wherever the energy of the shot appears in any equation giving the energy of the gases, the shot energy should be multiplied by $1 + \chi$. The effect on equation 29 is that $(\gamma - 1)$ has to be multiplied by $1 + \chi$.

[6] Cranz, *Ballistik*, vol. II (Berlin, 1926), p. 226.

Wherever the modification needs to be made (as, for example, in equation 4 of the next chapter), it can be done by using an "effective γ," namely, $\bar{\gamma}$, given by

$$\bar{\gamma} - 1 = (\gamma - 1)(1 + \chi) \qquad (33)$$

χ is biggest for small calibers and high muzzle velocities and rarely exceeds 0.3. γ is greatest for cool propellants, the practical range being 1.22 to 1.28. Hence $\bar{\gamma}$ may vary from 1.22 to 1.36. For large calibers and "hot" propellants a convenient figure is 1.25; for the majority of firings in guns of medium caliber $\bar{\gamma}$ can be taken as 1.3. The exact value is not of great importance in this method but can be calculated from § 10.41.

4.24 Summary of the working formulas

If $M > 1 - \theta$,

$$P_m = \frac{\lambda C\left(1 + \dfrac{C}{2W_1}\right)(1 + \theta)^2}{E\left(1 + \dfrac{C}{3W_1}\right)(eM + 4\theta)} \qquad (34)$$

Otherwise, the maximum pressure is

$$P_B = \frac{\lambda C\left(1 + \dfrac{C}{2W_1}\right)}{E\left(1 + \dfrac{C}{3W_1}\right)(1 + \theta)^{M/\theta}} \qquad (\theta \neq 0) \qquad (35)$$

$$= \frac{\lambda C\left(1 + \dfrac{C}{2W_1}\right)}{E\left(1 + \dfrac{C}{3W_1}\right)e^M} \qquad (\theta = 0) \qquad (35\text{A})$$

The position of "all burnt" is given by

$$x_B + l = l(1 + \theta)^{M/\theta} \qquad (\theta \neq 0) \qquad (36)$$

$$= le^M \qquad (\theta = 0) \qquad (36\text{A})$$

If the muzzle is at travel x and

$$r = \frac{x + l}{x_B + l} \qquad (37)$$

and

$$\Phi = \frac{2}{\bar{\gamma} - 1}(1 - r^{1-\bar{\gamma}}) \qquad (38)$$

then the muzzle velocity is derived from

$$V^2 = \frac{\lambda C(M + \Phi)}{W_1 + \frac{1}{3}C} \tag{39}$$

The central ballistic parameter M is related to the rate of burning by

$$M = \frac{A^2D^2\left(1 + \dfrac{C}{3W_1}\right)}{\beta^2 W_1 C\lambda\left(1 + \dfrac{C}{2W_1}\right)^2} \tag{40}$$

4.25 The efficiencies of gun and charge

Two "efficiencies" are in general use as expressions of the over-all behavior of a given gun-charge-projectile combination. The first is the "piezometric efficiency," which is connected with the flatness of the pressure-space curve. This "efficiency" is the ratio of the mean pressure to the peak breech pressure; the mean pressure is that which, applied to the shot base for the total shot travel, would give the observed muzzle velocity. The name "piezometric efficiency" was apparently introduced by Zaroodny, but the ratio itself has long been in use under the more cumbersome name of the ratio of mean to maximum pressures. The piezometric efficiency is chiefly of importance in the design of the barrel. A higher piezometric efficiency means a shorter and lighter barrel, though, if the factor of safety is uniform along the barrel, the saving of weight is not really great. Whether the complete piece will be lighter depends on whether the higher piezometric efficiency has been attained by an increase of chamber volume. If so, the walls of the chamber must weigh more; if the chamber length has been held constant, as often occurs in sketching alternative designs of gun, then the breech is bigger and heavier. Thus a higher piezometric efficiency is no guarantee of a lighter piece. In an example studied by the writer, in which the chamber volume was varied and the peak pressure, velocity, and regularity [7] held constant, the smallest piece weight occurred at a piezometric efficiency lower than the maximum attainable. This difference was particularly marked at high pressures.

A high piezometric efficiency implies a muzzle pressure high relative to the peak pressure, which usually means greater gun blast. A position of "burnt" well toward the muzzle gives a higher piezometric efficiency at the expense of inferior regularity. A charge that gives a peak pressure at "burnt" causes a lower efficiency because of the sharp peak on the pressure-space curve. Thus the successive charges in a howitzer give progressively higher and higher piezometric efficiencies as we proceed from small to large charges.

---

[7] For this calculation it was assumed that the regularity of the charge was a function chiefly of the expansion ratio from "burnt" to "muzzle," and it was this ratio that was held constant.

Piezometric efficiencies are usually of the order of 50 per cent. Low charges of howitzers and all charges where extreme regularity is important show lower values, of roughly 40 per cent. Muzzle-loading infantry mortars usually have efficiencies of up to 40 per cent. When high performance is more valuable than regularity of muzzle velocity, the efficiency of a gun can be put up to about 60 per cent by a combination of large chamber, tube or multitube charges, and "burnt" well toward the muzzle. This is the practice followed with antitank guns.

The highest piezometric efficiency of which we know is 75 per cent. This was obtained, as it happens, with a recoilless gun (see chapter 7), but it can be shown that this has an efficiency that cannot exceed that of an orthodox gun of the same dimensions by more than a few per cent, and that only when "burnt" is almost at the muzzle. There would be no difficulty in building an orthodox gun of the same efficiency.[8] This particular gun had, in fact, an unusually large chamber, amounting to 40 per cent of the total internal volume. Chambers are normally not larger than 20 per cent.

It can be shown from the theory of this chapter that piezometric efficiencies of almost 90 per cent are possible with big chambers, even if "burnt" is required to lie in the gun or at the muzzle. This assumes that the projectile starts at zero pressure. If initial resistance to motion is assumed, the limit changes somewhat. Although the exact upper limit to the piezometric efficiency depends on details of the particular ballistic method used, one and all agree that 85 per cent can be attained.

A second "efficiency," which is much used, refers to the utilization of the energy in the charge. Assuming an initial temperature of 300°K, the energy given out by the products of 1 g of propellant, in cooling to room temperature, is

$$\int_{300}^{T_0} C_V(T)\,dT = \int_{300}^{T_0} \frac{R\,dT}{\gamma(T) - 1}$$

Writing simply γ for the value of C_p/C_V at ballistic temperatures, in the range $0.6T_0$ to T_0, we see that this energy is closely related to $RT_0/(\gamma - 1)$, the "potential" of the propellant. Actually it may be seen from the energy equation of interior ballistics (§ 5.1) that $RT_0/(\gamma - 1)$

---

[8] A piezometric efficiency of 83 per cent has been quoted in German documents about certain trials with the 7.5-cm Pak 40.

is really the proper measure of the energy obtainable from 1 g of propellant in a normal gun. RT_0 is proportional to the mean RT used in this chapter and denoted by λ. We define the "ballistic efficiency," therefore, as the ratio of the translational energy of the emerging shot to the energy of the propellant, that is,

$$\text{Ballistic efficiency} = \frac{(\gamma - 1)WV^2}{2\lambda C} \tag{41}$$

This is, in practice, roughly one third. If it were to approach unity, it would be necessary to introduce the temperature dependence of γ and the relation between λ and RT_0, in order to prevent apparent efficiencies of more than 100 per cent. As things are, it is sufficient to use equation 41 for comparative purposes. When more refined theories are used, λ does not appear in the equations, and RT_0 should be used in its place in the definition of ballistic efficiency. This makes but little change in the calculated efficiencies, since λ is very close to RT_0 (see § 5.25).

The propellant gases generated earliest in the travel of the projectile give the longest expansion stroke and so give up more of their energy than those generated later. A high ballistic efficiency is obtained by burning the charge as early as possible in the shot travel. This is just the condition for a low piezometric efficiency.

By increasing the ratio of the total volume to the chamber volume (the "expansion ratio" of the gun), more work is obtained from the gas expansion; the ballistic efficiency goes up and the piezometric efficiency goes down. All these points will be illustrated by examples later in this chapter.

The highest possible ballistic efficiency obtainable from a given weight of propellant of a specified type in a given gun occurs when the web size is so small that the charge is completely burnt before the shot moves appreciably. In this case $M = 0$, and the ballistic efficiency is

$$\frac{(1 - r^{1-\gamma})W}{(1 + \chi)\left(W_1 + \dfrac{C}{3}\right)} \tag{42}$$

where

$$r = \frac{U + Ax_E - C\eta}{U - C\eta} \tag{43}$$

We have used the true covolume η instead of the approximation $1/\delta$, since in this particular case no inconvenience is caused. The travel to the muzzle has been written as x_E. The form 42 separates the various factors that influence the maximum ballistic efficiency: W/W_1 is slightly less than unity, because of the energy lost in resistance to motion down the bore and also the energy needed to rotate the shot; $(1 + \chi)^{-1}$ shows the loss of efficiency because of heat transfer to the walls of the gun; $[1 + (C/3W_1)]^{-1}$ corresponds to the energy appearing as kinetic energy of the propellant gases. Finally $(1 - r^{1-\bar{\gamma}})$ arises from the incomplete expansion of the gases. We may take $\bar{\gamma} = 1.3$ as a typical value; Table 4.1 shows the variation of $1 - r^{1-\bar{\gamma}}$ with r.

TABLE 4.1 MAXIMUM BALLISTIC EFFICIENCY FOR EXPANSION RATIO r

r	$1 - r^{-0.3}$
3	0.281
5	0.383
7	0.442
9	0.483

4.3 Comparison with experiment

4.31 Some typical ballistic solutions

We shall now discuss the observed ballistics of some typical guns, in the light of the approximate solution given in earlier sections of this chapter. The data from which we start are (1) the observed muzzle velocity, and (2) the pressure-time curve obtained from a piezo gage in the chamber. Although for gun design the pressure-space curve is more important than the pressure-time relation, the former cannot be obtained from the latter alone; the transfer from one to the other requires a space-time relation, which cannot be found from the pressure-time record without assumptions about bore resistance and the initial resistance to motion. There are ways of finding an experimental space-time curve, but these are devices of a research rather than of a routine nature.

The solutions of the earlier part of this chapter give the pressure P as a function of f up to "burnt," and thereafter P as a function of travel. To produce a $P(t)$ curve up to "burnt," it is best to start from equation 2 of § 4.21:

$$t = -\frac{D}{\beta}\int \frac{df}{P(f)} \tag{44}$$

Since $P(f)$ has to be computed in any case, $t(f)$ is obtained by only one additional numerical integration. After "burnt," P and V are computed as functions of the travel x, and t comes from a numerical integration of

$$t = \int \frac{dx}{V}$$

Near the start of the motion f is little less than unity, and P behaves like $1 - f$; the integral on the right of equation 44 diverges logarithmically. The origin of time is therefore best taken at "burnt," where $f = 0$.

In examples of this chapter the term $[1 + (C/2W_1)]/[1 + C/3W_1)]$, arising in equation 7 as a correction from mean to breech pressure, has been approximated by $1 + (C/6W_1)$. The error arising is roughly 1 part in 1000 in the rate of burning, 1 in 100 in the travel at "burnt," and a few feet per second in the muzzle velocity.

4.311 A typical AA gun

The example considered here is a 3.7-in. AA gun typical of those in use in most countries at the beginning of World War II. In general, a heavy AA gun has to have a high muzzle energy relative to its total volume. The errors at the target due to variations of velocity from round to round are usually swamped by errors of prediction, largely arising from evasive action by the target; no great stress need be laid on regularity of ballistics. Antiaircraft mountings are stiff and relatively heavy, and the weight of the barrel and chamber does not play much part in choosing the best ballistic solution. On the other hand, a short barrel is desirable because, for a given weight, the moment of inertia about the trunnions is reduced, and this makes easier the following of a high-speed target. When automatic loading is used, a small chamber and charge are particularly desirable.

The gun considered here has a bore area of 11.1 sq in., a shot travel of 160 in., and a chamber volume of 373 cu in. when the shot is seated. The expansion ratio is therefore about 5.7, a normal value for a gun of this type. In the round for which the pressure-time curve is given in Fig. 4.1, the charge was 8 lb 5 oz of a flashless propellant with covolume 1.0 cc/g, density 1.64 g/cc, $RT_0 = 61.7$ (tons/sq in.) × (cc/g), and $\gamma = 1.28$. We assume that up to shot ejection the heat loss to the walls is about 20 per cent of the energy of the shot; hence, we take, in round figures, $\bar{\gamma} = 1.34$. The density of loading is 0.62 g/cc. The quantity l, introduced in the theory, is 21.0 in. in this instance; the total travel is therefore about $7.6l$.

The propellant used for this round was prepared in a shape of nearly constant burning area, for which the "geometrical" θ is 0.15; this is the value that would be obtained if all the surfaces burned at the same rate and were ignited simultaneously. The web size D was 0.058 in. The only other details that need be given are that the shot weight was 28 lb, which is normal for the caliber d of 3.7 in. ($W/d^3 = 0.55$). The rifling twist is of the order of one turn in 30 calibers, and therefore we may write for the modified shot mass $W_1 = 28$ lb. The pressure-gradient effects are determined by the ratio C/W, which is 0.3 here.

The present-time curve is given in Fig. 4.1. The peak pressure is

21.4 tons/sq in. and the muzzle velocity 2701 ft/sec. The gun was in its first quarter of life. In most respects this is a typical ballistic solution for a nearly new heavy AA gun.

The mass of the recoiling parts is 4100 lb, almost 150 times the shot mass. The omission of the correction for recoil of the piece (§ 4.22) raises the calculated velocities by about 10 ft/sec. We shall be discussing much larger deviations, and the recoil effect can be neglected.

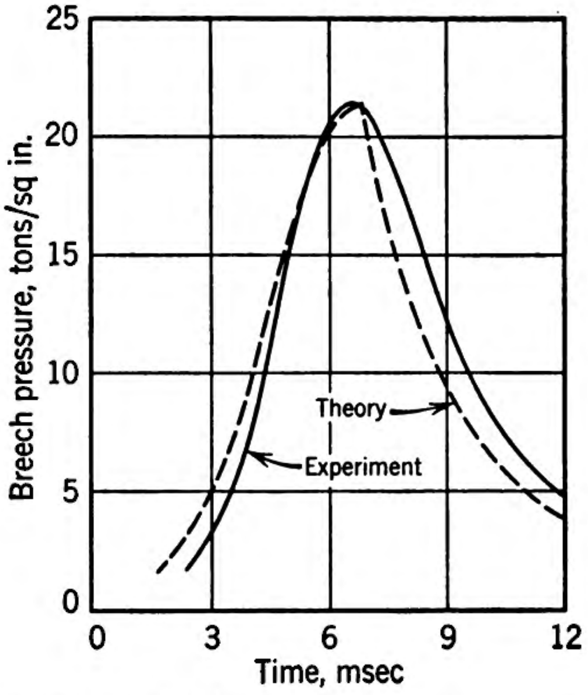

FIG. 4.1 Observed and calculated pressure-time curves for the heavy AA gun. The theoretical curve is the isothermal solution with $\theta = 0$, with constants chosen to give the observed peak pressure and muzzle velocity, and the zero of time chosen to make shot ejection occur at the observed moment.

Table 4.2 shows some solutions, all of which give the correct maximum pressure, and some of which have also the right MV. To compare

TABLE 4.2 SOME ISOTHERMAL SOLUTIONS GIVING THE CORRECT MAXIMUM PRESSURE IN THE 3.7-IN. AA GUN

θ	λ/RT_0	M	β (in./sec)/(ton/sq in.)	MV Calc.	MV Error	$x_B + l$, in.
0	1	1.101	0.824	2819	118	63.2
	0.9056	0.997	0.910	2701	0	57.0
	0.9	0.991	0.916	2694	−7	56.7
0.15	1	1.235	0.778	2850	149	66.5
	0.9	1.089	0.874	2724	23	58.1
	0.8817	1.064	0.893	2701	0	56.7
0.6	0.8314	1.460	0.785	2701	0	66.0

pressure-time curves, we begin with the solution for $\theta = 0$, and with M and λ/RT_0 chosen to produce the correct MV and peak pressure. The pressure-time curve of this solution is in Fig. 4.1. The zero of time in the theoretical curve has been chosen to give shot ejection at the observed time. The theoretical curve is obviously much too peaky—in this solution the central ballistic parameter M is less than $1 - \theta$, so that the maximum pressure occurs at "burnt." Some improvement would be obtained by using a larger θ. With $\theta = 0.15$, and λ/RT_0 and M chosen to reproduce P_m and MV, the pressure-time solution is that shown as I on Fig. 4.2. The shape of the observed peak is obviously more closely followed by this theoretical curve, though the agreement is still very imperfect.

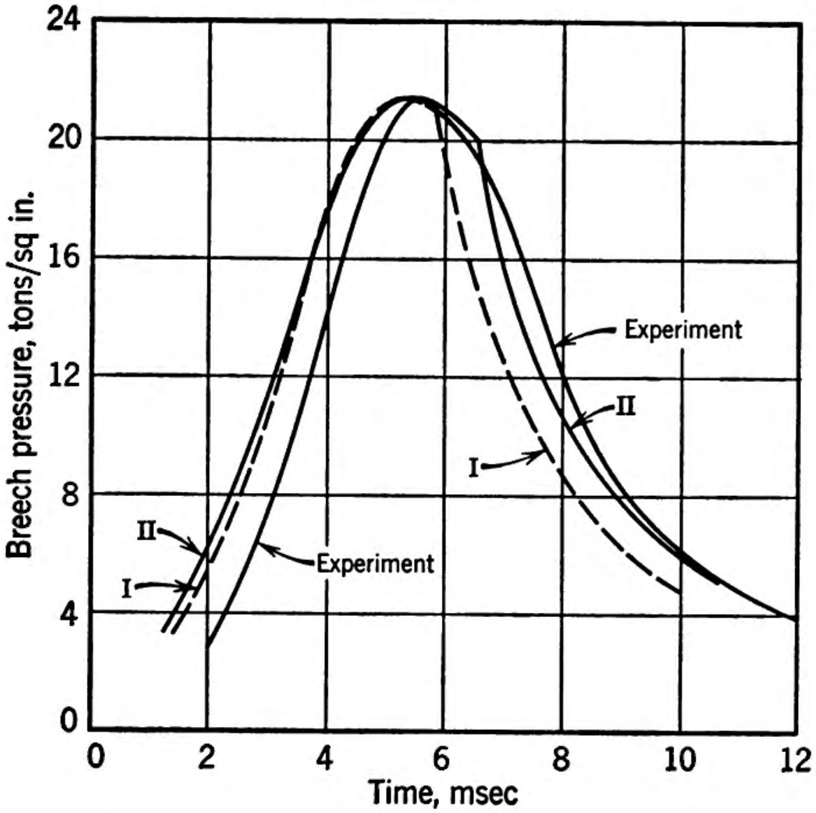

FIG. 4.2 Observed and calculated pressure-time curves for the heavy AA gun. I is the isothermal solution with $\theta = 0.15$, $W_1 = 28$ lb, and correct peak pressure, muzzle velocity, and instant of shot ejection; II is the result with $W_1 = 32$ lb.

A further increase of θ past the "geometrical" value of 0.15 leads to an improvement in the pressure-time curve. To secure really good agreement with the shape of the observed pressure-time curve one must go up to $\theta = 0.6$, for which the pressure-time relation is shown in Fig. 4.3. The time scales are still out of joint: the theoretical peak pressure occurs about 0.6 msec too early.

In view of the extremely simple theory it is not possible to deduce from this empirical θ much information on the burning rates on various surfaces of the propellant grain. Part of this increase of θ above the geometrical value is due to the neglect of covolume effects and the isothermal assumption; it is shown in the next chapter that an increase in the effective θ by about 0.15 is to be expected in this example. Part of the remaining change in θ may be attributed to neglect of resistance to motion down the bore and to our conventional correction for pressure gradient; both these are known from experiment to be in error at certain stages of the motion. By altering the shape of the pressure-time curve these effects alter the θ obtained by our empirical fitting. The fact that not all the propellant grains have the same web size is equivalent to an increase in θ, as may be most easily seen from the fact that both effects tend to smooth out the discontinuity of slope at "burnt." On the other hand, the general flow of gas out of the chamber past the burning propellant increases its rate of burning; this is most marked late in the burning, since the gas velocities are then highest; the effect is therefore usually equivalent to a decrease in θ, by as much as 0.2 in certain examples. Furthermore, since the rate of burning of this propellant is indicated by closed-vessel tests to be proportional to $P^{0.9}$ rather than P, this causes a lower rate late in the burning, that is, θ to be used in this theory must be increased.

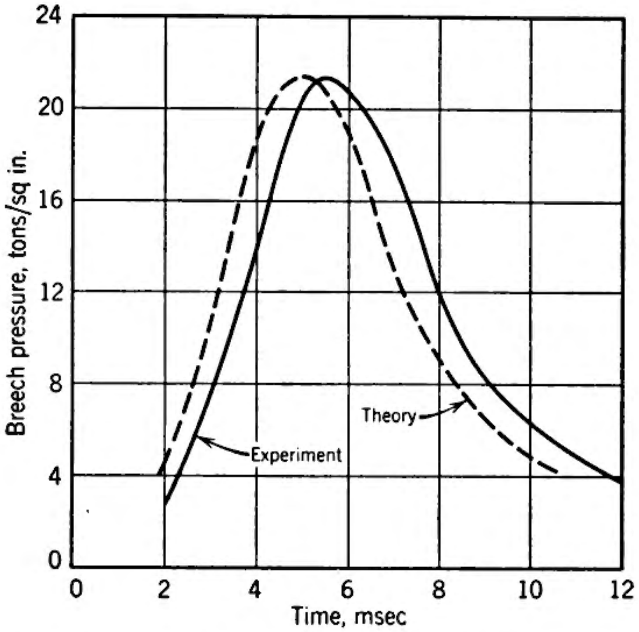

FIG. 4.3 Observed and calculated pressure-time curves for the heavy AA gun. The theoretical curve is the isothermal solution with $\theta = 0.6$ and correct muzzle velocity, peak pressure, and instant of shot ejection.

To sum up, if geometrical values of θ are used in ballistic analysis, then, in this example λ/RT_0 ought to be about 0.88 to give the right velocity. The shape of the pressure-time relation is reproduced only poorly. By going to $\lambda/RT_0 = 0.83$ and θ about 0.6, the shape of the pressure-time curve is much improved and the correct velocity maintained, but this set of parameters makes peak pressure occur too early. With the isothermal theory it is impossible to get P_m, MV, and the pressure-time curve correct for any plausible set of parameters λ/RT_0, θ, W_1; the theory finds its best use in teaching and in the *correlation* of data on velocity and maximum pressure.

In the next chapter it will be shown that (1) our neglect of the changes in gas temperature during burning and (2) the assumption that $\eta = 1/\delta$ can be compensated, as far as the peak pressure is concerned, by using $\lambda/RT_0 = 1$, when the peak pressure is in the neighborhood of 20 tons/sq in. We note that the velocity is then too high, by nearly 6 per cent for $\theta = 0.15$. To reduce this error to zero requires θ near -0.5, which gives a sharply peaked pressure-time curve quite unlike that observed. Thus it is better, if the pressure-time curve is to be considered, to use λ/RT_0 in the neighborhood of 0.85, say, and increase θ by about 0.4 above its geometrical value. The errors in the velocity and in the shape of the pressure-time curve will be small. These remarks apply to a propellant shape of roughly constant burning surface. It is true that the value of β which gives the correct maximum pressure will differ somewhat from that needed in a more adequate theory, but this is not an inconvenience in practice.

It is instructive to compare the values of β, deduced from the maximum pressure, with those obtained for the same propellant in a closed vessel. The latter value is $\beta = 0.64$ (in./sec)/(ton/sq in.). The sets of (θ, λ/RT_0) leading to correct maximum pressure and approximately correct velocity have β about 40 per cent greater than the closed-vessel result; this difference is least for the solution with $\theta = 0.6$, where the gap is only 23 per cent. Much of this difference is due to the initial resistance to the engraving of the band, completely omitted from this simple theory. This resistance reduces the acceleration of the projectile at a time when the pressure is beginning to build up rapidly, and, by reducing the free space to be filled by gas at this critical time, the resistance has a marked effect on the peak pressure. This can be simulated by an increase in β, which produces the same effect on the maximum pressure and therefore much the same effect on the velocity. It is worth pointing out here that a resistance near the start of motion increases the peak pressure, and this usually increases the kinetic energy of the shot by more than the energy lost against the resistance; thus initial resistance normally *in-*

creases the energy obtained from a given charge of a specified web size.[9] If, on the other hand, the web size is altered at the same time to preserve constant maximum pressure from a given weight of charge, then initial resistance tends to reduce velocity (in a gun with this density of loading), though the effect is small. A resistance occurring near the muzzle has no effect on peak pressure and merely reduces the velocity. A resistance varying with travel mixes the effects of initial resistance and muzzle resistance in proportions depending on the law of variation of resistance and on the ballistics—in particular, on the travel at which the peak pressure occurs. For this particular gun and charge, a constant resistance to motion raises the pressure and lowers the velocity.

A resistance proportional to the pressure is equivalent to an increase in shot weight. Figure 4.2 shows the effect of using $W_1 = 32$ lb with the "geometric" θ of 0.15. To reproduce the observed velocity and peak pressure, λ/RT_0 has to be taken as 1.015, which in the next chapter is shown to be reasonable in view of our isothermal model and our neglect of covolume terms. The rate of burning needed is only 14 per cent above the closed-vessel rate. The pressure-time curve (II of Fig. 4.2) is closer to experiment than that for the same geometric θ but W_1 equal to the shot weight. This makes it possible to get agreement with experiment for a value of θ not so far removed from the geometric value as the 0.6 previously used.

The difference between "gun" and "closed-vessel" rates of burning is not entirely due to neglect of resistance in our theory. Some effect must be expected from "erosion" of the propellant by the gas flowing over it and up the bore. In this gun the shot velocity at "burnt" is already 1700 ft/sec, at a travel of about 15 calibers, so that the gas velocities are fairly high. The propellant is a relatively cool type, which means, as pointed out in chapter 2, that the "erosion" effect is relatively severe. An increase of β by 10 per cent over the closed-vessel value is quite plausible in this example.

The piezoelectric gage provides pressure-time curves, and it is with these that we have dealt up to now. From the gun-design side, it is more important to have a pressure-space curve. In Fig. 4.4 we plot curves that give the correct maximum pressure and velocity, for $\theta = 0.15$ and 0.6, $W_1 = 28$ lb (curves I and II, respectively) and $\theta = 0.15$; $W_1 = 32$ lb (curve III). The differences are quite striking, and they demonstrate that for gun design it is important to find the most correct ballistic theory. For example, the hypothesis of a resistance to motion, expressed as a change of W_1 from 28 to 32 lb, makes a considerable difference to the pressure during the last three quarters of the travel. The importance of the pressure-space curve and the fact that relatively few have to be computed mean that, in practice, they are obtained from a more refined theory than the present one.

---

[9] A fuller discussion is given in the next chapter.

For gun design, only the pressure-space curve after maximum pressure is of interest; all sections of the barrel passed by the shot earlier in its travel are stressed by the maximum pressure itself. Another point is that the pressures plotted are breech pressures, whereas pressures at the shot are smaller. With our present assumptions about pressure gradient, the maximum pressure drop is 3.2 tons/sq in. The maximum pressure on any barrel section is not necessarily the pressure at the shot as the driving band passes that section; if, for example, the breech pressure were constant, then, when the shot were further toward the muzzle, the pressure at the section considered would be higher, being more nearly equal to the constant breech pressure. The curve of maximum pressure against position of the section is the envelope of the pressure-space curves for all times during the motion. It is usual for this curve to follow the shot-pressure curve from soon after peak pressure till the projectile reaches the muzzle. Going back toward earlier positions, the maximum pressure leaves from the shot-pressure curve in a smooth rise toward the peak breech pressure. The curve has the general nature of Fig. 4.5, which is not to be taken as more than qualitatively correct.

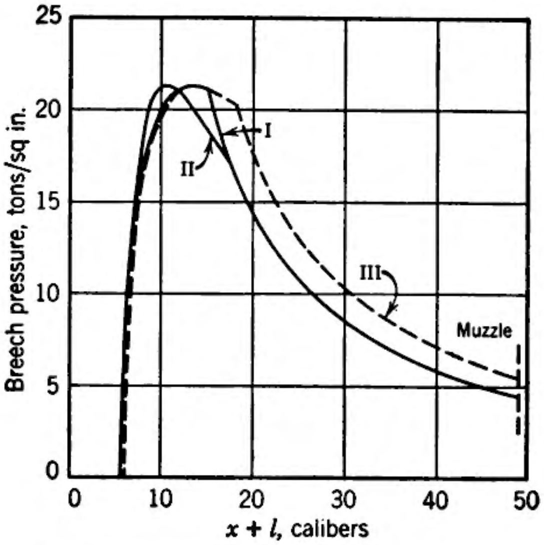

FIG. 4.4 Theoretical pressure-travel curves corresponding to Figs. 4.2 and 4.3. I and II have $W_1 = 28$ lb and $\theta = 0.15$ and 0.6, respectively; III has $W_1 = 32$ lb and $\theta = 0.15$. All these solutions give the observed peak pressure and muzzle velocity.

From Fig. 4.4 it can be seen that the value of $x + l$ at "burnt" is about 35 per cent of its value at shot ejection. This long expansion after "burnt" helps to reduce round-to-round variations of muzzle velocity. In this example more than half the kinetic energy of the projectile is acquired after "burnt." This early position of "burnt" also reduces the piezometric efficiency, which is only 45 per cent; that is, the mean accelerating pressure at the shot is only 45 per cent of the peak breech pressure. On the other hand, the ballistic efficiency, the efficiency of utilization of the energy in the charge, is correspondingly large, being 34 per cent, a figure that is not greatly exceeded in normal guns, except on reduced charges. The expansion ratio of this gun is 8.6, calculated on an initial free space of $U - C/\delta$; from Table 4.1 it appears that the maximum ballistic efficiency obtainable from a gun of this expansion ratio is about 47 per cent. Correcting for heat loss and pressure gradient reduces this to about 35½ per cent; this shows that the rate of burning is so rapid with this charge that the ballistic efficiency is almost the maximum possible for any web size, at this particular charge weight. The force of this conclusion would be reduced, however, if we have overestimated the heat loss. Rather higher efficiency might be obtained at smaller charges, for which both the relative heat loss and the pressure gradient are smaller; on the other hand, $U - C/\delta$ is larger and the expansion ratio less, and so there is really not much improvement in the ballistic efficiency. Observed values rarely go above 40 per cent.

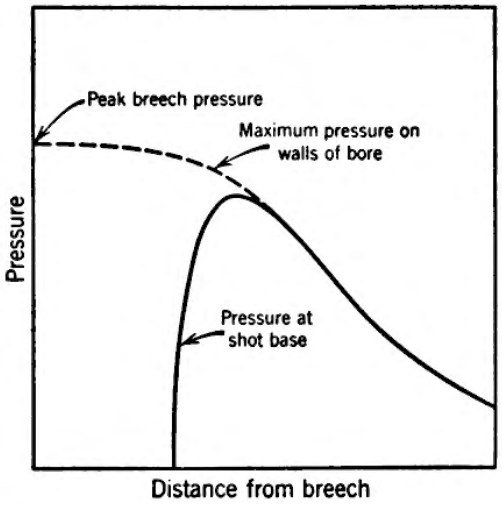

FIG. 4.5 Qualitative relation between the pressure-travel curve for the projectile and the maximum pressure experienced by the walls of the gun as a function of distance down the bore.

If we had omitted the correction for heat loss, using the thermochemical γ, calculated velocities would have been about 1 per cent higher. The heat loss used was 21 per cent of the shot energy at the epoch considered. It cannot be taken, however, that heat loss is responsible for a velocity drop of 1 per cent at constant maximum pressure; $\bar{\gamma}$ really alters the relation of our λ to RT_0. This is an effect that cannot be studied properly until the next chapter.

Figure 4.4 demonstrates that, as θ is increased, keeping the peak pressure and muzzle velocity constant, the maximum pressure occurs earlier in the travel and "burnt" at a later position.

Repetition of the calculations with the covolume η as the common value of covolume and solid density gives the results of Table 4.3. At constant λ/RT_0 and P_m, the use of η in place of $1/\delta$ raises the central ballistic parameter needed; that is, the web size has to be increased to hold P_m constant; at the same time the velocity rises, by 5.8 per cent in this example. At equal web size, $\lambda M/RT_0$ must be constant, from equation 15 of § 4.22; under these conditions λ/RT_0 is less if η is used in place of $1/\delta$, and the velocity is also less. To put it another way, if we use $1/\delta$ always, although in truth we ought sometimes to use η, then at a given rate of burning λ/RT_0 will have to be raised to get the right maximum pressure; the muzzle velocity will then be too high. Alternatively, if we use the true λ/RT_0 and obtain the rate of burning from the observed peak pressure, then our derived β will be too big and our velocity too small.

TABLE 4.3 SOLUTIONS USING $C\eta$ AND C/δ AS EXCLUDED VOLUME

$\theta = 0.15$; $P_m = 21.4$ tons/sq in.

Using	λ/RT_0	M	$\lambda M/RT_0$	$x_B + l$, in.	MV, ft/sec
$C\eta$	0.9	1.913	1.721	76.8	2882
	0.770	1.604	1.235	57.6	2708
C/δ	0.9	1.089	0.980	58.1	2724
	1	1.235	1.235	66.5	2850

These results have been obtained from one numerical example and one value of θ. In the next chapter they will be shown to be valid in general, and numerical values will be obtained for the effect.

4.312 Cord charges in a naval gun

This example is intended as a warning of the errors liable to occur in the predictions of this theory.

The gun is a naval gun of caliber 6 in., and a shot of normal weight (100 lb) for such a caliber: $W/d^3 = 0.463$. Naval guns of the larger calibers are designed for high but regular muzzle velocity, and considerations of stowage and particularly of the size of ammunition hoists make small charges desirable: such guns tend, therefore, to have small chambers, relative to the total volume of the gun, and high working pressures. This gun has a travel of 43.7 calibers and an expansion ratio of 5.3.

In Fig. 4.6 are given pressure-time curves for such a gun, firing 31- and 44-lb charges of the same propellant, in cord form with diameters 0.150 and 0.205 in., respectively. This gun was considerably worn, a point that has been taken into account in finding the dimensions. The ballistics of these rounds were (19.6 tons/sq in., 2850 ft/sec) and (29.0 ton/sq in., 3356 ft/sec), both pressures being from piezo gage. The piezometric efficiencies were 0.455 and 0.426. The densities of loading were 0.49 and 0.70 g/cc.

The propellant used is a relatively "hot" type, with $RT_0 = 70.9$ (ton/sq in.) × (cc/g), density 1.57 g/cc, and thermochemical $\gamma = 1.24$; allowing a heat loss of 25 per cent of the projectile energy, $\bar{\gamma} = 1.3$.

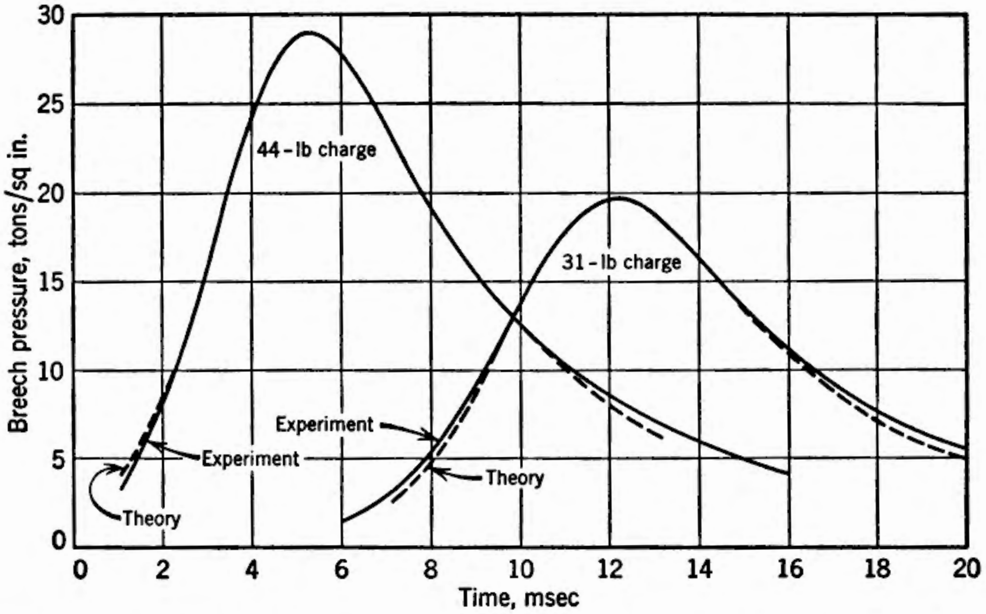

FIG. 4.6 Observed and theoretical pressure-time curves for two charges of cord propellant in a 6-in. gun.

Table 4.4 lists some isothermal solutions for the lower charge. First, with the uncorrected shot weight and the "geometrical" $\theta = 1$, the value of λ/RT_0 used in the previous example (0.8314) leads to a velocity about 80 ft/sec too high. This is 3 per cent of the muzzle velocity. Such a rise is to be expected in going from one propellant to another of greater θ. The error may be removed by a residual correction or by lowering

TABLE 4.4 ISOTHERMAL SOLUTIONS FOR THE 31-LB CHARGE

$l = 41.43$ in.; all solutions give correct peak pressure.

W_1	θ	λ/RT_0	M	$x_B + l$, in.	MV, ft/sec	Error
100	1	0.8314	1.861	150.5	2933	83
		0.78	1.655	130.4	2850	0
110	1	0.8314	1.846	148.9	2810	−40
		0.860	1.959	161.1	2850	0

λ/RT_0. In this case going down to $\lambda/RT_0 = 0.78$ is sufficient. Alternatively, we may correct for bore resistance by raising the effective shot weight. This gun had, in fact, been used for experiments on bore resistance, which had been found to be approximately constant during travel and about 1 ton/sq in. Thus a 10 per cent increase in W_1 seems to be of a reasonable order. This gives 2850 ft/sec at $\lambda/RT_0 = 0.86$ (Table 4.4).

Let us now use the same values of λ/RT_0 and W_1 to calculate the velocity given by the 44-lb charge. As Table 4.5 shows, the velocity turns out to be 2.3 per cent too high and not very different for the two alternative solutions. A more significant measure of the discrepancy is the error in the *change* of velocity between the 31-lb and 44-lb charges; this change is observed to be 506 ft/sec and calculated to be about 584 ft/sec. The error is unaltered by small decreases in θ. It is hoped that this example will show the size of the empirical corrections, which may have to be used with the isothermal theory.

TABLE 4.5 ISOTHERMAL SOLUTIONS FOR THE 44-LB CHARGE

$l = 33.50$ in.; all solutions give $P_m = 29.0$ tons/sq in.

W_1	θ	λ/RT_0	M	$x_B + l$, in.	MV ft/sec	Error
100	1	0.78	2.397	176.5	3438	82
110	1	0.86	2.674	213.8	3430	74

The pressure-time curves calculated from ($W = 100; \theta = 1; \lambda/RT_0 = 0.78$) are shown on Fig. 4.6. The agreement is extremely good and can be improved by a small increase in W_1, to, say, 105 lb.

The rates of burning, calculated from the observed central ballistic parameters, decrease as the peak pressure rises. The decrease is 8 and 5 per cent for the solutions with $W_1 = 100$ and 110 lb, respectively. The pressure changes meanwhile by 50 per cent.

4.32 Empirical corrections

The equations of burning of the propellant may be repeated here:

$$\phi = (1 - f)(1 + \theta f) \tag{45}$$

$$D\frac{df}{dt} = -\beta P \tag{46}$$

The value of θ has often been calculated from the geometry of the grain and the assumption that ignition is simultaneous and the rate of burning uniform on all surfaces. The θ so obtained is not that appropriate to firing in a gun. "Erosion" of the propellant, already discussed in § 2.4, is sufficient to alter θ by as much as 0.2 in a high-velocity gun; this effect is particularly noticeable for shapes with long perforations, but occurs to some extent for all shapes, including cord. Another factor which alters the "effective" θ is the assumption of a rate of burning proportional to pressure (equation 46). Since, in fact, the rate is usually more nearly proportional to the 0.9 power of the pressure, the propellant generates gas more slowly at high pressures than one expects from equation 46. For charges of nearly constant burning surface, peak pressure occurs just before "all burnt," so that the effect is nearly equivalent to an increase of θ by an amount of the order of 0.3. With normal cord charges the pressure falls during a large part of the later stages of burning, and the error in the pressure-time curve is not completely removed by any change in θ.

Heterogeneity of any kind increases θ. As an example of heterogeneity within the individual grain, one may take the eccentricity of the central perforation so often seen in tubular propellant. Differences of web size and rate of burning between different grains also have the result that the rate of evolution of gas falls off before the charge is completely burnt.

In view of these effects, the physical interpretation that was given to the auxiliary variable f collapses, and equations 45 and 46 must be replaced by the single equation:

$$\frac{d\phi}{dt} = \frac{\beta P}{D}\left[(1 + \theta)^2 - 4\theta\phi\right]^{1/2} \tag{47}$$

In this, θ is a parameter with absolute magnitude not greater than unity, chosen to give the best representation of the rate of generation of gas. ϕ and P are observables, and θ and β/D depend on the size and shape of the propellant and on its composition. It is convenient, however, to use a single β for all propellant of the same composition, choosing θ to be a function of shape and allowing D to be a function of shape and proportional to the linear dimension of the grain.

The possible choices are controlled by fitting to observed ballistics, though this obviously leaves considerable freedom. One process starts with the choice of θ and D for cord as unity and the diameter of the stick, respectively. The rate of burning β is then found by comparison with fired ballistics. Since this theory omits resistance to motion, β is found to depend on the details of the ballistics and on the gun and driving band. However, it is found empirically that the values β for different propellants at different pressures in the same gun can be written as (function of composition) × (function of maximum pressure). To deal with other shapes we choose, say, θ, and take β to be that already determined for the same propellant at the same peak pressure in the same gun. Then D is determined by fitting to firings, and θ is varied until D bears a constant relation to the geometrical scale of the propellant grain. For example, in British practice multitube is treated by taking $\theta = 0$, and then it is found that D should be calculated as 1.2 times the measured web. D for tube is taken to be the annulus, and θ is varied for best over-all fit. The value of θ is not critical, and $\theta = 0.2$ has been found quite satisfactory. The process can only be described as empirical, but this is inevitable in view of our neglect of initial resistance. The closed vessel plays no part here, because it does not reproduce the gas flow over the propellant in a gun; orthodox calculations of form factors and form functions are also used as no more than a guide, since they omit the influences mentioned previously.

It has been said that a satisfactory correlation with observed ballistics is possible with several values of θ. This is true so far as peak pressure and muzzle velocity are concerned. When the whole course of the pressure-time curve has to be fitted the process is less ambiguous, as was seen in § 4.311. However, in practice, questions involving pressure-time curves involve sufficient work to make it worth while to use a more sophisticated theory, such as one of those given in the next chapter.

Knowing β as a function of peak pressure for a given propellant composition in a given gun, we can calculate the central ballistic parameter for a charge, and, hence, the maximum pressure. We assume for the moment that λ/RT_0 is known. There is still an error in the muzzle velocity, depending on λ/RT_0 and on the details of the ballistics. How to reduce this error to an acceptable amount is a matter for statistical analysis. The most convenient method is to fix λ/RT_0 once and for all and to correlate the velocity error with such parameters as P_m and M. One way to choose λ/RT_0, which has much to commend it, is to ensure that the peak pressure of the theory can reach the peak pressure attained in a fast combustion, that is,

$$\frac{C\lambda}{U - \dfrac{C}{\delta}} \geq \frac{CRT_0}{U - C\eta} \tag{48}$$

For, if this equality is not obeyed, it is possible to come across gun firings whose pressures are too high to be ever explained by this ballistic system.

From equation 48,

$$\frac{\lambda}{RT_0} \geq 1 + \frac{C}{U}\left(\eta - \frac{1}{\delta}\right) = 1 + \frac{P_m}{RT_0}\left(\eta - \frac{1}{\delta}\right)$$

to the first order in $\eta - (1/\delta)$. Hence if we take $\lambda = 1.1RT_0$ we shall not have any unaccountably high pressures.

This relation is used in British practice, though since λ and peak pressures are quoted as copper-crusher pressures and RT_0 as true pressures, the values in the standard tables *appear* to obey $\lambda = 0.9RT_0$.

If we use $\lambda = 1.1RT_0$ and adjust our β to give the observed maximum pressure, then our calculated shot position at maximum pressure must be further toward the muzzle than really occurs. The theoretical pressure-travel curve has the correct peak pressure but too wide a hump, and the calculated velocity is always too high.

4.4 Ballistic effects of charge and design variables

4.41 The web size

As a typical example, we take the AA gun studied in § 4.311, using the parameters ($\theta = 0.6$, $\lambda/RT_0 = 0.8314$), which give a good fit to the observed pressure-time record. Figure 4.7 shows pressure-space curves for a charge of 8 lb 5 oz of three web sizes; the peak pressure and velocity are plotted in Fig. 4.8 as functions of D/β. Figure 4.9 gives the pressure-velocity relation at constant charge weight. The ballistic and piezometric efficiencies are shown in Fig. 4.10.

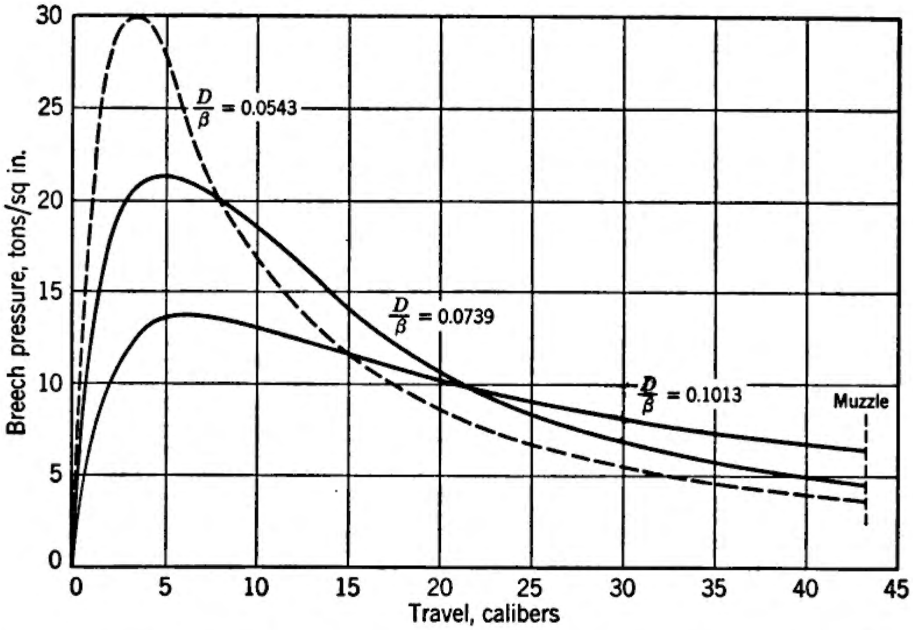

FIG. 4.7 Theoretical pressure-space curves for the heavy AA gun firing 8-lb 5-oz charges of three web sizes. Isothermal solutions with $\theta = 0.6$ and $\lambda/RT_0 = 0.8314$.

The most striking effect on the pressure-space curve is the wide movement of the position of "all burnt," compared with the small changes in the travel at maximum pressure. As D/β increases, the pressure-space curve becomes much flatter, an effect that is shown in the rapid rise of piezometric efficiency (Fig. 4.10). On the other hand, the ballistic efficiency, which measures the extent to which the energy of the chemical reaction is transformed into kinetic energy of the shot, stays almost constant at one third over a wide range of web sizes. This is equivalent to the velocity being nearly independent of web size (Fig. 4.8). From this isothermal model it follows, therefore, that 8 lb 5 oz of any size of this

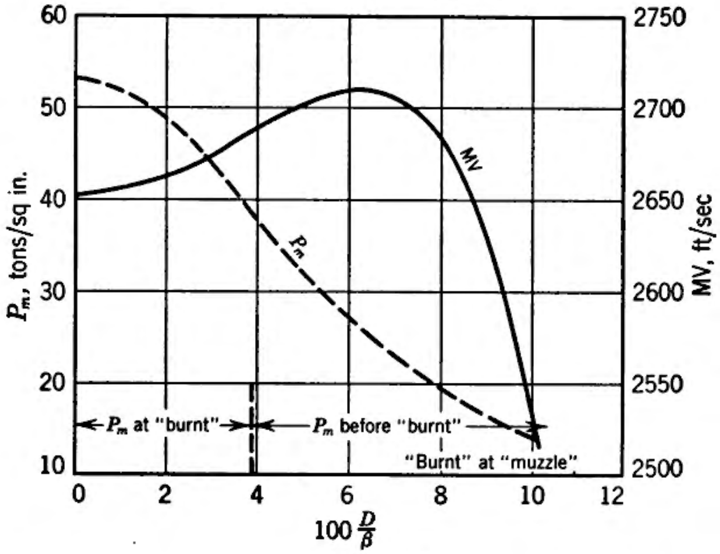

FIG. 4.8 Peak pressure and muzzle velocity as functions of web size in the heavy AA gun. Isothermal solutions with $\theta = 0.6$ and $\lambda/RT_0 = 0.8314$; the charge is 8 lb, 5 oz.

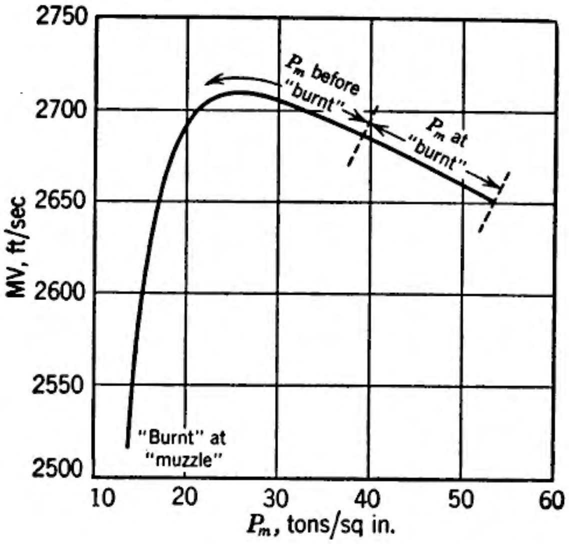

FIG. 4.9 Pressure-velocity relation at constant charge weight (8 lb, 5 oz) in the heavy AA gun. Isothermal solutions with $\theta = 0.6$ and $\lambda/RT_0 = 0.8314$.

propellant could not give more than 2710 ft/sec in this gun. This existence of such a flat maximum is very sensitive to the truth of the ballistic equations used; this is obvious when it is noticed that the peak pressure changes by a factor of two in the important region. In practice, this maximum would occur at smaller values of D/β, in a region that it would not be possible to investigate with a gun of normal strength. Extrapolation of observed velocities into this region suggests, however, that the maximum would probably not exist in this gun. Figure 4.8 is correct in suggesting that the velocity is insensitive to D/β for fast-burning charges, and becomes increasingly sensitive as the position of "burnt" approaches the muzzle.

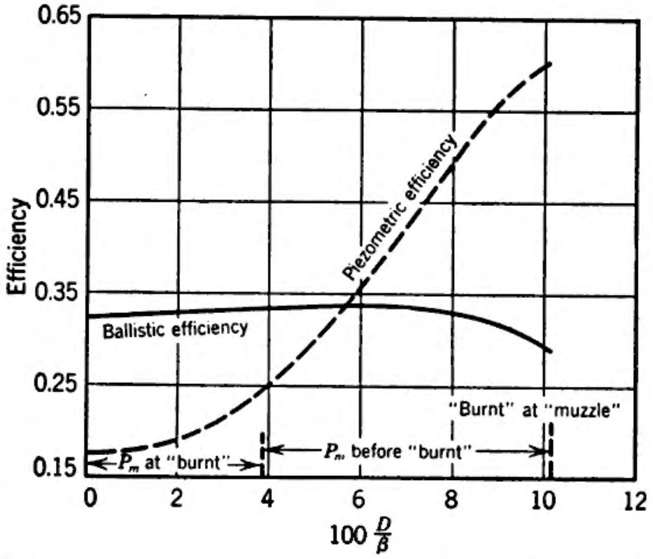

FIG. 4.10 Ballistic and piezometric efficiencies in the heavy AA gun firing constant charge weights of various web sizes.

The spread of the muzzle velocities obtained from a series of nominally identical charges arises from a variety of reasons, of which the most important are usually the variations in the average D and β and variations in the initial resistance to the shot. In service use one can expect also variations in the charge and shot weights, but in experimental work these can be so closely controlled (or allowed for if present) that they need not be considered here. The web size D of each unit of propellant can be measured, and, by a statistical analysis of the spread of D, it is easy to find the variability to be expected in the mean D of charges, each consisting of a known number of units. It is difficult, however, to do the same for β, the rate of burning.[10] Variations in the initial motion of the projectile are to be expected from small variations in ramming of separate-loaded projectiles, from small changes in free runup from fixed ammunition, and from the tolerances on the dimensions and contour of the driving band. In our isothermal model the initial resistance is taken into account by changing β; it follows that most of the sources of irregularity of ballistics can be taken into account by assuming that D/β has a distribution round its mean value.

---

[10] In one lot of solvent propellant studied by Dupuis and Chalvet, *Mém. artillerie franç.*, **18** (1939) 37, grading of the grains by web size left a considerable variability of behavior in a closed vessel.

If this is kept in mind while Fig. 4.8 is studied, it becomes clear that the position of "burnt" is of great practical importance; as "burnt" approaches the muzzle, the velocity rapidly becomes less regular.

The pressure when the shot is near the muzzle is greatest for the charge that has done least work; the muzzle pressure is greatest for the slowest-burning charge (Fig. 4.7).

4.42 The charge weight

We begin with some results, calculated with $\theta = 0.6$ and $\lambda/RT_0 = 0.8314$, for the same gun as in the previous section. First, some results

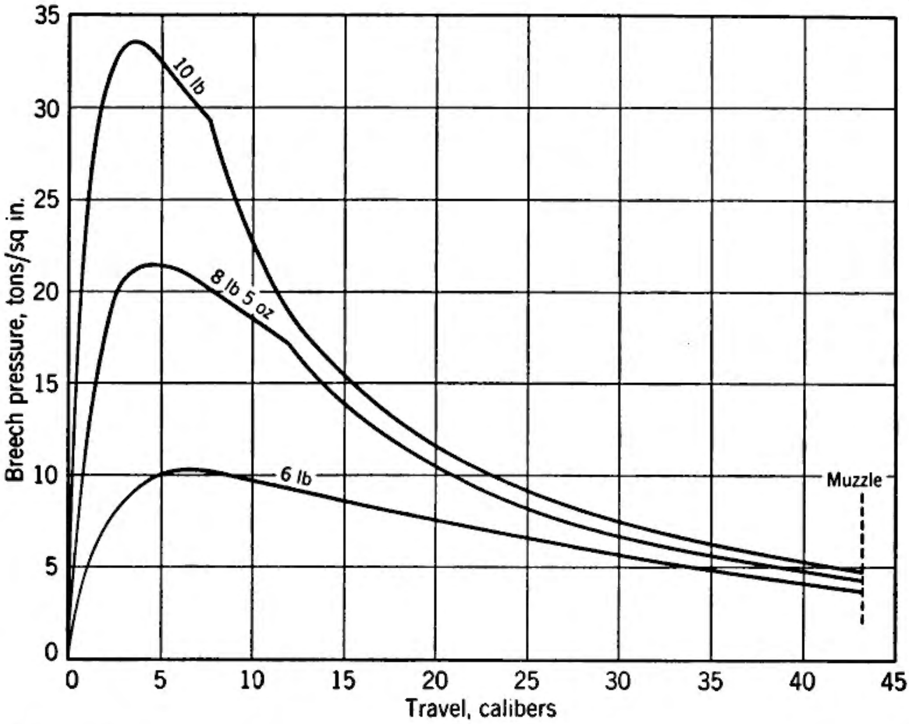

FIG. 4.11 Pressure-travel curves for the heavy AA gun firing charges of constant D/β. Isothermal solutions with $\theta = 0.6$ and $\lambda/RT_0 = 0.8314$.

at constant D/β are given in Figs. 4.11 to 4.14. Before looking at these it must be repeated that the values of β for one and the same propellant fired under different circumstances are not the same; this is a consequence

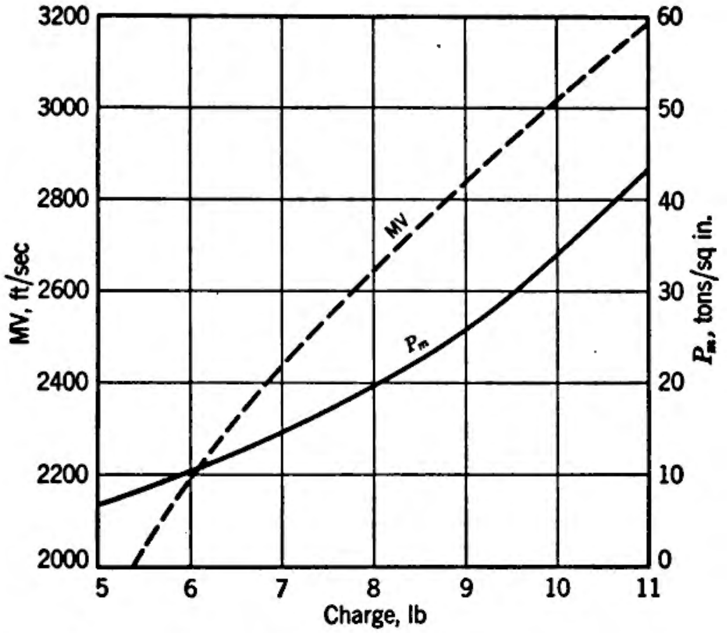

FIG. 4.12 Muzzle velocity as a function of charge weight (at constant D/β) in the heavy AA gun. Isothermal solutions with $\theta = 0.6$ and $\lambda/RT_0 = 0.8314$.

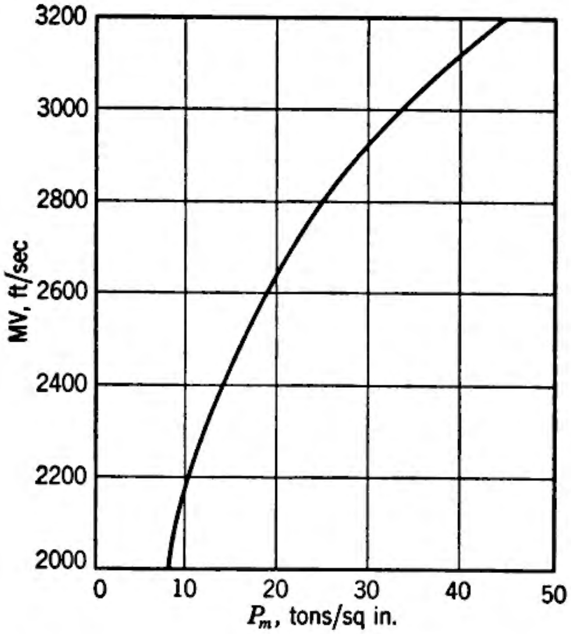

FIG. 4.13 Velocity-pressure relation at constant D/β in the heavy AA gun. Isothermal solutions with $\theta = 0.6$ and $\lambda/RT_0 = 0.8314$.

of the too simple assumptions made in this theory. β depends on the design of the rifling and driving band and in any one type of gun is almost entirely a function of peak pressure. In going from 10 to 20 tons/sq in. β may decrease by 10 per cent. Figures 4.11 through 4.14 do not represent the behavior of a gun firing increasing charge weights of the same web size. To find the latter we have to add, to the effects shown in Figs. 4.11 through 4.14, a certain amount of the effects produced by increasing D/β at constant charge weight (Figs. 4.7 to 4.10). The final result shows the same trends as in Figs. 4.11 to 4.14 but in a less intense form; exception must be made for the rising muzzle pressure with increasing charge, which is really a little more pronounced than in Fig. 4.11.

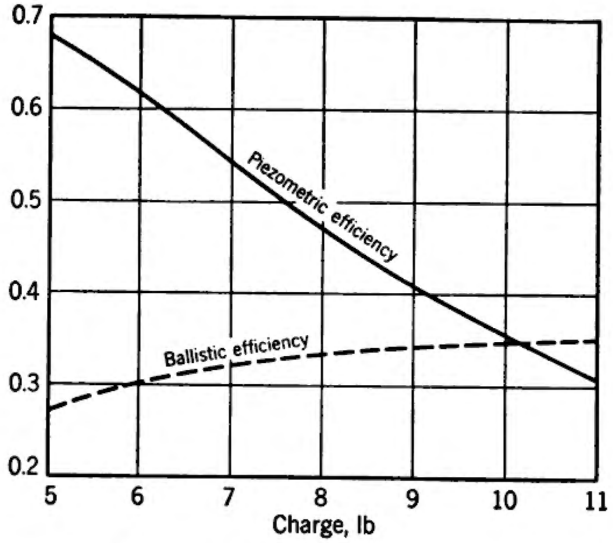

FIG. 4.14 Efficiencies of gun and charge for the heavy AA gun, at constant D/β. Isothermal solutions with $\theta = 0.6$ and $\lambda/RT_0 = 0.8314$.

The position at which maximum pressure is attained varies little with charge, whereas the position of "burnt" moves much more. Since the velocity at "burnt" is nearly constant, by equation 18, the wide variation in the peak pressure implies a large movement of "burnt."

At a given travel, the variation of pressure with charge is least near the muzzle. This arises from our assumption that the gas temperature at "burnt" is the same for all charges; the biggest charge has the biggest adiabatic expansion up to any assigned position, and has therefore the lowest temperature there. This helps to reduce the variation of muzzle pressure with charge.

Figure 4.12 shows that the velocity increases steadily with charge and that at constant D/β the rate of increase of velocity with charge is much the same at all charge weights—a point that makes easier the testing of guns and propellants.

It is often convenient to use the simple relation,

$$V \propto C^n \qquad \text{(constant } D\text{)} \qquad (49)$$

where n is a constant. Writing

$$n = \frac{d \log V}{d \log C}$$

we find that in this example n depends little on C, at constant D, until one approaches the boundary "burnt" at "muzzle." Here n increases sharply. For webs less than 0.06 in., n lies between 0.5 and 0.6, rising to about 0.8 on the curve "burnt" at "muzzle" at charges round 8 lb. For rough estimates of the effect of small changes in the charge weight, equation 49 with $n = 0.6$ would be satisfactory in this gun. As a mean over the whole range of types of guns found in practice, $n = 0.7$ is better.

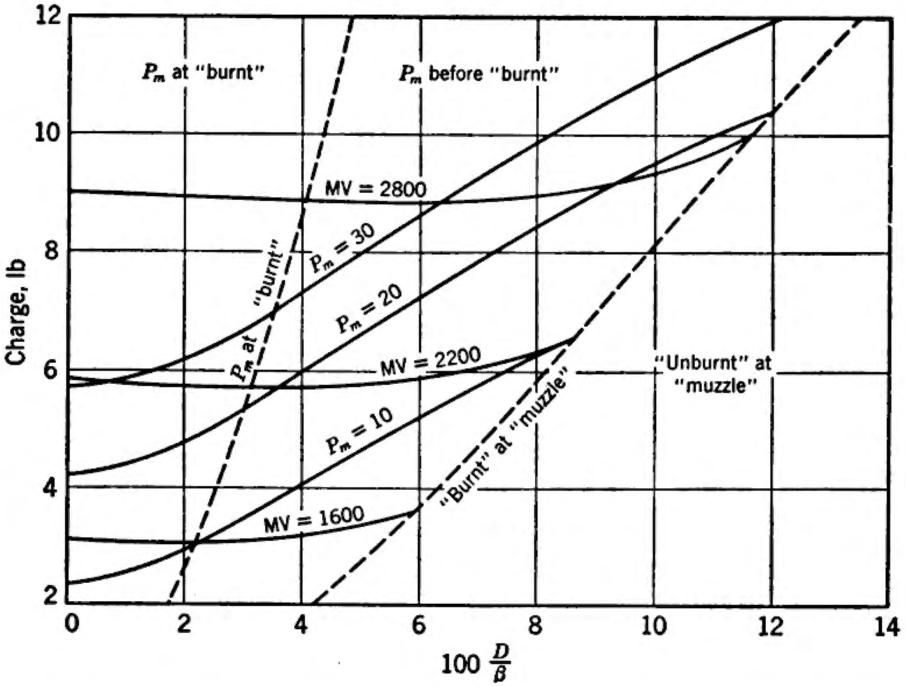

FIG. 4.15 Peak-pressure and muzzle velocity as functions of loading conditions in the heavy AA gun. Isothermal solutions with $\theta = 0.6$ and $\lambda/RT_0 = 0.8314$.

The ballistic efficiency varies a little with charge, increasing for large charges. The piezometric efficiency, which measures the flatness of the pressure-space curve, falls at the same time, in a much more decided manner. It may be noticed that even for this relatively small-chambered gun the piezometric efficiency can rise to nearly 70 per cent, although in normal use it is fired at 45 per cent.

We have combined the effects of charge and D/β in Fig. 4.15, which shows the curves of (1) constant velocity and (2) constant peak pressure, together with the boundaries along which (3) the peak pressure begins to occur after "all burnt," and (4) "burnt" is at the muzzle. We have indicated that the simple isothermal model cannot be expected to cover such a wide range of conditions without some empirical adjustments. These would transform Fig. 4.15 into something resembling Fig. 4.16. The changes are greatest at low pressures, for the resistance to motion is then largest relative to the gas pressure, and our simple treatment is least effective. The range of D is relatively wider at low charges than the range of D/β; that is, at small charge weights the gun can consume a wider range of web sizes than would be expected from the uncorrected theory.

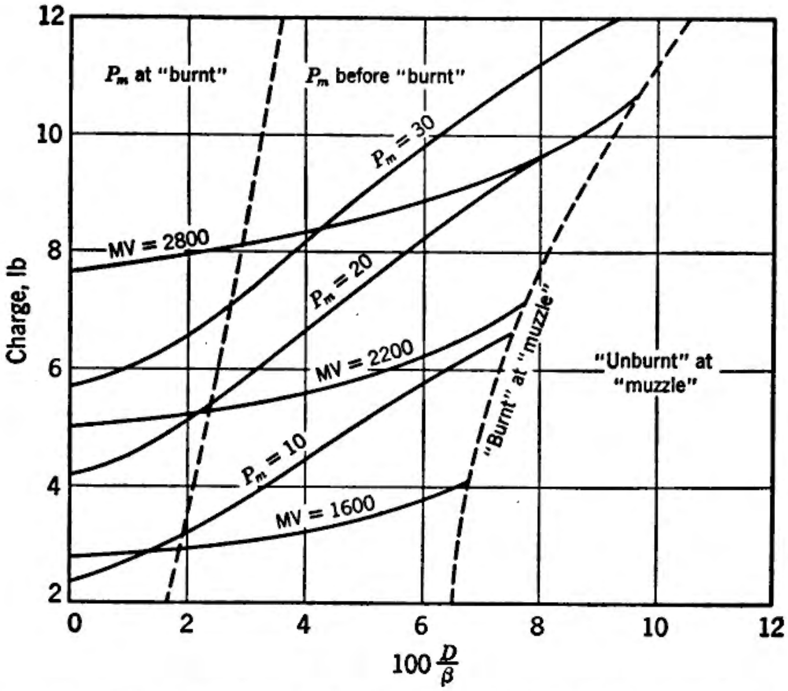

FIG. 4.16 Peak-pressure and muzzle-velocity relations of the type to be expected in the heavy AA gun.

The rate of change of velocity with D or D/β is primarily a function of D, increasing as D increases. Rather more exactly, it depends on the position of "burnt." This is shown in Fig. 4.17, together with a scale indicating the density of loading. In this gun with this shape of propellant it would be difficult to go higher than 0.8 g/cc. Figure 4.16 shows also that at a given pressure the regularity will be worst at high muzzle velocity.

In Fig. 4.18 are plotted the curves of constant ballistic and piezometric efficiencies. These are nearly parallel; thus, a high piezometric efficiency is, generally speaking, associated with a low muzzle energy per unit

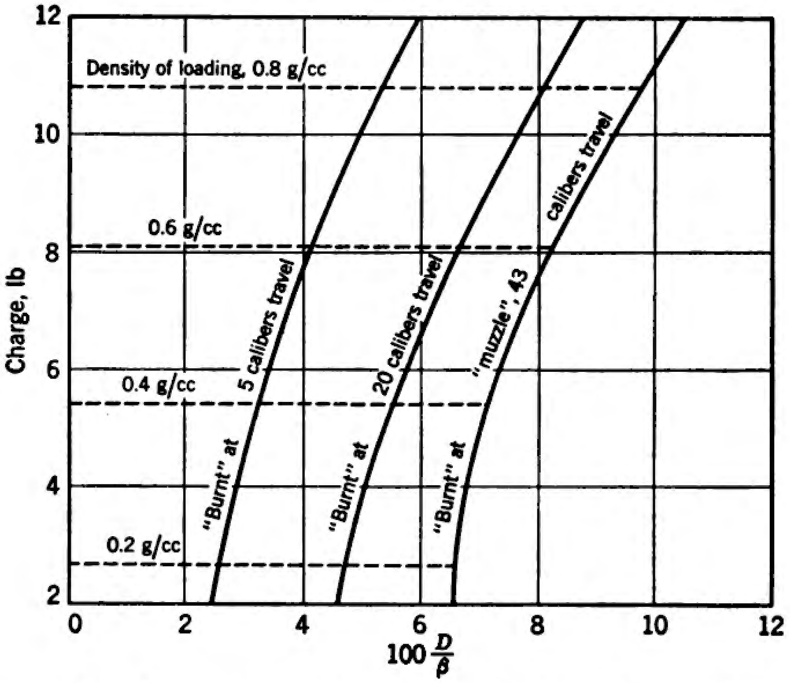

Fig. 4.17 Position of "all burnt" expected in the heavy AA gun.

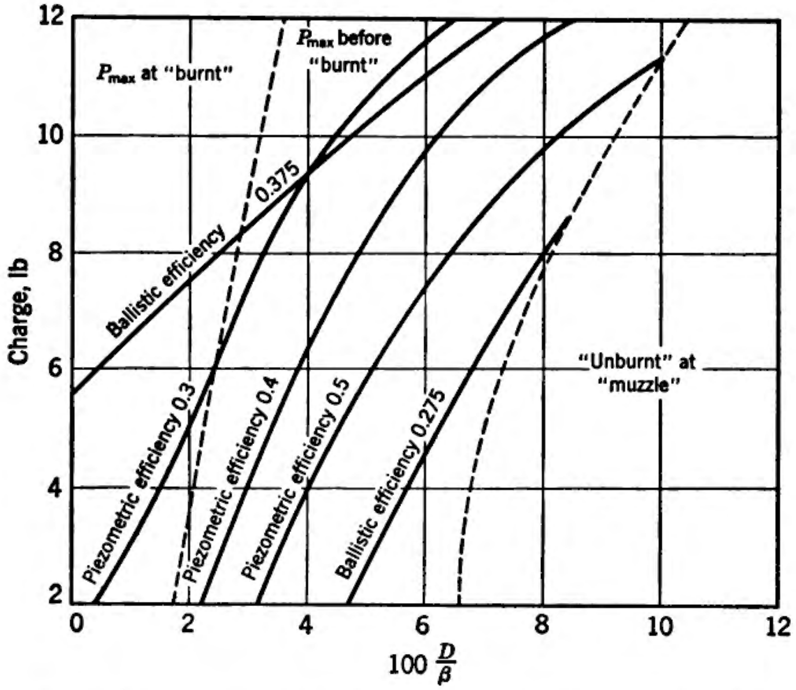

Fig. 4.18 Ballistic and piezometric efficiencies to be expected in the heavy AA gun.

weight of charge, though the variation in the piezometric efficiency is more than twice as large as in the ballistic efficiency. At given ballistic efficiency there is a maximum attainable piezometric efficiency; for example, at a ballistic efficiency of 0.325 the highest piezometric efficiency *in this gun* is about 0.48. In many cases, however, the maximum occurs at charges that could not be loaded.

The curves of constant ballistic efficiency run roughly parallel to the curves of constant peak pressure (Fig. 4.16). At each pressure there is a slight advantage in burning the charge as quickly as possible. The most striking resemblance is that between the curves of constant travel to "burnt" and the curves of constant ballistic efficiency. This shows again the practical importance of the position of "burnt" as an index of the general behavior of the propellant charge.

The temperature of the propellant affects the rate of burning β. This has the result that temperature corrections to velocity go hand in hand with irregularity of velocity. A gun-charge combination whose velocity is sensitive to temperature gives, by and large, a poor regularity.

One attraction of the isothermal model is the simple formula obtained for the effect of D/β on muzzle velocity. We have

$$\frac{dV}{dM} = \frac{V}{2(M + \Phi)}\left[1 - \frac{2r^{1-\bar{\gamma}}}{\theta} \ln (1 + \theta)\right] \qquad (\theta \neq 0) \qquad (50)$$

$$= \frac{V}{2(M + \Phi)}(1 - 2r^{1-\bar{\gamma}}) \qquad (\theta = 0) \qquad (50\text{A})$$

and

$$\frac{dV}{d(D/\beta)} = \frac{DV}{\beta(M + \Phi)}\left[1 - \frac{2r^{1-\bar{\gamma}}}{\theta} \ln (1 + \theta)\right] \qquad (\theta \neq 0) \qquad (51)$$

$$= \frac{DV}{\beta(M + \Phi)}(1 - 2r^{1-\bar{\gamma}}) \qquad (\theta = 0) \qquad (51\text{A})$$

where V is the muzzle velocity. Knowing the temperature dependence of β, one can estimate the rate of change of velocity with temperature.

The calculation of differential effects is a particularly useful application of all ballistic theories. Differential effects, such as the variation of velocity with ambient temperature, are much harder to determine by experiment than the pressure or velocity themselves. The number of rounds needed before a statistically significant answer can be obtained can be calculated from the observed dispersion of the quantity being measured, and is surprisingly high; for instance, if we try to determine the rate of change of velocity with temperature to the nearest foot per second per 10°F by firing pairs of 10-round series at 50°F apart, then, if our gun has a mean deviation, from round to round, of 5 ft/sec it will be necessary to fire 10 such double series. It is British practice to carry out only sufficient firing to fix the order of magnitude of the differential effect and then to accept the theoretical estimate unless a gross discrepancy has been revealed.

4.43 The total travel

If the total travel is reduced without other change in the gun, there is obviously a smaller muzzle energy at a given pressure. The curves of constant ballistic efficiency are moved to the left, but least of all if the piezometric efficiency is high. Piezometric efficiencies go up.

All these changes are normally small. For example, this gun, which gave 2701 ft/sec with a typical charge, would appear to give about 4100 ft/sec if one could increase the travel without limit; this velocity is, however, approached extremely slowly—doubling the existing travel raises the velocity by little more than 10 per cent.

4.44 Chamber capacity

This is related to the effect of total travel. It is sufficient to consider a change of capacity at constant loading density. Let the change be y per cent. Then the effect is the same as (1) increasing the whole internal volume by y per cent, while (2) reducing the travel by y per cent. The former increases the shot energy at the muzzle by y per cent, at a given peak pressure. The effect (2) has been discussed in the preceding section.

4.45 Shot weight

A change in effective shot weight W_1 may arise from a change in either the true mass W or in that part of the resistance to motion that is proportional to pressure. To compare the same gun firing two values of W_1, we need only correlate one solution with C, D, W_1 as the parameters with some other solution C', D', W_1', for any change ΔC, ΔD, ΔW_1 may then be obtained by superposition of the effects discussed in §§ 4.41 and 4.42.

Suppose that $C' = C$ and

$$\frac{D'}{D} = \left(\frac{W_1'}{W_1}\right)^{1/2} \left(\frac{1 + \dfrac{C}{3W_1'}}{1 + \dfrac{C}{3W_1}}\right)$$

Then $M' = M$ and $\Phi' = \Phi$, leading to

$$\frac{V'}{V} = \left(\frac{W_1}{W_1'}\right)^{1/2} \left(\frac{1 + \dfrac{C}{6W_1}}{1 + \dfrac{C}{6W_1'}}\right) \quad \text{and} \quad \frac{P_m'}{P_m} = \frac{1 + \dfrac{C}{6W_1'}}{1 + \dfrac{C}{6W_1}}$$

Thus, overlooking the slight trend due to the pressure-gradient corrections, we can say that, at equal charges and with webs proportional to $W_1^{1/2}$, the pressure and the energy of the shot at any given travel are unaltered.

If W_1 approaches the mass of the recoiling parts, the energy in the shot begins to fall. It is easy to show that $W_1 = (CM_0/3)^{1/2}$ gives the maximum shot energy from a given gun with charge C, total recoiling mass M_0, and D varying to keep $P_m[1 - (C/6W_1)]$ constant. This weight is much greater than normal projectile weights, except for a muzzle-loading infantry mortar; here the total recoiling mass may be no more than 100 lb, with $W_1 = 10$ lb and C a few ounces.

4.46 Propellant shape

We shall compare some solutions differing only in charge weight, web, and form factor θ. First, the case of constant peak pressure from a constant charge weight is shown in Table 4.6. Since the error in the velocity from the isothermal model varies with θ, these results give only an indication of what is to be expected in practice. The theory tends to overestimate the velocity most for cord. The results do show, nevertheless, that a greater velocity is obtained from a charge of cord ($\theta = 1$) than from one of constant-burning surface ($\theta = 0$). The solutions have roughly the same sensitivity to small changes of web and may be expected to give much the same regularity of velocity.

TABLE 4.6 SOLUTIONS WITH GIVEN PEAK PRESSURE AND CHARGE WEIGHT
Peak Pressure 21.4 tons/sq in.; Charge 8 lb 5 oz

θ	M	$100D/\beta$	$x_B + l$, in.	MV	Δ(MV)
0	0.911	5.84	52.3	2600	−5.1
0.6	1.460	7.39	66.0	2701	−2.9
1	2.189	9.05	95.9	2770	−4.3

Δ(MV) refers to a 2 per cent change in D/β.

Note that the web of the charge with $\theta = 0$ is about two thirds of that of the cord. This is a useful rough rule for mental comparison of the ballistic speeds of tubular and cord propellants.

The wide variation of the position of "burnt" in Table 4.6 suggests that we should compare solutions giving the same maximum pressure and constant travel to "burnt." Table 4.7 shows that under these conditions the shape with constant-burning surface enables a bigger charge to be consumed, giving a higher velocity; the gain of kinetic energy is less marked than the increase of charge weight. The difference of velocity between $\theta = 0$ and $\theta = 1$ would, in practice, be rather greater than indicated here.

TABLE 4.7 SOLUTIONS WITH GIVEN PRESSURE AND TRAVEL AT "BURNT"
Peak Pressure 21.4 tons/sq in.; "Burnt" at 45.0 in. Travel

θ	C, lb	M	$100D/\beta$	MV	Ballistic Efficiency	Δ(MV)
0	9.819	1.224	6.76	2817	0.309	−9.6
0.6	8.3125	1.460	7.39	2701	0.335	−2.9
1	7.432	1.589	7.71	2611	0.351	0.3

The solution with $\theta = 0$ is appreciably more sensitive to D/β than are the other solutions. The cord solution actually has a velocity increasing with increase of web. This comes from the behavior of the bracketed term in equations 51 and 51A, which makes $dV/d(D/\beta)$ zero at an expansion ratio:

$$r = \left[\frac{2}{\theta} \ln (1 + \theta)\right]^{1/(\bar{\gamma}-1)} \tag{52}$$

For $\bar{\gamma} = 1.34$, the critical ratios for $\theta = 0$ and 1 are 7.7 and 2.6, respectively. Both increase as $\bar{\gamma}$ is reduced; for example, $\bar{\gamma} = 1.25$ leads to values of 16 and 3.7. Thus for cord the curve $dV/dM = 0$ is well within the working range, so that if we keep to expansion ratios (from "burnt" to "muzzle") of about three, the gun should be very regular. For bigger r, D/β is smaller; hence this regularity of cord charges may be expected to hold for all expansion ratios of three or more.

4.47 Nature of propellant

There is little to be said here. At constant charge, with web adjusted to keep the same central ballistic parameter, both the maximum pressure and the kinetic energy given to the projectile are proportional to the force constant λ. The effect of a change in the specific heat of the products, that is, a change in $\bar{\gamma}$, cannot be found from this theory.

4.5 The history of the isothermal model

The idea that a useful approximation could be obtained by neglecting the variation of gas temperature during the motion appears very early in the literature. We find Moisson[11] making this approximation in 1887 for charges of gunpowder, though he also made the same assumption during the period after the charge had burned completely; he took $\eta = 1/\delta$, rate of burning proportional to pressure, no shot-start pressure, and the form function:

$$\phi = 1 - f^3$$

He was followed by Mata,[12] whose work attracted attention in Italy and France.[13] Mata's system differed from Moisson's in that the form functions considered were the general cubic in f, obtained for particular shapes by geometrical arguments, and in certain other details. Neither Moisson nor Mata obtained the simple formula 26 for the maximum pressure, leaving it at essentially equation 24.

During the First World War, it was discovered in Britain that the isothermal equations made a satisfactory basis for charge estimation, provided that the rate of burning were taken to be a function of band, rifling, and peak pressure, as well as propellant composition, of course. This was an empirical discovery, and the theory was studied by Sir Alwyn Crow. His transformation of initial resistance into a change of effective rate of burning has not survived later criticisms, but his simplification of the maximum pressure equation to the form 26 has been useful.

A very similar method has been published lately by Langweiler[14] and has apparently been much used in German ballistics. The essential differences are that Langweiler considers only the case $\theta = 0$ and that the initial resistance to motion is represented by a shot-start pressure, falling to zero as soon as the projectile moves. The former simplification is one that it is natural to make in German practice, where the great majority of propellant is made in the form of tube or ribbon, with θ therefore small, say, 0.2. The effect of shot-start pressure on the peak pressure is obtained as an approximate correction, and the effect on muzzle velocity is simulated by an appropriate change in the central ballistic parameter.

In its practical use, Langweiler's method has been supplemented by empirical corrections, which seem to be at least as large as those needed with the method used in this chapter.

---

[11] Moisson, *Pyrodynamique* (Paris, 1887), especially p. 104 onwards.

[12] Mata, *Rév. armée belge* (1890), 158; (1893), 128; (1894), 81; *Tradato de ballistica interior* (Madrid, 1890).

[13] Bravetta, *Z. ges. Schiess- u. Sprengstoffw.*, **1** (1906), 214, 249, 310; also *Mém. artillerie marine*, **30** (1902), 225, 287.

[14] Langweiler, *Z. ges. Schiess- u. Sprengstoffw.*, **33** (1938), 273, 305, 338.

EXAMPLES

1. Show that, if there is a coefficient of friction μ between the driving band and the rifling grooves in the gun, equation 10 should be replaced by

$$m = 1 + \frac{4\pi k^2}{nd^2}\left(\frac{\pi + n\mu}{n - \pi\mu}\right)$$

2. Show that, if the form factor θ cannot be negative and if unburnt propellant is not allowed at the moment of shot ejection, then the maximum possible piezometric efficiency is 88 per cent.

3. Show that, if the propellant is cord, there are no discontinuities of slope in the pressure-time curve.

4. Show that, if a given weight of charge is fired in a given gun, the travel at which the pressure is a maximum is less for any charge of cord than it is for a charge of constant-burning surface.

5. Show that, if a given weight of charge is fired in a given gun to produce a specified pressure, the travel to "burnt" will usually be greater for cord than for a charge of constant burning surface.

CHAPTER FIVE

More Advanced Ballistic Methods

The method explained in the previous chapter gives a valuable insight into the behavior of guns and can be converted from a qualitative to a quantitative treatment if supplemented by empirical corrections. The critical may, however, point to at least four ways in which the previous method deviates from physical reality.

(*a*) It is assumed that the rate of burning of the propellant is proportional to the pressure on it.

(*b*) Resistance to motion of the shot is taken into account only by an increase of the effective mass of the projectile and by an increase of the effective rate of burning; the former allows for a resistance proportional to the instantaneous pressure, whereas the latter produces much the same effect on the ballistics as the actual high resistance during the engraving of the band.

(*c*) It is assumed that the covolume η of the propellant gases is equal to the specific volume $1/\delta$ of the unburnt propellant.

(*d*) The progressive cooling of the gases by the work done on the shot is approximated, up to "burnt," by taking a mean temperature; after "burnt" the treatment is accurate.

For most propellants α, the pressure index of the rate of burning at gun pressures, is around 0.9, and it rarely falls below 0.8. Assumption *a* is, therefore, usually a good approximation. A theory that avoids this restriction is sketched later in this chapter.

We shall now discuss a solution, due to Coppock, which uses the approximations *a* and *b* but treats the points *c* and *d* in an accurate manner. We shall then sketch a method that also includes the effects of covolume and kinetic-energy terms and prefers to represent the initial resistance by a "shot-start pressure," with zero resistance after the pressure has attained this value.

5.1 The energy equation of interior ballistics

The kinetic energy of the shot at any time is $\frac{1}{2}WV^2$. If it is assumed that the propellant gas is distributed with uniform density between breech and shot and that its velocity at any point is proportional to the distance from the breech face, the kinetic energy of the gases is $\frac{1}{6}CV^2$. This is the conventional assumption and is consistent with our other assumptions about pressure gradient; whether it is accurate is discussed in chapter 9 (Lagrange corrections), but the matter is not important in practice until C/W approaches unity, that is, at muzzle velocities around 4000 ft/sec. The sum of these kinetic energies is

$$\tfrac{1}{2}(W + \tfrac{1}{3}C)V^2 \tag{1}$$

to which we must add corrections for rotation of the shot, resistance to motion, and recoil of the gun. These have been discussed in chapter 4, and the effect is to replace equation 1 by

$$\tfrac{1}{2}(W_1 + \tfrac{1}{3}C)V^2 \tag{2}$$

If it is assumed that the heat loss up to any time is a fraction χ of this kinetic energy, the total loss of energy by the propellant gases up to any particular time is

$$\tfrac{1}{2}(1 + \chi)(W_1 + \tfrac{1}{3}C)V^2$$

The specific heat, at constant volume, of these gases is $R/(\gamma - 1)$, and the temperature attained when the gases do no work is T_0. Hence, the temperature T at any time is given by

$$\frac{\phi CR}{\gamma - 1}(T_0 - T) = \frac{1 + \chi}{2}\left(W_1 + \frac{1}{3}C\right)V^2$$

Writing $T/T_0 = T'$, a "reduced temperature," and

$$\bar{\gamma} - 1 = (1 + \chi)(\gamma - 1) \tag{3}$$

we have

$$\phi(1 - T') = \frac{\bar{\gamma} - 1}{2}\left(\frac{W_1}{C} + \frac{1}{3}\right)\frac{V^2}{RT_0} \tag{4}$$

From this it is clear that a ballistically important property of a propellant is $RT_0/(\gamma - 1)$, which is usually known as the "potential" and has already been mentioned in § 3.4. This has the dimensions of energy per unit mass, or the square of a velocity, and the range covered by modern solid propellants is roughly from 3 to 6×10^7 (ft/sec)^2 or 600 to 1200 cal/g. If γ were constant from the temperatures attained in the gun, of the order of T_0, right down to 0°K, then $RT_0/(\gamma - 1)$ would

5.1 The energy equation of interior ballistics

The kinetic energy of the shot at any time is $\frac{1}{2}WV^2$. If it is assumed that the propellant gas is distributed with uniform density between breech and shot and that its velocity at any point is proportional to the distance from the breech face, the kinetic energy of the gases is $\frac{1}{6}CV^2$. This is the conventional assumption and is consistent with our other assumptions about pressure gradient; whether it is accurate is discussed in chapter 9 (Lagrange corrections), but the matter is not important in practice until C/W approaches unity, that is, at muzzle velocities around 4000 ft/sec. The sum of these kinetic energies is

$$\tfrac{1}{2}(W + \tfrac{1}{3}C)V^2 \tag{1}$$

to which we must add corrections for rotation of the shot, resistance to motion, and recoil of the gun. These have been discussed in chapter 4, and the effect is to replace equation 1 by

$$\tfrac{1}{2}(W_1 + \tfrac{1}{3}C)V^2 \tag{2}$$

If it is assumed that the heat loss up to any time is a fraction χ of this kinetic energy, the total loss of energy by the propellant gases up to any particular time is

$$\tfrac{1}{2}(1 + \chi)(W_1 + \tfrac{1}{3}C)V^2$$

The specific heat, at constant volume, of these gases is $R/(\gamma - 1)$, and the temperature attained when the gases do no work is T_0. Hence, the temperature T at any time is given by

$$\frac{\phi CR}{\gamma - 1}(T_0 - T) = \frac{1 + \chi}{2}\left(W_1 + \frac{1}{3}C\right)V^2$$

Writing $T/T_0 = T'$, a "reduced temperature," and

$$\bar{\gamma} - 1 = (1 + \chi)(\gamma - 1) \tag{3}$$

we have

$$\phi(1 - T') = \frac{\bar{\gamma} - 1}{2}\left(\frac{W_1}{C} + \frac{1}{3}\right)\frac{V^2}{RT_0} \tag{4}$$

From this it is clear that a ballistically important property of a propellant is $RT_0/(\gamma - 1)$, which is usually known as the "potential" and has already been mentioned in § 3.4. This has the dimensions of energy per unit mass, or the square of a velocity, and the range covered by modern solid propellants is roughly from 3 to 6 × 10^7 $(\text{ft/sec})^2$ or 600 to 1200 cal/g. If γ were constant from the temperatures attained in the gun, of the order of T_0, right down to 0°K, then $RT_0/(\gamma - 1)$ would be the internal energy of the products of combustion, formed without performance of work. The "calorimetric value (water liquid)" of the propellant is rather smaller than the "potential," partly because the former refers to the energy given up by the explosion gases in cooling to 300°K rather than to 0°K, partly because the specific heat of the products decreases as the temperature falls; these effects more than counterbalance the latent heat of condensation of the water vapor in the products. The potential is, in fact, about 5 per cent bigger than the calorimetric value for "hot" propellants, and the difference increases to some 15 per cent for cool flashless propellants.

RT_0 is usually quoted in (tons per square inch) per (gram per cubic centimeter). If the potential is required in calories per gram, the conversion factor is

$$\text{Potential} = \frac{3.69RT_0}{\gamma - 1}$$

The equation of state of the gas in the gun is

$$P\left[U + Ax - \frac{C(1-\phi)}{\delta} - C\phi\eta\right] = \frac{C\phi RT\left(1 + \dfrac{C}{2W_1}\right)}{1 + \dfrac{C}{3W_1}} \tag{5}$$

which enables equation 4 to be written in the form:

$$\phi = \frac{\bar{\gamma} - 1}{2}\left(\frac{W_1}{C} + \frac{1}{3}\right)\frac{V^2}{RT_0} + \frac{P\left(1 + \dfrac{C}{3W_1}\right)}{CRT_0\left(1 + \dfrac{C}{2W_1}\right)}\left[U + Ax - \frac{C(1-\phi)}{\delta} - C\phi\eta\right] \tag{6}$$

Either equation 4 or equation 6 may be regarded as the basic energy equation for orthodox guns. They were first introduced into interior ballistics by Résal,[1] and equation 6 is usually called the Résal equation. The first term on the right-hand side of equation 6 steadily increases in relative importance, and, when $\phi = 1$, this term is normally of the order of 0.2–0.3.

Heat losses to the walls of the bore have been taken into account by a suitable choice of $\bar{\gamma}$. A resistance to shot motion, proportional to the instantaneous pressure, requires an adjustment to W_1. A resistance varying in any other way with time or travel can be included in an obvious way, by adding a new term to equations 4 and 6.

---

[1] Résal, *Recherches sur le mouvement des projectiles dans les armes à feu* (Paris, 1864).

5.2 Coppock's solution

5.21 Assumptions

(*a*) The rate of burning is proportional to the pressure.

(*b*) The gases have a constant covolume η, not necessarily equal to $1/\delta$.

(*c*) The propellant burns at the breech pressure; that is, the propellant stays in the chamber.

(*d*) The law of burning away of the propellant grain is

$$\phi = (1 - f)(1 + \theta f)$$

(*e*) No account is taken of resistance to motion of the shot, though, of course, in the practical application of these results one may increase the rate of burning to simulate the effects of engraving resistance.

The other assumptions are so conventional that they need not be mentioned here: such are, for example, the assumption of a constant $\bar{\gamma}$ and the conventional assumptions about pressure gradient in the gun.

5.22 Equations of the problem

From *d* of the previous section,

$$\phi = (1 - f)(1 + \theta f) \tag{7}$$

and, from *a*,

$$D\frac{df}{dt} = -\beta P \tag{8}$$

From equation 6,

$$\phi\left[1 + \frac{P\left(1 + \dfrac{C}{3W_1}\right)}{RT_0\left(1 + \dfrac{C}{2W_1}\right)}\left(\eta - \frac{1}{\delta}\right)\right]$$
$$= \frac{\bar{\gamma} - 1}{2}\left(\frac{W_1}{C} + \frac{1}{3}\right)\frac{V^2}{RT_0} + \frac{P\left(1 + \dfrac{C}{3W_1}\right)}{CRT_0\left(1 + \dfrac{C}{2W_1}\right)}\left(U + Ax - \frac{C}{\delta}\right)$$

in which we write, in the notation of the previous chapter,

$$U - \frac{C}{\delta} = E = Al$$

so that

$$\phi\left[1+\frac{P\left(1+\frac{C}{3W_1}\right)}{RT_0\left(1+\frac{C}{2W_1}\right)}\left(\eta-\frac{1}{\delta}\right)\right]$$

$$=\frac{\bar{\gamma}-1}{2}\left(\frac{W_1}{C}+\frac{1}{3}\right)\frac{V^2}{RT_0}+\frac{AP(x+l)\left(1+\frac{C}{3W_1}\right)}{CRT_0\left(1+\frac{C}{2W_1}\right)} \tag{9}$$

Finally, the motion of the shot gives a fourth equation:

$$\left(W_1+\frac{1}{2}C\right)\frac{dV}{dt}=AP \tag{10}$$

Before we proceed further, it is well to have in mind the size of the various terms in equation 9. $\eta - (1/\delta)$ is about 0.3 cc/g, and RT_0 is usually around 60 tons/sq in. per (g/cc), so that the effect of the co-volume term is to increase the effective force constant by about 10 per cent at a pressure of 20 tons/sq in. The first term on the right increases in importance, relative to the second, as burning proceeds, and may reach as much as one third of the latter.

5.23 Solution of the equations

From equations 8 and 10 we derive

$$V=\frac{AD(1-f)}{\beta(W_1+\frac{1}{2}C)} \tag{11}$$

which is exactly the same as the corresponding result of the isothermal model (equation 13 of chapter 4). Write

$$b=\frac{\left(\eta-\frac{1}{\delta}\right)C}{E} \tag{12}$$

Into equation 9, in the form,

$$\phi=\frac{(\bar{\gamma}-1)(W_1+\frac{1}{3}C)V^2}{2CRT_0}+\frac{AP\left(1+\frac{C}{3W_1}\right)}{CRT\left(1+\frac{C}{2W_1}\right)}[x+l(1-b\phi)]$$

we substitute equations 8, 10, and 11, giving

$$Z\frac{dx}{df} + M(x + l) = Mbl\phi \tag{13}$$

where

$$Z = 1 - \frac{(\bar{\gamma} - 1)M}{2} + \theta_1 f \tag{14}$$

$$\theta_1 = \theta + \tfrac{1}{2}(\bar{\gamma} - 1)M \tag{15}$$

and

$$M = \frac{A^2D^2\left(1 + \frac{C}{3W_1}\right)}{\beta^2 W_1 CRT_0\left(1 + \frac{C}{2W_1}\right)^2}$$

Integrating equation 13 gives

$$x + l(1 - b\phi) = l\left(\frac{1+\theta}{Z}\right)^{M/\theta_1}\left[1 - \frac{\bar{\gamma}bM(1+\theta)^2}{(M+\theta_1)(M+2\theta_1)}\right] + \frac{blZ[\bar{\gamma}M(1+\theta) - 2\theta(M+\theta_1)(1-f)]}{(M+\theta_1)(M+2\theta_1)} \tag{16}$$

which relates the travel to the parameter f.

From equation 9, using equation 11, we obtain

$$P[x + l(1 - b\phi)] = \frac{CRT_0\left(1 + \frac{C}{2W_1}\right)}{A\left(1 + \frac{C}{3W_1}\right)}(1 - f)Z \tag{17}$$

We now seek the maximum breech pressure P_m. From equation 13 we have

$$\frac{dx}{df} = -\frac{MCRT_0\left(1 + \frac{C}{2W_1}\right)}{AP\left(1 + \frac{C}{3W_1}\right)}(1 - f) \tag{18}$$

and if we introduce the dimensionless quantity,

$$k = \frac{\left(\eta - \frac{1}{\delta}\right)P_m\left(1 + \frac{C}{3W_1}\right)}{RT_0\left(1 + \frac{C}{2W_1}\right)} \tag{19}$$

we can write equation 17 as

$$P(x + l) = \frac{CRT_0(1 - f)\left(1 + \dfrac{C}{2W_1}\right)}{A\left(1 + \dfrac{C}{3W_1}\right)}[Z + k(1 + \theta f)] \tag{20}$$

Differentiating equation 20 with respect to f, and using $dP/df = 0$, one obtains, as the parameter at maximum pressure,

$$f_m = \frac{\gamma' M + \theta - 1}{\gamma' M + 2\theta} \tag{21}$$

where

$$\gamma' = \frac{\bar{\gamma}}{1 + k} \tag{22}$$

For pressures up to 25 tons/sq in., RT_0 greater than 60 (tons/sq in.) × (cc/g), η less than 1.02 cc/g, and δ less than 1.67 g/cc, the maximum value of k is 0.175. It is convenient to introduce also a quantity:

$$\zeta = \gamma' - \bar{\gamma} + 1 \tag{23}$$

Then

$$1 - f_m = \frac{1 + \theta}{\xi M + 2\theta_1} \tag{24}$$

and

$$Z_m = \frac{(1 + \theta)(\xi M + \theta_1)}{\xi M + 2\theta_1} \tag{25}$$

To evaluate $x + l(1 - b\phi)$ at peak pressure, we shall need

$$\begin{aligned}\left(\frac{1 + \theta}{Z_m}\right)^{M/\theta_1} &= \frac{(\xi M + \theta_1)(\xi M + 2\theta_1)^{(M/\theta_1)+2}}{(\xi M + 2\theta_1)^2(\xi M + \theta_1)^{(M/\theta_1)+1}} \\ &= \frac{(\xi M + \theta_1)}{(\xi M + 2\theta_1)^2}(\xi e^{1/\xi} M + 4\theta_1)\end{aligned}$$

by the approximation already used in chapter 4 to pass from equation 24 to equation 26. Expanding in powers of k gives

$$\left(\frac{1 + \theta}{Z_m}\right)^{M/\theta_1} = \frac{(\xi M + \theta_1)}{(\xi M + 2\theta_1)^2}\left[eM\left\{1 + \frac{(k\bar{\gamma})^2}{2}\right\} + 4\theta_1\right]$$

Now $\bar{\gamma}$ is at most 1.35, and the term $\frac{1}{2}(k\bar{\gamma})^2$ is always less than 3 per cent and is usually much less than this limit. Thus it is sufficiently accurate to write

$$\left(\frac{1+\theta}{Z_m}\right)^{M/\theta_1} = \frac{(\xi M + \theta_1)(eM + 4\theta_1)}{(\xi M + 2\theta_1)^2} \tag{26}$$

Substituting in equation 16, we have

$$\frac{[x_m + l(1 - b\phi_m)](\xi M + 2\theta_1)^2}{\xi M + \theta_1} = l(eM + 4\theta_1)\left[1 - \frac{\bar{\gamma} bM(1+\theta)^2}{(M+\theta_1)(M+2\theta_1)}\right] + \frac{bl(1+\theta)^2[\bar{\gamma}M(\xi M + 2\theta_1) - 2\theta(M+\theta_1)]}{(M+\theta_1)(M+2\theta_1)} \tag{27}$$

From equations 17, 24, and 25,

$$\frac{P_m[x_m + l(1 - b\phi_m)](\xi M + 2\theta_1)^2}{\xi M + \theta_1} = \frac{CRT_0\left(1 + \dfrac{C}{2W_1}\right)}{A\left(1 + \dfrac{C}{3W_1}\right)}(1+\theta)^2 \tag{28}$$

Dividing equation 27 by equation 28 and expanding in powers of $\eta - 1/\delta$, we find that

$$\frac{(e + 2\bar{\gamma} - 2)M + 4\theta}{(1+\theta)^2} = \frac{C}{E}\left[\frac{RT_0\left(1 + \dfrac{C}{2W_1}\right)}{P_m\left(1 + \dfrac{C}{3W_1}\right)} + \left(\eta - \frac{1}{\delta}\right)F_1\left(\frac{\theta}{M}\right)\right] \tag{29}$$

where

$$F_1(\tau) = \frac{\bar{\gamma}(e + \bar{\gamma} - 2) + (3\bar{\gamma} + 1)\tau + 2\tau^2}{[\frac{1}{2}(\bar{\gamma} + 1) + \tau](\bar{\gamma} + 2\tau)} \tag{30}$$

The next term on the right of equation 29 involving $(\eta - 1/\delta)^2$ amounts to at most 3 per cent of the first term and may be neglected.

F_1 is a slowly varying function of $\bar{\gamma}$ and τ. Over the practical range of $\bar{\gamma}$, 1.25 to 1.35, F_1 varies by less than 1 per cent and may therefore be given the value for $\bar{\gamma} = 1.3$. In practice θ/M can take values ranging from small negative values to about unity. Over this range, F_1 can be represented by

$$F_1(\tau) = 1.755 - 0.749\tau + 0.343\tau^2 \tag{31}$$

which is in error by less than 1 per cent.

Equation 29 is the fundamental equation, which gives the maximum pressure in terms of the charge, gun dimensions, and the central ballistic parameter M. Conversely, if P_m is known, M can be obtained from equation 29 by successive approximation, which converges very rapidly.

The other interesting point of the solution is "burnt." Putting $f = 0$ in the general formulas previously obtained, we have

$$V_B = \frac{AD}{\beta(W_1 + \frac{1}{2}C)} \tag{32}$$

$$Z_B = 1 - \tfrac{1}{2}(\bar{\gamma} - 1)M \tag{33}$$

$$x_B + l(1 - b) = l\left(\frac{1 + \theta}{Z_B}\right)^{M/\theta_1}\left[1 - \frac{\bar{\gamma} b M(1 + \theta)^2}{(M + \theta_1)(M + 2\theta_1)}\right] + \frac{blZ_B[(\bar{\gamma} - \theta)M - 2\theta^2]}{(M + \theta_1)(M + 2\theta_1)} \tag{34}$$

and

$$P_B = \frac{CRT_0Z_B\left(1 + \dfrac{C}{2W_1}\right)}{A[x_B + l(1 - b)]\left(1 + \dfrac{C}{3W_1}\right)} \tag{35}$$

It only remains to give the solution for the adiabatic expansion after "burnt." The method is the same as in § 4.23, and the solution is

$$P = P_B r^{-\bar{\gamma}}$$

where

$$r = \frac{x + l(1 - b)}{x_B + l(1 - b)} \tag{36}$$

and

$$V^2 = \frac{CRT_0}{W_1 + \frac{1}{3}C}[M + Z_B\Phi] \tag{37}$$

where

$$\Phi = \frac{2}{\bar{\gamma} - 1}(1 - r^{1-\bar{\gamma}}) \tag{38}$$

5.24 Summary of the working formulas

The formulas most used in practice are the following.

A. The relation between P_m and M:

$$\frac{(e + 2\bar{\gamma} - 2)M + 4\theta}{(1 + \theta)^2} = \frac{C}{E}\left[\frac{RT_0\left(1 + \dfrac{C}{2W_1}\right)}{P_m\left(1 + \dfrac{C}{3W_1}\right)} + \left(\eta - \frac{1}{\delta}\right)F_1\left(\frac{\theta}{M}\right)\right] \tag{29}$$

with

$$F_1\left(\frac{\theta}{M}\right) = 1.755 - 0.749\,\frac{\theta}{M} + 0.343\left(\frac{\theta}{M}\right)^2 \tag{31}$$

provided

$$\bar{\gamma}M > (1-\theta)\left[1 + \left(\eta - \frac{1}{\delta}\right)\frac{P_m\left(1 + \dfrac{C}{3W_1}\right)}{RT_0\left(1 + \dfrac{C}{2W_1}\right)}\right]$$

otherwise peak pressure is at "burnt."

B. The travel and pressure at "burnt":

$$x_B + l(1-b) = l\left(\frac{1+\theta}{Z_B}\right)^{M/\theta_1}\left[1 - \frac{\bar{\gamma}bM(1+\theta)^2}{(M+\theta_1)(M+2\theta_1)}\right] + \frac{blZ_B[(\bar{\gamma}-\theta)M - 2\theta^2]}{(M+\theta_1)(M+2\theta_1)} \tag{34}$$

where

$$Z_B = 1 - \tfrac{1}{2}(\bar{\gamma}-1)M \tag{33}$$

$$b = \left(\eta - \frac{1}{\delta}\right)\frac{C}{E} \tag{12}$$

and

$$\theta_1 = \theta + \tfrac{1}{2}(\bar{\gamma}-1)M \tag{15}$$

Also,

$$P_B = \frac{CRT_0Z_B\left(1 + \dfrac{C}{2W_1}\right)}{A[x_B + l(1-b)]\left(1 + \dfrac{C}{3W_1}\right)} \tag{35}$$

C. The velocity at the muzzle:

$$V^2 = \frac{CRT_0}{W_1 + \frac{1}{3}C}\,(M + Z_B\Phi) \tag{37}$$

where

$$\Phi = \frac{2}{\bar{\gamma}-1}\,(1 - r^{1-\bar{\gamma}}) \tag{38}$$

and

$$r = \frac{x + l(1-b)}{x_B + l(1-b)} \tag{36}$$

5.25 The nature of the effects produced by covolume and kinetic-energy terms

When $\theta = 0$, the equation 29 for the maximum pressure is

$$\frac{CRT_0\left(1 + \dfrac{C}{2W_1}\right)}{EP_m\left(1 + \dfrac{C}{3W_1}\right)}\left[1 + \left(\eta - \frac{1}{\delta}\right)\frac{P_mF_1}{RT_0}\right]^{1/2} = (e + 2\bar{\gamma} - 2)M\left[1 + \left(\eta - \frac{1}{\delta}\right)\frac{P_mF_1}{RT_0}\right]^{-1/2} \tag{39}$$

M depends on RT_0 and is, in fact, inversely proportional to RT_0. Thus if we write

$$\lambda_1 = RT_0\left[1 + \left(\eta - \frac{1}{\delta}\right)\frac{P_mF_1}{RT_0}\right]^{1/2} \tag{40}$$

and denote M_1 as the value of M when calculated with this value of the force constant, then from equation 39 we have

$$\frac{C\lambda_1\left(1 + \dfrac{C}{2W_1}\right)}{EP_m\left(1 + \dfrac{C}{3W_1}\right)} = (e + 2\bar{\gamma} - 2)M_1 \tag{41}$$

which is the same form as would be obtained if $\eta = 1/\delta$. The effect of the $\eta - (1/\delta)$ term *on the maximum pressure* is therefore the same as an increase in the force constant by $\frac{1}{2}[\eta - (1/\delta)]P_mF_1$. This is independent of RT_0, almost independent of $\bar{\gamma}$, and it depends on the details of the ballistic solution only through P_m. For propellants in everyday use, $\eta - (1/\delta)$ ranges from 0.25 to 0.4 cc/g, with $\frac{1}{3}$ cc/g as an average; $F_1(0) = 1.755$; hence, at $P_m = 20$ tons/sq in. the effective increase in the force constant is about 6 (tons/sq in.) × (cc/g), which is slightly less than 10 per cent of a normal RT_0.

For cord $\theta = 1$, and an average θ/M is about 0.5, making $F_1 \simeq 1.5$. This is less than $F_1(0)$, but, owing to the 4θ term in equation 29, the effective increase in RT_0 is nearly the same as before. The increase in the force constant is in fact almost independent of propellant shape.

We now compare the maximum pressure calculated from this effective λ_1 and that obtained from the isothermal model of chapter 4. This will show how the λ of chapter 4 is related to λ_1 and RT_0.

From equation 26 of chapter 4,

$$P_m = \frac{\lambda^2 C(1+\theta)^2 \left(1 + \dfrac{C}{2W_1}\right)}{E(eM\lambda + 4\theta\lambda)\left(1 + \dfrac{C}{3W_1}\right)} \tag{42}$$

and, from equation 29 of this chapter,

$$P_m = \frac{\lambda_1{}^2 C(1+\theta)^2 \left(1 + \dfrac{C}{2W_1}\right)}{E[(e + 2\bar{\gamma} - 2)M_1\lambda_1 + 4\theta\lambda_1]\left(1 + \dfrac{C}{3W_1}\right)} \tag{43}$$

From the definition of the central ballistic parameter,

$$M\lambda = M_1\lambda_1$$

Consider first the case $\theta = 0$. The simpler theory gives the correct P_m if

$$\frac{\lambda}{\lambda_1} = \left(\frac{e}{e + 2\bar{\gamma} - 2}\right)^{1/2}$$

This varies little with $\bar{\gamma}$ over the range of interest in ballistics. For $\bar{\gamma} = 1.3$, $\lambda/\lambda_1 = 0.91$; that is, the mean temperature that gives the right peak pressure is 9 per cent less than the effective maximum temperature in a theory that includes the energy of the shot. Since also λ_1/RT_0 is about 1.1 at $P_m = 20$ tons/sq in., $\lambda \simeq RT_0$ for such pressures.

For cord, λ/λ_1 depends on M and in a typical case is 0.93. The dependence of λ/λ_1 on the shape of the propellant is therefore small.

To sum up, it has been shown that the proper λ to use *in the calculation of* P_m from the isothermal model is within 1 or 2 per cent of RT_0, if P_m is of the order of 20 tons/sq in. At lower maximum pressures, say around 10 tons/sq in., the appropriate λ falls below RT_0 by up to 5 per cent.

The contribution of $\eta - (1/\delta)$ and kinetic-energy terms to the muzzle velocity is not so easily picked out from the formulas, though they may be demonstrated by computations on typical examples. To this we shall return later. Here we shall consider only the muzzle velocity obtained from the isothermal model. If λ is chosen to give the correct P_m, the pressure later in the solution will be too big and the muzzle velocity too high. This is particularly so for cord charges, since, as can be seen from examples 4 and 5 at the end of chapter 4, it is for such charges that maximum pressure occurs earliest relative to "burnt." Therefore, the value of λ, which gives the correct velocity, will be less than RT_0, and the difference will be greatest for charges of cord. Alternatively, if a single value of λ is associated with each propellant composition, the velocity error (= calculated − fired) will be algebraically bigger for cord charges. This is indeed observed in practice.

From the peak pressures of various charges of a given propellant type in a given gun, one can calculate the central ballistic parameter and thence the effective rate of burning β. Since neither the theory of chapter 4 nor that used up to the present in this chapter takes explicit account of initial resistance, it is not surprising that the values of β calculated from both theories are found to depend on the details of the ballistics, though in rather different fashion for the two theories. In both, β is chiefly a function of the peak pressure, for a given gun and driving band.

The solution when the covolume term is omitted (that is, $\eta = 1/\delta$) is well known; see Lorenz [2] or other expositions listed by Cranz.[3] Closely related solutions are given by Desmazières.[4]

5.26 Comparison with experiment

The examples studied in the previous chapter will now be used to illustrate the results obtained in practice from this theory.

We consider first the 3.7-in. AA gun. Table 5.1 shows the details of the solutions for $\theta = 0.15$ (the "geometric" value) and $\theta = 0.3$. The central ballistic parameter M has been chosen to give the right maximum pressure; that is, the rate of burning has been chosen empirically. The error in the velocity is small. The pressure-time curve for $\theta = 0.3$ is shown in Fig. 5.1. The agreement is slightly better than was obtained (Fig. 4.3) from the isothermal model and is reached for a more plausible value of θ : 0.3 instead of 0.6. Moreover, the velocity is now correct to within 9 ft/sec in spite of there being one fewer arbitrary parameter.

TABLE 5.1 SOLUTIONS FOR THE 3.7-IN. AA GUN, GIVING CORRECT P_m

θ	M	β	Z_B	θ_1	MV, ft/sec	Error	x_B, in.
0.15	1.2333	0.778	0.7903	0.3597	2719	18	45.5
0.3	1.4379	0.720	0.7556	0.5444	2710	9	54.8

β is in (inches per second) per (ton per square inch); $W_1 = 28$ lb $= W$.

---

[2] Lorenz, *Ballistik*, 3d ed. (1935).

[3] Cranz, *Innere Ballistik* (Berlin, 1926).

[4] Desmazières, *Mém. artillerie franç.*, **1** (1922), 19.

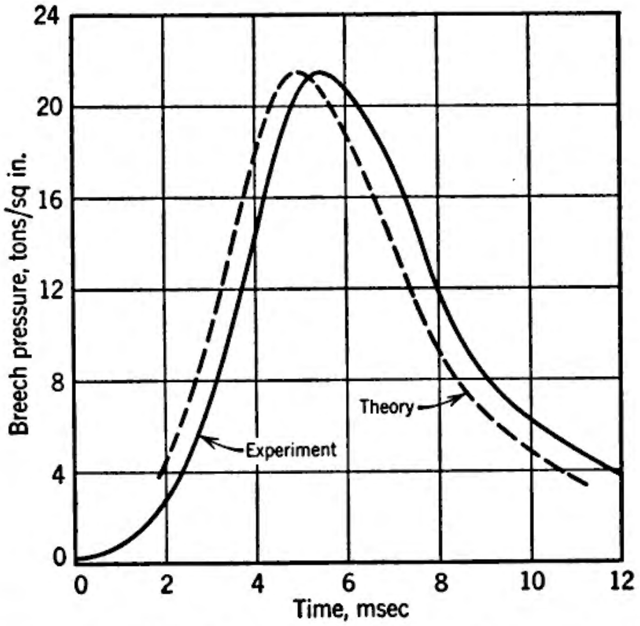

FIG. 5.1 Observed pressure-time curve for an AA gun, compared with the Coppock solution, with $\theta = 0.3$ and constants chosen to give correct peak pressure and instant of ejection.

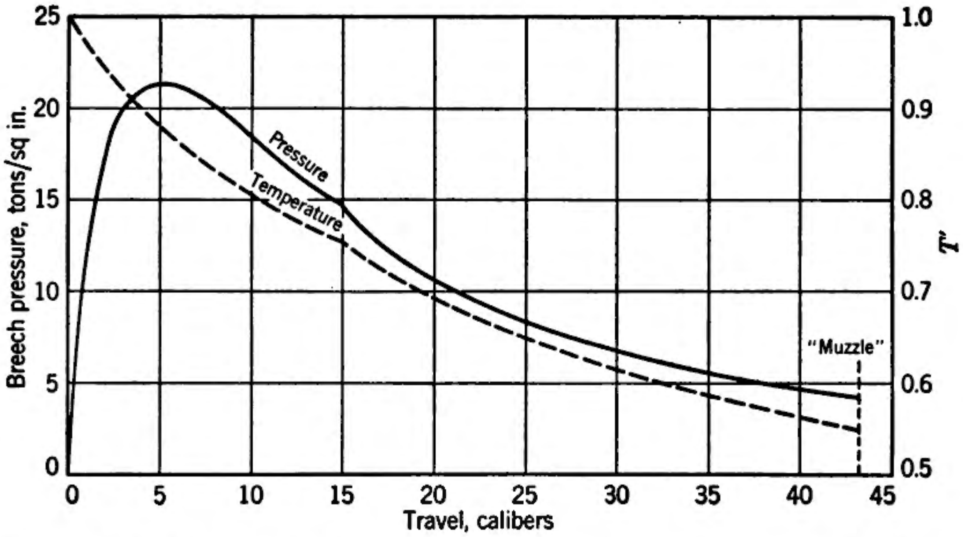

FIG. 5.2 Pressure and gas temperature (in reduced units) as functions of travel in the 3.7-in. AA gun, by the Coppock solution, with $W_1 = W$, $\theta = 0.3$, and rate of burning chosen to reproduce the observed peak pressure.

The pressure-travel and temperature-travel curves are shown in Fig. 5.2. The temperature given is actually the reduced temperature T' and is, at each instant, the mean throughout the gas at that time. T' is easily calculated from

$$T' = \frac{Z}{1 + \theta f} \tag{44}$$

The reduced temperature is initially 1 but falls to about 0.87 at maximum pressure and to 0.75 at the end of burning. At shot ejection the mean temperature is about 0.55, corresponding, for this cool propellant, to about 1350°K.

In Fig. 5.3 we give the observed and calculated pressure-time curves for two charges in a 6-in. naval gun, discussed in § 4.312. θ was assumed to be unity, and the effective shot mass W_1 was taken to be the same as the measured mass W. Table 5.2 shows some details of the solutions.

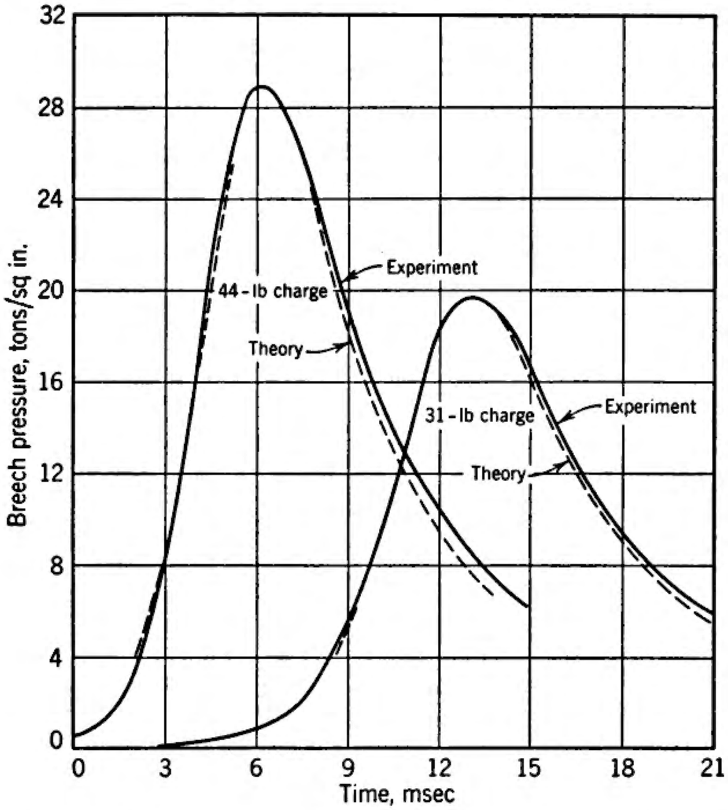

Fig. 5.3 Observed pressure-time relations with two charges in a 6-in. gun, compared with Coppock solutions, with $\theta = 1$, $W_1 = W$, and rates of burning chosen to give the observed peak pressures.

TABLE 5.2 SOLUTIONS FOR CORD CHARGES IN THE 6-IN. GUN

Charge, lb	Web, in.	M	β	θ_1	x_B, in.	MV, ft/sec	Error
31	0.150	2.457	0.953	1.3686	249.7	2884	34
44	0.205	3.454	0.886	1.5181	$\phi = 0.978$ at muzzle	3371	15

M chosen to give observed P_m; $\theta = 1$; $W_1 = 100$ lb; β is in (inches per second) per (ton per square inch).

The velocities are reproduced quite well, and if the fit to the pressure-time curves is not so good as on the isothermal model (Fig. 4.6), the agreement is obtained with one fewer arbitrary constant and could be improved by changes in θ and W_1.

The variation of β with the peak pressure is much the same as with the isothermal model (see Table 5.2).

This theory, with $W_1 = W$, gives velocities that are usually rather too high. The error is, for a given gun, more nearly constant than the error from the isothermal solution and is also less dependent on the shape of the propellant. The error may attain 3 per cent in a bad case.

5.27 The effect of heat losses

This theory takes full account of the specific heat of the gases, which enters the equations as $(\gamma - 1)$. Heat loss increases this to

$$\bar{\gamma} - 1 = (\gamma - 1)(1 + \chi)$$

where χ is the ratio of the heat loss at any time to the kinetic energy of shot and gas at that time. In the 3.7-in. AA gun we have used $\chi = 0.21$, which is perhaps slightly overestimated. Repetition of the calculations without heat loss shows that, to give the same peak pressure as before, the web size must be increased by 1.8 per cent. The travel at "burnt" increases by 2 in., and the velocity rises by 57 ft/sec. Thus at constant charge weight and constant pressure, the heat loss lowers the muzzle velocity by 57 ft/sec in 2700 ft/sec.

This is a fairly high heat loss, but would be exceeded if the velocity were higher, the caliber less, or the propellant a "hotter" composition. The effect of heat loss on muzzle velocity exceeds 100 ft/sec only for a few small antitank guns firing at velocities of about 4000 ft/sec.

5.3 A theory with a "shot-start pressure"

The ballistic theories discussed in chapter 4 and the preceding part of this chapter have represented the effects of resistance to initial motion of the shot by a change in the apparent rate of burning. This device is usually satisfactory in correlating experimental results, and is reasonably consistent; for example, a heavier band does alter the peak pressure in the same direction as an increase in the rate of burning. The initial resistance is so important in ballistics that it is desirable to investigate every promising representation of it. By analysis of firing data it will be possible to find which model leads to the best fit. This "best model" will continue to improve and at any one epoch will not necessarily be the same for all guns. We have in mind the jacketed shot fired in small arms, which engrave all along the body; these may be expected to show a resistance-travel relation quite different from that for a projectile with a band of normal width, say a quarter of a caliber.

The model to be used here may be called the "shot-start pressure" model. The shot is assumed not to move until the pressure reaches a value P_0, of the order of 2 ton/sq in. As soon as this gas pressure is reached, the projectile moves forward without resistance.

This model has been popular in all countries, especially with the French and German ballisticians. In England its development is associated chiefly with the names of Colonel F. R. W. Hunt and Brigadier G. H. Hinds. Recently a neater approximation to the solution of the same equations has been obtained by A. W. Goldie. This is the method given in the present chapter. Furthermore, the laborious but very necessary analysis of some hundreds of fired rounds has been carried out by Goldie, so that we have a good idea of how well this "shot-start model" accounts for the ballistics of various types of guns.

The shot-start model, as given here, can be improved by making an allowance for resistance, which occurs when the shot is in motion. This is most easily done by increasing the effective mass of the projectile, which would be an exact correction if the resistance were proportional at each instant to the pressure accelerating the shot. In the ballistic tables of Charbonnier-Sugot such a correction is made; it is assumed that the effective mass is 7 per cent greater than the true mass, and the shot-start pressure is taken to be 400 kg/sq cm.

The shot-start pressure can be found by working back from the observed peak pressure, provided we know the rate of burning of the propellant. If we take this from closed-vessel tests, any speeding up by "erosion" in the gun causes an increase in the "shot-start pressure" found by working back from the observed pressure. Thus we are led to expect that the shot-start pressure "observed" for a particular gun and composition of propellant will increase with the muzzle velocity and that the variation will be greatest for a cool propellant.

Alternatively we may assume zero shot-start pressure in a worn gun, which enables the rate of burning of the propellant to be calculated from the observed peak pressure in a worn gun. This process automatically allows for "cordite erosion," except for the small change in erosion due to the drop of velocity in going from new to worn guns. A snag in this otherwise attractive procedure is that allowance must be made for leakage past the shot and the increased volume of a worn gun. How to do this is explained in chapter 7. The labor involved is quite considerable, but it does give fairly reliable corrections for the two effects we have just mentioned. Without including these points there is, of course, no assurance that the apparent shot-start pressure can be taken to be zero.

In effect, we are here finding the rate of burning from guns instead of a closed vessel. The results for one propellant in various guns should show a correlation with muzzle velocity, with the closed-vessel rate corresponding to zero velocity.

A large number of firings have been analyzed by Goldie with the assumptions: neglect of heat loss, uncorrected shot mass, and a single rate of burning for a given composition in all shapes and for all guns. The shot-start pressures were found to be near 3 tons/sq in. and often almost independent of loading conditions. In other cases there was a tendency for the shot-start pressure to decrease as the peak pressure increased. Of the expected correlations with caliber, weight of band, and the like, the only one observed was the increase of P_0 with increasing weight of band on a given projectile in a given gun. The neglect of heat loss may have obscured a dependence on caliber, and this and the neglect of resistance may have had some effect on the variation of shot-start pressure.

From what we have said, it should be clear that not much physical significance can be attached to the "shot-start pressures" used by various writers. The most that can be claimed for any such value is that, after correcting for the effects omitted in the theoretical analysis (usually heat loss and resistance after shot start) and examining the credentials of the rate of burning, one can arrive at last at a pressure that is of the same order as the engraving resistance. Uncorrected shot-start pressures tend to range from 2 to 4 tons/sq in., whereas the engraving resistance, expressed as an equivalent pressure over the bore cross section, is unlikely to exceed 2 tons/sq in. The general tendency toward higher apparent resistance is due to the common use of closed-vessel rates of burning, which fail to include propellant "erosion."

5.31 Assumptions

(*a*) The rate of burning is proportional to the pressure.

(*b*) The gases have a constant covolume η, not necessarily equal to $1/\delta$.

(*c*) The propellant burns under the breech pressure P; that is, the propellant stays in the chamber.

(*d*) The law of burning away of the propellant is

$$\phi = (1 - f)(1 + \theta f)$$

(*e*) There is no motion of the shot until the "shot-start pressure" is reached. If there is any resistance to motion at later times, the resistance is proportional to pressure and so may be included by a change in the effective shot weight.

(f) We make the conventional assumptions about pressure gradient and the constancy of $\bar{\gamma}$.

5.32 Goldie's solution

The equations can be written down at once; they are the same as in Coppock's method. The difference lies only in the initial conditions. We have

$$\phi = (1 - f)(1 + \theta f) \tag{45}$$

$$D\frac{df}{dt} = -\beta P \tag{46}$$

$$(W_1 + \frac{1}{2}C)\frac{dV}{dt} = AP \tag{47}$$

$$AP[x + l(1 - b\phi)] + (\bar{\gamma} - 1)\left(W_1 + \frac{1}{2}C\right)\frac{V^2}{2} = C\phi RT_0\frac{\left(1 + \dfrac{C}{2W_1}\right)}{\left(1 + \dfrac{C}{3W_1}\right)} \tag{48}$$

where

$$b = \left(\eta - \frac{1}{\delta}\right)\frac{C}{E} \tag{49}$$

and

$$Al = E = U - \frac{C}{\delta} \tag{50}$$

We introduce the familiar ballistic parameter:

$$M = \frac{A^2D^2\left(1 + \dfrac{C}{3W_1}\right)}{\beta^2W_1CRT_0\left(1 + \dfrac{C}{2W_1}\right)^2} \tag{51}$$

Let suffix 0 denote quantities when the shot-start pressure is attained. P_0 is the breech pressure at that instant, and the pressure at the shot base is $P_0/[1 + (C/2W_1)]$. It is convenient to call P_0 the "shot-start pressure," bearing in mind that it is a pressure at the breech. In reality the pressure in the chamber at this epoch does not vary by nearly so much as the factor $1 + (C/2W_1)$ suggests, so that our assumptions about pressure gradient are physically incorrect here. This in itself warns us not to be too dogmatic in saying that $P_0/[1 + (C/2W_1)]$ "ought" to be more constant than P_0 when various charges are fired from the same gun.

Equations 46 and 47 give

$$V = \frac{AD(f_0 - f)}{\beta(W_1 + \frac{1}{2}C)} \tag{52}$$

equivalent to

$$V^2 = \frac{MCRT_0(f_0 - f)^2}{W_1 + \frac{1}{3}C} \tag{53}$$

and equation 48 becomes

$$\phi = \frac{AP[x + l(1 - b\phi)]\left(1 + \dfrac{C}{3W_1}\right)}{CRT_0\left(1 + \dfrac{C}{2W_1}\right)} + \frac{1}{2}(\bar{\gamma} - 1)M(f_0 - f)^2 \tag{54}$$

As in Coppock's method, we write

$$\theta_1 = \theta + \tfrac{1}{2}(\bar{\gamma} - 1)M \tag{55}$$

and introduce two new symbols,

$$\nu = \frac{4\theta_1\phi_0}{(1 + \theta)^2 - 4\theta\phi_0} \tag{56}$$

$$\epsilon = \frac{(1 + \nu)^{1/2} - 1}{(1 + \nu)^{1/2} + 1} \tag{57}$$

which are zero if there is no shot-start pressure. Also we write

$$l_2 = 1 - \theta + 2\theta f_0 \tag{58}$$

Equation 54 can now be expressed as

$$\frac{AP[x + l(1 - b\phi)]\left(1 + \dfrac{C}{3W_1}\right)}{CRT_0\left(1 + \dfrac{C}{2W_1}\right)} = \theta_1\left[\frac{l_2\epsilon}{\theta_1(1 - \epsilon)} + f_0 - f\right]\left[\frac{l_2}{\theta_1(1 - \epsilon)} - f_0 + f\right]$$

which by writing

$$\mu = \frac{\theta_1(1-\epsilon)(f_0-f)}{l_2} \tag{59}$$

becomes

$$\frac{AP[x+l(1-b\phi)]\left(1+\dfrac{C}{3W_1}\right)}{CRT_0\left(1+\dfrac{C}{2W_1}\right)} = (1-\mu)\left(\phi_0+\frac{\mu\phi_0}{\epsilon}\right) \tag{60}$$

For zero shot-start pressure, ϕ_0/ϵ tends to $(1+\theta)^2/\theta_1$.

We need an expression for the travel as a function of the fraction of charge burnt. From equations 46 and 47,

$$\frac{d}{df}[x+l(1-b\phi)] + bl\frac{d\phi}{df} = -\frac{DV}{\beta P} = -\frac{M(f_0-f)[x+l(1-b\phi)]}{(1-\mu)\left(\phi_0+\dfrac{\mu\phi_0}{\epsilon}\right)}$$

which integrates to

$$x + l(1-b\phi) = lH(f)[1-bG(f)] \tag{61}$$

where

$$\log H(f) = -\frac{M}{\theta_1(1+\epsilon)}\left[\log(1-\mu)+\epsilon\log\left(1+\frac{\mu}{\epsilon}\right)\right] \tag{62}$$

and

$$G(f) = \phi_0 + \int_{\phi_0}^{\phi}\frac{d\phi}{H} = \phi_0 + \frac{l_2{}^2}{\theta_1(1-\epsilon)}\int_0^{\mu}\left[1-\frac{2\theta\mu}{\theta_1(1-\epsilon)}\right]\frac{d\mu}{H} \tag{63}$$

Position of "burnt." Let suffix B denote values at "burnt," $f = 0$. Then

$$\mu_B = \theta_1(1-\epsilon)\frac{f_0}{l_2} \tag{64}$$

and $H(0)$ can be computed from equation 62 and a set of logarithm tables. To calculate the travel from equation 61 we need in addition only $G(0)$. This can be obtained from Table 5.3, of which the greater part has been taken from Goldie's work. Table 5.3 lists $G(0)$ and $dG(0)/d\phi_0$ for $\phi_0 = 0$, so that it covers any reasonable value of ϕ_0. Results for large ϕ_0 are not given accurately, but here the effect of the covolume term is small. The table covers values of M from 0 to 4, and linear interpolation causes errors of less than half a unit in the last place of $G(0)$. Four of the most important values of θ are listed, namely: $\theta = 0$, 0.2, 0.5, and 1; other values of θ can be obtained by interpolation. The remaining parameter is $\bar{\gamma}$. The table was computed for $\bar{\gamma} = 1.25$. Since $G(0)$ is multiplied by the covolume term, it is permissible to use this single value of $\bar{\gamma}$ in all cases. It can be shown that for the extreme value $\bar{\gamma} = 1.35$ the error in $G(0)$ causes an error of at most about 1 in 1000 in the muzzle velocity. This is most easily proved for the special case of zero shot-start pressure.

TABLE 5.3 $G(0)$, THE COVOLUME TERM IN THE TRAVEL

For $\bar{\gamma} = 1.25$

	$\theta = 0$		$\theta = 0.2$		$\theta = 0.5$		$\theta = 1$	
M	$G(0)$ at $\phi_0 = 0$	$\frac{dG(0)}{d\phi_0}$	$G(0)$ at $\phi_0 = 0$	$\frac{dG(0)}{d\phi_0}$	$G(0)$ at $\phi_0 = 0$	$\frac{dG(0)}{d\phi_0}$	$G(0)$ at $\phi_0 = 0$	$\frac{dG(0)}{d\phi_0}$
0	1	0	1	0	1	0	1	0
0.2	0.906	0.43	0.922	0.33	0.940	0.22	0.962	0.13
0.4	0.822	0.79	0.851	0.61	0.885	0.42	0.927	0.25
0.6	0.747	1.10	0.787	0.85	0.834	0.60	0.893	0.37
0.8	0.681	1.35	0.729	1.06	0.787	0.76	0.861	0.47
1.0	0.622	1.56	0.676	1.23	0.744	0.90	0.830	0.57
1.2	0.569	1.73	0.629	1.38	0.704	1.02	0.801	0.66
1.4	0.522	1.87	0.586	1.51	0.667	1.13	0.774	0.74
1.6	0.481	1.98	0.547	1.62	0.633	1.22	0.748	0.82
1.8	0.444	2.07	0.512	1.70	0.601	1.31	0.723	0.89
2.0	0.411	2.14	0.480	1.77	0.572	1.38	0.700	0.95
2.2	0.382	2.19	0.451	1.83	0.545	1.44	0.677	1.01
2.4	0.356	2.22	0.425	1.88	0.520	1.50	0.656	1.07
2.6	0.332	2.24	0.401	1.92	0.497	1.55	0.636	1.13
2.8	0.311	2.26	0.380	1.94	0.475	1.59	0.617	1.17
3.0	0.292	2.27	0.360	1.96	0.455	1.62	0.599	1.21
3.2	0.275	2.27	0.342	1.98	0.437	1.65	0.581	1.25
3.4	0.260	2.26	0.325	2.00	0.420	1.68	0.565	1.29
3.6	0.246	2.26	0.310	2.00	0.404	1.70	0.549	1.33
3.8	0.233	2.25	0.296	2.00	0.389	1.72	0.534	1.36
4.0	0.222	2.23	0.283	2.01	0.374	1.74	0.520	1.39

Calculation of the pressure-space curve up to "burnt." We take a number of values of f from f_0 to zero, and for each we determine the travel from equation 61 and the pressure from equation 60. To evaluate the latter we need only μ, given by equation 59 and the initial data of the problem. To get the travel we calculate $H(f)$ from equation 62 and the known μ; it only remains to find $G(f)$. Goldie suggests that the approximation,

$$G(f) = \phi_0 + \frac{1+\theta}{(M+\theta_1)(M+2\theta_1)}$$

$$\times \left[\bar{\gamma}M(1+\theta) - \left(\frac{1 - \frac{1}{2}(\bar{\gamma}-1)M + \theta_1 f}{1+\theta} \right)^{1+(M/\theta_1)} \right.$$

$$\left. \times \{M\bar{\gamma}(1+\theta) - 2\theta(1-f)(M+\theta_1)\} \right] \quad (65)$$

should be used. This is exact for $\phi_0 = 0$ and is most in error at $f = 0$, where the error may attain ±10 per cent. It is best to start by finding the error of equation 65 at $f = 0$ and to introduce this as a correction increasing as f decreases to zero.

Calculation of muzzle velocity. We have found the travel at "burnt." If this is less than the total travel, the muzzle velocity is calculated from the velocity at "burnt" and the usual adiabatic expansion. The explicit result is

$$V^2 = \frac{CRT_0}{W_1 + \frac{1}{3}C} \left[Mf_0{}^2 + \left\{ 1 - \frac{1}{2}(\bar{\gamma} - 1)Mf_0{}^2 \right\} \Phi \right] \quad (66)$$

where, as usual,

$$\Phi = \frac{2}{\bar{\gamma} - 1}(1 - r^{1-\bar{\gamma}}) \quad (67)$$

with

$$r = \frac{x + l(1-b)}{x_B + l(1-b)} \quad (68)$$

If the charge is unburnt at the muzzle, we calculate the travel for various values of f, interpolating to find f at the muzzle. Then the muzzle velocity comes from equation 53.

Tables for maximum pressure. For a ballistic solution to be useful in routine work, the maximum pressure must be expressed as a simple, even if not quite exact, formula, or else in an easily used table. The former method is exemplified by the simple result of Coppock's method: equations 29 and 30 of § 5.24. In the present theory the use of a set of tables is demonstrated.

We begin by reducing the number of variables that influence the maximum pressure. Goldie has shown that an increase of 0.03 in $\bar{\gamma}$ is nearly equivalent, *in its effect on maximum pressure,* to a 1 per cent decrease in β. The tables have therefore been computed for $\bar{\gamma} = 1.25$ and are used with the variable:

$$M_1 = M[1 + \tfrac{2}{3}(\bar{\gamma} - 1.25)] \tag{69}$$

The errors so caused are of order 1 in 1000 for $\bar{\gamma}$ between 1.2 and 1.3, rising a little toward the extreme $\bar{\gamma}$ of about 1.35.

The dependence on θ has now to be studied. Taking $\bar{\gamma}$ as a constant, we have

$$\epsilon = \text{function of } \frac{M}{\theta} \quad \text{and} \quad \frac{\theta\phi_0}{(1+\theta)^2} \tag{70}$$

from equations 55, 56, and 57. Differentiate equation 60 with respect to f, and put $dP/df = 0$. Let suffix m refer to the epoch of maximum pressure. We find

$$f_m = \frac{(\theta - 1)\left[1 + \dfrac{bEP_m\left(1 + \dfrac{C}{3W_1}\right)}{CRT_0\left(1 + \dfrac{C}{2W_1}\right)}\right] + f_0(M + 2\theta_1 - 2\theta)}{2\theta\dfrac{bEP_m\left(1 + \dfrac{C}{3W_1}\right)}{CRT_0\left(1 + \dfrac{C}{2W_1}\right)} + M + 2\theta_1} \tag{71}$$

which leads to

$$\mu_m = \frac{\theta_1(1 - \epsilon)\left[1 + \dfrac{bEP_m\left(1 + \dfrac{C}{3W_1}\right)}{CRT_0\left(1 + \dfrac{C}{2W_1}\right)}\right]}{2\theta\left[1 + \dfrac{bEP_m\left(1 + \dfrac{C}{3W_1}\right)}{CRT_0\left(1 + \dfrac{C}{2W_1}\right)}\right] + \bar{\gamma}M} \tag{72}$$

By equations 70 and 72,

$$\mu_m = \text{function only of } \frac{\mathrm{M}}{\theta}, \quad \frac{\theta\phi_0}{(1+\theta)^2}, \quad \text{and} \quad \frac{bEP_m\left(1 + \dfrac{C}{3W_1}\right)}{CRT_0\left(1 + \dfrac{C}{2W_1}\right)} \tag{73}$$

From equations 60 and 73,

$$\frac{\theta A P_m[x_m + l(1 - b\phi_m)]\left(1 + \dfrac{C}{3W_1}\right)}{(1+\theta)^2 CRT_0\left(1 + \dfrac{C}{2W_1}\right)} = \text{function only of } \frac{\text{M}}{\theta}, \quad \frac{\theta\phi_0}{(1+\theta)^2}$$

$$\text{and} \quad \frac{bEP_m\left(1 + \dfrac{C}{3W_1}\right)}{CRT_0\left(1 + \dfrac{C}{2W_1}\right)} \tag{74}$$

From equation 61,

$$x_m + l(1 - b\phi_m)$$

$$= lH(f_m)\left[1 - \frac{bEP_m\left(1 + \dfrac{C}{3W_1}\right)G(f_m)CRT_0\left(1 + \dfrac{C}{2W_1}\right)}{CRT_0\left(1 + \dfrac{C}{2W_1}\right)EP_m\left(1 + \dfrac{C}{3W_1}\right)}\right] \tag{75}$$

Now, by equations 62 and 73, $H(f_m)$ is a function of the same three variables as μ_m, whereas, from equation 63,

$$G(f_m)\,\frac{CRT_0\left(1 + \dfrac{C}{2W_1}\right)}{EP_m\left(1 + \dfrac{C}{3W_1}\right)}$$

$$= \left[\frac{\theta EP_m\left(1 + \dfrac{C}{3W_1}\right)}{(1+\theta)^2 CRT_0\left(1 + \dfrac{C}{2W_1}\right)}\right]^{-1}$$

$$\times\left(\frac{\theta\phi_0}{(1+\theta)^2} + \frac{\theta}{\theta_1(1-\epsilon)}\left[1 - \frac{4\theta\phi_0}{(1+\theta)^2}\right]\int_0^{\mu_m}\left[1 - \frac{2\theta\mu}{\theta_1(1-\epsilon)}\right]\frac{d\mu}{H}\right)$$

$$= \text{function only of } \frac{\theta EP_m\left(1 + \dfrac{C}{3W_1}\right)}{(1+\theta)^2 CRT_0\left(1 + \dfrac{C}{2W_1}\right)}, \quad \frac{\theta\phi_0}{(1+\theta)^2}, \quad \frac{M}{\theta},$$

$$\text{and}\quad \frac{bEP_m\left(1+\dfrac{C}{3W_1}\right)}{CRT_0\left(1+\dfrac{C}{2W_1}\right)} \tag{76}$$

Returning to equation 75, we see that $[x_m + l(1 - b\phi_m)]/l$ is a function of only the four variables listed previously; hence, from equation 74,

$$\frac{\theta EP_m\left(1+\dfrac{C}{3W_1}\right)}{(1+\theta)^2 CRT_0\left(1+\dfrac{C}{2W_1}\right)} = \text{function only of } \frac{M}{\theta},\quad \frac{\theta\phi_0}{(1+\theta)^2},$$

$$\text{and}\quad \frac{bEP_m\left(1+\dfrac{C}{3W_1}\right)}{CRT_0\left(1+\dfrac{C}{2W_1}\right)}.$$

This is a very useful result. It holds only if there is a true maximum. If the mathematical maximum occurs for negative f_m, the peak pressure observed is that at "burnt" and is

$$P_B = \frac{CRT_0\left(1+\dfrac{C}{2W_1}\right)\left[1-\dfrac{1}{2}(\bar{\gamma}-1)Mf_0{}^2\right]}{[x_B + l(1-b)]\left(1+\dfrac{C}{3W_1}\right)} \tag{77}$$

with the travel being taken from equation 61.

The criterion for a true maximum pressure is $f_m \geq 0$, that is,

$$M \geq \frac{1-\theta}{\bar{\gamma}f_0}\left[1 + \frac{bEP_m\left(1+\dfrac{C}{3W_1}\right)}{CRT_0\left(1+\dfrac{C}{2W_1}\right)}\right] \tag{78}$$

To calculate the true maximum pressure we need only tabulate

$$\frac{\theta EP_m\left(1+\dfrac{C}{3W_1}\right)}{(1+\theta)^2 CRT_0\left(1+\dfrac{C}{2W_1}\right)}$$

TABLE 5.4 VALUES OF $\frac{(M_1 + 2\theta)EPm[1 + (C/3W_1)]}{(1+\theta)^2 CRT_0[1 + (C/2W_1)]}$ FOR $\frac{bEP_m[1 + (C/3W_1)]}{CRT_0[1 + (C/2W_1)]} = 0$

M_1/θ	$\frac{\theta\phi_0}{(1+\theta)^2} = 0$		0.005		0.01		0.02		0.03	0.04
0	0.500		0.500		0.500		0.500		0.500	0.500
0.125	0.482		0.484		0.485		0.488		0.491	0.494
0.25	0.467		0.471		0.474		0.479		0.484	0.488
	16		15		14		13		12	11
0.5	0.444		0.451		0.457		0.466		0.475	0.484
	10		9		8		9		8	
0.75	0.427		0.437		0.445		0.458		0.471	0.483
1	0.414		0.426		0.436		0.454		0.470	0.485
1.25	0.403	(10)	0.418		0.430	8	0.452		0.471	0.489
1.5	0.394	(15)	0.412		0.427	11	0.451		0.473	0.495
	10		9							
2	0.381	(20)	0.403		0.422	13	0.452		0.480	0.507
2.5	0.371	(30)	0.398	8	0.420	15	0.456		0.490	0.522
3	0.364	(35)	0.395	9	0.419	15	0.461		0.501	0.538
3.5	0.359	(40)	0.394	11	0.420	16	0.468		0.513	0.555
4	0.354	(40)	0.393	12	0.422	18	0.476	8	0.526	0.573
5	0.347	(50)	0.394	15	0.429	23	0.493	9	0.554	0.611
6	0.342	(55)	0.396	16	0.437	26	0.510	9	0.582	0.649
7	0.338	(60)	0.398	17	0.445	29	0.528	9	0.609	0.686
8	0.335	(65)	0.401	18	0.454	31	0.547	10	0.636	0.723
9	0.332	(75)	0.405	20	0.463	33	0.566	11	0.664	0.760
10	0.330	(90)	0.410	22	0.473	36	0.586	10	0.693	0.798
12	0.327	(100)	0.420	25	0.493	40	0.626	10	0.752	0.876
14	0.325	(110)	0.430	27	0.513	43	0.666	10	0.811	0.954
16	0.323	(120)	0.440	29	0.533	46	0.706	11	0.870	1.032

Differences listed in both directions are sums of adjacent second differences, modified to allow for the effect of fourth differences.

against the three variables mentioned previously. This is done in Tables 5.4 and 5.5, where to reduce the variation of this function[5] we have actually given

$$\left(\frac{M_1}{\theta} + 2\right) \frac{\theta E P_m \left(1 + \dfrac{C}{3W_1}\right)}{(1+\theta)^2 CRT_0 \left(1 + \dfrac{C}{2W_1}\right)}$$

---

[5] Goldie's tables are in a form that is more convenient for practical work, and the present form was adopted only to give a compact synopsis.

TABLE 5.5 VALUES OF $\frac{(M_1 + 2\theta)EP_m[1 + (C/3W_1)]}{(1 + \theta)^2 CRT_0[1 + (C/2W_1)]}$ FOR $\frac{bEP_m[1 + (C/3W_1)]}{CRT_0[1 + (C/2W_1)]} = 0.1$

M_1/θ	$\frac{\theta\phi_0}{(1+\theta)^2} = 0$		0.005		0.01		0.02		0.03	0.04
0	0.550		0.550		0.550		0.550		0.550	0.550
0.125	0.534		0.536		0.537		0.540		0.543	0.546
0.25	0.520		0.524		0.527		0.533		0.538	0.543
	14		13		13		11		10	9
0.5	0.498		0.506		0.512		0.523		0.533	0.543
	10		8							
0.75	0.482		0.493		0.502		0.517		0.531	0.545
1	0.470		0.483		0.494		0.514		0.532	0.549
1.25	0.459		0.476		0.489	9	0.513		0.534	0.555
1.5	0.451	(10)	0.470		0.486	10	0.513		0.538	0.562
	9		8							
2	0.438	(15)	0.462		0.482	13	0.516		0.547	0.578
2.5	0.428	(25)	0.457	8	0.481	15	0.521		0.559	0.595
3	0.421	(35)	0.455	10	0.481	16	0.528		0.572	0.614
3.5	0.416	(40)	0.454	11	0.482	16	0.536		0.586	0.634
4	0.411	(40)	0.453	12	0.486	18	0.545		0.602	0.655
5	0.404	(45)	0.455	15	0.493	19	0.564		0.634	0.697
6	0.399	(50)	0.457	16	0.502	22	0.585	8	0.666	0.740
7	0.395	(60)	0.460	16	0.513	27	0.608	9	0.699	0.785
8	0.392	(70)	0.465	18	0.524	31	0.631	10	0.732	0.829
9	0.389	(80)	0.470	20	0.535	34	0.653	10	0.765	0.873
10	0.387	(90)	0.475	22	0.546	36	0.676	11	0.799	0.918
12	0.384	(100)	0.486	24	0.568	39	0.721	12	0.866	1.007
14	0.382	(110)	0.497	26	0.591	43	0.766	11	0.932	1.096
16	0.380	(120)	0.509	30	0.614	46	0.811	11	0.999	1.185

Differences listed in both directions are the sums of adjacent second differences, modified to include the effect of fourth differences.

M_1/θ goes from 0 to 16, which covers all practical cases. $\theta\phi_0/(1 + \theta)^2$ covers the range 0 to 0.04, so that for all θ the range of ϕ_0 goes up to at least 0.16. For P_0 of 3 tons/sq in. or less, this range of $\theta\phi_0/(1 + \theta)^2$ is sufficient for all but cord charges at densities of loading below 0.25 g/cc.

The differences listed are the sums of adjacent second differences, modified by a "throwback" to include fourth differences; if a function $f(a + nh)$ is to be calculated from $f(a)$, $f(a + h)$ and a printed difference D of this type, then

$$f(a + nh) = nf(a + h) + (1 - n)f(a) + DB''(n)$$

TABLE 5.6 VALUES OF $\dfrac{EP_m[1 + (C/3W_1)]}{CRT_0[1 + (C/2W_1)]}$ FOR $\theta = 0$; $\dfrac{bEP_m[1 + (C/3W_1)]}{CRT_0[1 + (C/2W_1)]} = 0$

M_1	$\phi_0 = 0$		0.025		0.05		0.1		0.15		0.2		0.25	0.3
0	1.000		1.000		1.000		1.000		1.000		1.000		1.000	1.000
	21		16		13		10							
0.1	0.893	(10)	0.905		0.913	9	0.925		0.936		0.944		0.952	0.958
	20		15		12		10							
0.2	0.796	(16)	0.817	9	0.832	16	0.855		0.875		0.891		0.905	0.917
	18		15		13		10							
0.3	0.709	(20)	0.737	11	0.757	20	0.790	10	0.818	8	0.841		0.861	0.878
	16		14		12		10							
0.4	0.630	(30)	0.664	13	0.689	24	0.729	11	0.764	10	0.793		0.818	0.840
	16		13		10		8							
0.5	0.559	(35)	0.598	14	0.626	27	0.673	13	0.713	10	0.747		0.777	0.804
	14		10		10									
0.6	0.496	(40)	0.538	15	0.568	27	0.620	13	0.665	11	0.704		0.738	0.770
	11		10		9									
0.7	0.439	(40)	0.482	14	0.515	27	0.571	13	0.620	11	0.663		0.701	0.737
	10		9		9									
0.8	0.387	(40)	0.432	15	0.466	27	0.525	13	0.577	9	0.623	8	0.666	0.704
0.9	0.344	(40)	0.388	13	0.422	23	0.483		0.536		0.585		0.631	0.673
	12		12		14		15							
1.0	0.310	(40)	0.354	14	0.386	22	0.446		0.500		0.549		0.597	0.643
	10		10		12		12		12					
1.1	0.282	(40)	0.325	13	0.357	21	0.416		0.470		0.523		0.572	0.614
	8		8		8		9		8		8			
1.2	0.258	(40)	0.301	13	0.333	21	0.391		0.445		0.497		0.547	0.597
1.3	0.238	(40)	0.280	12	0.312	21	0.370		0.423		0.475		0.525	0.575
1.4	0.221	(40)	0.263	13	0.294	20	0.351		0.404		0.456		0.506	0.556
1.5	0.207	(40)	0.248	13	0.279	19	0.335		0.388		0.439		0.490	0.539
1.6	0.194	(35)	0.235	13	0.265	18	0.321		0.374		0.425		0.475	0.524
1.7	0.182	(35)	0.223	13	0.253	19	0.309		0.361		0.412		0.462	0.511
1.8	0.172	(35)	0.213	13	0.243	19	0.298		0.350		0.401		0.450	0.500
1.9	0.163	(35)	0.203	12	0.233	18	0.288		0.340		0.391		0.440	0.489
2.0	0.155	(30)	0.194	11	0.224	17	0.279		0.331		0.381		0.431	0.479
2.2	0.141	(30)	0.180	11	0.209	17	0.264		0.315		0.365		0.414	0.463
2.4	0.129	(30)	0.168	11	0.197	17	0.251		0.302		0.352		0.401	0.450
2.6	0.119	(30)	0.157	10	0.186	16	0.240		0.291		0.341		0.390	0.439
2.8	0.111	(30)	0.148	10	0.177	15	0.230		0.281		0.331		0.380	0.429
			8		8		8		8		8		8	8
3.2	0.097	(30)	0.134	10	0.162	15	0.215		0.265		0.315		0.364	0.413
3.6	0.086	(30)	0.123	10	0.150	14	0.203		0.253		0.302		0.351	0.400
4.0	0.077	(30)	0.113	9	0.140	13	0.193		0.243		0.292		0.341	0.390

Differences listed in both directions are the sums of adjacent second differences.

TABLE 5.7 VALUES OF $\frac{EP_m(1 + C/3W_1)}{CRT_0(1 + C/2W_1)}$ FOR $\theta = 0$; $\frac{bEP_m(1 + C/3W_1)}{CRT_0(1 + C/2W_1)} = 0.1$

M_1	$\phi_0 = 0$		0.025		0.05		0.10		0.15		0.20	0.25	0.30
0	1.100		1.100		1.100		1.100		1.100		1.100	1.100	1.100
	22		18		15		13						
0.1	0.988	(10)	1.000		1.009	9	1.022		1.034		1.044	1.052	1.060
	20		16		13		11						
0.2	0.887	(18)	0.909	9	0.925	16	0.950		0.972		0.990	1.006	1.021
	18		15		12		9						
0.3	0.795	(25)	0.825	11	0.847	22	0.883	10	0.913		0.939	0.962	0.983
	18		14		12		8						
0.4	0.712	(30)	0.749	14	0.775	26	0.820	12	0.857		0.890	0.920	0.947
	16		12		11		8						
0.5	0.638	(35)	0.679	14	0.709	27	0.761	13	0.805	8	0.844	0.880	0.912
	13		12		10		8						
0.6	0.571	(40)	0.615	14	0.648	27	0.706	14	0.756	9	0.800	0.841	0.878
	12		11		10								
0.7	0.510	(40)	0.557	15	0.592	27	0.654	13	0.709	10	0.758	0.803	0.845
	11		9		8								
0.8	0.455	(40)	0.504	16	0.541	27	0.606	12	0.665	10	0.718	0.767	0.813
0.9	0.407	(40)	0.455		0.493	27	0.562	12	0.623	8	0.680	0.733	0.782
	16		16										
1.0	0.366	(40)	0.414	13	0.452	20	0.521		0.584	8	0.644	0.700	0.753
	13		13		14		14						
1.1	0.333	(40)	0.380	13	0.417	20	0.485		0.549		0.610	0.669	0.724
	10		10		11		11		11				
1.2	0.305	(40)	0.352	13	0.388	20	0.455		0.518		0.579	0.638	0.697
	8		8		8		9		9		9		
1.3	0.282	(40)	0.328	13	0.364	20	0.430		0.492		0.553	0.612	0.670
1.4	0.262	(40)	0.308	13	0.343	20	0.409		0.470		0.531	0.589	0.647
1.5	0.244	(40)	0.290	13	0.325	20	0.390		0.451		0.511	0.569	0.627
1.6	0.229	(40)	0.274	13	0.309	19	0.373		0.434		0.494	0.552	0.609
1.7	0.215	(40)	0.261	13	0.295	20	0.359		0.419		0.478	0.537	0.594
1.8	0.203	(40)	0.248	12	0.282	19	0.346		0.406		0.465	0.523	0.580
1.9	0.193	(35)	0.237	11	0.271	18	0.334		0.394		0.453	0.510	0.567
2.0	0.183	(35)	0.226	11	0.260	17	0.323		0.383		0.441	0.499	0.556
							8		8		8	8	
2.2	0.166	(35)	0.209	11	0.243	18	0.305		0.364		0.422	0.479	0.536
2.4	0.153	(30)	0.195	11	0.228	17	0.290		0.348		0.406	0.463	0.520
2.6	0.141	(30)	0.183	11	0.215	16	0.277		0.335		0.393	0.449	0.506
2.8	0.131	(30)	0.172	10	0.204	14	0.265		0.324		0.381	0.437	0.494
	10		10		10		10		10		10	10	10
3.2	0.114	(30)	0.155	11	0.187	15	0.247		0.305		0.362	0.418	0.474
3.6	0.102	(30)	0.142	10	0.173	13	0.232		0.290		0.347	0.403	0.458
4.0	0.092	(30)	0.131	9	0.162	13	0.221		0.278		0.334	0.390	0.446

Differences listed in both directions are sums of adjacent second differences.

where $B''(n)$ is the second Bessel interpolation coefficient,

$$B''(n) = \tfrac{1}{4}n(n-1)$$

A small table of $B''(n)$ is given in Appendix C, where reference is also made to tables of higher accuracy. Results interpolated in this way in Tables 5.4 and 5.5 will be in error by at most half a unit in the last place given, if the value of B'' is exact; if the table in Appendix C is used, the error may be doubled. Where no differences are given, linear interpolation is sufficient.

To include the dependence on $\dfrac{bEP_m[1 + (C/3W_1)]}{CRT_0[1 + (C/2W_1)]}$, separate tables are given with this parameter equal to 0 and 0.1. Its value is scarcely ever greater than 0.15. Goldie has shown that the maximum error in P_m caused by linear interpolation and extrapolation in this variable is 1 per cent, but this occurs only for a coincidence of three unfavorable factors; the average error is more nearly 1 in 1000.

Tables 5.4 and 5.5 give no information about the case $\theta = 0$, for which Tables 5.6 and 5.7 have to be used. They should be interpolated in the same way as the previous tables. Note the dotted boundary across Tables 5.6 and 5.7, showing the approximate position where the maximum pressure changes from a true maximum to a peak at "burnt." The location of the boundary can be calculated accurately from equation 78. The only inconvenience caused by the boundary arises when we cross the boundary during an interpolation. The error that can arise if no allowance at all is made during interpolation is only a few parts per thousand, and it is easy to estimate an approximate correction.

5.33 Ballistic effects of a shot-start pressure

The shot-start pressure prevents at first the motion of the shot in a way that is plausible, in the light of our knowledge of initial resistance. Once the shot-start pressure has been attained, the theoretical process diverges considerably from the practical behavior. In the first place, no work is done against the theoretical resistance, whereas a finite amount is done against the true resisting force. Now if we suppose that the resistance is equivalent to 1 ton/sq in. opposing pressure and acts for only half a caliber, whereas the mean gas pressure during the travel of, say, 40 calibers is about 10 ton/sq in., then the work done against initial resistance is only 0.1 per cent of the final energy of the shot. The neglect of this work in the "shot-start pressure" model is therefore sometimes reasonable. As the other extreme we may note that a nearly constant resistance all down the barrel would produce effects that would be hard to simulate by a shot-start pressure unless this were varied with the charge. There is evidence that, in fact, the resistance sometimes falls relatively slowly with travel, and this is probably why in certain guns the "shot-start pressure" deduced from the fired ballistics often shows a variation with peak pressure.

A second weakness of the "shot-start pressure" model is that the motion starts with a finite acceleration, whereas in practice the acceleration must increase continuously from zero. It is clear that the true effect of engraving on initial motion (and hence on peak pressure) is only partly simulated by a shot-start pressure.

The value of the "shot-start pressure" model is therefore a matter for practical trial. It is often very good, especially if energy losses are taken into account by raising the effective shot weight by a few per cent.[6] In this section we shall examine the ballistic effects of the shot-start pressure and shall show where they differ from those obtained by a simple modification of the rate of burning.

As an example we take the 3.7-in. AA gun discussed in connection with Coppock's method (§ 5.26). The data are the same as before, and some typical results, computed from Goldie's tables, are shown in Table 5.8.[7] It may be seen that in this case a shot-start pressure of 2 tons/sq in. produces the same effect on the peak pressure as an increase of 9 per cent in the rate of burning β. The velocities then differ by only 4 ft/sec. It is possible to reproduce the effect of the shot-start pressure on the peak pressure by altering other ballistic data, such as θ and W_1, but Table 5.8 shows how badly these changes reproduce the muzzle velocity. It is this kind of comparison with the shot-start pressure

TABLE 5.8 SOLUTIONS FOR THE 3.7-IN. AA GUN, FROM GOLDIE'S TABLES

All give the correct peak pressure of 21.4 tons/sq in.

Shot-start pressure, tons/sq in.	β, (in./sec) per (ton/sq in.)	MV, ft/sec	θ	W_1, lb
0	0.722	2715	0.3	28
2	0.660	2711	0.3	28
0	0.660	2790	0.71	28
0	0.660	2456	0.3	34.9

---

[6] As is done in the Charbonnier-Sugot tables, for example.

[7] The first solution of Table 5.8 refers to the same data as the second solution of Table 5.1. The values of β to give the same P_m are 0.722 and 0.720, respectively, and the velocities differ by 5 ft/sec. These small differences arise from the neglect of higher-order terms in the Coppock solution and various approximations noted when discussing the Goldie tables. In ballistic analysis with either method alone the change in the error between different solutions would be smaller.

model, as well as analysis of gun firings, that justifies (in most cases) the representation of initial resistance by a change in the rate of burning.

In general, if there is no other change in the conditions, a shot-start pressure always raises the peak pressure P_m, the relation being linear for small P_0. The muzzle velocity increases, the position of "burnt" moves toward the breech, and there is a trivial change in the position of the shot at the moment of peak pressure. These are the effects produced in practice by the small round-to-round variations in the shot-start pressure. Quite different results arise when we deliberately alter the shot-start pressure in search of an optimum, because then for the sake of the gun we must also change the web size to keep the peak pressure constant. For such combined changes of shot-start pressure and web thickness, the effect depends chiefly on the density of loading. At small densities of loading, say 0.4 g/cc, the muzzle velocity increases slightly as P_0 increases and falls off sharply when P_0 approaches P_m. At high densities of loading, around 0.8 g/cc, the muzzle velocity decreases slightly as P_0 increases from zero, the decline becoming more rapid at large P_0. At the same time, "burnt" occurs later in the travel, while the movements of the position of peak pressure are very small, and, in fact, both signs are found.

These conclusions about the effects of really large shot-start pressures were derived by mechanical integration on a differential analyzer (§ 5.6), since the existing tables, such as Tables 5.4 to 5.7, cover only the much smaller range of shot-start pressures that occur in conventional practice. The results themselves show that there is little reason to extend the existing tables.

5.4 Rate of burning not proportional to pressure

In all ballistic solutions given earlier in this book it has been assumed that the rate of burning of the propellant is proportional to the pressure. This is not far from the truth for present-day propellants at gun pressures, though a better law would be

$$\text{Rate} = \beta(P + P_1)$$

with P_1 a positive constant. No ballistic theory has yet used this law. Another relation which has been used, is

$$\text{Rate} = \beta P^{\alpha} \tag{79}$$

where α usually lies between 0.8 and 1. A more complete discussion of the rate of burning is given in § 2.37. Here we shall discuss equation 79 with $\alpha \neq 1$, to show how this alters the interior ballistics.

Liouville[8] studied ballistic theory with equation 79, obtaining complicated expressions, which found no practical application. Later Charbonnier[9] gave some approximate results to show the general nature of the effect. Numerical methods have often been used with α not unity; Centervall[10] used $\alpha = 0.9$, Bennett's tables[11] were computed for $\alpha = 2/3$, and Röggla[12] used $\alpha = 0.7$. The analytical solution of the general equation, without resistance to motion, and with $\eta = 1/\delta$, has been studied by Clemmow,[13] who has reduced the problem to certain standard forms of nonlinear differential equations and has obtained series expansions of the appropriate solutions. Dr. Clemmow has also computed the functions by numerical integration for the isothermal model for all form functions,

$$\phi = (1 - f)(1 + \theta f)$$

with θ from 0 to 1, though of his tables only that for ($\alpha = 1/2$, $\theta = 0$) has been published.

In this section we shall show how these theories have led to a useful formula for the peak pressure, and shall give tables of certain associated functions, due to Clemmow; the other ballistic effects, such as the effect on the muzzle velocity, are not so easily written explicitly, and we shall merely describe the qualitative effects of varying α, as found by using Clemmow's tables or by numerical integration.

We consider propellant burning as if it had constant burning surface, so that

$$\phi = 1 - f \tag{80}$$

We use the isothermal approximation, with mean force constant λ during the period of burning; with $\eta = 1/\delta$ we have

$$PA(x + l) = \frac{C\phi\lambda\left(1 + \dfrac{C}{2W_1}\right)}{\left(1 + \dfrac{C}{3W_1}\right)} \tag{81}$$

where

$$Al = U - \frac{C}{\delta} \tag{82}$$

---

[8] Liouville, *Mém. poudres*, **8** (1895), 25.

[9] Charbonnier, *Ballistique intérieure* (Paris, 1908), p. 308.

[10] Centervall, *Internal Ballistics* (Stockholm, 1902).

[11] Bennett, *ODD* 2039 (1922).

[12] Röggla, *Mitt. Gegenstände d. Artill. u. Geniewesens*, **45** (1914), 1, 149; *Neue Diagramme fur die angewandte innere Ballistik* (Pilsen, 1931); see also § 6.12.

[13] Clemmow, *Phil. Trans. Roy. Soc. (London)*, **227A** (1928), 345; **231** (1933), 263.

which is the initial air space behind the projectile. Also

$$\left(W_1 + \frac{1}{2}C\right)\frac{d^2x}{dt^2} = AP \tag{83}$$

and

$$D\frac{df}{dt} = -\beta P^{\alpha} \tag{84}$$

We note that $\left(\dfrac{\beta^2 W_1 C^2 \lambda^2}{A^3 l D^2}\right)^{1/(3-2\alpha)}$ has the dimensions of a pressure. This suggests that we should write

$$P(t) = g(t)\left[\frac{\beta^2 W_1 C^2 \lambda^2 \left(1 + \dfrac{C}{2W_1}\right)^3}{A^3 l D^2 \left(1 + \dfrac{C}{3W_1}\right)^2}\right]^{1/(3-2\alpha)} \tag{85}$$

where $g(t)$ is a numerical function, which may depend on such quantities as α and C/W_1. We find that by writing also

$$t = \frac{D}{\beta}\left[\frac{\beta^2 W_1 C^2 \lambda^2 \left(1 + \dfrac{C}{2W_1}\right)^3}{A^3 l D^2 \left(1 + \dfrac{C}{3W_1}\right)^2}\right]^{(1-\alpha)/(3-2\alpha)} \frac{Al\left(1 + \dfrac{C}{3W_1}\right)}{C\lambda\left(1 + \dfrac{C}{2W_1}\right)}\tau \tag{86}$$

$$\phi = \frac{Al\left(1 + \dfrac{C}{3W_1}\right)}{C\lambda\left(1 + \dfrac{C}{2W_1}\right)}\left[\frac{\beta^2 W_1 C^2 \lambda^2 \left(1 + \dfrac{C}{2W_1}\right)^3}{A^3 l D^2 \left(1 + \dfrac{C}{3W_1}\right)^2}\right]^{1/(3-2\alpha)} \Phi \tag{87}$$

and

$$x = l\xi \tag{88}$$

that equations 81 to 84 become

$$\Phi = (1 + \xi)g \tag{89}$$

$$\frac{d\Phi}{d\tau} = g^{\alpha} \tag{90}$$

and

$$\frac{d^2\xi}{d\tau^2} = g \tag{91}$$

with the initial conditions $\xi = 0$, $d\xi/d\tau = 0$, $\Phi = 0$, $g = 0$. Hence the maximum value of g is a function only of α, which we may write as $G(\alpha)$, arriving at

$$P_m = G(\alpha)\left[\frac{\beta^2 W_1 C^2 \lambda^2 \left(1 + \dfrac{C}{2W_1}\right)^3}{A^3 l D^2 \left(1 + \dfrac{C}{3W_1}\right)^2}\right]^{1/(3-2\alpha)} \tag{92}$$

If the variations of gas temperature during the firing are taken into account, G becomes a function of γ also. The result (equation 92) was first obtained by Gossot and Liouville,[14] who, in effect, found α for French propellant by fitting equation 92 to a set of observed pressures. They decided that $\alpha = 2/3$. The unknown factor $G(2/3)$ was determined in the same process of fitting. Röggla [15] did the same, arriving at $\alpha = 0.7$.[16] The first systematic attack on the set of equations 89 through 91 was made by Clemmow,[17] who integrated them by series expansions and numerical integration (for $\gamma = 1$). Only his solution for $\alpha = 1/2$ was published, apart from the table of $G(\alpha)$ from which we have extracted Table 5.9.

Table 5.9 The Clemmow Factor

For the isothermal equations with $\theta = 0$, $\eta = 1/\delta$, and no resistance. Maximum error from linear interpolation with respect to α is 1 in 500

α	$G(\alpha)$	α	$G(\alpha)$	α	$G(\alpha)$
0	0.993	0.5	0.824	0.8	0.605
0.1	0.966	0.55	0.796	0.85	0.553
0.2	0.939	0.6	0.766	0.9	0.497
0.3	0.908	0.65	0.732	0.95	0.435
0.4	0.870	0.7	0.693	1.0	0.368
0.45	0.848	0.75	0.651		

For $\alpha = 1$ we have the result already given as equation 24A of chapter 4, which shows that $G(1) = 1/e$.

Peak pressure occurs at a value of Φ which depends only on α, say $\Phi_m(\alpha)$. Then by equation 87 the peak pressure (equation 92) is attained only if

---

[14] Gossot and Liouville, *Mém. poudres*, **13** (1905), 1.

[15] Röggla, *Mitt. Gegenstände d. Artill. u. Geniewesens*, **45** (1914), 1, 149.

[16] It has been pointed out by Desmazières, *Mém. artillerie franç.*, **3** (1924), 1009, that Röggla fitted this formula to firings with small plates of propellant, although it refers to $\theta = 0$. Allowing for the degressivity of the propellant shape, α would be much closer to unity. This illustrates our remark in chapter 3 that effects due to changes of α and θ are not easily distinguished in practice.

[17] Clemmow, *Phil. Trans. Roy. Soc. (London)*, **227A** (1928), 345.

$$\frac{Al\left(1+\dfrac{C}{3W_1}\right)}{C\lambda\left(1+\dfrac{C}{2W_1}\right)}\left[\frac{\beta^2W_1C^2\lambda^2\left(1+\dfrac{C}{2W_1}\right)^3}{A^3lD^2\left(1+\dfrac{C}{3W_1}\right)^2}\right]^{1/(3-2\alpha)} \leq \frac{1}{\Phi_m(\alpha)} \tag{93}$$

If this is not satisfied, the peak pressure occurs at "burnt," that is, at $\phi = 1$. The peak pressure is then

$$P_m = g_m\left[\frac{\beta^2W_1C^2\lambda^2\left(1+\dfrac{C}{2W_1}\right)^3}{A^3lD^2\left(1+\dfrac{C}{3W_1}\right)^2}\right]^{1/(3-2\alpha)} \tag{94}$$

where g_m is now a function of the expression on the left of equation 93 as well as of α. To cover all possible cases one would have to give the Clemmow tables of the complete solutions.

A useful form of the Clemmow factor has been derived by Pike. Let β_1 be the rate to be used with a linear law, to give the same peak pressure as equation 92. Then since $G(1) = 1/e$,

$$\frac{\beta_1P_m}{\beta P_m{}^{\alpha}} = e^{1/2}[G(\alpha)]^{3/2-\alpha} = K(\alpha), \text{ say} \tag{95}$$

provided peak pressure occurs before "burnt" in *both* solutions. Hence to get the right pressure from a linear law, one should choose the parameter β_1 to give the true rate of burning at a pressure

$$P_m[K(\alpha)]^{-1/(1-\alpha)}$$

Table 5.10 gives values of the Pike factors $K(\alpha)$ and $[K(\alpha)]^{-1/(1-\alpha)}$

TABLE 5.10 THE PIKE FACTORS (FOR $\gamma = 1$, ZERO RESISTANCE, AND $\eta = 1/\delta$)
Maximum Error by Linear Interpolation 1 per cent in $[K(\alpha)]^{-1/(1-\alpha)}$ and 0.1 per cent in $K(\alpha)$

α	$[K(\alpha)]^{-1/(1-\alpha)}$	$K(\alpha)$
0.5	0.542	1.358
0.6	0.522	1.297
0.7	0.501	1.230
0.8	0.478	1.159
0.85	0.464	1.122
0.9	0.449	1.084
0.95	0.430	1.043
1.0	0.368	1

The latter varies only slowly with α, and for most propellants a value of 0.45 may be assumed as a rough guide in converting closed-vessel results for ballistic calculations with a linear rate of burning. Thus, if the peak pressure is to be 20 tons/sq in. (copper) in the gun, the rates should be adjusted at about 12 tons/sq in. (piezo) on the closed-vessel record.

Until now we have assumed that $\theta = 0$, that is,

$$\phi = 1 - f$$

The more general case

$$\phi = (1 - f)(1 + \theta f)$$

with $\theta \neq 0$ leads to one more parameter in the expression for the pressure. It is easy to show by the methods employed previously that

$$P_m = \frac{C\lambda\left(1 + \dfrac{C}{2W_1}\right)(1 + \theta)^2}{4Al\theta\left(1 + \dfrac{C}{3W_1}\right)} g_m' \tag{96}$$

where g_m' is a function only of α and of

$$\frac{\theta\beta^2 C\lambda W_1\left(1 + \dfrac{C}{2W_1}\right)^2}{A^2D^2\left(1 + \dfrac{C}{3W_1}\right)}\left[\frac{4\theta Al\left(1 + \dfrac{C}{3W_1}\right)}{C\lambda\left(1 + \dfrac{C}{2W_1}\right)(1 + \theta)^2}\right]^{2(1-\alpha)} \tag{97}$$

The significance of this parameter may be seen by taking $\alpha = 1$, when the parameter appears as θ/M, where M is the central ballistic parameter of the simple theory of chapter 4.

We may write the parameter in equation 97 as

$$\frac{\theta\beta^2 C\lambda W_1\left(1 + \dfrac{C}{2W_1}\right)^2}{A^2D^2\left(1 + \dfrac{C}{3W_1}\right)}\left(\frac{g_m'}{P_m}\right)^{2-2\alpha}$$

so that g_m' is a function only of α and $\dfrac{\theta\beta^2 C\lambda W_1[1 + (C/2W_1)]^2}{A^2D^2[1 + (C/3W_1)]P_m{}^{2-2\alpha}}$.

Suppose we compare two solutions, which both have a true peak pressure and which differ only in that one has $\alpha = 1$ and a rate β_1, chosen to give the same peak pressure as in the other solution. Then g_m' is the same in both solutions, and so $\dfrac{\theta\beta_1{}^2C\lambda W_1[1 + (C/2W_1)]^2}{A^2D^2[1 + (C/3W_1)]}$ is a function only of α and $\dfrac{\theta\beta^2C\lambda W_1[1 + (C/2W_1)]^2}{A^2D^2[1 + (C/3W_1)]P_m{}^{2-2\alpha}}$, that is, $\beta_1P_m{}^{1-\alpha}/\beta$ is a function only of α. Thus, the function $K(\alpha)$, already defined for $\theta = 0$ as $\beta_1P_m{}^{1-\alpha}/\beta$, is in fact independent of the form factor θ.

So far the isothermal approximation has been assumed. This is equivalent to writing $\bar{\gamma} = 1$ in the Résal equation. For a more general $\bar{\gamma}$, there is one more essential parameter in the ballistic equations, and $\beta_1P_m{}^{1-\alpha}/\beta$ becomes a function of $\bar{\gamma}$. Although this case can be discussed by the methods used previously, it is convenient to defer the matter until the next chapter, where we shall deal with the similarity rules of interior ballistics in more detail. The treatment given previously will then appear as a special and simple case.

By going from $\bar{\gamma} = 1$ to a more representative value, say, 1.3, changes in $\bar{\gamma}$ from 1.3 alter $K(\alpha)$ by an extremely small amount, at any rate for the practical values of α, between 0.8 and 1. Dr. Pike has indeed shown that the expansion of $K(\alpha)$ in powers of $(\bar{\gamma} - 1)$ starts with a term depending only on α, followed by a term proportional to $(\bar{\gamma} - 1)(1 - \alpha)$.

Resistance to motion alters $K(\alpha)$ slightly. It can be shown that $\beta_1P_m{}^{1-\alpha}/\beta$ then depends on P_0/P_m, if a shot-start pressure P_0 is used to simulate initial resistance. In unpublished work, Crank and Wood have evaluated the effect of a shot-start pressure of $0.1P_m$; they solved the equations numerically on a differential analyzer. Table 5.11 has been prepared from results of Clemmow, Crank and Wood, and the writer, and it gives $K(\alpha)$ for $\bar{\gamma} = 1.3$ and two values of the shot-start pressure, and for $\bar{\gamma} = 1$ with $P_0 = 0$. From this table $\beta_1P_m{}^{1-\alpha}/\beta$ can be estimated for any α and shot-start pressure, to ample accuracy for

TABLE 5.11 A WORKING TABLE OF PIKE'S FACTOR $K(\alpha) = \beta_1P_m{}^{1-\alpha}/\beta$

For $\eta = 1/\delta$, and any θ; P_0 = shot-start pressure

	$\bar{\gamma} = 1.3$		$\bar{\gamma} = 1$
α	$P_0 = 0$	$P_0 = 0.1P_m$	$P_0 = 0$
0.65	1.249	1.186	1.264
0.7	1.217	1.160	1.230
0.75	1.184	1.132	1.195
0.8	1.150	1.107	1.159
0.85	1.114	1.081	1.122
0.9	1.078	1.055	1.084
0.95	1.041	1.028	1.043
1.0	1.0	1.0	1.0

practical use. The values in this table refer to $\eta - (1/\delta) = 0$, but the covolume effect [18] on $K(\alpha)$ is small.

The effect of α on the muzzle velocity is not so easily given an explicit form, though it is easily calculated in any specific example by using Dr. Clemmow's tables. As α decreases from unity, the muzzle velocity rises; we are supposing, of course, that β is being altered to hold the peak pressure constant. This change of muzzle velocity is consistent with the movement of the travel at which peak pressure occurs. Dr. Clemmow has shown that this travel becomes less as α decreases from unity; hence ϕ, the fraction burnt, is less at peak pressure, and the charge is therefore a slower-burning type with a bigger piezometric efficiency and so a higher muzzle velocity. The changes are nevertheless very small and vary a good deal from one example to another.

Other burning laws with rate not proportional to pressure have been studied. A rate proportional to the gas density was examined by Crow and Grimshaw [19] and Wadley (unpublished), who obtained series expansions in terms of a perturbation parameter. The same type of analytical method was used by Desmazières,[20] for the form,

$$\text{Rate} = \frac{\beta P}{1 + \omega\psi_1(P) + \omega^2\psi_2(P) + \cdots} \tag{98}$$

as a perturbation on a basic solution, which included Résal and covolume terms but neglected resistance: in fact, a basic solution very similar to the Coppock solution (§ 5.2).

5.5 The ballistic effects of bore resistance [21]

The effects produced by the resistance during the engraving of the band have been discussed earlier in this chapter, the "shot-start pressure" being used as a simple model for the process. In the following sections we shall discuss the effects caused by the resistance that occurs after the engraving of the band and appears to persist for a large part of the travel of the shot. Evidence for such a resistance has accumulated from many directions; much of this evidence is only qualitative, though its bulk and its general consistency are impressive. The fitting of theoretical ballistics to observed results often leaves a discrepancy which could be attributed to a mean resistance equivalent to a pressure in the neighborhood of 1 ton/sq in. It is true that in many cases one might reduce the discrepancy by altering the details of the theory or by postulating small errors in some of the data assumed; however, such *ad hoc* manipulations are, in bulk, less plausible than the idea of a bore resistance. From the experimental side, the radial strain recorded in the barrel is sufficient to indicate an appreciable axial resistance, even when the coefficient of friction has fallen as low as 0.01. A resistance is also indicated when attempts are made to correlate measured space-time curves with pressure-time curves recorded at gages spaced along the barrel.

---

[18] See also example 3 at the end of this chapter.

[19] Crow and Grimshaw, *Phil. Mag.*, **15** (1933), 529, 729.

[20] Desmazières, *Mém. artillerie franç.*, **1** (1922), 19.

[21] Corner, *Quart. J. Mech. and Applied Maths.*, **II** (1949), 232.

It can be taken, then, that in many cases a substantial resistance does persist over a large part of the travel. It is desirable to investigate theoretically the ballistic consequences. Here we study the effect on the muzzle velocity. The changes in the peak pressure can be deduced by similar methods. The line followed is the choice of a standard form of resistance, the determination of its ballistic effects, and the construction of more realistic resistance laws by superposition of standard forms suitably spaced along the travel.

The reader can no doubt think of analogous methods in other subjects. In exterior ballistics, for example, the change in range due to perturbations such as head wind, which occur with varying strength at different heights, are obtained by integration over the actual distribution of wind, weighted by a factor that represents the effect of unit wind concentrated along unit length of the trajectory. This "weighting factor" for the effect of head wind on range is a function of position along the trajectory and is one of a series of analogous weighting factors that are computed from a set of equations adjoint to the primary ballistic equations.

In operational methods for sets of linear differential equations we find a similar practice. The behavior of the system is investigated for a standard impressed force, the Heaviside unit function. The response to a force varying in any way with time is obtained by splitting this force into a sum or integral of unit functions suitably spaced in time. The response to the complex force is, by the linearity of the system, equal to the sum of the responses to the individual unit functions. Since our system of ballistic equations is not linear, it cannot be taken for granted that the ballistic effects of a set of our "unit bore resistances" can be superposed; that the error involved is small has to be verified. There is one similarity between our "unit resistance" and the "Heaviside unit function" that should be pointed out: the usefulness of the latter is in no way impaired by its artificial character (for it is an idealization that can be approached but not attained in practice); likewise, we are free to take a very idealized standard bore resistance, so long as by superposition we can construct any bore resistance likely in practice.

As standard bore resistance we take a force AP_0, constant over a short travel Δx near the point x_0, and zero force at all other shot positions. The effect on the ballistics can be calculated, to the first order in $P_0 \Delta x$, by subtracting an energy $AP_0 \Delta x$ from the kinetic energy of the projectile as it passes through the point x_0. The ballistic equations from the point x_0 onward are exactly the same as before, except for a perturbing term linear in $P_0 \Delta x$. If the ballistic system is a simple one this perturbation can be integrated exactly. If not, numerical integration would be necessary, in which case it would probably be quicker to abandon weighting factors altogether.

We are led to consider to which ballistic system this method should be applied. As we have just seen, it must give an analytical solution, the simpler the better. A second point can be realized by taking the resistance of length Δx to occur at shot start. Then if P_0 is finite there is a finite change of muzzle velocity, even if Δx tends to zero. The weighting factor which multiplies $P_0 \Delta x$ must therefore tend to infinity as x_0 moves toward shot start. Hence the weighting-factor method fails to represent initial resistance at all, and must become increasingly inaccurate as the position of the resistance approaches shot start. It is therefore immaterial whether the basic equations, before the addition of the bore-resistance terms, are a good or a bad representation of initial resistance.

We use as our basic system Coppock's solution (§ 5.2), omitting also the covolume terms. These complicate the weighting factor and, being only a correction to a correction, probably have a negligible effect on the relation between bore resistance and velocity. When covolume terms are omitted, the solution becomes one known in the literature from early times.

In the next section we derive the analytical weighting factors for this solution. Then we describe some tests to check the validity of first-order theory, the linearity approximation, the error near shot start, and the error due to the omission of covolume.

5.51 Disturbance of muzzle velocity by the standard bore resistance

We use the equations of § 5.22 with, in addition, $b = 0$, that is, $\eta = 1/\delta$. Let suffix zero denote quantities at the moment the bore resistance acts; no confusion need be feared with the "force" RT_0. The bore resistance acts for a time $\Delta x / V_0$, which is assumed to be infinitesimal. The only immediate result is therefore a decrease of the kinetic energy of the shot by $AP_0 \Delta x$. Take first the case where the resistance occurs before "burnt." For travels less than x_0, the solution is the normal solution of the equations of § 5.22. For travel greater than x_0, only the energy equation 9 needs alteration, but there has also been an instantaneous drop in the velocity V.

Before going on, we note two limitations of this method, which occur even for a truly infinitesimal Δx. First, if V_0 is zero then $\Delta x/V_0$ is not infinitesimal; hence initial resistance cannot be represented by this model. Second, if the kinetic energy of the shot when it meets the resistance is less than $AP_0\,\Delta x$, the method breaks down, for it gives the projectile an imaginary velocity after crossing the resistance. In practice, the projectile would come to rest and would restart after the pressure had built up behind the shot, which would take a finite time. This is again a matter of $\Delta x/V_0$ being finite.

Just before reaching the resistance, the kinetic energy of the charge and projectile is $\frac{1}{2}(W_1 + \frac{1}{3}C)V_0^2$; immediately afterwards it is $\frac{1}{2}(W_1 + \frac{1}{3}C)V_0^2 - AP_0\,\Delta x$. The instantaneous drop of velocity of the projectile is transmitted through the gas with a finite velocity, namely a_0, the velocity of sound in the propellant gases, and the time taken for the waves to settle down is of the order of $(2/a_0)(U/A + x_0)$. This is comparable with the time scale of the whole ballistic phenomenon. We approximate to this delayed redistribution of energy by assuming that the process is immediate, so that the total kinetic energy is at all times $\frac{1}{2}(W_1 + \frac{1}{3}C)V^2$, where V is the velocity. Other extreme assumptions can be shown to make very little difference to the final results, except when C/W_1 approaches unity; in such a case, however, the conventional Lagrange correction is itself seriously in error.

Let the velocity of the shot just after the resistance be V_1. Then

$$\tfrac{1}{2}(W_1 + \tfrac{1}{3}C)V_1^2 = \tfrac{1}{2}(W_1 + \tfrac{1}{3}C)V_0^2 - AP_0\,\Delta x \tag{99}$$

Equations 7, 8, and 10 of § 5.22 are unaltered. Equation 4 of § 5.1 is replaced by

$$\phi(1 - T') = \frac{\bar{\gamma} - 1}{CRT_0}\left[\left(W_1 + \frac{1}{3}C\right)\frac{V^2}{2} + AP_0\,\Delta x\right] \tag{100}$$

From equations 8 and 10,

$$V = V_1 + \frac{AD(f_0 - f)}{\beta(W_1 + \frac{1}{2}C)} \tag{101}$$

so that equation 100 becomes

$$\frac{CRT_0\phi(1 - T')}{\bar{\gamma} - 1} = AP_0\,\Delta x + \frac{1}{2}\left(W_1 + \frac{1}{3}C\right) \times\left[V_1^2 + \left\{\frac{AD(f_0 - f)}{\beta(W_1 + \frac{1}{2}C)}\right\}^2 + \frac{2ADV_1(f_0 - f)}{\beta(W_1 + \frac{1}{2}C)}\right]$$

$$= \frac{1}{2}\left(W_1 + \frac{1}{3}C\right)\left[V_0^2 + \left\{\frac{AD(f_0 - f)}{\beta(W_1 + \frac{1}{2}C)}\right\}^2 + \frac{2ADV_1(f_0 - f)}{\beta(W_1 + \frac{1}{2}C)}\right] \tag{102}$$

Combining equations 5 of § 5.1 and 102 gives

$$CRT_0\phi = \tfrac{1}{2}(\bar{\gamma} - 1)(W_1 + \tfrac{1}{3}C) \times \left[V_0^2 + \left\{\frac{AD(f_0 - f)}{\beta(W_1 + \frac{1}{2}C)}\right\}^2 + \frac{2ADV_1(f_0 - f)}{\beta(W_1 + \frac{1}{2}C)}\right] + \frac{AP(x + l)(W_1 + \frac{1}{3}C)}{W_1 + \frac{1}{2}C} \tag{103}$$

Up to this point the equations have been exact; at least they have been exact transcriptions of our physical assumptions. We now keep only first-order terms in equations 99, 101, and 103:

$$V_1 = V_0 - \frac{AP_0\,\Delta x}{(W_1 + \frac{1}{3}C)V_0} \tag{99A}$$

$$V = \frac{AD(1 - f)}{\beta(W_1 + \frac{1}{2}C)} - \frac{AP_0\,\Delta x}{(W_1 + \frac{1}{3}C)V_0} \tag{101A}$$

$$CRT_0\phi = \tfrac{1}{2}(\bar{\gamma} - 1)(W_1 + \tfrac{1}{3}C) \times \left[\left\{\frac{AD(1 - f)}{\beta(W_1 + \frac{1}{2}C)}\right\}^2 - \frac{2AP_0\,\Delta x(f_0 - f)}{(W_1 + \frac{1}{3}C)(1 - f_0)}\right] + \frac{AP(x + l)(W_1 + \frac{1}{3}C)}{W_1 + \frac{1}{2}C} \tag{103A}$$

The latter can be written as

$$(1 - f)(1 + \theta f) = \frac{1}{2}(\bar{\gamma} - 1)M(1 - f)^2 - \frac{(\bar{\gamma} - 1)AP_0\,\Delta x(f_0 - f)}{CRT_0(1 - f_0)} - M(x + l)(1 - f)\frac{df}{dx} + \frac{AP_0\,\Delta x(x + l)}{CRT_0(1 - f_0)}\frac{df}{dx}$$

leading to

$$Z + M(x + l)\frac{df}{dx} = \frac{AP_0\,\Delta x}{(1 - f)(1 - f_0)CRT_0}\left[(x + l)\frac{df}{dx} - (\bar{\gamma} - 1)(f_0 - f)\right] \tag{104}$$

where

$$Z = 1 - \tfrac{1}{2}(\bar{\gamma} - 1)M + \theta_1 f \qquad (105)$$

$$\theta_1 = \theta + \tfrac{1}{2}(\bar{\gamma} - 1)M \qquad (106)$$

Equation 104 shows the first-order effect of the resistance on the equation,

$$Z + M(x + l)\frac{df}{dx} = 0 \qquad (107)$$

used in § 5.22 when $b = 0$, and we shall obtain a solution correct to terms of order $P_0\,\Delta x$ if we use equation 107 on the right of equation 104. This gives

$$Z + M(x + l)\frac{df}{dx} = -\frac{AP_0\,\Delta x}{CRT_0(1 - f_0)(1 - f)}\left[\frac{Z}{M} + (\bar{\gamma} - 1)(f_0 - f)\right]$$

and so

$$\int\frac{dx}{x + l} = -\int\frac{M\,df}{Z} + \frac{AP_0\,\Delta x}{CRT_0(1 - f_0)} \times\left[\int\frac{df}{Z(1 - f)} + (\bar{\gamma} - 1)M\int\frac{(f_0 - f)\,df}{Z^2(1 - f)}\right] \qquad (108)$$

The lower limit in these integrals is the point, suffix zero, at which the resistance occurred. The integrals are easily evaluated, and, when substituted in equation 108, results in

$$\ln\left(1 + \frac{x}{l}\right) = \frac{M}{\theta_1}\ln\left(\frac{1 + \theta}{Z}\right) + \frac{AP_0\,\Delta x}{CRT_0(1 - f_0)} \left[\frac{\{1 + \theta - (\bar{\gamma} - 1)M(1 - f_0)\}}{(1 + \theta)^2}\ln\left\{\frac{Z(1 - f_0)}{Z_0(1 - f)}\right\} + \frac{(\bar{\gamma} - 1)M}{\theta_1(1 + \theta)}\left(\frac{1}{Z_0} - \frac{1}{Z}\right)\{1 + \theta - \theta_1(1 - f_0)\}\right] \qquad (109)$$

Solution with "unburnt" at "muzzle." In this case the value of f at the muzzle is computed from equation 109, and the muzzle velocity follows by equations 99 and 101. This case is not of practical importance, and we shall not test the accuracy of superposition and higher-order terms in the way we shall for:

Solution for "burnt" inside gun. This is the important problem. It will be remembered that we are dealing here with a resistance during the period of burning. Resistance during the adiabatic expansion is discussed later.

We need the change in $\ln (x_B + l)$, where suffix B refers to conditions at "burnt." This change is

$$\Delta \ln (x_B + l) = \frac{AP_0\,\Delta x}{CRT_0(1 - f_0)} \times \left[\frac{\{1 + \theta - (\bar{\gamma} - 1)M(1 - f_0)\}}{(1 + \theta)^2} \ln \left\{\frac{Z_B(1 - f_0)}{Z_0}\right\} + \frac{(\bar{\gamma} - 1)M\{1 + \theta - \theta_1(1 - f_0)\}}{\theta_1(1 + \theta)}\left(\frac{1}{Z_0} - \frac{1}{Z_B}\right)\right] \tag{110}$$

Let suffix E refer to values at shot ejection. We have

$$V_E{}^2 = V_B{}^2 + \frac{AP_B(x_B + l)\Phi}{W_1 + \frac{1}{2}C} \tag{111}$$

where

$$\Phi = \frac{2}{\bar{\gamma} - 1}\,(1 - r^{1-\bar{\gamma}}) \tag{112}$$

and

$$r = \frac{x_E + l}{x_B + l} \tag{113}$$

In equation 111, V_B, $P_B(x_B + l)$, and Φ are all altered by the resistance. From equation 103A,

$$\frac{AP_B(x_B + l)}{W_1 + \frac{1}{2}C} = \frac{CRT_0[1 - \frac{1}{2}(\bar{\gamma} - 1)M]}{W_1 + \frac{1}{3}C} + \frac{(\bar{\gamma} - 1)AP_0 f_0\,\Delta x}{(1 - f_0)(W_1 + \frac{1}{3}C)} \tag{114}$$

Also

$$\Delta\Phi = 2r^{-\bar{\gamma}}\,\Delta r = -2r^{1-\bar{\gamma}}\,\Delta \ln (x_B + l) \tag{115}$$

and, from equation 101A,

$$\Delta(V_B{}^2) = -\frac{2AP_0\,\Delta x}{(W_1 + \frac{1}{3}C)(1 - f_0)} \tag{116}$$

so that

$$\Delta(V_E{}^2) = -\frac{2AP_0\,\Delta x(1 - f_0 + f_0 r^{1-\bar{\gamma}})}{(W_1 + \frac{1}{3}C)(1 - f_0)} - \frac{2r^{1-\bar{\gamma}}Z_B AP_0\,\Delta x}{(W_1 + \frac{1}{3}C)(1 - f_0)} \times \left[\frac{\{1 + \theta - (\bar{\gamma} - 1)M(1 - f_0)\}}{(1 + \theta)^2} \ln \left\{\frac{Z_B(1 - f_0)}{Z_0}\right\} + \frac{(\bar{\gamma} - 1)M\{1 + \theta - \theta_1(1 - f_0)\}}{\theta_1(1 + \theta)}\left(\frac{1}{Z_0} - \frac{1}{Z_B}\right)\right]$$

and finally

$$\begin{aligned}\frac{(W_1+\frac{1}{3}C)V_E(1-f_0)\,\Delta V_E}{AP_0\,\Delta x} &= -1+f_0-f_0r^{1-\bar{\gamma}}\\ &\quad - r^{1-\bar{\gamma}}Z_B\left[\frac{\{1+\theta-(\bar{\gamma}-1)M(1-f_0)\}}{(1+\theta)^2}\ln\left\{\frac{Z_B(1-f_0)}{Z_0}\right\}\right.\\ &\qquad\left. + \frac{(\bar{\gamma}-1)M\{1+\theta-\theta_1(1-f_0)\}}{\theta_1(1+\theta)}\left(\frac{1}{Z_0}-\frac{1}{Z_B}\right)\right] \qquad (117)\end{aligned}$$

This gives the change of muzzle velocity ΔV_E due to a bore resistance $AP_0\,\Delta x$ occurring at the point $(f_0,\ Z_0)$, in terms of the characteristics of the solution without resistance.

For resistance very early in the travel, f_0 is nearly unity, and

$$\frac{(W_1+\frac{1}{3}C)V_E\,\Delta V_E}{AP_0\,\Delta x} \sim \frac{r^{1-\bar{\gamma}}Z_B}{(1+\theta)(1-f_0)}\ln\left[\frac{1+\theta}{Z_B(1-f_0)}\right]$$

showing that for resistance occurring sufficiently early in the travel the muzzle velocity rises. For resistance at "burnt," $f_0 = 0$, and

$$\frac{(W_1+\frac{1}{3}C)V_E\,\Delta V_E}{AP_0\,\Delta x} = -1$$

and the muzzle velocity falls. When resistance occurs during the adiabatic expansion, the kinetic energy of the shot and the gases at the muzzle are reduced by the work done on the resistance, without other effect on the ballistics (except on the time to traverse the bore). Hence,

$$\frac{(W_1+\frac{1}{3}C)V_E\,\Delta V_E}{AP_0\,\Delta x} = -1$$

if the resistance occurs after "burnt."

5.52 Accuracy of first-order theory

The results of the preceding section were obtained by expansion in powers of $P_0\,\Delta x/V_0$, keeping only the first term. To show the magnitude of the error we take an example, and this is, of course, the 3.7-in. AA gun, which has appeared so often in these pages. A charge of 8 lb 5 oz, giving 20 tons/sq in., was assumed. With $\theta = 0.3$, $\bar{\gamma} = 1.34$, and no covolume term, the velocity from the basic method is 2642 ft/sec. Peak pressure occurs at a travel of about 4 calibers and "burnt" about 10 calibers farther on. A series of exact solutions, with exact allowance for the assumed resistance, was computed on a National accounting machine. To get sufficient accuracy in the differences ΔV_E, these solutions were computed to an accuracy of 0.1 ft/sec.

Table 5.12 shows the effect of increasing $P_0\,\Delta x$ at a given point early in the travel. At this point, where $x_0 = 0.58$ calibers and $f_0 = 0.9$, the shot would be brought to rest by an instantaneous $P_0\,\Delta x$ of 7.99 ton/in., so that one would not expect first-order theory to be other than very rough for such a value of $P_0\,\Delta x$. The agreement found is therefore encouraging. The error in first-order theory is only 7 per cent when $P_0\,\Delta x$ reaches half the value needed to stop the shot.

Table 5.12 Accuracy of First-Order Theory at 0.58 Calibers Travel

$f_0 = 0.9$

$P_0\,\Delta x/7.99$	$\dfrac{(W_1 + \frac{1}{3}C)V_E\,\Delta V_E(1 - f_0)}{AP_0\,\Delta x}$	Method
0	0.624	First-order theory
0.25	0.65½	Exact integration
0.5	0.67	Exact integration
1	0.85	Exact integration

Another way to show the agreement is to calculate the effect of $P_0\,\Delta x = 7.99$ ton/in. at various positions along the bore. Table 5.13 shows the comparison to be extremely satisfactory except when the resistance stops the shot. We can conclude that first-order theory is adequate to represent the effect of a *concentrated* bore resistance except when this is sufficient to halt the projectile.

Table 5.13 Standard Bore Resistance, $P_0\,\Delta x = 7.99$ ton/in., at Various Positions along the Bore

$$\frac{(W_1 + \frac{1}{3}C)(1 - f_0)V_E\,\Delta V_E}{AP_0\,\Delta x}$$

f_0	Exact Integration	First-Order Theory	Error
0.9	0.85	0.624	0.23
0.8	0.25	0.231	0.02
0.7	−0.02	−0.026	0.01
0.6	−0.22	−0.226	0.01
0.4	−0.53	−0.540	0.01
0.2	−0.78	−0.789	0.01
0	−1	−1	0

5.53 Calculation of the effect of long stretches of bore resistance

One often wishes to find the effect of a bore resistance extending over a large part of the travel. Such a resistance, no matter how it varies, can be represented as an integral over suitably chosen resistances of our standard type. To see the errors likely in this process we consider the special case of constant resistance, and, since the exact solution is known from "burnt" to "muzzle," we need consider only the part up to "burnt." This enables us to take f as the variable of integration. The weighting-factor theory makes

$$\Delta V_E = \int \frac{\Delta V_E}{\Delta x}\frac{dx}{df}\,df = -\int \frac{\Delta V_E}{\Delta x}\frac{M(x+l)}{Z}\,df$$

$$= \frac{-MA}{(W_1 + \frac{1}{3}C)V_E} \times \int \frac{(x+l)P_0}{(1-f)Z}\left[\frac{(1-f)(W_1+\frac{1}{3}C)V_E\,\Delta V_E}{AP_0\,\Delta x}\right] df \qquad (118)$$

This integral is easily evaluated. P_0 is a known function of x, which is itself a simple function of f. So is Z, and the "weighting factor" in brackets comes from equation 117. Thus, equation 118 is easily computed by a numerical integration, whatever the form of the bore resistance.

Table 5.14 shows the agreement between equation 118 and exact numerical integration of the equations with resistance, for $P_0 = 1$ ton/sq in. extending from "burnt" to $f = 0.5$, 0.7, and 0.9. The agreement is extremely good and shows that the effect of all reasonable forms of bore resistance can be calculated in this way with high accuracy in spite of the speed of the method.

TABLE 5.14 THE EFFECT OF A CONSTANT BORE RESISTANCE FOR A CONSIDERABLE PART OF THE TRAVEL

$P_0 = 1$ ton/sq in.

Position in Bore	Position in Unperturbed Solution	ΔV_E, ft/sec		
		Exact	Eq. 118	Difference
$x = 0.58$ to 13.43 cals	$f = 0.9$ to 0	−23.3	−23.5	0.2
2.02 to 13.43 "	0.7 to 0	−29.8	−30.7	0.9
4.96 to 13.43 "	0.5 to 0	−26.9	−27.5	0.6

Another simple test is the effect of $P_0 = 1$ ton/sq in. from 0.58 calibers travel to the muzzle. This is −115.9 ft/sec by exact integration and -116.1 ft/sec by using equation 118 up to "burnt" and thereafter the exact relation:

$$\frac{1}{2}\left(W_1 + \frac{C}{3}\right)\Delta(V_E^2) = -AP_0(x_E - x_B) \tag{119}$$

5.54 Effect of the covolume

The basic solution used here omits the covolume term $\eta - (1/\delta)$. The same process can be applied to Coppock's solution with covolume, but the algebra is more tedious. The best way to allow for covolume appears to be to follow a practice introduced by Dr. Pike and to increase the force constant of the propellant as explained in § 5.25, to give the correct effect of covolume on peak pressure. Such a modified force constant can be used in the equations of the preceding sections and appears to give the interaction of covolume and bore resistance to a sufficient accuracy.

5.6 Numerical and mechanical methods

Whatever the form of the interior-ballistic equations, they can be solved by numerical integration for any desired values of the parameters. This method was first employed by Centervall[22] (1902). The disadvantage of numerical integration is that each special case needs a complete new solution. Centervall therefore studied a sample of typical guns and constructed a short table of standard solutions; he also represented his computed results by formulas resembling those of Sarrau. Centervall's list of solutions is much too short to fulfil his aim. Later writers have constructed more elaborate tables based on other sets of theoretical equations and have used the similarity theory to make each solution as general as possible. The similarity principles are discussed in the next chapter. It is worth saying here that they are not just a matter of dimensional analysis, which was already used by Centervall, for example; the similarity rules arise from the structure of the particular equations used, and, roughly speaking, the more detailed the equations, the less general each solution becomes. As an example, we may take the "covolume term" $\eta - (1/\delta)$. If this is taken to be zero, there is obviously one fewer parameter in the equations, and the assumption $\eta = 1/\delta$ folds up a single infinity of numerical solutions into one solution of the simplified equations. Thus we may say that in general numerical integration is capable of dealing with the most complicated set of ballistic equations, but each increase in detail is paid for by a great increase in work, both for the original computer and for the user.

---

[22] Centervall, *Internal Ballistics* (Stockholm, 1902).

Numerical integration of the ballistic equations is easy and is described in Appendix A.

During World War II the differential analyzers at Cambridge and Manchester, England, were used for a time on interior ballistics. These are mechanical differential analyzers of fundamentally the original Bush model, and they have eight integrating units.[23] The capacity of such a machine is measured by the number of integrators, and eight is sufficient for most systems of ballistic equations. In the work done at Cambridge the equations were normally about as complicated as those of § 5.32, with covolume and Résal terms, and a shot-start pressure or bore resistance; the rate of burning was a tabulated function. Such a set of assumptions requires seven or sometimes six integrators. It is not often that more complicated equations are studied in interior ballistics, and those that arise can usually be solved approximately by taking slowly varying mean values of unimportant terms. This was done for recoilless guns, whose equations are a little too complicated to be set up properly on an 8-unit analyzer.

The differential analyzer is faster than a computer most strikingly when only an end value is required. Suppose, as an illustration, that we have a set of equations for the interior ballistics of a gun and that we have to find what rate of burning gives the observed peak pressure. The computer guesses a rate, works through the integration, step by step, and must write down the details of the working as he goes. This continues until peak pressure is reached, after which the process is repeated with other values of the rate of burning, and the correct rate is deduced by an interpolation. The solutions written down can now be thrown away. If the same problem were to be done by differential analyzer, one would run trial solutions in the same way, integrating out to peak pressure but not stopping to record any details of the solution except peak pressure itself. This ability to record no more than is absolutely necessary for the purpose in hand does make a considerable difference in the time spent on many problems.

It is difficult to give a general figure for the relative times for solution by differential analyzer and by computer, since there is as yet no "standard" analyzer: each new machine is faster than its predecessors. Experience in England during World War II showed that for interior ballistics a team of computers is cheaper than a differential analyzer, especially with regard to capital cost. Nevertheless, in an emergency an existing analyzer can be put to work on interior ballistics if no problem arises that is better suited to the analyzer. The accuracy of most present-day machines is about 1 part in 300 on problems of this size. This is sufficient for most work on interior ballistics, though for the production of "grids" of solutions a little smoothing of the results will usually be necessary. By contrast, the accuracy of a differential analyzer is inconveniently low for the central problem of exterior ballistics, and definitely much too low for producing grids of standard solutions between which one will wish to interpolate. When American analyzers were used on exterior ballistics during the Second World War, smoothing of the results was necessary to bring the nominal accuracy up to the level demanded in that subject.

---

[23] For a description of the Manchester machine, see Hartree, *Nature*, **135** (1935), 940.

The differential analyzer at Cambridge was used to explore certain ballistic problems of a general character, particularly the consequences of a shot-start pressure. Since a small shot-start pressure usually slightly improves the muzzle velocity of a given gun at a given peak pressure, it might seem that a really large shot-start pressure would improve the performance by an amount of some importance. It was shown, by using the analyzer, that the optimum shot-start pressure was usually quite small, and the performance dropped rapidly after this optimum was exceeded. The analyzer was also used for the tabulation of the Clemmow factors (§ 5.4) for certain conditions, for the study of optimum solutions, discussed in the next chapter, and for an investigation of ballistics when there is a substantial resistance to the motion of the shot down the bore.

EXAMPLES

1. Solve the ballistic equations by the method of § 5.23 when the propellant burns according to the geometric form function for spheres.

2. Calculate the change of peak pressure caused by bore resistance concentrated at one point.

3. Show that if $\eta \neq 1/\delta$, then $\beta_1 P_m^{1-\alpha}/\beta$ depends on $[\eta - (1/\delta)]P_m/RT_0$.

CHAPTER SIX Similarity Relations and Optimum Problems of Interior Ballistics

6.1 Introduction to ballistic similarity

The idea that a ballistic solution for one gun could sometimes be transformed to apply to another first appeared in Sarrau's approximate theoretical solution,[1] where the details of gun and charge were found to occur only in certain combinations. This was put to a more important use by Gossot and Liouville[2]; having written down their version of the fundamental equations of the gun, they discovered the essential parameters and hence obtained the functional form of the theoretical solution. The functions themselves were found by fitting to firing data and were approximated by simple mathematical expressions. These can be regarded as a convenient synopsis of past experience on normal guns, but their value for completely new types of guns depends on the accuracy of the basic theoretical equations.

Similarity of the ballistic solutions was first studied for its own sake by Emery[3] (1912), who examined the transformations possible in various sets of fundamental assumptions. A most useful advance was made by Röggla[4] in 1914, when he showed that solutions for propellants of different shapes could be correlated, at least up to "burnt." Since the solution is always simple after "burnt," this restriction does not cause any difficulty in practice. Röggla assumed $\eta = 1/\delta$ in proving his similarity law, but this too is not an essential feature.

Since that time the methods of finding similarity relations have been applied to other cases[5] and have been used to reduce the bulk of tables of numerical solutions. Röggla's transformation is particularly valuable when solutions are being found by numerical or mechanical integration, for, as we shall see, solutions for all possible values of the form factor θ can be deduced from the solutions for a certain three values. On the other hand, no new technique for finding additional similarity relations has been discovered since Röggla's day. Articles that have reviewed the concepts and results of similarity have not always made clear how simple the matter is; one of the best is a note by Pappas.[6]

---

[1] Sarrau, *Recherches théoriques sur le chargement des bouches à feu* (Paris, 1882).

[2] Gossot and Liouville, *Mém. poudres*, **13** (1905), 1.

[3] See Emery, *Mém. artillerie franç.*, **2** (1923), 21.

[4] Röggla, *Mitt. Gegenstände d. Artill. u. Geniewesens*, **45** (1914), 1, 149.

[5] A burning rate proportional to $P + P_1$ has been examined by Proudman, *Proc. Roy. Soc.* (*London*), **100A** (1921), 289, and various forms of bore resistance by Proudman and by Voituriez, *Mém. artillerie franç.*, **4** (1925), 131.

In this chapter we deal first with a fairly simple form of the ballistic equations, to make the methods stand out more clearly. Later we give in brief the results for a more detailed set of ballistic equations.

6.11 The similarity relations for a simple set of ballistic equations

We assume:

1. Rate of burning βP^{α}.
2. A form function $\phi = (1 - f)(1 + \theta f)$.
3. A resistance to motion represented by a "shot-start pressure" P_0, vanishing as soon as the shot moves.
4. We neglect the covolume term $\eta - (1/\delta)$.

Then the equations are, in the usual notation,

$$\phi = (1 - f)(1 + \theta f) \tag{1}$$

$$D\frac{df}{dt} = -\beta P^{\alpha} \tag{2}$$

$$\left(W_1 + \frac{1}{2}C\right)\frac{dV}{dt} = AP \tag{3}$$

$$P\left(U - \frac{C}{\delta} + Ax\right) = \frac{C\phi T' R T_0 \left(1 + \dfrac{C}{2W_1}\right)}{1 + \dfrac{C}{3W_1}} \tag{4}$$

and

$$\phi(1 - T') = \frac{(\bar{\gamma} - 1)(W_1 + \frac{1}{3}C)V^2}{2CRT_0} \tag{5}$$

where P is the pressure at the breech. The boundary conditions are that $(V = x = 0; P = P_0)$ at $t = 0$.

The first step is to replace all quantities in these equations by dimensionless variables. Obvious changes are

---

[6] Pappas, *Heerestechnik* (1930), 161; *Mém. artillerie franç.*, **10** (1931), 581.

$$P = \frac{CRT_0\left(1 + \dfrac{C}{2W_1}\right)}{\left(U - \dfrac{C}{\delta}\right)\left(1 + \dfrac{C}{3W_1}\right)}\pi \tag{6}$$

where π is the new variable, and

$$x = \left(U - \frac{C}{\delta}\right)\frac{\xi}{A} \tag{7}$$

which replace equation 4 by

$$(1 + \xi)\pi = \phi T' \tag{8}$$

To reduce equation 2 to a standard form, we write

$$t = B\tau$$

giving

$$\frac{df}{d\tau} = -\frac{\beta B}{D}\left(\frac{CRT_0}{U - \dfrac{C}{\delta}}\right)^{\alpha}\left(\frac{1 + \dfrac{C}{2W_1}}{1 + \dfrac{C}{3W_1}}\right)^{\alpha}\pi^{\alpha}$$

so that if

$$t = \frac{D}{\beta}\left(\frac{U - \dfrac{C}{\delta}}{CRT_0}\right)^{\alpha}\left(\frac{1 + \dfrac{C}{3W_1}}{1 + \dfrac{C}{2W_1}}\right)^{\alpha}\tau \tag{9}$$

then

$$\frac{df}{d\tau} = -\pi^{\alpha} \tag{10}$$

Now

$$V = \frac{dx}{dt} = \frac{\beta}{AD}\left(\frac{1 + \dfrac{C}{2W_1}}{1 + \dfrac{C}{3W_1}}\right)^{\alpha}\left(U - \frac{C}{\delta}\right)^{1-\alpha}(CRT_0)^{\alpha}\frac{d\xi}{d\tau} \tag{11}$$

and this gives, from equation 3,

$$\frac{d^2\xi}{d\tau^2} = \left(\frac{AD}{\beta}\right)^2\frac{\left(U - \dfrac{C}{\delta}\right)^{2\alpha-2}\left(1 + \dfrac{C}{3W_1}\right)^{2\alpha-1}}{W_1\left(1 + \dfrac{C}{2W_1}\right)^{2\alpha}(CRT_0)^{2\alpha-1}}\pi \tag{12}$$

Suppose that $\alpha = 1$, in which case this equation becomes

$$\frac{d^2\xi}{d\tau^2} = \left(\frac{AD}{\beta}\right)^2 \frac{\left(1 + \dfrac{C}{3W_1}\right)}{\left(1 + \dfrac{C}{2W_1}\right)^2 W_1 CRT_0} \pi$$

in which we recognize the "central ballistic parameter" of chapter 4 and the first part of chapter 5. In its generalized form, then, we write

$$M = \left(\frac{AD}{\beta}\right)^2 \frac{\left(U - \dfrac{C}{\delta}\right)^{2\alpha-2} \left(1 + \dfrac{C}{3W_1}\right)^{2\alpha-1}}{W_1(CRT_0)^{2\alpha-1}\left(1 + \dfrac{C}{2W_1}\right)^{2\alpha}} \tag{13}$$

leading to

$$\frac{d^2\xi}{d\tau^2} = M\pi \tag{14}$$

and, from equation 5,

$$\phi(1 - T') = \frac{\bar{\gamma} - 1}{2M}\left(\frac{d\xi}{d\tau}\right)^2 \tag{15}$$

All the equations are now in dimensionless form, with τ as the independent variable and π, f, ϕ, ξ, and T' as the dependent variables. In these equations we have only the following parameters: α, θ, M, and $\bar{\gamma}$. The initial conditions are

$$T' = 1, \quad \xi = \frac{d\xi}{d\tau} = 0, \quad \text{and} \quad \pi = \pi_0 = \frac{\left(U - \dfrac{C}{\delta}\right) P_0 \left(1 + \dfrac{C}{3W_1}\right)}{CRT_0\left(1 + \dfrac{C}{2W_1}\right)}$$

at $\tau = 0$, and the equations hold up to $f = 0$. Therefore the initial conditions introduce only one more parameter, π_0, the reduced value of the shot-start pressure.

Hence the solution of this set of equations has the form: π (or equally well f, ϕ, ξ, or T') = a function only of τ and (π_0, α, $\bar{\gamma}$, θ, M). This holds also for the function $d\pi/d\tau$, and, in particular, the equation,

$$\left(\frac{d\pi}{d\tau}\right)_m = 0$$

determines τ_m as a function of (π_0, α, $\bar{\gamma}$, θ, and M). Hence the peak breech pressure P_m is

$$P_m = \frac{CRT_0\left(1 + \dfrac{C}{2W_1}\right)}{\left(U - \dfrac{C}{\delta}\right)\left(1 + \dfrac{C}{3W_1}\right)} \times \text{a function of only } \pi_0,\ \alpha,\ \theta,\ \bar{\gamma}, \text{ and } M$$

provided $f(\tau_m) \geq 0$: this is itself one relation that can be written as

$$M \geq \text{a function of only } \pi_0,\ \alpha,\ \bar{\gamma}, \text{ and } \theta$$

At "burnt," $f = 0$, which gives τ $(= \tau_B)$ as τ_B = function of (π_0, α, $\bar{\gamma}$, θ, and M), and the velocity at "burnt" is given by

$$V_B{}^2 = \frac{CRT_0}{W_1 + \frac{1}{3}C} \times \text{a function of only } (\pi_0,\ \alpha,\ \bar{\gamma},\ \theta, \text{ and } M)$$

There are formulas of analogous type for such quantities as the travel to "burnt" and to peak pressure.

Solutions for different guns can be transformed one into another if they have the same values of π_0, α, $\bar{\gamma}$, θ, and M. This is one type of similarity between ballistic solutions. Other forms can be deduced by the same methods; for example, the influence of θ can be found as in the previous chapter. We have

$$(1 + \xi)\pi = \phi T' \tag{8}$$

$$\frac{d^2\xi}{d\tau^2} = M\pi \tag{14}$$

$$\phi(1 - T') = \frac{\bar{\gamma} - 1}{2M}\left(\frac{d\xi}{d\tau}\right)^2 \tag{15}$$

$$\frac{df}{d\tau} = -\pi^\alpha \tag{10}$$

$$\phi = (1 - f)(1 + \theta f) \tag{1}$$

of which the last two may be replaced by

$$\frac{d\phi}{d\tau} = (1 + \theta)\left[1 - \frac{4\theta\phi}{(1 + \theta)^2}\right]^{1/2} \pi^\alpha \tag{16}$$

To take account of θ, for $\theta \neq 0$, we replace ϕ throughout by

$$\Phi = \frac{4\theta\phi}{(1 + \theta)^2} \tag{17}$$

and then equation 8 indicates that π should be replaced by

$$\pi' = \frac{4\theta\pi}{(1 + \theta)^2} \tag{18}$$

giving

$$(1 + \xi)\pi' = \Phi T' \tag{19}$$

and

$$\frac{d\Phi}{d\tau} = \frac{(1 + \theta)^{2\alpha-1}}{(4\theta)^{\alpha-1}} (1 - \Phi)^{1/2}(\pi')^{\alpha} \tag{20}$$

Also

$$\frac{d^2\xi}{d\tau^2} = \frac{M(1 + \theta)^2}{4\theta} \pi' \tag{21}$$

We change the variable τ to τ' to simplify equation 21:

$$\tau' = (1 + \theta) \left(\frac{M}{4\theta}\right)^{1/2} \tau \tag{22}$$

giving

$$\frac{d^2\xi}{d\tau'^2} = \pi' \tag{23}$$

and

$$\frac{d\Phi}{d\tau'} = \left[\frac{(1 + \theta)^2}{4\theta}\right]^{\alpha-1} \left(\frac{4\theta}{M}\right)^{1/2} (1 - \Phi)^{1/2}(\pi')^{\alpha} \tag{24}$$

Finally equation 15 gives

$$\Phi(1 - T') = \frac{1}{2} (\bar{\gamma} - 1) \left(\frac{d\xi}{d\tau'}\right)^2 \tag{25}$$

The equations of the system have been reduced to equations 19, 23, 24, and 25, and the initial conditions are

$$\xi = \frac{d\xi}{d\tau'} = 0, \quad \pi' = \pi_0' \equiv \frac{4\theta\left(U - \dfrac{C}{\delta}\right) P_0 \left(1 + \dfrac{C}{3W_1}\right)}{(1 + \theta)^2 CRT_0 \left(1 + \dfrac{C}{2W_1}\right)} \qquad \text{at } \tau' = 0$$

and the solution holds only to $\Phi = 4\theta/(1 + \theta)^2$.

Hence the solution depends only on the parameters,

$$\bar{\gamma}, \quad \alpha, \quad \pi_0', \quad \text{and} \quad \frac{(1 + \theta)^{4(\alpha-1)}(4\theta)^{3-2\alpha}}{M} \tag{26}$$

while any quantity referring to "burnt" is also a function of $4\theta/(1 + \theta)^2$.

Compare this with the previous results, which showed that the essential variables were

$$\bar{\gamma}, \quad \alpha, \quad \pi_0, \quad \theta, \quad \text{and} \quad M \tag{27}$$

The transformation which led from expression 27 to expression 26 is a Röggla transformation. It holds only if $\theta \neq 0$ and shows that the solutions for various θ fall into essentially three types. Suppose that we want the solution for the parameters $\bar{\gamma}$, α, π_0, θ, and M, with $0 < \theta \leq 1$. Then the transformation given previously enables the solution to be found if we know the solution for the same $\bar{\gamma}$ and α, $\theta = 1$, π_0 multiplied by $4\theta/(1 + \theta)^2$, and M multiplied by $[(1 + \theta)/2]^{4-4\alpha}\theta^{2\alpha-3}$. The solution for $0 < \theta \leq 1$ has "burnt" at the point $\phi = 4\theta/(1 + \theta)^2$ in the solution for $\theta = 1$. Hence, if we know the solutions for $\theta = 1$ and all values of π_0 and M, we can obtain any solution we want for $0 < \theta \leq 1$. This shows that numerical integration need be carried out only for $\theta = 1$, and, if the complete solution up to "burnt" is needed, then only one set of solutions ($\theta = 1$) need be tabulated. It should be noted that, if only the peak pressure and the results at "burnt" are being tabulated, then we have the choice of either tabulating solutions for $\theta = 1$ but giving every point, or else first picking off the data at "burnt" for simple values of θ from the complete solutions ($\theta = 1$) and tabulating the "burnt" data for stated values of θ. This is a consequence of "burnt" occurring at $\phi = 4\theta/(1 + \theta)^2$ in the basic solutions. Usually the second course leads to more compact tables.

The transformation of one ballistic solution into another is by no means restricted to theoretical solutions. The similarity relations have long been used for building up families of guns from one standard model of medium caliber, whose performance has been thoroughly investigated by experiment. This scaling up or down is made much easier if the propellant composition and the density of loading are constant throughout the series. This is one reason why in the past the guns of one maker have often had nearly the same density of loading. Another interesting practical application of similarity is the construction of scale models of unorthodox monstrosities: examples which can be quoted are the model of 2-cm caliber, built to give data for the 400-ft-long *Hoch Druck Pumpe* of 15-cm caliber, which was to have bombarded London from Belgium; likewise the ballistics of the 80-cm-caliber *Schwere Gustav*, which fired 7-ton shell at 2300 ft/sec, were predicted from a model of 8-cm caliber.[7]

---

[7] It is difficult to see why theory was scorned in this case, for the gun was ballistically normal, except in size. Possibly the idea was to reduce the number of test rounds, for each full charge consumed 4000 lb of propellant! The life was not unduly short: from the wear in the first 50 rounds the life was estimated to be 300 rounds. This gun was used to reduce the Sebastopol forts in 1942.

If we neglect the shot-start pressure and use an isothermal model ($\bar{\gamma} = 1$), we see from expression 26 that the solution can be found when we know the two parameters α and $(1 + \theta)^{4(\alpha-1)}(4\theta)^{3-2\alpha}/M$, of which the second can be written in full as

$$\frac{\beta^2 W_1 CRT_0\left(1 + \dfrac{C}{2W_1}\right)^2 4\theta}{A^2D^2\left(1 + \dfrac{C}{3W_1}\right)}\left[\frac{4\theta\left(U - \dfrac{C}{\delta}\right)\left(1 + \dfrac{C}{3W_1}\right)}{CRT_0(1 + \theta)^2\left(1 + \dfrac{C}{2W_1}\right)}\right]^{2(1-\alpha)}$$

This result was given as equation 97 in § 5.4.

Another special case occurs when $\alpha = 1$. The essential parameters of the solution are, from expression 26,

$$\bar{\gamma}, \quad \frac{\theta}{M}, \quad \text{and} \quad \frac{4\theta P_0\left(U - \dfrac{C}{\delta}\right)\left(1 + \dfrac{C}{3W_1}\right)}{(1 + \theta)^2 CRT_0\left(1 + \dfrac{C}{2W_1}\right)}$$

These are the variables used in the Goldie tables of § 5.32, where also a term in $\eta - (1/\delta)$ was included.

The solutions for $\theta = 1$ include all the solutions for $0 < \theta \leq 1$ but not $\theta = 0$ itself; for θ close to zero, say, $\theta = 0.05$, though the transformation is still valid, yet the numerical factors involved (such as $(1 + \theta)^2/4\theta$ in equation 18) are large, and there is a considerable loss of accuracy in passing from the basic solution ($\theta = 1$) to the derived solution for $\theta = 0.05$. As θ tends to zero, the solution is obtained by greater and greater magnification of less and less of the basic solution, whose central ballistic parameter M tends to infinity at the same time.

For the case $\theta = 0$, we return to the set of equations:

$$(1 + \xi)\pi = \phi T' \tag{8}$$

$$\frac{d^2\xi}{d\tau^2} = M\pi \tag{14}$$

$$\phi(1 - T') = \frac{\bar{\gamma} - 1}{2M}\left(\frac{d\xi}{d\tau}\right)^2 \tag{15}$$

$$\frac{d\phi}{d\tau} = \pi^\alpha \tag{16}$$

Clearly we may multiply π, ϕ, and τ by factors chosen to give simple forms to any three of the foregoing equations. This has been done already in § 5.4, and the result is

$$\pi = \pi' M^{-1/(3-2\alpha)} \tag{28}$$

$$\phi = \Phi M^{-1/(3-2\alpha)} \tag{29}$$

and

$$\tau = \tau' M^{-(1-\alpha)/(3-2\alpha)} \tag{30}$$

giving the transformed equations

$$(1+\xi)\pi' = \Phi T' \tag{31}$$

$$\frac{d^2\xi}{d\tau'^2} = \pi' \tag{32}$$

$$\frac{d\Phi}{d\tau'} = (\pi')^\alpha \tag{33}$$

and

$$\Phi(1 - T') = \frac{1}{2}(\bar{\gamma} - 1)\left(\frac{d\xi}{d\tau'}\right)^2 \tag{34}$$

with the initial conditions

$$\xi = \frac{d\xi}{d\tau'} = 0, \qquad \pi' = \pi_0' \equiv \frac{M^{1/(3-2\alpha)}\left(U - \frac{C}{\delta}\right)P_0\left(1 + \frac{C}{3W_1}\right)}{CRT_0\left(1 + \frac{C}{2W_1}\right)}$$

and "burnt" occurring at $\Phi = M^{1/(3-2\alpha)}$.

Hence the solution depends on only three parameters: α, $\bar{\gamma}$, and π_0', whereas quantities at "burnt" depend also on M. All solutions with given α and $\bar{\gamma}$ can be obtained from the set of solutions with all values of the shot-start pressure, a single value of M, and the same values of α and $\bar{\gamma}$. This set of basic solutions should have the largest value of M that will be needed in practice.

For zero shot-start pressure we return to the results of § 5.4 for $\theta = 0$, in particular to the Gossot-Liouville law for the peak pressure:

$$P_m = \left[\frac{\beta^2 W_1 (CRT_0)^2 \left(1 + \frac{C}{2W_1}\right)^3}{A^2D^2\left(U - \frac{C}{\delta}\right)\left(1 + \frac{C}{3W_1}\right)^2}\right]^{1/(3-2\alpha)} G(\alpha, \bar{\gamma}) \tag{35}$$

whose consequences have been developed in the preceding chapter.

For $-1 < \theta < 0$, the same transformation applies as for $0 < \theta \leq 1$, and the similarity rules are the same. The basic solution must be one with a negative θ. The case $\theta = -1$ is special, and, as it does not occur in practice, it is not necessary to investigate it further. Usually a basic solution with $\theta = -0.5$ is sufficient. Thus all we need consider, in numerical integration, are the three values $\theta = -0.5$, 0, and 1.

6.12 The tabulation of ballistic solutions

We consider a ballistic system with the fundamental assumptions:

1. A rate of burning βP^{α}.
2. A form function $\phi = (1 - f)(1 + \theta f)$.
3. A resistance to motion represented by a pressure $R(x)$ per unit area of bore cross section.

These cover most cases that have been or are likely to be tabulated. The form function is sometimes a cubic instead of a quadratic, and the rate of burning is sometimes taken as $\beta(P + P_1)$. These extensions are easily included by the same methods.

The equations of the problem are

$$\phi = (1 - f)(1 + \theta f) \tag{36}$$

$$D\frac{df}{dt} = -\beta P^{\alpha} \tag{37}$$

$$W_1 \frac{dV}{dt} = \frac{AP}{1 + \dfrac{C}{2W_1}} - AR(x) \tag{38}$$

$$P\left[U - \frac{C}{\delta} + Ax - C\phi\left(\eta - \frac{1}{\delta}\right)\right] = \frac{C\phi RT_0T'\left(1 + \dfrac{C}{2W_1}\right)}{1 + \dfrac{C}{3W_1}}$$

and

$$\phi(1 - T') = \frac{1}{2}(\bar{\gamma} - 1)\left(W_1 + \frac{1}{3}C\right)V^2 + \frac{(\bar{\gamma} - 1)A}{CRT_0}\int_0^x R\,dx$$

of which the last two may be combined into

$$\begin{aligned} CRT_0\left(1 + \frac{C}{2W_1}\right)\phi = \left(1 + \frac{C}{3W_1}\right)P\left[U - \frac{C}{\delta} + Ax - C\phi\left(\eta - \frac{1}{\delta}\right)\right] \\ + \frac{1}{2}(\bar{\gamma} - 1)\left(1 + \frac{C}{2W_1}\right)\left(W_1 + \frac{1}{3}C\right)V^2 \\ + (\bar{\gamma} - 1)\left(1 + \frac{C}{2W_1}\right)A\int_0^x R\,dx \end{aligned} \tag{39}$$

As in the previous section, we write, for $\theta \neq 0$,

$$P = \frac{CRT_0\left(1 + \dfrac{C}{2W_1}\right)\pi(1 + \theta)^2}{\left(U - \dfrac{C}{\delta}\right)\left(1 + \dfrac{C}{3W_1}\right)4\theta} \tag{40}$$

$$R = \frac{CRT_0 r(1 + \theta)^2}{\left(U - \dfrac{C}{\delta}\right)\left(1 + \dfrac{C}{3W_1}\right)4\theta} \tag{41}$$

$$x = \frac{\left(U - \dfrac{C}{\delta}\right)\xi}{A} \tag{42}$$

$$M = \left(\frac{AD}{\beta}\right)^2 \frac{\left(U - \dfrac{C}{\delta}\right)^{2\alpha-2}\left(1 + \dfrac{C}{3W_1}\right)^{2\alpha-1}}{W_1(CRT_0)^{2\alpha-1}\left(1 + \dfrac{C}{2W_1}\right)^{2\alpha}} \tag{43}$$

$$t = \frac{\left(U - \dfrac{C}{\delta}\right)}{A}\left[\frac{4\theta\left(W_1 + \dfrac{1}{3}C\right)}{(1 + \theta)^2 CRT_0}\right]^{1/2}\tau \tag{44}$$

$$\Phi = \frac{4\theta\phi}{(1 + \theta)^2} \tag{45}$$

$$B = \frac{C\left(\eta - \dfrac{1}{\delta}\right)(1 + \theta)^2}{\left(U - \dfrac{C}{\delta}\right)4\theta} \tag{46}$$

which give

$$\frac{d^2\xi}{d\tau^2} = \pi - r \tag{47}$$

$$\Phi = (1 + \xi - B\Phi)\pi + (\bar{\gamma} - 1)\int_0^{\xi}\pi\,d\xi - \frac{\bar{\gamma} - 1}{\dfrac{3W_1}{C} + 1}\int_0^{\xi} r\,d\xi \tag{48}$$

and

$$\frac{d\Phi}{d\tau} = \left[\frac{(1 + \theta)^2}{4\theta}\right]^{\alpha-1}\left[\frac{4\theta}{M}(1 - \Phi)\right]^{1/2}\pi^{\alpha} \tag{49}$$

with the boundary conditions,

$$\xi = \frac{d\xi}{d\tau} = 0, \qquad \pi = r(\xi = 0) \quad \text{at } \tau = 0 \tag{50}$$

and "burnt" at

$$\Phi = \frac{4\theta}{(1+\theta)^2}$$

The essential parameters include:

1. B, a measure of the covolume effect.
2. $\left[\frac{(1+\theta)^2}{4\theta}\right]^{\alpha-1} \left(\frac{4\theta}{M}\right)^{1/2}$, which represents the effective speed of burning.
3. $\bar{\gamma}$, which is connected with the heat capacity of the propellant gases and the heat losses to the gun barrel.
4. $(\bar{\gamma} - 1)/[(3W_1/C) + 1]$, which arises as a correction from mean pressure to the pressure at the shot.
5. α, a property of the propellant, but depending also slightly on the details of the ballistics.
6. $4\theta/(1+\theta)^2$ as a further parameter when values are needed at "burnt."

The function r introduces at least one more parameter, the value of r at $\xi = 0$. r is derived from R, the resistance to motion, by equation 41. R will be a known or assumed function of travel. In the simplest possible case, R will be independent of travel, r will be a constant during any given ballistic solution, and this will be the only parameter introduced by resistance. More generally, R will be a function with two parameters or more, which it will probably be sufficiently general to write as

$$R = R_0 g \left[\frac{axA}{U - \frac{C}{\delta}}\right]$$

$$g(0) = 1$$

where g might be, for example, an exponential or linear decay; the parameter a is dimensionless. Then,

$$r = r_0 g(a\xi)$$

so that two parameters are involved, even if we stick to a single function g. If we like to take a constant value of a in all cases, only one parameter is needed. This implies that, if we change the loading conditions, the resistance at a given travel changes (except in the special case of g

being a constant); this variation of resistance from one solution to another goes in a direction that is physically plausible. Suppose C is increased; then at given x there is a bigger ξ and so a smaller resistance, since g will of course be a decreasing function; physically a bigger charge means a higher velocity at a given travel, and this higher velocity usually lowers the resistance. Thus a constant value of a produces a variation of resistance, with the loading conditions, in the physically correct direction. Any discrepancy would occur away from $\xi = 0$, since variations of initial resistance are represented exactly by r_0; hence any appreciable error arising from constant a could be corrected by a device similar to the method of § 5.5, which fails only near $\xi = 0$. All told, it is a reasonable approximation to take

$$r = r_0 g(\xi)$$

with a single function g in each set of ballistic tables.

We have isolated six ballistic parameters, whose relative importance will now be discussed. The covolume term,

$$B = \frac{C\left(\eta - \frac{1}{\delta}\right)(1 + \theta)^2}{\left(U - \frac{C}{\delta}\right)4\theta}$$

has a minimum value zero, approached in firings at low density of loading. The maximum value has no upper limit, for θ may approach zero as closely as we please; a practical limit is set by the fact that θ very close to zero makes the transformation factor $(1 + \theta)^2/4\theta$ very large, and the derived solution is much less accurate than the basic. If it is really necessary to use θ between 0 and 0.1, this could be more easily attained by interpolation between these values than by direct conversion from a basic grid with $\theta = 1$. A reasonable upper limit of B would therefore be $B = 3$. In most regions of a ballistic table the solution is not sensitive to B, and in such regions it is usually sufficient to deduce a quadratic relation from three values of B.

The parameter, $(M/4\theta)[(1 + \theta)^2/4\theta]^{2(1-\alpha)}$, runs from 0 to about 5, in practice, and has too strong an influence on the results to be taken into account in any approximate way. This parameter measures the influence of the increasing volume available for the propellant gases, relative to the evolution of gas from the propellant.

The pressure index α of the rate of burning has a considerable effect on the ballistic solution.

The nature of the propellant enters through α and also through $\bar{\gamma}$. The latter does not vary over a wide range, nor does it have a major effect on ballistics.[8] It is almost always sufficiently accurate to use simply the three values $\bar{\gamma} = 1.25$, 1.3, and 1.35.

In the term that represents the work done against bore resistance we find another parameter, $(\bar{\gamma} - 1)/[(3W_1/C) + 1]$. Usually the work done against resistance is small compared with the kinetic energy of the shot, and it is possible to use linear interpolation with respect to this minor parameter. Its limits are zero and $\bar{\gamma} - 1$, though this upper limit is attained very slowly as C/W_1 increases.

Finally, there is the parameter r_0, which measures the importance of the bore resistance relative to the peak pressure. This parameter has a major influence on the ballistic solution.

In general, not all these parameters will appear in any particular set of ballistic tables, which would then be intolerably bulky and awkward in use. Usually only one value of α is taken: for example, the Charbonnier-Sugot tables have $\alpha = 1$, Röggla used $\alpha = 0.7$, and the Bennett tables $\alpha = 2/3$. For analytical work $\alpha = 1$ is much the best single value, but for numerical tables it is possible to choose a better mean, at say 0.9.

By the approximation $\eta = 1/\delta$ and the assumption of universal values of $\bar{\gamma}$ and r_0, the number of ballistic parameters can be so reduced as to permit a graphical representation of the results. This is the basis of the Röggla graphs,[9] whose practical usefulness is, however, restricted by the low value of α $(= 0.7)$; it is also to be noted that, as published by Röggla, the peak pressure is the mathematical maximum, which may occur after "burnt," so that some care is needed in the use of these graphs. They have not become popular in Britain, where it is thought that the isothermal model of chapter 4 is as quick as the Röggla graphs, and the empirical corrections, necessary in any case, are a good deal smaller in the isothermal model. Of course, the formulas of the isothermal model could be graphed in exactly the same way as the results of Röggla's numerical integration, since the differences are basically only in the assumed values of α, $\bar{\gamma}$, and the "reduced shot-start pressure."

The set of reduced equations given previously is not applicable to $\theta = 0$, which needs a separate investigation on the same lines. The essential parameters are a little simpler in form when $\theta = 0$.

---

[8] This may be illustrated by various ballistic systems which have treated $\bar{\gamma}$ as a parameter to be used to adjust theoretical to observed ballistics. A small error in the assumptions requires a big change in $\bar{\gamma}$ as compensation. For example, Bianchi, *Balistica Interna* (Turin, 1910), had to use $\bar{\gamma}$ varying from 1.0 to 1.95! He used different values of $\bar{\gamma}$ to adjust peak pressure and muzzle velocity.

[9] Röggla, *Neue Diagramme fur die angewandte innere Ballistik* (Pilsen, 1931).

6.2 Optimum ballistic solutions

There are two classes of optimum problems: (1) the choice of a "best" charge for a given gun, and (2) the choice of a "best" gun for a given projectile. In the earliest days these were studied with "maximum muzzle velocity" as the criterion of the best solution. Charbonnier[10] took his analytical solution for $\alpha = 1$ and $\theta = 0$, without shot-start pressure or $\eta - (1/\delta)$ terms, and showed that:

1. Of all charges giving an assigned peak pressure, there was one that gave a maximum muzzle velocity; this "optimum charge" gave "all burnt" when the shot was at the muzzle.

2. For all guns of the same total internal volume and given peak pressure and projectile, each gun being fired with its optimum charge, there was one gun which gave the maximum velocity. This was the "optimum gun" of the specified total volume and peak pressure.

These results were extended to other values of α by Emery, using ballistic similarity. An elegant discussion on these lines is given by Sugot,[11] based on the ballistic parameters for $\theta = 0$, $\eta = 1/\delta$, and zero resistance. He demonstrates the following properties of the "optimum charge":

(*a*) For expansion ratios near unity, there is still unburnt propellant at the muzzle, and the corresponding density of loading is independent of P_m/RT_0; here the expansion ratio is defined as $1 + (x/l)$, where, as in chapter 4, $Al = U - (C/\delta)$.

(*b*) For large expansion ratios, "burnt" occurs at or before the muzzle, but not much before; the optimum density of loading increases with the expansion ratio and with P_m/RT_0.

For the "optimum gun":

1. The optimum expansion ratio decreases slowly as P_m/RT_0 increases.
2. The muzzle energy is proportional to the total volume of the gun and increases more slowly than P_m/RT_0.
3. The optimum density of loading increases with P_m/RT_0.

Taking a special progressive form function, Sugot shows that progressivity increases the optimum density of loading.

The practical application of these results is limited by the fact that in these "optima" the position of "burnt" is close to or past the muzzle. The regularity is therefore poor, usually too bad to be tolerated in a practical gun. A more realistic problem would be: Given P_m, velocity and regularity; find (1) the smallest charge, or possibly (2) the gun of smallest total internal volume, or perhaps (3) the shortest gun. Which of these three criteria to use would depend on the nature of the requirement. To go into these matters would involve the establishment of a formula for regularity in terms of the ballistic parameters. This we are not prepared to state in this book. It must be said that this question is fundamental to the study of optimum ballistic solutions.

---

[10] Charbonnier, *Balistique intérieure* (Paris, 1908), p. 255.

[11] Sugot, *Mém. artillerie franç.*, **5** (1926), 1131.

Another failing of the "optimum gun" as ordinarily given is that the conditions of given total volume and given maximum pressure do not ensure a constant weight of barrel. In reality, the weight of these guns depends also on the shot position at the time peak pressure is attained, and, in fact, also on the whole course of the (pressure-travel) curve after that point. It is easy to see that, if we specify the weight of the barrel, that gun that gives the highest velocity has a bigger expansion ratio than the "optimum gun" as ordinarily defined. No treatment taking account of this factor has been published.

In view of these shortcomings of the orthodox "optimum-gun" problem, it is not surprising to find that relatively few real guns are "optimum" in this sense. Nor need we go into the mathematical details of the orthodox solution. This is a straightforward matter of differentiation and after some laborious reduction ends with formulas that are quite complicated, even when derived from the most unsophisticated ballistic system. It is, in practice, quicker to determine the optima by direct numerical evaluation of neighboring solutions; this is indeed essential when one is using a refined ballistic method or a set of tables. Such a process cannot determine the position of the optimum very accurately, but this is needed only as a rough guide; the optimum performance, which is of more interest in practice, can be found with high accuracy by numerical evaluation.

We need not give here tables of the "optimum charge," since the charge that makes "burnt" occur at the muzzle is nearly the optimum and can be determined more easily in any ballistic system. The only appreciable difference between this and the optimum charge occurs in guns of small expansion ratio, where the optimum is so much less regular that it is actually better to use the charge giving "burnt" at the muzzle.

Tables of the "optimum gun" will be of more interest to the reader, for this optimum is not approximated by any simpler expression. Table 6.1, from Sugot,[12] shows the optimum as a function of RT_0/P_m, where, it should be noted, P_m is the maximum of the mean pressure in the gas, smaller than the breech pressure by a factor of $1 + (C/6W_1)$; actually Sugot uses rather different Lagrange corrections from this, but the inconsistency arising is not important. These optima have been calculated by assuming $\theta = 0$, $\eta = 1/\delta$, and no resistance. The piezometric

---

[12] Sugot, *Mém. artillerie franç.*, **5** (1926), 1131.

TABLE 6.1 OPTIMUM GUNS FOR $\theta = 0$

After Sugot; assuming $\eta = 1/\delta$ and no resistance. The expansion ratio ρ is defined as $1 + \dfrac{Ax}{U - C/\delta}$.

RT_0/P_m	ρ	Density of loading, g/cc	Piezometric Efficiency
2.5	3.1	0.675	0.78
3	3.3	0.63	0.79
4	3.7	0.565	0.80
5	3.95	0.51	0.80
6	4.15	0.465	0.81

efficiencies quoted are not the maximum possible, since the optimum gun maximizes $[1 - (1/\rho)] \times$ the piezometric efficiency, where ρ is the expansion ratio.

Very similar tables have been given by other workers, though apparently not in open publications. For 7-hole multitubular propellant, geometrical form function, covolume terms included, and a small shot-start pressure, the optimum density of loading has been found to be close to those in Table 6.1, though the optimum expansion ratio is almost two units greater. This is in part due to the flatness of the optimum, which results in the expansion ratio being sensitive to the details of the ballistic method.

Optimum solutions for cord charges have not been published. The only country that uses cord at all extensively is Britain, where optimum problems are of a more realistic type. It has been shown, however, that, when cord is used, the optimum charge always has unburnt remaining at the muzzle and that the optimum density of loading is less for cord than for tube. It is, in practice, easier to attain high densities of loading when cord is used. Since the optimum density of loading increases with peak pressure, we deduce that cord is most useful in high-pressure guns.

EXAMPLES

1. Find similarity relations when (*a*) the rate of burning is proportional to $P + P_1$, where P_1 depends only on the propellant composition; (*b*) there is a constant resistance to the motion of the shot [these cases were studied by Proudman, *Proc. Roy. Soc. (London)*, 100A (1921), 289]; (*c*) ϕ is a cubic in f.

2. If the propellant burns instantaneously, find the optimum charge weight and expansion ratio for a gun of given total volume and P_m. The existence of an optimum was first shown by Robins (1742). Show that the optimum expansion ratios for such guns are less than those quoted for slow burning in Table 6.1.

3. Solve the "optimum-charge" and "optimum-gun" problems on the isothermal model of chapter 4.

been of value in deciding what tolerances on bomb diameter ought to be allowed.

Although these two applications of the theory of guns with gas leakage are of some importance, the leakages considered are only of the order of 10 per cent. Thus very simple methods, such as that of § 7.36, are adequate. There is, however, another application in which more accurate methods are needed for reliable results. This occurs in work on recoilless guns (Figs. 7.1 and 7.2), in which a venturi in the breech discharges gas to counteract the recoil. A typical recoilless gun is shown in section in Fig. 7.3, which shows also the disk, usually of a thermosetting plastic, which provides the initial seal to the venturi.

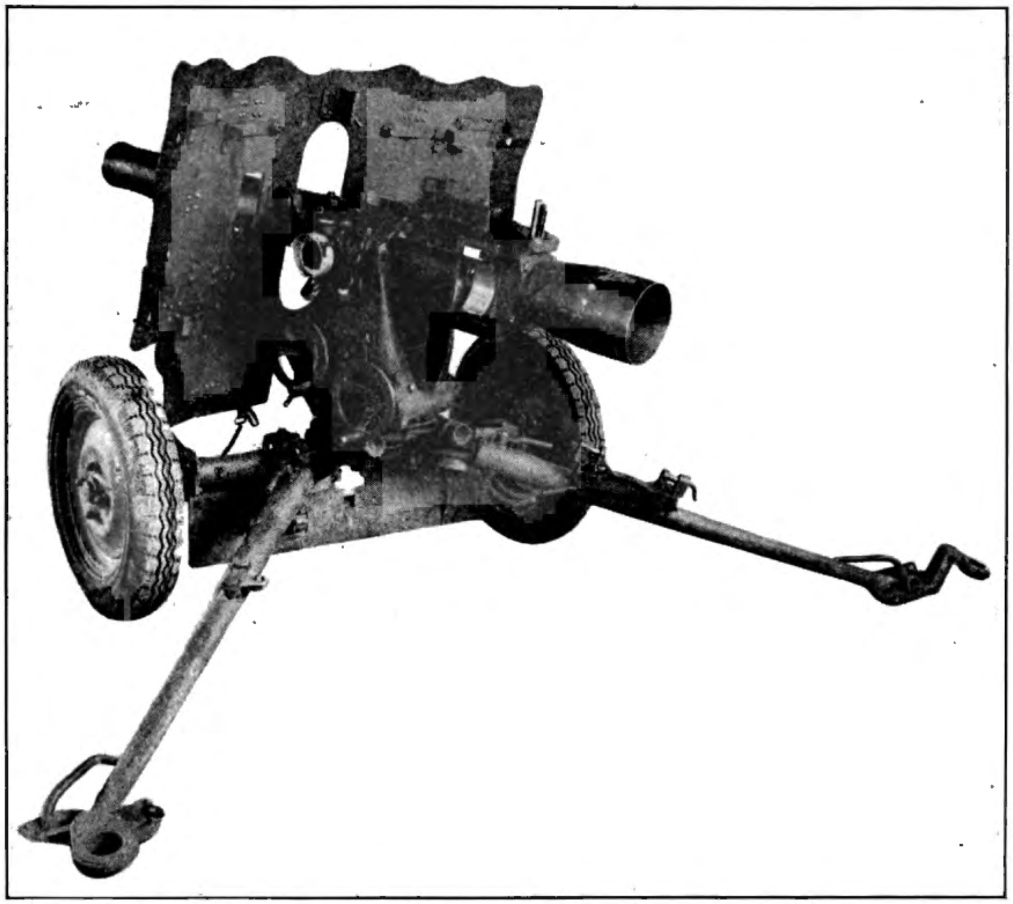

FIG. 7.1 A German 10.5-cm recoilless howitzer (LG 42) for airborne troops. Shell weight 33 lb, muzzle velocity 1140 ft/sec, weight of complete equipment 1100 lb.

We may approach the idea of this type of recoilless gun in several ways. For example, it may be considered as a rocket and gun built together, with a common propellant chamber. Again, we may think of a "drainpipe," which is obviously recoilless, and which was in fact

CHAPTER SEVEN

The Interior Ballistics of Leaking Guns

7.1 Introduction

Although the published literature of interior ballistics is quite extensive, and the confidential reports are still more innumerable, there has been little previous work on the subject to be treated in this chapter. Indeed, at the time the author began his own investigations, no other theory had been published. It is now known that parallel work was being carried out simultaneously in the United States, chiefly by Hirschfelder and Vinti, and also by Strecke in Germany. Until the present time, the only open publication in this field is a paper by the writer.[1] In this chapter we shall repeat the mathematical methods given in that paper, with a more expanded discussion of the practical consequences.

There are at least three fields of application of these theories. First, we can now calculate the ballistics of a worn orthodox gun, in which gas is able to leak past the projectile in the earliest stages of its motion. The leakage is particularly noticeable when the shot is held in the mouth of a cartridge case (fixed ammunition), for then in a worn gun there is a long "runup" before the band engages the rifling.

A second application, to be discussed later, is to smooth-bore guns without obturating device on the projectile. The most familiar example is the muzzle-loading smooth-bore mortar. Here the projectile is a finned bomb with a diameter less than the caliber of the mortar. The leakage of gas lowers the peak pressure and the muzzle velocity. This would be of little consequence if the bomb diameter were the same from round to round, but, in practice, a manufacturing tolerance must be allowed. This causes a spread of muzzle velocity, inflating the dispersion that would occur from variations of charge and shot weight. Although the existence of this effect was known, its quantitative evaluation had not been attempted before the treatment sketched in § 7.4. This has

---

[1] Corner, *Proc. Roy. Soc.* (*London*), **188A** (1947), 237.

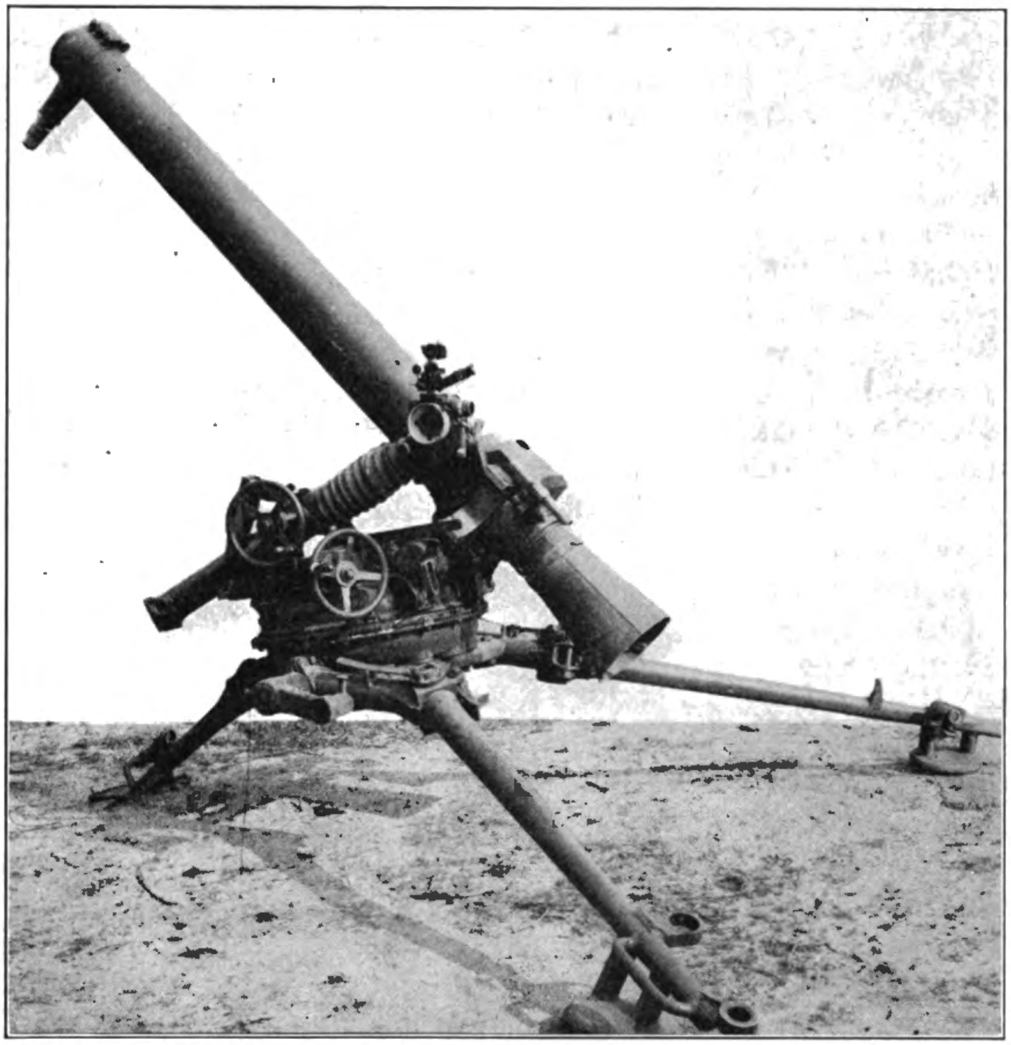

FIG. 7.2 A German 15-cm recoilless gun (LG 290) firing an 84-lb shell at 1020 ft/sec. Weight in firing position, as shown, 1400 lb.
Reproduced by permission of the Royal Society, London.

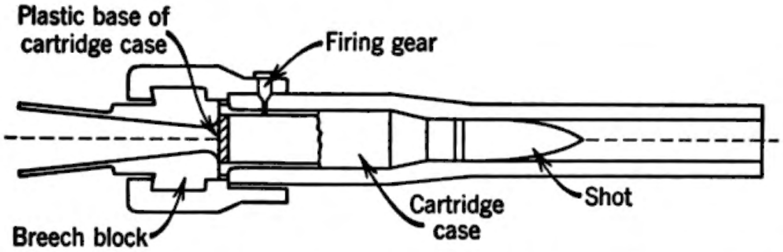

FIG. 7.3 Section through a typical recoilless gun, showing the plastic disk, which seals the base of the cartridge case until a certain pressure has been built up.
Reproduced by permission of the Royal Society, London.

used as a gun by Riabouchinsky.[2] By forming a constriction of suitable form in the pipe we arrive at the gun shown in Fig. 7.3; this form uses less charge than the plain drainpipe but can be made equally recoilless. Finally we can regard the recoilless gun as a Davis gun in which the counterprojectile thrown to the rear is propellant gas; this device reduces the weight of the counterprojectile and, what is equally important, the rear barrel is eliminated.

The history of this type of recoilless gun appears to begin with the work of Cooke.[3] German experiments began about 1937, and the first production types, the 10.5-cm and 7.5-cm LG 40, were used in the invasion of Crete. Other types built in Germany included the 5.5-cm MK 115 automatic, and 8.8-cm recoilless guns for light boats and aircraft.[4] The largest was the 28-cm DKM 44, a coast-defense gun firing a shell of 694 lb at 2450 ft/sec. American interest in recoilless guns dates from 1943,[5] and details have been published[6] of the 57-mm and 75-mm recoilless, low-pressure weapons.

In recoilless guns the leakage is far from being just a small correction to be added to the normal ballistic solution. While the charge is burning, about half the gas evolved goes out through the nozzle, only the other half remaining to increase the pressure in the gun. It will be clear that this enforces a more detailed solution than that which is adequate for the other applications we have mentioned earlier. The theories sketched in this chapter were in fact studied because of the appearance of recoilless guns in action.

7.2 The classical theory of nozzles

The flow of a *compressible* fluid through a nozzle, which first converges and then diverges, can be treated very simply by the classical one-dimensional approach. It is assumed that the condition of the fluid is a function only of the co-ordinate x measured along the axis of the channel and is therefore uniform across each normal cross section. Further assumptions that are made are (a) that loss of heat to the walls and turbulence and surface resistance can be neglected, and (b) that the fluid does not separate from the walls. For well-streamlined channels a gives results that are correct to a few per cent, and, as may be seen later, the error can be eliminated by using an empirical correction factor never far from unity; b is, in the same circumstances, true until the pressure in the gas as it leaves the nozzle falls to approximately the external pressure. As we shall not, in this book, have to deal with problems in which exit pressures are as low as this, we are spared the discussion of this more complicated region in which separation and shock waves can occur. The matter has some importance, however, in the design of rockets.

---

[2] Riabouchinsky, *Mém. artillerie franç.*, **2** (1923), 689.

[3] Cooke, U. S. patent 1,380,358.

[4] A sketch of the German development of recoilless guns for aircraft was given by Corner in *Aircraft Eng.*, **19** (1947), 378.

[5] Studler, *Army Ordnance*, **29** (1945), 232.

[6] *Army Ordnance* (Sept., 1945).

Let the cross-sectional area of the channel be $S(x)$, with p, ρ, T, and v as the values of pressure, density, temperature, and velocity at position x. Take suffix r to refer to quantities in the large reservoir where the fluid originates and where, therefore, the velocity is zero. Let suffix t refer to conditions at the throat.

We restrict our attention at first to gases obeying the equation of state of a perfect gas. As is conventional in ballistics, we write R for the gas constant divided by the average molecular weight of the propellant gases. We write γ for the ratio of the specific heats at constant pressure and volume. We treat R and γ as independent of temperature.

Finally, it must be emphasized that the following treatment is correct only for a steady state, though it can be used as an approximation for slowly varying flows.

Since there is no accumulation of gas at any section,

$$S\rho v = \text{constant } Q, \text{ say, } = S_t\rho_t v_t \tag{1}$$

The expansion of each element of gas being adiabatic,

$$p\rho^{-\gamma} = p_t\rho_t^{-\gamma} = p_r\rho_r^{-\gamma} \tag{2}$$

From the equation of energy for an element as it passes down the nozzle,

$$\frac{\gamma R}{\gamma - 1}(T_r - T) = \frac{v^2}{2} \tag{3}$$

The equation of state of the gas is

$$p = \rho RT \tag{4}$$

At the throat

$$\frac{dS}{dx} = 0$$

so that, from equation 1,

$$\frac{1}{\rho}\frac{d\rho}{dx} + \frac{1}{v}\frac{dv}{dx} = 0 \tag{5}$$

With a little reduction, this leads to

$$\frac{T_t}{T_r} = \frac{2}{\gamma + 1} \tag{6}$$

and, hence, the other properties of the fluid at the throat are given by

$$\frac{p_t}{p_r} = \left(\frac{2}{\gamma + 1}\right)^{\gamma/(\gamma-1)} \tag{7}$$

$$\frac{\rho_t}{\rho_r} = \left(\frac{2}{\gamma + 1}\right)^{1/(\gamma-1)} \tag{8}$$

$$v_t^2 = \frac{2\gamma R T_r}{\gamma + 1} \tag{9}$$

The rate of flow of mass through the system is

$$Q = \gamma^{1/2}\left(\frac{2}{\gamma + 1}\right)^{(\gamma+1)/2(\gamma-1)} \rho_r S_t (RT_r)^{1/2} \tag{10}$$

$$= \gamma^{1/2}\left(\frac{2}{\gamma + 1}\right)^{(\gamma+1)/2(\gamma-1)} p_r S_t (RT_r)^{-1/2} \tag{11}$$

We write, in general,

$$Q = \psi p_r S_t (RT_r)^{-1/2} \tag{12}$$

where ψ has the value indicated by equation 11 when there are no heat or energy losses. In practical cases with well rounded contours, ψ lies a few per cent below the theoretical value. It is remarkable and very useful that ψ is nearly independent of γ when this is near 1.25, the value typical of gun propellants. It can be shown, in fact, that ψ lies within 1 per cent of 0.66 for the whole range of values of γ given by the products of modern propellants.

We have assumed up to the present that the throat pressure as given by equation 7 is greater than the pressure in the space into which the nozzle exhausts. For $\gamma = 1.25$, $p_t/p_r = 0.55$. In this book we consider usually cases in which the reservoir pressure is some tons per square inch, while the external pressure is atmospheric, so that the throat pressure is far higher than the external pressure. The only exception occurs in the "high-low pressure" gun (§ 8.1). In the latter case equation 5 is replaced by the condition that the throat pressure is the external pressure, which with equations 1 to 4 determines a unique solution.

We return to the example in which the external pressure is less than the throat pressure. For $\gamma = 1.25$, the other characteristics of the gas at the throat are $\rho_t/\rho_r = 0.62$ and $v_t = 1.05(RT_r)^{1/2}$.

With a general value of γ, the conditions at any section can easily be written down. The most useful relations are

$$\left(\frac{p_r}{p}\right)^{2/\gamma} = \left(\frac{2}{\gamma - 1}\right)\left(\frac{\gamma + 1}{2}\right)^{(\gamma+1)/(\gamma-1)} \left(\frac{S}{S_t}\right)^2 \left[1 - \left(\frac{p}{p_r}\right)^{(\gamma-1)/\gamma}\right] \tag{13}$$

which gives the pressure at any expansion ratio S/S_t, and

$$\left(\frac{T_r}{T}\right)^{2/(\gamma-1)} = \left(\frac{2}{\gamma - 1}\right)\left(\frac{\gamma + 1}{2}\right)^{(\gamma+1)/(\gamma-1)} \left(\frac{S}{S_t}\right)^2 \left[1 - \frac{T}{T_r}\right] \tag{14}$$

which gives the temperature at any cross section. Another useful equation is

$$v^2 = \frac{2\gamma}{\gamma - 1} RT_r \left[1 - \left(\frac{p}{p_r}\right)^{(\gamma-1)/\gamma}\right] \tag{15}$$

These equations 13, 14, and 15 are true only so long as p is greater than the external pressure.

In many applications the reservoir in which the gas is at rest may not exist, but the "reservoir" pressure, density, and temperature always do. T_r is defined by equation 3 with T, v, any corresponding values of temperature and velocity; ρ_r and p_r then follow from equations 2 and 4.

For the gases produced by gun propellants the mean molecular weight is almost independent of temperature, as was pointed out in § 3.22, and R is therefore the same at all points in the flow. Slowly varying states are usually treated by the steady-state equations, and in such problems R is also independent of time.

If the gases are in a chemical equilibrium, which is a function of temperature, γ depends both on the rate of attainment of equilibrium and on the temperature. For some rocket fuels this raises such difficulties in the definition of a suitable mean γ that it is better to return to first principles and to rewrite equations 2 and 3 in terms of heat contents. For guns there is less difficulty. At equilibrium with respect to the water-gas reaction, γ does not vary greatly with temperature and is not much affected by the lag, in reaching this equilibrium, which appears below about 2000°K. It is easy to choose a mean γ for any particular case, using of course the tables of chapter 3.

7.21 Covolume corrections

The results of the preceding section apply only to perfect gases. Rateau [7] has obtained the analogous results when the equation of state is

$$p\left(\frac{1}{\rho} - \eta\right) = RT \tag{16}$$

where η is a covolume, independent of pressure and temperature. The equation of state of propellant gases has been discussed in chapter 3, where it was shown that the conventional equation 16 is less accurate than a certain equally simple alternative. However, equation 16 is sufficiently accurate for the present calculations.

Write

$$\epsilon = \frac{\eta\rho_r}{1 - \eta\rho_r} \tag{17}$$

This dimensionless parameter ϵ is a measure of the effect of the covolume. A reservoir pressure of 25 tons/sq in. corresponds to $\epsilon \simeq 0.35$.

The adiabatics of equation 16 are

$$p\left(\frac{1}{\rho} - \eta\right)^{\gamma} = \text{constant} \tag{18}$$

Rateau has obtained the correction terms for the special case $\gamma = 1.25$, which is close to the value for the gases used in guns. The equation 6 is replaced by

$$\frac{T_t}{T_r} = \frac{2}{\gamma + 1}\left[1 - 0.050\epsilon + 0.018\epsilon^2 + 0(\epsilon^3)\right] \tag{19}$$

and equation 7 by

$$\frac{p_t}{p_r} = \left(\frac{2}{\gamma + 1}\right)^{\gamma/(\gamma-1)}\left[1 - 0.248\epsilon + 0.117\epsilon^2 + 0(\epsilon^3)\right] \tag{20}$$

It should be noted that the equation of energy, formerly equation 3, is now

$$\frac{v^2}{2} = \frac{\gamma R}{\gamma - 1}(T_r - T) + (p_r - p)\eta \tag{21}$$

so that

$$v_t = \left(\frac{2\gamma}{\gamma + 1} RT_r\right)^{\frac{1}{2}}(1 + 0.599\epsilon - 0.128\epsilon^2) \tag{22}$$

---

[7] Rateau, *Comp. rend.*, **168** (1919), 330; also *Mém. artillerie franç.*, **11** (1932), 5.

The rate of flow through the nozzle is

$$Q = \gamma^{1/2}\left(\frac{2}{\gamma+1}\right)^{(\gamma+1)/2(\gamma-1)} p_r S_t (RT_r)^{-1/2}(1 - 0.224\epsilon + 0.104\epsilon^2) \quad (23)$$

At the highest ϵ reached in normal ballistics, $\epsilon = 0.35$, the correction terms in equation 23 amount to only 6½ per cent. Thus this correction can almost always be neglected.

In calculating the thrust obtained from a nozzle (§ 7.22), it turns out that we need the quantity v/v_t, where v is the velocity where the cross section is S. The following equation,

$$\left(\frac{v}{v_t}\right)^2 = \frac{\gamma+1}{(\gamma-1)(1+1.2\epsilon)}\left[1 + 0.2\epsilon - \frac{2}{\gamma+1}\left(\frac{v_tS_t}{vS}\right)^{\gamma-1} \times \left[1 + \left\{0.281\left(\frac{v_tS_t}{vS}\right) - 0.206\right\}\epsilon\right]\right] \quad (24)$$

is correct to terms of order ϵ and can be solved numerically by successive approximations.

7.22 Thrust on a nozzle

Let the velocity and pressure at the exit section of area S_e be v_e and p_e, respectively. Let p_a be the atmospheric pressure.

From momentum considerations, the force F on the nozzle is

$$F = Qv_e + S_e(p_e - p_a) \quad (25)$$

and, if we neglect the atmospheric pressure, as may always be done in the applications we shall make, we have

$$F = Qv_e + S_ep_e \quad (26)$$

It is of interest to consider first a channel that converges to a throat, with no diverging part. In this case,

$$F = Qv_t + S_tp_t \quad (27)$$

which, from equations 20, 22, and 23, reduces to

$$F = (\gamma+1)\left(\frac{2}{\gamma+1}\right)^{\gamma/(\gamma-1)} p_rS_t(1 + 0.097\epsilon - 0.036\epsilon^2) \quad (28)$$

where, as usual, the terms in ϵ are correct only for $\gamma = 1.25$. The momentum term on the right of equation 27 is just γ times the pressure term (omitting terms in ϵ). The factor $(\gamma + 1)[2/(\gamma + 1)]^{\gamma/(\gamma-1)}$ varies from 1.242 to 1.255 as γ is changed from 1.2 to 1.3.

Now suppose that the nozzle throat is gradually widened until it is of the same diameter as the reservoir, until, in short, the whole system is simply a pipe of uniform section, open at one end and closed at the other. The only thrust on the pipe comes from the pressure on the closed end, and the thrust is therefore $p_r S_t$. This shows that equation 28 cannot be used in all circumstances. Only for a small throat area (relative to that of the reservoir) can equation 28 be used, and it is obvious that equation 28 is an overestimate when the throat area is greater than 80 per cent of the area in the main channel before the throat. It is probable, however, that the accuracy of equation 28 becomes rapidly greater as the throat area is reduced beyond this value and is sufficient for work on recoilless guns.

Table 7.1 Thrust Coefficient of a Nozzle, $\zeta = F/p_r S_t$

	$\gamma = 1.2$		$\gamma = 1.3$	
S_e/S_t	$\epsilon = 0$	$\epsilon = 0.2$	$\epsilon = 0$	$\epsilon = 0.2$
1	1.242	1.266	1.255	1.280
1.2	1.318	1.355	1.327	1.336
1.4	1.369	1.403	1.374	1.381
1.6	1.408	1.440	1.409	1.414
1.8	1.439	1.470	1.438	1.440
2	1.466	1.494	1.461	1.462
2.5	1.516	1.540	1.505	1.503
3	1.554	1.575	1.537	1.534
3.5	1.583	1.602	1.562	1.556
4	1.607	1.624	1.582	1.575
5	1.644	1.657	1.612	1.603
6	1.673	1.683	1.635	1.624
8	1.713	1.720	1.667	1.654
10	1.742	1.747	1.689	1.675
∞	2.247	2.211	1.964	1.934

When there is a divergent part to the nozzle, the thrust, to terms of order ϵ, is given, in terms of a dimensionless "thrust coefficient," by

$$\zeta \equiv \frac{F}{p_r S_t} = \gamma \left(\frac{2}{\gamma + 1}\right)^{\gamma/(\gamma-1)} \frac{v_e}{v_t} (1 + 0.375\epsilon) + \left(\frac{S_t}{S_e}\right)^{\gamma-1} \left(\frac{v_t}{v_e}\right)^{\gamma} \left(\frac{2}{\gamma + 1}\right)^{\gamma/(\gamma-1)} \left[1 - \left(1.029 - 0.780 \frac{v_t S_t}{v_e S_e}\right) \epsilon\right] \tag{29}$$

For given S_e/S_t, γ, and ϵ, the right-hand side can be evaluated by using the results of equation 24. Table 7.1 gives the results for $\gamma = 1.2$ and 1.3 and for $\epsilon = 0$ and 0.2 and is intended to be used for linear interpolation between $\epsilon = 0$ and 0.3 and γ from 1.2 to 1.3. Although the results are smooth to the three decimal places given, the last place is intended only to prevent the accumulation of rounding-off errors in interpolated values. Two decimal places represent the real accuracy of the calculations, except that for $\epsilon = 0.3$ the neglect of terms in ϵ^2 is likely to cause an error of a little more than 1 per cent. The intervals of tabulation have been so chosen that linear interpolation with respect to ϵ, γ, and S_e/S_t leads to errors of less than 1 per cent. Both the ϵ^2 errors and the errors of interpolation are less than the deviations between real nozzles and our simple theory.

A point that is shown clearly by Table 7.1 is that the thrust increases very slowly after S_e/S_t has reached, say, 6.

7.3 The equations of interior ballistics of a leaking gun

7.31 Assumptions of the theory

In chapter 1 we have discussed the various gradations between ballistic "schemes" and "theories," and examples with claims to simplicity and accuracy have been given in chapters 4 and 5 respectively. In the present chapter we start by finding a set of equations that generalize those of chapter 5 and are of essentially the same order of accuracy. We sketch the method of solution by numerical integration. A simpler solution is then presented for the case where the rate of burning is proportional to pressure. A still simpler method consists in a reduction to an "isothermal" model, which is closely related to the simple but useful methods already explained in chapter 4. This reduction is particularly valuable for grasping the connection between the ballistics of leaking and of orthodox guns, and, accordingly, we place this method immediately after the most general equations have been derived.

To begin with the assumptions underlying the most accurate equations, we may list

1. The use of a rate of burning (of the web) βP^{α};
2. The inclusion of a covolume, independent of temperature;
3. Bore resistance is neglected, though it is not difficult to include it, and this is indeed done in § 7.513; for the present, however, we replace the resistance by either a shot-start pressure vanishing immediately after engraving or an equivalent "correction" of β in the rate of burning.

The following assumptions are associated with the features peculiar to a leaking gun.

4. No unburnt propellant is lost through the nozzle. This is obviously true for smooth-bore guns with a small leakage area between shot and bore and also for worn orthodox guns. In many types of recoilless guns the propellant is effectively trapped by the cartridge case. Even in

the most unfavorable type, that of guns shown in Fig. 7.3, the losses of unburnt propellant are small unless the charge burns very slowly. It will be shown in § 9.51 that this result is to be expected from a consideration of the forces acting on the propellant. The assumption may be expected to break down for charges of chopped propellant.

5. We assume that the bursting of the disk, which closes the nozzle, and the setting up of the flow out of the gun can be represented by the use of the familiar equations for quasisteady flow through nozzles (§ 7.2) beginning instantaneously at a certain pressure, which we shall call the "nozzle-start pressure."

The use of this idealization requires a certain amount of care. For guns with thin bursting disks, such as the paper or sheet brass used in certain designs, the breaking of the disk occurs at a time when the rate of increase of pressure is small; hence in the time taken by the flow through the nozzle to start and settle down the pressure in the chamber does not rise much. The nozzle-start pressure is low—indeed such guns can usually be treated on the assumption of a zero nozzle-start pressure. Thickening the disk delays the initial nozzle flow until an epoch when the pressure is rising rapidly, and the "nozzle-start pressure" under these conditions is considerably greater than that needed to break the disk. The apparent "nozzle-start pressure" would therefore be expected to show a very rapid increase with disk thickness, once this has passed a certain critical value. This appears to be borne out by experiments with German recoilless guns, where plastic disks as thick as a third of a caliber have been used. A theoretical analysis appears to be possible, following a method of Carrière.[8]

If we follow out the consequences of our assumption that the steady flow out of the nozzle is set up immediately the nozzle opens, then it is found that, if this nozzle-start pressure is zero, the initial temperature must be slightly less than T_0, the temperature of uncooled explosion (see chapter 3 for definition). This is a defect of the assumption, since the initial temperature is certainly equal to T_0, if we neglect heat loss to the walls. However, the errors in the pressure are small and occur only during the earliest part of the firing.

In our basic equations and in the more exact of the methods of handling them (§ 7.37), we do not assume that the leakage area is constant during the firing. In most recoilless guns the area is in fact constant. In certain other vented weapons the area does vary; the most obvious example is a worn orthodox gun, firing fixed ammunition, where the leakage area is greatest at the start of shot motion and decreases rapidly to zero as the projectile moves along. The Germans have also carried out trials of a recoilless gun whose vent area was varied in rough relation to the bore resistance; the idea was to reduce the momentary resultant thrust on the carriage, a point that will be discussed in § 7.61. The most noticeable effect seen in these trials was erosion of the mechanism.

---

[8] Carrière, *Proc. 7th Intern. Congr. Applied Mech.* (*London*, 1948).

We come next to our more rapid method (§ 7.38), which uses a rate of burning proportional to pressure and represents initial resistance by a "shot-start pressure." This is no doubt a violent idealization, but, as the justification is the same as for an orthodox gun, we may refer to the discussion of § 5.3.

7.32 Notation

Let the area of the cross section of the bore be A and the chamber volume, measured out to the throat of the nozzle, be U. Let the charge weight be C and effective shot weight W—in the latter one can include corrections for rotational inertia and the motion, if any, of the gun barrel. We take S as the area of the throat through which the gas escapes. We write the shot travel at time t as x and the velocity as V. Let the function of charge burnt be ϕ, and the mass of gas present in the gun be NC. As in our treatment of orthodox guns, we denote the remaining least dimension of propellant grain by fD, where D is the initial web size. The quantities ϕ and f are connected by the form function, usually written as

$$\phi = (1 - f)(1 + \theta f) \tag{30}$$

where θ is the "form factor" of the grain.

Let the propellant have covolume η, density δ, diametral rate of burning βP^{α} at pressure P, and let the uncooled explosion temperature (without performance of external work) be T_0°K. Let RT_0 be the "force constant" of the propellant. The equation of state of the products of uncooled explosion is therefore

$$P(v - \eta) = RT_0$$

where v is the volume per gram. We have also

$$D\frac{df}{dt} = -\beta P^{\alpha} \tag{31}$$

7.33 Pressure and density distributions in the gun

The conventional approximate theory of the pressure gradient in an orthodox gun assumes that the density of gas is independent of position in the gun. This theory is sketched in chapter 9, and some of its consequences have already been used in earlier chapters. The results that we wish to use here are that the

$$\text{Space-mean pressure} = \frac{1 + \dfrac{C}{3W}}{1 + \dfrac{C}{2W}} P \tag{32}$$

where P is the pressure at the breech, and the

$$\text{Pressure at shot} = \frac{P}{1 + \dfrac{C}{2W}} \tag{33}$$

For a gun with leakage some allowance must be made for the fact that the quantity of gas in the gun does not increase up to the full value C. Allowance must also be made for the velocity distribution in the gun being altered if the leakage is backwards through the breech; this occurs in recoilless guns of the type shown in Fig. 7.3, but not in smooth-bore mortars or worn orthodox guns. To cover these possibilities, we may replace C in equations 32 and 33 by $kC(N + 1 - \phi)$, where the numerical factor k will be unity for forward leakage and should be reduced considerably for free venting through the breech. A more detailed investigation shows that k varies during the motion of the shot, owing to the movement of the stagnation point in the gun. To follow up this effect would lead us rather far from our main theme, and so we simply use k here as a semiempirical factor.

It is possible to use, instead of $kC(N + 1 - \phi)$, the alternative expression kCN, which is analogous to the replacement of C by $C\phi$ in equations 32 and 33 for orthodox guns. The form kCN is more convenient in application, and its use instead of $kC(N + 1 - \phi)$ alters muzzle velocity and peak pressure by not much more than 1 per cent in most cases. We use, therefore,

$$\text{Space-mean pressure} = \frac{P}{1 + \dfrac{kCN}{6W}} \tag{34}$$

and

$$\text{Pressure at shot} = \frac{P}{1 + \dfrac{kCN}{2W}} \tag{35}$$

where P is the maximum pressure anywhere inside the gun at the instant considered.

We assume that the gas density is uniform along the gun. Let this density be ρ. Then,

$$\rho\left[U + Ax - \frac{C(1-\phi)}{\delta}\right] = NC \tag{36}$$

Let T°K be the mean temperature of the gases at the instant considered. We have, from equation 34,

$$P\left(\frac{1}{\rho} - \eta\right) = RT\left(1 + \frac{kCN}{6W}\right)$$

which, with equation 36, becomes

$$P\left[U + Ax - \frac{C(1-\phi)}{\delta} - CN\eta\right] = NCRT\left(1 + \frac{kCN}{6W}\right) \tag{37}$$

Numerical examples have shown that for guns with a substantial leak, such as recoilless guns, this equation may usually be replaced by

$$P\left(U + Ax - \frac{C}{\delta}\right) = NCRT\left(1 + \frac{kCN}{6W}\right) \tag{38}$$

with ample accuracy, right up to the time when the charge is all burnt, $\phi = 1$. In a typical case, the error in the pressure due to the use of equation 38 was at most ½ per cent, which occurred in the early stages; the error decreased with time until $\phi = 1$ and was 0.3 per cent when $\phi = \frac{1}{2}$. This is about one tenth of the corresponding error in an orthodox gun at the same stage of burning.

In exceptional cases we have found errors of as much as 10 per cent in pressure due to this approximation. It has been found that for a given gun and projectile these percentage errors are almost independent of the loading and initial conditions and are substantially constant over the important period of high pressures in the firing. These observations justify the following method of correction; we use equation 38 always, and on our first calculation with a new type of gun we find the percentage error at maximum pressure due to the use of equation 38 instead of equation 37. If this error is appreciable, we correct all future runs by this factor. In the exact method it is necessary only to multiply $NCRT$ by the appropriate factor to get the corrected pressure. In our approximate method (§ 7.38) we absorb the correction into RT_0, using the corrected value, say RT_{01}, to replace RT_0 only in equations 72, 84, 85, 90, and 91.

Where the leakage is small, as in smooth-bore guns and eroded guns, the approximation 38 is no more accurate than in orthodox interior ballistics.

After $\phi = 1$, the approximate equation 38 becomes inadequate in all cases, and in this part of the solution we shall use the exact equation 37.

The equation of motion of the shot is

$$W_1 \frac{d^2x}{dt^2} = AP \tag{39}$$

where W_1 is a modified shot mass, which from equation 35 is equal to

$$W_1 = W + \tfrac{1}{2}kCN \tag{40}$$

Corrections for recoil, if any, of the gun and for rotational inertia and bore resistance may be added to W_1 if desired.

7.34 Nozzle flow and energy relations

It has been shown in §§ 7.2 and 7.21 that the rate of flow through the nozzle is

$$Q = \psi p_r S(RT_r)^{-\frac{1}{2}} \tag{41}$$

where p_r and T_r refer to the reservoir conditions, and ψ is a numerical factor, which would be 0.66 if there were no energy losses and which lies a few per cent lower for leakage channels of good shape. Covolume corrections reduce the flow only slightly, by only 6½ per cent even at pressures around 25 tons/sq in. and thus may be neglected. Their mean effect can be taken into account by a slight change in ψ between high- and low-pressure firings in the same gun. We may now identify p_r with P and T_r with T, the latter introducing a relative error in Q of order $kCN/30W$. Hence,

$$C\frac{dN}{dt} = C\frac{d\phi}{dt} - \frac{\psi SP}{(RT)^{\frac{1}{2}}} \tag{42}$$

We come now to the equation of energy. In time dt the gas gives kinetic energy $AP\,dx$ to the shot and the gas in front of the stagnation point; a mass $C\,d\phi$ is evolved from the propellant, and $C(d\phi - dN)$ passes out through the nozzle. We divide this process into three steps.

1. The gas, of internal energy $NCE(T)$, provides kinetic energy $AP\,dx$; in this stage the temperature changes by

$$dT = -\frac{AP\,dx}{CNc_v} \tag{43}$$

where c_v is the specific heat (at constant volume) of the gases, at temperature T; since $c_v = R/(\gamma - 1)$, equation 43 can be written as

$$N\,dT = -\frac{(\gamma - 1)AP\,dx}{CR} \tag{44}$$

2. A mass $C\,d\phi$, with internal energy $E(T_0)C\,d\phi$, enters the gas; hence,

$$C\,d\phi\,E(T_0) = CNc_v\,dT + C\,d\phi\,E(T)$$

and so

$$dT = \frac{d\phi}{N}(T_0 - T) \tag{45}$$

if c_v is constant over the range T to T_0.

3. A mass $C(d\phi - dN)$ escapes through the nozzle. Since the expansion is adiabatic, we have

$$d(\log T) = -(\gamma - 1)\,d\log\left(\frac{1}{\rho} - \eta\right)$$

or

$$\frac{dT}{T} = \frac{(\gamma - 1)\,d\rho}{(1 - \eta\rho)\,\rho}$$

Also

$$\frac{d\rho}{\rho} = \frac{dN - d\phi}{N}$$

Hence,

$$\frac{dT}{T} = (\gamma - 1)(1 + \epsilon)\left(\frac{dN - d\phi}{N}\right) \tag{46}$$

Summing all three effects 44, 45, and 46 gives

$$N\frac{dT}{dt} = -(\gamma - 1)\frac{AP}{CR}\frac{dx}{dt} + (T_0 - T)\frac{d\phi}{dt} + (\gamma - 1)(1 + \epsilon)T\left(\frac{dN}{dt} - \frac{d\phi}{dt}\right)$$

and using equation 42 yields

$$\frac{d}{dt}(NT) = -(\gamma - 1)\frac{AP}{CR}\frac{dx}{dt} + T_0\frac{d\phi}{dt} - [\gamma + (\gamma - 1)\epsilon]\frac{\psi SP}{CR}(RT)^{1/2} \tag{47}$$

The term in ϵ can be omitted with a relative error of 7 per cent at $\epsilon = 0.35$, which is almost exactly compensated by the error in using a single ψ throughout a solution.

Heat losses can be included in the way explained by Kent and Vinti (see § 4.23); if the loss can be approximated by $\frac{1}{2}\chi W_1 V^2$, with χ constant during the firing, then one writes

$$\bar{\gamma} - 1 = (\gamma - 1)(1 + \chi)$$

and replaces γ by $\bar{\gamma}$ in that term of equation 47 which involves dx/dt. Thus one arrives at

$$\frac{d}{dt}(NT) = -(\bar{\gamma} - 1)\frac{AP}{CR}\frac{dx}{dt} + T_0\frac{d\phi}{dt} - \frac{\psi\gamma SP(RT)^{1/2}}{CR} \qquad (48)$$

7.35 Summary of the equations

With nozzle open, shot in motion, and charge not completely burnt, we have

$$\left.\begin{array}{ll}
(38) & P\left(U + Ax - \dfrac{C}{\delta}\right) = NCRT\left(1 + \dfrac{kCN}{6W}\right) \\[2ex]
(39) & W_1 \dfrac{d^2x}{dt^2} = AP \\[2ex]
(40) & W_1 = W + \tfrac{1}{2}kCN \\[2ex]
(31) & D\dfrac{df}{dt} = -\beta P^{\alpha} \\[2ex]
(30) & \phi = (1 - f)(1 + \theta f) \\[2ex]
(42) & \dfrac{dN}{dt} = \dfrac{d\phi}{dt} - \dfrac{\psi SP}{C(RT)^{1/2}} \\[2ex]
(48) & \dfrac{d(NT)}{dt} = -(\bar{\gamma} - 1)\dfrac{AP}{CR}\dfrac{dx}{dt} + T_0\dfrac{d\phi}{dt} \\[2ex]
 & \qquad\qquad - \dfrac{\gamma\psi SP(RT)^{1/2}}{CR}
\end{array}\right\} \qquad (49)$$

Various special cases are derived thus: before the nozzle opens, $S = 0$; before the shot starts, $x = 0$; after "all burnt," $\phi = 1$, and equation 38 is replaced by

$$P(U + Ax - CN\eta) = NCRT\left(1 + \frac{kCN}{6W}\right) \qquad (50)$$

7.36 The equivalent nonleaking ballistic problem

In this section we shall deal with a simplified version of the set of equations 49, and by comparison with the analogous equations for an orthodox gun we shall show the nature of the effects produced by gas leakage. The level of approximation is essentially that of the "isothermal" model discussed in chapter 4.

We assume that the shot finds no initial resistance to motion and that the nozzle flow is established at a low pressure. In practical applications it is possible to make partial correction for these approximations by adjusting the rate of burning. We assume, also, that the rate of burning is proportional to pressure and that the leakage area S is constant.

Placing $S = 0$ in equation 49, we return to the equations of an orthodox gun. The variation of the gas temperature with time is decided by the competition between the two terms remaining on the right of equation 48: the first term represents the lowering of the energy of the gas by the work done on the projectile; the second term corresponds to the increase of energy by the burning of the propellant. The competition between these terms leads, as has been illustrated in chapter 5, to a gas temperature that falls only slowly from the initial value T_0, though the decrease becomes rather more marked toward the end of burning; after the propellant has been consumed, there is of course a further drop of temperature during the adiabatic expansion of the gases.

When there is a constant leakage area S, there is an additional term on the right of equation 48, tending to lower the temperature because of the work done in pushing gas out of the nozzle. The effect on the (temperature-time) relation depends chiefly on the ratio S/A, where A is the cross-sectional area of the bore. For recoilless guns with nozzles of reasonably good shape, S/A lies near 0.65, and in such cases the temperature shows a rapid drop after the nozzle opens, thereafter flattens out, and later shows the increasing rate of decline characteristic of normal guns. For most of the period of burning the gas temperature in the recoilless gun lies near 0.9 of the mean temperature in the corresponding period of an ordinary gun.

We shall approximate to both leaking and sealed guns by equations in which the temperature is given a mean value during the period of burning. For a normal gun this mean should be about 0.9 T_0 (see § 5.25), whereas, if we neglect $\eta - (1/\delta)$, the proper mean rises to about T_0 at 20 tons/sq in. The mean to be used with leakage depends chiefly on S/A, decreasing to about $0.85T_0$ at $S/A = 0.7$. Thus we may express one effect of leakage as a decrease in the effective force constant of the propellant, by as much as 10 per cent in a fully recoilless gun.

We write the mean value of RT as λ. Then, by integration of equation 49, using $\alpha = 1$, we find

$$P\left(U + Ax - \frac{C}{\delta}\right) = C\lambda(1 - f)(1 - \Psi + \theta f) \tag{51}$$

after omitting a factor $(1 + kC\overline{N}/6W)$ from the right; this factor is never far from unity. We have written

$$\Psi = \frac{\psi SD}{\beta C\lambda^{1/2}} \tag{52}$$

The dimensionless parameter Ψ is, as we shall show, the fundamental quantity expressing the effect of leakage on the interior ballistics. The values of Ψ found in practice fall into two distinct classes. In the first, appropriate to smooth-bore guns and mortars and leakage due to erosion, Ψ is of the order of 0.1. We shall see that in this region the deviations of the ballistics from that of normal guns can be expressed as linear functions of Ψ. Larger values of Ψ do not appear in practice, at least not in our experience, until we reach values in the range 0.4–0.6. These are obtained in firings of recoilless guns with tubular propellant. When cord is used, rather larger values of Ψ are found. However, cord is but little used in recoilless guns, for a reason that will appear soon.

We may write equation 51 as

$$P\left(U + Ax - \frac{C}{\delta}\right) = C(1 - \Psi)\lambda(1 - f)(1 + \theta' f) \tag{53}$$

where

$$\theta' = \frac{\theta}{1 - \Psi} \tag{54}$$

An orthodox gun with a charge $C(1 - \Psi)$ of propellant with mean force constant λ and form factor θ' would have, instead of equation 53, the equation

$$P\left[U + Ax - \frac{C(1 - \Psi)}{\delta}\right] = C(1 - \Psi)\lambda(1 - f)(1 + \theta' f) \tag{55}$$

which differs from equation 53 in a term that is important only for high densities of loading. Indeed the term $C(1 - \Psi)/\delta$ is correct only at the start of motion in an orthodox gun, this term later increasing to $C(1 - \Psi)\eta$, which is about 60 per cent greater. Thus, up to "all burnt" the leaking gun behaves almost as if it were an orthodox gun with the *same dimensions*, the *smaller charge* $C(1 - \Psi)$, the *bigger form factor*

$\theta' = \theta/(1 - \Psi)$, and a *force constant reduced* as described in an earlier paragraph.

Since θ' is numerically greater than θ, it is clear that a propellant shape that is degressive in an orthodox gun is even more so in a leaking gun—hence the tendency not to use cord in recoilless guns. For the same reason, the virtues of a progressive burning shape are especially pronounced in recoilless guns.

It is also possible to approximate to the recoilless gun by a normal gun with the same charge C, form factor $\theta'/(1 - \Psi)$, and smaller force constant $\lambda(1 - \Psi)$. However, the variation of force constant between different existing propellants is small, and therefore this large change of force constant is rather outside the experience of the working ballistician, unless he is familiar with charges of gunpowder.

The "effective charge,"

$$C' = C(1 - \Psi) = C - \frac{\psi SD}{\beta\lambda^{1/2}} \tag{56}$$

This may be recast into a form that brings out more clearly the significance of the separate terms. We have, from equations 31 and 39,

$$D(1 - f) = \frac{\beta \overline{W}_1 V}{A} \tag{57}$$

and so, if we write V_B for the velocity when the propellant is just burnt,

$$\frac{D}{\beta} = \frac{\overline{W}_1 V_B}{A}$$

For a typical gun, V_B is about 80 to 90 per cent of the muzzle velocity V_E, and so one may use

$$\frac{D}{\beta} = \frac{0.8\overline{W}_1 V_E}{A} \tag{58}$$

For an orthodox gun with an expansion ratio of the order of 5, the energy of the shot at the muzzle is

$$\frac{1}{2} W_1 V_E^2 \simeq \frac{C'RT_0}{3(\gamma - 1)} \simeq \frac{4C'\lambda}{3} \tag{59}$$

Substituting from equations 58 and 59 in equation 56 gives

$$C' = \frac{3}{8}\frac{W_1 V_E^2}{\lambda} + 0.8\,\frac{\psi S \overline{W}_1 V_E}{A\lambda^{1/2}}$$

These terms may be regarded as the "part that pushes" and the "part that leaks," respectively. For a recoilless gun, $S/A \simeq 0.65$, and $\psi \simeq 0.63$, so that

$$C' \simeq \frac{3W_1 V_E^2}{8\lambda} + \frac{\overline{W}_1 V_E}{3\lambda^{1/2}} \tag{60}$$

The second term on the right may be regarded as the charge thrown backwards to balance the muzzle momentum of the shot.

A formula of the same type as equation 60 was used by certain German engineers for the design of recoilless guns and was based on the argument that part of the charge pushes and the rest balances the recoil. Actually the coefficient of $W_1 V_E^2/\lambda$ was taken to be rather greater than $3/8$, and the coefficient of $\overline{W}_1 V_E/\lambda^{1/2}$ was determined by fitting to firings with "reasonable" charges. It can be seen that this is not exact, though it does give a useful guide in preliminary design. The basic reduction to an orthodox gun holds only up to the end of burning. Afterward, as will appear in § 7.39, the pressure-space curve shows a much more rapid drop than in a normal gun. It is clear that the factor $3/8$ ought to be increased on this account, as was indeed done by the Germans. Another reason why this factor ought to be increased when dealing with practical recoilless guns is that, as the charge is larger than in normal guns, the expansion ratio tends to be smaller than normal, and the muzzle energy per unit of effective charge C' is therefore lower than in most orthodox guns.

A formula that is fairly satisfactory up to velocities around 2000 ft/sec is

$$\frac{C}{W} = \frac{x^2}{2} + \frac{x}{2.3} \tag{61}$$

where $x = V_E/(RT_0)^{1/2}$.

It is possible to attack the problem of Lagrange corrections from an empirical standpoint, by starting from an equation of the form of equation 60.

Strecke[9] has constructed a theory based on the assumptions we have used in our present reduction to an orthodox gun: mean gas temperature during burning, rate proportional to pressure, effective covolume equal to the volume of the initial charge, and nozzle opening at the same time as the shot starts. His work is more general in that he uses a shot-start pressure to represent initial resistance, and is more special in that he considers only propellant with constant burning surface. Since he makes considerable use of the balance of momentum during firing, his method is applicable only to fully recoilless guns; the methods given in the present chapter can be used whatever the extent of the leakage.

---

[9] Strecke, *DWM—FMB* no. 13.

In an orthodox gun the muzzle velocity is, for small changes in the charge weight, proportional to the charge to the power n, where n depends on the details of gun, charge, and projectile. A common value for n is 0.7. When there is leakage, the effective charge is $C(1 - \Psi)$. Hence for the effect of a small leak when the charge or web size is not altered, we have

$$V_E \propto (1 - \Psi)^n \simeq 1 - n\Psi \tag{62}$$

in which, it is to be noted, n is certainly nonzero; actually the inefficiency of a leaking gun after "all burnt" causes n to be rather larger than for the orthodox gun with the same "effective" charge.

The peak pressure can be treated similarly. For propellants with θ nearly zero and not too fast a rate of burning, the maximum pressure is, by equation 24A of chapter 4, proportional to the square of the charge; hence,

$$\text{Peak pressure} \propto (1 - \Psi)^2 \simeq 1 - 2\Psi \tag{63}$$

Exceptions to this rule are fast charges, in which the pressure has its peak at "burnt," and charges of cord. These can also be treated by the reduction to a nonleaking gun, followed by the use of the formulas of chapter 4.

The central ballistic parameter of orthodox ballistics is, omitting corrections for pressure gradient,

$$M = \frac{A^2D^2}{\beta^2CWRT_0} \qquad \text{(see equation 15 of chapter 4)}$$

which for small Ψ behaves as

$$M \propto 1 + \Psi \tag{64}$$

An important and useful point is that these ballistic quantities are all linear in Ψ.

When we consider not small Ψ but small changes in a large Ψ, we find that such quantities as $(1/V_E)(dV_E/d\Psi)$ have a factor $(1 - \Psi)$ in their denominators. It follows that recoilless guns, where Ψ is of the order of 0.5, are more than normally sensitive to changes in web size or rate of burning. Furthermore, the lower the velocity, the bigger is Ψ, so that low-performance weapons are the most troublesome in this respect. A factor that enters in all low-pressure guns is the unusually big influence of engraving conditions, since the ratio of shot-start pressure to maximum pressure is large. If we combine these facts, it is easy to see why low-pressure, low-velocity recoilless guns are a headache for the ballistician.

7.37 Numerical integration

The set of equations 49 can always be integrated numerically in a straightforward way. It is convenient to write these equations in terms of nondimensional variables. We write

$$x = l\xi \quad \text{with} \quad l = \frac{U - \frac{C}{\delta}}{A}$$

$$S = \mu A$$

$$t = \frac{ADl}{\beta CRT_0}\tau$$

so that

$$V = \frac{\beta CRT_0}{AD}\frac{d\xi}{d\tau}$$

$$T = T_0T'$$

$$P(t) = \frac{CRT_0\pi(\tau)}{U - \frac{C}{\delta}}$$

and we put

$$M = \frac{A^2D^2}{\beta^2WCRT_0} \quad \text{and} \quad \Psi = \frac{\psi SD}{\beta C(RT_0)^{1/2}} \tag{65}$$

The set 49 becomes

$$\left.\begin{aligned}
\pi(1 + \xi) &= NT'\left(1 + \frac{kCN}{6W}\right) \\
\frac{d^2\xi}{d\tau^2} &= \frac{M\pi}{1 + \frac{kCN}{2W}} \\
\frac{df}{d\tau} &= -\left(\frac{CRT_0}{Al}\right)^{\alpha-1}\pi^\alpha \\
\phi &= (1 - f)(1 + \theta f) \\
\frac{dN}{d\tau} &= \frac{d\phi}{d\tau} - \Psi\pi(T')^{-1/2} \\
\frac{d}{d\tau}(NT') &= -(\bar{\gamma} - 1)\pi\frac{d\xi}{d\tau} + \frac{d\phi}{d\tau} - \gamma\Psi\pi(T')^{1/2}
\end{aligned}\right\} \tag{66}$$

After "all burnt,"

$$\pi\left(\xi + \frac{U - CN\eta}{U - \dfrac{C}{\delta}}\right) = NT'\left(1 + \frac{kCN}{6W}\right) \tag{67}$$

These variables increase the generality of each computed solution. They are also useful in deriving relations of similarity.

The equations can be solved by a step-by-step integration proceeding in steps of equal $\Delta\tau$. The method is straightforward. It is possible to reduce the labor of computation by the following approximations: if we use Δ to denote increments over a step of the integration, and bars to denote mean values over the step,

$$\Delta N = \Delta\phi - \overline{(T')^{-1/2}}\Psi\,\Delta\left(\int \pi\,d\tau\right) \tag{68}$$

$$\Delta(NT') = -\frac{\bar{\gamma} - 1}{2M}\left(1 + \frac{kC\bar{N}}{2W}\right)\Delta\left[\left(\frac{d\xi}{d\tau}\right)^2\right] + \Delta\phi - \gamma\Psi\overline{(T')^{1/2}}\,\Delta\left(\int \pi\,d\tau\right) \tag{69}$$

Since $\overline{(T')^{1/2}}$ and $[1 + (kC\bar{N}/2W)]$ vary only slowly, it is possible to use the same average values for several steps in succession.

Numerical integration is suitable when the nozzle throat area S is varying during the firing or when bore resistance has to be taken into account; an example where both points arise is the treatment of a worn gun (§ 7.5). The set of equations 66 is easily modified to include bore-resistance terms. Numerical integration seems to be necessary also when α the pressure index of the rate of burning differs substantially from unity. This occurs most noticeably at low pressures (see the discussion of § 2.37). The class of recoilless guns does, however, include quite a large number with peak pressures as low as 1 to 2 tons/sq in.

Numerical integration can always be carried out, no matter how one may choose to represent initial resistance. The integration need not be carried past "burnt." An analytical solution of ample accuracy is available for the period after "burnt" and is explained in § 7.39.

We see that the leakage introduces two new parameters into the ballistic equations: (1) Ψ, which is a constant if the throat area is constant during the firing; (2) the epoch of opening of the nozzle.

7.38 Solution with linear rate of burning

A more rapid method than numerical integration can be used if $\alpha = 1$. This has been built up in a semiempirical manner by a study of a large number of numerical integrations and offers a considerable saving of time. We assume that the throat area S is independent of time, and the initial conditions are represented by nozzle-start and shot-start pressures. We denote conditions at these epochs by suffixes NS and SS.

We shall work in ordinary units except that the temperature T will be written as T_0T'. The equations of the system are

$$D\frac{df}{dt} = -\beta P \tag{70}$$

$$\phi = (1 - f)(1 + \theta f) \tag{71}$$

$$P\left(U + Ax - \frac{C}{\delta}\right) = CNRT_0T'\left(1 + \frac{kCN}{6W}\right) \tag{72}$$

$$W_1V\frac{dV}{dt} = AP \tag{73}$$

$$W_1 = W + \tfrac{1}{2}kCN \tag{74}$$

$$\frac{dN}{dt} = \frac{d\phi}{dt} - \frac{\psi SP}{C(RT_0)^{1/2}}(T')^{-1/2} \tag{75}$$

$$\frac{d}{dt}(NT') = -\frac{\bar{\gamma} - 1}{2CRT_0}\frac{d}{dt}(W_1V^2) + \frac{d\phi}{dt} - \frac{\gamma\psi SP(T')^{1/2}}{C(RT_0)^{1/2}} \tag{76}$$

Eliminating P from equations 70 and 75 and integrating gives

$$N = \phi + \frac{\psi SD}{\beta C(RT_0)^{1/2}}\frac{(f - f_{NS})}{\nu_1}$$

where

$$\frac{1}{\nu_1} = \frac{1}{(f - f_{NS})}\int_{f_{NS}}^{f}(T')^{-1/2}\,df$$

It is convenient to write, as in § 7.36,

$$\Psi = \frac{\psi SD}{\beta C(RT_0)^{1/2}} \tag{77}$$

leading to

$$N = \phi + \frac{\Psi(f - f_{NS})}{\nu_1} \tag{78}$$

Inspection of a number of accurate solutions has shown that it is sufficiently accurate to take

$$\nu_1 = \tfrac{1}{4}[1 + 3(T')^{1/2}] \tag{79}$$

From equations 70 and 73,

$$V = \frac{AD}{\beta \overline{W}_1}(f_{SS} - f)$$

or, with the central ballistic parameter,

$$M = \frac{A^2D^2}{\beta^2 WCRT_0} \tag{80}$$

we have

$$V^2 = \frac{MCRT_0W(f_{SS} - f)^2}{(\overline{W}_1)^2}$$

This holds from "shot-start" to "burnt." It is sufficient to take for $\overline{W}_1$ over any interval the mean of the values of W_1 at the ends of the interval, so that

$$V^2 = \frac{MCRT_0(f_{SS} - f)^2}{W_1} \tag{81}$$

A relation which is useful in practice is

$$\frac{M}{\Psi^2} = \left(\frac{A}{\psi S}\right)^2 \frac{C}{W} \tag{82}$$

From equations 70 and 76,

$$NT' = (NT')_{NS} + \phi - \phi_{NS} - \frac{(\bar{\gamma} - 1)W_1V^2}{2CRT_0} + \gamma\Psi(f - f_{NS})\nu_2$$

where

$$\nu_2 = \frac{1}{f - f_{NS}} \int_{f_{NS}}^{f} (T')^{1/2}\, df$$

Since $N = \phi$ at nozzle start, and T'_{NS} is accurately unity if $P_{NS} \leq P_{SS}$ and never far from unity under any conditions,

$$NT' = \phi - \frac{(\bar{\gamma} - 1)W_1V^2}{2CRT_0} + \gamma\Psi(f - f_{NS})\nu_2$$

which with equations 78 and 81 reduces to

$$T'\left[\phi + \frac{(\gamma - 1)\Psi(f_{NS} - f)}{\nu_3}\right] = \phi - \frac{\bar{\gamma} - 1}{2} M(f_{SS} - f)^2 \tag{83}$$

where

$$\frac{\gamma - 1}{\nu_3} = \frac{\gamma\nu_2}{T'} - \frac{1}{\nu_1}$$

Equation 83 holds after the opening of the nozzle. If the shot starts first, equation 83 is used, until the nozzle opens, with $\Psi = 0$.

We need also a relation between the travel and the fraction of charge burnt. Eliminating P from equations 72 and 73 yields

$$\frac{A\,dx}{U + Ax - \dfrac{C}{\delta}} = \frac{W_1 V\,dV}{CNRT_0T'\left(1 + \dfrac{kCN}{6W}\right)}$$

$$= -\left(\frac{AD}{\beta\overline{W}_1}\right)^2 \frac{W_1(f_{SS} - f)\,df}{CRT_0\left(1 + \dfrac{kCN}{6W}\right)NT'}$$

so that

$$\int \frac{A\,dx}{U + Ax - \dfrac{C}{\delta}} = -\left(\frac{AD}{\beta}\right)^2 \frac{1}{CWRT_0\nu_4} \int \frac{(f_{SS} - f)\,df}{N} \tag{84}$$

where ν_4 is a certain average reduced temperature.

This result is true whether shot start occurs before or after the opening of the nozzle. We must now distinguish between these two cases.

Case A. $\boldsymbol{P_{NS} \leqq P_{SS}}$

In this case N is given by equation 78 for the whole of the period of motion of the shot. Substituting into equation 84 and integrating from shot start onward yields

$$\ln\left(1 + \frac{Ax}{U - \dfrac{C}{\delta}}\right) = \frac{MI}{\nu_4} \tag{85}$$

where

$$I = \int_f^{f_{SS}} \frac{(f_{SS} - f)\,df}{\phi - \dfrac{\Psi(f_{NS} - f)}{\nu_1}}$$

In the integrand ν_1 is a function of T', and to make progress one must average ν_1. We find that, writing the average value of Ψ/ν_1 as Ω, *For* $\theta \neq 0$:

$$I = \frac{1}{2\theta} \ln \left[\frac{1 - \Omega f_{NS} + (\theta + \Omega - 1) f_{SS} - \theta f_{SS}^2}{1 - \Omega f_{NS} + (\theta + \Omega - 1) f - \theta f^2} \right]$$
$$+ \frac{\theta + \Omega - 1 - 2\theta f_{SS}}{[4\theta(1 - \Omega f_{NS}) + (\theta + \Omega - 1)^2]^{\frac{1}{2}}}$$
$$\times \left[\tanh^{-1} \left\{ \frac{2\theta f - (\theta + \Omega - 1)}{[4\theta(1 - \Omega f_{NS}) + (\theta + \Omega - 1)^2]^{\frac{1}{2}}} \right\} \right.$$
$$\left. - \tanh^{-1} \left\{ \frac{2\theta f_{SS} - (\theta + \Omega - 1)}{[4\theta(1 - \Omega f_{NS}) + (\theta + \Omega - 1)^2]^{\frac{1}{2}}} \right\} \right] \tag{86}$$

This is true only if the arguments of the $\tanh^{-1}$ terms are less than unity. Where any argument is greater than unity, $\tanh^{-1}$ should be replaced by $\coth^{-1}$.

For $\theta = 0$:

$$I = \frac{f_{SS} - f}{1 - \Omega} - \frac{[1 - \Omega f_{NS} - (1 - \Omega) f_{SS}]}{(1 - \Omega)^2} \ln \left[\frac{1 - \Omega f_{NS} - (1 - \Omega) f}{1 - \Omega f_{NS} - (1 - \Omega) f_{SS}} \right] \tag{87}$$

We have found that pressures correct to a few per cent can be obtained by taking

$$1 - \nu_4 = \frac{50(1 - T')^2(T' - 0.78)}{1 + 2.5(1 - T')} \tag{88}$$

$$\Omega = \frac{2\Psi}{3(T')^{\frac{1}{2}} - 1} \tag{89}$$

The fact that ν_4 is greater than unity for T' less than 0.78 is due to Ω being least accurate in this region. The pair of formulas 88 and 89 have been chosen to compensate for each other's deficiencies even at these low temperatures. The integral I becomes infinite for $\Omega = 1$ and correspondingly sensitive to Ω if Ω is near unity. This approximate method is unreliable for Ω greater than 0.8. In such cases the pressure-space curve is very flat, and it is better to integrate equation 73 in large steps, using equation 81 and mean values of P; one finds x thereby, and P from equation 72, correcting the integration if necessary. This is much simpler than carrying out the numerical integration of the full set of equations, though the process is of course restricted to fairly flat pressure-space curves. The process was suggested by Mr. T. Vickers.

Case B. $P_{NS} > P_{SS}$

Before the opening of the nozzle $N = \phi$, and so

$$\ln\left(1 + \frac{Ax}{U - \frac{C}{\delta}}\right) = \frac{I(\Omega = 0)}{\nu_4} \tag{90}$$

After nozzle opening N is taken from equation 78 and

$$\ln\left(\frac{U - \frac{C}{\delta} + Ax}{U - \frac{C}{\delta} + Ax_{NS}}\right) = \frac{MJ}{\nu_4} \tag{91}$$

where

$$J = \int_f^{f_{NS}} \frac{(f_{SS} - f)\,df}{\phi - \frac{\Psi(f_{NS} - f)}{\nu_1}}$$

This integral can be evaluated:

For $\theta \neq 0$:

$$\begin{aligned} J = {} & \frac{1}{2\theta}\ln\left[\frac{1 + (\theta - 1)f_{NS} - \theta f_{NS}{}^2}{1 - \Omega f_{NS} + (\theta + \Omega - 1)f - \theta f^2}\right] \\ & + \frac{\theta + \Omega - 1 - 2\theta f_{SS}}{[4\theta(1 - \Omega f_{NS}) + (\theta + \Omega - 1)^2]^{1/2}} \\ & \times \left[\tanh^{-1}\left\{\frac{2\theta f - (\theta + \Omega - 1)}{[4\theta(1 - \Omega f_{NS}) + (\theta + \Omega - 1)^2]^{1/2}}\right\}\right. \\ & \left. - \tanh^{-1}\left\{\frac{2\theta f_{NS} - (\theta + \Omega - 1)}{[4\theta(1 - \Omega f_{NS}) + (\theta + \Omega - 1)^2]^{1/2}}\right\}\right] \end{aligned} \tag{92}$$

For $\theta = 0$:

$$J = \frac{f_{NS} - f}{1 - \Omega} - \frac{[1 - \Omega f_{NS} - (1 - \Omega)f_{SS}]}{(1 - \Omega)^2}\ln\left[\frac{1 - \Omega f_{NS} - (1 - \Omega)f}{1 - f_{NS}}\right] \tag{93}$$

with the usual caution about the replacement of $\tanh^{-1}$ by $\coth^{-1}$ if the argument is greater than unity.

We give now a summary of the use of these equations. We have introduced various mean values such as Ω and the ν's, and we shall give rules for their estimation. These were derived by analysis of a number of accurate solutions for various initial conditions, and it is not suggested that they are the only rules that will work. However, these formulas are simple, and our experience has shown that pressures, velocities, and travels can be computed in this way to within 3 per cent. This is sufficiently accurate for routine ballistic calculations, being usually less than the error arising from uncertainties in the nozzle-start and shot-start pressures.

Case A. $P_{NS} \leq P_{SS}$

Solution at nozzle start. Equation 72 with $P = P_{NS}$, $T' = 1$, and $x = 0$ gives $N_{NS} = \phi_{NS}$. From equation 71 we derive f_{NS}.

Solution at shot start. We guess T'_{SS}. Equation 72 with $P = P_{SS}$ and $x = 0$ gives N_{SS}. If we calculate ν_1 from equation 79, ϕ_{SS} and f_{SS} follow from equations 71 and 78. We take, in this part of the computation,

$$\nu_3 = 1 - \frac{6(1 - T')}{2 + 10^3(1 - T')^3} \tag{94}$$

and obtain T'_{SS} from equation 83 with $V = 0$. The process is now repeated until a self-consistent set of values is reached.

Solution for any desired f less than f_{SS}. We guess T' at this value of f. We estimate ν_3 here as

$$\nu_3 = 1.75T' - 0.75 \tag{95}$$

and then T' can be calculated from equation 83. We repeat until the results are self-consistent.

To calculate the corresponding travel we use equations 88, 89, and 85, with either equation 86 or 87. N can then be computed from equations 78 and 79 and the pressure calculated from equation 72.

Maximum pressure. By calculating the pressure at three or four evenly spaced values of f, the maximum pressure can be found by interpolation.

Case B. $P_{NS} > P_{SS}$

Solution at shot start. Equation 72 with $P = P_{SS}$, $x = 0$, and $T' = 1$ gives $\phi_{SS} = N_{SS}$, and f_{SS} follows from equation 71.

Solution at nozzle start. We guess f_{NS}, obtaining V from equation 81, $\phi = N$ from equation 71, T' from equation 83 with $\Psi = 0$, and x from equation 90 with ν_0 from equation 88. The pressure can now be calculated from equation 72. We repeat with other values of f and interpolate for $P = P_{NS}$.

Solution after nozzle start. The only difference from the procedure in case A is that equations 92 and 93 replace equations 86 and 87.

7.39 Solution after "burnt"

This is so much simpler than the problem during burning that an approximate analytical solution can be derived by modifying the method used for the same period in the orthodox gun.

From the exact equations, we have

$$\frac{d}{dt}(NT') = -(\bar{\gamma} - 1)\frac{AP}{CRT_0}\frac{dx}{dt} - \frac{\gamma\psi SP(T')^{1/2}}{C(RT_0)^{1/2}}$$

$$= -\frac{KNT'A}{U + Ax - CN\eta}\frac{dx}{dt} \tag{96}$$

where

$$K = \left(1 + \frac{kCN}{6W}\right)\left[\bar{\gamma} - 1 + \frac{\gamma\psi S(T')^{1/2}(RT_0)^{1/2}}{AV}\right] \tag{97}$$

Let suffix B denote conditions at "all burnt." We can integrate equation 96 by taking mean values of K and $\eta CN/U$, giving

$$\log\left[\frac{NT'}{(NT')_B}\right] = \bar{K}\log\left(\frac{U + Ax_B - C\bar{N}\eta}{U + Ax - C\bar{N}\eta}\right) \tag{98}$$

We can write equation 96 in the alternative form

$$\frac{d}{dt}(NT') = -\frac{KAPV}{CRT_0\left(1 + \dfrac{kCN}{6W}\right)} = -\frac{KW_1V}{CRT_0\left(1 + \dfrac{kCN}{6W}\right)}\frac{dV}{dt}$$

leading to

$$V^2 - V_B{}^2 = \frac{2CRT_0}{\bar{K}(W + \frac{1}{3}kC\bar{N})}[(NT')_B - NT'] \tag{99}$$

Finally,

$$\frac{dN}{dt} = -\frac{\psi SW_1(T')^{-1/2}}{AC(RT_0)^{1/2}}\frac{dV}{dt}$$

giving

$$N_B - N = \psi\frac{S}{A}\frac{\bar{W}_1}{C(RT_0)^{1/2}}\overline{(T')^{-1/2}}(V - V_B) \tag{100}$$

From these equations can be calculated close approximations to the conditions at any desired travel after "burnt," and in particular the muzzle velocity is easily derived. The detailed working runs thus. We know T_B', x_B, V_B, and N_B, from which we compute K_B. We guess $(T')^{1/2}$ and V and N at the assigned value of x. K follows from equation 97, and we take

$$\bar{K} = \tfrac{1}{2}(K_B + K)$$

$$\bar{N} = \tfrac{1}{2}(N_B + N)$$

then obtaining NT' from equation 98. We calculate $W + kC\bar{N}/3$ from $\bar{N}$ and then find V from equation 99. Finally, N is obtained from equation 100, using the mean value

$$\overline{(T')^{-1/2}} = \tfrac{1}{2}[(T')_B^{-1/2} + (T')^{-1/2}]$$

The cycle is repeated until self-consistent. The number of cycles necessary depends on the success of the first guess but is normally two.

Errors in V, N, and T' in a typical calculation of this type for a fully recoilless gun were found to be 0.2, -4, and -16 per cent, respectively, of the change from "burnt" to "shot-ejection," that is, about 0.1, -2, and -5 per cent, respectively, of the values at ejection. The error in muzzle velocity is only a few feet per second, which is usually a trivial price to pay for the reduction of computation effected by this method.

The shape of the pressure-space curve during the adiabatic expansion, which in ordinary guns is determined by $\bar{\gamma} - 1$, is settled here by the quantity $\bar{K}$. For a typical recoilless gun $\bar{K}$ is of the order of 2, whereas $\bar{\gamma} - 1$ is only about 0.3; hence, after "all burnt" the pressure-space curve falls much more rapidly than in an orthodox gun.

The process of successive approximations given previously fails to converge if the expansion goes so far that almost all the gas passes through the vent before the shot reaches the muzzle. In such cases the change in K from "burnt" to "ejection" is so large that it is not possible to reach the muzzle in one step of computation. There is no reason, however, why one should not divide the process into several steps, each taking as its initial conditions the final results of the previous step. Although expansion down to almost zero pressure and temperature is an inefficient way of using a gun, it does occur in practice in low-velocity rounds from a recoilless howitzer, such as that shown in Fig. 7.2. When such a gun, giving about 1000 ft/sec at top charge, is fired at a velocity of about 400 ft/sec, we have the following circumstances: to be sure of starting the shot, the peak pressure must be near 4 tons/sq in.; therefore, to keep down the muzzle velocity to 400 ft/sec, the charge must burn out very rapidly; hence, there is a long travel after "burnt," during which T' falls greatly; because V is small, K is large at "burnt"; because $(T')^{1/2}$ is small when the shot reaches the muzzle, K is then small; hence, this is a case where K varies greatly between "burnt" and "ejection," and this interval must be broken into two or three steps. Of course, the muzzle velocity in such cases can be estimated from equation 99 with $NT' = 0$, provided again that one can estimate $\bar{K}$. If the gain in energy of the shot after "burnt" is sufficiently small, the uncertainty in $\bar{K}$ will lead to an uncertainty in the muzzle velocity, which is adequate for many purposes. It should be remembered that such low-velocity results are very sensitive to the initial conditions assumed in the calculations, so that analysis of such firings is at best a tricky business.

The formulas of this section are useful when it is proposed to drill the gun near the muzzle. This has been suggested, from time to time, as a cure for various difficulties. The effect on muzzle velocity can be found by the formulas given previously, the initial conditions being taken to be those computed by orthodox ballistics for the shot position at which venting starts. Questions involving that old favorite, the smooth-bore muzzle extension, can be treated in the same way.

7.4 Gas leakage in a smooth-bore mortar

The history of the "mortar" is long, and an attempt to define this class is further complicated by the name having been debased through its use for many of the more exotic weapons developed in World War II. For our present purpose we restrict attention to what is really only one subclass but is in fact much the most important. This is the muzzle-loading, smooth-bore mortar. The same treatment could be applied to any smooth-bore gun without obturating device on the projectile. The only smooth-bore gun that is at all common is, however, the infantry mortar.

The question discussed here arises from the weapon being in use in such great numbers. Mortar bombs are produced in quantities that, although small compared with the astronomical totals of small arms ammunition, are much larger than any other type of artillery projectile. This means that in wartime there is a constant urge to speed production by relaxing tolerances in the specification. This results in a larger number of bombs, which, unfortunately, have a bigger dispersion at the target. The net result may or may not be an improvement. One step toward a decision is to know how the tolerances on the weight and dimensions of the bomb are connected with the dispersions of muzzle velocity and range. Here we shall discuss only the former.

The connection between weight of bomb and muzzle velocity can be calculated from the simple ballistic theory of chapter 4, and it is unnecessary to repeat what was said there. Tolerances on bomb dimensions lead to variations in two ballistic parameters. The first is the effective chamber volume, which depends on the position of the guide band on the body and on the shape of the body behind the band. Surprisingly large variations do occur in the chamber volume as a result. The associated dispersion of velocity can be found by the equations of chapter 4. The second and more important effect of dimensional changes is the variation of the leakage between bomb and mortar. This leakage is controlled by the diameter of the "guide band" of the bomb.

To study this problem it is convenient to begin by combining all mortars in a single expression.

Let V now denote the muzzle velocity, with other notation as before. The loss of velocity ΔV due to a leakage area S, constant during travel, is given, according to § 7.36, by

$$\frac{\Delta V}{V} = -n\Psi = -n\,\frac{\psi SD}{\beta C\lambda^{1/2}} \tag{101}$$

where n varies somewhat with details of gun and charge but is usually around 0.7. Furthermore,

$$\frac{D}{\beta} = \frac{WV_B}{A} = \frac{mWV}{A}$$

with m around 0.8–0.9. Also,

$$C = q(\gamma - 1)\,\frac{WV^2}{\lambda}$$

where q depends a little on the ballistic details and is about $1\frac{1}{2}$. To sum up, equation 101 yields

$$\Delta V = -\frac{\epsilon S}{A} \tag{102}$$

where ϵ is of the order of 2000 ft/sec and varies with the propellant used and with such matters as the expansion ratios at "burnt" and "ejection." The possible variation in ϵ is a factor of 2, if all the variables are given their extreme values. As a matter of fact, experience suggests that the differences between various types of mortar are smaller than the variety seen in "real" artillery. For many purposes ϵ can be taken to be the same for all mortars.

When the bore area A remains unaltered and the diameter of the projectile is reduced to create the leakage area S, the accelerating force on the bomb (at equal pressures) falls in the ratio $(A - S)/A$. This causes a further drop in velocity, which is approximately $VS/2A$ and may be regarded as included in equation 102 if ϵ is allowed to depend on velocity. Since the leakage ϵ is much larger than $V/2$, ϵ is only a slowly varying function of velocity, and the ratio $A\,\Delta V/S$ is practically the same for all mortars. This is a most useful result.

To carry the matter further, a calculation was made of the effect of leakage on a typical 8-cm mortar. The methods used were those explained in §§ 7.38 and 7.39. The following data were used: shot weight 10 lb, total travel 35 in., bore area 8.09 sq in. A charge of $3\frac{1}{2}$ oz of mortar propellant gave a calculated pressure (at zero leakage) of 2.54

tons/sq in. piezo, "all burnt" at 13.8 in. travel, and a muzzle velocity of 767 ft/sec.

A solution was then computed for a bomb diameter of 3.16 in., corresponding to a clearance of 0.049 in. in diameter. It was assumed that $\psi = 0.55$; that is, the leakage was taken to be 17 per cent less than the theoretical value for no friction. This, it will appear, is a fairly good estimate of the resistance to flow past the guide band of the bomb.

The velocity was found to be 690 ft/sec. About 15 per cent of this drop is due to the reduced area of the projectile, the rest to the leakage. At "burnt" 12 per cent of the charge has escaped, and, when the shot is at the muzzle, 18 per cent has leaked away.

These results give $\epsilon = 2500$ ft/sec for the constant of equation 102. We may rewrite this equation in another form. Let d be the caliber of the mortar and Δd the clearance, on diameter, between bomb and mortar. Then,

$$\Delta V = -2\epsilon \frac{\Delta d}{d} \tag{103}$$

A value of 2500 ft/sec for ϵ is seen, from equation 101, to be reasonable if n is about 1; this is greater than the 0.7 that would be expected from our reduction to an "effective charge" acting in an orthodox gun. The reason is that this reduction is true only up to "burnt," after which the leaking gun is relatively less efficient.

For this mortar,

$$\frac{\Delta V}{\Delta d} = -1.57 \text{ (ft/sec) per (thousandth inch)} \tag{104}$$

This is a convenient unit for practical calculations. Suppose, for example, that the bombs have a mean deviation in diameter of 0.002 in.; assuming a rectangular frequency distribution, which is a fair approximation, this mean deviation corresponds to a total tolerance of 0.008 in. on the diameters of accepted bombs. This gives an md in velocity of 3.1 ft/sec, which is a substantial part of the observed deviations. The associated range dispersion can be estimated from the known range for such a bomb at a velocity of this order. It can be taken that the bomb would give about 3300 yards at 700 ft/sec. Working back via the ballistic coefficient, the mean deviation in range is found to be about 21 yards, and the 50 per cent zone is 37 yards.

There is some experimental evidence to check these calculations. Statistical analyses have been made of firings in 6-cm, 8-cm, and 10.5-cm mortars. It is convenient to reduce the observed rate of change of velocity with bomb diameter to what it would be in a caliber of 8.1 cm, for comparison with equation 104. The 10.5-cm mortar firings gave, when reduced to 8-cm caliber, 1.54 (ft/sec) per (10^{-3} in.). A trial in an 8-cm mortar was shown by the present writer to yield 1.7 (ft/sec) per (10^{-3} in.). Finally, American firings of a 6-cm mortar have given a mean value of 1.6 (ft/sec) per (10^{-3} in.). These three sets of results are in excellent agreement with each other and with the theoretical value, showing that the coefficient ϵ of equations 102 and 103 is indeed insensitive to the details of the interior ballistics. That it is little altered by changes of muzzle velocity (within the practical range for mortars) has been verified by computation and is supported by the experimental results for the 6-cm mortar with three of its standard charges: the regression coefficients were 1.3, 1.8, and 1.4 (ft/sec) per (10^{-3} in.) (when converted to 8-cm caliber), in which no statistically significant trend can be seen.

Guide bands of mortar bombs are often given a series of circumferential grooves, whose function is usually stated to be the reduction of gas leakage by the setting up of turbulence. Of the three mortars quoted previously, only the 6-cm has grooved bombs, but ϵ does not show any diminution on that account. This and the fact that $\psi = 0.55$ gives good agreement with observation suggest that the flow past the band suffers a good deal of resistance, even when the band is ungrooved, and a few more grooves make little difference.

7.5 The ballistics of a worn gun

In a gun firing separate-loading ammunition, the gradual wearing of the gun is reflected in an increased length of ramming. The ballistic effects are due to the extra chamber capacity and a rather smaller engraving resistance. Gas leakage is very small, and the drop of ballistics in a worn gun can be calculated quite well from the two effects mentioned.

When the gun fires fixed ammunition, the situation is quite different. Figure 7.4 shows the relative dimensions of lands and grooves of the bore and the driving band in a very badly eroded gun. The scales are, of course, different in the axial and radial directions. The new gun conditions are shown for comparison.

The propellant used during most of the life of this gun had the relatively high explosion temperature of about 3300°K. This is responsible for the marked concentration of wear near the commencement of rifling. Cooler propellants give a wear that is more evenly distributed than that shown here, though there is always most wear near the commencement of rifling (C of R).

In the new gun the undeformed band engages the shot seating slope at a point 0.13 caliber back from the C of R. The length of the cartridge case is arranged to bring the band almost to this position. When the pressure in the cartridge case rises, the crimping of the case to the shot fails, and the band of the projectile engraves after an extremely short free run. The pressure needed to release the shot from the case is small by ballistic standards, of the order of $\frac{1}{10}$ ton/sq in.

In a gun worn to the extent shown in Fig. 7.4 the case positions the shot at the same point as before. On its release from the case the projectile travels about 2.7 calibers before the band meets the lands; during this period, which occupies a relatively long time by reason of the low velocity of the projectile, the gas is able to leak between the band and the walls of the bore. Even after the band has engaged the rifling, there is a considerable travel, approaching 2 calibers, during which gas may still escape down the grooves. This leakage lowers peak pressure and muzzle velocity, and it is these aspects that we shall now discuss, but the erosive effects have equal practical importance.

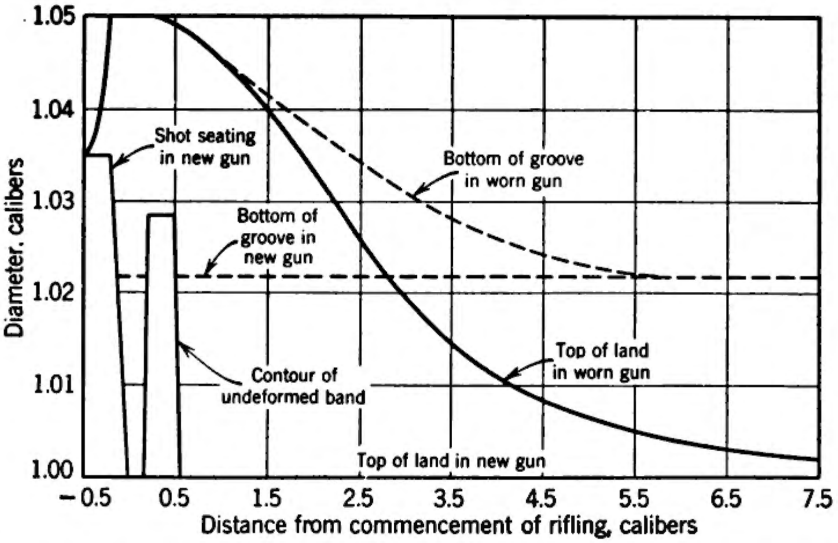

FIG. 7.4 The grooves and lands of the bore in new and badly worn guns firing fixed ammunition with a propellant of high explosion temperature. Note the difference of scale in radial and axial directions. The contour, before engraving, of the driving band of the normal shot is also shown.

The loss of ballistics as a gun wears is also due in part to the loss of initial resistance and to the enlargement of chamber capacity. We shall sketch a theoretical analysis, based on the equations of a leaking gun developed earlier in this chapter, of some trials designed to separate these effects. The peak pressure and muzzle velocity were measured in a new gun and in the gun whose wear curve is shown in Fig. 7.4, when firing (*a*) normal shot with band as shown in Fig. 7.4, and (*b*) special shot, designed to fit this particular worn bore and of such a form that it seemed plausible that gas leakage was prevented, while at the same time but little change was caused in the resistance to motion. These latter projectiles differed slightly from the normal shot in weight and in protrusion into the cartridge case. Assuming that gas leakage was negligible for normal projectiles in a new bore, the ordinary methods of interior ballistics were used to correct the "new-gun" performance to what it would have been if these heavier and bulkier special shot had been fired. This correction amounted to only a few feet per second and about 0.7 ton/sq in. To sum up, the experimental data available were pressure and velocity in the worn gun with gas leakage and pressure and velocity in the new and worn guns with, it was hoped, no gas escape. From these data it is possible, by a theoretical analysis, to check whether any substantial leakage did occur, and to throw some light on the initial resistance to motion of the shot. We give first (§ 7.51) the equations used in problems of this type, then (§ 7.52) the observations and a theoretical discussion, followed (§ 7.53) by a note on some other aspects of the ballistics of worn guns.

7.51 Equations of interior ballistics of a worn gun

7.511 Basic assumptions

We shall explain the assumptions made, and then any new notation, and lastly the equations will be written down. The terms that arise from the gas leakage are taken from § 7.34. The only special point to be noticed is that the leakage passages open from the base of the shot instead of from the breech as in a recoilless gun. We allow for this by using the pressure at the shot base in the formula for the rate of leakage. Frictional losses in the leakage channels are taken into account in the following equations; so are covolume effects, except in the rate of flow through the leakage area. In our example this effect amounts to about 2 per cent at the average pressure while leakage is occurring.

We assume that most of the propellant stays in the chamber for the greater part of the time of burning; that is, the pressure under which it burns is the breech pressure. This question has been mentioned in earlier chapters and is more fully discussed in § 9.51.

Bore resistance, expressed as an equivalent pressure, is included in the equations. The bore area and the area of the base of the shot are written as functions of the travel.

7.512 Notation

Let x be the travel of the projectile up to time t, and $S(x)$ the leakage area between shot and bore. We write $A_0(x)$ for the maximum area of any normal cross section of the shot; A_0 is a function of the travel because the deformation of the band takes place over a considerable travel in a worn gun. Let the volume behind the shot be $U + xA'(x)$. The form $U + xA'(x)$ is convenient for computation, since $A'(x)$ is a slowly varying function, which need be tabulated only at fairly wide intervals; for a new gun A' is constant, being equal to the bore cross section A''; in a worn gun $A'(x)$ has to be computed from the wear curve, such as that in Fig. 7.4, but, once the shot has reached a practically unworn part of the bore, it is possible to write the volume as $U' + xA''$, where U' is a new constant, somewhat larger than U. The computation can then be carried along without reference to tables of $A'(x)$.

Other notation is the same as in earlier parts of this chapter. It is perhaps worth repeating that $P(t)$ is written for the breech pressure, whereas $T(t)$ is the space-mean temperature of the propellant gases.

7.513 Equations of the problem

We have, as usual,

$$\phi = (1 - f)(1 + \theta f) \tag{105}$$

and

$$D\frac{df}{dt} = -\beta P^{\alpha} \tag{106}$$

Let

$$F = (1 - f)(2 - \theta + 3\theta f) \tag{107}$$

We shall assume that the pressure gradient down the bore is such that

$$\frac{P\text{ (chamber)}}{P\text{ (shot)}} = 1 + \frac{C}{2W}F \tag{108}$$

which may be compared with the classical result

$$\frac{P\text{(chamber)}}{P\text{(shot)}} = 1 + \frac{C}{2W} \tag{109}$$

For $\theta = 0$, $F = 2\phi$, so that it is possible for equations 108 and 109 to differ considerably in the early stages of the motion.

Equation 108 has a theoretical origin and was suggested by Mr. E. P. Hicks and Mr. C. K. Thornhill. We cannot enter here into a discussion of its derivation and the experimental backing. At "burnt," $f = 0$, equation 108 gives

$$\frac{P(\text{chamber})}{P(\text{shot})} = 1 + \frac{C}{2W}(2 - \theta) \tag{110}$$

After this epoch equation 109 seems to be more satisfactory. If the transition from equation 108 to equation 109 is carried out at $f = 0$, we have a discontinuity of pressure, except for a charge of cord. This is due to the deficiencies of equation 108 in the later stages of burning. To eliminate this discontinuity and reduce computation, we have used equation 108 only until $F = 1$, with equation 109 thereafter. In our example this occurs when the charge is roughly half burnt, near the time of maximum pressure.

The effect of this novel Lagrange correction is discussed in § 7.521; it may be said here, however, that the effects on the peak pressure and muzzle velocity are almost the same as those of a change in the rate of burning β. The differences in the details of the solution are most marked for small F, that is, in the earliest stages of the motion. As this is the most important period in regard to gas leakage, it was thought to be worth while to use this elaborate Lagrange correction. The form is intractable for analytical work, but as our treatment of this problem is completely numerical, the form is not particularly inconvenient in the present context.

The equation of motion of the shot is

$$W\frac{d^2x}{dt^2} = \frac{PA_0(x)}{1 + \dfrac{CF}{2W}} - A_0(x)B(x) \tag{111}$$

where $A_0(x)B(x)$ is the resistance to motion of the shot; $B(x)$ is a pressure, introduced to make the magnitude of the resistance more easily visualized. The equation of state of the gas in the gun is

$$P\left[U + xA'(x) - \frac{C}{\delta} - C\left(N\eta - \frac{\phi}{\delta}\right)\right] = CNRT\frac{1 + \dfrac{CF}{2W}}{1 + \dfrac{CF}{6W}} \tag{112}$$

where the term $[1 + (CF/2W)]/[1 + (CF/3W)]$ appears because P is the breech pressure and here has to be corrected to the space-mean pressure.

The equation expressing the leakage of gas past the shot is

$$\begin{aligned}\frac{dN}{dt} &= \frac{d\phi}{dt} - \frac{\psi S(x)}{C}\left(\frac{P}{(RT)^{1/2}}\right)_{\text{shot}} \\ &= \frac{d\phi}{dt} - \frac{\psi SP}{C(RT)^{1/2}}\left[1 - \frac{(2\gamma+1)}{6\gamma}\frac{CF}{W}\right] \qquad (113)\end{aligned}$$

The "discharge coefficient" ψ is a dimensionless factor, which depends on the smoothness and shape of the leakage channels. For flow without resistance, ψ lies within 1 per cent of 0.66 for all modern propellants (§ 7.2). The passages through which the gas escapes in a worn gun are only moderately rough, from a hydrodynamic point of view, and, therefore, we have assumed a value of $\psi = 0.6$ in our numerical calculations. When $(1 - f)(3\theta f + 2 - \theta) > 1$, we replace F in equation 113 by unity. This also applies to equation 114, which follows.

Finally we come to the equation that relates the cooling of the gas to the work done on the shot, on the bore resistance, and on the escaping gas. This equation is

$$\begin{aligned}\frac{d}{dt}(NT) = T_0\frac{d\phi}{dt} - \frac{\bar{\gamma}-1}{CR}\frac{d}{dt}\left(\frac{WV^2}{2} + \frac{CFV^2}{6}\right) - \frac{(\gamma-1)A_0(x)B(x)V}{CR} \\ - \frac{\gamma\psi SP(RT)^{1/2}}{CR}\left[1 - \frac{(2\gamma+1)CF}{6\gamma W}\right] \qquad (114)\end{aligned}$$

We have written $\bar{\gamma}$ in the kinetic-energy term to denote that an allowance for heat losses may be included.

The equations to be solved are equations 105, 106, 107, 111, 112, 113, and 114. This can always be done by numerical integration in steps of t. Certain auxiliary functions have to be known: $A_0(x)$ and $A'(x)$ have to be computed from the internal shape of the gun and the height of the band; $B(x)$, related to the bore resistance, must also be assumed. The computations themselves are quite straightforward.

7.514 Solution after "all burnt"

It will usually happen that "all burnt" occurs when the projectile is in an effectively unworn section of the bore. The rest of the motion can then be solved analytically instead of by a numerical process, provided that the bore resistance is constant during this part of the motion. Let suffix B refer to quantities at "burnt." In this part of the travel the volume behind the shot can be written as $U' + xA''$, where A'' is the cross-sectional area of an unworn bore and U' is a constant. A'' is also the value of $A_0(x)$ in this region. We write

$$\nu = (U' + xA'' - CN_B\eta)^{\bar{\gamma}-1} \tag{115}$$

It can be shown that

$$(W + \tfrac{1}{3}C)(V^2 - V_B{}^2)$$
$$= \left[\frac{2CN_BRT_B}{\bar{\gamma} - 1} - \frac{2B(U' + x_BA'' - CN_B\eta)}{\bar{\gamma}(\bar{\gamma} - 1)}\left\{\bar{\gamma} - \gamma + (\bar{\gamma} - 1)\frac{C}{3W}\right\}\right]$$
$$\times\left(1 - \frac{\nu_B}{\nu}\right) - \frac{2BA''}{\bar{\gamma}}(x - x_B)\left(\gamma + \frac{C}{3W}\right) \tag{116}$$

which gives the muzzle velocity in terms of quantities known from the step-by-step integration up to "all burnt." The proof is left as an exercise for the reader.

7.515 Approximate solution near the start

When there is a shot-start pressure of the order of 2 tons/sq in., the integration in steps of the independent variable t proceeds quite normally. If, on the other hand, we start at a low pressure, say, ¼ ton/sq in., it is obvious from the computation that many of the terms are not contributing to the solution; furthermore, the pressure builds up slowly, so that we must use either a large number of t steps or frequent changes in the size of the step. On both grounds it is better to use an approximate solution up to pressures near 1 ton/sq in. We give here the solution for the useful particular case where (*a*) the rate of burning is proportional to pressure, and (*b*) there is no bore resistance acting during this part of the motion, but (*c*) there is a leakage area, and (*d*) there is a shot-start pressure P_0.

From equation 105, neglecting a term of the order of $(1 - f)^2$, we have

$$\phi = (1 + \theta)(1 - f)$$

and so, with equation 106,

$$\frac{d\phi}{dt} = \frac{\beta(1 + \theta)}{D}P \tag{117}$$

We assume that

$$P = P_0e^{\mu t} \tag{118}$$

so that the shot starts at $t = 0$. Integrating equation 117 from $t = 0$ gives

$$\phi - \phi_{SS} = \frac{\beta(1 + \theta)(P - P_0)}{D\mu} \tag{119}$$

Equation 107 makes $F = (2 + \theta)(1 - f) + O[(1 - f)^2]$, which enables us to omit all Lagrange corrections in this approximate solution.

In equation 114 we can omit the term representing the kinetic energy of the shot, which it is easy to show is of higher order in $(P - P_0)$ than the other terms. We assume that there is no leak until after shot start. This is true in our application to "runup" in a worn gun; here "shot start" is the release of the shot from the cartridge case. We have then

$$NT = \phi T_0 - (\gamma - 1)\frac{A_0(0)B(0)x}{CR} - \frac{\gamma\psi S(0)(RT_0)^{1/2}(P - P_0)}{\mu CR} \tag{120}$$

From equation 112,

$$P\left(U - \frac{C}{\delta}\right) = CNRT \tag{121}$$

and, from equations 120 and 121,

$$\phi - \phi_0 = \frac{(P - P_0)\left(U - \frac{C}{\delta}\right)}{CRT_0} + \frac{\gamma\psi S(0)(P - P_0)}{\mu C(RT_0)^{1/2}} + \frac{(\gamma - 1)A_0(0)B(0)x}{CRT_0} \tag{122}$$

If $B(0)$ is zero or small, the last term may be omitted and the result combined with equation 119 to give

$$\frac{\beta(1 + \theta)(P - P_0)}{D\mu} = \frac{(P - P_0)\left(U - \frac{C}{\delta}\right)}{CRT_0} + \frac{\gamma\psi S(0)(P - P_0)}{\mu C(RT_0)^{1/2}} \tag{123}$$

Thus, a solution of the form $P = P_0 e^{\mu t}$ is indeed possible, and μ has the value

$$\mu = \frac{(1 + \theta)\beta CRT_0}{D\left(U - \frac{C}{\delta}\right)} - \frac{\gamma\psi S(0)(RT_0)^{1/2}}{U - \frac{C}{\delta}} \tag{124}$$

Normally this solution will be used to pass from the pressure P_0 to a selected pressure P in the region where numerical solution is necessary. It is convenient, therefore, to write the formulas for such quantities as ϕ or the travel in terms of P and P_0. Integrating equation 111 yields

$$\frac{W\mu V}{A_0(0)} = P - P_0 - B(0) \ln\left(\frac{P}{P_0}\right) \tag{125}$$

and

$$\frac{W\mu^2 x}{A_0(0)} = P - P_0 - P_0 \ln\left(\frac{P}{P_0}\right) - \frac{1}{2} B(0) \left[\ln\left(\frac{P}{P_0}\right)\right]^2 \tag{126}$$

From equation 122 we obtain ϕ; NT comes from equation 120, and N from the integrated form of equation 113:

$$N = \phi - \frac{\psi S(0)(P - P_0)}{\mu C(RT_0)^{1/2}} \tag{127}$$

The resistance terms in equations 122, 125, and 126 are not a full expression of the effect of resistance. They are intended only as a check: if these terms are appreciable, the reduction of equation 122 to equation 123 fails, and numerical solution must be used.

We have used these formulas to shorten our solutions in badly worn guns. Here there is a shot-start pressure associated with the release from the cartridge case; a P_0 of ¼ ton/sq in. was assumed, though this is certainly higher than the pressure at which the shot is released from the case; the muzzle velocity and maximum pressure are not much altered by the difference between this P_0 and the true value, and the labor is reduced by taking P_0 high. After shot-start the leakage area comes into operation, and there is a considerable "runup" in which bore resistance is small. Test solutions have shown that up to 1 ton/sq in. the approximate solution is correct to within 2 per cent, in the worst case. The absolute magnitude of the error at this stage is of the order of ½ ft/sec in velocity, 0.005 in. in travel, and less than 10^{-3} in ϕ, N, and f. Beyond 1 ton/sq in. the errors increase rapidly. Although the solution could be pushed to higher pressures by running an occasional check solution by numerical integration, it is simpler to abandon the approximate solution at a pressure in the neighborhood of 1 ton/sq in.

7.52 Analysis of the experimental data on new and worn guns

TABLE 7.2 OBSERVED BALLISTICS

Gun	Leakage	Max. Pressure, tons/sq in. Piezo	Muzzle Velocity, ft/sec
New	No	24.5	2752
Worn	No	18.8	2623
	Yes	17.6	2587
Difference		1.2	36

These results are means from a large number of rounds. The details of charge, chamber capacity, and the like need not be given here, except for the form factor, which was 0.15; thus the surface of the propellant decreases only slowly during burning. The thermochemical data on the propellant were well known, leaving in all only two uncertain quantities in the calculations. The rate of burning in the closed vessel was known, but, as explained in chapters 5 and 9, this gives only a rough indication of the effective rate in such a high-velocity gun as this; the cool propellant used in these trials had an explosion temperature $T_0 = 2400°\text{K}$ (although the gun had been worn by a much hotter propellant), and so the effect of erosion of the propellant may be expected to be considerable in this example. Further, the nature of the resistance to motion of the shot was not known except in a very qualitative way. The parameter β and the bore resistance were, therefore, determined by fitting to the observed ballistics, in the way to be described.

7.521 Ballistics of the new gun

Heat losses to the bore were omitted at first; that is, we replaced $\bar{\gamma}$ by the thermochemical γ. We shall discuss in § 7.522 the changes produced by including these losses, which up to shot-ejection amount (in this gun) to some 20 per cent of the energy given to the projectile.

The resistance to motion was taken to be a shot-start pressure dropping, immediately the shot moves, to a constant resistance acting up to the muzzle. This is only a rough model, but it does possess some features that are physically plausible: the higher initial resistance, for example, is here counterfeited by the shot-start pressure, whereas our assumption of a constant resistance during travel is supported by certain experimental evidence. We write the shot-start pressure as P_0 and the bore resistance as $A_0(x)B$, where $A_0(x)$ is the area of the greatest cross section of the shot when at a travel x; thus the constancy of B, the pressure equivalent of the bore resistance, implies a slight, but only a very slight, decrease in the bore resistance in the early stages of shot motion. By their definitions, $P_0 \geq B$.

The rate of burning of this propellant is, by closed-vessel observations, proportional to P^α, where α lies between 0.9 and 1.0. There is no appreciable error in taking the convenient value $\alpha = 1$.

There were thus three arbitrary parameters in the calculations for a new gun, namely, β, P_0, and B. The results of the computations[10] can be represented by

[10] For assistance with the computations underlying this analysis I am indebted to Mr. T. Vickers and Mrs. H. N. Wilkinson.

$$\left.\begin{aligned} P_{\max} &= 1.684P_0 + 2.76B + 70.47\beta - 31.96 \text{ tons/sq in.} \\ \text{MV} &= 29.9P_0 - 72.2B + 1205\beta + 1886 \text{ ft/sec} \end{aligned}\right\} \quad (128)$$

where P_0 and B are in tons per square inch and β in (inches per second) per (ton per square inch). These linear formulas fit our set of results with root-mean-square deviation 0.05 ton/sq in. and 1 ft/sec, which are of the same order as the accumulated errors of computation that we tolerated in the numerical integration.

For $P = 3$ tons/sq in., the new gun data are reproduced by $B = 0.86$ ton/sq in. and $\beta = 0.696$. This is a very plausible value for B; this β is 9 per cent higher than the accepted closed-vessel rate.

The lowest bore resistance is found for a low shot-start pressure, and the smallest allowable pair is $B = P_0 = 0.840$ ton/sq in. with $\beta = 0.748$.

One of our new gun solutions was repeated with the conventional Lagrange correction, which amounts to a replacement of F by unity throughout our formulas. In the example studied, the peak pressure was raised from 24.5 to 26.4 tons/sq in., with an increase in the MV of 29 ft/sec. This rise of maximum pressure can be counteracted by a suitable reduction of β, which brings the muzzle velocity back to only 4 ft/sec less than its former value. Thus the newer Lagrange correction would not produce significant effects in routine ballistics. On the other hand, the leakage past the shell is increased by about 10 per cent in this example, by using the newer Lagrange correction.

We shall now turn to the data on the worn gun in order to pick the best of the one-parameter set of solutions allowed by the new-gun ballistics.

7.522 Ballistics of the worn gun

The shape of the important part of the bore of the worn gun has been shown in Fig. 7.4. The free runup is about 2.7 calibers. From these curves were calculated the volume behind the shot, as a function of travel, and, in particular, the increase of chamber volume, which is only 0.2 per cent.

The maximum cross-sectional area of the shot $A_0(x)$ is needed in the computations. $A_0(x)$ is the cross section at the band and for the normal shot was calculated on the assumption that the lands wipe away the upstanding copper without altering the height of the copper in the grooves, until the groove comes down to meet the band. This assumption is far from sufficient as a basis of band design, but its results should be adequate for our ballistic calculations. For firings with the special projectiles, it was assumed that $A_0(x)$ was equal to the full bore area at the band.

The leakage area has been written $S(x)$ and is, in our example, the area between band and bore. It has to be verified that this is the minimum and therefore the controlling cross section in the annular passage by which the gas escapes from back to front of the shot. The other possible minimum is at the head of the cylindrical proof shot, which is in a less worn part of the bore. The cross section for leakage is here, in our example, about twice as large as the leakage area at the band.

A number of solutions were computed for various combinations of bore resistance and rate of burning, for normal and special shot. In all solutions a shot-start pressure of $\frac{1}{4}$ ton/sq in. was assumed. This is probably an overestimate of the force required to overcome the indentation into the cartridge case, but the difference is not important in this connection. In runs with leakage, a nozzle discharge coefficient of $\psi = 0.6$ was used. This is about 10 per cent smaller than the theoretical result without resistance to flow.

The band does not meet the rifling until a travel of 2.7 calibers. Up to this travel there may be a small resistance from friction of the shot against the lower wall of the bore. Beyond this travel there should be some bore resistance, rising in the later stages of motion to a value comparable with that found in a new gun. In our calculations we have used the same bore resistance as in the new gun, assuming that the resistance enters when the band first engages the worn rifling. At a travel of 2.7 calibers in a worn gun the pressure is about 12 tons/sq in., and it follows that a bore resistance of 0.8 ton/sq in. has little effect on the peak pressure, while making a considerable difference to the muzzle velocity. In a typical case the effects were found to be +0.24 ton/sq in. and −96 ft/sec, respectively.

Table 7.3 shows the nature of the theoretical results obtained.

The first set ($B = 0.86$ ton/sq in.; $\beta = 0.696$) fits the new gun with a shot-start pressure of 3 tons/sq in. The second set fits the new gun if the shot-start pressure is no larger than the bore resistance. On comparing with the experimental results of Table 7.2, it is clear that the theoretical effect of leakage on pressure is in excellent agreement with the firings, and this is true for both sets of theoretical results. On the other hand, the observed saving of velocity is 36 ft/sec, which is less than even the lower of the two theoretical results. Considering now the ballistics with normal shot, it may be seen that the results for ($B = 0.84$ ton/sq in.; $\beta = 0.748$) are the better and are in quite good agreement with the observed loss of ballistics: this is 6.9 tons/sq in. and 165 ft/sec, whereas the theoretical is 7.5 tons/sq in. and 211 ft/sec.

As mentioned previously, some allowance should be made for the heat loss, which amounts to 20 per cent of the muzzle energy. The effect on the new-gun ballistics has been computed. The result is to emphasize the trends indicated by the earlier work. Thus, the new-gun ballistics can be obtained by $P_0 = B = 0.314$ ton/sq in., which improves the fit to the worn gun with and without leakage, while at the same time β has to be raised to 0.794, which is even further from the closed-vessel results than the values of β previously obtained.

Taking all these points into consideration, it can be concluded that the firings, in new and old guns, with normal and special shot, are in good agreement with the hypothesis that the resistance to motion can be represented by a constant bore resistance without any special shot-start pressure. The only disturbing features are that (1) this implies a rate of burning some 20 per cent higher than closed-vessel results, and (2) the calculated saving of MV by the suppression of leakage is about 50 per cent larger than that observed. In considering item 2 it should be noticed that the theoretical saving of maximum pressure is in very good agreement with that observed. We take these results to mean that the steps adopted to prevent gas leakage have protected the driving band proper from gas wash in the early stages of motion, causing a higher bore resistance at the later stages of the travel. Thus, our calculations of maximum pressure are correct, but our theoretical velocity without leakage ought to be lowered. We conclude, also, that the methods used to prevent gas leakage do indeed produce substantially all the saving of ballistics that can be expected from a sealing device.

TABLE 7.3 THEORETICAL RESULTS IN WORN GUN

Bore Resistance Used only after Free Runup

B, ton/sq in.	β, (in./sec) per (ton/sq in.)	Leakage	Max. pressure, tons/sq in.	MV, ft/sec
0.86	0.696	No	15.82	2501
0.86	0.696	Yes	14.59	2428
			1.2	73
0.84	0.748	No	18.32	2596
0.84	0.748	Yes	17.03	2541
			1.3	55

Figure 7.5 shows pressure-space curves typical of those calculated for the new gun (without leakage) and worn gun (with and without leakage). In Fig. 7.6 is given the development of the leakage with shot travel, in a typical solution for the worn gun. The total amount of gas lost is little more than 1 per cent of the total charge. All but 4 per cent of the total leakage occurs during free runup.

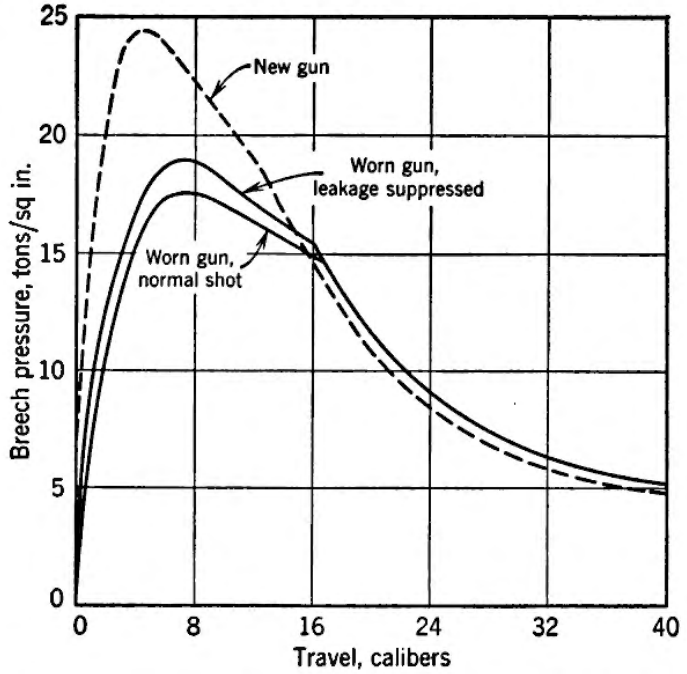

FIG. 7.5 Pressure-travel curves for new and worn guns.

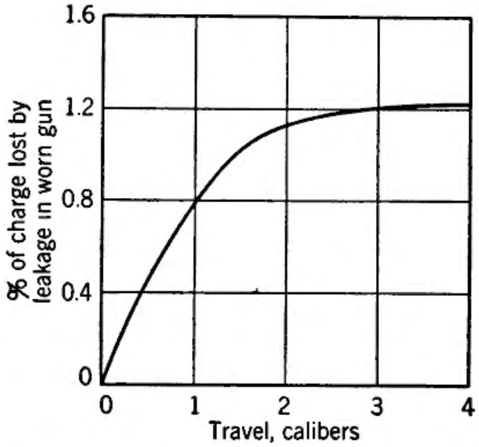

FIG. 7.6 Weight of gas lost by leakage, as a function of travel, in the worn gun with normal shot.

Calculations were made of the behavior of this well-worn gun when used with separate-loading ammunition. The increase of chamber capacity and reduction of shot travel cause a drop of ballistics (relative to the same gun with fixed ammunition) of 4.2 tons/sq in. and 210 ft/sec, when there is no leakage in either case. The elimination of leakage saves only 0.3 ton/sq in. and 10 ft/sec when used with separate-loading ammunition; in these calculations a shot-start pressure of 1 ton/sq in. was used to represent the slow engraving by the worn rifling. It has to be remembered that a gun used exclusively with such ammunition would develop a different internal contour; it seems clear, however, that the reduction of performance by gas leakage is small with separate-loading ammunition.

One of the solutions for a worn gun was repeated with the same leakage area as before, but with the chamber capacity, bore area, and projectile cross section being replaced by those characteristic of the new gun. The performance was raised by 0.9 ton/sq in. and 25 ft/sec. We can use this result to apportion the blame for the fall in ballistics, sharing it among loss of initial resistance, gas leakage, and the changes of internal dimensions. We have theoretical results for the second, third, and the total; by subtraction we find that the drop of muzzle velocity is divisible among these three in the ratio 64, 24, and 12 per cent. Firing trials have given the second and the total, and, if we use our theoretical result for the third, we arrive at 66, 19, and 15 per cent for the three contributions. We may take it that, when this gun is almost worn out, its drop of velocity from the new-gun value is divisible into these three parts in the ratio of, roughly, 65, 20, and 15 per cent. This refers to a gun worn mainly by a hot propellant but now fired with a cooler propellant.

7.53 Changes in ballistics during the life of the gun

Having obtained an idea of the resistance to shot motion from the results for this gun, we may proceed to a discussion of the changes in ballistics during the life of the gun. For this purpose we consider a gun worn exclusively by the cooler propellant. Wear curves at various stages of the life were compiled, and ballistic solutions were computed for $B = P_0 = 0.84$ ton/sq in., with and without leakage. The results are shown in Fig. 7.7. The values at 600, 900, and 1200 rounds were fitted by a smooth curve, which was then extrapolated to meet the known

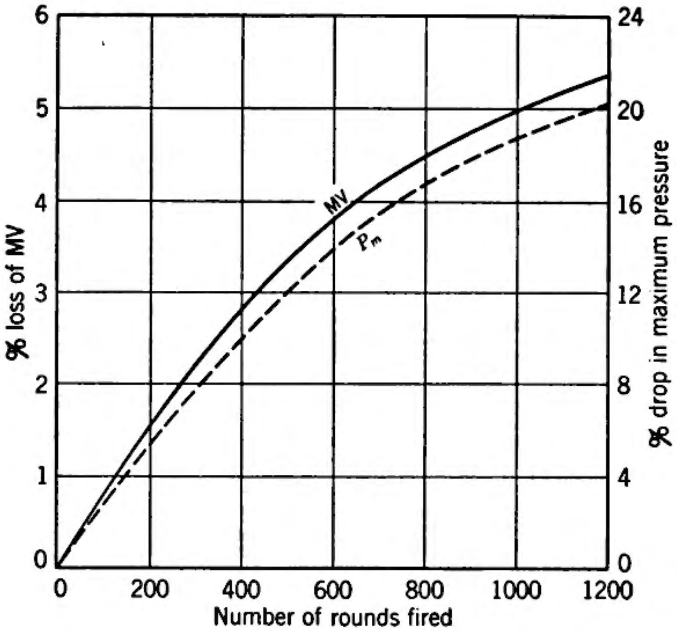

FIG. 7.7 Theoretical change of ballistics during the life of this gun.

result at zero rounds. This could be done without straining the fit to the calculated points. The rate of drop of ballistics with rounds fired is not constant, the rate falling off toward the end of the life of the gun.

In Fig. 7.8 the theoretical drop of velocity is plotted against the wear at 1 in. from the C of R, superposed on experimental data for this nature of gun. Our results appear to be too high by about 20 per cent. They lie on a straight line whose continuation passes fairly near the origin.

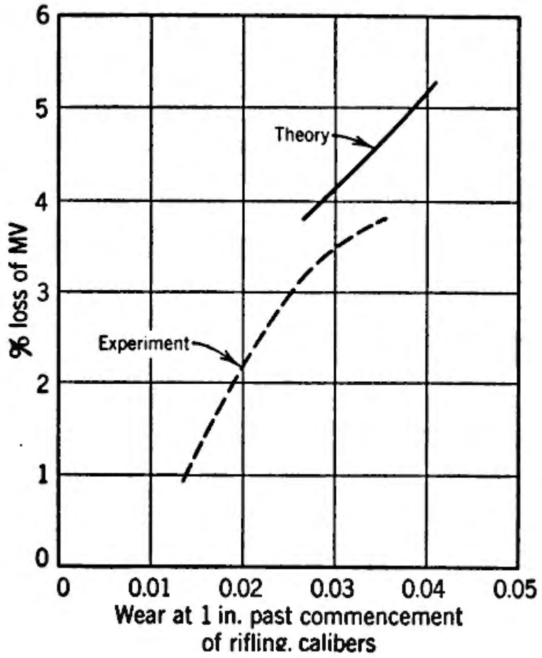

FIG. 7.8 Loss of velocity with wear; comparison of theory and observations.

We attribute the fact that the theoretical drop of velocity is larger than that observed to the decreased bore resistance of a well-eroded band; this factor had to be omitted from our calculations, since we had no knowledge of its magnitude. Allowing for this, our theoretical drop of velocity would be reduced, and most of all in the later stages of life. Hence our theoretical line would be lowered and its slope reduced. Both changes would bring better agreement with the observations. Such an interpretation requires an average bore resistance lower, in a well-worn gun, by about ¼ ton/sq in. This seems a reasonable value.

7.54 Rapid estimation of the effect of leakage

It is possible to make a rapid estimate of the loss of ballistics due to leakage in a gun in any stage of wear.

Knowing the internal shape of the bore, we begin by finding the maximum area through which gas can leak past the shot. This will usually occur as the shot leaves the cartridge case. Let this area be S. Write

$$\Psi = \frac{0.3SD}{C(RT_0)^{1/2}} \tag{129}$$

which is a dimensionless parameter that has appeared earlier in this chapter. Equation 129 for Ψ differs from that quoted for a constant leak, in that we have here used $S/2$ as an average value of the leakage area. From equations 62 and 63 we know that

$$\frac{\text{MV with leak}}{\text{MV without}} = 1 - n\Psi \tag{130}$$

where $n \sim 0.7$, and that

$$\frac{\text{Max. pressure with leak}}{\text{Max. pressure without}} = 1 - 2\Psi \tag{131}$$

These are valid only for small Ψ.

In our example of a worn gun, equations 130 and 131 agree very well with both our numerical integrations and the trial results. This is shown in Table 7.4.

TABLE 7.4 EXACT AND APPROXIMATE RESULTS FOR EFFECT OF LEAKAGE

Ratio of	Equations 130 and 131	Numerical Integration	Trials
MV	0.975	0.979	0.986
Max. pressure	0.927	0.930	0.936

7.6 Ballistic properties of recoilless guns

In the rest of this chapter some of the general properties of recoilless guns are discussed. The results quoted have all been derived from the set of equations given in § 7.35, and in most cases the method of numerical integration was used.

We have used the ideas of a "nozzle-start pressure" and a "shot-start pressure," which are convenient idealizations of complicated processes. Consider, first, the use of a "shot-start pressure." This is no doubt a violent approximation, and the considerations of § 7.522 have led us to believe that it has less physical justification than we supposed at the time we carried out our researches on the recoilless gun. In orthodox ballistics there are three justifications for the "shot-start pressure": it is easily included in most ballistic solutions; physically more accurate assumptions might lead to more parameters, which would be difficult to evaluate by working back from fired ballistics; in any case, the calculated ballistics are not sensitive to the way in which the resistance to motion is taken into account; for example, the replacement of a shot-start pressure by a modification of the rate of burning, chosen to give the same maximum pressure, has little effect on the muzzle velocity and pressure-space curve.

In dealing with recoilless guns the nature of the initial motion of the shot affects not only the peak pressure and muzzle velocity, but also the resultant recoil momentum. The nature of the initial motion of gas and shot has, unfortunately, a more marked effect on the momentum. An important point affected by this is the question of the maximum impulsive load on the mounting. It is possible that, when the nozzle-start and shot-start pressures have been chosen to reproduce the observed ballistics, the impulsive forces may be in error by a large fraction. In a gun of 3-in. caliber the impulsive load can be as much as 10 tons. The calculation of such effects, depending in a critical manner on the physical accuracy of the assumptions made about the initial processes, is likely to be the least satisfactory of the results calculated from our model of the initial conditions.

7.61 "Recoillessness"

Two kinds of "recoillessness" are possible:

(*a*) If the flow out of the nozzle begins at the same time as the shot starts and there is no resistance to motion afterwards, then it is possible to find a nozzle throat area that gives zero resultant force on the gun at all times during the firing, including the post-ejection period.

(*b*) If the flow through the nozzle is established at a pressure different from the shot-start pressure, then only a more restricted recoillessness can be achieved. Suppose, for example, that the gas flow starts before the shot moves. It is obvious that until the shot starts there is a resultant forward thrust on the gun. To get zero momentum of the gun after the firing is over, there must be a resultant backward thrust while the shot is in motion. The zero final momentum means a negligible total movement, since the forces last for only a short time. This state of affairs would be described in trials reports as "recoillessness"; it is clear that, nevertheless, the carriage would have to withstand large impulsive forces.

Recoillessness of type *a* is obviously a very special case, implying a particular form of resistance to motion as well as a certain suitable choice of bursting disk. However, it can be approached sufficiently nearly, for all practical purposes, to justify our separating such cases into a separate class.

Both types of recoillessness are considered in this book. Case *b* is by far the more common.

The stress on the carriage depends on whether this is rigidly attached to the ground. If it is so attached, for example by spades, then the whole of the momentary thrust on the gun is transmitted to the carriage. If, on the other hand, the carriage is free to move, only a part of the thrust appears at the gun-carriage junction; the rest is used in acceleration of the piece itself. A carriage weighing as much as the piece would receive half the resultant thrust on the piece.

Some of the ballistic properties of a recoilless gun depend quite strongly on the relation between nozzle-start and shot-start pressure. It is useful, therefore, to be able to detect whether one is working in region *a* or *b*, and in the latter case to say which pressure is the larger. In §§ 7.623 to 7.624 we shall discuss the effects of changes in charge and shot weights on recoillessness. It will appear that if a certain gun has been adjusted to be recoilless at normal charge, with nozzle opening before the shot starts, then if fired with a smaller charge of the same propellant the gun will move forward. This is quite obvious, since in the latter case the period during which $P_{NS} < P < P_{SS}$, in which therefore the system is acting as a rocket, is longer than before. This is the simplest practical test for the relative timing of nozzle opening and shot start. Other similar tests can be based on the results quoted later, for example, on the effect of change of shot weight, but the easiest to apply is the change of charge weight. The gun movements to be expected are not very large—an inch or two if mounted on a rubber-tired carriage on smooth ground.

7.611 The calculation of recoil momentum

When the shot is rigidly held in the shot seating, the thrust forward on the gun is, by the theory of § 7.22, ζSP, where the dimensionless thrust coefficient ζ $(= F/S_t p_r)$ has been tabulated in Table 7.1. When the shot is free to move along the bore, the thrust on the gun falls by AP, reducing the net forward thrust to $(\zeta S - A)P$; writing $\mu = S/A$, this thrust is $(\mu\zeta - 1)AP$.

The coefficient ζ depends on the γ of the propellant gases and, more strongly, on the expansion ratio of the nozzle used. These characteristics of propellant and gun are effectively constant during the firing. ζ has also a small dependence on ϵ, the parameter measuring the covolume effect:

$$\epsilon = \frac{\eta\rho}{1 - \eta\rho}$$

For the most accurate work, this dependence on ϵ can be taken into account by using a ζ, which is a function of time, perhaps in the form of different mean ζ in various parts of the solution. In the formulas that follow we shall not explicitly distinguish the various ζ.

Using NS, SS, and E to denote conditions at nozzle start, shot start, and shot ejection, respectively, we have, for the total backward momentum of the gun at shot ejection,

$$A(1-\mu\zeta)\int_{SS}^{E} P\,dt - A\mu\zeta\int_{NS}^{SS} P\,dt$$

For all solutions of good ballistic regularity, "burnt" occurs before shot ejection, and we can take the system after shot ejection as a reservoir of gas exhausting through nozzles in parallel, of throat areas S and A. By Hugoniot's theory (see § 9.22), we have

$$P = \frac{CN_E RT_E}{U_0}\left(1+\frac{t}{\Omega}\right)^{-2\gamma/(\gamma-1)}$$

where t is measured from shot ejection, U_0 is the total internal volume of the gun, and

$$\Omega = \left(\frac{2}{\gamma-1}\right)\left(\frac{U_0}{A+S}\right)\left[\frac{1}{\gamma RT_E}\left(\frac{\gamma+1}{2}\right)^{(\gamma+1)/(\gamma-1)}\right]^{1/2}$$

These formulas neglect the effect of covolume. The gain in backward momentum after shot ejection is

$$\begin{aligned} A(1-\mu\zeta)\int_0^{\infty} P\,dt &= A(1-\mu\zeta)\,\frac{CN_E RT_E}{U_0}\left(\frac{\gamma-1}{\gamma+1}\right)\Omega \\ &= \frac{(1-\mu\zeta)CN_E}{(1+\mu)}\left(\frac{RT_E}{\gamma}\right)^{1/2}\left(\frac{\gamma+1}{2}\right)^{(3-\gamma)/2(\gamma-1)} \qquad (132) \end{aligned}$$

The function of γ, which occurs in equation 132, is equal to 1.34 within 3 per cent for all modern propellants.

It is convenient to write the total momentum of the gun after firing as WV_1, where V_1 is a "virtual shot velocity." For a gun with exactly balanced recoil, V_1 is zero. From the previous formulas,

$$WV_1 = \int_{SS}^{E} AP\,dt - \mu\zeta\int_{NS}^{E} AP\,dt + \frac{1.34(1-\mu\zeta)CN_E(RT_0)^{1/2}(T_E')^{1/2}}{1+\mu} \qquad (133)$$

In terms of the reduced units introduced in § 7.37,

$$WV_1 = \frac{AD}{\beta}\int_{SS}^{E} \pi\,d\tau - \frac{AD\mu\zeta}{\beta}\int_{NS}^{E} \pi\,d\tau + \frac{1.34(1-\mu\zeta)CN_E(RT_0)^{1/2}(T_E')^{1/2}}{1+\mu} \qquad (134)$$

Up to "burnt" in a numerical integration, $\int \pi \, d\tau$ can be found by a summation, since increments of this quantity appear in the computation. After "burnt,"

$$\frac{AD}{\beta}(1 - \mu\zeta)\int_B^E \pi \, d\tau = (1 - \mu\zeta)\overline{W}_1(V_E - V_B)$$

where $\overline{W}_1$ is a mean from "burnt" to "shot ejection."

When the rate of burning is proportional to pressure,

$$WV_1 = \frac{AD}{\beta}(f_{SS} - \mu\zeta f_{NS}) + (1 - \mu\zeta)\overline{W}_1(V_E - V_B) + \frac{1.34(1 - \mu\zeta)CN_E(RT_0)^{1/2}(T_E')^{1/2}}{1 + \mu} \tag{135}$$

If a bore resistance, depending on travel, is preferred to an instantaneous collapse of the "shot-start pressure," the formulas of this section must be rewritten, but the changes to be made are quite obvious.

7.62 The influence of design variables and loading conditions on the interior ballistics of a typical recoilless gun

There are two kinds of variation to be considered. Let us take, for example, a gun with balanced recoil and alter the shot-start pressure. If we leave the nozzle area unchanged, the gun will, in general, now show a nonzero recoil. This change could occur in practice by the band of the shot not being quite standard; the change in ballistics *at constant nozzle area* has, therefore, a bearing on the regularity of the gun. On the other hand, suppose that a new type of shot with a new band system were to be introduced; then firing trials would determine the correct throat area to give zero recoil with the new shot-start pressure. The change in ballistics caused by the new band design would be a change during which nozzle area would be adjusted to keep zero recoil. In general, then, we calculate two types of variation: changes at constant throat area and changes at zero recoil; the former are useful in studying regularity of the weapon, the latter in deciding the design to give the best standard performance. In settling design it is necessary to pay attention to both factors, but as their relative importance depends on the purpose of the weapon it is convenient to distinguish sharply between these two classes.

We consider changes in the following quantities: nozzle-start and shot-start pressures, web size or rate of burning, charge and shot weights, chamber capacity, shot travel, nature of propellant, and nature of the venturi. The effects on maximum pressure, muzzle velocity, position of "burnt," and recoil velocity (or throat area) are obtained in each case.

The example considered here is typical of the class with pressure in the neighborhood of 5 tons/sq in. and muzzle velocities of the order of 1500 ft/sec. It is thought that the effects of the variables on this gun will be a qualitative guide to the results produced by similar changes in other guns. The pressure index of the rate of burning was taken to be unity in these calculations, but small changes in this should not seriously alter the general nature of the results.

7.621 Effect of nozzle-start and shot-start pressures

The effects at constant nozzle throat area are plotted in Figs. 7.9, 7.10, and 7.11, and at zero recoil in Figs. 7.12, 7.13, 7.14, 7.15, and 7.16. Examination of these shows that on crossing the boundary $P_{NS} = P_{SS}$ the results have a discontinuity of slope. This is most marked with the peak pressure (Figs. 7.9 and 7.12) and the position of "all burnt" (Figs. 7.11 and 7.13). The muzzle velocity is not strongly affected in this way when the nozzle throat area is constant (Fig. 7.10), but when adjustment is made to give zero recoil in all cases the muzzle velocity has the same sharp bend as the other quantities at the critical boundary $P_{NS} = P_{SS}$ (see Fig. 7.13).

This type of discontinuity, though likely to be somewhat smoothed in practice, has some important results. In the first place, it prevents extrapolation from the region $P_{NS} < P_{SS}$ into the zone $P_{NS} > P_{SS}$, or vice versa.

A more useful consequence is that we have here another way of determining the relative timing of nozzle opening and shot start. The maximum pressure is almost independent of nozzle-start pressure (at constant throat area), provided $P_{NS} < P_{SS}$. If, however, P_{NS} passes the shot-start pressure, the maximum pressure set up in the gun immediately becomes sensitive to P_{NS}. Figure 7.17, which illustrates this statement, was derived from Fig. 7.9. The maximum pressure is here plotted against nozzle-start pressure. The experimental method is, therefore: make a series of cartridge cases with stronger and stronger blowout disks; record maximum pressures of these rounds, plot peak pressure against disk thickness; the curve should show the characteristic form of Fig. 7.17, provided that at each thickness the number of rounds fired is sufficient to eliminate random variations of ballistics. The position of the bend in the curve shows the disk thickness at which shot-start and nozzle-opening pressures are equal, and, hence, one can estimate the relation between these pressures for the standard thickness of disk. In

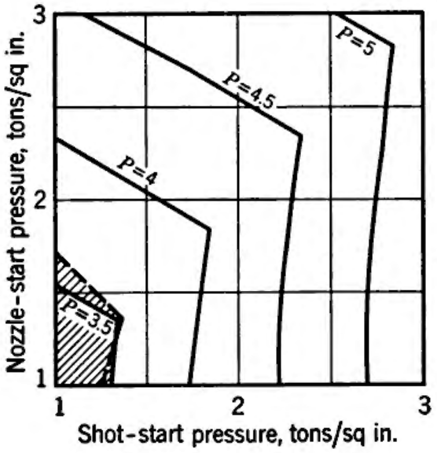

FIG. 7.9

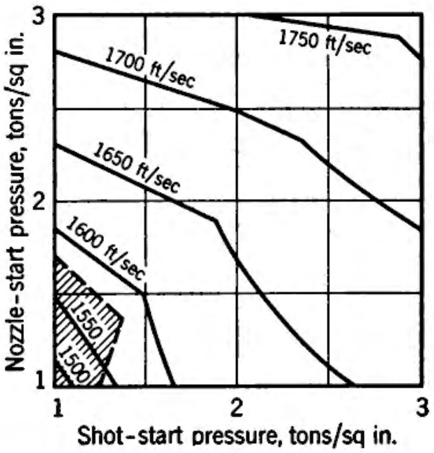

FIG. 7.10

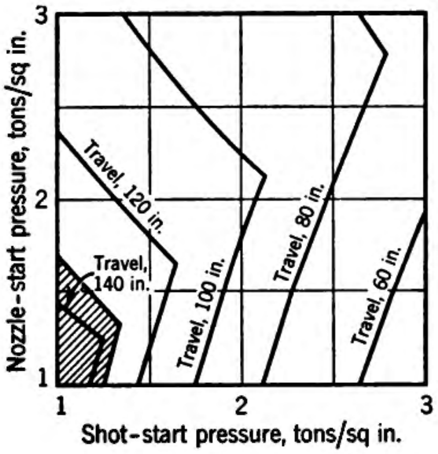

FIG. 7.11

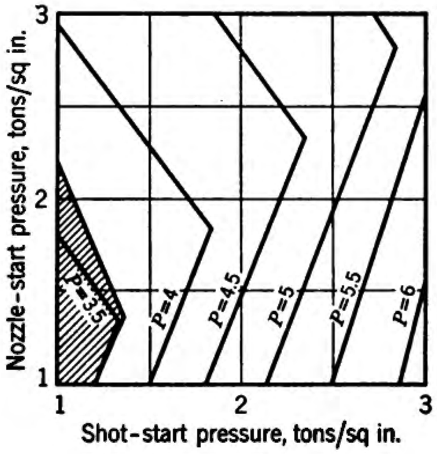

FIG. 7.12

British Crown copyright reserved.

FIG. 7.9 Peak pressure as a function of starting pressures, at constant nozzle throat area, in a typical recoilless gun. In this and Figs. 7.10–7.16 shaded areas indicate solutions with some propellant still unburnt when the shot reaches the muzzle.

FIG. 7.10 Muzzle velocity as a function of starting pressures, at constant nozzle throat areas.

FIG. 7.11 Shot travel at "burnt" as a function of starting pressures, at constant nozzle throat area.

FIG. 7.12 Peak pressure as a function of starting pressures, adjusting nozzle area to preserve zero recoil.

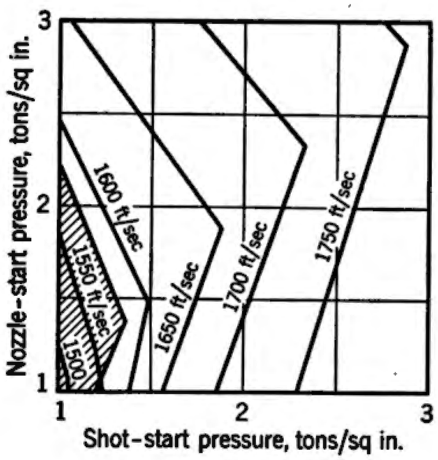

FIG. 7.13

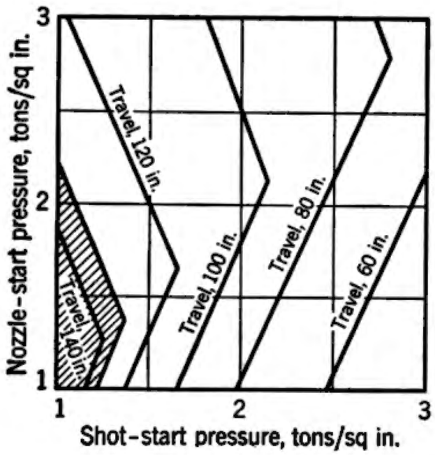

FIG. 7.14

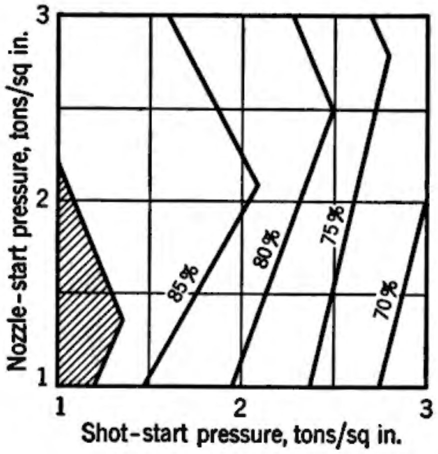

FIG. 7.15

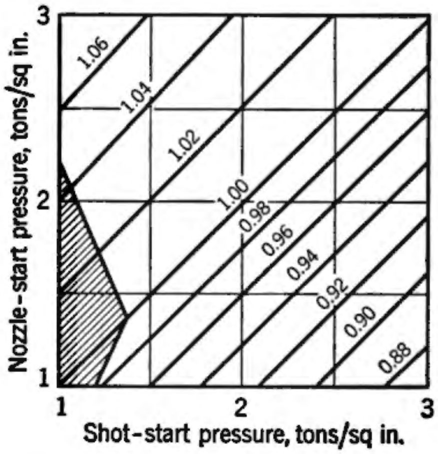

FIG. 7.16

British Crown copyright reserved.

FIG. 7.13 Muzzle velocity as a function of starting pressures, adjusting nozzle area to keep zero recoil.

FIG. 7.14 Travel to "burnt" as a function of starting pressures, adjusting nozzle area to preserve zero recoil.

FIG. 7.15 Ratio of mean to maximum pressures as a function of initial conditions. Nozzle area adjusted to keep zero recoil.

FIG. 7.16 Nozzle throat area for zero recoil, relative to the value when nozzle-opening pressure = shot-start pressure.

practice, the fact that the setting up of the nozzle flow and the engraving of the shot are not instantaneous serves to blur the sharp changes calculated from our idealizations of these processes. Figure 7.10 shows that the muzzle velocity cannot be used as an indicator instead of maximum pressure, for the discontinuity of slope on crossing the boundary $P_{NS} = P_{SS}$ is very small.

The influence of nozzle-start and shot-start pressures depends on their magnitude in relation to the normal maximum pressure of the gun. Thus low-pressure guns are more sensitive in this respect than high-pressure weapons. It should be noted that the variations of initial pressures shown in these diagrams, from 1 to 3 tons/sq in., are considerable when compared with the peak pressures, which are around 5 tons/sq in.

The shaded area at the bottom left corner of each of Figs. 7.9 to 7.16 shows the region of solutions that have unburnt propellant remaining as the shot passes the muzzle. A more complete picture of the position of "burnt" is shown in Figs. 7.11 and 7.14. A closely related feature is the piezometric efficiency, that is, the ratio of mean to maximum pressure, shown in Fig. 7.15. Comparison with Fig. 7.14 shows how the ratio of mean to maximum pressure is improved by having "burnt" further toward the muzzle. This is, of course, a well-known effect in normal guns.

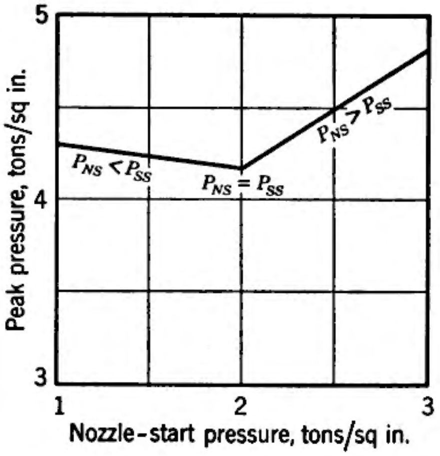

FIG. 7.17 Variation of peak pressure with nozzle-start pressure, at a shot-start pressure of 2 tons/sq in. British Crown copyright reserved.

From Fig. 7.10 we conclude that round-to-round variations of muzzle velocity due to given variations of nozzle-start pressure will be much the same, whatever the nozzle-start pressure. We can combine this with the plausible assumption that round-to-round variations of disk-bursting pressure will increase with this pressure; hence, it follows that round-to-round variations of muzzle velocity *due to this effect* will be least for cases that burst early.

Round-to-round variations of maximum pressure are of less importance. Figure 7.9 or 7.17 shows that the part of such variations due to variations of disk-bursting pressure is greatly reduced by having the disk burst before the shot moves.

Variations of shot-start pressure must occur in both orthodox and recoilless guns. In the latter, however, the variations are probably smaller than the variations of nozzle-start pressure. Figure 7.9 shows that the variation in maximum pressure due to a given change in shot-start pressure is least when the nozzle opens after shot start. Figure 7.10 proves that the variations of muzzle velocity are much the same whatever the nozzle-start pressure.

We turn now to the diagrams showing the effect of changes of nozzle-start and shot-start pressures when the nozzle area is adjusted to preserve zero recoil velocity after firing. Figure 7.16 shows how this nozzle area varies. There is little to be said about these curves, beyond the obviously simple nature of the relation. The crossing of the critical line $P_{NS} = P_{SS}$ does affect the spacing of the lines, a point clearly shown by the lines marked 1.02, 1.00, 0.98. The other figures of this series, Figs. 7.12, 7.13, 7.14, and 7.15, have many resemblances one to another. Their general shape is useful in estimating the best nozzle-start and shot-start pressures to reproduce experimental results in various guns.

7.622 Effect of rate of burning or web size

The following results give an idea of the order of magnitude of the effect produced by a change of web size, which has the same effect as a change of rate of burning.

TABLE 7.5 EFFECT OF WEB SIZE ON A TYPICAL RECOILLESS GUN

Web Size, in.	Max. Pressure, tons/sq in. Piezo	Muzzle Velocity, ft/sec	Travel at "Burnt," in.	Mean/Max. Pressure
0.064	4.16	1667	104	0.860
0.060	4.96	1739	66	0.785

The effects are qualitatively the same as in a normal gun. A smaller web gives higher peak pressure and muzzle velocity, and the pressure-space curve becomes less flat because "burnt" occurs at a smaller travel. These two examples have the same nozzle throat area, because the fact that $P_{NS} = P_{SS}$ means that the change of web size does not alter the recoillessness. If the nozzle-start pressure differs from the shot-start pressure, then a change of web size entails a change of throat area if we are to preserve recoillessness. Table 7.6 illustrates an example in which P_{NS} was 1 ton/sq in. less than P_{SS}. Compared with Table 7.5, the changes in muzzle velocity and travel to "burnt" are halved, while the changes in maximum pressure and mean/maximum pressure are much the same as before.

In connection with regularity of ballistics, it is necessary to know the changes produced by a change of web size when no attempt can be

TABLE 7.6 EFFECT OF WEB SIZE ON BALLISTICS AND RECOIL IF $P_{NS} < P_{SS}$

Nozzle Throats Adjusted to Give Zero Recoil Velocity

Web Size, in.	Max. Pressure, tons/sq in. Piezo	MV, ft/sec	Travel at "Burnt," in.	Mean/Max. Pressure	Nozzle Area
0.064	5.80	1780	58	0.704	1.000
0.060	6.58	1815	47	0.645	1.011

made to adjust for zero recoil. This corresponds to the random variations of effective web size encountered in the field. Table 7.7 shows the effect for an example with P_{NS} 1 ton/sq in. less than P_{SS}.

TABLE 7.7 EFFECT OF WEB SIZE ON BALLISTICS AT CONSTANT NOZZLE AREA IF $P_{NS} < P_{SS}$

Small Unbalanced Recoil in Both Cases

Web Size, in.	Max. Pressure, tons/sq in. Piezo	MV, ft/sec	Travel at "Burnt," in.	Mean/Max. Pressure
0.064	5.27	1709	61	0.714
0.060	6.04	1757	49	0.658

Comparison of Tables 7.5 and 7.7 shows that the effect on the muzzle velocity is less in the latter case. This has an important bearing on the consistency of ballistics.

The rate of burning of the propellant varies with its temperature. The normal change is about 3 per cent per 10°C. Assuming this, a nozzle-start pressure of 2 tons/sq in. and a shot-start pressure of 3 tons/sq in., we find that in this example the throat area for zero recoil must increase at the rate of 0.3 per cent per 10°F. If shot start and nozzle opening are simultaneous, there is no change necessary in the nozzle area.

7.623 Effect of charge weight on nozzle throat area for zero recoil

If nozzle start and shot start are simultaneous, the nozzle area for recoillessness is independent of the charge weight. We take $P_{NS} = 2$ and $P_{SS} = 3$ tons/sq in. as a typical case where this condition is not satisfied.

In Table 7.8 we show the effect of increasing the charge by 25 per cent. This requires an increase of throat area of 4.2 per cent to preserve recoillessness. Since a difference in nozzle-start and shot-start pressures

TABLE 7.8 EFFECT OF CHARGE WEIGHT, KEEPING ZERO RECOIL

Charge, lb	Nozzle Throat for Zero Recoil	Max. Pressure, tons/sq in. Piezo	MV, ft/sec	Travel at "Burnt," in.	Mean/Max. Pressure
8	1.000	5.80	1780	58	0.704
10	1.042	9.50	2110	44	0.604

of 1 ton/sq in. is quite possible, we have here a strong argument for arranging an approximate equality of these two pressures, if the gun is to fire at several charge weights. This is necessary in a howitzer but not in an antitank gun.

7.624 Effect of shot weight on nozzle area for zero recoil

An increase of shot weight from 20 to 24 lb alters the ballistics in the same way as for normal guns: the peak pressure goes up, and the muzzle velocity and travel at "all burnt" decrease. If nozzle opening and shot start occur together, the balance of recoil is not affected by the change of shot weight. As an example of the case of nozzle opening before shot start, we take $P_{NS} = 2$, $P_{SS} = 3$ tons/sq in. Table 7.9 shows the effect on the throat area for zero recoil. The change is only 0.3 per cent.

TABLE 7.9 EFFECT OF SHOT WEIGHT, KEEPING ZERO RECOIL

Shot Wt., lb	MV, ft/sec	Max. Pressure, tons/sq in. Piezo	Travel at "Burnt," in.	Mean/Max. Pressure	Nozzle Throat for Zero Recoil
24	1596	6.30	45	0.625	1.000
20	1780	5.80	58	0.704	1.003

7.625 Effect of changes of chamber capacity

Such changes, keeping nozzle throat area constant, correspond to one source of round-to-round variation in ballistics: the variations of shot seating. These variations are, however, of little importance in the normal gun and are not very different for the recoilless gun. Table 7.10 illustrates an extreme case.

TABLE 7.10 CHANGES OF CHAMBER CAPACITY AT CONSTANT NOZZLE AREA

Chamber, cu in.	Max. Pressure, tons/sq in. Piezo	MV, ft/sec	Travel to "Burnt," in.	Mean/Max. Pressure
815	5.27	1709	61	0.714
500	7.08	1878	58	0.642

In this example there are unbalanced recoil momenta. Correcting to zero recoil in both cases, we find that this change in chamber capacity requires a considerable change of throat area (see Table 7.11). If nozzle start and shot start occurred together, the nozzle area would not be affected by change of chamber volume.

TABLE 7.11 EFFECT OF CHANGES OF CHAMBER CAPACITY AT ZERO RECOIL

Chamber, cu in.	Nozzle Throat for Zero Recoil	Max. Pressure, tons/sq in. Piezo	MV, ft/sec	Travel to "Burnt," in.	Mean/Max. Pressure
815	1.000	5.80	1780	58	0.704
500	1.037	7.60	1926	55	0.629

7.626 Changes in total shot travel

Here, too, the interest lies chiefly in the ranges of throat area needed to preserve zero recoil. The interior ballistics change in the same way as in a normal gun. If $P_{NS} = P_{SS}$, no change is needed in the nozzle area. An instance where these pressures differ by 1 ton/sq in. is shown in Table 7.12.

TABLE 7.12 EFFECT OF TOTAL SHOT TRAVEL ON NOZZLE AREA FOR ZERO RECOIL

Shot Travel, in.	Nozzle Throat Area for Zero Recoil
134	1.000
84.5	0.995

7.627 Effect of nature of propellant

This alters the rate of burning and the thermodynamic properties of the propellant gases. In changing to another propellant we have at our disposal two parameters, the charge weight, and the web size. These will be chosen to satisfy two conditions. The most natural choice would be to reproduce the previous muzzle velocity and maximum pressure. Other conditions are equally possible, and, in general, the effect on the recoil will depend on which conditions we take. In the special case of simultaneous shot starting and nozzle opening, the throat area alters only because of the change in C_p/C_v ($= \gamma$) of the propellant gases. If γ is altered from 1.24 to 1.26, which is a change of the right order, then the throat area has to be increased by less than 1 per cent. Where nozzle opening and the shot start do not occur together, the necessary variations of throat area may be somewhat larger but will be of the same order.

7.628 Influence of nozzle design

The diverging part of the nozzle is subjected to a forward thrust by the gases passing out and therefore helps to counteract the recoil of the gun. Alternatively, we may think in terms of momenta rather than pressures and can then describe the effect of the divergent part of the nozzle as a speeding up of the gases that have escaped through the throat. An important point is raised by the question: what do we gain by an increase in the expansion in the diverging part? We can use a smaller throat area and still retain zero recoil; maximum pressure and muzzle velocity must go up. Suppose we reduce the charge to return the maximum pressure to its value when the less efficient nozzle was fitted; is the muzzle velocity then higher or lower than it is with the less efficient nozzle? The answer is not very obvious, though one may guess that the change will be relatively small. It can be shown that a more efficient nozzle allows the charge to be reduced, if a certain maximum pressure is to be preserved, and the muzzle velocity drops very slightly, though there is a better utilization of the available energy in the charge.

7.63 The optimum pressure for opening of the nozzle

This pressure is more easily controlled by the designer than is the shot-start pressure. We have, therefore, some hope that, if we can decide on the optimum pressure, we shall be able to obtain this in our guns. Unfortunately, the optimum must be a compromise among various considerations. The points that follow have all been discussed in previous sections and are assembled here for convenience.

If nozzle opening and shot start occur together, there are no resultant thrusts on the gun at any stage of the firing. This means a lighter carriage. Furthermore, in this case, the nozzle area, for zero recoil, depends only on the nature of the propellant, varying by not much more than 0.5 per cent. If the nozzle opens at a pressure other than the shot-start pressure, then the throat area varies also with web size, charge weight and temperature, and shot weight; the extent of the variation depends on the difference between shot-start and nozzle-start pressures and may attain several per cent.

The smaller the nozzle-starting pressure, the smaller are likely to be the variations in the muzzle velocity and maximum pressure due to round-to-round variations in the strength of the disk.

In considering the nozzle-start pressure which gives the best ballistics as distinct from the best regularity, it is necessary to remember that an increase of muzzle velocity obtained from a particular nozzle-opening pressure may be associated with a higher maximum pressure or a longer travel to "burnt." If this is so, the advantage could be simulated by an increase of charge weight or web size. The best basis of comparison of nozzle-start pressure appears to be the comparison of the mean/maximum pressure ratio and the travel to "burnt." Figures 7.14 and 7.15 show that there is little to be gained in this respect by any special choice of nozzle-start pressures.

7.64 The value of a muzzle brake on a recoilless gun

It was suggested by Cooke, in one of the first patents on recoilless guns,[11] that a muzzle brake should be used on a recoilless gun. More is said about muzzle brakes in § 9.3. Here it is sufficient to explain that, by deflecting sideways or backwards part of the gases leaving the gun behind the shot, the muzzle brake reduces the total momentum imparted to the barrel after the shot has left. The addition of a muzzle brake has only a trivial effect on the muzzle velocity of a normal gun and, of course, no effect at all on the pressure-space curve. The advantage of a muzzle brake lies in the reduction of the carriage weight associated with a given energy of projectile.

In a recoilless gun the brake alters the charge as well as the weight of equipment needed for a given performance. This arises from the fact that a muzzle brake alters the interior ballistics of a recoilless gun; if we add a muzzle brake to a gun adjusted for zero recoil, we must reduce the nozzle throat at the back of the chamber if we wish to retain zero recoil. This change of throat alters the interior ballistics. To show the value of the muzzle brake we must adjust our interior ballistics.

One way to express the results is as follows. We add the brake, and adjust our four variables, charge weight, web size, nozzle-throat area, and total shot travel, to secure:

1. Zero recoil momentum after firing.
2. Same maximum pressure.
3. Same ballistic regularity.
4. Same muzzle velocity.

The reasons for items 1 and 4 are obvious. The reason for item 2 is the sensitivity of barrel weight to changes in peak pressure. It is, therefore, essential that none of the weight difference between the guns with and without brake should come from changes in maximum pressure; such weight changes could be produced without a muzzle brake and ought not to be credited to its use.

The gun thus produced has a weight that differs from that of the original gun without muzzle brake, and the new gun gives the same ballistics with a smaller charge than before. It can be shown that the changes in the weight of equipment are trivial, so that in effect the value of the muzzle brake is expressed as a saving in propellant. An example treated in detail by the author showed that the fitting of a medium-efficiency brake to a recoilless gun of muzzle velocity about 3500 ft/sec could be expected to save about 10 per cent of the propellant charge. The use of this brake on a normal antitank gun would give the same velocity, pressure, and regularity (the conditions satisfied by our recoilless-gun solutions with and without muzzle brake) with no change of charge and a saving of about 25 per cent on total weight of the whole weapon.

---

[11] Cooke, U. S. patent 1,380,358.

A recoilless gun with muzzle brake suffers bigger unbalanced momentary thrusts than a gun made recoilless by a breech nozzle alone.

It can be concluded that a muzzle brake ought to be fitted to a recoilless gun only if a saving of 10 per cent of the charge is considered valuable; however, in such circumstances one would probably not tolerate the three times normal charge demanded by the recoilless gun. It seems to be a safe conclusion that recoilless guns will never carry muzzle brakes.

This conclusion, based purely on theoretical work, checks with the German doctrine, arrived at by practical test.

For the possibilities of making a gun recoilless by use of a muzzle brake alone, see § 9.32. It is there shown that such a gun has the same (but more marked) disadvantages as the recoilless gun with breech venturi and no new virtues.

EXAMPLES

1. Show that the velocity of the gas at the throat of a nozzle is equal to the local velocity of sound $(dp/d\rho)^{1/2}$. [Osborne Reynolds, *Phil. Mag.* (March 1886).]

2. Can the velocity of efflux of the gas from a nozzle exceed the mean random velocity of the molecules in the reservoir?

3. Prove equation 24.

4. Prove the thrust formula, as regards the divergent part of the nozzle, by integration of the pressure on the walls from throat to exit.

5. A recoilless gun is to be compared with an orthodox gun of the same dimensions, firing the same shot at the same peak pressure. Which would you expect to have the higher muzzle velocity?

6. Integrate the isothermal equations of a recoilless gun when $1 < \Psi < 1 + \theta$, starting from equation 51 and using the methods of chapter 4. Show that there is always unburnt propellant at shot ejection. What is the mathematical solution if $\Psi > 1 + \theta$? What would be the physical behavior?

7. Find the similarity relations for a recoilless gun.

8. Estimate the order of magnitude of the velocity of the pieces of plastic nozzle seal when ejected from a recoilless gun. What contribution would this make to the balancing of recoil?

9. Prove equation 116.

10. Obtain a formula for the loss of velocity due to a small gas leakage occurring after "burnt," by expanding the formulas of § 7.39 up to the term in S/A. An 8-cm mortar barrel firing an 8-lb bomb at 700 ft/sec is vented by 16 holes of ½-in. diameter, arranged in sets of 4 every 3 in. along the last foot of the barrel. Make an estimate of the resulting loss of MV.

11. A certain recoilless gun has a peak pressure of 5 tons/sq in., a shot-start pressure of the order of 1 ton/sq in., and a much smaller nozzle-start pressure. The barrel has to be proved without dismantling from its rather flimsy carriage, and without altering the nozzle area. The methods suggested are (1) heavier shot, (2) heating the charge, (3) increase of charge weight. Which of these would impose least stress on the carriage for a given increase of peak pressure?

CHAPTER EIGHT Some Special Types of Gun

We shall now discuss some weapons that cannot be covered by the methods of chapters 4, 5, and 6. There we dealt with the normal, simplest type of gun. Here we shall show how the methods can be adapted to more complicated problems. Our aim is to illustrate some useful techniques, but the examples studied are important on their own account. They show also that the future of interior ballistics is not confined to reworking of the old classical problems.

8.1 The high-low-pressure gun

The design of a projectile often depends on the maximum acceleration it receives in the gun. For example, the lower the peak pressure the more explosive can be carried in an HE shell of given total weight, and the greater the lethal effect against most targets. Similarly, the effect of a hollow-charge projectile against armor is not strongly dependent on the weight of the metal casing of the projectile; thus a lower peak pressure means a lighter projectile for a given penetration, and the result is a lighter weapon. A low peak pressure is therefore desirable from the point of view of projectile design. An objection is the greater length of the gun, to which there are limits set by convenience in handling. A low peak pressure implies a low muzzle energy per unit of volume, and, if the volume of gun and cartridge case are to be practicable, the muzzle energy of the gun must be low. A really low peak pressure is possible only if the projectile is light in relation to its caliber (small W/d^3) and if the velocity is low.

Low-pressure weapons show difficulties of ignition, presumably because the pressure builds up so slowly, and the round-to-round variations of velocity are apt to be large.

A notable advance in low-pressure guns was made during World War II by German engineers. The front of the cartridge case was closed by a plate pierced by one or several nozzles, usually in the form of plain holes. By choice of the nozzle area the pressure in the chamber was kept considerably higher than that in the bore. The projectile was exposed to only a low pressure; the bore had to be as long as in an orthodox low-pressure gun; on the other hand, the propellant burned under a pressure two or three times that in the bore, and ignition and regularity were improved. Finally, the volume of the cartridge case was much smaller than in an orthodox low-pressure gun of the same muzzle energy. The nozzle plate was an integral part of the case and could be used several times.

To sum up, this *hoch- und niederdruck Kanone* is claimed to have the advantages, over the orthodox gun of equal muzzle energy and peak bore pressure, of better regularity and smaller cartridge.

Two examples of this kind of gun were built, the 8-cm PAW 600 and the 10.5-cm PAW 1000; the former was produced in some numbers and was nearly ready for service at the end of the war. Both were antitank guns firing hollow-charge projectiles at pressures of approximately 3 tons/sq in., and the "H/L principle" was adopted to improve the regularity.

Recoilless guns are often of a low-pressure type, and they appear to be suitable for the application of the high-low-pressure system. The only German example known is the 8.8-cm W71, which was built on the "three-pressure principle." The chamber vented into a space from which the gas passed either through the rearward jets or forward into the bore by another nozzle. It is not clear what ballistic advantages were expected from these complications, but, with its three nozzle areas to adjust, as well as charge and shot weight and web size, it made an excellent toy for the ballistician.

We shall use the high-low-pressure gun as an example[1] to show how easily the isothermal solution can be applied to the more unorthodox guns. Incidentally, the analysis is equally valid for mortars firing on primary charge only, when this is housed in the tail of the bomb in the conventional manner.

8.11 Notation

The gun can be idealized to the form shown in Fig. 8.1. Let the projectile and charge weights be W and C. Let W_1 be the effective mass of the shot, allowing for friction. The charge is contained in the first chamber, of volume U_1, and before the shot moves there is a total volume $U_1 + U_2$ behind it. Let S be the throat area of the venturi or nozzles connecting the two chambers, and let A be the bore area.

---

[1] Corner, *J. Franklin Inst.*, **246** (1948), 233.

Let P_1 be the pressure in the main chamber, assumed uniform throughout the chamber, and let P_2 be the space-mean pressure in the bore and second chamber. We write V for the velocity at travel x. Let $C\phi(t)$ be the amount of propellant burnt up to time t, and let $CN(t)$ be the amount of gas in the first chamber. Let η and δ be the covolume and density of the propellant.

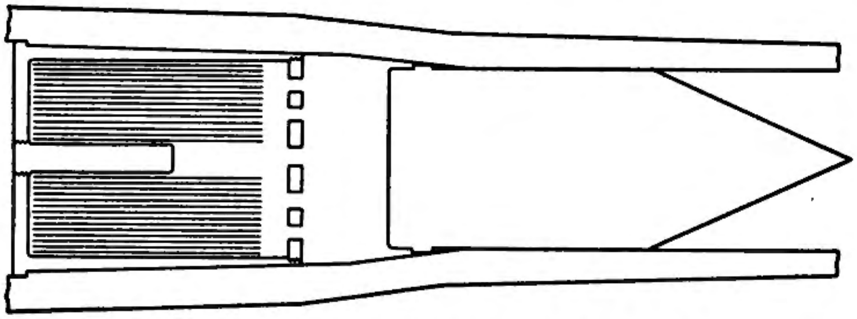

FIG. 8.1 Basic diagram of the *hoch-und-niederdruck Kanone*.
J. Franklin Inst. Reproduced by permission of the Franklin Institute.

8.12 Assumptions

We assume the form function,

$$\phi = 1 - f \tag{1}$$

The common shapes, tube, ribbon, and multitube, have effective form factors θ sufficiently close to zero to make a successful practical analysis possible with $\theta = 0$. Only for charges of cord is equation 1 far from sufficient.

We assume the conventional Lagrange correction, which ought to be little more inaccurate than in an orthodox gun. Hence,

$$W_2 \frac{dV}{dt} = AP_2 \tag{2}$$

where

$$W_2 = W_1 + \frac{C}{3} \tag{3}$$

We assume a rate of burning proportional to pressure, that is,

$$D \frac{df}{dt} = -\beta P_1 \tag{4}$$

We adopt the isothermal approximation, in which a mean temperature of the propellant gases is assumed throughout the period of burning of the charge. Let the corresponding force constant be λ. This applies throughout both chambers and bore, and we neglect the small regions near the venturi where other conditions hold.

We represent the initial resistance to motion of the shot by a change of effective rate of burning. The rate β is the adjusted rate. It may be seen that in this and the preceding assumption that we are following the basic level of accuracy of chapter 4.

The pressures at inlet and exit of the nozzle are P_1 and P_2, as near as matters. Let γ be the ratio of the specific heats at constant pressure and constant volume, for the propellant gases. If

$$\frac{P_2}{P_1} < \left(\frac{2}{\gamma + 1}\right)^{\gamma/(\gamma-1)} \tag{5}$$

then the rate of flow is settled by P_1 alone. This is a familiar result in the one-dimensional theory of nozzles. There should, as a matter of fact, be a covolume correction to this critical ratio, the magnitude of which has been worked out by Rateau and discussed in § 7.21. The correction amounts to about 7 per cent for $\gamma = 1.25$ and $P_1 = 25$ tons/sq in. For this value of γ, the condition 5 is

$$\frac{P_2}{P_1} < 0.555$$

The covolume also alters the rate of flow at a given pressure; it can be shown that the error is less than 7 per cent for pressures up to 25 tons/sq in. Thus we shall omit covolume effects on the flow between the two chambers, but not the direct effect on the equation of state.

For P_1 and P_2 satisfying equation 5, the rate of flow is

$$\frac{\psi S P_1}{\lambda^{1/2}} \tag{6}$$

where ψ is a numerical factor, which depends on γ but which lies within 1 per cent of 0.66 for all normal propellants. A correction for friction and heat losses in the nozzle should be added to ψ: a 5 per cent reduction, which is reasonable, makes ψ about 0.63.

If P_2/P_1 is greater than the limit mentioned in equation 5, the rate of flow is, for $\gamma = 1.25$,

$$\frac{zSP_1}{\lambda^{1/2}}\left(\frac{P_2}{P_1}\right)^{0.8}\left[1 - \left(\frac{P_2}{P_1}\right)^{0.2}\right]^{1/2} \tag{7}$$

where z is 3.162 for no friction losses. With allowance for friction, one may take $z = 3.00$. Another way to express the difference between equations 6 and 7 is by their ratio, which can be regarded as the factor representing the effect of back pressure on the flow. Table 8.1 shows some typical values and will be found useful in approximate calculations when P_2/P_1 exceeds 0.55.

TABLE 8.1 THE BACK-PRESSURE FACTOR

P_2/P_1	Factor	P_2/P_1	Factor
0.56	1	0.94	0.507
0.6	0.995	0.96	0.419
0.7	0.948	0.98	0.300
0.8	0.840	0.99	0.214
0.85	0.755	0.997	0.117
0.9	0.638	1	0

We shall assume that P_2/P_1 remains throughout at less than the critical value, equation 5. The simplicity that this introduces into the mathematics will be seen later. This assumption seems to be usually obeyed in the practical examples of the high-low-pressure gun.

We assume that no unburnt propellant passes the nozzle. This is probably true in the later types of H/L gun with a number of small nozzles in parallel between the two chambers. With normal ignition no appreciable error is expected from this assumption.

8.13 Equations of interior ballistics up to "burnt"

The first chamber. The equation of state for the gas in the first chamber is

$$P_1\left[U_1 - \frac{C(1-\phi)}{\delta} - CN\eta\right] = CN\lambda \tag{8}$$

and for that in the second chamber and bore is

$$P_2[U_2 + Ax - C(\phi - N)\eta] = C\lambda(\phi - N) \tag{9}$$

Also,

$$\frac{dN}{dt} = \frac{d\phi}{dt} - \frac{\psi S P_1}{C\lambda^{1/2}} \tag{10}$$

$$= \left(\frac{\beta}{D} - \frac{\psi S}{C\lambda^{1/2}}\right)P_1 \tag{11}$$

since

$$\frac{d\phi}{dt} = \frac{\beta P_1}{D} \tag{12}$$

Hence,

$$N = (1 - \Psi)\phi \tag{13}$$

where

$$\Psi = \frac{\psi SD}{\beta C\lambda^{1/2}} \tag{14}$$

This dimensionless parameter Ψ was found to play a fundamental part in the ballistics of recoilless guns, where S was the throat area of the venturi in the breech. Ψ is equally important in the theory of the H/L gun, where Ψ is of the order of 0.5.

Substituting from equation 13 into equation 8, we have

$$C\lambda(1 - \Psi)\phi = P_1\left[U_1 - \frac{C}{\delta} - C(1 - \Psi)\phi\left\{\eta - \frac{1}{\delta(1 - \Psi)}\right\}\right] \tag{15}$$

Thus the pressure builds up in the first chamber as if it were a closed vessel with charge $C(1 - \Psi)$, covolume η, density $\delta(1 - \Psi)$, and web size D.

From equations 12 and 15,

$$\frac{d\phi}{dt} = \frac{\beta C\lambda(1 - \Psi)\phi}{D\left[U_1 - \dfrac{C}{\delta} - C\phi\left\{\eta(1 - \Psi) - \dfrac{1}{\delta}\right\}\right]} = \frac{\mu\phi}{1 + b\phi} \tag{16}$$

where

$$\mu = \frac{\beta C\lambda(1 - \Psi)}{D\left(U_1 - \dfrac{C}{\delta}\right)} \tag{17}$$

and

$$b = \frac{C\left[\dfrac{1}{\delta} - \eta(1 - \Psi)\right]}{U_1 - \dfrac{C}{\delta}} \tag{18}$$

Note that b may have either sign. Taking the origin of time when $\phi = 1$, the solution of equation 16 is

$$\phi e^{b(\phi - 1)} = e^{\mu t} \tag{19}$$

The pressure in the first chamber is

$$P_1 = \frac{C\lambda(1 - \Psi)\phi}{\left(U_1 - \dfrac{C}{\delta}\right)(1 + b\phi)} \tag{20}$$

whose maximum value is

$$P_{1m} = \frac{C\lambda(1 - \Psi)}{\left(U_1 - \dfrac{C}{\delta}\right)(1 + b)} \tag{21}$$

The second chamber and bore. The equations for the second chamber and bore are simply

$$W_2 \frac{dV}{dt} = AP_2 \tag{22}$$

and

$$P_2 = \frac{C\Psi\lambda\phi}{U_2 + Ax - C\Psi\eta\phi} \tag{23}$$

Hence,

$$\frac{dV}{d\phi} = \frac{\lambda C\Psi(1 + b\phi)}{W_2\mu\left(\frac{U_2}{A} + x - \frac{\eta C\Psi\phi}{A}\right)} \tag{24}$$

If $U_2 \neq 0$, then, for small ϕ,

$$P_2 = \frac{C\Psi\lambda\phi}{U_2} \quad \text{and} \quad P_1 = \frac{C\lambda(1 - \Psi)}{U_1 - \frac{C}{\delta}}$$

so that initially

$$\frac{P_2}{P_1} = \left(\frac{\Psi}{1 - \Psi}\right)\left(\frac{U_1 - \frac{C}{\delta}}{U_2}\right) \qquad (U_2 \neq 0) \tag{25}$$

Returning to equation 24, we write

$$X = \mu\left(\frac{W_2}{\lambda C\Psi}\right)^{1/2}\left(\frac{U_2}{A} + x\right) \tag{26}$$

which, with equation 24, leads to

$$\frac{d}{d\phi}\left(\frac{\phi}{1 + b\phi}\frac{dX}{d\phi}\right) = \frac{1 + b\phi}{X - \nu\phi} \tag{27}$$

where

$$\nu = \frac{\mu\eta}{A}\left(\frac{W_2 C\Psi}{\lambda}\right)^{1/2} \tag{28}$$

b and ν will both be small. It is easy to show that ν is roughly $2\eta\bar{P}/\lambda$, where $\bar{P}$ is the space-mean pressure on the shot up to "burnt." For a gun working at $\bar{P} = 8$ tons/sq in., which is not likely to be exceeded in H/L guns, ν is less than 0.3. The value of b increases with the density of loading, and, for a density of loading of 0.8 g/cc, the limits of b are -0.6 and $+1$. For practical values of ν the range of values of b is -0.5 to 0.5. We may expect, therefore, that for H/L guns b will usually be small but larger than ν.

The solution that passes through $X = 0$ at $\phi = 0$ is

$$X = 2\phi^{1/2} + \frac{\nu}{5}\phi + \left(\frac{4b}{5} + \frac{4\nu^2}{125}\right)\phi^{3/2} + \frac{44}{425}b\nu\phi^2 + \frac{19}{325}b^2\phi^{5/2}$$

$$+ 0(b\nu\phi^{5/2}) + 0(\nu^3\phi^2) \quad (29)$$

This, then, is the solution for $U_2 = 0$.

In terms of X and ν, we have, for all solutions,

$$P_2 = \frac{\mu(W_2C\Psi\lambda)^{1/2}\phi}{A(X - \nu\phi)} \quad (30)$$

For the particular solution 29,

$$P_2 = \frac{\mu(W_2C\Psi\lambda)^{1/2}}{2A}\left[1 + \frac{2\nu}{5}\phi^{1/2} + \left(\frac{18\nu^2}{125} - \frac{2b}{5}\right)\phi\right.$$

$$\left. - \frac{158}{425}b\nu\phi^{3/2} + \frac{17}{130}b^2\phi^2 + \cdots\right] \quad (31)$$

The maximum of P_2 occurs at $\phi = 1$ unless b is greater than $5/6$, and even then only if ν is small. For the high density of loading of 0.9 g/cc, b is greater than $5/6$ only if $\Psi > 0.74$, and for lower and more practical densities of loading, Ψ must be still greater; for example, at a density of loading of 0.7 g/cc the peak of P_2 always occurs at $\phi = 1$. Hence it is only in the most extreme cases that $P_2(\phi = 1)$ will not be the maximum pressure P_{2m}, and even here they will agree closely. Therefore,

$$P_{2m} = \frac{\mu(W_2C\Psi\lambda)^{1/2}}{2A}\left(1 + \frac{2\nu}{5} + \frac{18\nu^2}{125} - \frac{2b}{5} + \cdots\right) \quad (32)$$

and

$$\frac{P_{2m}}{P_{1m}} = \frac{\beta(1 + b)(\lambda C W_2\Psi)^{1/2}}{2AD}\left(1 + \frac{2\nu}{5} + \frac{18\nu^2}{125} - \frac{2b}{5} + \cdots\right) \quad (33)$$

For values of ϕ less than unity, P_2/P_1 is nearly proportional to $\phi^{-1/2}$. If we go back in the solution toward smaller values of ϕ, we arrive always at a state in which our basic assumption,

$$\frac{P_2}{P_1} < 0.555$$

is violated. This means that our particular solution 29 is not a physically acceptable solution for small ϕ, though it is of course an exact solution of equation 27. The paradox that P_2/P_1 tends to infinity as ϕ

tends to zero is of no physical significance; this behavior would be eliminated in a real gun by Ψ tending to zero as P_2/P_1 approached unity.

For the velocity corresponding to equation 29, we have

$$\begin{aligned} V &= \frac{\phi}{1+b\phi}\left(\frac{\lambda C\Psi}{W_2}\right)^{1/2}\frac{dX}{d\phi} \\ &= \left(\frac{\lambda C\Psi}{W_2}\right)^{1/2}\left[\phi^{1/2} + \frac{\nu}{5}\phi + \left(\frac{b}{5} + \frac{6\nu^2}{125}\right)\phi^{3/2}\right. \\ &\qquad \left. + \frac{3b\nu}{425}\phi^2 - \frac{7}{130}b^2\phi^{5/2} + \cdots\right] \end{aligned} \tag{34}$$

and the velocity at "burnt" is

$$V_B = \left(\frac{\lambda C\Psi}{W_2}\right)^{1/2}\left[1 + \frac{\nu}{5} + \frac{b}{5} + \frac{6\nu^2}{125} + \frac{3b\nu}{425} - \frac{7b^2}{130} + \cdots\right] \tag{35}$$

The particular solution obtained up to the present applies only if $U_2 = 0$. A series solution can be obtained if $U_2 \gg Ax_B$. This is

$$\begin{aligned} X = X_0 &+ \frac{\phi}{X_0} + \left(\frac{3b}{4X_0} + \frac{\nu X_0 - 1}{4{X_0}^3}\right)\phi^2 + \left[\frac{(\nu X_0 - 1)^2}{9{X_0}^5} - \frac{\nu X_0 - 1}{36{X_0}^5}\right. \\ &\left. - \frac{b}{12{X_0}^3} + \frac{5b(\nu X_0 - 1)}{18{X_0}^3} + \frac{b^2}{6X_0}\right]\phi^3 + \cdots \end{aligned} \tag{36}$$

The corresponding pressure is

$$\begin{aligned} P_2 = \frac{\mu\phi(W_2C\lambda\Psi)^{1/2}}{AX_0}&\left[1 + \frac{\nu X_0 - 1}{{X_0}^2}\phi\right. \\ &+ \left\{\frac{1 - \nu X_0}{4{X_0}^4} + \frac{(1 - \nu X_0)^2}{{X_0}^4} - \frac{3b}{4{X_0}^2}\right\}\phi^2 + \left\{\frac{(\nu X_0 - 1)^3}{{X_0}^6}\right. \\ &\left.\left. - \frac{7(\nu X_0 - 1)^2}{12{X_0}^6} + \frac{b}{12{X_0}^4} + \frac{16b(1 - \nu X_0)}{9{X_0}^4} - \frac{b^2}{6{X_0}^2}\right\}\phi^3 + \cdots\right] \end{aligned} \tag{37}$$

and the velocity is

$$\begin{aligned} V = \frac{\phi}{X_0(1 + b\phi)}\left(\frac{\lambda C\Psi}{W_2}\right)^{1/2}&\left[1 + \left(\frac{3b}{2} + \frac{\nu X_0 - 1}{2{X_0}^2}\right)\phi + \left\{\frac{(\nu X_0 - 1)^3}{3{X_0}^4}\right.\right. \\ &\left.\left. - \frac{\nu X_0 - 1}{108{X_0}^4} - \frac{b}{4{X_0}^2} + \frac{5b(\nu X_0 - 1)}{6{X_0}^2} + \frac{b^2}{2}\right\}\phi^2 + \cdots\right] \end{aligned} \tag{38}$$

For $X_0 \geq 5$, this solution is convenient and accurate. For nonzero values of X_0 such that these series do not converge sufficiently rapidly, it is best to integrate equation 27 numerically. The boundary conditions are that $\phi \dfrac{dX}{d\phi} = 0$ and $X = X_0$ at $\phi = 0$. Since we are interested in the pressure, velocity, and travel only at $\phi = 1$, the results can be tabulated very simply, as in Tables 8.2, 8.3, and 8.4. Here we tabulate X

TABLE 8.2 VALUES OF $X/(2 + X_0)$ AT BURNT, AS A POWER SERIES IN b AND ν

The coefficients should be interpolated linearly with respect to X_0.

X_0					
0	1.000	$+0.400b$	$+0.032b^2$	$+0.100\nu$	$+0.05b\nu$
0.05	0.964				
0.1	0.928				
0.15	0.894				
0.2	0.861	$+0.355b$			
0.25	0.830			$+0.095\nu$	
0.3	0.801				
0.35	0.773				
0.4	0.747	$+0.308b$			
0.45	0.724				
0.5	0.703		$+0.030b^2$	$+0.085\nu$	$+0.05b\nu$
0.55	0.687				
0.6	0.674	$+0.262b$			
0.65	0.662				
0.7	0.651	$+0.239b$			
0.75	0.642			$+0.065\nu$	
0.8	0.634	$+0.218b$			
0.9	0.621	$+0.198b$			
1.0	0.611	$+0.181b$	$+0.025b^2$	$+0.045\nu$	$+0.03b\nu$
$1\frac{1}{8}$	0.604	$+0.162b$			
$1\frac{1}{4}$	0.600	$+0.146b$		$+0.033\nu$	
$1\frac{3}{8}$	0.600	$+0.132b$			
$1\frac{1}{2}$	0.602	$+0.120b$	$+0.020b^2$	$+0.025\nu$	
$1\frac{3}{4}$	0.609	$+0.100b$			
2	0.618	$+0.084b$	$+0.016b^2$	$+0.015\nu$	$+0.01b\nu$
$2\frac{1}{2}$	0.641	$+0.061b$	$+0.013b^2$	$+0.009\nu$	
3	0.665	$+0.047b$	$+0.010b^2$	$+0.005\nu$	
$3\frac{1}{2}$	0.688	$+0.037b$	$+0.007b^2$	$+0.002\nu$	
4	0.708	$+0.030b$	$+0.005b^2$	$+0.000\nu$	
$4\frac{1}{2}$	0.726	$+0.025b$	$+0.003b^2$		
5	0.743	$+0.021b$	$+0.002b^2$	$+0.000\nu$	$+0.01b\nu$

Digitized by Google

Original from
UNIVERSITY OF MICHIGAN

TABLE 8.3 VALUES OF $\left(\frac{1 + X_0}{1 + b}\right) \frac{dX}{d\phi}$ AT "BURNT"

The coefficients should be interpolated linearly with respect to X_0.

X_0					
1.1	1.425	$+0.515b$	$-0.081b^2$	$+0.401\nu$	$+0.07b\nu$
1.3	1.410	$+0.542b$		$+0.378\nu$	
1.5	1.392	$+0.560b$	$-0.070b^2$	$+0.350\nu$	$+0.125b\nu$
$1\frac{3}{4}$	1.368	$+0.576b$			
2	1.344	$+0.585b$	$-0.054b^2$	$+0.285\nu$	$+0.12b\nu$
$2\frac{1}{4}$	1.322	$+0.590b$			
$2\frac{1}{2}$	1.301	$+0.593b$	$-0.034b^2$	$+0.234\nu$	$+0.115b\nu$
3	1.264	$+0.592b$	$-0.016b^2$	$+0.200\nu$	$+0.10b\nu$
$3\frac{1}{2}$	1.234	$+0.587b$	$-0.008b^2$	$+0.174\nu$	$+0.09b\nu$
4	1.210	$+0.580b$	$-0.000b^2$	$+0.152\nu$	$+0.08b\nu$
$4\frac{1}{2}$	1.191			$+0.135\nu$	
5	1.175	$+0.564b$	$+0.037b^2$	$+0.123\nu$	$+0.05b\nu$

TABLE 8.4 VALUES OF $\frac{1}{1 + b} \frac{dX}{d\phi}$ AT "BURNT"

The coefficients should be interpolated linearly with respect to X_0.

X_0					
0	1.000	$+0.217b$	$-0.070b^2$	$+0.210\nu$	$+0.00b\nu$
0.05	1.018				
0.1	1.027	$+0.226b$		$+0.235\nu$	
0.15	1.029				
0.2	1.025	$+0.234b$		$+0.253\nu$	
0.25	1.015				
0.3	1.000	$+0.241b$		$+0.264\nu$	
0.4	0.965	$+0.247b$		$+0.268\nu$	
0.5	0.924	$+0.251b$	$-0.056b^2$	$+0.265\nu$	$+0.01b\nu$
0.6	0.881	$+0.253b$		$+0.257\nu$	
0.7	0.837	$+0.254b$		$+0.247\nu$	
0.8	0.795	$+0.253b$		$+0.233\nu$	
0.9	0.754	$+0.252b$		$+0.220\nu$	
1.0	0.715	$+0.249b$	$-0.042b^2$		$+0.03b\nu$
1.1	0.678	$+0.245b$		$+0.191\nu$	

and $dX/d\phi$, both at $\phi = 1$. From these can at once be obtained

$$P_{2m} = \frac{\mu(W_2 C \Psi \lambda)^{1/2}}{A(X - \nu)} \tag{39}$$

$$\text{Travel at "burnt"} = \frac{(X - X_0)}{\mu} \left(\frac{\lambda C \Psi}{W_2}\right)^{1/2} \tag{40}$$

and

$$\text{Velocity at ``burnt''} = \frac{1}{1+b}\left(\frac{\lambda C\Psi}{W_2}\right)^{1/2}\frac{dX}{d\phi} \tag{41}$$

Linear interpolation leads to errors of, at most, 0.002 in $X_B/(2 + X_0)$ and 1 in 400 in $(dX/d\phi)_B$. Other errors can arise from our approximate representation of the computed results, so that the possible errors are doubled. This accuracy is ample, in view of the simplifying assumptions made in our theory.

We have shown that, if $U_2 = 0$, the maximum of P_2 occurs at "burnt" except in extreme cases. Now an increase of the chamber volume of a gun causes the maximum pressure to occur at larger values of ϕ. Hence we see, and this can also be verified from the numerical solutions, that it is only in the most extreme cases that the peak bore pressure does not occur at "burnt."

8.14 Interior ballistics after "burnt"

So long as $P_2/P_1 < 0.555$, the gas flow from the first chamber is the same as if P_2 were zero, and the rate of decay of pressure is given by Hugoniot's theory with Rateau's corrections for covolume (see chapter 9). It is probable, however, that covolume corrections will be small in all practical high-low-pressure guns. In such a case,

$$P_1 = \frac{C(1-\Psi)\lambda}{U_1 - \eta C(1-\Psi)}\left(1 + \frac{t}{\theta_1}\right)^{-2\gamma/(\gamma-1)} \tag{42}$$

and

$$N = (1-\Psi)\left(1 + \frac{t}{\theta_1}\right)^{-2/(\gamma-1)} \tag{43}$$

where

$$\theta_1 = \frac{2U_1}{(\gamma-1)\psi S\lambda^{1/2}} \tag{44}$$

The gas in the second chamber and bore also expands adiabatically. The equations are:

$$P_2 = \frac{C\lambda T'(1-N)}{U_2 + Ax - C(1-N)\eta} \tag{45}$$

$$W_2\frac{dV}{dt} = AP_2 \tag{46}$$

together with the equation of energy,

$$\frac{C\lambda}{\gamma-1}[\Psi - (1-N)T'] = \frac{W_2}{2}\left[\left(\frac{dx}{dt}\right)^2 - \left(\frac{dx}{dt}\right)_B^2\right] \tag{47}$$

We have written T' for the ratio of the gas temperature to the mean value it had during burning. Suffix B refers to conditions at "burnt." Differentiating equation 47 and using equations 45 and 46, we have

$$T'\frac{dN}{dt} - (1 - N)\frac{dT'}{dt} = \frac{(\gamma - 1)(1 - N)T'A}{[U_2 + Ax - C(1 - N)\eta]}\frac{dx}{dt}$$

which integrates to

$$\log\left[\frac{(1 - N)T'}{\Psi}\right] = -(\gamma - 1)\log\left[\frac{U_2 + Ax - C(1 - \bar{N})\eta}{U_2 + Ax_B - C(1 - \bar{N})\eta}\right] \tag{48}$$

To obtain the muzzle velocity, therefore, we guess $\bar{N}$ for the period after "burnt," and determine $(1 - N)T'$ from equation 48 and the muzzle velocity from equation 47. The mean velocity after "burnt" gives the epoch of shot ejection and so, from equation 43, the value of N at that instant. We then verify that our first $\bar{N}$ was sufficiently accurate.

Finally we insert our value of $(1 - N)T'$ in equation 45 and our estimate for the time of shot ejection in equation 42 and examine whether P_2/P_1 is still less than 0.555 at the muzzle.

Although equations 43 and 44 apply only if P_2/P_1 is less than 0.555, the equations 47 and 48 are always true. If P_2/P_1 is greater than 0.555 for all or part of the period after "burnt," ψ in equation 44 should be multiplied by an appropriate "back-pressure factor" from Table 8.1. Equation 43 can still be used, as an approximation, with the new and larger value of θ_1, when finding $\bar{N}$ for the period after "burnt."

8.15 Summary of the working formulas

In practice, one is often interested only in certain salient features of the ballistic solution. The first of these is the peak pressure in the propellant chamber:

$$P_{1m} = \frac{C\lambda(1 - \Psi)}{\left(U_1 - \dfrac{C}{\delta}\right)(1 + b)} \tag{21}$$

where

$$\Psi = \frac{\psi SD}{\beta C\lambda^{1/2}} \tag{14}$$

and

$$b = \frac{C\left[\dfrac{1}{\delta} - \eta(1 - \Psi)\right]}{U_1 - \dfrac{C}{\delta}} \tag{18}$$

If P_2/P_1 is later found to be greater than 0.555 for all or part of the time, ψ is multiplied by an appropriate "back-pressure factor" from Table 8.1.

We calculate

$$\mu = \frac{\beta C\lambda(1 - \Psi)}{D\left(U_1 - \frac{C}{\delta}\right)} \tag{17}$$

and, from the initial volume U_2 of the second chamber, we find

$$X_0 = \frac{\mu U_2}{A}\left(\frac{W_2}{\lambda C\Psi}\right)^{\frac{1}{2}} \tag{26}$$

where

$$W_2 = W_1 + \tfrac{1}{3}C \tag{3}$$

We work out

$$\nu = \frac{\mu\eta}{A}\left(\frac{W_2 C\Psi}{\lambda}\right)^{\frac{1}{2}} \tag{28}$$

From Tables 8.2 through 8.4 we obtain X and $dX/d\phi$ at "burnt." Then the peak pressure in the bore is

$$P_{2m} = \frac{\mu(W_2 C\Psi\lambda)^{\frac{1}{2}}}{A(X - \nu)} \tag{39}$$

the travel at "burnt" is

$$x_B = \frac{(X - X_0)}{\mu}\left(\frac{\lambda C\Psi}{W_2}\right)^{\frac{1}{2}} \tag{40}$$

and the velocity at "burnt" is

$$\frac{1}{1 + b}\left(\frac{\lambda C\Psi}{W_2}\right)^{\frac{1}{2}}\frac{dX}{d\phi} \tag{41}$$

It remains only to find the muzzle velocity. At "burnt," $N = 1 - \Psi$. We guess $\bar{N}$ for the period from "burnt" to shot ejection and calculate $(1 - N)T'$ from

$$\log\left[\frac{(1 - N)T'}{\Psi}\right] = -(\gamma - 1)\log\left[\frac{U_2 + Ax - C(1 - \bar{N})\eta}{U_2 + Ax_B - C(1 - \bar{N})\eta}\right] \tag{48}$$

The muzzle velocity then comes from

$$V^2 = V_B{}^2 + \frac{2C\lambda}{(\gamma - 1)W_2}[\Psi - (1 - N)T'] \tag{47}$$

The mean velocity after "burnt" gives the epoch of shot ejection, and so the value of N at that time, from

$$N = (1 - \Psi)\left(1 + \frac{t}{\theta_1}\right)^{-2/(\gamma-1)} \tag{43}$$

where

$$\theta_1 = \frac{2U_1}{(\gamma - 1)\psi_1 S\lambda^{1/2}} \tag{44}$$

$\bar{N}$ is calculated and, if necessary, the muzzle velocity repeated with this better $\bar{N}$.

8.16 The maximum possible piezometric efficiency

Some German ballisticians have claimed that a high-low-pressure gun can be designed with a higher piezometric efficiency than any orthodox gun. The theoretical maximum piezometric efficiency obtainable from orthodox guns depends to some extent on the details of the theory used, and, in particular, on the type of resistance that is assumed to oppose the motion of the shot. The theory of chapter 4 gives a maximum of 88 per cent, if "burnt" must lie inside the gun or at the muzzle; other theories give results between 85 and 90 per cent. It is clear that in any event 85 per cent is possible, so that the room for improvement by the H/L principle is small.

Consider now an H/L gun for which P_2/P_1 is less than 0.555 throughout the firing. Then Ψ is a constant, and our theory is as accurate as, say, that of chapter 4. The maximum piezometric efficiency of a given gun obviously occurs when "burnt" coincides with shot ejection. The muzzle energy of the shot is then

$$\frac{\lambda C\Psi}{2(1 + b)^2}\frac{W_1}{W_2}\left(\frac{dX}{d\phi}\right)_B^2 \tag{49}$$

The maximum value of W_1/W_2 is unity. Also the peak pressure in the bore is

$$P_{2m} = \frac{\mu(W_2 C\Psi\lambda)^{1/2}}{A(X_B - \nu)}$$

and the travel is

$$x_B = \frac{(X_B - X_0)}{\mu}\left(\frac{\lambda C\Psi}{W_2}\right)^{1/2}$$

so that the work done by P_{2m} acting through a distance x_B would be

$$\lambda C\Psi\left(\frac{X_B - X_0}{X_B - \nu}\right) \tag{50}$$

From equations 49 and 50 the piezometric efficiency is

$$\mathrm{PE} = \frac{X_B - \nu}{2(1 + b)^2(X_B - X_0)}\left(\frac{dX}{d\phi}\right)_B^2 \tag{51}$$

For $b = \nu = 0$, this is a function of X_0 alone. The PE starts at 0.5 for $X_0 = 0$, rises to a maximum of about 0.6 near $X_0 = \frac{1}{4}$, and then falls to 0.5 again as X_0 tends to infinity. Increase of b increases the upper limit of the PE. For $b = 0.5$, which is not likely to be exceeded in practice, the maximum PE is still less than 0.75. ν has very little influence on this limit, a value of $\nu = 0.2$ changing the piezometric efficiency by only 0.01.

Hence for H/L guns in which P_2/P_1 is always less than 0.555, the piezometric efficiency cannot exceed 0.8, which is less than can be obtained from orthodox guns.

Although our equations can be applied as a guide when P_2/P_1 exceeds 0.555 for part or all of the solution, they become increasingly inaccurate as this ratio approaches unity; indeed, our solution does not include that of chapter 4 as a special case, in spite of having the same basic approximations. This arises from our having assumed that the parameter Ψ is constant during the solution. An orthodox gun can, if we like, be regarded as having a propellant chamber, a vanishingly small second chamber, and a connecting nozzle of full bore area. The equations for such a system are included in our fundamental set, but as the variation of Ψ is important our method of solution fails.

If any H/L gun has a better piezometric efficiency than can be obtained from an orthodox gun, then the ratio P_2/P_1 must be greater than 0.555 for a large part of the motion.

8.2 Small arms

The class of "small arms" is defined as consisting of those weapons whose recoil is sufficiently small to be taken directly by the firer and whose weight enables them to be carried by one man. Ballistically, the differences between "small arms" and "guns" are well marked, so that it is possible to recognize in a given weapon either "small-arms behavior" or "gun behavior."

The most important special features of small arms are the following:

1. The ballistics are much more sensitive to the details of the ignition.
2. Cooling to the walls of the bore is more important, because of the greater surface/volume ratio.
3. S.A. projectiles are normally not banded. The outside layer is a relatively soft metal, which is pressed into the rifling by deformation of

Digitized by Google Original from UNIVERSITY OF MICHIGAN

the whole bullet under the high acceleration in the bore. In calibers of 20 mm and over, however, ordinary bands are used.

4. The propellants are often "moderated," that is, coated with slowly burning layers.

When the third effect is present it makes a great difference to the form of the resistance to motion of the shot. Instead of a high resistance at the start, dropping rapidly to a much smaller value, the resistance is now small at the start, building up to a maximum somewhat before peak pressure; thereafter the resistance decreases slowly.[2] Of the simple ways to represent resistance in the theory, the best appears to be the increase of effective shot mass. Even so, predictions based on such a model are not always successful.

Moderated propellants also complicate the theory, to which the modifications are indeed of an obvious type, but inconvenient in most analytical solutions.

The need to consider ignition as an important factor makes an accurate theory of small arms more elaborate than a corresponding theory for guns. At the same time the simple "working schemes" are handicapped by not being able to allow for this important factor, which, indeed, it is not easy to put into numerical form. Ballistic methods for small arms are accordingly more empirical than for guns and rarely more sophisticated than the isothermal model of chapter 4.

A point of some interest is raised by the development of recoilless guns, which have been produced as one-man weapons in calibers as large as 9 cm. Are these to be called guns or small arms? Although from the points of recoil and weight they may appear to be "small arms," in calibers over 4 cm, at least, their ballistic behavior is that typical of a gun.

8.3 Composite charges

Throughout this book up to this point we have assumed that all the pieces of the charge have the same nominal dimensions and uniform composition through the depth of the grain. We have referred briefly to the effects produced by the real variation of web size from one grain to another, which makes the charge more degressive than one would expect from its nominal shape. The discussion of chapter 2 was intended to cover only small variations in the size. The "composite charges," which we are now to consider, consist of a mixture of grains of two or more nominal sizes, usually with the same composition but quite often with different shapes. The practical application is to the successive charges of howitzers. Here the bottom charge has to be small in weight in order to keep the muzzle velocity low; to start the shot with certainty needs a peak pressure of at least 3 tons/sq in. and preferably 4 tons/sq in., which can be attained on a small charge only if the web is very small. Thus the bottom charge is a small weight of a small size. The higher charges cannot be formed by addition of more of the same size, since the peak working pressure of the gun would soon be exceeded. The higher charges are therefore a mixture of various weights and sizes and even of shapes: mixtures of cord and tube have been used. It must be added that the top charge is often a completely separate charge of a single large web size, to get the utmost performance out of the gun.

---

[2] For experimental results on the resistance of S.A. projectiles, see Bodlien, **Z.** *ges. Schiess- u. Sprengstoffw.*, **34** (1939), 33, 65, 97, and references therein.

Such composite charges are usually of a single chemical composition. An example where this is not so occurs in the treatment of an ignition system as a partial charge of different force and web size to the main charge.

Closely related problems occur when the propellant charge is composed of nominally identical grains, each of which is "moderated." This means that the first part to be burnt is a cool, slow-burning type, which covers a core of much faster propellant. This gives the same ballistic effects as a progressive shape. Moderated propellants are found chiefly in small-arms practice; one reason is that the optimum density of loading for a progressive charge is greater than for cord or tube and can be attained only with difficulty in a gun cartridge. It is easier to obtain a high density of loading in a small-arms cartridge.

Propellants could be made with a "negative moderation," but the ballistic effects could be obtained more easily by using cords or thin plates. Other surface treatments of grains include glazing with graphite, to reduce the risks of static electricity during loading, and coating with a thin film of catalyst for ignition. Both surface films are too thin to play a part in the central problem of interior ballistics; the catalyst merely helps to make our normal assumptions about the start of burning more nearly correct.

8.31 Reduction of a composite charge to a single effective web size

We shall deal first with a charge consisting of several nominal sizes, each grain being unmoderated. We shall attempt to find a charge of a single web size that would give the same ballistics.

In the equations of interior ballistics appear eight characteristics of the charge: its weight C, covolume η, density δ, force constant RT_0, effective ratio of specific heats γ, index of the rate of burning α, form factor θ, and finally D/β, which is related to the burning time. These parameters occur as (1) CRT_0, $C[\eta - (1/\delta)]$ and C/δ in the equation of state; (2) $CRT_0/(\gamma - 1)$ in the energy equation; (3) C in the Lagrange pressure-gradient corrections; (4) α, θ, and D/β in the equations of burning.

Suppose we mix two charges, C_1 and C_2, of different sizes, shapes, and compositions. We wish to find an equivalent composite charge of the same shapes and sizes but of a single composition. We can assume that the two compositions have the same index of the rate of burning, for, if not, then the index of one can be altered with a nearly counterbalancing change in the form function—this change will be, of course, somewhat different for each ballistic solution. Let the new charge weights be C_1' and C_2', and let their density be $\bar{\delta}$ and their force constant $\overline{RT}_0$. Then, if we define

$$\overline{RT}_0 = \frac{C_1RT_{01} + C_2RT_{02}}{C_1 + C_2} \tag{52}$$

$$\frac{1}{\bar{\delta}} = \frac{\dfrac{C_1}{\delta_1} + \dfrac{C_2}{\delta_2}}{C_1 + C_2} \tag{53}$$

$$C_1' = \frac{C_1RT_{01}}{\overline{RT}_0} \tag{54}$$

and

$$C_2' = \frac{C_2RT_{02}}{\overline{RT}_0} \tag{55}$$

we have

$$C_1' + C_2' = C_1 + C_2$$

and so the Lagrange terms are the same in the two systems. The equations of state differ at most in the covolume correction terms, which agree if both (*a*)

$$\frac{\left(\eta - \dfrac{1}{\delta}\right)_1}{RT_{01}} = \frac{\left(\eta - \dfrac{1}{\delta}\right)_2}{RT_{02}} \tag{56}$$

and (*b*) a mean $\overline{\eta - 1/\delta}$, defined by

$$\frac{\overline{\eta - \dfrac{1}{\delta}}}{\overline{RT}_0} = \frac{\left(\eta - \dfrac{1}{\delta}\right)_1}{RT_{01}} \tag{57}$$

is used for the mean composition. Alternatively, we can arrange

$$\bar{\eta} = \frac{C_1\eta_1 + C_2\eta_2}{C_1 + C_2}$$

as an alternative to equation 53, but there is no way to make the equations of state agree exactly unless a is satisfied. For all that, the difference is small in practice.

The energy equations agree only if $\gamma_1 = \gamma_2$; here again the difference is only rarely of importance. This completes the reduction to a single composition.

We have now to find a single charge C, of web size D and form factor θ, which gives the same ballistic equations as a composite charge (C_1, C_2) of webs (D_1, D_2) and form factors (θ_1, θ_2). We shall consider the special case where both θ_1 and θ_2 are zero, which is roughly true for tube or multitubular propellant. Other cases can be treated by the same process with differences only in the algebra. These we leave as an exercise for the reader.

Suppose, then, that

$$D_1 \frac{d\phi_1}{dt} = \beta P^\alpha = D_2 \frac{d\phi_2}{dt}$$

with D_1 less than D_2. The equivalent charge weight C must be

$$C = C_1 + C_2 \tag{58}$$

to give the same equations after "burnt." Let ϕ be the fraction of this charge burnt at time t, and let Df be the corresponding remaining part of the initial web D. The composite charge completes its burning at a time T given by

$$\int_0^T \beta P^\alpha \, dt = D_2$$

and the single equivalent charge at a time given by

$$\int_0^T \beta P^\alpha \, dt = D$$

Hence, D must be equal to D_2, and $f = f_2$.

The faster part of the composite charge burns out when

$$f_2 = 1 - \frac{D_1}{D_2}$$

Before this time the rate of generation of gas is, for the composite charge,

$$C_1 \frac{d\phi_1}{dt} + C_2 \frac{d\phi_2}{dt} = -\left(\frac{C_1}{D_1} + \frac{C_2}{D_2}\right) D_2 \frac{df}{dt}$$

and for the single equivalent charge is

$$(C_1 + C_2) \frac{d\phi}{dt}$$

To ensure that gas is evolved at the same rate by both charges we must take

$$(C_1 + C_2) \frac{d\phi}{dt} = -\left(\frac{C_1}{D_1} + \frac{C_2}{D_2}\right) D_2 \frac{df}{dt}$$

giving

$$\phi = \frac{(C_1 D_2 + C_2 D_1)(1 - f)}{D_1(C_1 + C_2)} \tag{59}$$

for

$$f \geq 1 - \frac{D_1}{D_2}$$

When

$$f < 1 - \frac{D_1}{D_2}$$

it is found that

$$\phi = \frac{C_1 + C_2(1 - f)}{C_1 + C_2} \tag{60}$$

Thus, the (ϕ, f) relation is a pair of straight lines meeting at

$$f = 1 - \frac{D_1}{D_2}$$

where there is a discontinuity of slope. When the charge of smallest web is in cord form the (ϕ, f) curve has no discontinuity of slope.

The relation 59–60 is now to be approximated by one of the form functions used for single charges. When this is done, the ballistic solution for the composite charge can be obtained from any of our previous methods for single charges. We take our usual form function,

$$\phi = (1 - f)(1 + \theta f)$$

which we shall fit to the relation 59–60. The fitting cannot be exact and consequently is a little arbitrary. One plausible way is to choose θ to give the same area under the (ϕ, f) curve as the pair of lines 59–60. The area,

$$\int_0^1 \phi \, df = \frac{1}{2} + \frac{\theta}{6}$$

The area under the true form function is

$$\frac{1}{2} + \frac{C_1(D_2 - D_1)}{2D_2(C_1 + C_2)}$$

so that the equivalent form factor is

$$\theta = \frac{3C_1(D_2 - D_1)}{(C_1 + C_2)D_2} \tag{61}$$

This can be used in a normal ballistic method only if $\theta \leq 1$, that is, if

$$3\frac{D_1}{D_2} + \frac{C_1}{C_2} \leq 2 \tag{62}$$

In practice equation 62 is nearly always satisfied. In the exceptional cases where the composite charge is more degressive than a single charge of cord, a form function more complicated than the standard type must be used. The obvious choice is

$$\phi = (1 - f)(1 + \theta f + \theta' f^2)$$

which would cover all strengths of degression up to and including spheres or cubes ($\theta = \theta' = 1$). As we have said, the need for such a degressive form rarely arises except with composite charges and also with chopped cord, used a little in weapons not usually given a theoretical analysis.

It is interesting to calculate from equation 61 the increase of θ caused by a small heterogeneity of web. Suppose, for example, that 20 per cent of the tubes have a web 20 per cent smaller than the nominal size, then θ will be 0.1.

Moderated propellants can be treated by using a suitable form function in the orthodox equations. Normally the form function will be less degressive than an unmoderated propellant of the same geometrical shape. This prevents any difficulty from θ becoming greater than unity. Since the variation of burning rate between different layers of the grain is achieved by a variation of the composition, causing a variation of the force constant, the reduction to a uniform composition has to allow for both factors. The correction to a single force is closely related to the process by which we reduced the problem of a mixture of two compositions to a single mean composition.

Digitized by Google

Original from
UNIVERSITY OF MICHIGAN

8.4 Tapered-bore guns

The first conception of a gun with a bore cross section varying along its length is due to Puff[3] (1903). His bore was to be a section of a converging cone, and the projectile was to have a form that could be swaged down during the travel. Apparently Puff was never able to construct such a weapon. Toward the end of the 1920's Gehrlich announced a supervelocity rifle, which turned out to be a coned-bore gun. His claims led to a vigorous discussion[4] of just what had been achieved. The discussion did show that the high muzzle energy of his gun was in line with orthodox weapons of the same charge weight and bore volume; the coned-bore gun was shorter than the orthodox gun with the same performance and emergent caliber; alternatively, the shot from a coned-bore weapon had better exterior ballistics than an orthodox shot of the same weight fired at the same velocity from a normal gun of equal length.

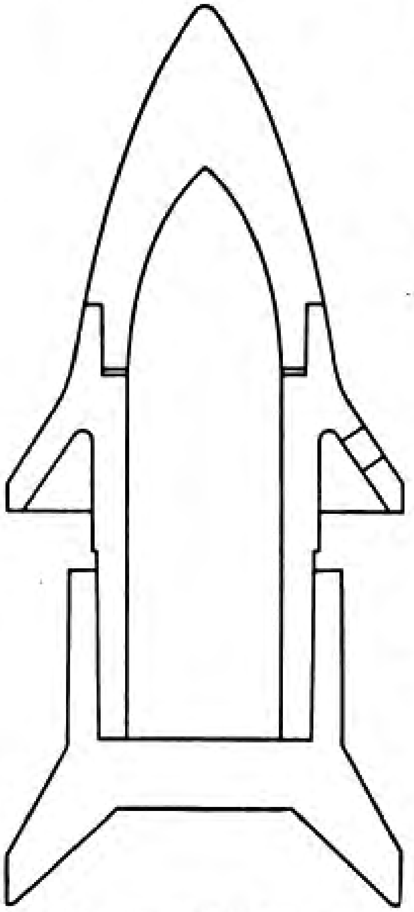

FIG. 8.2 The 28/20-mm armor-piercing shot in section showing the collapsing flanges, which are swaged back by the tapering bore.

This having been made clear, the tapered-bore gun fell out of the literature, and no more was heard of it until 1941. In June of that year a specimen of the first such gun to go into service was captured in Libya. In Fig. 8.2 is shown the shot used by this gun, the 28/20-mm Pz B 41, in the expanded state before firing. The initial caliber was 28 mm and the final caliber 20 mm, and the contraction took place over most of the central part of the shot travel. The bore was rifled throughout. The shot itself had an armor-piercing core of tungsten carbide, sheathed in a free-cutting steel. The two flanges shown are wide enough to support the shot at the start of its motion and fold backward as the bore narrows. A few holes are pierced through the front flange to prevent gas being trapped during the swaging, which considerably reduces the available volume between the flanges. The pressure of any trapped gas is sufficient to balloon the front flange as the shot leaves the muzzle, causing high retardation or loss of accuracy, and in a bad case, such as firing from an oily bore, the projectile may come to pieces at the muzzle.

---

[3] Puff, *DRP*, 183,614; 199,365.

[4] Gehrlich, *Heerestechnik* (1929), 261. Justrow, Z. *VDI* (1935), 1417; *Wehrtech. Monatshefte*, **40** (1936), 80. Schmitz, *Wehrtech. Monatshefte*, **39** (1935), 149.

Several other coned-bore antitank guns were developed in Germany before the end of 1943, when the shortage of tungsten made it not worth while to continue. Development in other countries went on to the end of World War II. The direction of development may be briefly indicated. The rifling of the cone (as in the 28/20) was difficult and was found to be unnecessary. Later guns had a short steeply rifled initial stretch of full caliber; then a smooth-bore slow cone, of slope about 1 in 30; and a short muzzle section of constant caliber. The projectile was spun in the rifled section and increased its spin in the smooth bore simply by the reduction of its axial moment of inertia.

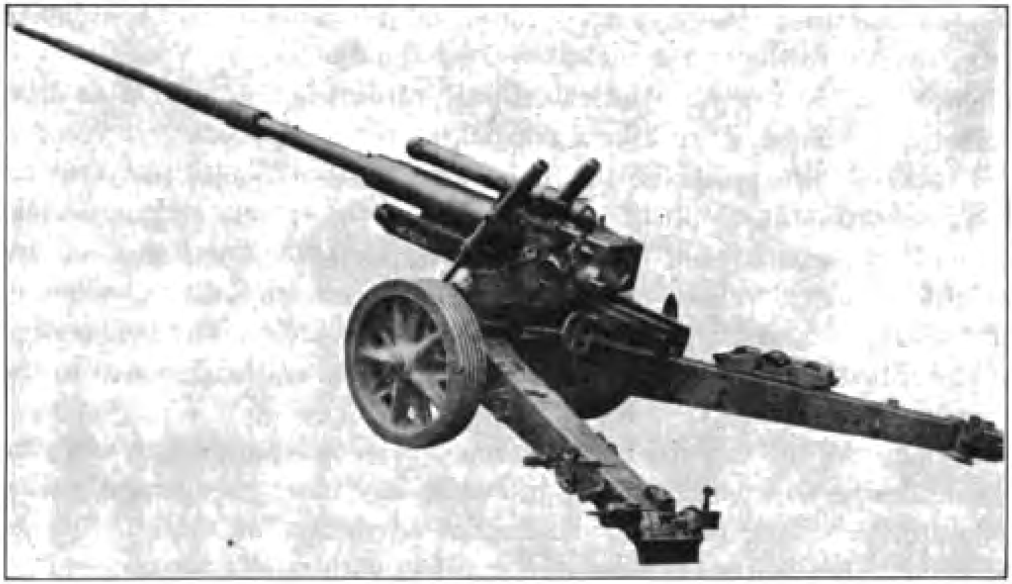

FIG. 8.3 An experimental German muzzle squeeze on a 10.5-cm gun giving an emergent caliber of 8.8 cm.

A further step along the same line was the muzzle adapter (Fig. 8.3), which was the convergent section and final parallel, made as a separate section to be attached to the muzzle of a full-caliber weapon. This division of the gun enabled the tapered part, which wore most rapidly, to be replaced independently of the rest of the barrel. Such a construction was used in British antitank guns and in German AA guns, in both cases with the aim of improving the usefulness of existing equipments. The largest gun turned into a coned bore in this way was a German 24 cm; in this example a flanged shell was given a squeeze to 17 cm diameter.

Digitized by Google Original from UNIVERSITY OF MICHIGAN

A 2/1 reduction in area of section was normal. HE shell were fired successfully.

The advantage gained by the tapered bore can be expressed in several ways. In the first place, we can get a normal muzzle energy from a larger gun volume working at a lower pressure: this means a longer life, due to the lower heat transmission per unit area; the barrel weight can also be reduced a little, although this increases the recoil energy and gives very little reduction in total weight of the whole equipment, except for a recoilless gun. Disadvantages of the coned bore are the more complicated projectile and a reduction of the ratio of HE content to total weight, owing to the metal used for the flanges.

Once outside the gun, the coned-bore projectile has normal exterior ballistics. Indeed, if we take a normal muzzle energy per unit volume, the tapered-bore projectile has a better exterior-ballistic performance than its orthodox competitor. This latter virtue was emphasized in its earliest applications; for example, the Germans used shot of low weight/(caliber)^3 in their orthodox and coned-bore guns, giving velocities of 4000 ft/sec and high penetrations near the muzzle. The penetration of the coned-bore shot, however, fell less rapidly as the distance to the target increased.

To sum up, the tapered-bore gun enables us to separate gun and projectile design to a large extent, and so satisfy more requirements than would otherwise be possible. Just what advantage we take of this depends on what feature is most important in each particular project.

8.41 The equations of interior ballistics for a tapered-bore gun

There are three points that need special attention:

1. The modification of the equations to allow for the variation of the cross section along the bore.
2. The pressure gradient and hydrodynamic behavior of the gas in a coned bore.
3. The axial resistance caused by the swaging of the flanges.

We may dispose of point 2 very quickly. The problem has never been studied properly. The light shot used in such guns give C/W of the order of unity; under these conditions the pressure gradient is not known accurately even for orthodox guns, as may be seen in the next chapter. The most that has been done for the tapered-bore gun is to carry over certain conventional approximations from the theory for the orthodox gun, as was done, for example, by Schmitz.[5] In this way it appears that the coned-bore gun has a smaller pressure-gradient loss than an orthodox gun of the same charge and shot weights. This arises from less of the gas moving with velocity of the order of the shot velocity. The advantage is small, however, and less than the probable error of such a simple theory.

---

[5] Schmitz, *Wehrtech. Monatshefte*, **39** (1935), 149.

The ballistic effects produced by the resistance due to swaging of the shot are the same as the results of bore resistance in a normal gun. This has been discussed in § 5.5. If the cone is merely a muzzle squeeze, the burning of the charge will have been completed before the shot begins to deform. The effect on the muzzle energy is simply a reduction by the amount of work done against the resistance. This cannot be found by quasistatic forcing experiments, because of the great difference between the rates of strain and because of the change of friction with velocity. The work done against resistance is most easily found by firing with and without the muzzle squeeze. Static forcing does serve to indicate whether the wear is likely to be distributed evenly along the taper, and the design of bands and particularly the contours of the cone can be adjusted to eliminate peaks in the resistance.

Swaging can occur during burning only if the coning of the bore extends over most of the travel. The effect is qualitatively the same as in an orthodox gun: if resistance occurs before peak pressure, the latter is increased, whereas the muzzle velocity is increased only if the cone begins really early in the travel. As it happens, the resistance lowers the velocity in all the tapered-bore guns we have seen.

We come now to the modification to the equations caused by the variation of the bore cross section A with the travel x. In the ballistic equations, the cross section appears in only two places: in the equation of motion,

$$WV\frac{dV}{dx} = \frac{A(x)P}{1 + \dfrac{C}{2W}} \tag{63}$$

and in the equation of state of the gas,

$$P\left(U + \int A\,dx - \frac{C}{\delta}\right) = C\phi\lambda\left(1 + \frac{C}{6W}\right) \tag{64}$$

For simplicity we are assuming that $\eta = 1/\delta$ and are using the isothermal model. Our conclusions will be equally true for ballistic theories of all levels of accuracy.

Let $U + \int A\,dx - C/\delta$ be written as $L(x)$. Then equations 63 and 64 become

$$WV\frac{dV}{dL} = \frac{P}{1 + \dfrac{C}{2W}} \tag{65}$$

and

$$PL = C\phi\lambda\left(1 + \frac{C}{6W}\right) \tag{66}$$

Write

$$\tau = \int A \, dt$$

The equations of the problem are completed by the pair

$$V = \frac{dL}{d\tau} \tag{67}$$

and

$$\frac{d\phi}{d\tau} = \frac{1}{A}\frac{d\phi}{dt} = \frac{g(\phi, P)}{A} \tag{68}$$

where g is a known function. We have now eliminated the varying cross section except from the equation of burning. It follows that the solution with a cross section varying in any manner corresponds, point by point, with the solution for the orthodox problem differing only by having a constant bore area. The velocities, fractions burnt, and pressures are equal when the volumes behind the projectile are equal; the time scales in the problems are related by a factor which varies during the travel. In a bore of decreasing area things take longer to happen near the muzzle.

This transformation includes the correspondence between orthodox guns differing only in bore area, which is a special case of the similarity discussed in chapter 6.

We see that the tapered-bore gun introduces nothing new into the central problem of interior ballistics. There are, of course, many interesting theoretical problems connected with the rapid deformation of the projectile, as well as the almost unexplored hydrodynamic problems.

EXAMPLES

1. Prove equation 7.
2. Modify the theory of the H/L gun to apply to cord charges.
3. The German 8.8-cm W 71 had a high-pressure propellant chamber venting into a second chamber from which the gas passed either to a rear-facing nozzle or through another nozzle into the bore. Write down the equations of an isothermal model for such a gun, and investigate the reduction to an equivalent recoiling H/L gun.
4. Find a single charge equivalent to a composite charge of tube and cord, assuming that both burn with their "geometrical" form factors.

CHAPTER NINE

The Hydrodynamic Problems of Interior Ballistics

9.1 Introduction to Lagrange's ballistic problem

One-dimensional theory is adequate for most hydrodynamic problems of the orthodox gun. In this theory it is assumed that across any one section normal to the axis of the bore the conditions are uniform, except for a thin boundary layer near the wall. This is likely to be a good approximation in most problems and is certainly adequate for a general understanding of the phenomena. Some of the newer systems, such as tapered-bore guns and weapons with nozzles, appear to need two-dimensional hydrodynamics for a detailed explanation of all the observations, though even here a simpler theory accounts for much of the behavior. In regard to orthodox guns, there is no reason to suppose that we shall quickly reach a stage at which we should begin to consider the small variation of conditions across a normal section. For the consequences of the one-dimensional theory are by no means completely explored at present. It is true that progress is likely to be more rapid in future, because of the recent development of computing machines of revolutionary speed; as we shall explain in § 9.14, this is likely to make a considerable difference to the method of approach.

The first and most important of the hydrodynamic problems of the gun is of respectable age, having been studied first by Lagrange in 1793.[1] This problem is to find the distribution of pressure, density, and gas velocity between the breech and the base of the shot at all times during the firing. That there will be usually a higher pressure at the breech is obvious from the fact that the propellant gases have themselves to be accelerated by this difference of pressure. On further examination, it is not obvious why the acceleration of *all parts* of the gas should be directed down the bore at *all times*, so that it is not necessarily true that the pressure at the breech is always higher than that everywhere else in the gas. This introduces the theory of waves of finite amplitude, associated particularly with the names of Riemann and Hugoniot. The latter studied Lagrange's problem in detail,[2] because of its importance as one of the simplest standard problems of hydrodynamics. His work was extended by Gossot and Liouville,[3] and this line of attack was pushed to the limit by Love,[4] in a classic paper, which is summarized in § 9.12.

---

[1] Published in *J. école polytech.* (*Paris*), **21** (1832), 13.

Lagrange did little more than begin the problem, but he introduced an approximation that is remarkably useful. The "Lagrange approximation" assumes that the velocity of the gas at any instant increases linearly with distance along the bore, from zero at the breech to the full shot velocity at the base of the projectile. The consequences of this assumption were developed more fully by Piobert and later by Sébert, in the first and second halves of the nineteenth century. The numerical coefficients at which they arrived are still known by their names, and the results are still an accepted convention of interior ballistics. All the more detailed theories put forward up to the present time give only slightly different results, and so it is proper that we give here the conventional treatment. The problem is only just becoming accessible to experiment, but it is already clear that the deviations from this simple theory are quite large. However, there is at present no theory that comes nearer the empirical results.

Before starting to discuss some of the work that has been done on Lagrange's problem, one should mention certain conventional approximations. The first is that the heat conductivity of the gas is so small that it has a negligible effect on the distribution of temperature along the bore. This may easily be verified.[5] Another effect, which is small though not so extremely trivial as the first, is the pressure drop needed to force the gas down the bore against the skin friction of the walls. The subject of the transfer of heat and momentum in an accelerating flow such as this, is not yet in a final form. We shall follow an approximate treatment (shortly to be published) by Hicks and Thornhill. As the flow in the gun is entirely "inlet length," in the language of hydrodynamics, they consider the flow as that over a flat plate parallel to the stream. Let x be the distance from the breech, y the coordinate of the base of the projectile, and d the caliber. Let μ be the viscosity of the gas, ρ its density, and v its velocity at position x. By Lagrange's approximation, sufficiently accurate here, ρ is independent of x, and

---

[2] Hugoniot, *J. école polytech.* (*Paris*), **58** (1889), 1.

[3] Gossot and Liouville, *Mém. poudres*, **17** (1914), 34.

[4] Love and Pidduck, *Phil. Trans. Roy. Soc.* (*London*), **222** (1921–22), 167.

[5] Considering gases at rest under a typical distribution of temperature attained in their state of motion, we have the temperature at any point changing at the rate $\lambda\, d^2T/\rho C\, dx^2$, where ρ is the density, C the specific heat per unit mass, at constant volume, and λ the thermal conductivity of the gas. In ballistic problems ρC is of the order of 0.1 cal/cm^3 deg, λ is about 2×10^{-4} (cal/cm^{2}sec) per (deg/cm), and d^2T/dx^2 is at the most 10 deg/caliber^2. Hence, the temperature is being equalized at the rate of 2×10^{-2} deg per sec per (caliber/cm)^2. For a caliber of 1 cm the times involved in the ballistic phenomena are of the order of 1 msec. Thus, the heat conductivity of the gas is sufficiently small to have a negligible effect on the temperature differences generated by adiabatic compressions and expansions in different parts of the system. This conclusion remains true, even if we allow for heat transfer by turbulence multiplying λ by a factor of as much as 10^3.

$$v = \frac{x}{y}\frac{dy}{dt} \tag{1}$$

The viscosity is also independent of x. By using the boundary-layer momentum integral, as described in the next chapter, Hicks and Thornhill have shown that the logarithmic velocity distribution[6] applicable in the boundary layer at Reynolds numbers of 10^6 and upward gives a skin-friction drag per unit area τ_0 approximating closely to

$$\tau_0 = 0.0126\rho v^2 R_x{}^{-0.14} \tag{2}$$

where R_x is the Reynolds number at distance x, namely:

$$R_x = \frac{\rho v x}{\mu} \tag{3}$$

The pressure gradient needed to balance this drag is given by

$$\frac{\pi d^2}{4}\frac{dp}{dx} = -\pi\tau_0 d \tag{4}$$

Integrating this with the help of equations 1, 2, and 3, we find

$$p(x) = p\ (\text{breech}) - 0.0185x\,\frac{\rho}{d}\left(\frac{x}{y}\right)^2\left(\frac{dy}{dt}\right)^2\left(\frac{\rho x^2}{\mu y}\frac{dy}{dt}\right)^{-0.14} \tag{5}$$

The total drop of pressure down the gun is greatest when the shot is at the muzzle; dy/dt is then the muzzle velocity V, and y is L, the total length of the bore and chamber. Then,

$$\Delta p = 0.0185\,\frac{\rho V^2 L}{d}\left(\frac{\rho V L}{\mu}\right)^{-0.14} \tag{6}$$

For ballistically similar guns, Δp is proportional to $d^{-0.14}$. Thus in going from a 15-in. gun to a rifle the pressure drop increases by a factor 1.7. At constant caliber, charge, and velocity, the pressure drop is independent of the length of the barrel. For given dimensions, the ratio of this pressure drop to the pressure difference arising from inertia is proportional to $C^{0.86}V^{-0.14}$, where C is the charge weight. From these results we can say that the frictional drag is most important at small calibers and high velocities—but not if the latter are obtained by using a lightweight shot of small W/d^3. In any case, the effect is always small. For a gun of 3 in. caliber and total length 50 calibers, giving 3000 ft/sec to a normal shot of 17 lb weight, the pressure drop due to friction is at most 30 atm. The inertia pressure drop is about five times as big at this moment. For earlier times in the firing the inertia drop is bigger and the frictional drop much less.

---

[6] Prandtl, in *Aerodynamic Theory*, vol. III (ed. Durand), p. 150.

These considerations have assumed that the surface of the bore is hydrodynamically smooth. The rifling tends to disturb the flow, and some increase of the drag may be expected. Evidence on this point is contradictory, but it has never been suggested that the drag is more than 50 per cent greater on this account. Such an increase would not raise the frictional effects into real importance. When it is desired to take them into account this can be done with ample accuracy by simply adding the pressure drop shown in equation 5 to the inertia pressure drop derived later.

A point that is almost always assumed, for simplicity, in studying Lagrange's problem, is that the recoil of the barrel can be neglected. This is plausible, since recoil velocities and distances are of the order of 1 per cent of the corresponding quantities for the shot—except in certain low-velocity projectors where there is in any case no measurable Lagrange gradient. Dr. Hepner has obtained the recoil corrections to Pidduck's solution of § 9.13, and his results show how small is the effect.

Another common assumption is that the chamber, of rather greater diameter than the bore, can be replaced by a cylindrical continuation of the bore, with the correct total volume. The present writer is not aware of any study of Lagrange's problem that has not used this simplification, although Winter, *Mém. artillerie franç.*, **18** (1939), 775, has described qualitatively the effect produced by the chamber diameter being greater than the bore diameter.

9.11 The conventional solution

It is assumed that all the propellant charge is in the gaseous form at the time considered. It is assumed also that at any time the gas density ρ is the same at all points:

$$\frac{\partial \rho}{\partial x} = 0 \tag{7}$$

The equation of continuity is therefore

$$\frac{d\rho}{dt} + \frac{\partial}{\partial x}(\rho v) = 0$$

which, with equation 7, gives

$$\frac{1}{\rho}\frac{d\rho}{dt} = -\frac{\partial v}{\partial x}$$

The left side is independent of x; hence, the right-hand side integrates to

$$v = \frac{x}{y}\frac{dy}{dt} \tag{8}$$

when we remember that $v = 0$ at the breech ($x = 0$) and $v = dy/dt$ at the shot.

The term "Lagrange approximation" is applied to equation 7 or 8. It has been shown that equation 7 leads to equation 8, but it is not true that equation 8 necessarily implies equation 7.

The energy and momentum of the gas stream can now be found. The energy is

$$\int_0^y \tfrac{1}{2}A\rho v^2\,dx = \tfrac{1}{6}CV^2$$

where V is the velocity of the shot and C is the weight of the propellant. The total kinetic energy of projectile and charge is

$$\tfrac{1}{2}(W + \tfrac{1}{3}C)V^2 \tag{9}$$

The momentum is

$$\int_0^y A\rho v\,dx = \tfrac{1}{2}CV$$

and the total momentum of shot and propellant is

$$WV\left(1 + \frac{C}{2W}\right) \tag{10}$$

More exact analytical solutions usually give for velocity and density the Lagrange approximations with other terms of higher order in C/W. Hence it is usual to find that the energy and momentum differ from those in equations 9 and 10 by terms of the relative order of $(C/W)^2$; that is, the Lagrange corrections derived from equations 9 and 10 are correct to the order of C/W, if the common assumptions of these theories are correct.

For the pressure distribution we integrate the equation of motion of the gas:

$$\frac{\partial v}{\partial t} + v\frac{\partial v}{\partial x} = -\frac{1}{\rho}\frac{\partial p}{\partial x} \tag{11}$$

which reduces, from equations 7 and 8, to

$$\frac{\partial p}{\partial x} = -\rho\frac{x}{y}\frac{d^2y}{dt^2}$$

With

$$\rho = \frac{C}{Ay}$$

where A is the bore area, we find

$$p = g(t) - \frac{C}{2A}\left(\frac{x}{y}\right)^2\frac{d^2y}{dt^2} \tag{12}$$

Let the pressure at the shot be p_S, at the breech be p_B, and let the resistance to the motion of the shot be written as an equivalent pressure p_R over the bore area A. Then,

$$W\frac{d^2y}{dt^2} = A(p_S - p_R)$$

and, from equation 12 with $x = y$,

$$g(t) = \left(1 + \frac{C}{2W}\right)p_S - \frac{C}{2W}p_R$$

giving the pressure as a function of distance:

$$p = p_S + \frac{C}{2W}\left(1 - \frac{x^2}{y^2}\right)(p_S - p_R) \tag{13}$$

In particular, the breech pressure is

$$p_B = \left(1 + \frac{C}{2W}\right)p_S - \frac{C}{2W}p_R \tag{14}$$

and the mean pressure is

$$\bar{p} = \frac{1}{y}\int_0^y p\,dx = p_S + \frac{C}{3W}(p_S - p_R) \tag{15}$$

If there is no bore resistance,

$$\frac{\bar{p}}{p_S} = 1 + \frac{C}{3W} \tag{16}$$

which should be compared with the ratio of the kinetic energy of the system to the kinetic energy of the shot alone:

$$\frac{\text{Total KE}}{\text{Shot KE}} = 1 + \frac{C}{3W} \tag{17}$$

The similarity of equations 16 and 17 holds only to this order of approximation.

From equations 14 and 15 we find the ratio of breech to mean pressure, already used many times in this book,

$$\frac{p_B}{\bar{p}} = \frac{1 + \dfrac{C}{2W}\left(1 - \dfrac{p_R}{p_S}\right)}{1 + \dfrac{C}{3W}\left(1 - \dfrac{p_R}{p_S}\right)} = 1 + \frac{C}{6W}\left(1 - \frac{p_R}{p_S}\right) \tag{18}$$

since this approximate theory is valid, if at all, only as far as the first power of C/W.

If we write the equation of motion of the shot in terms of the breech pressure and a modified shot mass W_m, that is,

$$W_m \frac{d^2y}{dt^2} = Ap_B$$

instead of

$$W \frac{d^2y}{dt^2} = A(p_S - p_R)$$

then

$$\frac{W_m}{W} = 1 + \frac{C}{2W} + \frac{p_R}{p_S - p_R} \tag{19}$$

The coefficient whose value turns out here to be one half is often called Sébert's factor. If, like some writers on ballistics, we had used the mean pressure everywhere in our equations, the appropriate modified shot mass W_m' would have been

$$\frac{W_m'}{W} = 1 + \frac{C}{3W} + \frac{p_R}{p_S - p_R} \tag{20}$$

The set of coefficients ⅓, ½, and ⅙, which keep appearing in these equations, are the approximate numerical values of what are sometimes called Piobert's first, second, and third coefficients, respectively.

Up to this point we have assumed that all the charge has been converted into gas. Before this state the theory applies without alteration if it is assumed that the unburnt charge moves with the gas, the distribution of solid along the bore being the same as the distribution of gas. This is a convenient assumption, but it is not supported by an examination of the forces acting on the burning propellant (§ 9.5). It is conventional, however, to apply the formulas we have obtained to all stages of the ballistic solution.

It is possible to obtain very simply an idea of the error caused by applying these formulas before "burnt." Assume, as before, that the gas density ρ is uniform through the bore, and that the propellant stays in the chamber, whose length is L. Then,

$$\rho = \frac{C\phi}{Ay - \dfrac{C(1-\phi)}{\delta}} \tag{21}$$

In the space beyond the chamber, equation 2 leads to

$$v = \frac{dy}{dt} + (x - y)f(t) \tag{22}$$

which is more general than equation 8. At the junction between chamber and bore,

$$(\rho v)_{x=L} = \frac{d}{dt}[\rho(y - L)]$$

which with equation 22 gives

$$v = \frac{dy}{dt} + \frac{(y - x)}{\rho}\frac{d\rho}{dt}$$

which may be transformed by equation 21 to

$$v = \left[\frac{Ax - \dfrac{C(1-\phi)}{\delta}}{Ay - \dfrac{C(1-\phi)}{\delta}}\right]\frac{dy}{dt} + \frac{y - x}{\phi}\left[\frac{Ay - \dfrac{C}{\delta}}{Ay - \dfrac{C(1-\phi)}{\delta}}\right]\frac{d\phi}{dt} \tag{23}$$

This is a satisfactory generalization of equation 8; after "all burnt," ϕ is unity, $d\phi/dt$ is zero, and equation 23 reduces to equation 8.

We may now integrate $\frac{1}{2}A\rho v^2$ with respect to x to find the kinetic energy of the gas; if we use equation 23 for $x = L$ to y, and a linear variation for the part $x = 0$ to L, we can obtain a rough estimate of the deviation from the conventional value $\frac{1}{6}CV^2$. The second term on the right of equation 23 is substantial and makes the gas velocity at some parts of the bore considerably higher than the velocity of the projectile, dy/dt. Numerical examples show that this effect sometimes more than balances the loss of energy arising because the moving mass is only $C\phi$. Over a large part of the period of burning, $\frac{1}{6}CV^2$ is close to the computed kinetic energy.

The conclusion to be drawn from this rough treatment is that, if the propellant is stationary, this does not necessarily make a substantial difference to the total kinetic energy, except in certain short periods of the motion.

9.12 The results of Love and Pidduck

The theory of waves of finite amplitude in a gas was given a substantial advance by Riemann in 1858. A little later Hugoniot contributed to the general theory and applied it to Lagrange's problem.[7] Hugoniot studied the case where all the charge is present as gas when the shot begins to move; he followed the resulting wave of rarefaction on its journey to the breech. His methods were extended by Gossot and Liouville [8] to follow the wave as it travels back toward the shot. Finally, Love [9] carried the analysis of the same problem as far as the third wave traveling toward the breech, and Pidduck evaluated the formulas in a special case. Their work has been of great value, and, as it closes one line of attack, it should be discussed in some detail.

Their assumptions were: (1) that the propellant had completed its burning before the shot started; (2) adiabatic expansion of each element of gas; (3) initially uniform pressure, density, and temperature, and shot at rest; (4) a constant covolume. They assumed also that γ took one of a discrete set of values, chosen to permit easy solution:

$$\gamma = \frac{2n+1}{2n-1} \qquad (n \text{ an integer})$$

with $\gamma = {}^{11}\!/_{9}$ in the numerical example;[10] Platrier [11] has generalized some of Love's results to other values of γ. In addition, Love and Pidduck assumed that the chamber was a cylindrical continuation of the bore.

---

[7] Hugoniot, *J. école polytech. (Paris)*, **58** (1889), 1.

[8] Gossot and Liouville, *Mém. poudres*, **17** (1914), 34.

[9] Love and Pidduck, *Phil. Trans. Roy. Soc. (London)*, **222A** (1921–22), 167.

[10] $\gamma = {}^{9}\!/_{7}$ and ${}^{11}\!/_{9}$ give a sufficiently good idea of the behavior of the complete range of modern propellants.

[11] Platrier, *Comp. rend.*, **199** (1934), 770; also *Mém. artillerie franç.*, **15** (1936), 431.

Heat transfer to the bore might be taken into account, very roughly, by using an effective γ in the adiabatic law. The constant covolume is also unobjectionable. The really important points are 1 and 2. They are not good approximations to real guns, but they do specify an exact problem to which an exact solution has been found.

Love's formulas are in general form; that is, the solution can be found for any particular case by substituting numbers in the general formulas. However, a certain amount of interpolation and trial and error is needed, and we have the evidence of Pidduck that the computation is laborious. An alternative method is to solve the partial-differential equations numerically by the method of characteristics,[12] in any desired case. The labor involved is not much greater than that required for the substitution in Love's formulas; in fact, it has been contended [13] that, if carried out graphically, the method of characteristics is actually quicker. This seems to depend on the accuracy required.[14] At the very least, it must be agreed that Love's formulas are extremely complicated, in spite of the simplicity of his basic problem. Thus it is almost certain that problems more nearly related to actual guns, with slow burning of the propellant, will not be solved by analytical solution.

Nevertheless, Love and Pidduck's results make clear some of the phenomena to be expected in practice. Figure 9.1 shows the pressure-space curves at a number of successive instants, in a typical gun with $C/W = 0.24$ and a muzzle velocity near 2500 ft/sec. The rarefaction wave can be seen to leave the base of the shot as the latter starts; this wave speeds up the gas it engulfs, and, as the wave passes down to the breech, more and more gas is set into motion to follow the shot. The wave is reflected at the breech as another rarefaction wave, which travels toward the projectile, slowing down gas on the way. At the shot this wave is reflected again, and Love and Pidduck follow the wave through one more reflection at the breech and one more at the base of the projectile. Of the earlier workers, Hugoniot had studied the first wave passing back down the bore, and Gossot and Liouville had indicated how the wave reflected from the breech could be followed toward the shot. The waves appearing in this problem are all rarefaction waves, in which, at the head of the wave, there is a discontinuity only in the pressure gradient. In particular, shock waves do not occur; these (see § 9.15) are marked by a sudden rise in the pressure itself, and, as they increase the entropy of the gas, their occurrence would have vitiated the assumption that all the elements of gas expand along a common adiabatic. Although shock waves do not occur in the problem studied by Love and Pidduck, they have been found in guns, under conditions of inefficient ignition.

---

[12] For the mathematical theory of characteristics, see Goursat, *Leçons sur les équations aux dérivées partielles du seconde ordre*, or Hadamard, *Leçons sur la propagation des ondes* (Paris, 1903). Its use as a numerical method for the solution of hyperbolic partial-differential equations can be understood without study of its deeper significance. A typical example is Prandtl and Busemann, *Stodola Festschrift* (Zurich, 1929), p. 499. A good introduction to the subject is provided by Courant and Friedrichs, *Supersonic Flow and Shock Waves* (New York, 1948), chapters II and IIIA.

[13] de Haller, *Proc. 6th Intern. Congr. Applied Math.* (*Paris*, 1946).

[14] The accuracy of a solution by characteristics falls off rapidly as the computation proceeds farther and farther from the region of the initial conditions. In general, even "graphical accuracy" may be unattainable far from the initial boundary if graphical *methods* have been used throughout. Where graphical accuracy is called for, it is usually permissible to use graphical methods only in the later parts of the computation. In the case of the Lagrange problem the flow rapidly settles down to a simple pattern, and this helps in the smoothing out of errors.

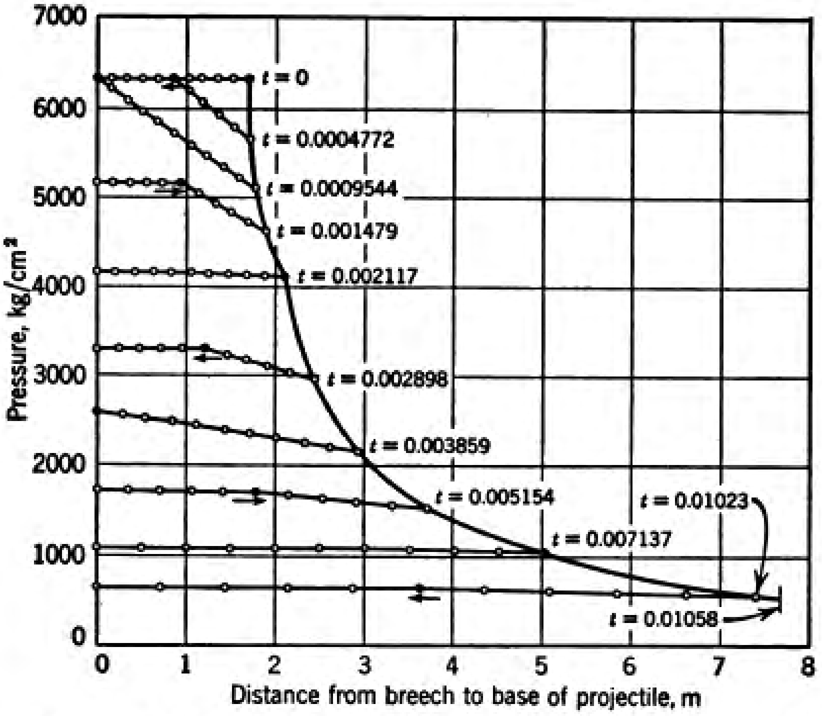

FIG. 9.1 Pressure distribution behind the projectile at various stages of its motion, in the example studied by Love and Pidduck.
Phil. Trans. Roy. Soc. A. Reproduced by permission of F. B. Pidduck and the Royal Society, London.

It is clear from Fig. 9.1 that the rarefaction waves damp down fairly rapidly into an almost smooth distribution of pressure. The ratio of

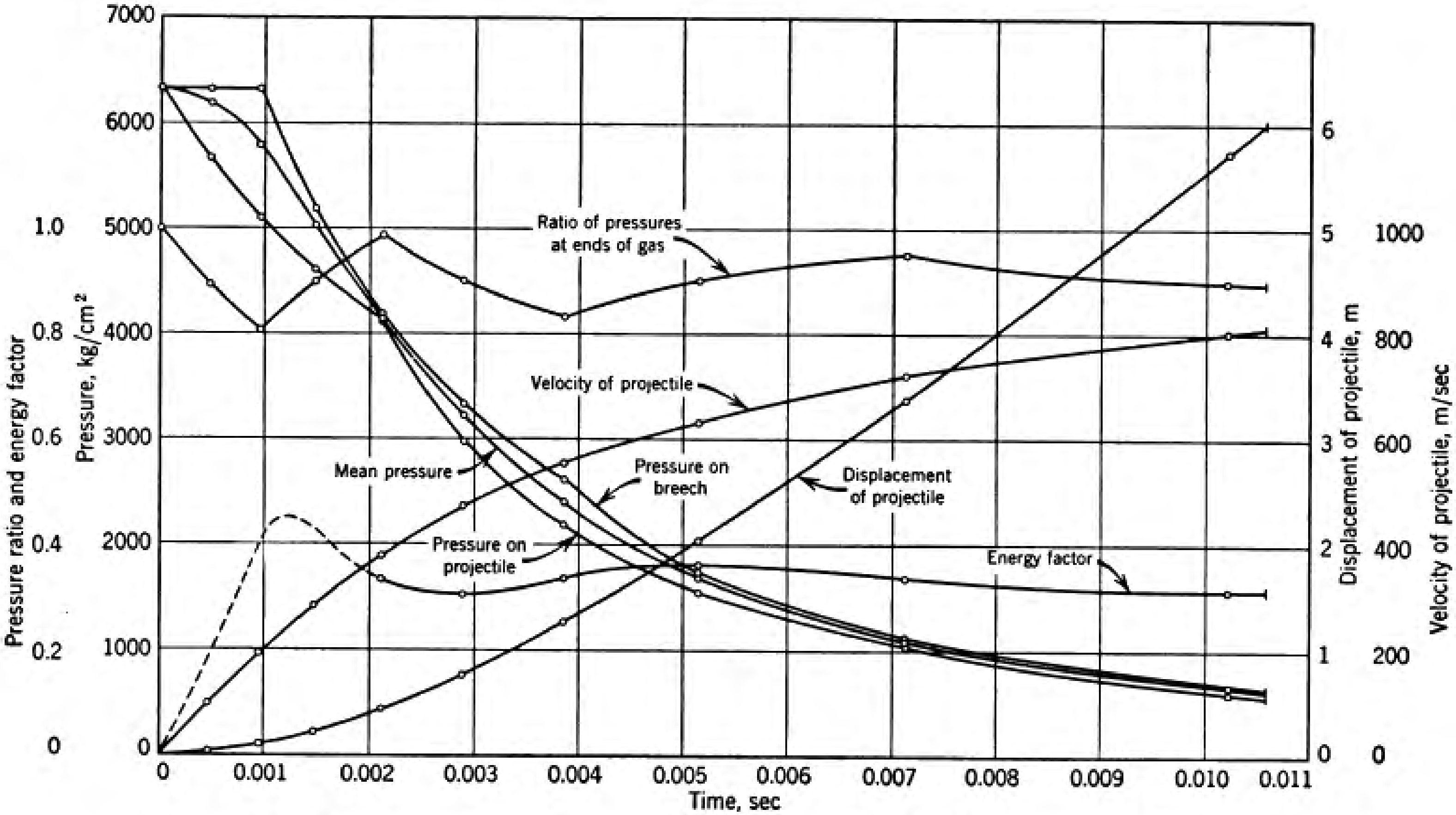

FIG. 9.2 Time variation of main results, in the example studied by Love and Pidduck. *Phil. Trans. Roy. Soc. A.* Reproduced by permission of F. B. Pidduck and the Royal Society, London.

breech and shot pressure and the kinetic energy of the gas relative to that of the shot are shown in Fig. 9.2. As time goes on, the variations of these quantities decrease, and they approach very closely the values given in the preceding section (for zero resistance).

9.13 Pidduck's limiting solution

It was noticed by Pidduck (*loc. cit.*) that the features of the solution special to the assumed initial conditions were rapidly damped out; for example, the rarefaction waves generated by the starting of the shot die away quickly. It may be supposed that other assumptions, more realistic than those of Love and Pidduck, would lead to solutions that would tend to become the same toward the end of shot travel. Pidduck therefore attempted to find a limiting solution, which would be an approximation to the later stages of all likely solutions. His limiting solution was derived later in a rather different way by Kent,[15] whose method we shall follow here.

Let the position of the element of gas originally at x_0 be x at time t. All distances are measured from the breech. The position of the base of the shot is $y(t)$, and its initial position is b. Let $\rho(x_0, t)$ be the density at time t of the element of gas, which was at x_0 initially. Let $p(x_0, t)$ be the pressure of this element. Let γ be the ratio of the specific heats at constant pressure and constant volume, and η the covolume of the gas. Then, if we neglect heat loss to the bore,

$$p\left(\frac{1}{\rho} - \eta\right)^{\gamma} = \text{function of } x_0 \text{ only}$$

To make the problem more tractable it is necessary to assume that all elements follow the *same* adiabatic, so that

$$p\left(\frac{1}{\rho} - \eta\right)^{\gamma} = K \tag{24}$$

The equation of continuity of the gas is

$$\rho(x_0, t)\,\frac{\partial x}{\partial x_0} = \rho(x_0, 0) \tag{25}$$

and its equation of motion is

$$\rho(x_0, t)\,\frac{\partial^2 x\,(x_0, t)}{\partial t^2} = -\,\frac{\partial p\,(x_0, t)}{\partial x} \tag{26}$$

---

[15] Kent, *Physics*, **7** (1936), 319. Pidduck, *J. Applied Phys.*, **8** (1937), 144. Kent, *ibid.*, **8** (1937), 144; **9** (1938), 734.

The projectile of mass W is assumed to suffer no resistance to motion, so that

$$W\frac{d^2y}{dt^2} = Ap(y, t) \tag{27}$$

Integrating equation 26 and using equation 27, we find

$$\begin{aligned}\frac{p(0, t)}{p(y, t)} &= 1 + \frac{A}{W}\int_0^y \rho(x_0, t)\,\frac{\partial^2 x\,(x_0, t)}{\partial t^2}\left(\frac{d^2y}{dt^2}\right)^{-1} dx \\ &= 1 + \frac{A}{W}\int_0^b \rho(x_0, 0)\,\frac{\partial^2 x\,(x_0, t)}{\partial t^2}\left(\frac{d^2y}{dt^2}\right)^{-1} dx_0 \end{aligned}\tag{28}$$

From equations 24 and 25, equation 26 becomes

$$\rho(x_0, 0)\,\frac{\partial^2 x\,(x_0, t)}{\partial t^2} = -K\frac{\partial}{\partial x_0}\left(\frac{1}{\rho(x_0, t)} - \eta\right)^{-\gamma} \tag{29}$$

It is convenient to introduce in place of x a new variable z, defined by

$$z = x - \int_0^{x_0} \eta\rho(x_0, 0)\,dx_0 \tag{30}$$

leading to

$$\frac{\partial z}{\partial x_0} = \frac{\partial x}{\partial x_0} - \eta\rho(x_0, 0) = \rho(x_0, 0)\left(\frac{1}{\rho(x_0, t)} - \eta\right) \tag{31}$$

Using this in equation 29, we find

$$\frac{\partial^2 z}{\partial t^2} = \gamma K[\rho(x_0, 0)]^{\gamma-1}\left(\frac{\partial z}{\partial x_0}\right)^{-(\gamma+1)}\left[\frac{\partial^2 z}{\partial {x_0}^2} - \frac{1}{\rho(x_0, 0)}\frac{\partial\rho(x_0, 0)}{\partial x_0}\frac{\partial z}{\partial x_0}\right] \tag{32}$$

A solution is attempted in the form

$$z = f(z_0)\phi(t) \tag{33}$$

in which, without loss of generality,

$$\phi(0) = 1$$

If we write $t = 0$ in equation 33, $f(z_0) = z_0$. Hence we have

$$z = z_0\phi(t) \tag{34}$$

and

$$\frac{\partial z}{\partial x_0} = \frac{dz_0}{dx_0}\phi(t) = [1 - \eta\rho(x_0, 0)]\phi(t) \tag{35}$$

which, from equation 31, implies that

$$\frac{1}{\rho(x_0, t)} - \eta = \left(\frac{1}{\rho(x_0, 0)} - \eta\right)\phi(t) \tag{36}$$

Also, from equation 35,

$$\frac{\partial^2 z}{\partial {x_0}^2} = -\eta \frac{\partial \rho}{\partial x_0} \phi(t) \tag{37}$$

Substituting these results in equation 32, we have

$$\phi^\gamma \frac{d^2\phi}{dt^2} = -\gamma K[1 - \eta\rho(z_0, 0)]^{-\gamma}[\rho(z_0, 0)]^{\gamma-2} \frac{d\rho(z_0, 0)}{z_0\, dz_0} \tag{38}$$

The left side is independent of z_0, the right of t. Both sides are therefore equal to a constant B, say. The time factor is a solution of

$$\phi^\gamma \frac{d^2\phi}{dt^2} = B \tag{39}$$

into which we need not enquire yet. Of more interest is the density. Integrating equation 38 gives

$$\frac{1}{\rho(z_0, 0)} - \eta = \left(\frac{1}{\rho(0, 0)} - \eta\right) \times \left[1 - \frac{B(\gamma - 1){z_0}^2}{2\gamma K}\left(\frac{1}{\rho(0, 0)} - \eta\right)^{\gamma-1}\right]^{-1/(\gamma-1)} \tag{40}$$

At the shot,

$$z_0 = b - \frac{\eta C}{A}$$

For convenience we write

$$\Omega = \frac{B(\gamma - 1)}{2\gamma K}\left(\frac{1}{\rho(0, 0)} - \eta\right)^{\gamma-1}\left(b - \frac{\eta C}{A}\right)^2 \tag{41}$$

so that, with equation 36,

$$\frac{1}{\rho(z_0, t)} - \eta = \left(\frac{1}{\rho(0, 0)} - \eta\right)\phi(t)\left[1 - \Omega\left(\frac{z_0}{b - \dfrac{\eta C}{A}}\right)^2\right]^{-1/(\gamma-1)} \tag{42}$$

We find the initial distribution of density by writing $t = 0$ in this equation, and we see that the *initial* density decreases from breech to shot base. This shows that the Pidduck-Kent solution cannot represent the conditions in a real gun throughout the motion, nor indeed does it represent the early stages of the Love solution. It is supposed, however, that all more realistic solutions will approach the Pidduck-Kent solution as a limiting form as the shot moves down the bore. The pressure follows from equation 24:

$$p(z_0, t) = K\left(\frac{1}{\rho(0, 0)} - \eta\right)^{-\gamma} \phi^{-\gamma}(t) \left[1 - \Omega\left(\frac{z_0}{b - \dfrac{\eta C}{A}}\right)^2\right]^{\gamma/(\gamma-1)} \tag{43}$$

and the gas temperature from the equation of state,

$$p\left(\frac{1}{\rho} - \eta\right) = RT$$

giving

$$RT(z_0, t) = RT(0, 0)\phi^{1-\gamma}(t) \left[1 - \Omega\left(\frac{z_0}{b - \dfrac{\eta C}{A}}\right)^2\right] \tag{44}$$

Finally, the position of any element is

$$x(x_0, t) = x_0 + z_0[\phi(t) - 1] \tag{45}$$

and its velocity is $z_0\, d\phi/dt$.

There are two parameters in these formulas: Ω and $\rho(0, 0)^{-1} - \eta$. To fix these we have the equation of motion of the shot and the condition that the total amount of gas present is the charge mass C. From equations 45 and 39,

$$W\frac{d^2y}{dt^2} = W\left(b - \frac{\eta C}{A}\right)B\phi^{-\gamma}$$

while from equation 43,

$$Ap(y) = AK\left(\frac{1}{\rho(0, 0)} - \eta\right)^{-\gamma}(1 - \Omega)^{\gamma/(\gamma-1)}\phi^{-\gamma}$$

so that

$$W\left(b - \frac{\eta C}{A}\right)B = AK\left(\frac{1}{\rho(0, 0)} - \eta\right)^{-\gamma}(1 - \Omega)^{\gamma/(\gamma-1)} \tag{46}$$

The second condition is

$$C = A\int_0^b \rho(x_0, 0)\, dx_0 = A\int_0^{b-(\eta C/A)} \frac{\rho(x_0, 0)\, dz_0}{1 - \eta\rho(x_0, 0)}$$

$$= A\left(\frac{1}{\rho(0,\,0)} - \eta\right)^{-1}\int_0^{b-(\eta C/A)}\left[1 - \Omega\left(\frac{z_0}{b - \frac{\eta C}{A}}\right)^2\right]^{1/(\gamma-1)} dz_0$$

$$= A\left(b - \frac{\eta C}{A}\right)\left(\frac{1}{\rho(0,\,0)} - \eta\right)^{-1}\int_0^1 (1 - \Omega\mu^2)^{1/(\gamma-1)}\, d\mu \tag{47}$$

Hence,

$$\int_0^1 (1 - \Omega\mu^2)^{1/(\gamma-1)}\, d\mu = \frac{(\gamma-1)C}{2\gamma W}\frac{(1-\Omega)^{\gamma/(\gamma-1)}}{\Omega} \tag{48}$$

This gives Ω in terms of γ and C/W. Also,

$$\frac{1}{\rho(0,\,0)} - \eta = \frac{A(\gamma-1)}{2\gamma}\left(b - \frac{\eta C}{A}\right)\frac{(1-\Omega)^{\gamma/(\gamma-1)}}{W\Omega} \tag{49}$$

For practical values of C/W, Ω can be expanded as a power series in C/W; from equation 48, one obtains

$$\Omega = \frac{(\gamma-1)C}{2\gamma W}\left[1 + \left(\frac{1}{6\gamma} - \frac{1}{2}\right)\frac{C}{W} + \left(\frac{1}{4} - \frac{1}{10\gamma} + \frac{1}{180\gamma^2}\right)\left(\frac{C}{W}\right)^2 + \cdots\right] \tag{50}$$

giving

$$\frac{1}{\rho(0,\,0)} - \eta = \left(\frac{Ab}{C} - \eta\right)\left[1 - \frac{C}{6\gamma W} + \left(\frac{1}{45\gamma^2} + \frac{7}{120\gamma}\right)\left(\frac{C}{W}\right)^2 + \cdots\right] \tag{51}$$

The ratio of the pressures at the ends of the gas is of interest. In this solution it follows from equation 43 that at all times

$$\begin{aligned}\frac{p\ (\text{shot})}{p\ (\text{breech})} &= (1-\Omega)^{\gamma/(\gamma-1)} \\ &= 1 - \frac{C}{2W} + \left(\frac{1}{4} + \frac{1}{24\gamma}\right)\left(\frac{C}{W}\right)^2 \\ &\quad - \left(\frac{1}{8} + \frac{13}{240\gamma} + \frac{1}{360\gamma^2}\right)\left(\frac{C}{W}\right)^3 + \cdots\end{aligned} \tag{52}$$

The inverse result,

$$\frac{p\ (\text{breech})}{p\ (\text{shot})} = 1 + \frac{C}{2W} - \frac{1}{24\gamma}\left(\frac{C}{W}\right)^2 + \left(\frac{1}{80\gamma} + \frac{1}{360\gamma^2}\right)\left(\frac{C}{W}\right)^3 + \cdots \tag{53}$$

is very close to the simple conventional approximation,

$$\frac{p\ (\text{breech})}{p\ (\text{shot})} = 1 + \frac{C}{2W}$$

Other interesting features can be calculated easily. For example, the ratio of the kinetic energy of the gas to that of the projectile is

$$\frac{A}{W\left(\frac{dy}{dt}\right)^2}\int_0^y \rho(x, t)\left(\frac{\partial x}{\partial t}\right)^2 dx = \frac{A\left(\frac{d\phi}{dt}\right)^2}{W\left(\frac{dy}{dt}\right)^2}\int_0^b z_0{}^2\rho(x_0, 0)\, dx_0$$

$$= \frac{2\gamma\Omega}{\gamma - 1}(1 - \Omega)^{-\gamma/(\gamma-1)}\int_0^1 \mu^2(1 - \Omega\mu^2)^{1/(\gamma-1)}\, d\mu \qquad (54)$$

For small values of C/W, this expression is

$$\frac{1}{3}\frac{C}{W}\left[1 - \frac{2}{15\gamma}\frac{C}{W} + \frac{4(3\gamma + 1)}{315\gamma^2}\left(\frac{C}{W}\right)^2 + \cdots\right] \qquad (55)$$

which differs only slightly from the result 17 of the Lagrange approximation.

The mean pressure in the gun at any given time depends to some extent on the definition of the mean. If we weight pressures according to the density of the gas, that is,

$$\bar{p}(t) = \frac{A}{C}\int_0^y p(x, t)\rho(x, t)\, dx$$

We find

$$\frac{\bar{p}(t)}{p\ (\text{breech})} = \frac{I(\gamma + 1)}{I(1)}$$

when we define

$$I(n) = \int_0^1 (1 - \Omega\mu^2)^{n/(\gamma-1)}\, d\mu$$

Expanding the integrals as a power series in C/W gives

$$\frac{\bar{p}(t)}{p\ (\text{breech})} = 1 - \frac{C}{6W} + \frac{30\gamma^2 + 13\gamma - 12}{360\gamma^2}\left(\frac{C}{W}\right)^2 + \cdots \qquad (56)$$

It remains to solve equation 39 for $\phi(t)$. Since the shot velocity is $[b - (\eta C/A)]\, d\phi/dt$ and the shot position is $[b - (\eta C/A)]\phi$, we see that we need find only the relation between $d\phi/dt$ and ϕ. This is a velocity-distance relation. The connection between ϕ and t, that is, the time to reach any given distance, is of little interest in ballistics. Integrating equation 39 yields

$$\left(\frac{d\phi}{dt}\right)^2 = \frac{2B}{\gamma - 1}(1 - \phi^{1-\gamma}) \qquad (57)$$

which is the equation of energy of the system, as may be verified from equation 54 and an integration of RT over all the elements of gas.

9.14 Experimental results and future theoretical research

It may be seen that the theory of Lagrange's problem has given the following solutions: (1) Love's analysis for the case where the propellant burns very rapidly; (2) the alternative numerical treatment of particular cases by the method of characteristics, assuming that the unburnt propellant moves with the gas; (3) the Lagrange approximation from the assumption of constant density; (4) Pidduck's special solution. The last is not physically exact, for it implies an initial nonuniform distribution of density before the shot moves, but it is hoped that the real solution approaches this special solution toward the end of shot travel. As far as terms of the order of C/W, Pidduck's solution is equivalent to the Lagrange approximation. A further solution that is equivalent to this order is Pfriem's analysis [16] by splitting off space-mean values of the quantities appearing in the equations.

Love's analysis is not expected to be a good representation of a real gun near shot start, since its physical assumptions are here wide of the mark. It can be foreseen that it will be better in the later stages, in which, however, Pidduck's solution is a close approximation. Thus, we can say that all the theoretical work done until now leads one to expect that, to terms of the order of C/W,

$$\frac{p\ (\text{breech})}{p\ (\text{shot})} = 1 + \frac{C}{2W} \tag{58}$$

Experiments on the distribution of pressure behind the shot have become feasible only in the most recent times, and the techniques used are still undergoing development. Such experiments have been carried out in the United States (published only in the classified literature) on a 3-in. gun of medium velocity, by Rossmann [17] in Germany, and by Goode and Lockett (unpublished) in England. Their methods were rather different, and the values of C/W cover fairly well the range up to 0.44. A detailed comparison of their results is made difficult by the different propellant shapes used. It is quite clear, nevertheless, that equation 58 is not correct, even for these small values of C/W. The ratio of breech to shot pressure is in no case constant during the firing. The ratio is in fact less than $1 + C/2W$ at first, and greater than $1 + C/2W$ toward the end of shot travel. The time at which equation 58 is correct appears to come a little after peak pressure. The contribution of the frictional pressure drop (§ 9.1) is greatest at shot ejection and accounts for only part of the discrepancy.

---

[16] Pfriem, *Z. ges. Schiess- u. Sprengstoffw.*, **38** (1943), 1, 21, 165.

[17] Rossmann, *Jahrb. deut. Akad. LFF*, **1940/41**.

Here, then, there is encouragement for further theoretical work. It is obvious that one important factor omitted from previous work is the gradual burning of the propellant. Considering the possible lines of attack, it is likely that Love's analysis represents the highest point that will be reached in the way of an analytical solution unless there is some revolutionary advance in methods. Love's solution is laboriously attained, and computation from it is not easy; neither does the solution carry that sudden illumination for which we look to analytical solutions. In fact, not until some typical examples have been worked out is it easy to see just what the analysis implies. Now it is highly unlikely that analytical solutions can be obtained when the propellant burns slowly, and, even if they could be found, it would still be necessary to evaluate them numerically in selected cases, a proceeding that appears

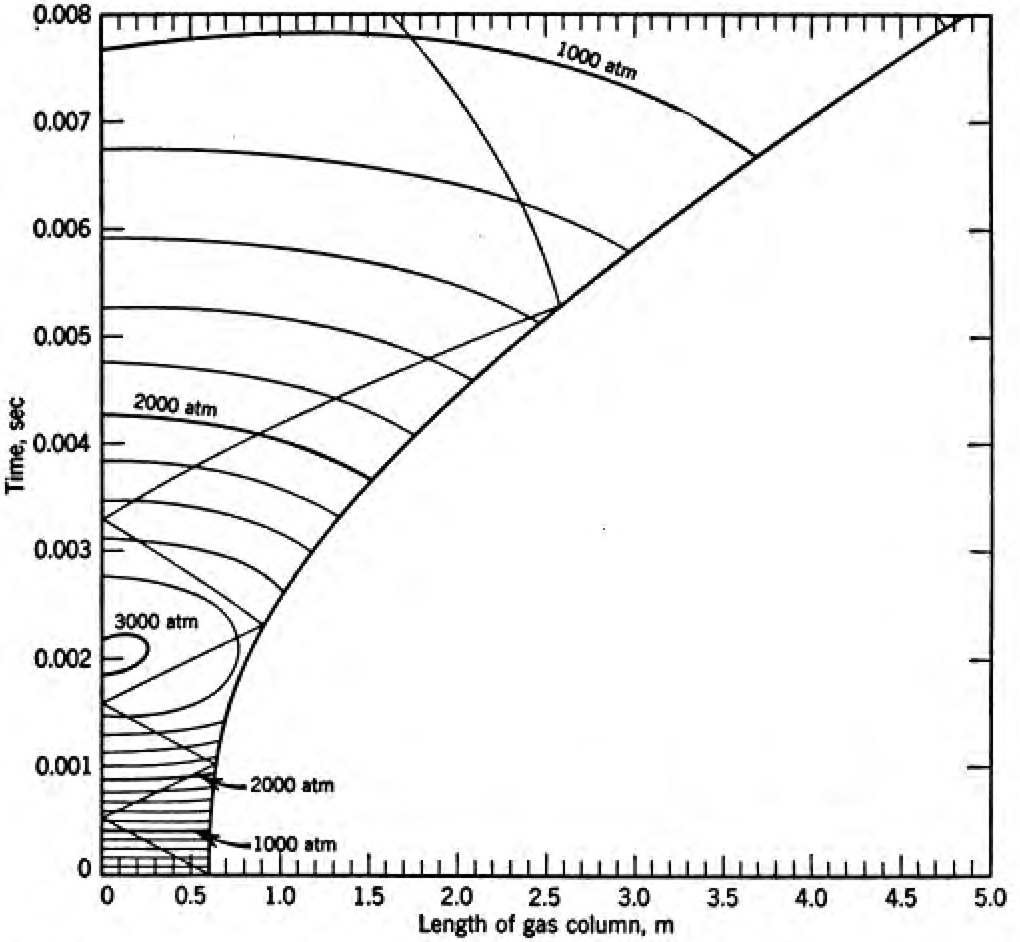

FIG. 9.3 The pressure in the propellant gas as a function of time and position, in an example computed by de Haller using the method of characteristics. *Bull. tech. Suisse Romande.* Reproduced by permission of Dr. P. de Haller.

clearly, from Love and Pidduck's paper, to be very laborious. It is far more promising to solve a few typical problems by a completely numerical process, using the method of characteristics. This is more certain and probably much less work in the end than analytical research. Work on these lines has been done by de Haller,[18] who neglected the variation of entropy with position at a given time, and later, without this approximation, by Carrière.[19] We expect that such work will close the substantial gap between theory and experiment.

Figure 9.3 shows the pressure as a function of position and time in an example solved by de Haller. In this case the rate of burning was assumed independent of pressure, but results of qualitatively the same nature have been computed by Carrière on more realistic assumptions.

9.15 The shock-wave equations

Needed for the next section and § 9.4 are the main formulas for shock waves. An arbitrary disturbance traveling through a compressible medium changes its form as it proceeds; the velocity with which the high-pressure regions are propagated is greater than that of adjacent regions of lower pressure, for the pressure raises the temperature and so the velocity of sound, and in the high-pressure regions the medium itself has a forward velocity. Hence, if not eaten away by a pursuing rarefaction, the regions of higher pressure become steeper and eventually form into sudden jumps of pressure. Strictly speaking, the rise of pressure occurs in a thin but finite zone, in which viscosity and thermal conduction effects are enhanced by the rapidity of the changes; these irreversible changes convert mechanical energy into heat. A shock wave, then, which is a single, almost discontinuous jump of pressure, leaves behind it gas at higher temperature, indeed hotter than by adiabatic compression to the same pressure. The loss of mechanical energy is seen as a decay of the pressure jump, unless some agency such as a piston or a shot serves to maintain the shock. In such a case the net result is that work is done by the piston against resistance, and the gas which is crossed by the shock is heated.

For further details of the properties of shock waves we refer to standard texts.[20] Here we shall simply assume the pressure to rise in a discontinuous jump at a certain plane, the shock front. This is a very good approximation in the applications we shall make. We deal only with shocks in which the medium flows normal to the shock front.

---

[18] de Haller, *Bull. tech. de la Suisse Romande* (January 1948).

[19] Carrière, *Proc. 7th Intern. Congr. Applied Mech.* (London, 1948).

[20] Taylor and Maccoll, in *Aerodynamic Theory*, vol. III (ed. Durand, Berlin, 1934). Courant and Friedrichs, *Supersonic Flow and Shock Waves* (New York, 1948).

Digitized by Google Original from UNIVERSITY OF MICHIGAN

Let the velocity of the medium be u, its density ρ, and pressure p. Let suffix 1 denote conditions in front of the plane shock wave and suffix 2 the conditions just behind. Let D be the velocity of the shock. The conservation of mass, applied to unit cross sections parallel to the shock front, gives

$$\rho_1(D - u_1) = \rho_2(D - u_2) \tag{59}$$

and the conservation of momentum requires

$$\rho_1(D - u_1)(u_2 - u_1) = p_2 - p_1 \tag{60}$$

Let E_1 and E_2 be the intrinsic energies of the medium just before and just after the shock. The conservation of energy gives

$$\rho_1(D - u_1)(E_2 - E_1 + \tfrac{1}{2}u_2^2 - \tfrac{1}{2}u_1^2) = p_2u_2 - p_1u_1 \tag{61}$$

These three equations may be put into various forms, for example:

$$D = u_1 + \left[\frac{p_2 - p_1}{\rho_1\left(1 - \dfrac{\rho_1}{\rho_2}\right)}\right]^{\frac{1}{2}} \tag{62}$$

$$u_2 = u_1 + \left[(p_2 - p_1)\left(\frac{1}{\rho_1} - \frac{1}{\rho_2}\right)\right]^{\frac{1}{2}} \tag{63}$$

$$E_2 - E_1 = \frac{1}{2}(p_1 + p_2)\left(\frac{1}{\rho_1} - \frac{1}{\rho_2}\right) \tag{64}$$

If the initial state is given, there are three equations to determine the final state (p_2, ρ_2, u_2, E_2) and the velocity D of the shock wave. There is also a known relation between E_2, p_2, and ρ_2. Thus there is one degree of freedom in the system. If D is specified, then all the other properties of the medium behind the shock can be computed. Similarly if the shock pressure p_2 is given, one can find the rest of the solution, including the speed at which the shock is traveling.

Equation 64 is the "Rankine-Hugoniot relation." If p_1 and ρ_1 are given, the states satisfying equation 64 lie on the "Hugoniot curve" in a pressure-density plot. If one may take a mean γ over the range of temperatures T_1 to T_2, and if the medium is a perfect gas,

$$E_2 - E_1 = \frac{R(T_2 - T_1)}{\gamma - 1} \tag{65}$$

and equation 64 can be put into the form,

$$\frac{\rho_2}{\rho_1} = \frac{(\gamma + 1)p_2 + (\gamma - 1)p_1}{(\gamma + 1)p_1 + (\gamma - 1)p_2} \tag{66}$$

We may check the arithmetic, to some extent, by going to an infinitely weak shock. If we write $\rho_2 - \rho_1 = d\rho$, and so on, equation 66 gives

$$\gamma \frac{d\rho}{\rho} = \frac{dp}{p}$$

which is the adiabatic relation that one would expect in this limit. The Hugoniot curve and the adiabatic through (p_1, ρ_1) are therefore tangential at that point. It is also easy to show, from equations 64 and 65 that the temperature rise $T_2 - T_1$ is always greater for a shock than for an adiabatic compression to the same pressure.

9.16 The maximum possible muzzle velocity

This is a matter of considerable interest. That there must be some limit is clear from the fact that the energy of the propellant has to supply among other things the kinetic energy of its own gases, which must therefore have some limiting velocity.

One way to approach the matter is to make the shot weight tend to zero in some theory of Lagrange's problem. Suppose we do this in Pidduck's limiting solution. From equation 57, for a gun of infinite length ($\phi \to \infty$), the maximum velocity V_m is given by

$$V_m{}^2 = \frac{2B\left(b - \dfrac{\eta C}{A}\right)^2}{\gamma - 1}$$

which, by equation 41, is

$$\begin{aligned} V_m{}^2 &= \frac{4\gamma\Omega K}{(\gamma - 1)^2}\left(\frac{1}{\rho(0, 0)} - \eta\right)^{1-\gamma} \\ &= \frac{4\gamma\Omega RT(0, 0)}{(\gamma - 1)^2} \end{aligned}$$

From equation 48, $\Omega = 1$ for $W/C = 0$. Also $RT(0, 0)$ is RT_0, the usual force constant of the propellant. Hence,

$$V_m = \frac{2}{\gamma - 1}(\gamma RT_0)^{1/2} \tag{67}$$

For the typical values $\gamma = 1.25$, $(RT_0)^{1/2} = 3300$ ft/sec, this limit is 29,500 ft/sec. A result of the same class arises from the less sophisticated Lagrange approximation. The kinetic energy of the gas is $CV^2/6$, while the chemical energy of the propellant is $CRT_0/(\gamma - 1)$, with a suitable mean γ. Hence,

$$V_m = \left(\frac{6RT_0}{\gamma - 1}\right)^{1/2} \tag{68}$$

which for $\gamma = 1.25$ is only 55 per cent of equation 67.

A different line was followed by Langweiler,[21] who thought that the limit would be that attained by the propellant gas expanding to zero pressure in a nozzle. This velocity is obtained from the classical one-dimensional theory of nozzles (§ 7.2), and its basis is simply that the kinetic energy is $CV_m^2/2$; thus,

$$V_m = \left(\frac{2RT_0}{\gamma - 1}\right)^{1/2} \tag{69}$$

that is, 58 per cent of equation 68.

Langweiler fired a rifle with smaller and smaller projectiles, using a constant weight of fast-burning propellant; C/W ranged from 0.8 to 44. Extrapolating to zero shot weight, Langweiler estimated that the limiting velocity for his propellant was 9150 ft/sec, agreeing with his theoretical result within 1 per cent.

This agreement, however, does not mean that equation 69 can be accepted without modification. As Langweiler mentioned, the expansion is not down to zero pressure or even to 1 atm (which itself lowers the limit substantially) but to the pressure behind a shock wave of velocity V_m traveling into air at 1 atm; at $V_m = 9000$ ft/sec this pressure is about 100 atm. Another criticism is that it is not clear why all the propellant gas need attain the limiting velocity; the fact that in Pidduck's solution only part does so is the reason why the limit from equation 67 is more than three times the Langweiler limit.

All these theories neglect the air in front of the shot. The effects produced are discussed in § 9.4. We can give here a result for the velocity limit, due to Pfriem,[22] without presuming too much knowledge of what is to follow in the more complete discussion later. Pfriem considers that the limiting velocity will be attained when the propellant burns with infinite speed. This fills the chamber instantaneously. A shock wave is then generated at the interface between the gas in the chamber and the air in the barrel. This shock passes through the air toward the muzzle, while at the same time a rarefaction travels back from the interface towards the breech. It is assumed that the chamber is so long that the reflection of this wave at the breech does not over-take the shock wave in the time interval of interest. The maximum possible projectile velocity is then the particle velocity behind the compression shock.

---

[21] Langweiler, *Z. tech. Physik.*, **19** (1938), 416.

[22] Pfriem, *Z. tech. Physik*, **22** (1941), no. 10. The equations had been given earlier by Schardin, *Physik. Z.*, **33** (1932), 60, for the case when the high-pressure medium is compressed air.

Let γ be the ratio of the specific heats for the propellant gases, γ_1 the ratio for air at the relevant temperatures. Referring to Fig. 9.4, let P_0 and P_1 be the initial pressures of gas and air, and let P be the pressure behind the shock wave. Similarly let ρ_0 and ρ_1 be the initial densities of the gas and the air in the barrel and ρ the density behind the shock front. Heat loss to the walls being neglected, conditions are the same from the shock wave right back through the air to the air-gas interface.

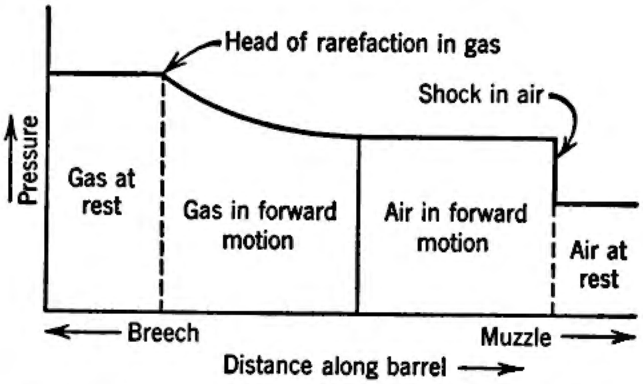

Fig. 9.4 Pressure distribution along the gas column, in the case considered by Schardin and by Pfriem.

The shock wave in the air accelerates the air over which it has passed, to a velocity V. Likewise the rarefaction traveling back to the breech sets into motion more and more of the gas, giving it a velocity (toward the muzzle) varying with the position; at the gas-air interface the gas velocity must be V.

From the adiabatic law applied to the transition suffered by an element at this interface,

$$\frac{P}{P_0} = \left(\frac{\rho}{\rho_0}\right)^{\gamma} \tag{70}$$

It will be shown in § 9.42, from Riemann's theory, that, in a rarefaction traveling backwards into gas at rest,

$$V = \frac{2(\gamma R T_0)^{1/2}}{\gamma - 1}\left[1 - \left(\frac{\rho}{\rho_0}\right)^{(\gamma-1)/2}\right] \tag{71}$$

giving

$$\frac{P}{P_0} = \left[1 - \frac{(\gamma - 1)V}{2(\gamma R T_0)^{1/2}}\right]^{2\gamma/(\gamma-1)} \tag{72}$$

Turning to the shock wave in the air, from equation 63 of the preceding section, one has

$$V^2 = (P - P_1)\left(\frac{1}{\rho_1} - \frac{1}{\rho}\right)$$

and, from equation 66,

$$\frac{\rho_1}{\rho} = \frac{(\gamma_1 - 1)P + (\gamma_1 + 1)P_1}{(\gamma_1 + 1)P + (\gamma_1 + 1)P_1}$$

so that

$$V^2 = \frac{2R_1T_1\left(\frac{P}{P_1} - 1\right)^2}{(\gamma_1 + 1)\frac{P}{P_1} + \gamma_1 - 1} \tag{73}$$

where R_1 is the gas constant per gram for the air in the barrel.

The two unknowns V and P are obtained from equations 72 and 73 by successive approximations. The highest material velocity in the system is V; this, then, is the maximum possible projectile velocity attainable from the given values of P_0 and P_1.

As a special case, consider $P_1 = 0$, that is, an evacuated barrel. The maximum velocity is

$$V_m = \frac{2}{\gamma - 1}(\gamma R T_0)^{1/2} \tag{74}$$

which is identical with equation 67, obtained from Pidduck's limiting solution. The present derivation is more satisfying, since it is shown to arise exactly from a physically possible initial state.

Langweiler's experimental limit can also be verified from these equations. With $\gamma = 1.25$, $\gamma_1 = 1.4$, $P_0 = 80$ tons/sq in., $P_1 = 1$ atm, $T_1 = 288$°K, and Langweiler's assumed RT_0 of 1000 m/sec, the maximum theoretical velocity is 10,400 ft/sec. In view of the experimental difficulties and the neglect of heat loss and frictional drag in the theory, this is as good agreement as could be expected, and the deviation is in the plausible direction. The pressure behind the shock wave is 147 atm, and the temperature is over 7000°K. At such temperatures γ_1 for air is well down from its low-temperature value of 1.4, and this reduces the temperature considerably. Nevertheless the temperature is strikingly high, particularly when compared with the 1200°K obtained by an adiabatic compression from 1 to 147 atm.

9.2 The interior ballistics of a gun after shot ejection

The problem of the motion of the gas in a gun after the shot has left is rather similar to Lagrange's ballistic problem, and is connected with the latter by the fact that the final state in Lagrange's problem, with the shot just at the muzzle, is the initial state in the present work. The emptying of a gun was apparently first discussed by Hugoniot,[23] in a form that has been repeated in many other applications to the emptying of a reservoir of gas. In regard to their use in interior ballistics, Hugoniot's results show how the breech pressure dies away after shot ejection and, hence, by integration, how the gas increases the momentum of the recoiling parts after the shot has left the gun. However, for a long time these results were not applied in the design of recoil systems, which was carried out with the help of empirical factors drawn from accumulated experience. The proposal to use muzzle brakes made it necessary to pay more attention to the theoretical details of the flow from the gun, partly because of the larger number of empirical factors needed to cover the more complicated behavior, and also because of the lack of empirical knowledge of such systems. With this aim, Rateau [24] improved Hugoniot's work by (1) including the effect of the covolume, and (2) correcting for the initial distribution of gas velocity along the barrel at the moment of shot ejection. Rateau's theory will be sketched later.

During World War II the use of muzzle brakes became almost universal on certain classes of guns, and theoretical calculations were made on certain aspects of their behavior. The solution given in the following sections [25] arose from a desire to check the Rateau-Hugoniot formulas in a typical application. It was found that Rateau's formulas are sufficiently accurate for the design of recoil systems assisted by muzzle brakes.

Our results do not cover the example of a low muzzle velocity, where the hydrodynamic behavior is relatively more complicated. This is, however, a region where the forces acting after ejection are small compared with the total momenta concerned, so that our results do cover the range of practical interest. We have also neglected terms of relative size $(C/W)^2$, which is about 0.2 for a typical antitank gun. Our results are therefore not necessarily true for hypervelocity guns with C/W of the order of unity. It should be noted that the initial state of our problem is itself not known to terms of this order, except in the artificial case where the propellant burns very rapidly.

9.21 The initial state of the gas in the barrel

We shall assume that the internal volume of the gun has the form of a circular cylinder of cross-sectional area A and volume U. In applications to real guns U will be the total capacity of the gun and A the bore area. The length of the real gun will then be somewhat less than U/A, because of the larger cross section of the chamber, but the error in our results will be small for all normal guns.

---

[23] Hugoniot, *Comp. rend.*, **103** (1886), 1002.

[24] Rateau, *Comp. rend.*, **168** (1919), 330, 435, 581; *Mém. artillerie franç.*, **11** (1932), 5.

[25] Published in *Proc. Roy. Soc. (London)*, **188A** (1947), 255.

Let the charge mass be C, shot mass W, and muzzle velocity V_0. Let x denote distance from the breech, t the time from the instant of shot ejection. At this point and time, the pressure is p, velocity of the gas v, temperature T, and density ρ. It is convenient to introduce nondimensional units of distance and time, defined by

$$\xi = \frac{xA}{U}; \qquad \tau = \frac{V_0At}{U} \tag{75}$$

We shall assume that the charge is completely burnt before the shot reaches the muzzle. At $t = 0$ the base of the projectile is at the muzzle section, and the velocity and pressure distribution along the barrel is the end state of Lagrange's problem. It has been shown in § 9.14 that the theory of this is not in its final form. We may suppose, however, that we shall not be far wrong in using the Pidduck solution for the instant of shot ejection and keeping only terms of the order of C/W. For $C/W = \frac{1}{2}$, corresponding to muzzle velocities of the order of 3000 ft/sec, the $(C/W)^2$ term, in the ratio of breech pressure to pressure at shot, is 3 per cent of the C/W term; therefore, we shall neglect terms of order $(C/W)^2$ throughout our calculations. It is, of course, true that the $(C/W)^2$ terms, certainly small in the initial state, may increase relatively to the other terms as time goes on; this seems unlikely, since the terms of the order of C/W do not increase much, and they later die down. In any case, the physical correctness of the C/W term in the initial state is itself not completely above suspicion.

We shall not neglect the covolume, which would indeed not be very plausible in the practical example we shall discuss later, for which the breech pressure at shot ejection is almost 10 ton/sq in. Let the covolume be denoted by η. It is useful to introduce the ratio,

$$\epsilon = \frac{\eta}{\dfrac{U}{C} - \eta} \tag{76}$$

which is the definition 17 of chapter 7, specialized to our particular case. ϵ is a measure of the effects produced by the covolume. There are practical limits on the muzzle pressure, and ϵ is therefore rarely more than 0.2. We shall expand certain terms as power series in ϵ, neglecting terms of the order of ϵ^2. The error will be of the same importance as the neglect of terms in $(C/W)^2$. The terms of the order of ϵ continually decrease, as would be expected.

Let T_e be the gas temperature at the instant of shot ejection, averaged over the whole of the gas. Let R be, as usual, the gas constant per gram of the propellant gas; to the accuracy of our calculations R can be taken to be constant. Further, let γ be the ratio of specific heats for the gases. A mean value must be taken, appropriate to the temperature range being considered.

To the accuracy of this work the covolume is independent of temperature (see chapter 3). It follows then, from the equation of state of the propellant gases, namely,

$$p\left(\frac{1}{\rho} - \eta\right) = RT \tag{77}$$

that the equation of the adiabatics is

$$p\left(\frac{1}{\rho} - \eta\right)^{\gamma} = \text{constant} \tag{78}$$

In § 9.13 it was assumed that $p[(1/\rho) - \eta]^{\gamma}$ is independent of position along the barrel, though it is, of course, a function of time. The results for the instant of shot ejection are, to terms of the order of C/W,

$$p = \frac{RT_e}{\dfrac{U}{C} - \eta}\left[1 + \frac{C}{6W}(1 - 3\xi^2)\right] \tag{79}$$

$$\frac{1}{\rho} - \eta = \left(\frac{U}{C} - \eta\right)\left[1 + \frac{C}{6\gamma W}(3\xi^2 - 1)\right] \tag{80}$$

$$T = T_e\left[1 + \frac{(\gamma - 1)C}{6\gamma W}(1 - 3\xi^2)\right] \tag{81}$$

$$p\left(\frac{1}{\rho} - \eta\right)^{\gamma} = RT_e\left(\frac{U}{C} - \eta\right)^{\gamma - 1} \tag{82}$$

and, for the velocity distribution,

$$v = V_0\xi \tag{83}$$

These follow immediately from equations 42, 43, and 44 with 50.

These equations give the pressure, density, and velocity distributions in terms of the muzzle velocity, gun dimensions, covolume, and RT_e.

The last can be calculated from the energy of reaction of the propellant, the energy of the shell as it leaves the muzzle, and the heat and friction losses to the barrel; that is to say, in terms of muzzle velocity, known properties of the propellant, and certain properties, rather more doubtful, of the gun. However, these results and those that follow can be applied without needing a solution of the ordinary equations of interior ballistics for the gun under consideration.

The pressure drop down the gun due to gas friction is neglected in these formulas.

9.22 Earlier work

The problem of the emptying of a reservoir of perfect gas by expansion through a nozzle was first treated by Hugoniot,[26] by assuming that the state of flow at any instant was the same as would be set up eventually in steady flow with the reservoir pressure existing at that instant. This hypothesis of quasisteady flow is plausible, provided the reservoir pressure is not falling too rapidly. Rateau [27] used the same assumption about quasisteady flow and introduced the covolume into the calculations. He assumed that the gun barrel acted as a convergent nozzle with throat area equal to that of the bore, so that the gas velocity at the muzzle was equal to the local velocity of sound. He pointed out that the gun was an unusual type of reservoir, with its cross section no bigger than the throat area of the nozzle; also the initial state, at the instant that flow through the nozzle began, was a nonuniform distribution of pressure and velocity down the reservoir. He suggested that this initial state could be taken into account in the following way. The gas can be imagined to start from rest at an effective pressure P_i and temperature T_i, such that by adiabatic expansion the gas would arrive at the true pressure p_e, the right temperature T_e, and the correct total kinetic energy for the instant when the shot passes the muzzle. This statement is not unambiguous, with regard to such questions as whether to take breech or mean pressures, for example. This theory will be compared with experiment in § 9.25. The correction by using such an effective pressure is by no means sufficient to give agreement with experiment, and, as the formulas are much simpler when the correction is omitted, we state only such results here: for the mean density at time t,

$$\frac{1}{\rho} + 1.07\eta = \left(\frac{U}{C} + 1.07\eta\right)\left(1 + \frac{t}{\theta}\right)^{2/(\gamma-1)} \tag{84}$$

---

[26] Hugoniot, *Comp. rend.*, **103** (1886), 1002.

[27] Rateau, *Comp. rend.*, **168** (1919), 330, 435, 581; *Mém. artillerie franç.*, **11** (1932), 5.

where

$$\theta = \frac{2U}{(\gamma - 1)A}\left(1 + 0.13\,\frac{\eta C}{U}\right)\left[\frac{1}{\gamma}\left(\frac{\gamma + 1}{2}\right)^{(\gamma+1)/(\gamma-1)} \frac{C}{Up_e\left(1 - \dfrac{\eta C}{U}\right)^{\gamma}}\right]^{1/2} \tag{85}$$

and, hence, the breech pressure follows as

$$p = p_e\left(\frac{U}{C} - \eta\right)^{\gamma}\left(\frac{1}{\rho} - \eta\right)^{-\gamma} \tag{86}$$

Using the expression 79 with $\xi = 0$ to give p_e, we may write equation 85 as

$$\theta = \frac{2U}{(\gamma - 1)A}\left(1 + 0.13\,\frac{\eta C}{U}\right) \times \left[\frac{1}{\gamma}\left(\frac{\gamma + 1}{2}\right)^{(\gamma+1)/(\gamma-1)} \frac{1}{RT_e\left(1 + \dfrac{C}{6W}\right)\left(1 - \dfrac{\eta C}{U}\right)^{\gamma-1}}\right]^{1/2} \tag{87}$$

This sometimes appears in the literature with the C/W terms omitted or given other values, arising from different interpretations of the "pressure," which occurs in the equation for the nozzle flow. We have assumed that the flow is the same as that from a reservoir pressure equal to the *breech* pressure.

Omitting the covolume terms, we arrive at what are effectively Hugoniot's results:

$$p = \frac{CRT_e}{U}\left(1 + \frac{C}{6W}\right)\left(1 + \frac{t}{\theta}\right)^{-2\gamma/(\gamma-1)} \tag{88}$$

with

$$\theta = \frac{2U}{(\gamma - 1)A}\left[\frac{1}{\gamma}\left(\frac{\gamma + 1}{2}\right)^{(\gamma+1)/(\gamma-1)} \frac{C}{Up_e}\right]^{1/2} \tag{89}$$

It is often important to know the momentum imparted to the gun after the projectile has left. If we integrate the Hugoniot formula, the momentum is

$$\left(\frac{\gamma + 1}{2}\right)^{(3-\gamma)/2(\gamma-1)} C\left(\frac{RT_e}{\gamma}\right)^{1/2}\left(1 + \frac{C}{12W}\right) \tag{90}$$

which for the typical value $\gamma = 1.25$ is

$$1.35C(RT_e)^{1/2}\left(1 + \frac{C}{12W}\right) \tag{91}$$

Digitized by Google
Original from
UNIVERSITY OF MICHIGAN

9.23 Discussion of the problem

We assume that each element of gas expands adiabatically, so that $p[(1/\rho) - \eta]^\gamma$ is independent of time and depends only on the element considered. Now, on the assumptions of § 9.21 this quantity is the same for all elements at the moment of shot ejection, and hence

$$p\left(\frac{1}{\rho} - \eta\right)^\gamma = RT_e\left(\frac{U}{C} - \eta\right)^{\gamma-1} \tag{92}$$

for *all* values of x and t.

The assumption of adiabatic expansion after the instant of shot ejection involves two factors: (1) we neglect heat loss to the barrel after shot ejection; (2) we assume that no shock waves occur in the gas inside the gun. Of these the second is certainly justifiable. As the projectile passes out of the gun a rarefaction wave enters the barrel and moves toward the breech; this wave cannot give rise to a discontinuity of pressure. It may happen, in certain peculiar guns, that shock waves are present in the propellant gas even before the shot leaves, in which case our assumption would break down; in such a case it would also be untrue that the elements of gas lie on a common adiabatic before shot ejection, and the whole treatment would collapse.

The heat loss to the barrel is not easily included in the calculations. Its effect can be expected to be less than its effect on the Lagrange problem, in which heat loss has been neglected up to the present day. It will be shown in § 9.25 that, as a matter of fact, the neglect of heat loss helps to compensate certain other approximations in our treatment.

Since all elements of the gas follow a common adiabatic throughout the solution, it is convenient to use the Eulerian equations of hydrodynamics. The equation of continuity is

$$\frac{\partial \rho}{\partial t} + \frac{\partial}{\partial x}(\rho v) = 0 \tag{93}$$

and the equation of motion is

$$\frac{\partial v}{\partial t} + v\frac{\partial v}{\partial x} = -\frac{1}{\rho}\frac{\partial p}{\partial x} \tag{94}$$

The velocity of sound at time t and position x is

$$c = \left(\frac{dp}{d\rho}\right)^{1/2} = \frac{(\gamma RT_e)^{1/2}}{1 - \eta\rho}\left(\frac{\dfrac{U}{C} - \eta}{\dfrac{1}{\rho} - \eta}\right)^{(\gamma-1)/2} \tag{95}$$

The influence of the conditions outside the muzzle section is transmitted through the gas toward the breech with velocity $c - v$ relative to the barrel. This is assured by the fact that it is a rarefaction wave that is passing through the gas, not a wave of compression, which might develop into a shock. Let Z be the value of ξ ($= xA/U$) at the point reached by the front of the wave at time t; that is, for $\xi \leq Z$, the behavior of the gas is settled entirely by the state of the gas inside the gun at the instant of shot ejection, whereas for $\xi > Z$ it is necessary to take into account conditions outside the muzzle. The motion of the wave front satisfies the equation,

$$\frac{U}{A}\frac{dZ}{dt} = v - c \tag{96}$$

the right-hand side being evaluated at $\xi = Z$.

It will be clear that the motion of the gas is simplest in the region $\xi \leq Z$. We shall first obtain a solution for this zone, and use this to integrate equation 94, thereby showing how far the rarefaction wave from the muzzle has progressed at any time. In § 9.26 we shall discuss the nature of the flow in the region $\xi > Z$. The solution in the region of ξ less than Z is obviously not applicable at the muzzle except for guns of velocity greater than 3500 ft/sec, and then only for a short time; hence the solution for this region is not of much use by itself for the calculation of rates of outflow. For these the wave of rarefaction is an essential feature. However, this wave often takes a relatively long time to reach the breech; for example, the breech pressure of the gun studied later falls to one third of its initial value before the rarefaction wave hits the breech. Thus questions of recoil can often be settled by using the simpler solution up to this time and some rough approximation for the pressure at later times. The extent to which this is possible in a typical antitank gun may be seen from a later example.

9.24 Solution before the arrival of the wave from the muzzle

We assume that the gas velocity is a linear function of the distance along the gun and that the pressure is a quadratic function. These forms are suggested by the initial distributions. To attempt a solution on these lines we write

$$v = V_0\xi f(\tau)\left[1 + \epsilon g(\tau) + \frac{C}{W}h(\tau)\right]$$

and

$$\frac{1}{\rho} = \left(\frac{U}{C} - \eta\right)k(\tau)\left[1 + \epsilon l(\tau) + \frac{C}{W}m(\tau) + \xi^2\left\{n(\tau) + \epsilon p(\tau) + \frac{C}{W}q(\tau)\right\}\right]$$

where the functions $f(\tau) \cdots q(\tau)$ are to be chosen to satisfy equations 92, 93, and 94 for all τ, and the initial conditions 79 to 83 at $\tau = 0$. It is possible to satisfy all these equations with errors of the order of ϵ^2, $\epsilon C/W$, and $(C/W)^2$. The process is simple, though the details are a little laborious, and the solution is

$$v = \frac{\xi V_0}{1+\tau}\left[1 + \frac{C}{W}\frac{RT_e}{V_0^2(2-\gamma)}\left\{(1+\tau)^{1-\gamma} - (1+\tau)^{-1}\right\}\right] \tag{97}$$

$$\begin{aligned} p = \frac{RT_e}{\left(\frac{U}{C} - \eta\right)(1+\tau)^{\gamma}} & \left[1 + \frac{C}{6W} - \frac{\epsilon\gamma\tau}{1+\tau} - \frac{C}{W}\frac{\xi^2}{2(1+\tau)^2}\right. \\ & \left. - \left(\frac{\gamma}{2-\gamma}\right)\frac{C}{W}\frac{RT_e}{V_0^2}\left\{\frac{2-\gamma}{\gamma-1} + \frac{1}{1+\tau} - \frac{1}{(\gamma-1)(1+\tau)^{\gamma-1}}\right\}\right] \end{aligned} \tag{98}$$

$$\begin{aligned} \frac{1}{\rho} = \left(\frac{U}{C} - \eta\right)(1+\tau) & \left[1 - \frac{C}{6\gamma W} + \epsilon + \frac{C}{W}\frac{\xi^2}{2\gamma(1+\tau)^2}\right. \\ & \left. + \frac{C}{W}\frac{RT_e}{V_0^2(2-\gamma)}\left\{\frac{2-\gamma}{\gamma-1} + \frac{1}{1+\tau} - \frac{1}{(\gamma-1)(1+\tau)^{\gamma-1}}\right\}\right] \end{aligned} \tag{99}$$

The terms in C/W and ϵ stay small at all times, and so the neglect of higher powers is almost certainly correct at all times.

The velocity of sound is

$$\begin{aligned} c = \frac{(\gamma RT_e)^{1/2}}{(1+\tau)^{(\gamma-1)/2}} & \left[1 + \epsilon\left\{1 - \frac{(\gamma+1)\tau}{2(1+\tau)}\right\}\right. \\ & \left. + \frac{C}{W}\frac{RT_e}{V_0^2}\left\{\frac{1}{2(2-\gamma)(1+\tau)^{\gamma-1}} - \frac{1}{2} - \frac{\gamma-1}{2(2-\gamma)(1+\tau)}\right\}\right] \end{aligned} \tag{100}$$

Here the terms in ϵ^2 and $(C/W)^2$ have been neglected as usual, and also a term proportional to C/W and depending on ξ and τ, whose sum is at most $C/30W$.

Substituting from equations 100 and 97 into equation 96, we find that the boundary of the rarefaction wave satisfies the equation,

$$\begin{aligned} \frac{dZ}{d\tau} - \frac{Z}{1+\tau} & \left[1 + \frac{C}{W}\frac{RT_e}{(2-\gamma)V_0^2}\left\{(1+\tau)^{1-\gamma} - (1+\tau)^{-1}\right\}\right] \\ & + \frac{(\gamma RT_e)^{1/2}}{V_0(1+\tau)^{(\gamma-1)/2}}\left[1 + \epsilon\left\{1 - \frac{(\gamma+1)\tau}{2(1+\tau)}\right\}\right. \\ & \left. + \frac{C}{W}\frac{RT_e}{V_0^2}\left\{\frac{1}{2(2-\gamma)(1+\tau)^{\gamma-1}} - \frac{1}{2} - \frac{\gamma-1}{2(2-\gamma)(1+\tau)}\right\}\right] = 0 \end{aligned} \tag{101}$$

of which the general solution is

$$\begin{aligned}
&\frac{Z}{1+\tau}\left[1+\frac{C}{W}\frac{RT_e}{(2-\gamma)V_0^2}\left\{\frac{1}{(\gamma-1)(1+\tau)^{\gamma-1}}-\frac{1}{1+\tau}\right\}\right]\\
&\quad=\frac{1}{1+\tau_0}\left[1+\frac{C}{W}\frac{RT_e}{(2-\gamma)V_0^2}\left\{\frac{1}{(\gamma-1)(1+\tau_0)^{\gamma-1}}-\frac{1}{1+\tau_0}\right\}\right]\\
&\qquad+\frac{2(\gamma RT_e)^{1/2}}{(\gamma-1)V_0(1+\tau)^{(\gamma-1)/2}}\left[1-\frac{\epsilon(\gamma-1)\tau}{2(1+\tau)}\right.\\
&\qquad\left.+\frac{C}{W}\frac{RT_e}{V_0^2}\left\{\frac{\gamma+1}{6(2-\gamma)(\gamma-1)(1+\tau)^{\gamma-1}}-\frac{1}{2}-\frac{\gamma-1}{2(2-\gamma)(1+\tau)}\right\}\right]\\
&\qquad-\frac{2(\gamma RT_e)^{1/2}}{(\gamma-1)V_0(1+\tau_0)^{(\gamma-1)/2}}\left[1-\frac{\epsilon(\gamma-1)\tau_0}{2(1+\tau_0)}\right.\\
&\qquad\left.+\frac{C}{W}\frac{RT_e}{V_0^2}\left\{\frac{\gamma+1}{6(2-\gamma)(\gamma-1)(1+\tau_0)^{\gamma-1}}-\frac{1}{2}-\frac{\gamma-1}{2(2-\gamma)(1+\tau_0)}\right\}\right]
\end{aligned}\tag{102}$$

The new constant τ_0 is the value of τ when $Z = 1$, that is, when the boundary of the rarefaction starts from the muzzle. There are two cases to be considered.

Case I. Shot velocity less than local velocity of sound

The relevant velocity of sound is the velocity just behind the shot as it leaves the muzzle. Case I is much the more common, and the condition for it to occur is, from equation 100,

$$V_0 \leq (\gamma RT_e)^{1/2}\left[1+\frac{\eta}{\dfrac{U}{C}-\eta}\right]\tag{103}$$

In this instance the rarefaction moves in from the muzzle immediately after shot ejection, and, therefore, $\tau_0 = 0$. This simplifies equation 102 sufficiently to justify repeating the solution for this particular case:

$$\begin{aligned}
&\frac{Z}{1+\tau}\left[1+\frac{C}{W}\frac{RT_e}{(2-\gamma)V_0^2}\left\{\frac{1}{(\gamma-1)(1+\tau)^{\gamma-1}}-\frac{1}{1+\tau}\right\}\right]\\
&\quad=1+\frac{C}{W}\frac{RT_e}{(\gamma-1)V_0^2}-\frac{2(\gamma RT_e)^{1/2}}{(\gamma-1)V_0}\left[1+\frac{C}{W}\frac{RT_e}{3(\gamma-1)V_0^2}\right]\\
&\qquad+\frac{2(\gamma RT_e)^{1/2}}{(\gamma-1)V_0(1+\tau)^{(\gamma-1)/2}}\left[1-\frac{\epsilon(\gamma-1)\tau}{2(1+\tau)}\right.\\
&\left.+\frac{C}{W}\frac{RT_e}{V_0^2}\left\{\frac{\gamma+1}{6(2-\gamma)(\gamma-1)(1+\tau)^{\gamma-1}}-\frac{1}{2}-\frac{\gamma-1}{2(2-\gamma)(1+\tau)}\right\}\right]
\end{aligned}\tag{104}$$

Case II. Muzzle velocity greater than the local velocity of sound

That is,

$$V_0 > (\gamma RT_e)^{1/2}\left[1 + \frac{\eta}{\dfrac{U}{C} - \eta}\right] \tag{105}$$

This occurs for guns of very high muzzle velocity, of the order of 3500 ft/sec or more. Just after shot ejection the gas velocity at the muzzle is greater than the local velocity of sound, and so the conditions inside the gun are completely independent of what is happening outside. The gas velocity at the muzzle soon falls to the local velocity of sound, and at this time the rarefaction wave starts from the muzzle toward the breech. The value of τ_0 is given by the condition that $V = c$ for $\xi = 1$ and $\tau = \tau_0$ and can be found numerically from equations 97 and 100 in any particular case. An explicit formula for τ_0 can be given, but it is not illuminating. Having found τ_0 numerically, we can substitute it in equation 102 to give the relation between Z and τ.

Our solution for case II is valid only if the initial conditions 79 to 83 are true. It seems possible that, when the velocity of the projectile exceeds the velocity of sound in the gas behind it, the initial distribution of gas in the barrel may well be considerably different from that assumed here.

9.25 Comparison with an experimental breech pressure record

In applications, most of the parameters can be found without difficulty. RT_e can be calculated from Résal's equation, the energy equation of interior ballistics, using the kinetic energy of shot and gases, the thermochemical properties of the propellant, and estimates of the heat loss to the barrel and of the work done against friction. In our example we know the experimental breech pressure at shot ejection, from which we find RT_e immediately.

We consider an example for which $C/W = 0.474$, $\epsilon = 0.197$, $V_0 = 3130$ ft/sec, and $\gamma = 1.275$. The breech pressure as the shot leaves is about 9½ tons/sq in. By equations 95 and 80 the velocity of sound just behind the shot as it leaves the muzzle is about 3640 ft/sec; hence this is an example of case I, and the rarefaction wave starts from the muzzle at $\tau_0 = 0$. From equation 104 we can calculate Z, the position of the rarefaction boundary, at any time. The result is shown in Fig. 9.5. The boundary starts from the muzzle at a fairly low speed, of the order of 500 ft/sec and accelerates as it approaches the breech, chiefly owing to the lower velocity of the gas in this region. The wave reaches

Digitized by Google Original from UNIVERSITY OF MICHIGAN

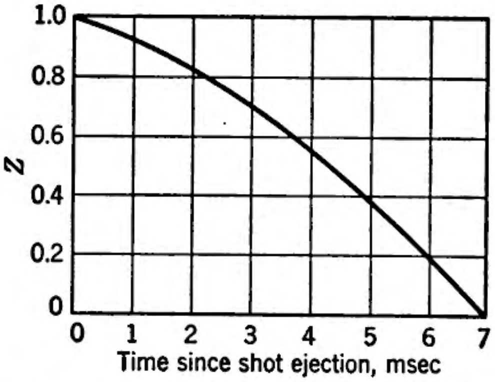

FIG. 9.5 Motion of the rarefaction boundary.
Reproduced by permission of the Royal Society, London.

the breech after 7 msec, which is roughly equal to the time taken for the projectile to travel through the gun.

Figure 9.6 shows the breech pressure for times after shot ejection. The results of the present theory are in good agreement with the experimental results. The error in the pressure at any time is best stated as a fraction of the pressure drop from ejection up to that time. In this case the error is everywhere less than 5 per cent. It is interesting that the theoretical curve lies below the experimental results. The error is due to:

1. Neglect of terms of order ϵ^2 and $(C/W)^2$.

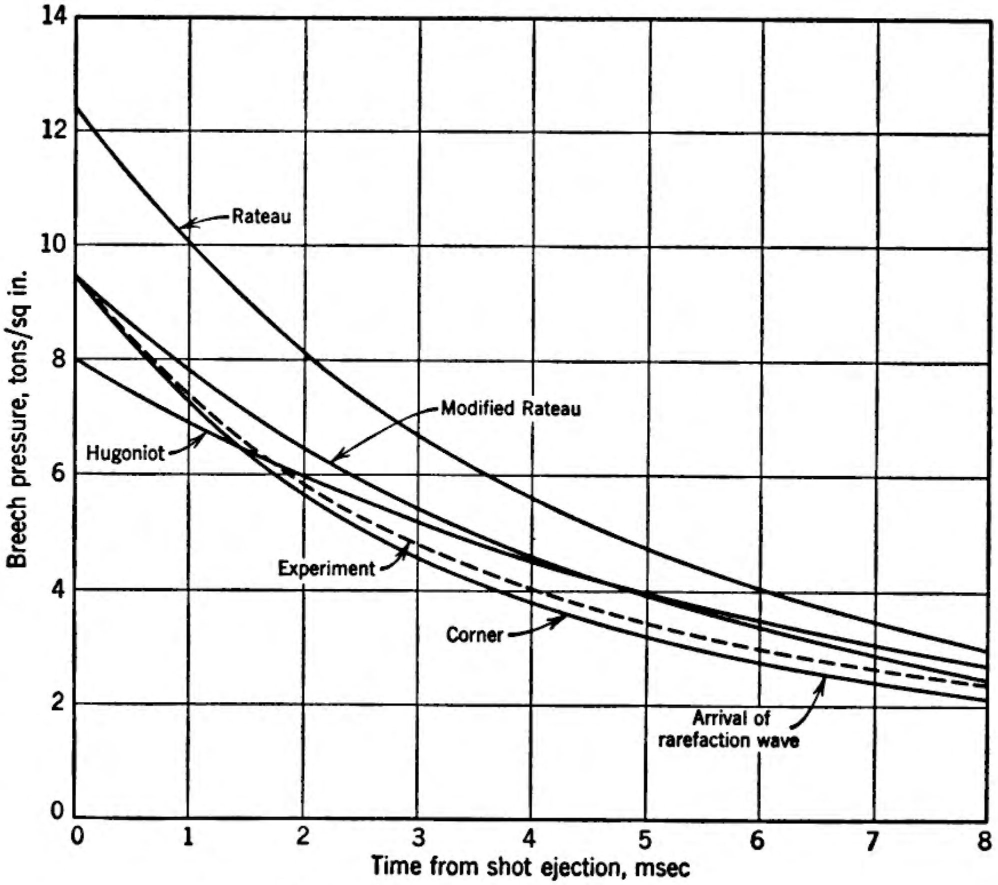

FIG. 9.6 Breech pressure after shot ejection.
Reproduced by permission of the Royal Society, London.

2. The assumption that the cross section is constant along the gun.
3. The neglect of heat loss to the barrel after the shot has left.

It seems obvious that 3 must cause our theoretical pressures to be higher than the true ones; therefore 1 and 2 together must be responsible for lowering the theoretical pressure. The agreement within 5 per cent must therefore arise by partial compensation of opposing errors but is nevertheless very satisfactory.

This theory has been tested on guns with muzzle velocities from 2000 to 4400 ft/sec and initial pressures from 3 to 10 tons/sq in. and has been found to give pressures correct to a few per cent. As it happens, in nearly all these examples the pressure at which the rarefaction wave hits the breech is close to 1 ton/sq in.

The results of other theories are also shown on Fig. 9.6. The curve marked "Rateau" was calculated with his correction for the initial motion of the gas. The "modified Rateau" curve (equations 84 to 87) without this correction is seen to be in much better agreement with experiment. Hugoniot's formulas 88 and 89 are calculated by omitting all covolume terms and using the same RT_e as before, which accounts for the pressure lying considerably below the experimental values at the start. This is partly offset by the theoretical pressure being too big later. A more consistent treatment, with RT_e chosen to make the Hugoniot pressure correct at $t = 0$, would give poor agreement.

The formulas for the breech pressure given in this chapter hold until the rarefaction reaches the breech. An exact treatment for later times would be difficult, and fortunately it is usually unnecessary. It is sufficient to complete the postejection period by one of the simpler theories. This has been done in Fig. 9.6 by using Hugoniot's formulas, with time measured from the instant at which the rarefaction wave reaches the breech. It can be seen that in this case there is no appreciable kink in the pressure-time curve at this point. There does not appear to be any discontinuity of slope in this particular experimental record either. Such a kink can often be detected on pressure-time curves for high-velocity guns.

In many applications the important quantity to be derived from breech pressures after ejection is the *total* momentum caused by the gas pressure on the breech. The curves in Fig. 9.6, labeled "modified Rateau" and "Hugoniot," differ considerably in shape, while their total momenta in the postejection period are only 1 per cent apart. For certain purposes they are effectively identical.

We shall therefore list some momenta to show the differences among various theories. The momentum acquired up to shot ejection = $(W + \frac{1}{2}C)V_0 = 2046$ lb wt × sec.

TABLE 9.1 SUMMARY OF MOMENTA FROM BREECH PRESSURE

Momenta in lb wt × sec

	Experiment	Present Theory	Rateau	Modified Rateau	Hugoniot
First 8.8 msec after ejection	629	596	862	686	653
Error, per cent		−5	+37	+11	+4
After first 8.8 msec		261	335	281	322
Total		2902	3242	3011	3020

In this gun the postejection period contributes about 32 per cent of the total momentum. It is clear that the "modified Rateau" results are practically as accurate as those of the present work, and omission of the covolume (which leads to the Hugoniot formulas) alters the results by a negligible amount. The latter formulas are much the simplest. It must be remembered, however, that the Hugoniot formulas are favored by the choice of RT_e in this comparison.

Details of the velocity and pressure distributions along the gun are given at the end of the next section, after an approximate treatment of the rarefaction zone.

9.26 The rarefaction zone

We consider first case I (shot velocity less than local velocity of sound), in which the rarefaction starts back from the muzzle as soon as the shot leaves. We can calculate Z, the position reached by the rarefaction boundary, by equation 104; substitution in equations 97 and 99 gives the density and gas velocity at this boundary. We denote these by $\rho_1(\tau)$ and $v_1(\tau)$. Let $\rho_2(\tau)$ and $v_2(\tau)$ be the corresponding quantities at the muzzle; these are as yet unknown.

While $Z > 0$, it is possible to carry through the following approximate treatment of the motion inside the rarefaction zone. We assume a particular form for the way the density varies along the zone at any time, in terms of its values at the ends: $\rho_1(\tau)$ at the boundary $\xi = Z$, and $\rho_2(\tau)$ at the muzzle. The latter is a function not yet determined. We then take the equation of continuity,

$$\frac{\partial \rho}{\partial t} + \frac{\partial}{\partial x}(\rho v) = 0 \tag{106}$$

and integrate with respect to x, from the rarefaction boundary to the muzzle. If we return to the variables $\tau = V_0At/U$ and $\xi = xA/U$, the result is

$$\rho_2 v_2 - \rho_1 v_1 = -V_0 \int_Z^1 \frac{\partial \rho}{\partial t}\, d\xi \tag{107}$$

This gives $v_2(\tau)$. Also from $\rho_2(\tau)$ we know $c_2(\tau)$, the velocity of sound at the muzzle. When $\tau = 0$, c_2 is greater than v_2, for this is the definition of case I, which we are considering. In steady flow through a nozzle, $c = v$ at the throat, provided the pressure at entry is more than about twice the pressure in the region into which the nozzle is discharging. It is evident that v_2 must rapidly approach c_2; this condition decides the form of $\rho_2(\tau)$ and so the values of density and velocity throughout the rarefaction zone. For the prediction of muzzle-brake thrusts, to which we come in § 9.31, we need also $\rho_2 v_2{}^2$, which is likewise obtained by this method.

The accuracy of this treatment depends on choosing a good form for the variation of density in the rarefaction zone. The form must also be mathematically convenient. A suitable assumption appears to be that the density is a linear function of distance in the rarefaction zone, so that

$$\rho(\xi, \tau) = \frac{(1 - \xi)\rho_1(\tau) + (\xi - Z)\rho_2(\tau)}{1 - Z} \tag{108}$$

From equation 96,

$$V_0 \frac{dZ}{d\tau} = v_1 - c_1 \tag{109}$$

We introduce a ratio:

$$\theta(\tau) = \frac{\rho_1(\tau)}{\rho_2(\tau)} \tag{110}$$

Equation 107 then leads to

$$v_2 = \theta v_1 - \frac{1}{2} V_0(1 - Z) \left[(1 + \theta) \frac{d}{d\tau} \ln \rho_1(\tau) - \frac{d}{d\tau} \ln \theta \right] + \tfrac{1}{2}(\theta - 1)(c_1 - v_1) \tag{111}$$

while

$$c_2 = \frac{(\gamma R T_e)^{1/2}}{1 - \eta\rho_2} \left[\frac{\dfrac{U}{C} - \eta}{\dfrac{1}{\rho_2} - \eta} \right]^{(\gamma-1)/2} \tag{112}$$

We have said that $\theta(\tau)$ must be chosen to make $c_2 - v_2$ rapidly approach zero from its initial positive value. It does not seem easy to do this in the general case, and so we shall now take as an example the firing mentioned in § 9.25. We assume that

$$\theta = (1 + \tau)^n \tag{113}$$

The behavior of c_2 and v_2, until the time the rarefaction reaches the breech, shows that n must be taken to be 0.6. A more general form such as $\theta = (1 + m\tau)^n$ would be preferable, but it would be much more laborious to determine the best pair of values of m and n; moreover, c_2 is not sensitive to θ, and hence the "best" v_2 would probably not be much altered by using the extra parameter m.

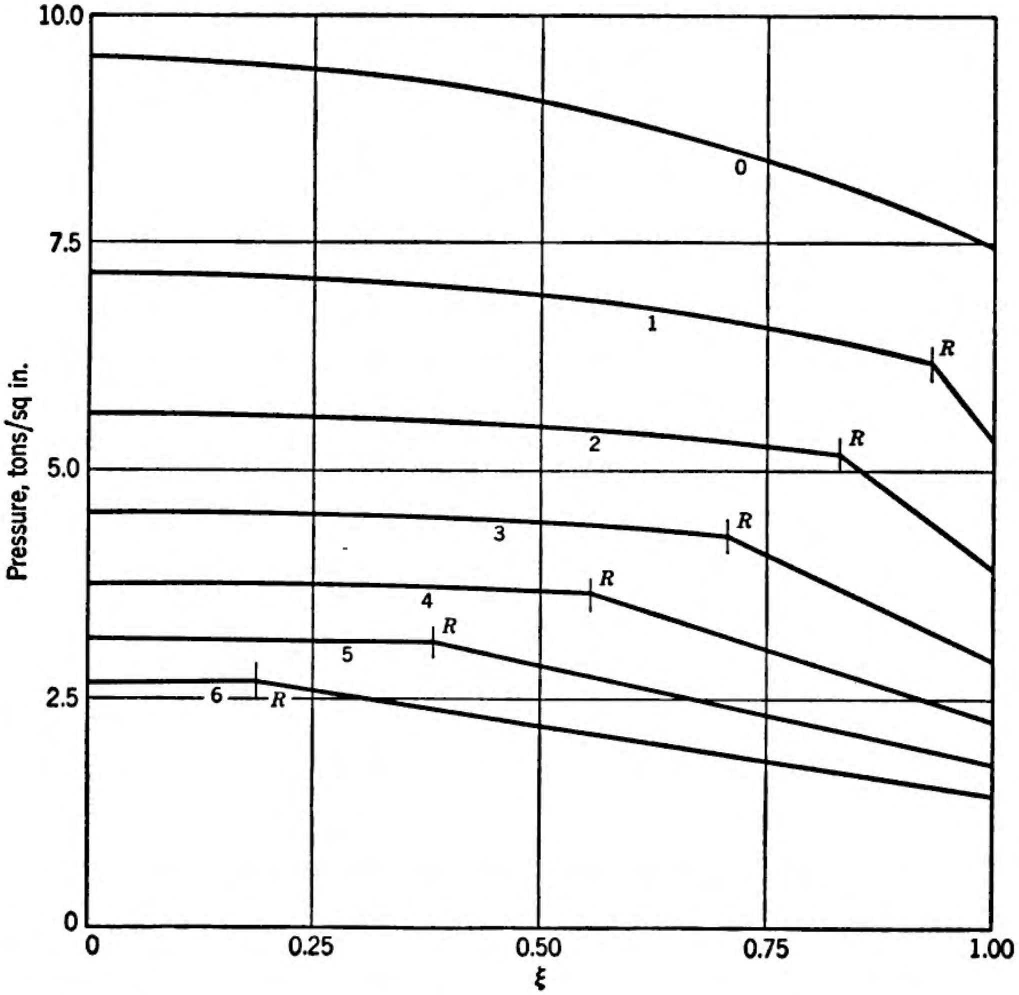

FIG. 9.7 Theoretical pressure distributions at various times. R denotes boundary of rarefaction wave. Numbers on the curves denote time in milliseconds after shot ejection.

Reproduced by permission of the Royal Society, London.

The value of $n = 0.6$ applies to this example only, though n can be expected to have the same order of magnitude for all guns.

Figure 9.7 shows the theoretical pressure distribution along the barrel at various times after shot ejection. The values in the rarefaction zone were calculated from the treatment of this section with $n = 0.6$, and those closer to the breech by the equations of § 9.24. It can be seen how the pressure drop down the barrel, which is about 2 tons/sq in. when the shot is at the muzzle, is rapidly damped thereafter. There is, of course, a marked fall of pressure in the rarefaction wave near the muzzle; this drop attains about 1.2 tons/sq in. in 2 msec and stays practically constant for later times.

In Fig. 9.8 are plotted local gas temperatures, calculated from coexisting values of pressure and density. The temperature at the muzzle drops by 500°C during the first 6 msec. The temperature drop in the rarefaction zone reaches nearly 200°C.

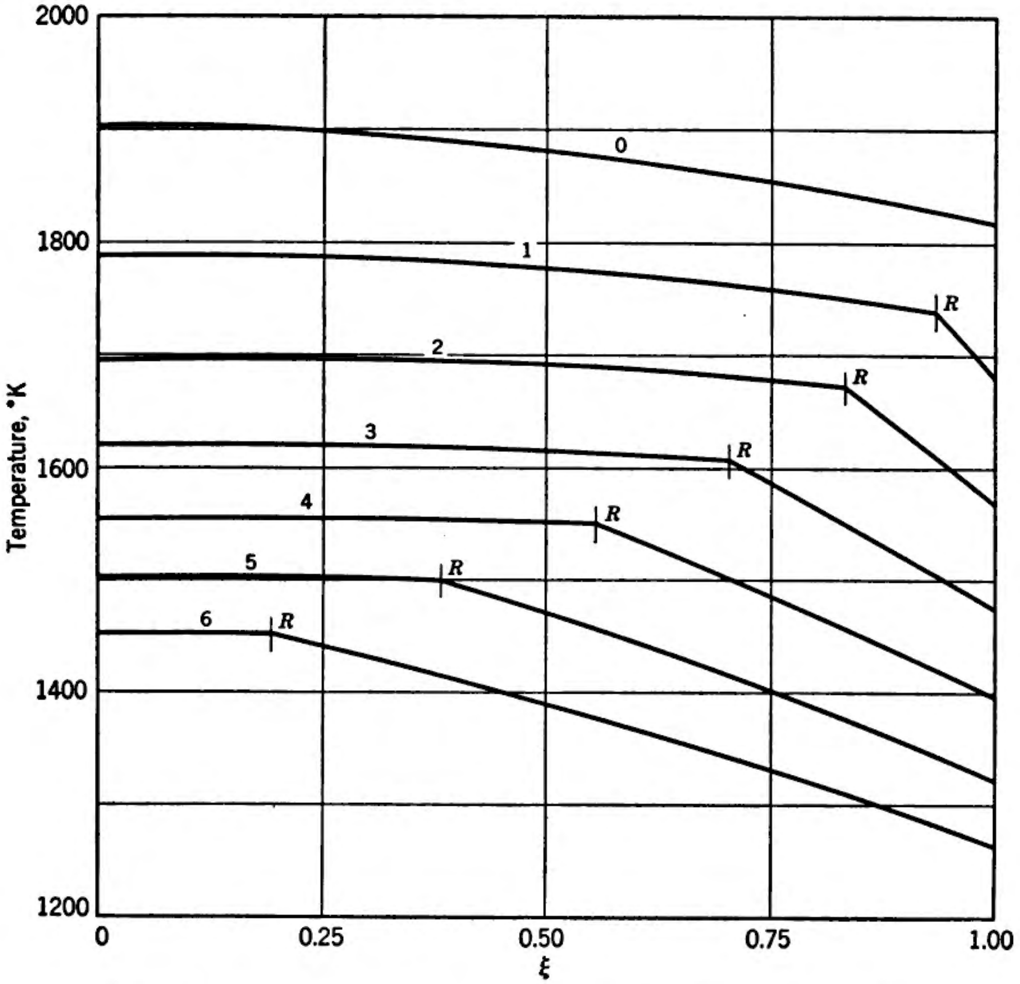

FIG. 9.8 Local gas temperatures at various times. Notation as in Fig. 9.7. Reproduced by permission of the Royal Society, London.

Figure 9.9 shows the local velocity of sound as a function of position and time. This was calculated from the density distribution. The gas velocities are also shown. To get the velocity at a point ξ in the rarefaction wave it is necessary to integrate equation 106 from the boundary Z to ξ. We do not give the rather complicated formulas here. The velocities computed in this way cross in a rather confusing way in Fig. 9.9; this behavior is due to the imperfections of our treatment of the rarefaction zone. The general trend is sufficiently clear, as is the fact that the gas velocity at the muzzle does indeed approach the local velocity of sound more closely as time goes on.

In theoretical prediction of muzzle-brake thrusts it is necessary to know the momentum of the gas entering the brake through the muzzle section. The momentum per second is $A\rho_2 v_2^2$. Table 9.2 shows the results of the present work (with $n = 0.6$), the "modified Rateau" theory with covolume, and the Hugoniot formulas. The first two theories dif-

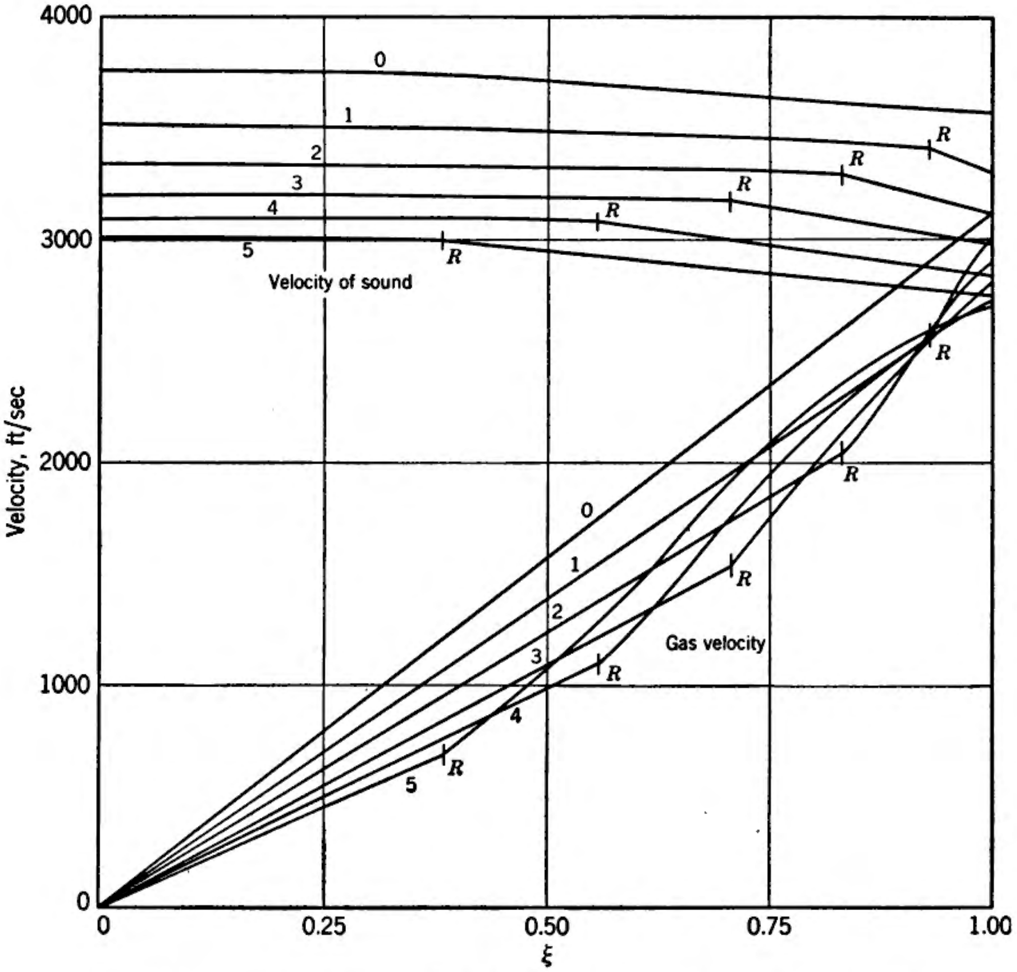

FIG. 9.9 Local velocities at various times. Notation as in Fig. 9.7. Reproduced by permission of the Royal Society, London.

TABLE 9.2 RATES OF OUTFLOW, BY VARIOUS THEORIES

Time from ejection, msec	0	1	2	3	4	5	6
$A\rho_2 v_2^2$, present theory, in tons wt	64.1	46.5	34.5	26.4	20.9	17.1	14.3
"Modified Rateau"	50.8	41.3	34.0	28.3	23.8	20.0	17.0
Hugoniot	38.3	33.0	28.5	24.6	21.4	18.6	15.8

fer by 25 per cent at the start and 20 per cent (in the opposite direction) after 6 msec. The significant measure of difference is, however, the total momentum of the gas crossing the muzzle section. This is only 1 per cent different in these two examples. The work of the present section applies only to the time before the rarefaction wave reaches the breech. We shall not attempt a theory of the conditions inside the gun at a later time. We may accept the modified Rateau formulas as applicable at all times to within the accuracy needed for calculation of muzzle-brake thrusts, which include rather uncertain corrections for friction loss in the brake itself.

It will appear when we discuss muzzle brakes in detail in the next section, that while the projectile is passing through the brake this is acting with higher efficiency than later. Therefore the total momentum produced by the muzzle brake will be rather more than 1 per cent different in these two instances. This initial period lasts about ¼ msec, in our example, and it is easy to show that the difference between the two theories cannot be more than 3 per cent for any likely design of brake. However, the stresses on the material are probably greatest in the period while the shot is passing through the brake, and, if calculations of strength are to be derived from the modified Rateau formulas, suitable corrections must be applied.

By omitting the covolume terms we pass from the Rateau to the Hugoniot formulas. The total momentum of the gas is about 15 per cent too small on this theory. This is an unfortunate failure, since the theory is much simpler than when covolume is included, and the simpler theory appears to be adequate for the calculation of breech pressures.

We must now consider case II. As the projectile passes the muzzle, the gas velocity just behind the shell is greater than the local velocity of sound. The solution inside the gun is determined by the initial conditions inside the gun only up to the time at which the gas velocity at the muzzle has fallen to the local velocity of sound. Until this time the solution of § 9.24 is valid everywhere inside the gun. From this solution we see that the gas velocity at the muzzle decreases much faster than the local velocity of sound, and so it is no long time before the rarefaction wave starts in from the muzzle. The conditions inside the rarefaction wave can be treated in the same approximate way as for case I. The only difference is that one can impose the rigid condition $c_2 = v_2$ for τ greater than τ_0, and, hence, by the analogues of equations 111 and 112, one can obtain a differential equation for ρ_2 (the density at the muzzle), which is a function of τ.

In case I we have a more qualitative condition to satisfy, which can best be examined by using a trial form for $\rho_2(\tau)$. In case II it is not so necessary to take a trial form for $\rho_2(\tau)$, but it is still a quick way to get a rough answer. The exact differential equation for ρ_2 is a complicated nonlinear type.

9.3 Muzzle brakes

The idea that a baffle just outside the muzzle should be used to provide a thrust to reduce the recoil momentum was first put forward in the 1880's by de Place. At that time the gun barrel was rigidly attached to the carriage, and the whole equipment had to be hauled back into position and aimed afresh after each round. However, the hydraulic buffer had already been invented by Siemens (1860) and had been used on a few fixed mountings, and the application of the hydraulic buffer to field guns accomplished completely what the muzzle brake could have done only in part.[28]

The idea of the muzzle brake was taken up again in the war of 1914–18, by the French. This time the aim was to reduce the work to be done by the recoil system. The development was not completed in time for service use, and, although various Continental firms, especially Schneider, tried to sell muzzle brakes in the period between the two world wars, they were never accepted as other than very special devices. Nevertheless, the idea was becoming more familiar.

World War II was marked by rapid and competing developments in tanks and antitank guns. The virtues of the muzzle brake are shown later to be greater at high muzzle velocities; the antitank gun is therefore a very suitable weapon to be fitted with a brake. The recoil system can be made lighter, and for equal stability and strength the fitting of a muzzle brake enables the carriage itself to be lightened. Typical antitank guns with efficient muzzle brakes have a muzzle energy about 20 per cent greater than equipments of equal weight but without muzzle brake. This is a striking advantage. The snag of the muzzle brake is its blast backward toward the gun crew, who must be protected by a shield. This is, however, already present on all antitank guns.

It is therefore not surprising that the muzzle brake was soon in service on German and Russian antitank guns (of the former, first on the 5-cm Pak 38). The German brakes included a few with only one baffle, but most were of the two-baffle form illustrated in Figs. 9.10 and 9.11. This is a workmanlike brake of medium-high efficiency, widely copied by other nations. On the other hand, after the collapse of Germany its artillery testing grounds were found to be littered with brakes of the most bizarre designs. Some of these may have been intended to perform in addition other functions such as flash suppression; it is clear that for good braking effect at any desired level of blast there is no need to depart from relatively simple designs.

---

[28] See Challeat, *Histoire technique de l'artillerie de terre en France*, vol. II (Paris, 1935), p. 135.

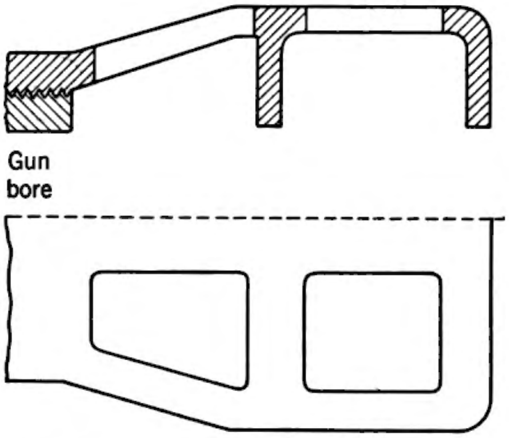

FIG. 9.10 Outer view and internal construction of a two-baffle muzzle brake. Reproduced by permission of the Royal Society, London.

The flow inside a muzzle brake has not been studied much from the theoretical side. The most interesting work known to the writer is that of Oswatitsch in Germany. He studied experimentally and theoretically (by the method of characteristics) the flow inside two- and three-dimensional brakes of simple form. The kind of question studied was, for example, where to place a single baffle of given area to produce most thrust. This work was tackled in other countries by experiments on model brakes.

For brakes of streamlined internal form one can obtain a good idea of the factors affecting the thrust of the brake by simple assumptions about the distribution of the flow. Before discussing this, we shall deal with the question of which guns are most suitable for muzzle brakes.

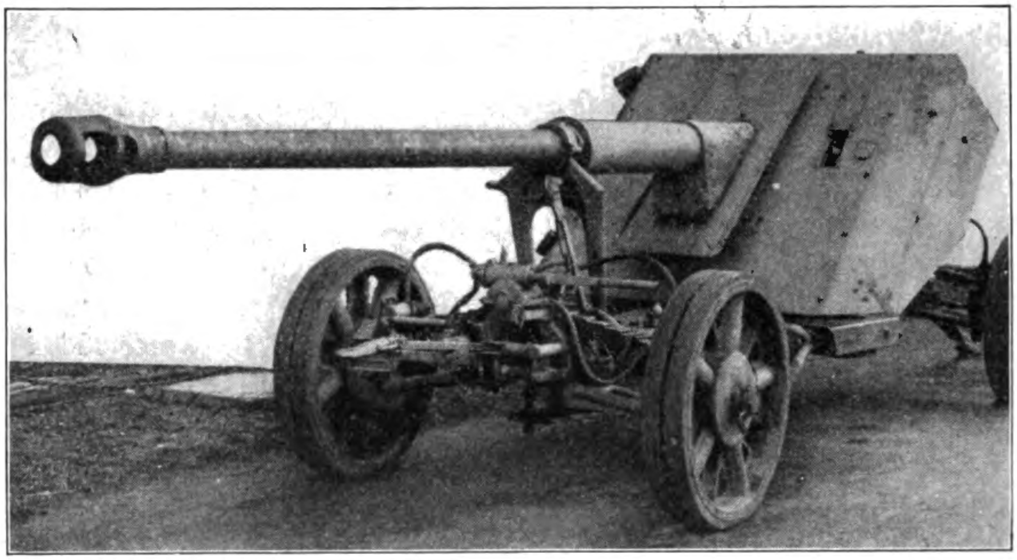

FIG. 9.11 A German two-baffle muzzle brake on the 8.8-cm Pak 43.

The greater the momentum supplied to a gun after shot ejection when there is no muzzle brake, the greater the braking momentum that can be supplied by a given muzzle brake. This suggests that a criterion for the suitability of a gun is the ratio

$$\frac{\text{Momentum from breech pressure after shot ejection}}{\text{Momentum from breech pressure up to shot ejection}}$$

both taken in the gun without brake. By the Hugoniot formulas of § 9.22 this ratio is proportional to

$$\frac{C(RT_e)^{1/2}}{(W + \frac{5}{12}C)V_0}$$

Let T_0 be the temperature of uncooled explosion of the propellant, at constant volume. Since T_e/T_0 is much the same for all guns, we may use as a simple criterion of suitability the quantity,

$$\beta = \frac{C(RT_0)^{1/2}}{(W + \frac{5}{12}C)V_0} \tag{114}$$

The larger β, the more effective will be a muzzle brake of given geometrical design—the larger, too, will be the blast. It should be noted that β is not a property of the gun alone but depends also on the weight and type of propellant used.

A point of some interest is the extent to which we can increase β by increase of C/W. Langweiler[29] has published muzzle velocities of a rifle with values of C/W from 0.86 to 44 and the same copper crusher pressure in all cases; actually the charge weight C was kept constant while the shot weight W was reduced to smaller and smaller values. In using such extreme values of C/W it must be remembered that the standard corrections for gas inertia are less correct than ever, though Langweiler's results show that the errors are not very large *in his case.* The error in Hugoniot's formula for the momentum after shot ejection is also known to increase with velocity. With these provisos in mind, it can be said that the criterion corresponding to β increases steadily with C/W, at constant crusher pressure.

9.31 The calculation of muzzle-brake thrusts

An accurate calculation would be a laborious business, which fortunately is hardly ever necessary. The essential points can be illustrated by a very simple treatment.

The flow through the brake is assumed to "run full" everywhere, which is usually a reasonable assumption. The first step is to draw streamlines (actually surfaces) separating the elements, which pass into

---

[29] Langweiler, *Z. tech. Physik,* **19** (1938), 416.

Digitized by Google Original from UNIVERSITY OF MICHIGAN

different channels of the brake. This division can usually be done in a plausible way by mere inspection of the brake section. The area available for the gas passing into each section of the brake is now known, being the area between streamlines until these merge with the walls of the brake. The gas may be imagined to be passing down a nozzle with an area varying in this way with distance down the axis. The smallest area is almost always at the muzzle section. This implies that the velocity of sound is attained there or sooner and that therefore the rate of outflow across the muzzle section is unaffected by the fitting of a muzzle brake.

For each channel, straightened out in this way, we can calculate the total thrust from Table 7.1, knowing (1) the ratio of the area at the exit to the area A_1 occupied by this section of the flow at the muzzle, and (2) the parameter ϵ, measuring the covolume effect, which may be derived from an estimate of the mean pressure in the gun during the important period of its emptying. Now we have pointed out in § 7.22 that the gun is not really the kind of reservoir that is implied in classical nozzle theory and that for the throat (that is, the muzzle) the thrust listed in Table 7.1 is too big. The thrust should really be $A_1 p_r$, where p_r is the breech pressure. However, the part of the thrust due to the nozzle downstream from the throat is correctly given by the difference of the corresponding entries in Table 7.1. This partial thrust is therefore

$$(\zeta_e - \zeta_1) A_1 p_r$$

where ζ_e and ζ_1 are the dimensionless thrust coefficients of Table 7.1, corresponding to the exit and the throat.

Let the mean angle of the flow from the brake channel considered be α measured from the axis of the bore. Then the total backward thrust on the gun due to the gas flowing in this channel is

$$(\zeta_e - \zeta_1 + 1) A_1 p_r \cos \alpha$$

and, by summing over all the channels, the total thrust is

$$A p_r \Sigma (\zeta_e - \zeta_1 + 1) \left(\frac{A_1}{A}\right) \cos \alpha$$

where A is the bore area. We have shown in § 9.22 that Hugoniot's formula gives

$$A \int_0^\infty p_r \, dt = 1.35 C (R T_e)^{1/2} \left(1 + \frac{C}{12W}\right) \tag{115}$$

Rateau's formula, which would be more accurate, does not appear to be integrable in a simple form.

The fitting of the muzzle brake reduces the postejection momentum to the fraction 1 − B, where

$$B = 1 - \Sigma(\zeta_e - \zeta_1 + 1)\left(\frac{A_1}{A}\right)\cos\alpha \tag{116}$$

The "momentum index" B may be negative; for example, an axial venturi attached to the muzzle has $\zeta_e > \zeta_1$, $A_1 = A$, $\alpha = 0$, and so B is negative. This occurs in practice with the flash hiders fitted on some small-caliber weapons. The true muzzle brake has B positive, but it is possible to find brakes with B less than unity; that is, there may still be some resultant backward thrust after shot ejection. For brakes of medium efficiency B is rather greater than unity, running up to over 1.6 for practical brakes.

B is a function of the shape of the brake, but not of its scale, except insofar as this affects the frictional losses. This slight dependence on the Reynolds number of the flow is not likely to matter in going from one gun to another. The effect may be more noticeable in extrapolating from model tests in rifle caliber.

B also depends slightly on the value of γ for the propellant gases, and to a slight extent on the pressure at shot ejection. Otherwise B is independent of the charge.

Suppose we now write down the total recoil momentum given to the gun, using equation 115 for the postejection term in a gun without muzzle brake. The result when there is a brake is

$$(W + \tfrac{1}{2}C)V_0 + 1.35(1 - B)C(RT_e)^{1/2} \tag{117}$$

where the notation is the same as in earlier sections. If we use this to analyze recoil experiments, finding B from the observed momentum, then B will *not* be completely independent of the charge. For the simple formula 115 is wrong by different amounts at different velocities, and the apparent value of B alters slowly with velocity. This difficulty can be eliminated by finding the postejection recoil momentum by control firings in the same gun without a muzzle brake.

9.32 The "efficiency" of a muzzle brake

There are two distinct processes in the development of muzzle brakes. In the first, one tries to assess the relative merits of various brakes, which are usually tested on a single standard type of gun. Now the recoil momentum is altered by the mere weight of a brake, even if the latter gives no thrust at all. We need, therefore, some figure of merit which will separate this effect.

In the second stage one picks the most suitable brake for various equipments. This will involve questions of blast, reduction of momentum, and possibly other factors. Once the design is chosen, it is necessary to predict its performance on the new equipment, which in ballistics and carriage design may be quite different from the standard gun used for brake testing.

It is clear that the "efficiency" of a brake has two applications: in the first stage it is used as a figure of merit; in the second as a device to predict performance. The properties required in these cases will now be listed.

In the first stage these are:

1. The efficiency should be independent of the weight of the brake, for various designs differ considerably in this respect.

2. It should be easy to deduce the efficiency from measurements of recoil velocity and trunnion pull, and in particular there can be no objection if we need a firing in a gun without a brake.

In the second stage we have:

(*a*) The efficiency should be independent of the weight of the recoiling parts.

(*b*) The efficiency should not refer to any particular gun, charge, projectile, recuperator, or buffer.

(*c*) The efficiency should depend on the shape of the brake but not on its scale.

(*d*) It should be easy to use the "efficiency" in a recoil calculation.

Points *a*, *b*, and *c* are obviously essential if we are to use the efficiency for prediction of performance. Point *d* is necessary if our definition is to be adopted by carriage designers. Although we ask that the efficiency shall be easy to use, we do not stipulate that it must be easy to derive from experiment. The reason is that the property *c* assures us that only a relatively small number of efficiencies will have to be worked out.

Let the work done by the action of the gas on a gun without a muzzle brake be S_0, and that in the same gun modified only by the addition of a muzzle brake be S_B. Let the weight of the recoiling parts of the ordinary gun be W_0, and let the weight of the brake be W_B.

In his unpublished work on muzzle brakes, Goode has defined the "gross efficiency" of the brake as $1 - (S_B/S_0)$ and the "intrinsic efficiency" as $1 - \left(\frac{W_0 + W_B}{W_0}\right)\frac{S_B}{S_0}$. He has shown that the latter is independent of W_B, provided that the gas action is of short duration compared with the trunnion pull. Trial computations have shown that even when this assumption is badly violated the variation of intrinsic efficiency with W_B is of the order of 0.1 per cent and therefore negligible.

The "intrinsic efficiency" satisfies conditions 1 and 2 and is therefore well adapted to serve as a figure of merit for muzzle brakes, provided, of course, that all the efficiencies have been measured on the same gun and mounting and with the same charge.

The "intrinsic efficiency" satisfies *a*, but not *b*, for variations of more than 5 per cent can occur when the same brake is fired with different charges giving nearly the same muzzle velocity; variations by a factor of two can be caused by substantial changes of velocity. Point *c* is probably obeyed fairly well. With regard to *d*, the intrinsic efficiency is convenient for only some of the calculations that arise in carriage design.

It is natural to ask whether the "momentum index" *B*, introduced in the previous section, is a good measure of muzzle brake efficiency. From Hugoniot's theory, *B* satisfies all four conditions *a* to *d*, except for a trivial dependence on the γ of the propellant gases and the muzzle pressure. The error in this theory depends on the muzzle pressure and the muzzle velocity. Although the remarks of § 9.25 show that the error of Hugoniot's theory is not large for a typical antitank gun firing at 3000 ft/sec, still it is evident from experiment that the error changes fairly rapidly with velocity in this region. Thus, if *B* is deduced from firings by using the formula 117, *B* will satisfy *a*, *c*, and *d*, but not *b* completely. For a criterion of efficiency in the second stage of brake design, *B* is nevertheless rather better than the "intrinsic efficiency." Of course, if equation 117 is replaced by a more accurate formula, the *B* deduced will depend less on velocity. It is not possible to write *B* in terms of the momentum given to guns with and without muzzle brake, since in the second stage much of the work is concerned with projected guns for which neither momentum is known from experiment. Some formula has to be used for prediction, and for consistency it ought to be used throughout.

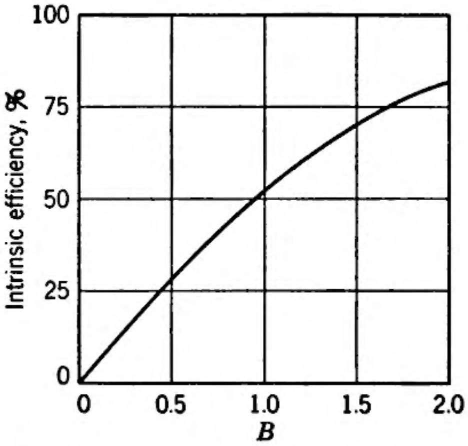

FIG. 9.12 Approximate relation between *B* and intrinsic efficiency. British Crown copyright reserved.

Although there is no exact relation between *B* and the intrinsic efficiency, it is useful to have a rough correlation. This can be taken from Fig. 9.12, which is roughly correct for velocities around 3000 ft/sec. To illustrate that this curve must not be applied except to normal guns and for this order of velocity, we shall now discuss whether the recoil velocity of a gun could be canceled by using a muzzle brake. It will appear that this is indeed possible for large but practical values of B, say, $B = 1.6$. This implies an intrinsic efficiency close to 100 per cent, instead of the value of 75 per cent shown by Fig. 9.12 to apply to normal guns. The reason is that a gun that could be made recoilless by using a brake of $B = 1.6$ would have to be of most abnormal dimensions, as we shall see.

Let the charge weight be C, shot weight W, muzzle velocity V, and "force" of the propellant RT_0. Let T_e be the mean temperature of the gas in the gun when the shot leaves. The conservation of energy gives

$$\frac{C}{\bar{\gamma} - 1}(RT_0 - RT_e) = \frac{1}{2}\left(W + \frac{1}{3}C\right)V^2$$

where we have neglected the work done against bore resistance. Write $T_e' = T_e/T_0$, so that

$$T_e' = 1 - \frac{1}{2}(\bar{\gamma} - 1)\left(\frac{W}{C} + \frac{1}{3}\right)\frac{V^2}{RT_0} \tag{118}$$

The Lagrange correction in equation 118 is the conventional approximation for small C/W, whereas in our calculations C/W will go up to values of the order of 5. However, the disadvantages revealed by our results are much bigger than any changes that might be made by more accurate Lagrange corrections.

We consider now the recoil forces. Up to shot ejection the gun acquires a momentum $(W + \frac{1}{2}C)V$, and later the breech pressure supplies a backward momentum $1.35C(RT_e)^{1/2}$ (§ 9.22), while the muzzle brake provides a forward momentum B times as great. For zero recoil momentum at the end of gas action,

$$(W + \tfrac{1}{2}C)V = 1.35(B - 1)C(RT_e)^{1/2}$$

that is,

$$\left(\frac{W}{C} + \frac{1}{2}\right)\frac{V}{(RT_0)^{1/2}} \doteq 1.35(B - 1)(T_e')^{1/2} \tag{119}$$

The solution of equations 118 and 119 has been computed for $B = 1.6$ and 1.8, with $V/(RT_0)^{1/2}$ up to 1.6; for normal propellants this corresponds to velocities up to 5000 ft/sec. The values of $B = 1.6$ and 1.8 would give, on normal antitank guns, intrinsic efficiencies of about 73 and 78 per cent. The lower value is attained on several existing brakes. $B = 1.8$ is probably the upper limit for brakes of practical weight and blast.

The results are shown in Figs. 9.13 and 9.14, which give C/W and the temperature of the gases at shot ejection, respectively. From the first of these diagrams it is clear that even a small increase in the efficiency of the muzzle brake reduces considerably the charge needed to cancel the recoil. The charge for an orthodox gun, shown on the same diagram, was calculated by assuming a ballistic efficiency of one third.

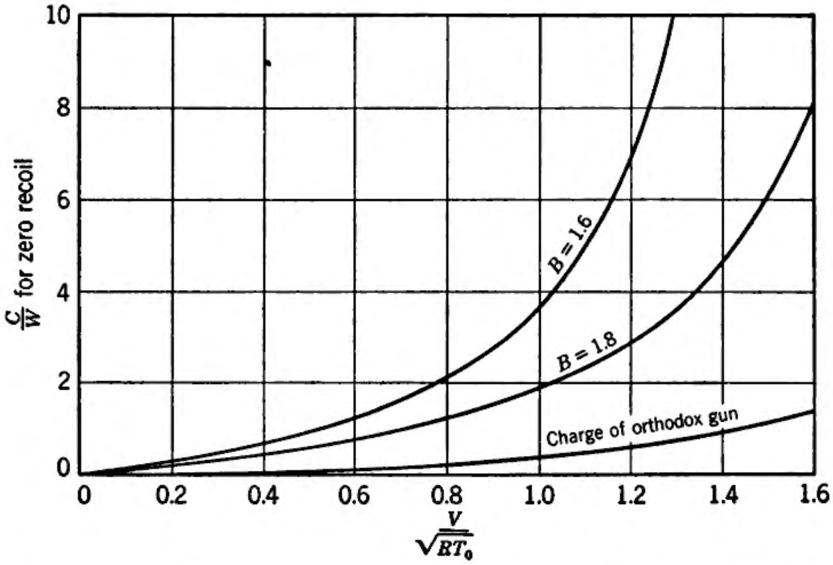

FIG. 9.13 Charges to produce recoillessness in guns with muzzle brakes. British Crown copyright reserved.

On Fig. 9.14 we show the ejection temperature for $B = 1.8$. It can be seen that the ballistic solution must be very different from that of an

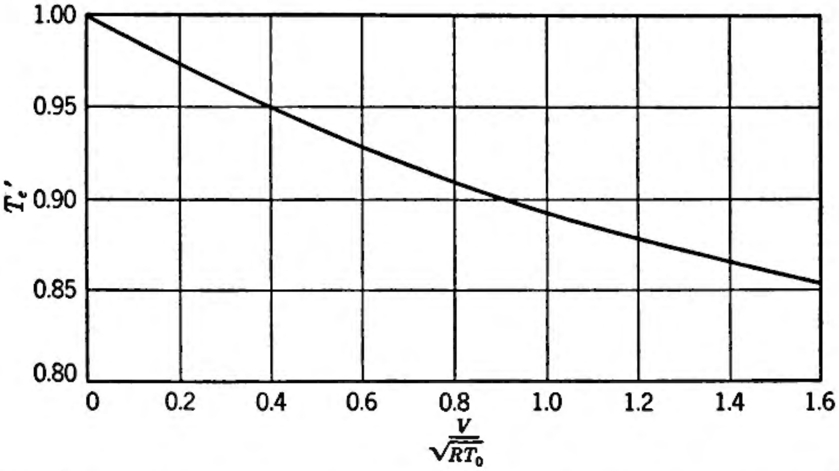

FIG. 9.14 Temperature at shot ejection in guns made recoilless by a muzzle brake with $B = 1.8$.
British Crown copyright reserved.

orthodox gun, which would have T_e' of 0.7 or less. The gun made recoilless by a muzzle brake has a very small ballistic efficiency; that is, the charge has to be increased several-fold over what would suffice to give the muzzle energy required. This increase is necessary to provide sufficient thrust from the brake. The large charge needs an enlarged chamber and therefore a heavier piece.

As the velocity rises, it becomes necessary to provide a greatly increased charge, until for $V/(RT_0)^{1/2}$ beyond about two (for $B = 1.8$) it is no longer possible to obtain recoillessness. This limiting velocity increases with B.

Thus it is possible to secure recoillessness with an efficient brake at all practical velocities, but the charge weights required are high, and this leads to many disadvantages. If the brake is used with a normal charge, to give partial reduction of recoil, the advantage gained increases continuously with velocity, within the practical range.

9.4 Conditions ahead of the shot

These conditions have some importance in practice. Without going into technical details, some applications may be cited. First, the shock wave and the blast of hot gas, which precede the projectile, are important when gun flash is to be separated into components and causes. Second, the behavior of various mechanical devices, which have at times been attached to gun muzzles, requires a rather similar knowledge.

Tapered-bore guns have been discussed in the preceding chapter. The swaging down of the flanges on the projectile reduces the volume enclosed by the two flanges and the body of the projectile, and any air or gas that may be trapped there is compressed. In many guns of this type the initial pressure of the trapped gas is the same as the air pressure in front of the shot at the time the latter enters the taper. The multiplication by adiabatic compression is considerable, and if not tapped off in some way the pressure will stretch open any press fits in the construction of the projectile and will balloon the front band at the moment of ejection. Steps are in fact taken to vent these gas traps, and for rational design one must know the theoretical air pressures in front of the shot.

Apart from these practical applications, the problem is interesting as a standard case in the one-dimensional flow of a compressible gas. Imagine the projectile to be given an arbitrary motion down the barrel. A complex pressure wave will set out from the shot, with a front of rising pressure, which is unstable and after a certain time becomes a discontinuity of pressure—that is, a shock wave. The history of this shock depends on the whole form of the motion of the shot. Suppose, for example, that the shot is brought to rest again. A rarefaction spreads out into the gas, overtaking and eating up the shock wave. The final state is a degenerate low-amplitude shock, in fact a sound wave, traveling out through air, which is otherwise at rest. If, on the other hand, the projectile is kept at high velocity, the shock wave will be maintained or strengthened. We can expect, therefore, the shot to be preceded by a strong shock wave if the shot velocity is greater than the velocity of sound for a substantial part of the travel, though it should be emphasized that, when moving along a gun-barrel, quite a noticeable shock wave can be set up without the projectile ever reaching the velocity of sound. For motion in the open air the results are considerably different.

9.41 Steady motion

For an introduction to the subject it is helpful to consider a shot moving along a tube at a constant velocity V. The treatment is due to Hugoniot.[30] The notation is illustrated in Fig. 9.15. The conditions before the arrival of the shock wave are p_0, ρ_0, T_0, and zero velocity. The shock front moves with velocity D, say, and immediately behind it the conditions are p_1, ρ_1, T_1, and material velocity V_1. At the head of the shot the velocities of gas and shot are equal, say, V, and the pressure, density, and temperature are p, ρ, and T.

Give the whole system a velocity V to the left. The shot is at rest in this system of coordinates. The shock wave travels at velocity $D - V$ into air coming at velocity V toward the shot. After the shock the gas velocity is $V - V_1$, reducing by adiabatic compression to zero at the head of the projectile.

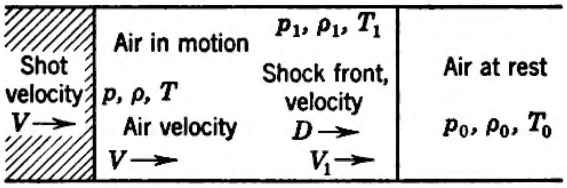
Shot velocity $V \rightarrow$
Air in motion
p, ρ, T
Air velocity $V \rightarrow$
p_1, ρ_1, T_1
Shock front, velocity $D \rightarrow$
$V_1 \rightarrow$
Air at rest
p_0, ρ_0, T_0

FIG. 9.15 Notation for flow ahead of a shot in a tube.

Rayleigh[31] was interested in the resistance to a projectile in free air. In this case the argument applies only to a streamline along the axis of the shot, and obviously D must be taken equal to V; otherwise, the shot and its associated shock wave would eventually part company. Then, from equations 62 and 66 of § 9.15,

$$\frac{p_1}{p_0} = \frac{2}{\gamma + 1}\frac{V^2}{RT_0} - \frac{\gamma - 1}{\gamma + 1} \tag{120}$$

and

$$\frac{\rho_1}{\rho_0} = \frac{(\gamma + 1)V^2}{(\gamma - 1)V^2 + 2\gamma RT_0} \tag{121}$$

---

[30] Hugoniot, *J. école polytech.*, **57** (1887), 3; **58** (1889), 1.

[31] Rayleigh, *Proc. Roy. Soc. (London)*, **84A** (1910), 247.

with, of course,

$$\frac{p_1}{\rho_1 T_1} = \frac{p_0}{\rho_0 T_0}$$

The compression from p_1, ρ_1, T_1 to p, ρ, T is adiabatic, and reduces the velocity from $V\rho_1/\rho_0$ to zero. From the equation of energy for the compression,

$$\frac{\gamma R}{\gamma - 1}(T_2 - T_1) = \frac{V^2 \rho_1{}^2}{2\rho_0{}^2}$$

and with the help of equations 120 and 121 one can obtain the convenient form:

$$\frac{T_2}{T_1} = \left(\frac{p_2}{p_1}\right)^{(\gamma-1)/\gamma} = \frac{(\gamma+1)^2}{4\gamma}\left[1 + \left(\frac{\gamma-1}{\gamma+1}\right)\frac{p_0}{p_1}\right] \tag{122}$$

All this applies only to the conditions just ahead of a projectile in free air. When the shot is in the bore, the air cannot escape sideways, and in the steady state the shock wave must be such as to reduce the velocity of the air to the velocity of the shot, that is, to zero in the present coordinates.

From equation 63 of § 9.15, together with equation 66, we find

$$\frac{p_1}{p_0} = 1 + \frac{(\gamma+1)V^2}{4RT_0} + \frac{V}{(RT_0)^{1/2}}\left[\gamma + \frac{(\gamma+1)^2 V^2}{16RT_0}\right]^{1/2} \tag{123}$$

and the density can be calculated from

$$\frac{\rho_1}{\rho_0} = \frac{(\gamma+1)p_1 + (\gamma-1)p_0}{(\gamma+1)p_0 + (\gamma-1)p_1} \tag{124}$$

while the shock velocity relative to the barrel is given by

$$D^2 = \frac{1}{2}RT_0\left[(\gamma+1)\frac{p_1}{p_0} + \gamma - 1\right] \tag{125}$$

and its velocity relative to the shot is $D - V$. This is positive; the zone of compressed air in front of the projectile becomes longer as time goes on.

The results of equations 123 to 125 are due to Hugoniot and are markedly different from those of equations 120 to 122. For example, take a projectile moving at 2600 ft/sec, in air of normal density and temperature: say 1 atm and 288°K, for which RT_0 would be roughly $(1120)^2/1.41$ (ft/sec)^2. Because of the heating in the shock wave the appropriate γ is rather less than 1.41, and should be rather different in the two cases. However, this has only a small effect on the difference between the two results. For simplicity we take $\gamma = 1.38$ in both cases. Then we arrive at the results of Table 9.3. The differences can well be

TABLE 9.3 CONDITIONS AHEAD OF A PROJECTILE WITH STEADY VELOCITY 2600 FT/SEC

$P_1 = 1$ atm; $T_1 = 288°$K

	In Free Air	In Gun Barrel
Pressure behind shock	6.23 atm	11.08 atm
Pressure at shot	7.50 atm	11.08 atm
Temperature behind shock	560°K	786°K
Temperature at shot	589°K	786°K
Velocity of shock	2600 ft/sec	3450 ft/sec

described as striking. It is easy to show that at very high velocities the divergence becomes small, whereas it is relatively more marked at low velocities. At the velocity of sound the head pressures differ by a factor of two. At lower velocities equation 120 is not applicable, since then no shock wave is formed; equation 122 then fails, and the pressure rise is only $\rho_0 V^2/2$. On the other hand, equations 123 to 125 are valid right down to zero velocity. The reason for these differences is that it is not possible to have a shock velocity less than the velocity of sound; when the projectile is enclosed in a barrel, however, the important quantity is the material velocity behind a shock wave, and this velocity can go right down to zero.

9.42 Riemann's method for the solution of the hydrodynamic equations

This discussion is restricted to the one-dimensional case. Extensions to two and three dimensions have been made lately in unpublished work. Let x be the co-ordinate, and v, p, and ρ the velocity, pressure, and density of the gas at position x at time t. The Eulerian equations of hydrodynamics are:

$$\frac{\partial v}{\partial t} + v\frac{\partial v}{\partial x} = -\frac{1}{\rho}\frac{\partial p}{\partial x} \tag{126}$$

and

$$\frac{\partial \rho}{\partial t} + v\frac{\partial \rho}{\partial x} = -\rho\frac{\partial v}{\partial x} \tag{127}$$

It is assumed that p is uniquely determined by ρ. This covers adiabatic changes but not shock waves, for there the transition through the shock front is accompanied by a shift from one adiabatic to another. The method to be described is therefore valid up to a shock but not across it.

If shock waves are present, it is usually possible to use Riemann's method in all the intervening regions, fitting together the solutions by appropriate shocks.

Write the local velocity of sound as c,

$$c = \left(\frac{dp}{d\rho}\right)^{1/2}$$

and define

$$\omega = \int c \frac{d\rho}{\rho} \tag{128}$$

where the lower limit is a constant, chosen for convenience. ω is a velocity. Then equations 126 and 127 can be written as

$$\left[\frac{\partial}{\partial t} + (v + c)\frac{\partial}{\partial x}\right](\omega + v) = 0$$

$$\left[\frac{\partial}{\partial t} + (v - c)\frac{\partial}{\partial x}\right](\omega - v) = 0$$

that is, $\omega + v$ is constant at a point moving with velocity $v + c$, whereas $\omega - v$ is constant at a point moving with velocity $v - c$. The curves

$$\frac{dx}{dt} = v \pm c \tag{129}$$

along which

$$d\omega \pm dv = 0 \tag{130}$$

are the "characteristics" of the original partial-differential equations. By integrating along these curves, finding their direction as we proceed, the solution can be built up from the boundaries where $v + c$ or $v - c$ are known.

If

$$p = \alpha\rho^{\gamma}$$

then

$$\omega = \frac{2c}{\gamma - 1} + \text{constant} \tag{131}$$

An important special case occurs when a rarefaction wave passes into gas originally at rest in a uniform state. Suppose that the wave is passing toward negative x. Then values of $\omega + v$ are being propagated backward into the wave with velocity $v - c$. But at $t = 0$, $v = 0$ everywhere, and ω is the same everywhere. Hence at points in the wave,

$$v = \omega(t = 0) - \omega = \frac{2}{\gamma - 1}(c_0 - c)$$

$$= \frac{2(\gamma R T_0)^{1/2}}{\gamma - 1}\left[1 - \left(\frac{\rho}{\rho_0}\right)^{(\gamma-1)/2}\right] \tag{132}$$

a relation already used in § 9.16.

Integration along characteristics is a useful method for obtaining numerical solutions and is applicable to other partial-differential equations with real characteristics, that is, equations of "hyperbolic type." The mathematical theory of characteristics is a wide subject, covered for example, in Goursat, *Cours d'Analyse*, volume 3. The numerical method can be applied without study of its deeper meaning.

9.43 Accelerated motion

We are now ready to consider the building up of air pressure in front of an accelerating shot. Riemann's method has been applied by Hugoniot [32] to the case of constant acceleration, among others, giving an analytical solution up to the time at which the first discontinuity of pressure appears in the field. This method is equally applicable to other acceleration-time relations with moderately simple analytical expressions. After the appearance of the shock an analytical solution is more difficult. Until recently all that had been obtained in this zone was a numerical solution; this being so, it was reasonable to use a numerical acceleration-time curve for the shot. A solution of this class has been obtained by Schardin.[33] Recently an analytical solution for the early stages of the motion after a shock has developed has been published by Pillow.[34]

In this section we shall give the solution for constant acceleration, to show how the shock first appears ahead of the shot. The later development of the shock will be sketched from Schardin's example.

Let the projectile move from left to right, with velocity $V(t)$, and let the velocity of the gas be $v(x, t)$. The position of the shot at time t is written as $X(t)$. The (x, t) plane is useful in visualizing the solution (Fig. 9.16). At time $t = 0$, $v = 0$ and c is a constant c_0 everywhere. ω is a constant too and may be taken equal to zero. The characteristics (α, of Fig. 9.16)

$$\frac{dx}{dt} = v - c \tag{133}$$

---

[32] Hugoniot, *J. école polytech.*, **58** (1889), 1.

[33] Schardin, *Jahrb. deut. Akad. LFF*, **1940/41**.

[34] Pillow, *Proc. Cambridge Phil. Soc.*, **45** (1949), 558.

carry the constant values of $\omega - c$ from the x axis into the region of positive t. But $\omega - v$ is zero everywhere on the x axis. Hence $\omega - v$ is zero at every point in the (x, t) plane that can be reached from the x axis by proceeding along a curve of type 133 without passing through a shock wave; therefore

$$v = \omega = \int_{\rho_0}^{\rho} \left(\frac{dp}{d\rho}\right)^{1/2} \frac{d\rho}{\rho} \qquad (134)$$

Along

$$\frac{dx}{dt} = v + c$$

(curves β in Fig. 9.16), $\omega + v$ is constant, and hence, from equation 133, v and ω are each constant. The velocity along a characteristic of type β is therefore equal to the shot velocity at the time τ at which β intersects the travel-time curve of the projectile. The equation of such a characteristic is

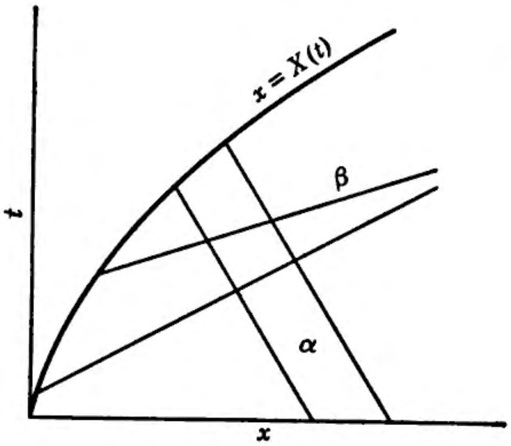

FIG. 9.16 Position-time curve of the projectile and the characteristics of the gas-flow field.

$$x - X(\tau) = (t - \tau)[V(\tau) + c(\tau)] \qquad (135)$$

and, along it,

$$v = V(\tau) \qquad (136)$$

and so, from equations 131 and 134, also

$$c(\tau) - c_0 = \tfrac{1}{2}(\gamma - 1)V(\tau) \qquad (137)$$

We have now a solution for each point of the (x, t) plane ahead of the shot. Each point lies on some characteristic (equation 135), and the appropriate value of τ gives the local gas velocity and density from equations 136 and 137.

The appearance of a shock wave is shown in this method by the crossing of a pair of characteristics of type β. This means that two values of pressure are possible at the same point; in other words, the solution is no longer valid. Physically a discontinuity of pressure has formed, and the assumption of adiabatic flow has broken down. The first infinitesimally small discontinuity appears when two characteristics first touch. This point is obtained by differentiating equation 135 with respect to τ and solving with the use of equation 135. The differentiated equation is

$$c(\tau) = \frac{1}{2}(\gamma + 1)(t - \tau)\frac{dV}{d\tau} \tag{138}$$

and the envelope of the characteristics (equation 135) is

$$x = X(\tau) + \frac{2[V(\tau) + c(\tau)]c(\tau)}{(\gamma + 1)\dfrac{dV}{d\tau}} \tag{139}$$

$$t = \tau + \frac{2c(\tau)}{(\gamma + 1)\dfrac{dV}{d\tau}} \tag{140}$$

We wish to find the first value of t on this curve. This does not always correspond to $\tau = 0$. Suppose the projectile has a constant acceleration a. Then,

$$V(\tau) = a\tau$$

and

$$t = \tau + \frac{2[c_0 + \frac{1}{2}(\gamma - 1)a\tau]}{(\gamma + 1)a}$$

whose minimum occurs at $\tau = 0$, giving

$$t = \frac{2c_0}{(\gamma + 1)a} \tag{141}$$

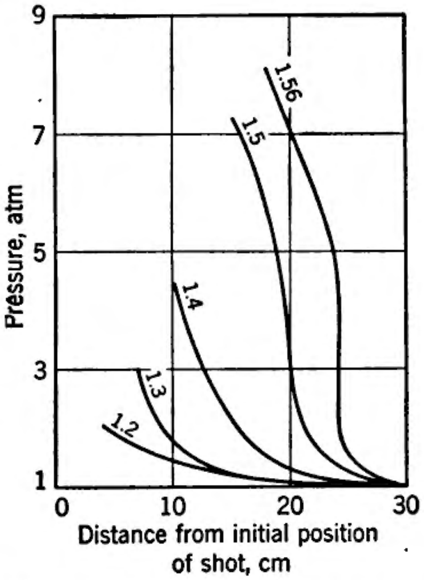

FIG. 9.17 Development of a shock wave ahead of an accelerated projectile, in an example typical of small arms. The numbers on the curves gives the time in milliseconds.

The first trace of discontinuity occurs, therefore, at the front of the pressure wave in this case, at a time given by equation 141 and a position

$$x = \frac{2c_0^2}{(\gamma + 1)a} \tag{142}$$

If the shot has retained its constant acceleration until the shock appears, the velocity of the shot is then $2c_0/(\gamma + 1)$. This velocity has nevertheless no particular significance. There is indeed no reason why the acceleration should remain constant; the shot could settle down to any constant speed without altering the time at which the first discontinuity appears. The later history of the wave does, of course, depend on the whole velocity-time curve of the projectile.

Figure 9.17 (after Schardin) shows a typical set of pressure-distance relations for the motion in front of a rifle bullet, up to the first appearance of a shock. The discontinuity in this case first appears some distance behind the front of the wave. This is connected with the fact that in this instance the acceleration at first increases with time (see also example 12 at the end of this chapter). The discontinuity occurs 7 calibers in front of the head of the shot, when the latter has moved about 25 calibers.

Once the discontinuity appears, the integration along the characteristics has to be carried out numerically. The position and strength of the shock are found as one goes along, by adjusting to give the correct velocity all along the shot travel curve.

In Schardin's example the shock reached the muzzle about 10 calibers in front of the head of the projectile. In this example the muzzle velocity was about 2500 ft/sec.

9.5 The motion of propellant in a gun

When the propellant burns slowly, its distribution between breech and shot base is a matter of some importance in Lagrange's problem. It is almost always assumed that the propellant moves with the gas, so that the local density of unburnt propellant is proportional to the local gas density; the ratio decreases as time goes on. This assumption is plausible and has the merit of helping the solution. Nevertheless, this is not the most accurate of the simple assumptions that one might make. The analysis of the motion of the propellant is not easy, if an exact solution is called for; however, we can very quickly reach significant results, if we ask for an *upper limit* to the motion.

The movement of the burning propellant is important for another reason too. The rate of burning of propellant increases when there is a transverse blast across it, as pointed out in § 2.4. If the propellant moves with the gas in a gun, there is no relative velocity. If the propellant remains stationary, the relative velocity attains, by the end of burning, a value that is sufficient to increase considerably the rate of burning. By finding an upper limit to the motion of the propellant, we find a lower limit to the erosion effect.

Since we seek only an upper limit, we may omit the mutual tangling of the pieces of propellant and the impedance caused by the walls of the gun. We take also the conventional Lagrange distribution of pressure, modified by using an effective charge $C\phi(t)$, the amount present as gas, in place of the total charge; that this is a reasonable estimate during most of the period of burning has been confirmed by recent experimental work.

We have also probably overestimated the drag forces on the propellant. These forces are important near the end of burning. We have taken the drag to be the same as that on a solid body of the same size as the propellant stick at the instant considered. It seems probable that the emission of gas from the propellant would reduce the drag. This is a problem that could probably be treated from existing knowledge on aerodynamics, but such a refinement is not necessary here.

(*a*) *Cord propellant.* Let t be time and x the co-ordinate down the barrel, measured from the breech. Let $p(x, t)$ be the gas pressure, $\rho(x, t)$ its density, and $v(x, t)$ its velocity. Let $V(t)$ and $X(t)$ be the shot velocity and position, respectively. Let C and W be the masses of charge and shot. We take $\phi(t)$ as the fraction burnt and $r(t)$ as the radius of the cord. The density of the propellant is denoted by δ and the length of the stick by L.

We shall discuss later the effects produced by using propellant shapes other than cord.

For simplicity we assume that the chamber has the same cross-sectional area A as the bore. We assume also that the stick remains parallel to the axis of the bore. Let $y(t)$ be the position of the center of the propellant stick at time t.

The resultant force on a stick due to the pressures on its ends is

$$F_1 = \pi r^2 \left[L \left(\frac{\partial p}{\partial x} \right)_y + O\left(L^3 \frac{\partial^3 p}{\partial x^3} \right) \right]$$

for the mean pressure on an end lies between p and $p + \frac{1}{2}\rho V^2$; the former limit gives F_1 and the other gives a smaller accelerating force. We shall use the form,

$$p = \alpha(t) - x^2 \beta(t)$$

so that

$$F_1 = \pi r^2 L \left(\frac{\partial p}{\partial x} \right)_y \tag{143}$$

We write μ for the viscosity of the propellant gases. Let R_z be the Reynolds number at a distance z from the upstream end of the propellant. In a stream of uniform velocity the appropriate Reynolds number is that for flow over a flat plate parallel to a stream, namely:

$$\begin{aligned} R_z &= \frac{(\text{relative velocity of gas})\ \rho z}{\mu} \\ &= \frac{\rho z}{\mu} \left(v - \frac{dy}{dt} \right) \end{aligned} \tag{144}$$

In our problem the relative velocity is itself a function of z, though the variation with z is relatively slow, and our formulas cannot be more than approximately correct.

For propellant products, μ is about 6×10^{-4} g/c sec.

The surface drag on a ring, width dz, of the surface of the stick is

$$\rho(z, t)\pi r\left(v(z) - \frac{dy}{dt}\right)^2 C_f(R_z)\, dz \tag{145}$$

where [35]

$$\left.\begin{aligned} C_f &= 1.328R_z^{-1/2} \quad \text{for } R_z < 3 \times 10^5 \\ C_f &= 0.455(\log_{10} R_z)^{-2.58} \quad \text{for } R_z > 3 \times 10^5 \end{aligned}\right\} \tag{146}$$

The density $\rho(z, t)$ may be replaced by the mean throughout the volume behind the shot, since the density varies relatively little along the bore. This mean is

$$\rho(t) = \frac{C\phi(t)}{AX - \dfrac{C(1 - \phi)}{\delta}} \tag{147}$$

We have to integrate equation 145 along the length of the cord, from $z = 0$ to L. For a cord of full chamber length a reasonable approximation is obtained by calculating a mean C_f from the Reynolds number at $z = 0.7L$ and using this C_f in the integration of equation 145. It follows that the total surface drag is

$$F_2 = \rho(t)\pi\, r\, \bar{C}_f \left[\frac{1}{3}\left(\frac{LV}{X}\right)^2 - \frac{LV}{X}\zeta + \zeta^2\right] \tag{148}$$

where

$$\zeta = \frac{dy}{dt} - (y - 0.5L)\frac{V}{X} \tag{149}$$

Also,

$$\bar{C}_f = C_f(\bar{R})$$

with

$$\bar{R} = \frac{\rho}{\mu}\left(y\frac{V}{X} + 0.2\frac{LV}{X} - \frac{dy}{dt}\right) \tag{150}$$

This gives the total acceleration with errors of the order of 2 per cent, which is better than the real accuracy of our physical model. In deriving equation 148 we have made the conventional assumption that

$$v(y) = y\frac{V}{X} \tag{151}$$

This is likely to be considerably in error in the earliest stages of firing. The gas drag is, however, important only when the propellant is nearly burnt, and under these conditions equation 151 is a good approximation.

---

[35] Prandtl, in *Physics of Solids and Fluids*, pp. 298, 299.

We assume also that

$$p(x,\, t) = p_0(t)\left[1 - \frac{C\phi(t)}{2W}\left(\frac{x}{X}\right)^2\right] \tag{152}$$

leading to

$$\frac{d^2y}{dt^2} = \frac{p_0(t)\phi(t)C}{WX^2\delta}\, y + \frac{\rho(t)\bar{C}_f}{r(t)\delta}\left[\frac{1}{3}\left(\frac{LV}{X}\right)^2 - \frac{LV}{X}\,\zeta + \zeta^2\right] \tag{153}$$

Note that this holds only for a cord whose end is initially near the breech.

For illustration we take a differential-analyzer solution for a high-velocity gun with $C/W = 0.64$, giving a peak pressure of 29 tons/sq in. and a velocity of 2475 ft/sec at "all burnt," at a travel of about 20 calibers. For this solution the functions occurring in equation 153 have been tabulated, and this equation has been solved by numerical integration, starting from the boundary conditions $y = y_0$, $dy/dt = 0$ at $t = 0$, the instant of shot start.

An apparent difficulty arises from the buckling of the cord under the acceleration stresses. This is equivalent to the buckling of a beam with pin ends under distributed axial loading, and the critical acceleration is given by[36]

$$\frac{L^3\delta}{Er^2}\frac{d^2y}{dt^2} = 4.6 \tag{154}$$

where E is the modulus of elasticity of the propellant. For a typical solventless propellant at temperatures near 60°F, we can take $E = 5 \times 10^9$ dyne/sq cm. For a stick the length of the chamber, the buckling criterion is exceeded even at shot start. Presumably the presence of other grains of propellant and the support of the walls of the gun restrict the buckling sufficiently to prevent breaking of the stick. Under these conditions, equation 153 for the motion of the cord is not likely to be seriously affected.

Numerical results are shown in Figs. 9.18 to 9.20. In Fig. 9.18 the travel and velocity of the cord are shown as ratios to the corresponding quantities for the shot. As the cord radius r tends to zero, the velocity tends to infinity like log $(1/r)$, but the travel remains finite. The total travel is only 2.3 calibers.

A more striking demonstration of the unimportance of the motion of the propellant is shown in Fig. 9.19, where the motion is plotted against $rP^{0.9}$. P is the breech pressure in tons per square inch and r is the radius of the cord; since the rate of burning of this propellant was taken to be

[36] See, for example, Timoshenko, *Elastic Stability* (1936), p. 122.

proportional to $P^{0.9}$ in this ballistic solution, $rP^{0.9}$ is proportional to the rate of generation of gas from the charge. It is clear that, in the region of most importance for interior-ballistic calculations (namely, that of large $rP^{0.9}$), the travel is of the order of half a caliber.

Another point of interest is the ratio of drag force to total force on the stick of propellant. This is plotted in Fig. 9.20, which shows that the final rapid acceleration when the cord is nearly burnt is due to the increasing effect of the gas drag.

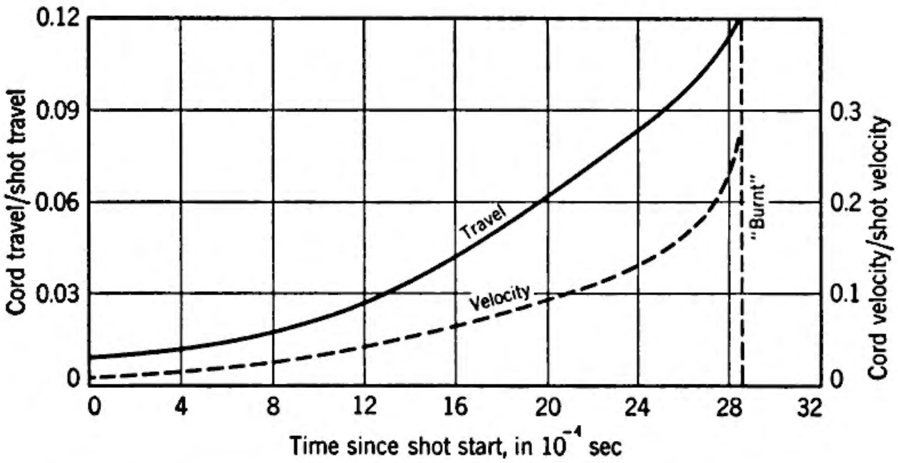

FIG. 9.18 Motion of cord of full chamber length in high-velocity gun. British Crown copyright reserved.

(*b*) *Tubular propellant.* If the internal and external diameters are $D_1(t)$ and $D_2(t)$, then the mass of the tube is $\frac{1}{4}\pi L\delta(D_1 + D_2)(D_2 - D_1)$, and the perimeter of any normal section is $\pi(D_1 + D_2)$. The equation of motion is

$$\frac{d^2y}{dt^2} = \frac{p_0(t)\phi(t)C}{WX^2\delta}\,y + \frac{2\rho(t)C_f(\bar{R})}{(D_2 - D_1)\delta}\left[\frac{1}{3}\left(\frac{LV}{X}\right)^2 - \frac{LV}{X}\zeta + \zeta^2\right] \quad (155)$$

where

$$\zeta = \frac{dy}{dt} - \left(y - \frac{1}{2}L\right)\frac{V}{X} \quad (156)$$

and

$$\bar{R} = \frac{\rho}{\mu}\left[(y + 0.2L)\,\frac{V}{X} - \frac{dy}{dt}\right] \quad (157)$$

We have made the same approximations as in dealing with long cords, and equation 156 reduces to equation 153 if we write $D_1 = 0$ and $D_2 = 2r$. Since $(D_2 - D_1)/2$ decreases during burning in the same way as the radius of a cord burning under the same pressure-time relation, it follows that the motion of a long tube shows no essentially new feature compared with cord. However, the rate of generation of gas is now simply proportional to $P^{0.9}$, and the epoch of greatest travel of the propellant is now a period of considerable importance to the ballistics. Even so, the travel of actually 2 calibers is not sufficient to be worth taking into account.

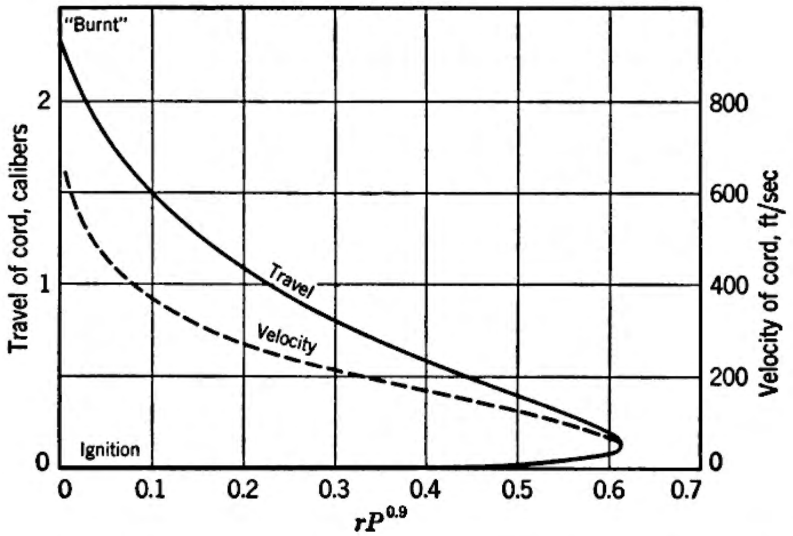

FIG. 9.19 Motion of cord of full chamber length, compared with rate of generation of gas, which is proportional to $rP^{0.9}$, where P tons/sq in. is the breech pressure and the cord radius is r cm.
British Crown copyright reserved.

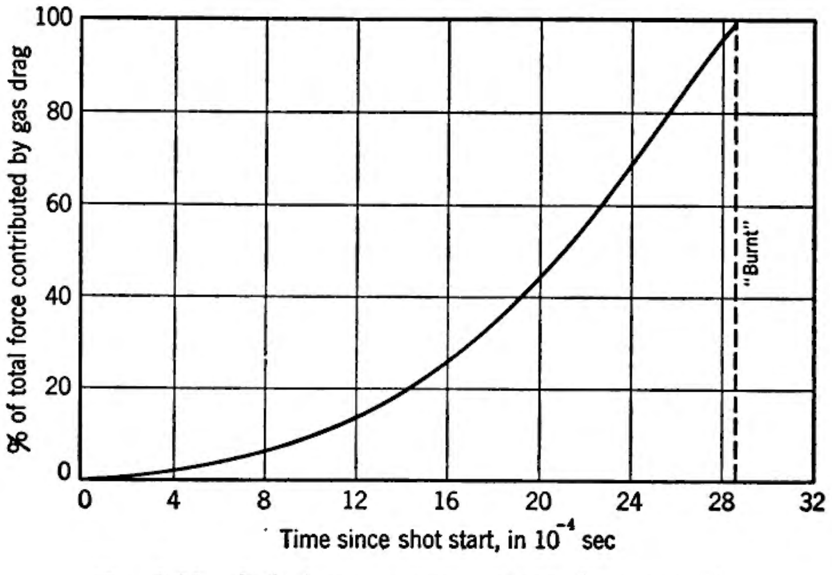

FIG. 9.20 Relative importance of gas drag on cord.
British Crown copyright reserved.

(c) *Short grains.* In this case the chief interest is in the motion of the pieces of propellant nearest to the shot. We return to the equations for short pieces of cord, though, as seen previously, there would be very similar results for chopped tube or multitubular. Equation 153 is true only for long cords of full chamber length; the more general equation is

$$\frac{d^2y}{dt^2} = \frac{p_0(t)\phi(t)C}{WX^2\delta}y + \frac{\rho(t)}{Lr(t)\delta}\int_0^L \left[\left(y + z - \frac{1}{2}L\right)\frac{V}{X} - \frac{dy}{dt}\right]^2 C_f(R_z)\,dz \tag{158}$$

with

$$R_z = \frac{z\rho(t)}{\mu}\left[\left(y + z - \frac{1}{2}L\right)\frac{V}{X} - \frac{dy}{dt}\right] \tag{159}$$

Numerical calculations have shown that, for lengths of, say, half a caliber, it is possible to replace the integral of C_f by a mean $\overline{C}_f$, calculated

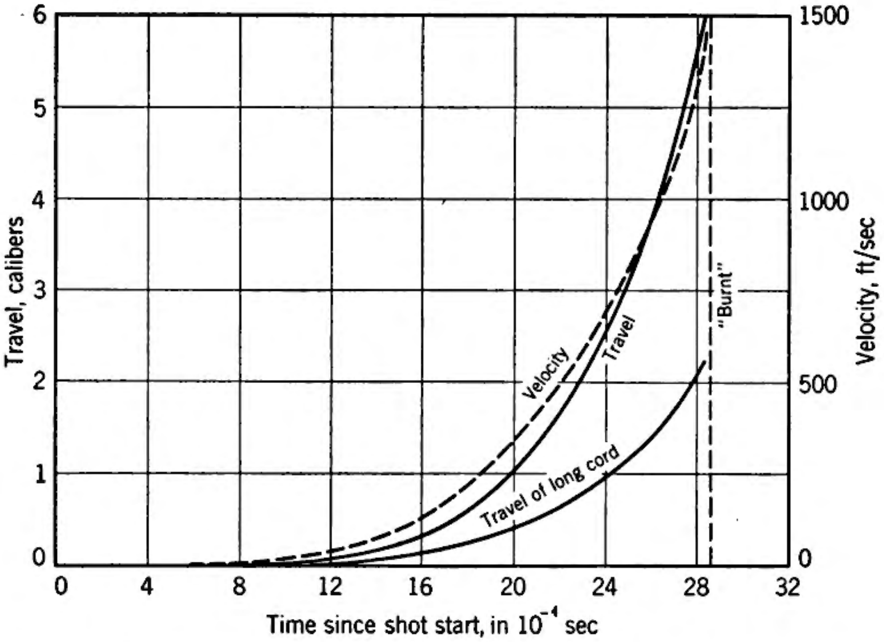

FIG. 9.21 Motion of a short cord originally at shot end of chamber. British Crown copyright reserved.

at $z = L/2$; the error in the total acceleration is only a few per cent. Hence, for chopped cord,

$$\frac{d^2y}{dt^2} = \frac{p_0(t)\phi(t)C}{WX^2\delta}y + \frac{\rho(t)}{r(t)\delta}\left(\frac{yV}{X} - \frac{dy}{dt}\right)^2 C_f(\overline{R}) \tag{160}$$

with

$$\overline{R} = \frac{L\rho(t)}{2\mu}\left(y\frac{V}{X} - \frac{dy}{dt}\right) \tag{161}$$

The motion of a length of ½ caliber, initially at the shot end of the chamber, has been followed by numerical integration. The results are shown in Fig. 9.21, together with, for comparison, the travel-time curve of a single long cord. Although the travel is about twice as large for the short length, it cannot be said that these travels of 5 calibers are likely to be of ballistic significance.

In short, a charge of propellant in small pieces will spread out, but even the grains nearest the shot will travel only about a quarter as far as the projectile.

9.51 Ballistic consequences

The first is that the rate of burning at any time is controlled by the pressure in the chamber more nearly than by the mean pressure in the whole volume behind the shot.

The velocities attained by the propellant, though small compared to the velocity of the projectile, are sufficient to explain why "unburnt" propellant, if present, comes out at the muzzle.

The forces on propellant in a recoilless gun are somewhat similar to those in an orthodox gun. There is a stagnation point, which is at first at the shot but which later moves backward. The gas velocities in the chamber and the pressure gradient in it are therefore not substantially different from those of an orthodox gun, though of course they are reversed in sign, and one need not expect propellant to be blown through the nozzle unless the web size is large. This is in agreement with observation. "Unburnt" picked up behind recoilless guns has, in our experience, always been short pieces of almost initial thickness, believed to be splinters broken off by violent ignition and thrown out with the plastic sealing disk.

From the known dependence of the rate of burning on the transverse relative velocity, the mean increase in the rate of burning has been found to be about 10 per cent for a typical propellant in this ballistic solution. A cool flashless propellant would give a much larger effect. It is to be remembered that this example has rather a high shot velocity at "burnt," almost 2500 ft/sec. Nevertheless the increase is significant even for more normal guns. Some of the consequences for orthodox ballistic theory have been pointed out in § 2.22. The idea that the rate of burning in a gun is affected in this way by velocity and nature of propellant has been found to be useful in explaining anomalies of various kinds.

Finally, we may add that the motion of the propellant is sufficiently small to allow us to take it as stationary in work on Lagrange's problem; this is not exact, but seems to be the most accurate of the simple assumptions we might make.

EXAMPLES

1. Calculate the Lagrange correction for a recoilless gun in the same order of approximation as carried through in § 9.11 for a normal gun.

2. Extend the German method of arriving at equation 60 of chapter 7, to include plausible Lagrange corrections. Show that the gun made recoilless by a nozzle in the breech uses less propellant than that made recoilless by a muzzle brake with $B = 1.8$.

3. Find the pressure distribution along the bore for the velocity distribution of equation 23.

4. Estimate the frictional pressure drop in Langweiler's firings at 9000 ft/sec, with charge weight 11 g, caliber 8 mm, equivalent length of the bore about 1 m.

5. Find the Rankine-Hugoniot curve for a gas with a constant covolume.

6. Repeat Pfriem's work on maximum MV, allowing for covolume. Assuming that, when covolume terms are included, RT_0 should be altered to keep constant energy of reaction, find the effect of a covolume on the maximum MV.

7. Calculate the velocity of the shock wave in Pfriem's theory of maximum MV, and compare with the material velocity behind the shock.

8. Centervall (*Internal Ballistics*, Stockholm, 1902) neglected the drop of temperature caused by the work done on the shot, using simply the relation between pressure p and density ρ taken from a closed vessel. He took the ratio of shot pressure to mean pressure to be $1 - (\rho V^2/2p)$. Show that these overestimates of the Lagrange correction and of the gas temperature nearly counterbalance in the guns he considered ($C/W \sim \frac{1}{4}$).

9. Rewrite the recoil equation of a vented-breech recoilless gun, to allow for the presence of a muzzle brake.

10. Find an upper limit to the possible values of B.

11. Bohler has proposed that flaps operated by gas pressure should be used to block the central exit of a muzzle brake as soon as the shot has left. Estimate the increase in B.

12. Find the position and time at which a shock first appears ahead of a projectile moving down the bore with acceleration proportional to time. Show that in this case the discontinuity does not appear first at the head of the compression wave.

CHAPTER TEN Heat Transfer to Gun Barrels

10.1 Introduction

This subject has two claims to importance. The first is the central place occupied by calculations and measurements of heat transfer in the investigation of gun erosion. It is now established that there are three main mechanisms of erosion in steel guns. The first is responsible for only a small rate of wear, but it can be the most important of the three in low-velocity weapons; this mechanism is connected with mechanical erosion of the bore and does not appear to be correlated with the temperature attained at the bore surface. The second mechanism enters at higher bore temperatures and increases fairly rapidly as the temperature rises. This effect is believed to be due to the brittleness of a surface layer of chemically transformed material, largely martensite, formed by rapid heating and cooling. Finally, in guns of large caliber and high velocity the temperatures reached are so high that products of a cementite nature are formed on the bore surface; because of its low melting point such a layer is easily swept away and the gun erodes rapidly. Though the subject of gun erosion is now too extensive and goes too far into metallurgy to be covered in this book, it should be apparent that calculations of bore temperature play a most important part.

The second use of a calculated heat transfer is in the Résal equation. Throughout this book we have assumed that the heat loss at any time is proportional to the energy of the shot at that instant, the constant of proportionality depending on the gun, charge, and projectile. In this chapter we explain how this convenient assumption can be tested and the constant factor estimated.

The calculation of the flow of heat through the system, from the gas out to the atmosphere, falls into three parts. The flow of heat in the metal barrel is one division and can be solved once we know the flow of heat at the inner and outer walls. The transfer of heat from propellant gases to bore surface occurs chiefly by forced convection through the highly turbulent boundary layer; it is easy to see that radiation has a much smaller effect than convection. The theory of this convection is the second main division of the subject. In a single round from a cold gun the penetration of heat into the barrel is small, and, when considering single rounds or low rates of fire, it is sufficient to take the outer boundary condition in the metal to be "atmospheric temperature at the outer surface." For guns fired at higher rates an equilibrium state is set up, in which the whole of any given section of metal, normal to the bore axis, is at about the same temperature, while transient peaks appear at the bore surface. The loss of heat by convection at the outer surface is then a third part of the problem.

In this chapter we shall illustrate the methods used by treating the simpler case, that of single rounds in a cold gun. Convection at the outer surface can then be neglected. We begin with the transfer of heat in the boundary layer, and then show how the heat flow in the barrel can be solved.

The theory of heat transfer in guns was studied in England during the war by Hicks and Thornhill, whose treatment we follow here. Parallel work was carried out in the United States by Hirschfelder and Nordheim and their collaborators. Until now none of this work has been published openly, though the Hicks-Thornhill treatment is in course of publication.

10.2 The heat-transmission coefficient

We assume that the bore surface is smooth in the hydrodynamic sense, and we correct for this approximation at the end of the section.

The rate at which heat is transferred through the boundary layer per unit area of the wall is written as $h(T_g - T)$, where T is the temperature of the bore surface and T_g is the temperature of the main gas flow, well outside the boundary layer. All three quantities, h, T_g, and T, depend on time as well as on position along the barrel. The difficulties of the problem occur mainly in the calculation of the heat-transmission coefficient h.

The flow in the boundary layer is neither uniform with regard to distance along the barrel nor steady in time; the Reynolds numbers are very high, compressibility effects occur, and there is a big drop of temperature across the boundary layer itself. The solution for the main stream is itself not completely understood, as was seen in chapter 9. Clearly a vigorous simplification of the problem is necessary. We begin with some of the more reasonable of the approximations. The first is the conventional replacement of the actual chamber and shot seating, with their tapered surfaces and greater diameter than the bore, by a cylindrical continuation of the bore of the correct volume. We measure all distances from this idealized breech position and assume that the gas velocity in the main stream rises linearly from breech to shot base. This Lagrange approximation can be expected to be better than the approximations made later in regard to the boundary layer, though the error is probably not negligible. When more is known about the real solution of the Lagrange problem, it will be easy to incorporate this in the heat-transfer calculations.

It will be shown later that the boundary-layer thickness is small compared with the radius of the bore, except in high-velocity guns and then only for a short time near the muzzle. It is therefore possible to consider the flow in and near the boundary layer to be the same as near a flat plate edge-on to the stream, the plate being of infinite extent perpendicular to the flow. The appropriate Reynolds number at a distance x from the breech is

$$R(x, t) = \frac{x\rho(x, t)V(x, t)}{\mu(x, t)}$$

where ρ is the gas density, μ the viscosity and V the velocity of the gas in the main flow. The viscosity depends on the temperature, but the variation with distance at any time is small. The density can also be taken to be independent of position at any given time; this is in fact the basic assumption of the Lagrange approximation. Thus we have

$$R(x, t) = \frac{x\rho(t)V(x, t)}{\mu(t)} \tag{1}$$

As typical magnitudes we may take $V = 1000$ ft/sec, $x = 5$ ft, $\rho = 0.1$ g/cc, and $\mu = 6 \times 10^{-4}$ g/cm sec; then the Reynolds number is 8×10^8. The range covered in all guns at all positions and times is from zero to 10^{10}, with $10^5 - 10^{10}$ as the important region. For smaller values of the Reynolds number the heat transfer is relatively small, and there is negligible error in applying everywhere the formulas that we shall derive for the higher Reynolds numbers.

Let C_p be the specific heat of the propellant gases, at constant pressure, and let λ be their thermal conductivity. Then the "Prandtl number" σ is defined as

$$\sigma = \frac{\mu C_p}{\lambda} \tag{2}$$

Reynolds' analogy between the transfer of momentum and heat in turbulent flow has been extended by von Kármán[1] to cover Prandtl numbers other than unity. For the heat-transfer coefficient h, his solution leads to

---

[1] von Kármán, *Proc. 4th Intern. Congr. Applied Mech.* (1934), p. 77; also *Modern Developments in Fluid Dynamics* (ed. Goldstein) (Oxford, 1938), p. 657.

$$\frac{\rho C_p V}{h} = \frac{\rho V^2}{\tau_0} + 5\left(\frac{\rho V^2}{\tau_0}\right)^{1/2} [\sigma - 1 + \ln\{1 + 0.83(\sigma - 1)\}] \tag{3}$$

where τ_0 is the skin friction drag per unit area.[2]

The Prandtl number is a slowly varying function of temperature, and enters the formula 3 only in the second term, which is no more than 10 to 20 per cent of the first. Moreover equation 3 is not necessarily correct at high velocities or in nonsteady or nonuniform flow. It is therefore sufficient to give σ a mean value for all gas temperatures and all propellants:

$$\frac{\rho C_p V}{h} = \frac{\rho V^2}{\tau_0} - 3\left(\frac{\rho V^2}{\tau_0}\right)^{1/2} \tag{4}$$

The composition and C_p of the gases at any specified temperature can be computed from the tables of chapter 3, neglecting minor products. The viscosity, which is nearly independent of pressure, can be estimated at ballistic temperatures by Sutherland's law:

$$\mu \propto \frac{T^{3/2}}{T + S} \tag{5}$$

where S depends on the gas and is of the order of 100°K for propellant products (Table 10.1). The viscosity of the mixture can be taken, with sufficient accuracy for this problem, to be a linear sum of the individual values, weighted according to mole fractions.

TABLE 10.1 DATA FOR VISCOSITY AND THERMAL CONDUCTIVITY OF PROPELLANT PRODUCTS

Gas	H_2	H_2O	CO	CO_2	N_2
Viscosity at 273°K, 10^{-4} gm/cm sec	0.84	1.27	1.66	1.37	1.65
Sutherland constant S, °K	94	120	156	240	114

We come now to the most difficult part of the whole calculation of heat transfer: the determination of the skin friction τ_0. This has been solved theoretically when the flow over the surface is uniform, steady, and incompressible and the temperature difference across the boundary layer is small. In the present case all these assumptions are violated. The flow is varying rapidly with time, the velocity increases with distance from the breech, and the gas velocities in the main stream are smaller but of the same order as the velocity of sound in the gas. Furthermore, the temperatures at the bore surface and the outer side of the boundary layer differ by more than 1000°C nearly all the time, and so there must be a large variation in thermal conductivity and viscosity inside the boundary layer itself. This makes a formidable problem, which has so far not been solved exactly. The most that has been done is to make a plausible guess, based on certain empirical results.

---

[2] In the technical literature the skin friction is often expressed in terms of the "Fanning coefficient" $2\,\tau_0/\rho V^2$.

If we take first the steady uniform flow, let z be distance measured from the surface perpendicularly into the stream. Writing

$$V_*^2 = \frac{\tau_0}{\rho} \tag{6}$$

and

$$\eta = \frac{\rho V_* z}{\mu} \tag{7}$$

then the velocity v at distance z from the wall can be shown to have the form

$$v = V_* \psi(\eta) \tag{8}$$

The function ψ can be determined from experiment, starting with forms suggested by theory. At high Reynolds numbers the velocity distribution ψ can be shown theoretically to take a logarithmic form, which has been fitted to experiment to give [3]

$$\psi = 2.495 \ln (1 + 8.93\eta) \tag{9}$$

For many calculations a more tractable form is

$$\psi = a\eta^{1/n} \tag{10}$$

of which a special case is the Blasius formula,

$$\psi = 8.74\eta^{1/7}$$

valid for Reynolds numbers up to 10^5. At higher Reynolds numbers it is possible to represent equation 9 by a "best" power law 10 by fitting the skin friction calculated from the two expressions in the special case of steady uniform flow. To obtain the skin friction we use the boundary-layer momentum integral,[4] which for steady flow and uniform velocity V gives

---

[3] Prandtl, in *Aerodynamic Theory*, vol. III (ed. Durand) (Berlin, 1934), p. 150.

[4] See, for example, *Modern Developments in Fluid Dynamics* (ed. Goldstein) (Oxford, 1938), p. 133.

$$\tau_0 = \rho \frac{\partial}{\partial x} \int_0^\delta (V - v)v \, dz \tag{11}$$

where δ is the thickness of the boundary layer. If we use equations 5 to 7 and define

$$\eta_1 = \frac{\rho V_* \delta}{\mu} \tag{12}$$

so that

$$V = V_* \psi(\eta_1) \tag{13}$$

then equation 11 leads to

$$\frac{dx}{d\eta_1} = \frac{d\psi(\eta_1)}{d\eta_1} \frac{\mu}{\rho V} \int_0^{\eta_1} \psi^2(\eta) \, d\eta \tag{14}$$

For $\psi = a\eta^{1/n}$ we have

$$x = \frac{\mu a^3 \eta_1{}^{(n+3)/n} n}{\rho V(n+2)(n+3)} \tag{15}$$

since $\eta_1 = 0$ at $x = 0$. This result may be written as a relation between the local Reynolds number,

$$R = \frac{x\rho V}{\mu}$$

and the local value of $\tau_0/\rho V^2$:

$$R = \frac{n}{a^n(n+2)(n+3)} \left(\frac{\rho V^2}{\tau_0}\right)^{(n+3)/2} \tag{16}$$

From the more accurate velocity distribution (equation 9), we obtain

$$R = 8.93(2.495)^3 \left[6\eta_1 - \frac{6}{8.93} \ln (1 + 8.93\eta_1) - 4\eta_1 \ln (1 + 8.93\eta_1) + \frac{1 + 8.93\eta_1}{8.93} \{\ln (1 + 8.93\eta_1)\}^2 \right]$$

where

$$1 + 8.93\eta_1 = \exp \left\{ \frac{1}{2.495} \left(\frac{\rho V^2}{\tau_0}\right)^{1/2} \right\} \tag{17}$$

By adjusting a and n in the power law, to give best agreement between equations 16 and 17 in the range $R = 10^6 - 10^9$, Hicks and Thornhill have found

$$\psi = 12.4\eta^{1/11.3} \tag{18}$$

as a "best" power law for heat transfer in guns. The deviation is less than 3 per cent in this range.

The skin friction drag deduced from this law in equation 16 is true only for steady uniform incompressible flow with small temperature changes across the boundary layer. We should now take account of the rapid changes in the flow, in both space and time, and the compressibility and the rapid changes in physical properties in the boundary layer. The generalization of Blasius' formula to apply to steady incompressible but nonuniform flow has been carried out by Buri,[5] whose result for the skin friction is within a few per cent of what would be deduced for a uniform flow at the *local* Reynolds number, assuming the normal velocity distribution across the layer.

The experiments of Frossel [6] show that at a given Reynolds number it matters little to the skin friction whether the flow is subsonic or supersonic, and it is reasonable to assume that this is true also for the heat transfer.

Hicks and Thornhill have therefore assumed that the disturbing factors, which at present have not been included accurately, would have only a small effect on the velocity distribution in the boundary layer. The next step, then, is to calculate $\tau_0/\rho V^2$ from the boundary-layer momentum integral, including now the terms due to the nonsteady and nonuniform nature of the flow, and using the velocity distribution found to be the "best" power law in the steady uniform flow.

The boundary-layer momentum integral is

$$\tau_0 = \rho \frac{\partial}{\partial x} \int_0^\delta (V - v)v\, dz + \rho \frac{\partial V}{\partial x} \int_0^\delta (V - v)\, dz + \rho \frac{\partial}{\partial t} \int_0^\delta (V - v)\, dz$$

which reduces to

$$\frac{\rho V^2}{\mu} = \frac{\partial V}{\partial x} \psi(\eta_1)[\eta_1 \psi^2(\eta_1) - \int_0^{\eta_1} \psi^2(\eta)\, d\eta] + V \frac{d\psi\,(\eta_1)}{d\eta_1} \frac{\partial \eta_1}{\partial x} \int_0^{\eta_1} \psi^2(\eta)\, d\eta + \eta_1 \psi^2(\eta_1) \frac{d\psi\,(\eta_1)}{\partial \eta_1} \frac{\partial \eta_1}{\partial t} \tag{19}$$

Let y be the position of the base of the shot. By the Lagrange approximation,

$$V = \frac{x}{y} \frac{dy}{dt}$$

and using also

$$\psi = a\eta^{1/n}$$

---

[5] Buri, Zurich dissertation, 1931.

[6] Frossel, *Forsch. Gebiete Ingenieurw.*, **7** (1936).

we find

$$\frac{\rho}{\mu}\left(\frac{x}{y}\right)^2\left(\frac{dy}{dt}\right)^2 = \frac{2a^3}{n+2}\,\eta_1{}^{(n+3)/n}\,\frac{1}{y}\frac{dy}{dt} + \frac{a^3}{n+2}\,\eta_1{}^{3/n}\,\frac{x}{y}\frac{dy}{dt}\frac{\partial\eta_1}{\partial x} + \frac{a^3}{n}\,\eta_1{}^{3/n}\,\frac{\partial\eta_1}{\partial t} \quad (20)$$

This determines η_1 as a function of x and t, if we know ρ and dy/dt as functions of t. The boundary conditions are that $\eta_1 = 0$ at $x = 0$ for all time and that $\eta_1 = 0$ everywhere at $t = 0$. The solution is

$$\eta_1{}^{(n+3)/n} = \frac{(n+2)(n+3)K(t)R}{na^3} \quad (21)$$

where R is the local Reynolds number at the time considered and

$$K(t) = \frac{n\int_0^t y^{(2n+2)/(n+2)}\left(\frac{dy}{dt}\right)^2 dt}{(n+2)y^{(3n+4)/(n+2)}\,\frac{dy}{dt}} \quad (22)$$

is the dimensionless factor, which shows the effect of the nonsteady and nonuniform nature of the flow. Equation 15 shows that in steady uniform flow $K(t)$ is unity. In all guns $K(t)$ starts from zero and increases rapidly at first, finally approaching 0.3, its behavior being little affected by the details of the ballistics.

It is now possible to calculate the heat-transfer coefficient h at all points of the bore at all times. We compute η_1 from equation 21, thence,

$$\frac{\rho V^2}{\tau_0} = a^2\eta_1{}^{2/n}$$

substituting in equation 14 to find h. The quantities needed from the ballistic solution are the velocity, fraction burnt, and gas temperature as functions of time.

This completes the Hicks-Thornhill treatment of the heat-transfer coefficient. They have also calculated the thickness of the boundary layer, to verify that it is indeed small compared with the bore radius. The ratio of boundary layer thickness δ to bore caliber d is

$$\frac{\delta}{d} = \left[(n+2)\left(1+\frac{3}{n}\right)K(t)x\right]^{(n+1)/(n+3)}\frac{1}{a^{2n/(n+3)}d}\left(\frac{\mu}{\rho V}\right)^{2/(n+3)} \quad (23)$$

which is largest at the muzzle, of course, and for small calibers, high velocities, and high pressures. For a fairly extreme case, we may take an antitank gun of 3 in. caliber, 60 calibers long, with muzzle velocity 3000 ft/sec and a muzzle pressure of 5 tons/sq in. Then δ/d attains 0.2 as the shot leaves the muzzle. The error arising from the approximation of a plane boundary layer is therefore trivial except in small-caliber, high-performance guns, and even there the effect occurs only near the muzzle toward the end of travel. The error is probably smaller than that arising from the effect of the nonsteady and nonuniform flow on the velocity distribution.

It has been assumed until this point that the bore surface is hydrodynamically smooth. The pressure drops measured when air is forced through gun barrels have suggested that the effect of the roughness of the bore is only a few per cent, although the Reynolds numbers have not been pushed up to the full ballistic values. It is clear, however, that the heat-transfer coefficient as calculated previously has to be increased by a substantial amount to give agreement with measured heat inputs to gun barrels. This increase is about 20 per cent in guns and up to 40 per cent in small arms. If the increase is attributed to roughness of the bore, the increasing size of the effect in small arms is explained by the depth of the rifling being here a larger fraction of the caliber. It is probable that some part of the effect is due to the approximations in this theory of the boundary layer.

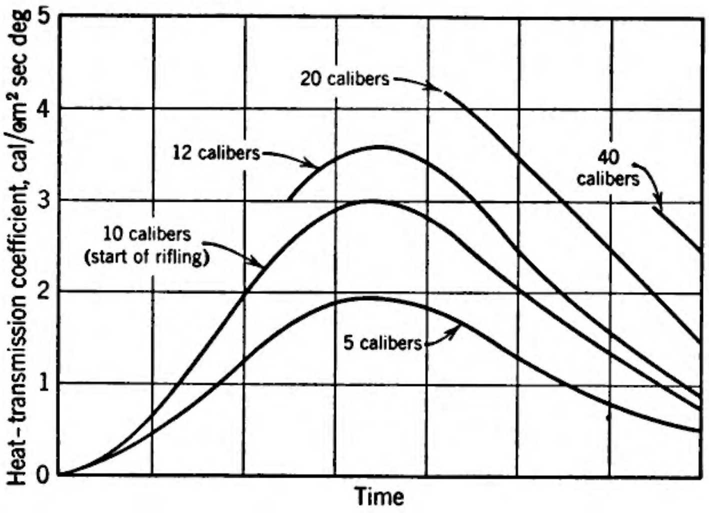

FIG. 10.1 Typical form of heat-transfer coefficient as a function of time during a gun firing. Each curve refers to a specified distance from the breech.

In a worn gun the surface near the shot seating becomes covered with a network of cracks whose appearance depends on the temperature of the propellant products. In all cases the result must be to increase the hydrodynamic roughness of the surface and so to increase the heat transfer. This is one reason, at least, why the rate of wear of a gun increases rapidly toward the end of its life.

Figure 10.1 shows the heat-transmission coefficient calculated in this way for various positions in a gun of fairly high velocity. The order of magnitude of h in guns is seen to be a few calories per square centimeter per second per degree.

10.3 The conduction of heat in the barrel

During the firing of a single round in a cold gun the temperature rise is confined to a layer of the order of 1 mm thick. It is permissible, therefore, to treat the heating as that of a plane wall. Heat flow along the barrel can also be neglected. The boundary condition at the outer wall can likewise be taken to be simply: ambient temperature at infinity.

Let z now be the distance measured into the plane metal wall, with $z = 0$ at the heated surface. Let $T(z, t)$ be the temperature, relative to the ambient temperature, and let $k(T)$ be the thermal conductivity, $\rho_s(T)$ the density, and $C_s(T)$ the specific heat of the metal. Let $T_g(t)$ be the temperature of the propellant gases at the position considered. This temperature is known from the space-mean temperature, which occurs in the ballistic solution, together with an assumed temperature distribution along the barrel, taken from chapter 9; it would often be sufficiently accurate to use merely the mean temperature in the space behind the shot. The heat-transfer coefficient $h(t)$ is a known function of the time, depending on the position considered along the barrel.

The equation of heat conduction is

$$\rho_s C_s \frac{\partial T}{\partial t} = \frac{\partial}{\partial z}\left(k \frac{\partial T}{\partial z}\right) \tag{24}$$

and the boundary conditions are

$$\left.\begin{aligned} &\text{at } z = 0, && k\frac{\partial T}{\partial z} = -h(T_g - T) \\ &\text{at } t = 0, && T = 0 \text{ for all } z \\ &\text{as } z \to \infty, && T \to 0 \text{ for all } t \end{aligned}\right\} \tag{25}$$

To solve equation 24 numerically, it is usual to replace the derivatives with respect to time or distance by finite differences. To obtain an analytical solution in this problem it is better to eliminate the time derivative. To permit an analytical solution it is also necessary to give k and $\rho_s C_s$ single mean values over the whole range of temperatures considered. To take account of the rapid changes in the specific heat at the transformation point, around 700°C, would require a more completely numerical approach. Let $T_n(z)$ and $T_{n+1}(z)$ be the temperature distributions at the beginning and end of the nth time interval (t_n, t_{n+1}), of length Δt. Then, by equation 24,

$$\frac{T_{n+1} - T_n}{\Delta t} = \frac{k}{2\rho_s C_s} \frac{d^2}{dz^2} (T_n + T_{n+1})$$

If we write

$$q^2 = \frac{2\rho_s C_s}{k\,\Delta t}$$

then

$$\frac{d^2}{dz^2} (T_n + T_{n+1}) = q^2(T_n + T_{n+1}) - 2q^2 T_n \tag{26}$$

with boundary conditions,

at $z = 0$,

$$h_{n+1}[T_g(t_{n+1}) - T_{n+1}] = -k \frac{d}{dz} T_{n+1}$$

and, as $z \to \infty$,

$$T_{n+1} \to 0$$

The function $T_n(z)$ can be supposed to be known and satisfies

at $z = 0$,

$$h_n[T_g(t_n) - T_n] = -k \frac{dT_n}{dz}$$

and, as $z \to \infty$,

$$T_n \to 0$$

Hence, at $z = 0$,

$$\left.\begin{aligned} k \frac{d}{dz} (T_n + T_{n+1}) &= -[h_{n+1} T_g(t_{n+1}) - h_n T_g(t_n)] \\ &\qquad + h_{n+1} T_{n+1} + h_n T_n \\ \text{and, as } z \to \infty, \quad T_n + T_{n+1} &\to 0 \end{aligned}\right\} \tag{27}$$

The solution of equation 26, which satisfies the conditions 27, is

$$\begin{aligned} T_n + T_{n+1} &= q e^{-qz} \int_0^z e^{qu} T_n(u)\, du + q e^{qz} \int_z^\infty e^{-qu} T_n(u)\, du \\ &\quad + e^{-qz} \left[\frac{h_n T_g(t_n) + h_{n+1} T_g(t_{n+1})}{h_{n+1} + kq} + \frac{(h_{n+1} - h_n) T_n(0)}{h_{n+1} + kq} \right. \\ &\quad \left. - \left(\frac{h_{n+1} - kq}{h_{n+1} + kq} \right) q \int_0^\infty e^{-qu} T_n(u)\, du \right] \end{aligned} \tag{28}$$

At points of the barrel which are exposed to the gases from the start, the transfer coefficient $h(t)$ starts at zero. At places nearer the muzzle than the initial position of the driving band, the heat-transfer coefficient jumps suddenly to a finite value as the band passes. We deal first with the former case. The initial state is then $T_1(z) = 0$ for all z, which satisfies the boundary conditions because $h_1 = 0$. By equation 28, the solution at the end of the first interval Δt is

$$T_2(z) = \frac{h_2 T_g(t_2) e^{-qz}}{h_2 + kq}$$

and the temperature at the end of the second and all later intervals can be found in analytical form. The solution T_n has the form

$$T_n(z) = e^{-qz}\left[a_0 + a_1(2qz) + \cdots + \frac{a_{n-2}}{(n-2)!}(2qz)^{n-2}\right] \tag{29}$$

where $a_0 \cdots a_{n-1}$ are independent of z and depend on the history of the heat-transfer coefficient up to the time t_n. The solution at time t_{n+1} is then

$$T_{n+1}(z) = e^{-qz}\left[b_0 + b_1(2qz) + \cdots + \frac{b_{n-1}(2qz)^{n-1}}{(n-1)!}\right] \tag{30}$$

where

$$\left.\begin{aligned} b_0 &= \frac{\begin{aligned}h_n T_g(t_n) + h_{n+1}T_g(t_{n+1}) &- (h_n + kq)a_0 \\ + kq(a_0 + a_1 + \cdots &+ a_{n-2})\end{aligned}}{h_{n+1} + kq} \\ b_r &= -a_r + \tfrac{1}{2}(a_{r-1} + a_r + \cdots + a_{r-2}) \quad \text{for } 1 \leq r \leq n-2 \\ b_{n-1} &= \tfrac{1}{2}a_{n-2} \end{aligned}\right\} \tag{31}$$

These recurrence relations enable the solution to be computed at all times and depths into the metal.

When the heat-transfer coefficient rises instantaneously from zero to a finite value at the moment the shot passes, the boundary condition,

$$k\frac{dT}{dz} = -h(T_g - T) \quad \text{at } z = 0 \tag{32}$$

is not satisfied by the initial solution $T_1(z)$ used up to now. The exact analytical solution is, however, well known. If $h(t)$ and $T_g(t)$ are replaced over the time interval $(0, \Delta t)$ by the mean values $\frac{1}{2}(h_1 + h_2)$ and $\frac{1}{2}[T_g(0) + T_g(\Delta t)]$, the solution is

$$T_2(z) = \frac{1}{2}\left[T_g(0) + T_g\,(\Delta t)\right]\left[\operatorname{erfc}\left(\frac{qz}{2\sqrt{2}}\right)\right.$$
$$\left. - \exp\left\{\frac{(h_1+h_2)^2}{2k^2q^2} + \frac{(h_1+h_2)z}{2k}\right\}\operatorname{erfc}\left(\frac{h_1+h_2}{kq\sqrt{2}} + \frac{qz}{2\sqrt{2}}\right)\right] \tag{33}$$

where

$$\operatorname{erfc}\,(w) = \frac{2}{\sqrt{\pi}}\int_w^\infty e^{-u^2}\,du \tag{34}$$

is a function tabulated in many places.

Formula 33 is not in a form that permits analytical solution at later times. It is therefore to be approximated by a series of type 29, of which the first two terms are normally sufficient. The first term is obtained by fitting $T_2(0)$ from equation 33,

$$a_0 = T_2(0)$$

and the second term is then fixed by equation 32, as

$$a_1 = \frac{(h_2 + kq)a_0 - h_2T_g(t_2)}{2kq}$$

If a comparison between the two-term approximation and the exact solution 33 indicates that a third term is needed, this can be found by equating the exact and approximate values of d^2T/dz^2 at $z = 0$.

To calculate the rate of transfer of heat, only the first term of the solution is needed. The rate of loss of heat per unit area is

$$h(t)[T_g(t) - a_0(t)]$$

and this can be integrated numerically with respect to time to obtain the total heat loss per unit area at the bore position being considered. A further numerical integration from breech to muzzle gives the complete heat loss to the gun.

An alternative method of solution of the flow of heat into a semi-infinite solid with a plane face starts from the well-known solution,

$$T(z,\,t) = (\pi\rho_s C_s k)^{-\frac{1}{2}}\int_0^t h(\lambda)[T_g(\lambda) - T(\lambda)](t-\lambda)^{-\frac{1}{2}}e^{-z^2\rho_s C_s/4k(t-\lambda)}\,d\lambda \tag{35}$$

where $T(\lambda)$ is the surface temperature at time λ, that is, $T(0,\,\lambda)$. The integral equation 35 must also be solved numerically by successive approximation and in some respects is more convenient than the process already given. The integral equation is useful also for finding rough solutions for simple forms of the heat-transfer coefficient $h(\lambda)$.

10.4 Results of the heat transfer in guns

The temperature at the bore surface is sketched in Fig. 10.2 for various positions along a typical gun with muzzle velocity 2600 ft/sec. The ambient temperature is 300°K in this example. Curves of the same general form are obtained in all guns. The highest temperature of all is attained near the commencement of rifling, which is clearly one reason why erosion is most severe in this region. As we move toward the muzzle, the maximum surface temperature falls off, relatively slowly at first. The temperatures reached in this example are toward the upper limit of those calculated for various guns. They should be increased somewhat to improve agreement with measured heat transfers. To correlate this temperature region with the phenomena of gun erosion, we note that most gun steels melt around 1500°C. The temperatures found by calculation are therefore usually lower, but not much lower, than the melting point of the unchanged metal and are normally higher than the melting point of some of the conceivable transformation products.

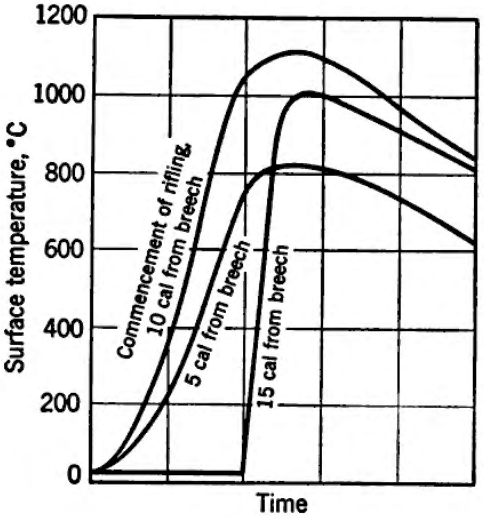

FIG. 10.2 Typical surface-temperature histories of bore wall at positions in the chamber, at the start of rifling and in the bore.

The variation of temperature in the metal near the commencement of rifling is shown in Fig. 10.3 for the time at which the surface temperature reaches its maximum. Later in the firing the zone of appreciable temperature rise extends further into the metal, though even so the depth is rarely more than 0.005 caliber. This refers to single rounds in a cold gun.

Turning now to the heat inputs to the barrel, Fig. 10.4 shows a typical example of the total heat transfer per unit area, as a function of position in the bore. These are heat inputs for the whole of the firing, including the part after shot ejection. The deviations from two straight lines are never very marked.

The heat transfer after the shot has left is not easy to obtain by this solution, since the heat flow continues for many intervals and a wide extrapolation is necessary. The heat supplied to the barrel after shot ejection is about 20 per cent of the total at the commencement of rifling and increases until at the muzzle it supplies the whole of the effect.

The heat loss to the barrel up to any time t during the firing is proportional to the energy of the shot at time t, with errors scarcely ever more than 20 per cent. This verifies the assumption made throughout this book, to the accuracy needed for what is after all only a correction to the ballistic solution.

The heat transfer under different ballistic conditions can be compared very simply, at least in regard to qualitative effects. From equation 3, if we neglect the correction term in $\sigma - 1$,

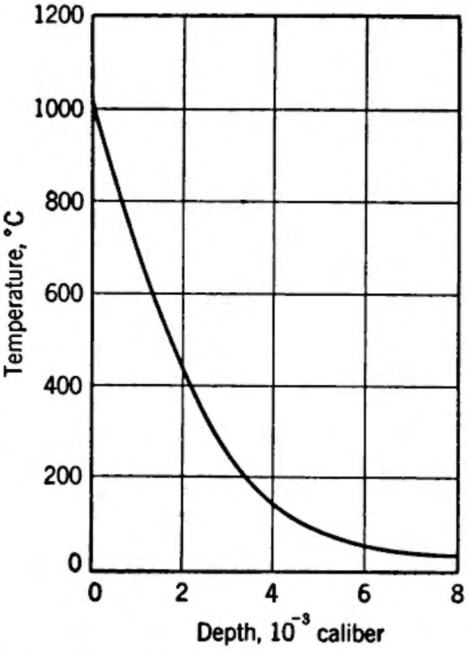

FIG. 10.3 Penetration of temperature into barrel wall, in a typical example.

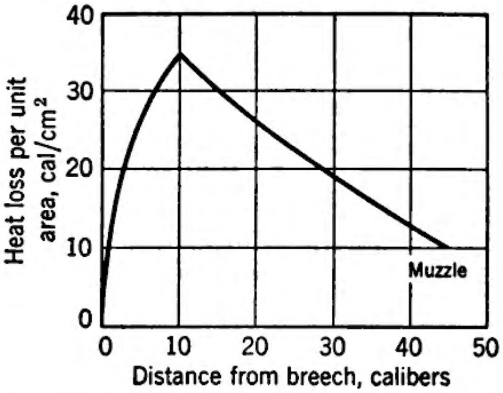

FIG. 10.4 Total heat loss per unit area as a function of position along bore.

$$h \simeq \frac{\rho C_p V}{\dfrac{\rho V^2}{\tau_0}} \propto \rho C_p V {\eta_1}^{-2/n} \propto \rho C_p V R^{-2/(n+3)}$$

since $K(t)$ is not a strongly varying function. The local rate of heat transfer is thus

$$h(T_g - T) \propto \frac{\rho V(T_g - T)}{\gamma - 1}\left(\frac{\mu}{\rho V x}\right)^{1/4} \propto \frac{\rho^{3/4}(T_g - T)x^{5/4}}{\gamma - 1}\left(\frac{1}{y}\frac{dy}{dt}\right)^{3/4}\mu^{1/4}$$

$\mu^{1/4}$ varies only a little from one propellant to another and may be taken as a constant. The heat loss per unit area at a given point, up to the instant of shot ejection, is

$$\int h(T_g - T)\,dt \propto \frac{x^{5/7}(\bar{T}_g - \bar{T})}{\gamma - 1}\int \left(\frac{\rho}{y}\frac{dy}{dt}\right)^{6/7} dt \tag{36}$$

where the gas and surface temperatures have been given mean values. The lower limit of integration is $t = -\infty$, if the point x is in the chamber, and depends on x, if the point is ahead of the commencement of rifling. The heat loss per unit area is greatest at this point, where it is H, say. For ballistically similar guns, with length L calibers,

$$H \propto \frac{\bar{T}_g - \bar{T}}{\gamma - 1}\frac{C}{d^2}\left(\frac{d^2}{CV_0}\right)^{1/7} \tag{37}$$

Here we have assumed that the guns have the same expansion ratio. To find the effect of expansion ratio on heat transfer, a more refined treatment is necessary.

Equation 37 is adequate to show the direction of the changes of H produced by changes in caliber and velocity. The heat transferred after shot ejection is only some 20 per cent of the total, at the commencement of rifling, so that the fact that this part of the heat transfer varies rather differently with the ballistic parameters is not of much importance. H, the total heat loss per unit area at the commencement of rifling, is a criterion of the severity of erosion in certain guns, where the failure is associated with general heating of the barrel. More usually the rate of erosion is correlated with the maximum surface temperature. It can be shown from the integral equation solution that this temperature depends on the maximum rate of heat transfer at the commencement of rifling, multiplied by the square root of the time scale. Hence, we are led to consider the parameter,

$$\zeta = \frac{\bar{T}_g - \bar{T}}{\gamma - 1}\frac{C}{d^2}\left(\frac{d^2}{CV_0}\right)^{1/7}\left(\frac{V_0}{Ld}\right)^{1/2} \tag{38}$$

from which can be estimated the effects of the ballistic variables. For example:

(*a*) At given peak pressure, projectile, and caliber, ζ increases rather less rapidly than the length of the gun.

(*b*) A change of scale makes ζ increase rather less rapidly than $d^{1/3}$.

(*c*) A change of peak pressure in a given gun increases ζ in roughly the same ratio.

(*d*) When different projectiles are fired at the same maximum pressure from the same gun, ζ increases as $V_0^{1/3}$, roughly.

The corresponding changes in H are easily worked out.

It can be shown from equation 38 why a cool propellant reduces erosion, even when the same muzzle energy is obtained. The latter condition requires that $C\overline{T}_g/(\gamma - 1)$ be constant.[7] In a given gun, for given muzzle velocity, ζ behaves like $\dfrac{C\overline{T}_g}{\gamma - 1}\left(1 - \dfrac{\overline{T}}{\overline{T}_g}\right)$ roughly, that is, as $1 - \overline{T}/\overline{T}_g$. This increases as $\overline{T}_g$ increases, and, when the erosion is severe, the dependence on $\overline{T}_g$ is marked. Consider, for example, a heavily worked gun with $\overline{T} = 1000°\text{C}$ above an ambient temperature of 300°K. Then, by going from $\overline{T}_g = 3000°\text{C}$ to 2000°C we reduce ζ by 25 per cent, which would increase several-fold the life of a gun with such a high $\overline{T}$.

10.41 Semiempirical formulas for heat loss

Thornhill has fitted formulas, whose form has a rough theoretical backing, to the heat transfers calculated for a number of guns. His results are as follows. Let d in. be the caliber, C lb the charge, T_0°K the temperature of uncooled explosion of the propellant, U cu in. the total internal volume of the gun, and A sq in. its bore area. Let θ°K be the maximum rise of temperature at the commencement of rifling (above the ambient temperature of 300°K). Then Thornhill finds, as a best representation of a number of theoretical results,

$$\theta = \frac{T_0 - 300}{1.7 + 0.38 d^{1/2} \left(\dfrac{d^2}{C}\right)^{0.86}} \tag{39}$$

The heat transfer at this point, up to shot ejection, is H cal/sq cm per round, where

$$H = 1.27 \times 10^{-2}\, \theta d^{1/2} \Omega \tag{40}$$

with Ω a roughness factor, greater than unity, which is usually about 1.25 in guns, rising to 1.4 or more in small arms.

The total heat loss to the barrel up to shot ejection can be estimated by taking the heat transfer to increase linearly with distance along the chamber, from zero at the breech to H at the start of the rifling, and to decrease linearly in the bore, down to zero at the muzzle. The total heat loss up to shot ejection is then

$$\frac{U}{2A}\,\pi\, dH \times 6.451 \text{ cal} = \frac{10.13 U\, Hd}{A} \text{ cal} \tag{41}$$

The kinetic energy of the shot and charge at the muzzle is

$$5.03 \times 10^{-3}\,(W + \tfrac{1}{3}C)V^2 \text{ cal} \tag{42}$$

---

[7] Strictly speaking, T_g here should be (T_g + the ambient temperature), but the error is small.

where W is in pounds and V in feet per second. The factor χ used in this book for heat loss/kinetic energy is therefore, at the muzzle,

$$\chi = \frac{25.6 U d^{3/2} (T_0 - 300) \Omega}{A V^2 \left(W + \frac{1}{3} C \right) \left[1.7 + 0.38 d^{1/2} \left(\frac{d^2}{C} \right)^{0.86} \right]} \tag{43}$$

To calculate an approximate value for the total heat loss over the whole of the firing, Thornhill uses a heat transfer varying linearly in the chamber from zero to $1.2H$, falling linearly in the bore to $\frac{2}{3}H$ at the muzzle.

EXAMPLES

1. The heat transfer per square centimeter from the propellant gas to the bore by radiation is

$$1.4 \times 10^{-12} \epsilon_g \epsilon_s (T_g{}^4 - T_s{}^4)$$

where ϵ_g and ϵ_s are the coefficients of emissivity of gas and surface and T_g and T_s the corresponding temperatures. Giving their emissivities their maximum values, unity, show that radiation plays a negligible part in the heating of a gun barrel.

2. Show from the integral solution that for ballistically similar guns the maximum bore surface temperature is proportional to the maximum rate of heat transfer per unit area, multiplied by the square root of the time scale of the phenomena.

3. A given projectile is to be fired at the same velocity from (*a*) a normal gun, (*b*) an abnormally long gun, (*c*) as a subcaliber projectile from a gun of greater caliber. In which will the erosion be worst?

4. Evaluate the function $K(t)$ introduced in equation 22, near the end of shot travel, neglecting the initial value of y, and assuming (*a*) constant shot velocity, (*b*) constant acceleration. Show that the effect of the initial nonzero value of y is to reduce $K(t)$. From these results deduce the general behavior of $K(t)$, stated in § 10.2.

Appendix A

The Numerical Solution of the Equations of Interior Ballistics

We have in several parts of this book referred to numerical solution of sets of ordinary differential equation. It will perhaps be useful if we explain one such process here, without any attempt to compare with other formulas, in fact, merely laying down one of the possible rules.

The numerical solution of partial differential equations can be a tricky matter, and the method depends essentially on the type of equations and the nature of the boundary conditions. Fortunately, partial differential equations are not common in this subject. Sets of ordinary differential equations can also raise difficult questions when one is computing near singularities. The equations of interior ballistics are, however, of a simple type, and the most elementary methods will suffice.

The formulas used depend on whether the computer has a calculating machine at hand. If so, it is best to work in terms of function values rather than of their differences. We shall take this case first.

A.1 Method of solution on a calculating machine

By introducing new dependent variables the set of equations may be reduced to a set of the form

$$\frac{dx}{dt} = f_1(t, x, y, z \cdots); \qquad \frac{dy}{dt} = f_2(t, x, y, z \cdots)$$

and so on, where t is the independent variable and $x, y, z \cdots$ the dependent variables. In ballistics t will usually be the time and $x, y, z \cdots$ the travel, velocity, fraction burnt, gas temperature, and so on. There will be algebraic relations between some of these: for example,

$$\phi = (1 - f)(1 + \theta f)$$

The set of equations reduces, in its simplest form, to the single equation,

$$\frac{dx}{dt} = f(t, x) \tag{1}$$

which we shall now discuss.

Let $t_0, t_1, t_2 \cdots$ be a set of values of t separated by a constant interval h, and let $x_0, x_1, x_2 \cdots$ be the corresponding values of x and $f_0, f_1, f_2 \cdots$ the corresponding values of $f(t, x)$. Then,

$$x_3 - x_2 = \tfrac{1}{12}h(5f_3 + 8f_2 - f_1) \tag{2}$$

and

$$x_3 - x_2 = \frac{h}{12}(23f_2 - 16f_1 + 5f_0) \tag{3}$$

both with an error proportional to $h(\Delta'''f)_{2\frac{1}{2}}$, where the third difference $(\Delta'''f)_{2\frac{1}{2}}$ is that which appears between lines t_2 and t_3 in a difference table of f at equal intervals of t. Equation 2 is much more accurate than equation 3, having $\frac{1}{9}$ of the error of the latter. These formulas enable a solution, known at t_0, t_1, and t_2, to be continued indefinitely. For from equation 3 we can compute x_3 and so f_3, and hence a better value of x_3 by applying equation 2. The value of f_3 is then computed afresh and equation 2 applied again, the process being repeated until convergent. Now that x_3 has been found, the whole affair is repeated to find x_4 and so on.

The number of times equation 2 has to be used per step is itself a good criterion for the accuracy of the whole process. Not more than two cycles should be necessary. An even better indication is the accuracy with which equation 3 predicts x_3. The difference between equation 3 and the final value of x_3 should be only a few units in the last place; in fact, if this prediction error is too large or too erratic to be guessed within two or three units, the size of interval h ought to be decreased.

More precisely, the errors in the process are as follows. For equation 2,

$$x_3 - x_2 = \frac{h}{12}(5f_3 + 8f_2 - f_1) - \frac{h}{24}(\Delta'''f)_{2\frac{1}{2}} + O(h^5) \tag{4}$$

and equation 3 is more correctly written as

$$x_3 - x_2 = \frac{h}{12}(23f_2 - 16f_1 + 5f_0) + \frac{3h}{8}(\Delta'''f)_{2\frac{1}{2}} + O(h^5) \tag{5}$$

Halving the size of step is simple. Suppose we know the solution at t_0, t_{-1}, t_{-2}, and so on, and that we want it at $t_{\frac{1}{2}}$, t_1, $t_{\frac{3}{2}}$, and so on. Then we begin by predicting $x_{\frac{1}{2}}$ from

$$x_{\frac{1}{2}} - x_0 = \frac{h}{24}(17f_0 - 7f_{-1} + 2f_{-2}) \tag{6}$$

calculating $f_{\frac{1}{2}}$ and computing a better $x_{\frac{1}{2}}$ from

$$x_{\frac{1}{2}} - x_0 = \frac{h}{72}(16f_{\frac{1}{2}} + 21f_0 - f_{-1}) \tag{7}$$

This equation is used until $x_{\frac{1}{2}}$ and $f_{\frac{1}{2}}$ are consistent. To predict x_1, we use

$$x_1 - x_{\frac{1}{2}} = \frac{h}{72}(64f_{\frac{1}{2}} - 33f_0 + 5f_{-1}) \tag{8}$$

and, as soon as f_1 has been obtained, we continue with

$$x_1 - x_{\frac{1}{2}} = \frac{h}{24}(5f_1 + 8f_{\frac{1}{2}} - f_0) \tag{9}$$

From this point the standard formulas 2 and 3 can be used.

Doubling the size of interval is needed when it becomes obvious that the errors in the process have fallen, compared with an earlier part of the solution. Suppose that we know the solution at t_0, t_{-1}, t_{-2}, and that we propose to continue in steps of double size, finding the solution at t_2, t_4. This can be done by the standard process, using the values t_0, t_{-2}, and t_{-4}. It often happens that the errors in this process are considerable, even though the error is small from t_0 onward. If the computer is anxious to double the interval size as soon as possible, the following formulas are useful.

For forward extrapolation,

$$x_2 - x_0 = \frac{h}{3}(19f_0 - 20f_1 + 7f_{-2}) \tag{10}$$

and, for integration,

$$x_2 - x_0 = \frac{h}{9}(7f_2 + 15f_0 - 4f_{-1}) \tag{11}$$

It has not been explained how to obtain the values x_0, x_1, x_2, which were assumed as the known solution at t_0, t_1, t_2. The value x_0 is certainly known, being one of the boundary conditions that specify the solution. How best to obtain x_1 and x_2 depends on the set of equations being solved, and there seem to be no general rules. One way is to try a series expansion of the solution. This has the disadvantage that a short series will carry one only a little way from t_0, so that $t_2 - t_1$ and $t_1 - t_0$ may have to be a good deal smaller than needed in the main computing process; this means a number of stages of doubling the interval. A long series may make it unnecessary to use short intervals at the start but is more laborious to find and compute. The finding of a series solution is an effort that is worth while only if a large number of solutions of the same equations are to be computed. However, the use of an expansion may be essential if there is some singularity at t_0.

The equations of interior ballistics are simple in form, and the behavior of the solution is easy to guess. In this field it is almost always best to estimate x_1 and x_2 and to work round the first two intervals until self-consistent. The integration needs no new formulas: $x_1 - x_0$ comes from the reversed form of equation 2,

$$x_1 - x_0 = \frac{h}{12}(5f_0 + 8f_1 - f_2)$$

Starting the solution can present difficulty when the shot is assumed to start without any "shot-start pressure." The solution then begins at zero pressure, which usually occurs at $t = -\infty$. To get to a finite pressure one tries first to approximate the dependent variable as $Ae^{\mu t}$, where A and μ are determined by the particular equations being solved. Such a change of independent variable usually enables one to reach a pressure at which a straightforward solution is possible. It is often simpler and equally effective to use ϕ or f as the independent variable.

It is essential that the computation be checked as it proceeds. The difference of extrapolated and computed values for the increment in an interval is itself proportional to the third difference, and the difference ought to be so small (for requirements of accuracy) that errors in it are obvious. This checks increments but not the addition of increments. This requires a high-order difference to be computed and either

$$\Delta'' x = x_2 - 2x_1 + x_0$$

or

$$\Delta''' x = x_3 - 3x_2 + 3x_1 - x_0$$

should be calculated and written on the computing sheet. For most work $\Delta''' x$ is better. Certainly the omission of all differencing is foolish. So too is the idea that errors can always be picked out by differencing the final result, say the peak pressure or muzzle velocity; this shows up some errors but may mean many wasted intervals of computation. Furthermore, differencing of the final results is possible only if a fair number of solutions have been computed. It is far better to check each solution as it is calculated.

There are two kinds of error to be considered: systematic and random. The former arises in the error in equation 2, which has been stated already to be $h(\Delta''' f)_{2\frac{1}{2}}/24$. The total of such errors can be estimated; if the equations are complicated, some care should be taken that all the interactions have been included. The sum of all systematic errors during the solution should be estimated and reduced by choice of interval size until the systematic error is less than the random error.

Random errors are those that arise by cutting short the number of decimals in the solution. These rounding-off errors in the last n intervals add to form a frequency distribution of errors with a spread $n^{\frac{1}{2}}$ times as large. This holds only if n is small. For the effect of a rounding-off error near the start of a solution will usually be cumulative; an error in the position of a solution affects its direction, and the effect on the position at a later time may come more from the early errors in direction than from those in position. An estimate of these errors must be made for each set of equations studied. The number of decimal places kept during the computation should be chosen to reduce the total random error below the specified upper limit.

A.2 Solution without a computing machine

The essential difference is that the formulas should now be written in terms of differences, so that the computer may work with smaller numbers. The formula for the prediction of x_3 from x_0, x_1, x_2 is

$$x_3 - x_2 = h[f_2 + \tfrac{1}{2}(\Delta f)_{1\frac{1}{2}} + \tfrac{5}{12}(\Delta'' f)_1] \tag{12}$$

and, for the accurate integration,

$$x_3 - x_2 = h[f_2 + \tfrac{1}{2}(\Delta f)_{2\frac{1}{2}} - \tfrac{1}{12}(\Delta'' f)_2] \tag{13}$$

Computing with differences means that rather more has to be written down by the computer. For example $\Delta''' x$ will be obtained (for checking) by writing down Δx, $\Delta''x$, $\Delta'''x$ in succession whereas the computer with a machine would calculate $\Delta'''x$ directly from

$$\Delta'''x = x_3 - 3x_2 + 3x_1 - x_0$$

Our previous discussion of checking and accuracy applies without change. The error term in equation 13 is

$$-\frac{h}{48}[(\Delta'''f)_{2\frac{1}{2}} + (\Delta'''f)_{1\frac{1}{2}}]$$

Appendix B

Some Constants Used in Ballistics [1]

1 ft = 30.480 cm; 1 lb/cu in. = 27.681 g/cc

$\pi = 3.1416$; $e = 2.71828$

The gas constant, $R = 8.205 \times 10^{-2}$ liter·atm/deg·mole = 8.314×10^{7} erg/deg·mole

1 $\text{cal}_{15} = 4.1855 \times 10^{7}$ ergs

1 ton/sq in. = 152.42 atm = 157.48 kg/sq cm, at the standard value of g = 32.174 ft/sec^2

1 (ton/sq in.) × (cc/g) = 1.6624×10^{5} (ft/sec)^2

---

[1] Birge, *Rev. Modern Phys.*, **13** (1941), 233.

Appendix C

Interpolation Coefficients

The tables in this book are designed for interpolation by Bessel's formula:

$$f(a + nh) = nf(a + h) + (1 - n)f(a) + B''(n)D$$

where D is printed in the table and is the sum of adjacent second differences, sometimes including a correction for higher-order differences. In this book D is usually so small that B'' need not be known to more than two decimal places, so that the accompanying table will often be sufficient. The error in any inter-

Table of $B''(n)$

n	$B''(n)$
0	
	−0.00
0.020	
	−0.01
0.064	
	−0.02
0.112	
	−0.03
0.168	
	−0.04
0.235	
	−0.05
0.326	
	−0.06
0.673	
	−0.05
0.764	
	−0.04
0.831	
	−0.03
0.887	
	−0.02
0.935	
	−0.01
0.979	
	−0.00
1	

The value of B'', lying between any two entries in the column of n, is the B'' to be used with all intermediate values of n. The B'' to be used with a value of n which appears in the list is the entry above and to the right.

polated value $f(a + nh)$ in this book due to the error in B'' from this table is never more than 0.6 of a unit in the last place. As the tables in the text have errors up to half a unit because of differences above the second not being taken into account exactly, the total error can attain one unit. Where the loss of half a unit of accuracy is important, the short table of B'' given here should be replaced by a table to one more place of decimals, such as is given in, for example, *Interpolation and Allied Tables* (H.M. Stationery Office, London, 1936 and 1942).

Digitized by Google Original from UNIVERSITY OF MICHIGAN

Name Index

Abel, 100
Altman, 121
Ambler, 94
Aunis, 44

Beattie, 104
Becker, 94
Belajev, 48
Bennett, 22, 207, 239
Bianchi, 239
Bichowsky, 94, 95
Birge, 90
Blasius, 415
Bodlien, 12, 328
de Boer, J., 105, 106
Bohler, 408
Booth, 53
Boulengé, 9
Boys, 45, 48
Bravetta, 172
Buri, 415
Burlot, 88, 102

Carrière, 254, 359
Cassini, 18
Centervall, 207, 223, 408
Challeat, 383
Chalvet, 36, 72, 161
Chapman, A. T., 124
Chapman, S., 67
Charbonnier, 3, 20, 38, 39, 41, 134, 190, 207, 239, 240
Clayton, 93
Clemmow, 207, 209, 212, 213
Cooke, 246, 309
Coppock, 174, 213
Corner, 45, 48, 74, 105, 106, 213, 243, 246, 313, 372
Courant, 348, 359
Cowling, 67
Crank, 212
Cranz, 2, 3, 20, 39, 130, 140, 186
Crawford, 49
Crow, 43, 45, 46, 88, 103, 172, 213
Curtiss, 62

Davis, 93, 124
Dawson, 93, 124
Desmazières, 3, 186, 209, 213
Devonshire, 123
Dryden, 77, 78, 79
Dupuis, 21, 36, 38, 39, 72, 161
Durand, 77
Duttenhofer, 25
Dwyer, 95

von Elbe, 93, 95, 124
Emery, 21, 226, 240
Enskog, 67

Fage, 77
Fanning, 412
Fiocke, 95
Fowler, 68, 69
Frank-Kamenetsky, 49
Friedrichs, 348, 359
Frossel, 415

Gallwitz, 26
Gehrlich, 334
Giauque, 93
Goldie, 190, 191
Goldstein, 77, 411
Goode, 357, 388
Gordon, 93, 124
Gossot, 3, 21, 38, 134, 209, 226, 234, 340, 347, 349
Goursat, 348, 397
Grimm, 107
Grimshaw, 43, 45, 46, 88, 103, 213
Guggenheim, 68

Hadamard, 348
de Haller, 348, 358, 359
Hartree, 224
Hélie, 19

Henkel, 62
Hepner, 342
Herzberg, 95
Heydenreich, 19
Hicks, 341, 410
Hinds, 47, 190
Hirschfelder, 62, 91, 93, 102, 105, 124, 243, 410
Hugoniot, 20, 323, 340, 347, 349, 360, 365, 368, 393, 397
Hummel, 62
Hunt, 47, 190

Johnston, 93, 124
Justrow, 334

von Kármán, 76, 78, 80, 411
Kassel, 91, 93, 124
Kent, 88, 140, 351
Kharasch, 94
Kilpatrick, 124
Kleider, 36, 37
Kratz, 83
Krupps, 85

Lagrange, 134, 339
Laidler, 26
Langweiler, 134, 137, 172, 362, 364, 385
Leduc, 19
Lesauskis, 45
Létang, 43, 46
Lewis, B., 93, 95, 124
Liebessart, 86
Liouville, 3, 20, 21, 38, 134, 207, 209, 226, 234, 340, 347, 349
Lockett, 357
Lorentz, 104
Lorenz, 186
Love, 340, 347, 357–359

Maccoll, 359
Mansell, 72, 73
Mata, 172
Mayer, J. E., 106
McClure, 105
McMahon, 93, 124
Michels, 105, 106
Moisson, 20, 172
Montroll, 106
Muraour, 25, 42–45, 47, 72, 88

Noble, 8, 14, 19, 85, 100
Nordheim, 410

Oswatitsch, 384

Pappas, 227
Penner, 121
Petavel, 88
Pfriem, 357, 362
Pidduck, 340, 347, 349, 351, 357, 359, 361, 366
Pike, 66, 70, 91, 94, 121, 210, 212, 223
Pillow, 397
Piobert, 38, 340, 346
Pitzer, 124
de Place, 383
Platrier, 347
Poisson, 19
Prandtl, 76, 77, 79–81, 341, 402, 411, 413
Prettre, 94
Proudman, 226, 242
Puff, 334

Rankine, 360
Rateau, 250, 315, 323, 365, 368, 376
Rayleigh, 393
Résal, 19, 176
Reynolds, 310
Riabouchinsky, 246
Rice, O. K., 49
Riemann, 340, 347, 363, 395
Rinkenbach, 94
Robins, 14, 18, 87, 242
Röggla, 22, 207, 209, 226, 232, 239
Rosecrans, 83
Rossini, 94, 95, 124
Rossmann, 13, 357

Sarrau, 19, 21, 226
Schardin, 362, 397, 399
Schmidt, A., 43, 94
Schmitz, 71, 85, 334, 336
Schönbein, 24
Schumacher, 43
Schweikert, 43, 88
Sébert, 20, 340, 343
Siemens, 383
Slater, N. B., 69
Spaulding, 62
Stephenson, 93, 124

Stockmayer, 104
Strecke, 243, 264
Studler, 246
Sugot, 3, 22, 134, 190, 239–241
Sutherland, 62, 75, 412

Takahasi, 80
Taylor, Sir Geoffrey, 76, 359
Taylor, H. S., 124
Thomson, Sir J. J., 15
Thornhill, 341, 410, 425
Timoshenko, 403
Townend, 77

Vallier, 19
Vickers, 271
Vieille, 15, 25, 85, 87
Vinti, 88, 140, 243
Voituriez, 226

van der Waals, 67
Wadley, 213
Wagman, 124
Walker, 93
Weeks, 105
Wilson, E. B., 93, 124
Winter, 73, 342
Wolf, 107
Wood, A. M., 212

Yamaga, 43, 45, 46

Zaroodny, 142
Zeldowitsch, 49

Subject Index

Acetone, 25, 94
Activation energy of propellant reactions, 65
Adiabatic flame temperature, 44, 90
"All burnt," 138, 142, 152, 159, 162, 164, 167
Ammonia, 89, 99
Antitank guns, 143, 313, 335, 336, 383
Auxiliary igniters, 28

Back-pressure factor, 316
Ballistic efficiency, 142, 144, 145, 153, 160, 162, 164, 166, 167, 184, 264, 305
Ballistic pendulum, 14, 18
Bennett tables, 239
Blättchenpulver, 33
Blending, 4
BL guns, 27
Bl P, 33
Bore resistance, 12, 136, 156, 237, 337
  ballistic effects, 213
Bore surface, 417
Boulengé chronograph, 9
Boundary-layer momentum integral, 415
Boys-Corner theory of burning, 45, 47
Breech pressure, 134
Burning, high explosive, 73
  high pressure, 66
  in closed vessel, 132
  laws, 40, 70
  of volatile explosives, 49
  theory, 43–45
"Burnt," 138, 142, 152, 159, 162, 164, 167
  solution after, 139, 182, 196, 274, 284, 323

Calorie, 92
Calorimetric value, 96, 127, 128, 176
Carbamite, 25
Catalyst, 329
Cementite, 409
Central ballistic parameter, 137, 181
Chalk, 89
Chamber volume, 143
  ballistic effects, 169, 307
Characteristics, 348, 358, 396, 398
Charbonnier burning law, 41
Charbonnier-Sugot tables, 22, 134, 190, 205, 239
Charge, composite, 328
  optimum, 240
  recoilless guns, 264, 305
Charge weight, ballistic effects, 162
Chopped cord propellant, 33, 38, 333
Chronograph, Boulengé, 9
Clemmow factor, 209, 225
Closed vessel, 35, 70, 85
  burning in, 132
  cooling corrections, 87, 88
  ignition, 86
Combination products, 99
Combustion temperature at constant pressure, 47, 102
Commission of Metz, 18
Composite charges, 328
Compressibility of propellant, 66
Conduction of heat in gun barrel, 418
Cool propellants, 41, 83
Coppock solution, 177
Cord charge, optimum, 242
Cordite, 25
Corner pressure-decay formula, 372
Covolume, 101, 133, 366
  ballistic effects, 184
  effect on burning rate, 67
  in nozzle theory, 250, 315
  neglect of, 134
  observed, 111
  theory, 102, 113
Crusher gage, 7
  temperature correction, 8
Cubical grains, 32, 333

Davis gun, 246
Day-to-day variations, 5

Decomposition of propellant, low-temperature, 45
DEGN, 26
Degressive shape, 32
Density of loading, 132
  optimum, 242
Detonation of propellant, 72
Diethylene glycol dinitrate, 26
Differential analyzer, 206, 224, 225
Diffusion, at high pressures, 69
  in flames, 48
Diphenylamine, 30
Dispersion, mortar bombs, 276
Dissociation, 97
Drilled barrel, 276

Eccentric burning surfaces, 37
Eddy conductivity, 81
Efficiency, ballistic, 142, 144, 145, 153, 160, 162, 164, 166, 167, 184, 264, 305
  muzzle brake, 386, 388
  piezometric, 142, 153, 160, 164, 166, 167
Effective, γ, 141
Ejection of propellant, 407
Empirical corrections, 156
Energy equation, 175, 184
  for leaking gun, 258
Equation of state, 100
Equilibrium, after burning, 89
  at constant pressure, 115
  constants, 91, 107
  during expansion, 121
erfc, 421
Erosion, factor, 74
  of gun, 409
  of propellant, 35, 39, 73, 83, 133, 151, 190, 407
Ethyl centralite, 25
Expansion ratio of gun, 144
Explosion temperature at constant pressure, 44, 52
Explosives, burning of, 49, 73
Exponential integral, 55
Exterior ballistics, 16, 214, 225

Fanning coefficient, 412
Firing interval, 11, 29
Fixed ammunition, 27
Flake propellant, 33
Flame theory, 49
Flash radiography, 12
Flash-reducing salts, 29, 89
Force, 96, 126, 133
Force constant, 96, 126, 133
Form factor, 31, 132, 157
Form function, 31
  geometrical, 30
  true, 35
Freezing of equilibrium, 96, 121, 127
Frictional pressure gradient, 341

Gas trapped around projectile, 334, 392
Gaswash, 291
Gehrlich rifle, 334
Gelatinization, 112
Goldie solution, 192
Gossot-Liouville law, 209, 234
G-pulver, 26
Granular propellant, 27
Graphical methods, 131, 239
Graphite glaze, 27, 329
Gross efficiency, muzzle brake, 388
Gudol, 26
Guidebands, mortar bombs, 279
Gun proof, 5
Gunpowder, 24
Guns, 28/20-mm Pz B 41, 334
  5 cm-Pak 38, 383
  5.5-cm MK 115, 246
  7.5-cm LG 40, 246
  7.5-cm Pak 40, 143
  8-cm PAW 600, 313
  8.8-cm Pak 43, 384
  3.7-in. AA, 146
  10.5-cm LG 40, 246
  10.5-cm LG 42, 244
  10.5-cm PAW 1000, 313
  15-cm LG 290, 245
  28-cm DKM 44, 246

Head pressure on shot, 393
Heat conduction in barrel, 418
Heat loss, 140, 189, 425
Heat transfer, coefficient, 410
  results, 422
Heterogeneous charges, 36, 333
High-low-pressure gun, 312
  working formulas, 324

H/L gun, 312
Hoch Druck Pumpe, 232
Hoch-und niederdruck Kanone, 313
Howitzers, 136, 143
  charges, 28, 329
  recoilless, 275
Hugoniot curve, 360
Hugoniot pressure-decay formula, 323, 369, 376
Hydrodynamic nature of the bore surface, 417
Hyperbolic partial-differential equations, 348, 397

Ignition, 17, 28, 29, 86
  small arms, 328
Index law, ballistic methods, 206
Inhibition of burning, 35
Integral equation for heat flow, 421
Integration, numerical, 427
Intermediate products in burning, 47
Interpolation, 201
  coefficients, 433
Intrinsic efficiency of muzzle brake, 388
Isobaric flame temperature, 44
Isothermal solution, 132, 171

Jammed shot, 87

Lagrange approximation, 340, 343, 411
Lagrange corrections, 134, 282, 289
  in recoiling guns, 342
  in recoilless guns, 264
Lagrange's ballistic problem, 339
Laminar sublayer, 77
Langweiler solution, 134, 172
Lead crusher gage, 8
Leaking guns, effective charge, 263
  energy equation, 258
  equations of, 260
  reduction to nonleaking gun, 261
  solution after "burnt," 274
Long shell, 136
Loss of performance by wear, 293, 294
Lots, 4
Lot-to-lot variation, 5
Love-Pidduck solution, 347, 348
Low-pressure guns, 312
  recoilless, 265, 303

Manganin pressure gage, 9
Martensite, 409
Maximum pressure, position of, 153, 160
Maximum velocity, 361
Mean deviation, 5
Methane, 89, 99
Minor products, 108
Mixing length, 78
Moderated propellants, 328, 329, 333
Molecular weight of products, 96
Momentum index, muzzle brake, 386, 389
Momentum integral, boundary layer, 415
Mortar bombs, 279
Mortars, 143, 243, 376
  primary charge, 313
  secondary charge, 33
Multitubular propellant, 27, 34, 35, 158
Muraour theory of burning, 44
Muzzle adapter, 335
Muzzle brake, 365, 382–385
  efficiency, 386, 388
  on recoilless guns, 309
Muzzle extension, 276
Muzzle pressure, 164

NC, 24
Neutral grain shape, 32
NG, 25
Nitrocellulose, 24, 94
  as igniter, 29
Nitroglycerine, 25, 94
Nitroguanidine, 26, 42
Noble-Abel equation of state, 100
Nozzle-start pressure, 254, 300, 308
Nozzle theory, 246
  covolume effect, 250, 315
  thrust, 251
  thrust coefficient, 252
NSP, 29
Numerical integration, 223, 427
Nz Man P, 29

Obturation, 27, 86
Oiled bore, 335
Optimum ballistic solutions, 240
Optimum charge, 240
Optimum cord charge, 242
Optimum density of loading, 242
Optimum gun, 240

Optimum nozzle-start pressure, 308

Petavel gage, 86
Pidduck solution, 351, 366
Piezoelectric pressure gage, 9, 85
  in shot, 13
Piezometric efficiency, 142, 153, 160, 164, 166, 167, 326
Pike factors, 210, 212
Piobert coefficients, 340, 346
Piobert law, 38
POL, 25
Polymers, 17
Potential, 127, 128, 143, 175
Prandtl number, 77, 411
Pressure dependence of burning rate, 40
Pressure gradient, 133, 152, 336, 341, 357
  in recoilless guns, 256, 264
Pressure index of burning rate, 40, 71
Pressure-space curve, 151
Pressure waves, 86
Progressive grain shape, 32
Proof shot, 5
Propellant, constituents, thermochemical data for, 94
  grain, 25
  motion in gun, cord, 400
    short grains, 405
    tube, 404
  products, thermochemical data for, 95
  shape, ballistic effects, 170
Pyrotechnics, 53

QF gun, 27

Radial crusher gage, 8
Radiation effects, in burning, 66
  in heat transfer, 426
Radiography, 12
Rankine-Hugoniot equation, 360
Rarefaction waves, 347, 371, 377, 396
Rateau pressure-decay formula, 368, 376
Rate of burning, definition, 30
"R.D.38," 131
Reaction-zone thickness, 59
Recoil, correction to velocity, 136, 147, 170
Recoilless guns, 244
  ballistics, 300, 304
  charge weight, 264
Recoilless guns, effective charge, 263
  energy equation, 258
  equations of, 260
  howitzers, 275
  Lagrange corrections, 264
  loss of propellant, 253
  low pressure, 265, 303
  muzzle brake, 309
  recoil momentum, 297
  regularity, 303
  solution after "burnt," 274
  stress on carriage, 296
  with linear law of burning, 267
Recoillessness, 296
  by muzzle brake, 389
Recoil momentum, 376, 386
Recording crusher gage, 14, 85
Regularity of ballistics, 29, 168, 171, 240, 303, 310
Résal equation, 19, 130, 176, 374, 409
Resistance, bore, 12, 136, 156, 237, 337
  initial, 150
  muzzle, 151
Reynolds number, in gun bore, 411
  in propellant burning, 75
Ribbon propellant, 33
Riemann's method, 395
Ringpulver, 33
Rocket propellant, 26, 49, 72, 73, 120
Röggla graphs, 239
Röggla transformation, 232
Röhrenpulver, 33
Rosette propellant, 35
Rotational inertia, 135
Round-to-round variations, 162
RP, 33
Runup, 243, 280

SC, 25, 66
Schmitz process, 71
"Schwere Gustav," 232
SD, 25
Sébert coefficient, 340, 343
Sébert velocimeter, 13
Separate-loading ammunition, 27, 28
Seven-perforated propellant, 34
Shot ejection, ballistics after, 364
Shock waves, 349, 359, 392, 398
Shot-start pressure, 189, 300
  ballistic effects, 204, 206

Shot weight, ballistic effects, 169, 306
  effective, 136
Similarity, 21, 226
Sliver point, 83
Small arms, 327
  ignition, 328
  projectiles, 327
Smoke, 29
Smoke meter, 13
Solenoid velocity measurement, 10
Solventless propellant, 25
Solvent propellant, 24
Soot, 89, 128
Sound velocity, 97
Space-mean pressure, 134
Specific heats, 93
Specific impulse, 120
Spherical grains, 32, 333
Spring pressure gage, 14
Stability of projectile, 136
Stabilizer, 26
Stacked charges, 28
Strain gage, 11
Streifenpulver, 33
Strip propellant, 33
Str P, 33
Subcaliber projectile, 426
Sulphur, 30
Surface temperature of propellant, 63, 64
Surface theories of propellant burning, 43
Sutherland's law, 62, 75, 412
Swaging of flanges in tapered bore, 337

Tabulation of ballistic solutions, 232, 235, 239
Tapered bores, 334, 337
  ballistic solution, 337
Temperature, correction to crusher gage, 8
  effect, on burning rate, 69, 73
    on velocity, 168
Thermal model of flame, 50
Third virial coefficient, 106
Thring gage, 9
Throwback, 201
Thrust of muzzle brake, 385
Touch-off temperature, 46
Travel, effect on ballistics, 169, 307
Tungsten carbide, 334, 335
Twin-perforated propellant, 34

Uncooled explosion temperature, 44, 52 90
Upward creep, 6

Vapor-phase burning theory, 47
Variations, in burning rate, 36, 161
  in propellant, 36
Vent, 28
Vented vessel, 70
Virial coefficients, 104
  tables of, 105
V2, 129

Water-gas reaction, 107
Waves, of finite amplitude, 339
  of rarefaction, 347, 371, 377, 396
Web size, 30, 31, 159, 304
Working formulas, Coppock solution, 183
  high-low-pressure gun, 324
  isothermal solution, 141
Worn gun, ballistics, 279
  loss of velocity, 293, 294
  solution after "burnt," 284
  surface, 417